Aluminum Properties and Physical Metallurgy
John E. Hatch editor, p 1-24
DOI: 10.1361/appm1984p001

CHAPTER 1

PROPERTIES OF PURE ALUMINUM*

Aluminum exceeding 99.99% in purity, produced by the Hoopes (Ref 1) electrolytic process, was first available early in 1920. In 1925, Edwards (Ref 2) reported some of the physical and mechanical properties of this grade of aluminum. Taylor, Willey, Smith, and Edwards (Ref 3) published a paper in 1938 that gave several properties for 99.996% aluminum that was produced in France by a modified Hoopes process. The first international meeting to discuss very pure metals was held in October 1959 in Paris (Ref 4), and a seminar on ultrahigh-purity metals was sponsored by the American Society for Metals in 1961 (Ref 5). The first edition of this monograph was published in 1967.

In the intervening years, because of the relative ease of preparing the metal in high-purity form and because of its interesting properties as a pure material, many papers have been published on the subject of pure aluminum. Applications have been mainly in the fields of electrolytic capacitor foil, cryoelectrics, cryomagnetics, and semiconductors.

Newer methods of preparation include zone refining (Ref 6–9), crystallization from amalgams (Ref 10 and 11), and preparation from aluminum alkyls (Ref 9 and 12). Electrical resistivity at low temperatures has been developed as a measure of purity (Ref 9 and 13). Improved methods of analysis, including neutron activation, have extended the sensitivity and scope of analyses (Ref 9 and 14).

There is no generally adopted nomenclature for the various degrees of purity of aluminum. The following classification is appropriate:

Aluminum, %	Designation
99.50–99.79	Commercial purity
99.80–99.949	High purity
99.950–99.9959	Super purity
99.9960–99.9990	Extreme purity
Over 99.9990	Ultra purity

Similar designations and the term "U.S. wrought alloy 1199" are used in *World Aluminum Abstracts*. In *Chemical Abstracts*, information on the preparation and properties are found under the respective headings of "Aluminum Preparation and Aluminum Properties." This chapter reviews the properties of aluminum of 99.95% purity or more. The effects of

*This chapter was revised by a team comprised of W.B. Frank, Alcoa Technical Center; G.P. Koch, Reynolds Metals Co.; and J.J. Mills, Martin Marietta Laboratories. The original chapter was authored by J.L. Brandt, Alcoa Research Laboratories.

alloying additions and impurities on the properties of aluminum alloys are covered in Chapter 6 of this Volume.

MECHANICAL PROPERTIES

The mechanical properties of aluminum are discussed under several headings in this chapter, but only briefly in each case in view of the variety and scope of the studies that have been made. The normal mechanical properties of aluminum of several purities are shown in Table 1. In this case and in general, sets of data from different sources should not be compared directly. Major difficulties may occur in such cases because of problems of precise analysis, specimen preparation, and test methods.

TENSILE AND YIELD PROPERTIES

Tensile and yield properties have been studied for a range of purities and structures under a variety of test conditions. Deep and Plumtree (Ref 16) determined the tensile and yield values of rods of 99.7 and 99.99% purities extruded under identical conditions and related observed properties to structural characteristics. Iida *et al* (Ref 17) found an anomalous strain-rate sensitivity of yield stress in 99.99 and 99.999% purity metal at fractional values of the superconductivity temperature. Hamel (Ref 18) determined the effect of strain rate and orientation on the tensile properties and work hardening for samples of 99.99 and 99.3% aluminum sheet. Hammad and others (Ref 19) investigated work softening yield points in 99.995% aluminum in the temperature range of 100 to 450 °C (212 to 840 °F) after prestraining in tension at lower temperatures or a higher strain rate. Hamel (Ref 18) and Vainblat and Khayurov (Ref 20) have reported serrated yielding.

STRESS-STRAIN RELATIONSHIPS

Stress-strain curves have been used by a number of investigators because of their sensitivity to material and test conditions and the mathematical expressions that can be used to represent, analyze, and compare them. Kocks (Ref 21) studied 99.99% aluminum in this way, using an expanded Voce equation to describe the dependence on temperature and strain rate, grain size, and purity for 99.99 and 99.5% aluminum. Polakovic and Taborsky (Ref 22 and 23) studied the effects of deformation rate, grain size, and purity for 99.99 and 99.5% aluminum. These authors, together with Hyross (Ref 24), performed similar studies over a

Table 1. Mechanical Properties of Pure Aluminum at Room Temperature

Purity, %	Tensile yield strength (0.2% offset) MPa	ksi	Tensile strength MPa	ksi	Elongation in 50 mm (2 in.), % (a)	(b)
99.99(a)	10	1.4	45	6.5	50	65
99.8(a)	20	2.9	60	8.7	45	55
99.6(a)	30	4.4	70	10.2	43	...

(a) From Chapter 9, Table 3 of this Volume. (b) From Ref 15.

temperature range of 20 to −90 °C (68 to −130 °F). Sellars and McG.Tegart (Ref 25) made such studies at 400 °C (750 °F). Roberts (Ref 26) has reported the effects of strain rate on work hardening in the temperature range of 77 to 425 K.

CREEP

Parker and Wilshire (Ref 27) studied the effect of a sudden reduction in applied stress. The instantaneous contraction can be greater than the elastic modulus predicts. Negative creep occurs immediately after the instantaneous specimen contraction with large reductions in stress. Positive creep behavior is determined by the full applied stress, not by an effective stress. Radhakrishnan (Ref 28–31) compared the effect of an oscillating stress on the steady-state creep rate to that for a static stress. Young, Robinson, and Oleg (Ref 32) found that the creep strength at a given strain rate increases as the subgrain size decreases. Myshlyaev and others (Ref 33) determined the stress dependence of the steady-state creep rate at 18 and 600 °C (64 and 1110 °F). At high temperatures and low stresses, the rate is parabolic and a function of stress. At lower temperatures and high stresses, the rate dependence changes to an exponential law. Prasad *et al* (Ref 34) studied creep at low temperatures of 87 and 200 °C (190 and 390 °F) and found the effects of stress increments and decrements to be different.

Table 2. Isotopes of Aluminum (Ref 36)

Isotope	Abundance, %	Mass(a)	Half-life, s	Decay products	Decay products with absorption of other particles	Particles absorbed
23	...	...	0.13	Mg + proton		
24	...	24.007 6	2.7	...	^{24}Mg + proton	Neutron
25	$<1.5 \times 10^{-4}$	24.998 3	7.5	^{24}Mg + proton + γ rays	^{25}Mg + proton	Neutron
26	$<1.5 \times 10^{-4}$	25.996 1	7.0	^{25}Mg + proton + γ rays	^{23}Na + He_4	Neutron
					^{25}Mg + H_2	Neutron
					^{26}Mg + proton	Neutron
					^{27}Al + γ rays	Neutron
26	...	...	10^6 years			
27	~100	26.989 74	stable	...		
28	$< 5 \times 10^{-5}$	27.997 8	144.0	^{28}Mg + electron	^{16}O + ^{14}N	2 protons
				^{27}Al + neutron + γ rays	^{25}Mg + ^{4}He	1 proton
					^{27}Al + ^{14}N	^{13}N
					^{27}Al + ^{2}H	1 neutron
					^{28}Si + β	
					^{28}Si + neutron	1 proton
					^{29}Si	1 proton
					^{31}P + neutron	^{4}He
					Cl + proton	Neutron
29	$<2 \times 10^{-5}$	28.989 7	396.0	...	^{26}Mg + ^{4}He	Proton
					^{27}Al + ^{3}H	Proton
					^{27}Al + ^{4}He	2 protons
					^{29}Si + neutron	Proton
					^{30}Si + γ rays	Proton
					^{31}P + γ rays	2 protons

(a) Mass calculated on basis of ^{16}O = 16.000 00.

PHYSICAL PROPERTIES

Atomic Structure and Nuclear Properties. Aluminum has an atomic number of 13, and the latest accepted values for the atomic weight are 26.981 5 based on ^{12}C and 26.989 74 based on ^{16}O (Ref 35). The main isotope is ^{27}Al, which is stable and consists of 14 neutrons and 13 protons. Apart from one isotope, ^{26}Al which has a half life of 10^6 years, all the isotopes have short half lives and negligible abundance (Table 2) (Ref 36). The valence of aluminum in chemical compounds is 3, with the 13 electrons distributed as follows: $1s^2$, $2s^2$, $2p^6$, $3s^2$, and $3p^1$.

The naturally occurring aluminum isotope has a low cross section for thermal neutrons of 0.232 ± 0.003 b* (Ref 37), increasing in an irregular manner to ~0.6 b at 700 to 800 MeV. Between 20 and 50 keV, there are various resonance peaks with maxima up to 15 (Ref 38). The nuclear mass absorption coefficient for γ-rays is dominated by the photoelectric

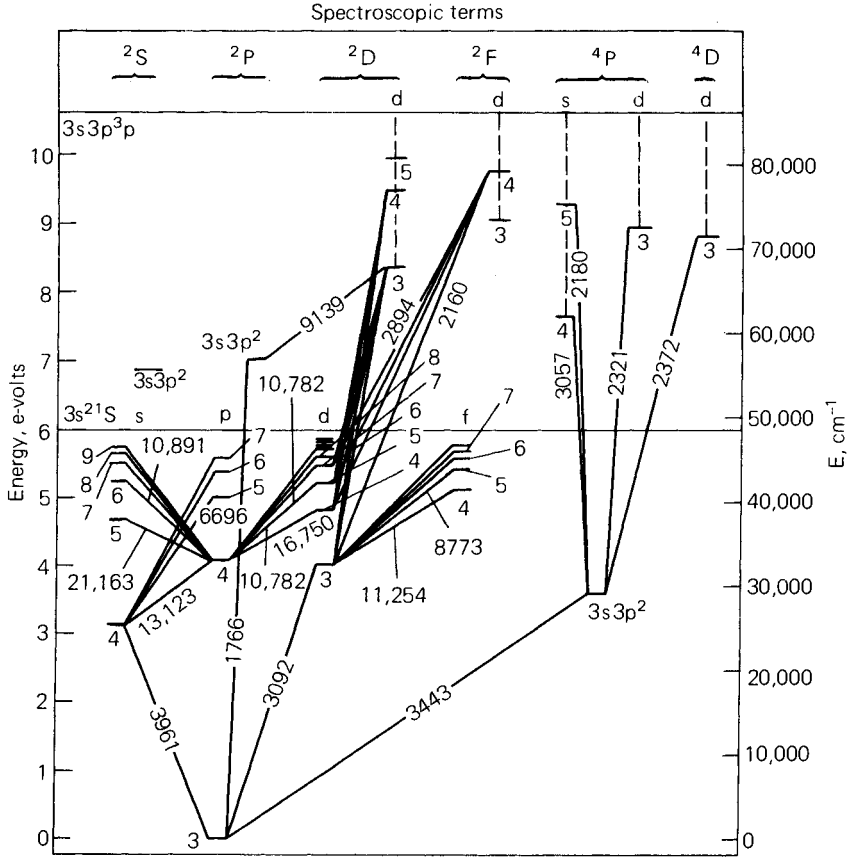

Fig. 1. Term diagram for Aluminum I. All combinations observed in this work are shown, except for the higher part of the sharp and diffuse series. Wavelengths are given in Angstroms. (Ref 43)

*A barn is a unit of area equal to 10^{-24} cm^2.

effect up to 0.04 MeV, at which energy the Compton effect begins to dominate up to 10 MeV. Above 30 MeV, the pair production mechanism dominates. The coefficient falls from ~2.5 m^2/kg at 0.01 MeV to 0.05 m^2/kg at 0.04 MeV and then decreases relatively slowly with increasing γ-ray energy falling from 0.02 m^2/kg at 0.1 eV to ~0.002 m^2/kg at 100 MeV (see Ref 39 for details). The nuclear magnetic and quadropole moments are +3.6414 nuclear magnetons and +0.15 b, respectively (Ref 40). The resonance energy for the absorption of protons through the $Al^{27}(p,\gamma)Si^{28}$ reaction is 991.9 ± 0.04 KeV with a half width of 0.10 ± 0.02 keV, and the threshold energy for the $Al^{27}(p,n)Si^{27}$ reaction is 5796.9 ± 3.8 KeV (Ref 41).

Atomic Spectrum. The atomic spectrum of aluminum has recently been reviewed by Martin and Zalukas (Ref 42), who give the spectral lines of all species from atomic aluminum, Al I, to fully ionized aluminum, Al XIII. The minimum ionization potential is 3.13 V and the first three ionization energies are 5.98580 ± 0.00002 eV, 18.82873 ± 0.00006 eV, and 28.44787 ± 0.00008 eV. The strongest line in the spectrum is the $3p^2P_{3_2} - 4s^2S_1$ transition at 396.15200 nm (3961.5200 Å) (Ref 43). The term diagram for Al I derived from the observations of Eriksson and Isberg (Ref 43) is presented in Fig. 1.

Crystal Structure. Aluminum crystallizes in the face-centered cubic lattice that is stable from 4 K to the melting point. Previous discoveries of allotropes have proven to be false. The coordination number of aluminum is 12, with four atoms to the unit cell. The accepted edge length of the unit lattice cube for pure aluminum is $4.049\ 596 \times 10^{-10}$ m at 298 K. Hence, the atomic diameter of aluminum is 2.86×10^{-10} m and its atomic volume 9.999×10^{-6} m^3/g at. The lattice parameter is only slightly affected by impurities (Ref 44).

Density. Theoretical density based on lattice spacing is 2698.72 kg/m^3 (Ref 44). Experimental values range from 2696.6 to 2698.8 kg/m^3 for polycrystalline material with the densities of single crystals lying 0.34% higher (Ref 44). The density of molten 99.996% aluminum is presented below (Ref 45):

Temperature, K	ρ(Kg/m³)	ρ (lb/ft³)
933	2368	148
973	2357	147
1023	2345	146
1073	2332	146
1123	2319	145
1173	2304	144

Thermal Expansion. The recommended values for the coefficient of thermal expansion (CTE) are listed on the following page. These values are for well-annealed 99.99% aluminum and are accurate to 5% between 100 K and the melting point. The CTE is thought to be isotropic, and values for metal of commercial purity lie within the experimental error of those of the pure metal (Ref 46). Willey (Ref 47) has developed three

Temperature, K	α ($\times 10^{-6}$ K^{-1})
25	0.5
50	3.5
75	8.1
100	12.0
150	17.1
200	20.2
250	22
293	23
350	24.1
400	24.9
500	26.5
600	28.2
700	30.4
800	33.5
900	37.3

equations that are useful in calculating approximate linear expansions over the temperature ranges indicated:

$$L\,(213 \text{ to } 373 \text{ K}) = L_0\,[1 + C\,\{22.17\,(T-273) + 0.012\,[T-273]^2\}\,10^{-6}]$$

$$L\,(273 \text{ to } 473 \text{ K}) = L_0\,[1 + C\,\{21.57\,(T-273) + 0.00443\,(T-273)^2 - 0.000124\,(T-273)^3\}\,10^{-6}]$$

$$L\,(273 \text{ to } 773 \text{ K}) = L_0\,[1 + C\,\{22.34\,(T-273) + 0.00997\,(T-273)^2\}\,10^{-6}]$$

where L_0 equals the length at 273 K, L is the length at temperature T (in degrees kelvin) within the range indicated, and C equals the alloy constant, which is 1 for pure aluminum (Ref 47). Alloy constants for aluminum alloys are given in Ref 48. Further details of the influence of alloying elements on the coefficient of thermal expansion are given in Touloukian (Ref 49).

Thermal Conductivity. At moderate to high temperatures such as >100 K, the true thermal conductivity, k, of well-annealed, high-purity (99.99+%) aluminum is relatively insensitive to the impurity level. Below 100 K, aluminum becomes highly sensitive to the impurity level, measured by the residual resistivity, ρ_0 (the resistivity at 0 K). For well-annealed, high-purity aluminum with a ρ_0 of $5.94 \times 10^{-12}\,\Omega \cdot$ m, the recommended value for thermal conductivity is listed in Tables 3a and 3b (Ref 50). The values in Tables 3a and 3b are thought to be accurate to within ±5% below room temperature to within ±2 to ±3% above room temperature and to within ±8% above the melting point (Ref 50). For samples with other ρ_0, the thermal conductivity, k, at temperatures below 1.5 T_m (where T_m is the temperature of the maximum in K) is given by

$$k = [\alpha' T^n + \beta T^{-1}]^{-1}$$

where $\alpha' = \alpha''\,[\beta/n\alpha'']^{(m-n)/(m+1)}$

with $\alpha'' = 4.79 \times 10^{-6}$, $m = 2.62$, and $n = 2$, and

$\beta = \rho_0/L_0$

L_0 is the theoretical Lorenz number (Ref 51).

Electrical Properties. The accepted value for the electrical resistivity of super-purity aluminum (99.990%) at 20 °C (68 °F) is 2.6548×10^{-8}

Table 3a. Recommended Thermal Conductivity of Aluminum (Solid)(a)

Temperature (*T*), K	Thermal conductivity (κ), W cm^{-1} K^{-1}	Temperature (*T*), K	Thermal conductivity (κ), W cm^{-1} K^{-1}
0	0	80	4.32
1	41.1	90	3.42
2	81.8	100	3.02
3	121	123.2	2.62
4	157	150	2.48
5	188	173.2	2.41
6	213	200	2.37
7	229	223.2	2.35
8	237	250	2.35
9	239	273.2	2.36
10	235	298.2	2.37
11	226	300	2.37
12	214	323.2	2.39
13	201	350	2.40
14	189	373.2	2.40
15	176	400	2.40
16	163	473.2	2.37
18	138	500	2.36
20	117	573.2	2.33
25	75.2	600	2.31
30	49.5	673.2	2.26
35	33.8	700	2.25
40	24.0	773.2	2.19
45	17.7	800	2.18
50	13.5	873.2	2.12
60	8.50	900	2.10
70	5.85	933.52	2.08

(a) Recommended values are for well-annealed high-purity aluminum, but those below 150 K are applicable specifically to samples having residual electrical resistivity of 0.000 594 μΩ cm. (Ref 50)

Ω · m or 64.94% of the International Annealed Copper Standard (IACS) (Ref 52). The electrical resistivity of aluminum of various purities is shown in Fig. 2 and given in Table 4 (Ref 53). The conductivity is isotropic unless oriented dislocations are present (Ref 54). The effect of grain size in commercial materials is negligible (Ref 54). Cold worked material, however, exhibits 0.5 to 1% better conductivity in the direction of deformation (Ref 54). Aluminum exhibits no photoconductive effect (Ref 54).

The resistivity of pure aluminum at very low temperatures (<100 K) is highly sensitive to its degree of purity. Hence, the ratio of the resistivity at 290 K to that at 4.2 K is sometimes used as a measure of purity. Values as high as 30,000 have been reported for 99.999% pure material (Ref 55). The degree of purity influences the electron mean free path, λ, with more pure materials having a higher λ. Hence, for high-purity materials at low temperatures, λ can become comparable to the specimen size, and a significant size effect can occur. For very pure specimens, the product ρλ, where ρ is the resistivity, should be constant because it is proportional to the number of valence electrons. This has been found to be true by Førsvoll and Hollvech (Ref 56 and 57) and by Montariol (Ref 58); the

Table 3b. Recommended Thermal Conductivity of Aluminum (Liquid)(a)

Temperature (T), K	Thermal conductivity (κ), W cm^{-1} K^{-1}	Temperature (T), K	Thermal conductivity (κ), W cm^{-1} K^{-1}
933.52	0.907	2873.2	1.13
973.2	0.921	3000	1.13
1000	0.930	3073	1.12
1073.2	0.955	3200	1.11
1100	0.964	3273	1.10
1173.2	0.986	3400	1.09
1200	0.994	3473	1.07
1273.2	1.01	3600	1.05
1300	1.02	3673	1.05
1373.2	1.04	3800	1.03
1400	1.05	3873	1.02
1473.2	1.07	4000	0.997
1500	1.07	4073	0.986
1573.2	1.08	4273	0.952
1600	1.09	4500	0.912
1673.2	1.10	4773	0.861
1700	1.11	5000	0.818
1773.2	1.11	5273	0.764
1800	1.12	5500	0.719
1873.2	1.13	5773	0.662
1900	1.13	6000	0.614
1973.2	1.14	6273	0.555
2000	1.14	6500	0.505
2073.2	1.14	6773	0.444
2173.2	1.15	7000	0.392
2200	1.15	7273	0.329
2273.2	1.15	7500	0.275
2400	1.15	7773	0.210
2473.2	1.15	8000	0.156
2600	1.15	8273	0.0915
2673.2	1.15	8500	0.0365
2800	1.14	8650(b)	···

(a) Except for 0.921, 0.930, 0.955, 0.964, 0.986, 0.994, and 1.01 W cm^{-1} K^{-1}, all liquid thermal conductivity values are estimated. (b) Critical point.

value is approximately 7×10^{-16} $\Omega \cdot m^2$. An extensive review on this subject has been published by Montariol (Ref 58).

Aluminum is superconducting at temperatures close to absolute zero. The superconducting transition variables have been reviewed by Caplan and Chavin who found transition temperatures, T_c, ranging from 1.164 to 1.200 K (Ref 59). Their own measurements produced $T_c = 1.175 \pm 0.001$ K and a parabolic critical field curve with

$$H_c = H_0 [1 - (T/T_c)^2]$$

and $H_0 = 8340 \pm 5$ A/m and $(dH_c/dT)_{T_c} = 12570 \pm 30$ A($m^{-1}K^{-1}$) (Ref 59). Increasing low-level impurity content decreases T_c, and Boato *et al* reviews these increases for the addition of chromium, manganese, and iron (Ref 60). High concentrations of impurities can result in an increase in T_c (Ref 61).

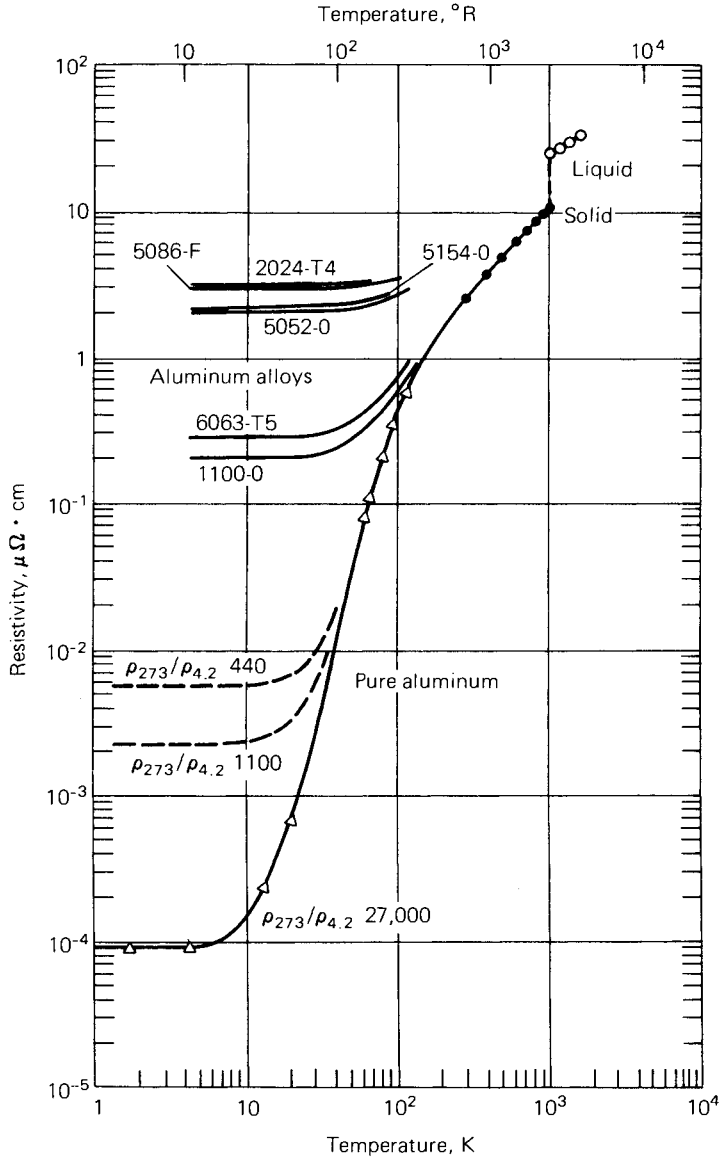

Fig. 2. Electrical resistivity of pure aluminum and aluminum alloys as a function of temperature. (Ref 62)

The temperature dependence of the resistivity of aluminum at low temperatures (<100 K), $\rho(T)$, can be expressed as

$$\rho(T) = \rho(0) + AT^2 + BT^5$$

where $\rho(0)$ is the residual resistivity, T is in degrees kelvin, and A and B are constants that should be determined for each purity. The T^2 term arises from electron-electron scattering, while the T^5 arises from electron-

Table 4. Electrical Resistivity of Pure Aluminum

Symbol(a)	Temperature, K	ρ/ρ 273 K	ρ, μΩ·cm(b)	dρ/dT, μΩ·cm/K(b)	Sample
—△—	1.65	3.69×10^{-5}	9.25×10^{-5}	···	99.9998% aluminum,
	4.22	3.69×10^{-5}	9.25×10^{-5}	···	single crystal,
	14	1.04×10^{-4}	2.61×10^{-4}	···	large diameter
	20.4	2.94×10^{-4}	7.33×10^{-4}	···	(~10 mm)
	58	3.48×10^{-2}	8.70×10^{-2}	···	
	63.5	4.68×10^{-2}	0.117	···	
	77.4	9.34×10^{-2}	0.210	···	
	90.31	0.140	0.351	···	
	111.6	0.246	0.614	···	
—●—	273	1	2.50	0.0109	99.9% aluminum, 0.05%
	373	1.448	3.62	0.0114	silicon 127-μm (5-mil)
	473	1.911	4.78	0.0119	diam wire
	573	2.400	6.00	0.0124	
	673	2.915	7.29	0.0130	
	773	3.453	8.63	0.0139	
	873	4.036	10.10	0.0154	
	923	4.361	10.90	0.0166	
—○—	933	···	10.95 (solid)	···	99.99% aluminum
	933	···	24.2 (liquid)	···	
	973	···	24.75	···	
	1073	···	26.25	···	
	1173	···	27.75	···	
	1273	···	29.2	···	
	1373	···	30.65	···	
	1473	···	32.15	···	
----	4.2	···	5.7×10^{-3}	···	5–9s purity commercial
	77	···	0.22	···	aluminum annealed at 150 °C (300 °F) for 4 h
	4.2	···	2.3×10^{-3}	···	6–9s purity commercial
	77	···	0.22	···	aluminum annealed at 150 °C (300 °F) for 4 h

(a) From Fig. 2. (b) Assuming ρ = 2.50 μΩ·cm at 273 K. (Ref 53)

photon scattering (Ref 62). Between 273 and 573 K, the temperature dependence of aluminum of various purities is approximately linear with a coefficient of $1 \cdot 15 \times 10^{-8}$ Ω · m per degree kelvin (Ref 53).

Hall Coefficient and Magnetoresistance. The Hall coefficient (R_H) and the magnetoresistance coefficient, $\Delta\rho/\rho(0)$, where $\rho(0)$ is the electrical resistivity in zero magnetic field have been and are currently being intensively studied because they can be used to derive information on the Fermi surface and electron scattering behavior (Ref 63–66). Most reported values, however, are for low temperatures of <20 K.

Being a metal with free electrons, R_H and $\Delta\rho/\rho(0)$ are strongly dependent on the magnitude of the variable B/ρ_0, where B is the magnetic field (in Wb/m^2) and ρ_0 is the resistivity (in Ω · m) at a temperature of absolute zero. There are two magnetic field regions of interest: the low field, where $B/\rho_0 \ll 10^2$ and the high field, where $B/\rho_0 \gg 10^2$. In low magnetic fields, the Hall coefficient of pure and dilute alloys of aluminum is independent of magnetic field and isotropic, with a value varying between

-0.4×10^{-2} mm^3/A.s. and $+0.8 \times 10^{-2}$ mm^2/As at 4.2 K, depending on the type but not the concentration of lattice defect on impurity present (Ref 63 and 64). Very few studies of R_H in aluminum at higher temperatures have been reported; the values reported by Mondolfo (Ref 65) for various temperatures are summarized below:

Temperature, K	R_H ($\times 10^2$ mm^3/A.s.)
4.2	−1.1
100	−2
293	−3.44
800	−3.89
933	−4

In the high field region, R_H again becomes independent of field, but is large and positive and approaches the theoretical value for metals of $+10.23 \times 10^{-2}$ mm^3/A.s. (Ref 66). At intermediate fields ($B/\rho_0 \sim 10^2$), it varies smoothly with field (Ref 66).

In low magnetic fields, both longitudinal and transverse magnetoresistance coefficients are given by $\Delta\rho/\rho(0) = K B^n$, where n approaches

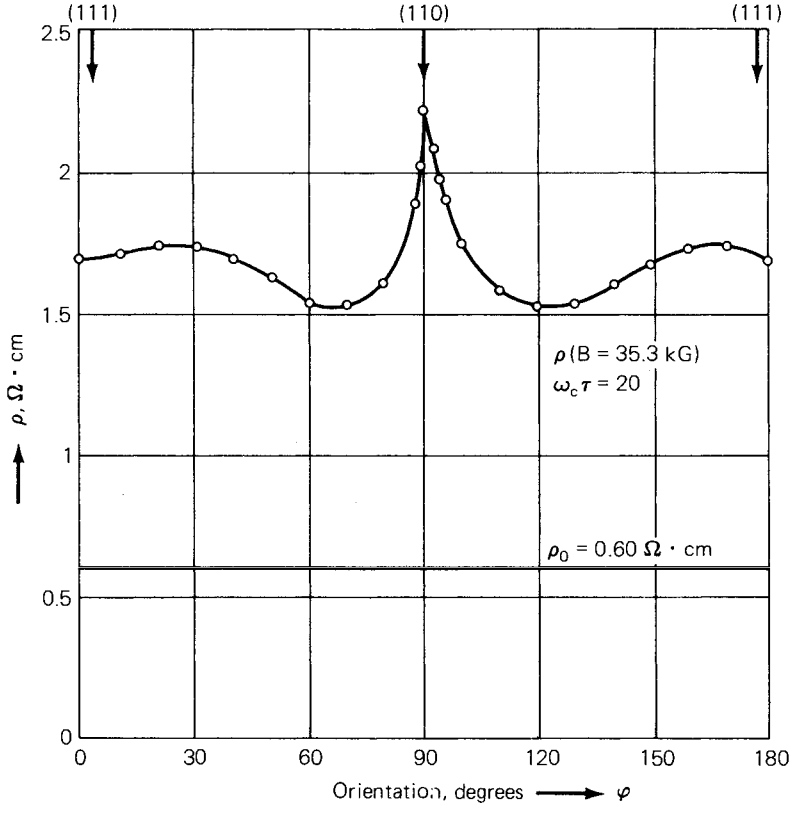

Fig. 3. High magnetic field anisotropy of magnetoresistance. (Ref 66)

the theoretical value of 2 and K is a constant that depends on the type of defect present. Both coefficients are almost isotropic, that is, variation in $\Delta\rho/\rho(0)$ is reportedly <2% (Ref 63). In highly magnetic fields ($B/\rho_0 \gg 10^2$), $\Delta\rho/\rho_0$ becomes highly anisotropic (Fig. 3) (Ref 66). There is some controversy over whether the coefficients saturate at high fields as required by theory for metals with a closed Fermi surface (Ref 66). Kesternich suggests that the portions of $\Delta\rho/\rho(0)$ that increase with field are attributable to geometrical effects caused by imperfect current distributions and sample alignment, such artifacts increasing with increasing sample purity (Ref 66). Values for the transverse $\Delta\rho/\rho(0)$ at saturation range from 1.2 to 30 at 4.2 K depending on orientation and defect type. For details, see Ref 66.

Magnetic Susceptibility. Because aluminum has an odd number of valence electrons (3), it is paramagnetic. The variation of magnetic susceptibility with temperature from 0 to 1000 K is presented in Fig. 4 (Ref 67). Small additions of iron and manganese raise the susceptibility only slightly, while other additions tend to lower it (Ref 65). The influence of deformation is still controversial, with some reports of 5 to 15% decreases at 50% deformation (Ref 65). Quenched dislocations reportedly reduce the susceptibility by several percent (Ref 65).

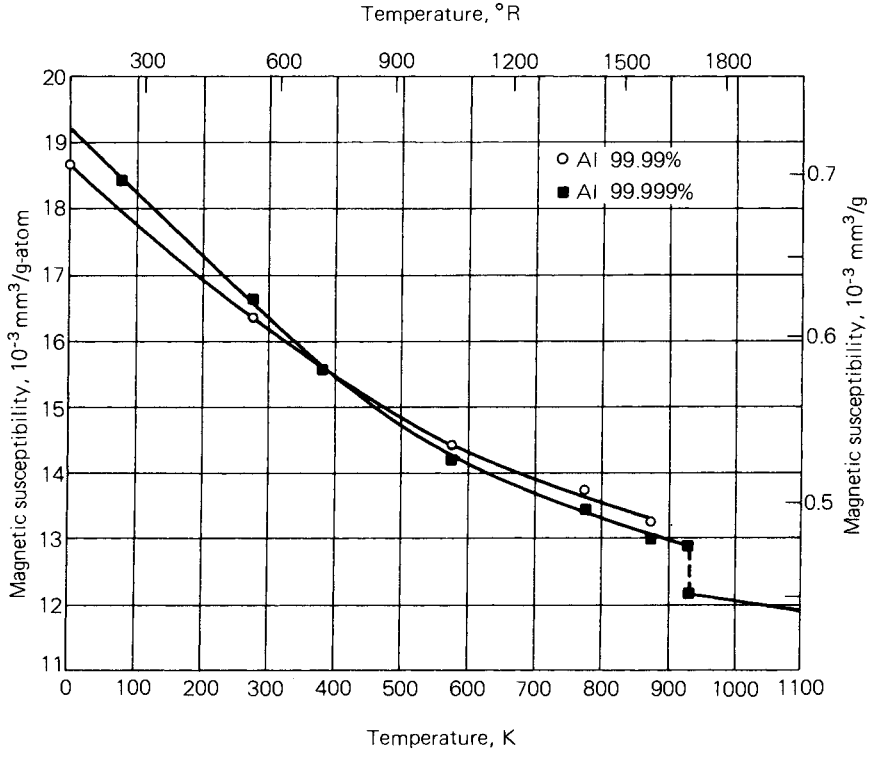

Fig. 4. Magnetic susceptibility of aluminum as a function of temperature and purity. (Ref 67)

COMPRESSIBILITY

Vaidya and Kennedy (Ref 68) determined the volume compression of aluminum of 99.999% purity to 45 kbar. The ratios of volume at high pressure to volume at ambient pressure are given in the following table:

Pressure, kbar	Volume compression, V/Vo
5	0.9937
10	0.9876
15	0.9817
20	0.9760
25	0.9704
30	0.9650
35	0.9597
40	0.9546
45	0.9497

Roy and Steward (Ref 69) report a partial structure transformation of aluminum at 205 kbar from cubic to hexagonal close-packed. At 200 kbar V/Vo = 0.85. Mondolfo (Ref 70), in reviewing measurements of the compressibility of aluminum at room temperature, indicates an average value of 13.3 m^2/TN for both high purity and commercial metal. Reported values range from 12 to 13.7 m^2/TN. Compressibility at 0 K is of the order of 12 m^2/TN and in the liquid at the melting point about 20 m^2/TN.

OPTICAL PROPERTIES

Mondolfo (Ref 71) indicates the reflectivity of smooth aluminum surfaces to light is more than 90% for wavelengths from 0.9 to 12.0 μm (0.04 to 0.5 mil). At wavelengths below 0.2 μm (0.008 mil), at which wavelength the reflectivities of smooth aluminum surfaces are about 70%, reflectivity decreases drastically. Highest reflectivity is obtained by vapor deposition, which can produce very smooth surfaces. Vapor-deposited films required a minimum thickness of about 10^{-5} cm (4×10^{-6} in.) for maximum reflection. The reflecting power of an aluminum surface decreases with roughness. A sandblasted aluminum surface may exhibit only 15 to 25% of the reflectivity of a polished surface of metal of the same composition. Figure 5 presents the normal spectral reflectances for various pure aluminum surfaces (Ref 72). Emissivity of polished aluminum at room temperature is only several percent of that of a blackbody (Ref 71). Rough finishes may raise the emissivity to about 20 to 30%. Emissivity increases with temperature to reach values of 15 to 20% for the liquid state. The total hemispherical emissivity of highly polished 99.999% aluminum has been reported as 1.0% at 180 K and 1.8% at 290 K (Ref 73). Literature on optical properties of aluminum has been reviewed by Mondolfo (Ref 71), and critical evaluation of data on thermal radiative properties of aluminum of various grades of purity is provided by Touloukian and DeWitt (Ref 72).

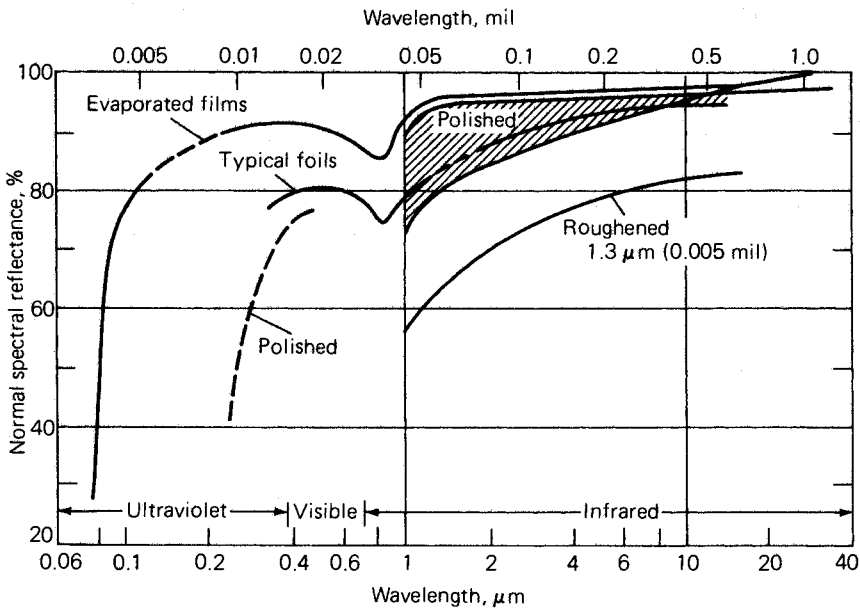

Fig. 5. Spectral reflectance of aluminum. (Ref 72)

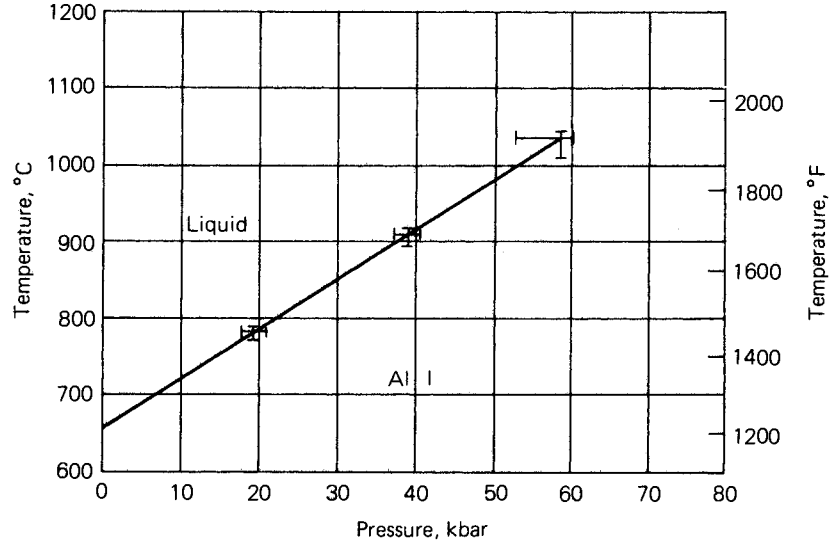

Fig. 6. Phase diagram for aluminum. (Ref 76)

MELTING POINT—HEAT OF FUSION

The melting point is quite sensitive to purity. Mondolfo (Ref 74) states that "the most accurate determinations on aluminum 99.996% give a melting point of 933.4 K." The freezing point of aluminum, a secondary reference point assigned 660.37 °C (1220.67 °F) on the International

Table 5. Heat Capacities, Entropies, and Heat Contents of Pure Crystalline Aluminum

Temperature, K	Heat capacity, C_p°, cal mole^{-1} deg^{-1}	Entropy, S°, cal mole^{-1} deg^{-1}	Heat content, $H^\circ - H^\circ_{298}$, kcal mole^{-1}
0	0.000	0.000	−1.094
100	3.116	1.650	−0.988
200	5.158	4.572	−0.546
298	5.806	6.769	0.000
300	5.814	6.805	0.011
400	6.163	8.528	0.610
500	6.450	9.934	1.241
600	6.717	11.134	1.900
700	6.999	12.190	2.585
800	7.370	13.147	3.302
900	7.901	14.044	4.064

Practical Temperature Scale of 1968, has been used for several decades to calibrate thermocouples (Ref 75). The phase diagram (Ref 76) for aluminum (Fig. 6) illustrates the effect of pressure on melting point. The JANAF Thermochemical Tables (Ref 77) select a value of 2.56 ± 0.05 kcal mol^{-1} (397 J g^{-1}) for the heat of fusion of pure aluminum.

Thermochemical Properties. Critically evaluated thermochemical data for aluminum in the solid, liquid, and gaseous states are compiled in the JANAF tables (Ref 77). The heat capacities, entropies, and heat contents of pure crystalline aluminum are given in Table 5. The recommended value of heat capacity of liquid aluminum from the melting point to the boiling point is a constant 7.59 cal mol^{-1} deg^{-1}.

Vapor Pressure. There is poor agreement in measurements of vapor pressure of aluminum at high temperatures. From critical evaluation of the determinations of vapor pressure, a boiling point of 2767 K and a heat of vaporization of 69.5 kcal mol^{-1} are recommended in the JANAF tables (Ref 77). Calculations from thermochemical data for liquid and gaseous aluminum in the JANAF tables give the following vapor pressures:

Temperature, K	Vapor pressure, atm
1000	7.4×10^{-11}
1200	3.7×10^{-8}
1400	3.0×10^{-6}
1600	7.8×10^{-5}
1800	9.8×10^{-4}
2000	0.007
2200	0.037
2400	0.143
2600	0.442
2700	0.728

SURFACE TENSION

Mondolfo (Ref 78) provides a review of measurements and calculations of interfacial energies of aluminum. Surface tensions of molten aluminum

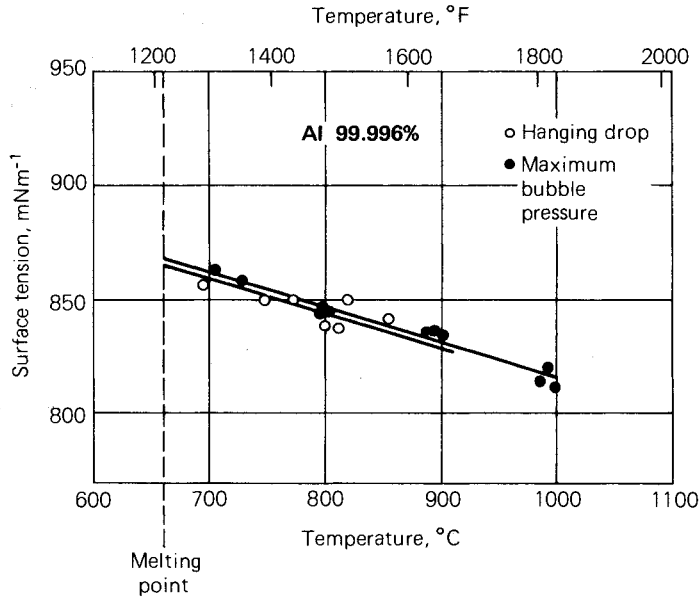

Fig. 7. Temperature dependence of surface tension of pure aluminum determined by two methods. (Ref 80)

are quite sensitive to the atmosphere and to even trace levels of impurities. Calculations of surface tensions from theoretical considerations also yield contrasting results. An absolute value for the surface tension of pure aluminum in any atmosphere is difficult to determine. Lang (Ref 79) evaluates earlier work on surface tension of high-purity aluminum, presents measurements for four samples of super-purity aluminum, and develops equations for the influence of small amounts of alloying elements on surface tension. The following expression was developed for the sample having the highest values of surface tension near the melting point:

$$\sigma = 868 - 0.152\,(t - t_m)$$

where σ is the surface tension in dyne cm^{-1}, t is the temperature in °C, and t_m is the melting point of aluminum. Lang *et al* (Ref 80) report measurements of the surface tension of aluminum of 99.996% purity by the sessile drop method and the maximum bubble method (Fig. 7) and also review earlier determinations of the surface tension of molten aluminum in various atmospheres.

VISCOSITY

The results of measurements of the viscosity of molten aluminum differ substantially among the various published investigations. The viscosity of liquid aluminum is increased significantly by small amounts of solid impurities such as aluminum oxide and by traces of dissolved impurities. The *Metals Reference Book* (Ref 81) gives the following equation for the viscosity of liquid aluminum:

$$\eta = 0.1492 \exp(1984.5/T)$$

where η is the viscosity in mNs/m^2, R is the gas constant, 8.3144 J/K

mol, which is a part of the exponential constant, and T is the temperature in degrees kelvin. Arsentev and Polyakova (Ref 82) report measurements at 670 to 1000 °C (1240 to 1830 °F) for the viscosity of molten aluminum of various degrees of purity by a viscosimeter. The results for zone-refined aluminum, the purest specimen investigated, can be represented by the equation:

$$\log \eta = \frac{720}{T} - 2.68$$

where η is the viscosity in poise and T is the temperature in degrees kelvin.

OXIDATION OF ALUMINUM

Although aluminum is one of the least noble of the common commercial metals, it is remarkably stable in many oxidizing environments. It owes its stability to the continuous film of aluminum oxide that rapidly grows on a nascent aluminum surface that is exposed to oxygen, water, or other oxidants. The molecular volume of the oxide is about 1.3 times greater than that of the aluminum consumed in the oxidation reaction. The surface layer is, therefore, under compressive stress and rapidly heals when damaged. In dry oxygen, the surface layer attains a limiting thickness that is a function of temperature. At room temperature, the limiting thickness is about 2.5 to 3.0 nm (25 to 30 Å). Logarithmic time laws have been determined by several workers for the range of low and moderate temperatures, indicating that ion transport is field controlled.

Film thickness increases in the presence of water vapor. At room temperature and 100% relative humidity, about twice as much oxide is formed as in dry oxygen. In both cases, however, the same rate laws apply. A duplex film generally forms in wet environments; the continuous oxide layer closest to the metal surface changes to hydroxylated film at the solid/gas interface. At higher temperatures and on aluminum alloys, especially those containing magnesium and copper, more complex film structures develop. Oxide growth can no longer be described by simple time laws (Ref 83).

GASES AND ALUMINUM

Hydrogen is appreciably soluble in both solid and molten aluminum. Other gases reported to be present occur when nonmetallics in the melt react with the environment (Ref 84). Molten aluminum reacts readily with carbon monoxide and carbon dioxide, and it also reacts with water vapor in the furnace atmosphere, adsorbed water, water present as hydrated oxide films on scrap, and water adsorbed on or combined in refractories. Solid aluminum also reacts with moisture in a furnace atmosphere to form oxides and hydrogen. Such reactions are a source of hydrogen in solid materials caused by diffusion from the surface. The amount of hydrogen present in molten aluminum can be significantly greater than the equilibrium solubility amount, because of the driving force of the metal-moisture reactions. The amount found in solid aluminum can also be greater than the solid solubility amount, either because of the presence during solidification of such excess amounts, or because of reactions of furnace

Table 6. Solubility of Hydrogen in Molten Aluminum with 1 atm of Hydrogen over the Melt

Temperature °C	Temperature °F	Solubility(a) (b)	Solubility(a) (c)	Solubility(a) (d)
660	1220	0.69	0.83 (0.78 STP)	0.46
700	1290	0.91	1.07 (1.00 STP)	0.63
800	1470	1.68	1.86 (1.74 STP)	1.23
850	1560	2.18	2.40 (2.24 STP)	1.66

(a) In cubic centimeters of hydrogen at NTP (20 °C or 68 °F and 760 mm pressure) per 100 g of aluminum. (b) From Ref 85. (c) From Ref 86. (d) From Ref 87.

moisture on the surface of the metal and subsequent diffusions of hydrogen into the body of the solid.

Ransley and Neufeld (Ref 85), Opie and Grant (Ref 86), and Eichenhauer, Hattenbach, and Pebler (Ref 87) have measured the solubility of hydrogen in molten aluminum. Equations representing the effect of temperature as established by these authors are given below, and the values are compared in Table 6:

$$\log S = \frac{-2760}{T} + 2.796 \qquad \text{(Ref 85)}$$

$$\log S = \frac{-2550}{T} + 2.62 \qquad \text{(Ref 86)}$$

$$\log S = \frac{-3086}{T} + 2.969 \qquad \text{(Ref 87)}$$

S is solubility of hydrogen in cubic centimeters per 100 g of metal and T is temperature in degrees kelvin.*

Ransley and Neufeld (Ref 85) and also Eichenauer *et al* (Ref 87) have reported solubilities in solid aluminum. Equations relating solubility, temperature, and pressure of hydrogen over the specimen are:

$$\log S = \frac{-2080}{T} + \frac{\log p}{2} - 0.652 \qquad \text{(Ref 85)}$$

$$\log S = \frac{-3042}{T} + \frac{\log p}{2} + 0.521 \qquad \text{(Ref 87)}$$

S is the solubility in cubic centimeters (NTP) per 100 g, T is the absolute temperature, and p is the pressure in torr. Solubilities calculated from these equations are in good agreement, as shown in the following table:

Temperature °C	Temperature °F	Solubility(a) (b)	Solubility(a) (c)
660	1220	0.04	0.05
600	1110	0.025	0.03
500	930	0.01	0.01
400	750	0.004	0.003

(a) In cubic centimeters of hydrogen at NTP (20 °C or 68 °F and 760 mm pressure) per 100 g of aluminum. (b) From Ref 85. (c) From Ref 87.

*In Ref 85 and 87, results are given in cubic centimeters of H_2 at NTP (20 °C or 68 °F) and 860 mm pressure, and in Ref 86 results are in cubic centimeters of H_2 at STP (0 °C or 32 °F) and 760 mm pressure.

The solubility-pressure relationship for both molten and solid aluminum follows the square root law. Eichenauer (Ref 88) carried out solid solubility measurements on hydrogen and also included deuterium in his experiments. For hydrogen, he found a decrease with time for the solubility coefficients and considerably lower values than previously reported. A provisional relationship to structure is assumed.

Hydrogen in aluminum in excess of the solid solubility is generally considered deleterious (Ref 89). Much work has been done on methods of removal and control for both the molten and solid conditions. Hydrogen can be determined by vacuum hot extraction (Ref 90), nitrogen carrier fusion, and vacuum fusion. The effects of hydrogen on the properties of commercial aluminum alloys is discussed by Hess and Turnbulls (Ref 91).

A summary of the physical properties of aluminum is provided in the following table:

Property	Value
Thermal neutron cross section	0.232 ± 0.003 barns
Lattice constant (length of unit cube)	4.0496×10^{-10} m at 298 K
Density (solid)	2699 kg m^{-3} (theoretical density based on lattice spacing)
	2697–2699 kg m^{-3} (polycrystalline material)
Density (liquid)	2357 kg m^{-3} at 973 K
	2304 kg m^{-3} at 1173 K
Coefficient of expansion	23×10^{-6} K^{-1} at 293 K
Thermal conductivity	2.37 W cm^{-1} K^{-1} at 298 K
Volume resistivity	2.655×10^{-8} Ω · m
Magnetic susceptibility	16×10^{-3} m^{-3} g $atom^{-1}$ at 298 K
Surface tension	868 dyne cm^{-1} at the melting point
Viscosity	0.012 poise at the melting point
Melting point	933.5 K
Boiling point	2767 K
Heat of fusion	397 J g^{-1}
Heat of vaporization	1.08×10^{-4} J g^{-1}
Heat capacity	0.90 J g^{-1} K^{-1}

REFERENCES

1. F.C. Frary, The Electrolytic Refining of Aluminum, *Transactions of American Electrochemical Society*, Vol 47, 1925, p 275–286
2. J.D. Edwards, The Properties of Pure Aluminum, *Transactions of American Electrochemical Society*, Vol 47, 1925, p 287–300
3. C.S. Taylor, *et al*, The Properties of High-Purity Aluminum, *Metals & Alloys*, Vol 9, 1938, p 189–192
4. "Nouvelles Properties Physiques et Chimiques des Metaux de Tres Haute Purete", Colloques Internationaux, Paris, 1959, Centre National de la Recherche Scientifique, Paris, 1960
5. "Ultra High Purity Metals", American Society for Metals, 1962
6. K. Akerman, *et al*, Zone Melting of Aluminum, *Rudy Metale Niezelazne*, Vol 9 (No. 9), 1964, p 483–485
7. R. Splitek, Zone Refining of Aluminum, *Hutnicke Listy*, Vol 17, 1962, p 495–503

8. S.E. Maraev, N.I. Elina, and E.I. Mudrova, Distribution of Impurities During Zone Purification of Aluminum, *Poluchenie i Analiz Veschchestv Osoboi Chistoly—Materialy Vsesoyuznoi Konferentsii*, Gorky, USSR, 1963 (published 1966) (Russian)

9. W.D. Hannibal, *et al*, Ultrapure Aluminum Production, Processing and Properties, Bonn, West Germany: Light Metal Research Institute, Vereinigte Aluminum-Werke AG, *Metall*, Vol 27 (No. 3), 1973, p 203–211

10. "Continuous Purification of Aluminum", Pechiney-Campaigne de Produits Chimiques et Electrometallurgiques, Neth. Appl. 6, 408,185 (Cl.C 22b), 20 Jan 1965, Fr. Appl. 10 July 1963; 23 pages

11. "Purification of Scrap Aluminum", Pechiney-Compagnie de Produits Chimiques et Electromettalurgiques, Belg. 650, 686, 28 Jan 1965; Fr. Appl. 19 July 1963; 28 pages

12. W.D. Hannibal *et al*, *Bundesministerum fuer Forschung und Technologie, Forschungsberichte Technologische Forschung und Entwicklung*, 1974

13. G. Revel, Application of Electrical Resistivity at Low Temperature to Purity Control of Aluminum, *Memoires Scientifique de la Revue de Metallurgie*, Vol 65 (No. 2), 1908, p 181–184

14. *Encyclopedia of Industrial Chemical Analysis*, Vol 5, New York: John Wiley & Sons, 1967, p 110–158

15. T.G. Pearson and H.W.L. Phillips, The Production and Properties of Superpurity Aluminum, *Metallurgical Reviews*, Vol 2, 1957, p 305–360

16. G. Deep and A. Plumtree, Yield Point Behavior in Extruded Aluminum Rod, *Metallurgical Transactions A.*, Vol 6A (No. 2), Feb 1975, p 359–366

17. F. Iida, *et al*, Anomalous Strain-Rate Sensitivity of Flow Stress in Superconducting Al and Al-Mg Alloys, *Acta Metallurgica*, Vol 27 (No. 4), April 1979, p 637–647

18. H.J. Hamel, The Influence of Rate of Extension on the Properties of Polycrystalline Aluminum and Aluminum Alloys, *Metall*, Vol 28 (No. 3), March 1974, p 238–245

19. F.H. Hammad, C.N. Ahlquist, and W.D. Nix, High-Temperature Work-Softening Yield-Point Phenomena in Polycrystalline Aluminum, *Metallurgical Transactions*, Vol 1 (No. 8), Aug 1970, p 2179–2183

20. M. Yu. Vainblat and S.S. Khayurov, Serrated Yielding on the Extension Diagram of Polygonized Aluminum, *Fizica Metallov i Metalloved*, Vol 35 (No. 3), 1973, p 530–534 (Russian)

21. U.F. Kocks, Laws for Work-Hardening and Low-Temperature Creep, *Journal of Engineering Materials and Technology*, Vol 98 (No. 1), Jan 1976, p 76–85

22. A. Polakovic and L. Taborsky, The Influence of Rate of Deformation, Grain Diameter, and Purity of Aluminum and Copper on the Stress-Strain Curves, *Metall*, Vol 25 (No. 1), Jan 1971, p 12–14

23. L. Taborsky and A. Polakovic, The Increase in Strength of Polycrystalline Aluminum at Low Temperature and High Performance Rate, *Metall*, Vol 29 (No. 3), March 1975, p 273–275

24. A. Polakovic, L. Taborsky, and H. Hyross, The Shape of Aluminum Stress-Strain Curve in Dependence on Deformation Rate, Temperature, and Material Purity, *Korove Materialy*, Vol 12 (No. 1), Jan 1974, p 89–94

25. C.M. Sellars and W.J. McG. Tegart, Hot Workability, *International Metals Review*, Vol 17 (No. 158), March 1972, p 1–24

26. W. Roberts, The Strain-Rate Sensitivity of Work Hardening in Pure Aluminum Polycrystals, Paper from 4th International Conference Strength of Metals and Alloys, Vol 1, 1976, p 146–150

27. J.D. Parker and B. Wilshire, Rate-Controlling Processes During Creep of Super-Purity Aluminum, *Philosophical Magazine A*, Vol 41 (No. 1), March 1972, p 50–54

28. V.M. Radhakrishnan, K.S. Raghavan, and R.G. Narayanamurthi, Creep Behavior Under Cyclic Stressing, *Transactions of the Indian Institute of Metallurgy*, Vol 25 (No. 1), March 1972, p 50–54

29. V.M. Radhakrishnan, Effect of Stress Change on Creep Deformation, *Indian Journal of Technology*, Vol 11 (No. 4), April 1973, p 160–163

30. V.M. Radhakrishnan, Creep Rupture Under Cyclic Stressing, *Indian Journal of Technology*, Vol 11 (No. 12), Dec 1973, p 728–731

31. V.M. Radhakrishnan, Creep Rupture Under Cyclic Stressing, Paper from International Symposium on Industrial Metallurgy, Indian Institute of Science, Bangalore, 1974, p 196–199

32. C.M. Young, S.L. Robinson, and O.D. Sherby, Effect of Subgrain Size on the High Temperature Strength of Polycrystalline Aluminum as Determined by Constant Strain Rate Tests, *Acta Metallurgica*, Vol 23 (No. 5), May 1975, p 633–639

33. M.M. Myshlyaev, W.A. Stepanov, and V.V. Shpeizman, Change in Creep Mechanism of BCC Metals at Transition From Low to High Temperatures, *Physica Status Solidi*, Vol 8 (No. 2), 16 Dec 1971, p 393–402

34. Y.V.R.K. Prasad, D.H. Sastry, and K.I. Vasu, A Study of Low-Temperature Creep in Aluminum by Change-In-Stress Experiments: Thermal Activation of Attractive Junctions, *Metal Science Journal*, Vol 4, March 1970, p 69–73

35. International Bulletin 14b, International Union of Pure and Applied Chemistry, 1961

36. L.F. Mondolfo, *Aluminum Alloys: Structure and Properties*, Boston: Butterworths, 1976, p 12

37. R.L. Heath, in *Handbook of Chemistry and Physics*, 61st ed., Edited by R.C. Wood, Cleveland: CRC Press, 1980–1981, p B262

38. R.L. Henkel and H.H. Borschall, Capture Cross-sections for Fast Neutrons, *Physical Review*, Vol 80, 1950, p 145

39. D.E. Gray, Ed., *The American Institute of Physics Handbook*, 3rd ed., New York: McGraw-Hill, 1972, p 8–205

40. D.E. Gray, Ed., *The American Institute of Physics Handbook*, 3rd ed., New York: McGraw-Hill, 1972, p 8–11

41. D.E. Gray, Ed., *The American Institute of Physics Handbook*, 3rd ed., New York: McGraw-Hill, 1972, p 5–8

42. W.C. Martin and R. Zalubas, Energy Levels of Aluminum, Al I through Al XIII, *Journal of Physical Chemistry, Reference Data*, Vol 8 (No. 3), 1979, p 817–864

43. K.B.S. Eriksson and H.B.S. Isberg, The Spectron of Atomic Aluminum, Al I, *Arkiv für Fysik*, Vol 23 (No. 47), 1963, p 527–541

44. L.F. Mondolfo, *Aluminum Alloys: Structure and Properties*, Boston: Butterworths, 1976, p 17

45. E. Gebhardt, M. Becker, and S. Dorner, The Properties of Metallic Melts: VIII the Density of Molten Aluminum and Some Aluminum Alloys, *Zeitschrift fuer Metallkunde*, Vol 44, 1953, p 573–575

46. Y.S. Touloukian and C.Y. Ho, Properties of Aluminum and Aluminum Alloys, Thermophysical Properties Research Center, Purdue University, West Lafayette, IN, Report 21, 1973, p 452

47. L.A. Willey, Alcoa Research Labs, 1957, cited in *Aluminum*, Vol I, 1967

48. *Alcoa Aluminum Handbook*, Aluminum Company of America, 1966

49. Y.S. Touloukian and C.Y. Ho, Properties of Aluminum and Aluminum Alloys, Thermophysical Properties Research Center, Purdue University, West Lafayette, IN, Report 21, 1973, p 462–514

50. Y.S. Touloukian and C.Y. Ho, Properties of Aluminum and Aluminum Alloys, Thermophysical Properties Research Center, Purdue University, West Lafayette, IN, Report 21, 1973, p 46

51. Y.S. Touloukian and C.Y. Ho, Properties of Aluminum and Aluminum Alloys, Thermophysical Properties Research Center, Purdue University, West Lafayette, IN, Report 21, 1973, p 43

52. Y.S. Touloukian and C.Y. Ho, Properties of Aluminum and Aluminum Alloys, Thermophysical Properties Research Center, Purdue University, West Lafayette, IN, Report 21, 1973, p 517

53. Y.S. Touloukian and C.Y. Ho, Properties of Aluminum and Aluminum Alloys, Thermophysical Properties Research Center, Purdue University, West Lafayette, IN, Report 21, 1973, p 518–519

54. L.F. Mondolfo, *Aluminum Alloys: Structure and Properties*, Boston: Butterworths, 1976, p 96

55. F.R. Fickett, Magnetoresistance of Very Pure Polycrystalline Aluminum, *Physical Review B, Solid State*, Vol 3 (No. 6), 1971, p 1941–1952

56. K. Førsvoll and I. Hollvech, Electrical Size Effect in Aluminum, *Proceeding of the Royal Society A275*, 1963, p 2230–2232

57. K. Førsvoll, A Refining Effect in Super Purity Aluminum, *Philosophical Magazine*, Vol 11, 1965, p 419–422

58. F. Montariol, Effect of Minute Additions of Foreign Elements on the Electrical Resistance of Zone Melted Aluminum at Low Temperatures, *Metaux Corrosion Industrie*, Vol 38 (No. 453), p 171–192; and Vol 38 (No. 454), p 223–242

59. S. Caplan and G. Chanin, Critical-Field Study of Superconducting Aluminum, *Physical Review*, Vol 138 (No. 5), 1965, p 1428–1433

60. G. Boato, *et al*, Effect of Transition Metal Impurities on the Critical Temperature of Superconducting Aluminum, Zinc, Indium and Tin, *Physical Review*, Vol 148 (No. 1), 1966, p 353–361

61. D.P. Seraphim, *et al*, The Critical Temperature of Superconducting Alloys, *Acta Metallurgica*, Vol 9 (No. 9), 1961, p 861–869

62. J.T. Milek and S.J. Welles, Properties of Aluminum and Aluminum Alloys, Thermophysical Properties Research Center, Purdue University, West Lafayette, IN, Report 21, 1973, p 516

63. W. Kesternich, H. Ullmaier, and W. Schilling, The Influence of Fermi Surface and Defect Structure on the Low Field Galvanomagnetic Properties of Al, *Journal of Physics, F. Metal Physics*, Vol 6 (No. 10), 1976, p 1867–1883

64. C. Papastaikoudis, D. Papadimitropoulos, and E. Rocofyllou, Low-Field Hall Coefficient R_H^0 of Dilute Al-3d Alloys at 4.2 K, *Physical Review B, Solid State*, Vol 22 (No. 6), 1980, p 2070–2076

65. L.F. Mondolfo, *Aluminum Alloys: Structure and Properties*, Boston: Butterworths, 1976, p 99

66. W. Kesternich, H. Ullmaier, and W. Schilling, High Field Magnetoresistance and Hall Effect in Aluminum Single Crystals, *Philosophical Magazine*, Vol 31 (No. 3), 1975, p 471–488

67. H. Borchers and W. Hepp, Magnetic Studies of Aluminum Alloys Without Ferromagnetic Phases, *Zeitschrift fuer Metallkunde*, Vol 60 (No. 9), 1969, p 722–729

68. S.N. Vaidya and G.C. Kennedy, *Journal of Physics and Chemistry of Solids*, Vol 31, 1970, p 2329–2345

69. N.N. Roy and E.G. Steward, *Nature*, London: Vol 224 (No. 522), 1969, p 905

70. L.F. Mondolfo, *Aluminum Alloys: Structure and Properties*, Boston: Butterworths, 1976, p 82

71. L.F. Mondolfo, *Aluminum Alloys: Structure and Properties*, Boston: Butterworths, 1976, p 108–111

72. Y.S. Touloukian and D.P. DeWitt, Eds., Thermophysical Properties of Matter, *Thermal Radiative Properties—Metallic Elements and Alloys*, Vol 7, New York: IFI/Plenum, 1970

73. E.A. Estalote and K.G. Ramanathan, *Journal of the Optical Society of America*, Vol 67, 1977, p 39–43

74. L.F. Mondolfo, *Aluminum Alloys: Structure and Properties*, Boston: Butterworths, 1976, p 56

75. G.T. Furukawa, *Journal of Research of the National Bureau of Standards*, Vol 78A (No. 4), 1974, p 477–495

76. J.F. Cannon, *Journal of Physical and Chemical Reference Data*, Vol 3 (No. 3), 1974, p 794

77. D.R. Stull and H. Prophet, JANAF Thermochemical Tables, 2nd ed., U.S. Dept. of Commerce, Washington, D.C., 1971

78. L.F. Mondolfo, *Aluminum Alloys: Structure and Properties*, Boston: Butterworths, 1976, p 49

79. G. Lang, *Aluminium*, Vol 50 (No. 11), 1974, p 731

80. G. Lang, *et al*, *Zeitschrift fuer Metallkunde*, Vol 68 (No. 2), 1977, p 113

81. C.J. Smithells and E.A. Brandes, Eds., *Metals Reference Book*, 5th ed., Boston: Butterworths, 1976, p 944

82. P.P. Arsentev and K.I. Polyakova, Soviet Nonferrous Metals Research, Vol 5, 1977, p 53–54

83. K. Wefers, Properties and Characterization of Surface Oxides on Aluminum Alloys, *Aluminium*, Vol 57, 1981, p 722–726

84. A.B. Nersesyants, *et al*, Gas Chromatographic Analysis of the Gases and Their Origin in Aluminum, *Trudy VAMI*, Vol 99, 1977, p 46–48

85. C.E. Ransley and H. Neufeld, The Solubility of Hydrogen in Liquid and Solid Aluminum, *Journal of the Institute of Metals*, Vol 74, 1947/1948, p 599–620

86. W.R. Opie and N.J. Grant, Hydrogen Solubility in Aluminum and Some Aluminum Alloys, *Transactions of AIME*, Vol 188, 1950, p 1237–1241

87. W. Eichenauer, K. Hattenbach, and Z. Pebler, The Solubility of Hydrogen in Solid and Liquid Aluminum, *Zeitschrift fuer Metallkunde*, Vol 52, 1961, p 682–684

88. W. Eichenauer, The Solubility of Hydrogen and Deuterium in High-Purity Aluminum at 400 to 630C, *Zeitschrift fuer Metallkunde*, Vol 59 (No. 8), Aug 1968, p 613–616

89. M.C. Celik and G.H.J. Bennett, Effects of Hydrogen and Inclusions on Blistering in High-Purity Aluminum Sheet and Foil on a Laboratory Scale, *Metals Technology*, Vol 6 (No. 4), April 1979, p 138–144

90. F. Degreve, J.C. Carle, and N. Gonzalez, New Methods for the Determination of Hydrogen Content of Aluminum and Its Alloys, Part I, Improvements in the Vacuum Extraction Method, *Metallurgical Transactions B*, Vol 68 (No. 12), Dec 1975, p 539–544

91. P.D. Hess and G.K. Turnbull, Effects of Hydrogen on Properties of Aluminum Alloys, Paper from *Hydrogen in Metals*, American Society for Metals, 1974, p 277–287

Aluminum Properties and Physical Metallurgy
John E. Hatch editors, p 25-57
DOI: 10.1361/appm1984p025

CHAPTER 2

CONSTITUTION OF ALLOYS*

Most of the metallic elements readily alloy with aluminum, but only a few are important major alloying ingredients in commercial aluminum-based alloys. Nevertheless, an appreciable number of other elements serve as supplementary alloying additions for improving alloy properties and characteristics.

TYPES OF SYSTEMS

A few generalizations, relating to the periodic system, can be made concerning the types of binary systems the various elements form with aluminum. Beryllium, silicon, zinc, gallium, germanium, tin, and mercury form simple eutectic-type systems with aluminum. Except for beryllium, these elements are in periodic groups IIb, IIIa, and IVa. Cadmium, indium, thallium, and lead of these groups; bismuth of group Va; and sodium and potassium (also probably rubidium and cesium) of group Ia are only partly miscible in liquid aluminum within an appreciable temperature range above its melting point. Therefore, they form simple, monotectic-type systems with aluminum. In binary combinations, aluminum forms no known intermetallic phases or compounds with these elements.

Available data indicate that the remaining metallic elements, including those of the lanthanide and actinide series, are miscible in the liquid state and form more complex binary systems, in which one or more intermetallic phases occur. In these systems, a eutectic reaction generally occurs involving the liquid, the aluminum terminal solid solution, and the aluminum-rich intermetallic phase. However, solid solution is formed near the extreme aluminum end of the system by peritectic reaction between the liquid and the aluminum-rich intermetallic phase with titanium, vanadium, chromium, zirconium, columbium, molybdenum, hafnium, and probably tantalum and tungsten (the elements of groups IVa, Va, and VIa in the fourth, fifth, and sixth periods).

Of the many binary intermetallic phases formed by the reaction of aluminum with the various metallic elements, a few solidify without the occurrence of compositional changes (congruent transformation). However, the majority form a liquid solution of the solid phase composition on cooling, by reaction between a previously existing solid phase and the remaining depleted liquid solution (peritectic reaction). Despite similarities, distinct relationships between the number or types of aluminum intermetallic phases and the elements within a periodic group are difficult to observe.

*This chapter was revised by a team comprised of E.M. Dunn, Kaiser Aluminum & Chemical Corp., *Chairman*; A.P. Davidson, Alcan International Ltd.; J.P. Faunce, Martin Marietta Laboratories; C.G. Levi, ATISA-ATKINS, S.A. de C.V.; S. Maitra, Alcoa Technical Center; and R. Mehrabian, National Bureau of Standards. The original chapter was authored by R.H. Brown and L.A. Willey of Alcoa Technical Center.

Table 1. Invariant Reactions in Binary Aluminum Alloys

Element	Temperature(a) °C	°F	Liquid solubility wt%	at.%	Solid solubility wt%	at.%
Ag	570	1060	72.0	60.9	55.6	23.8
Au	640	1180	5	0.7	0.36	0.049
B	660	1220	0.022	0.054	<0.001	<0.002
Be	645	1190	0.87	2.56	0.063	0.188
Bi	660(b)	1220(b)	3.4	0.45	<0.1	<0.01
Ca	620	1150	7.6	5.25	<0.1	<0.05
Cd	650(b)	1200(b)	6.7	1.69	0.47	0.11
Co	660	1220	1.0	0.46	<0.02	<0.01
Cr	660(c)	1220(c)	0.41	0.21	0.77	0.40
Cu	550	1020	33.15	17.39	5.67	2.48
Fe	655	1210	1.87	0.91	0.052	0.025
Ga	30	80	98.9	97.2	20.0	8.82
Gd	640	1180	11.5	2.18	<0.1	<0.01
Ge	425	800	53.0	29.5	6.0	2.30
Hf	660(c)	1220(c)	0.49	0.074	1.22	0.186
In	640	1180	17.5	4.65	0.17	0.04
Li	600	1110	9.9	30.0	4.0	13.9
Mg	450	840	35.0	37.34	14.9	16.26
Mn	660	1220	1.95	0.97	1.82	0.90
Mo	660(c)	1220(c)	0.1	0.03	0.25	0.056
Na	660(b)	1220(b)	0.18	0.21	<0.003	<0.003
Nb	660(c)	1220(c)	0.01	0.003	0.22	0.064
Ni	640	1180	6.12	2.91	0.05	0.023
Pb	660	1220	1.52	0.20	0.15	0.02
Pd	615	1140	24.2	7.5	<0.1	<0.02
Rh	660	1220	1.09	0.29	<0.1	<0.02
Ru	660	1220	0.69	0.185	<0.1	<0.02
Sb	660	1220	1.1	0.25	<0.1	<0.02
Sc	660	1220	0.52	0.31	0.38	0.23
Si	580	1080	12.6	12.16	1.65	1.59
Sn	230	450	99.5	97.83	<0.01	<0.002
Sr	655	1210	...	...	...	...
Th	635	1180	25.0	3.73	<0.1	<0.01
Ti	665(c)	1230(c)	0.15	0.084	1.00	0.57
Tm	645	1190	10.0	1.74	<0.1	<0.01
U	640	1180	13.0	1.67	<0.1	<0.01
V	665(c)	1230(c)	0.25	0.133	0.6	0.32
Y	645	1190	7.7	2.47	<0.1	<0.03
Zn	380	720	95.0	88.7	82.8	66.4
Zr	660(c)	1220(c)	0.11	0.033	0.28	0.085

(a) Eutectic reactions unless designated otherwise. (b) Monotectic reaction. (c) Peritectic reaction.

Liquid Solubility. Except for the partly miscible elements previously mentioned, all other metallic elements are completely miscible with aluminum in the liquid state. The solubility limits for a number of elements at temperatures above the melting point of aluminum are listed in Table 1. Of the semimetallic and nonmetallic elements, silicon is completely miscible with aluminum in the liquid state. Boron has a low solubility of about 0.02% at a eutectic temperature slightly below the melting point of aluminum. Its solubility increases with increasing temperature, but appears to be less than 1.5% at 1500 °C (2730 °F). Carbon has slight solubility in liquid aluminum; its solubility limits have not been completely established, but are indicated to be appreciably less than for boron.

Phosphorous and arsenic are nearly insoluble in aluminum. In hypothetical diagrams, sulfur has been indicated as having appreciable solubility in liquid aluminum. Early investigations indicated complete miscibility of selenium and tellurium with liquid aluminum. Although compounds are readily formed with aluminum, retention of more than trace amounts of these elements in the metal when melting and alloying are done under the usual atmospheric conditions is not possible. Three factors contribute to the difficulty of maintaining the composition: (1) high volatility of these elements at temperatures of liquid aluminum, (2) oxidation at the metal surface, and (3) formation of less dense compounds that separate to surface dross.

Except for hydrogen, common elemental gases and elements of the halogen group exhibit no detectable liquid solubility, but readily form compounds with aluminum. The solubility of hydrogen in both liquid and solid aluminum is discussed in Chapter 1 of this Volume. Figure 1 (Ref 1) shows the solubility of hydrogen in aluminum from 500 to 800 °C (930 to 1470 °F).

Solid Solubility. No element is known to have complete miscibility with aluminum in the solid state. Of all elements, zinc has the greatest solid solubility in aluminum (a maximum of 66.4 at.%). In addition to zinc, silver, magnesium, and lithium have solid solubilities greater than 10 at.% (in order of decreasing maximum solubility). Gallium, germanium, copper, and silicon (in decreasing order) have maximum solubilities of less than 10 but greater than 1 at.%. All other elements are less soluble. Solid solution limits for some elements in aluminum are recorded in Table 2.

The solid solution limits given for lithium are from recent investigations by Costa and Marshall (Ref 2) and by Levine and Rapperport (Ref 3). While the results of these investigators are in agreement, they differ considerably at temperatures below 500 °C (930 °F) from the results recently obtained by other investigators. Jones and Das (Ref 4) reported solubility limits of 4.2, 1.7, and 0.4% lithium, respectively, at the eutectic temperatures of 400 °C (750 °F) and 200 °C (390 °F).

With one known exception,* maximum solid solubility in aluminum alloys occurs at the eutectic, peritectic, or monotectic temperature. With decreasing temperature, the solubility limits decrease. This decrease from appreciable concentrations at elevated temperatures to relatively low concentrations at low temperatures is one fundamental characteristic that provides the basis for substantially increasing the hardness and strength of aluminum alloys by solution heat treatment and subsequent precipitation aging operations.

Intermetallic Phases. A feature of aluminum alloy systems is the wide variety of intermetallic phases, which occur because aluminum is highly electronegative and trivalent. The complete literature on intermetallic phases has been reviewed by Pearson (Ref 5). Intermetallic phases in aluminum alloy systems have also been discussed as part of a wider review by Mon-

*Tin shows a retrograde solid solubility between the melting point of aluminum and the eutectic temperature, 228.3 °C (442.9 °F), with a maximum of 0.10% at approximately 600 °C (1110 °F).

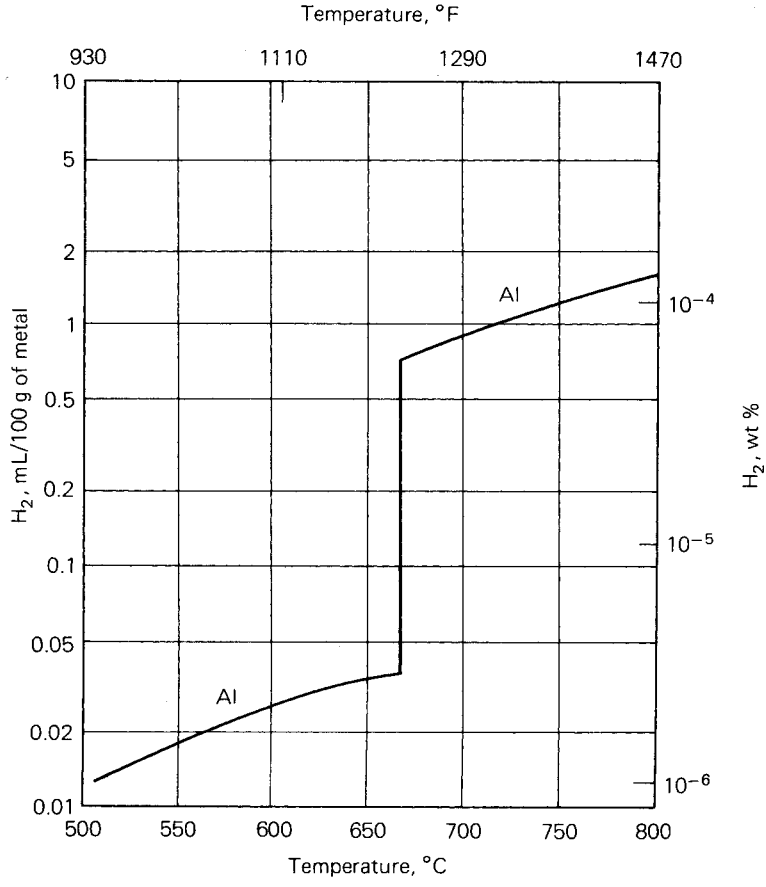

Fig. 1. Solubility of hydrogen at atmospheric pressure in aluminum and magnesium (Ref 1).

dolfo (Ref 6). The stability of such phases and the narrowness of their compositional range is determined by size and valency factors. In binary systems, some phases can be exactly stoichiometric, for example, AlSb. Other systems can have a very narrow compositional range not containing the composition of their formula, for example $CuAl_2$, thus containing lattice defects. Others such as Ag_2Al show wider compositional range. Transition metals often exhibit a succession with well defined and sometimes complex stoichiometry (Co_2Al_9, Co_4Al_{13}, $CoAl_3$, Co_2Al_5, and CoAl; and $MnAl_6$, $MnAl_4$, and $MnAl_3$). Transition metals also exhibit frequent metastability, in which one phase introduced during fast solidification transforms in the solid state to another, for example, $FeAl_6 \rightarrow FeAl_3$, or a metastable variant precipitates from supersaturated solid solution such as $MnAl_{12}$.

In ternary alloys, a few intermetallic phases of other binary systems can form a pseudobinary eutectic with primary aluminum solid solution, for example, Mg_2Si or $MgZn_2$. In quaternary systems, intermetallic phases

of the respective binary and ternary systems are occasionally isomorphous, forming continuous series of solid solutions in equilibrium with aluminum solid solution. An important example is in the aluminum-copper-magnesium-zinc quaternary system, where there are three such pairs: $CuMg_4Al_6$ + $Mg_3Zn_3Al_2$, Mg_2Zn_{11} + $Cu_6Mg_2Al_5$, and $MgZn_2$ + CuMgAl. The first pair have similar lattice parameters and form extensive mutual solid solution, the others less so. Neither $Cu_6Mg_2Al_5$ nor CuMgAl are equilibrium phases in aluminum-copper-magnesium, although both Mg_2Zn_{11} and $MgZn_2$ are equilibrium phases in aluminum-magnesium-zinc.

Table 2. Solid Solution Characteristics of Binary Aluminum Alloys

Element	ΔH_s(a) kJ/g-atom	μΩ/at.%(b)	$\Delta a/\Delta_Y$(c) m/at.% × 10^{10}	$\gamma_Y - \gamma_{Al}$(d) m × 10^{10}
Ag	26.7	1.15	Nil	+0.013
Au	87.5	2	...	+0.010
B	...	...	...	−0.449
Be	75.7	0.085	−0.0217	−0.306
Bi	...	...	...	+0.347
Ca	...	...	...	+0.541
Cd	82.0	0.057	−0.0067	+0.079
Co	...	...	...	−0.177
Cr	67.8	7.70	−0.0100	−0.153
Cu	41.0	0.785	−0.0051	−0.153
Fe	95.8	4.75	...	−0.169
Ga	19.2	0.250	+0.0012	−0.025
Gd	...	...	...	+0.375
Ge	40.6	0.775	+0.00155	+0.015
Hf	(77.8)	...	...	+0.156
In	...	...	...	+0.150
Li	26.8	0.89	−0.00016	+0.120
Mg	18.8	0.49	+0.00460	+0.169
Mn	60.7	5.97	−0.0066	−0.161
Mo	...	8.35	...	−0.043
Na	...	...	...	+0.467
Nb	...	6.85	...	+0.027
Ni	95.8	1.77	...	−0.185
Pb	...	1.5	...	+0.275
Pd	51.0	2.35	...	−0.056
Rh	...	...	...	−0.077
Ru	...	...	...	−0.093
Sb	...	...	...	+0.228
Sc	69.5	3.32	...	+0.191
Si	49.4	0.65	−0.0018	−0.054
Sn	...	1.1	...	+0.194
Sr	...	3.2	...	+0.719
Th	...	...	...	+0.366
Ti	64.0	5.10	−0.0105	+0.038
Tm	...	...	...	+0.330
U	...	...	...	+0.087
V	73.6	6.90	−0.0075	−0.091
Y	...	...	...	+0.368
Zn	8.5	0.211	−0.00075	−0.090
Zr	86.2	5.85	...	+0.168

(a) Heat of solution from slope of line for ln solubility versus 1/T (for dilute solutions for elements silver and zinc). (b) Increase in electrical resistivity per 1 at.% in solid solution. (c) Change in aluminum lattice parameter per 1 at.% in solid solution. (d) Difference between Pauling metallic radii of element and aluminum.

Table 3. Intermetallic Phases in Aluminum-Rich Aluminum Alloy Systems

Intermetallic phase	ASTM E157-61T designation	Other designation	Structure type		Space group	Lattice parameter, A		
						a	b	c
Binary Systems								
Ag_2Al	(Ag,Al)2*H*	ζ	A_3	Hex	$P6_3/mmc$	2.885	...	4.582
αAlB_{12}	(B,Al)52*N*	...	...	Mono	$C2/m$	8.522	11.002	7.393
βAlB_{12}	(B,Al)208*T*	...	...	Tet	...	12.58	...	10.20
AlB_2	(B,Al)3c*H*	...	C32	Hex	...	3.006	...	3.252
$CaAl_4$	(Al,Ca)10*U*	...	$D1_3$	bc Tet	$I4/mmm$	4.362	...	11.09
Co_2Al_9	(Al,Co)22*M*	...	...	Mono	$P2_1/c$	6.213	6.290	8.556
$CrAl_7$	...	...	...	Ortho	...	24.8	24.7	30.2
$Cr \cdot Al_{11}$	...	...	...	Ortho	...	24.8	24.7	30.2
$CuAl_2$	(Al,Cu)12a*U*	θ	C16	bc Tet	$I4/mcm$	6.066	...	4.874
		θ′	...	Tet	...	4.04	...	5.80
		GP[2] or θ″	...	Tet	...	4.04	...	7.68
$FeAl_4$	...	...	...	Mono	$C2/m$	15.520	8.099	12.501
$FeAl_6$	...	...	...	Ortho	$CCmm$	6.464	7.440	7.779
AlLi	(Al,Li)16*F*	...	B32	bcC	$Fd3m$	6.38	...	...
Mg_2Al_3	(Al,Mg)1166*F*	β	...	fcC	$Fd3m$	28.16	...	...
$MnAl_6$	(Al,Mn)28*Q*	...	...	Ortho	$Cmcm$	6.498	7.552	8.870
$MnAl_4$	...	...	...	Hex	...	28.41	...	12.38
$MnAl_{12}$	...	G	...	Cubic	...	~7.47	...	...
$NiAl_3$	(Al,Ni)16c*O*	ϵ	$D0_{20}$	Ortho	$Pnma$	6.611	7.366	4.812
Ni_2Al_3	(Al,Ni)5b*H*	δ	$D5_{13}$	Hex	$P3m1$	4.036	...	4.900
NiAl	(Ni,Al)2*B*	β	B2	bcC	$Pm3m$	2.887	...	...
AlSb	(Al,Sb)8*F*	...	B3	Cubic	$F43m$	6.096	...	...
$TiAl_3$	(Al,Ti)8*U*	...	$D0_{22}$	bc Tet	$I4/mmm$	3.848	...	8.596
UAl_4	(Al,U)20*P*	...	$D1_b$	bc Ortho	$Imma$	4.41	6.27	13.71
VAl_{11}	(Al,V)192*F*	...	...	fcC	$Fd3$	14.586	...	...
VAl_6	(Al,V)56*H*	...	...	Hex	...	7.718	...	17.15
$ZrAl_4$	(Al,Zr)16c*U*	...	$D0_{23}$	bc Tet	$I4/mmm$	4.013	...	17.320
TiB_2	(B,Ti)3*H*	...	C32	Hex	$P6/mmm$	3.028	...	3.228
Mg_2Si	(Mg,Si)12*F*	β	C1	fcC	$Fm3m$	6.351	...	...
		β′	...	Hex	...	7.05	...	4.05/12.15
Mg_2Zn_{11}	(Zn,Mg)39*C*	Z	...	Cubic	$Pm3$	8.552	...	...
$MgZn_2$	(Zn,Mg)12*H*	M	C14	Hex	$P6_3/mmc$	5.18	...	8.517
Ternary Systems								
$Cr_2Mg_3Al_1$	(Al,Mg,Cr)184*F*	E	...	fcC	$Fd3m$	14.55	...	...
$(Cr,Mn)Al_{12}$	(Al,Mn,Cr)26*B*	G	...	bcC	$Im3$	7.507	...	...
$Cr_4Si_4Al_{13}$	(Al,Cr,Si)84*F*	α	...	fcC	$F43m$	10.917	...	...
Cu_2FeAl_7	(Al,Cu,Fe)40*T*	β or N	...	Tet	$P4/mnc$	6.336	...	14.870
$(Fe,Cu)(Al,Cu)_6$	(Al,Fe,Cu)28*Q*	α	...	Ortho	$Cmcm$	7.464	6.441	8.786
$Cu_5Li_2Al_{15}$	...	T_B	C1	fcC	$Fm3m$	5.83	...	...
$CuLiAl_2$	...	T_1	...	Hex	...	4.96	...	9.35
$CuLi_3Al_6$	...	T_2	...	...	...	...	...	...
$CuMgAl_2$	(Al,Cu,Mg)16*S*	S	...	fc Ortho	$Cmcm$	4.01	9.25	7.15
CuMgAl	(Al,Cu,Mg)12*H*	U or M	C14	Hex	$P6_3/mmc$	5.07	...	8.29
$CuMg_4Al_6$	(Al,Mg,Cu)162*B*	T	...	bcC	...	14.31	...	...
$Cu_3Mg_6Al_7$	(Al,Mg,Cu)96*B*	Q or Y	...	Cubic	$Im3$	12.087	...	...
$Cu_6Mg_2Al_5$	(Cu,Al,Mg)39*C*	V or Z	...	Cubic	$Pm3$	8.311	...	...
$Cu_2Mn_3Al_{20}$	...	T	...	Ortho	...	24.11	12.51	7.71
Cu_3NiAl_6	(Al,Cu,Ni)250*B*	T	...	bcC	...	14.6	...	...
Cu_3ZnAl_3	...	T′	...	bcC	...	2.911	...	...
$FeNiAl_9$	...	...	...	Mono	...	...	...	...
Fe_2SiAl_8	...	αFeSi	...	Hex	$P6_3/mnc$	12.3	...	26.3
	$(FeM)_3Si_2Al_{15}$	α′FeSi		bcC	$Im3$	12.548	...	...
$FeSiAl_5$	...	βFeSi	...	Mono	...	6.12	6.12	41.48
$FeSi_2Al_4$	...	δFeSi	...	Tet	...	6.16	...	9.49
Mg_2MnAl_{10}	...	T	...	...	...	...	...	...
$Mg_3Zn_3Al_2$	(Mg,Zn,Al)162*B*	T	...	bcC	$Im3$	14.19	...	...
$Mn_3Si_2Al_{15}$	...	αMnSi	...	Cubic	...	12.652	...	...
Mn_3SiAl_{10}	(Al,Mn,Si)26*H*	βMnSi	...	Hex	$P6_3/mmc$	7.513	...	7.745
Quaternary Systems								
$Cu_2Mg_8Si_6Al_5$	...	...	...	Hex	...	10.32	...	4.05
$CuMg_5Si_4Al_4$	...	...	...	bcC	...	12.63	...	...
$FeMg_3Si_6Al_8$	(Al,Si,Mg,Fe)18c*H*	...	...	Hex	$P62m$	6.63	...	7.94

(a) Peritectic decomposition.

c/a, α or β	Atoms per unit cell	Density: Measured g/cm³	Density: Measured lb/in.³	Density: Calculated g/cm³	Density: Calculated lb/in.³	Melting temperature °C	Melting temperature °F
1.588	2	...	...	8.14	2.94	730(a)	1350(a)
143° 29′	52	...	...	2.53	0.913	...	...
0.811	208	...	...	2.58	0.931	~1350	~2460
1.082	3	...	...	3.17	1.14	~850(a)	~1560(a)
2.542	10	...	...	2.33	0.841	700(a)	1290(a)
94° 46′	22	3.60	1.30	3.60	1.30	1940(a)	1720(a)
...	1160	...	...	3.14	1.13	~725(a)	~1340(a)
...	1209	...	...	3.34	1.21	~940(a)	~1720(a)
0.803	12	4.34	1.57	4.35	1.57	590	1090
1.436	6	...	...	4.12	1.49	...	...
1.901	8	...	...	3.83	1.38	...	...
107° 43′	~100	3.77	1.36	3.78	1.36	1160(a)	2120(a)
...	42	3.45	1.25	3.45	1.25	...	...
...	16	...	...	1.725	0.6232	717	1322
...	1166	2.23	0.805	2.23	0.805	450	840
...	28	3.27	1.18	3.31	1.19	710(a)	1310(a)
0.436	...	...	...	...	...	820(a)	1510(a)
...	...	...	...	...	...	...	...
...	16	...	...	3.96	1.43	855(a)	1570(a)
1.214	5	...	...	4.76	1.72	1130(a)	2070(a)
...	2	...	...	5.91	2.13	1640	2980
...	8	4.34	1.57	...	...	~1050	~1920
2.234	8	3.31	1.19	3.37	1.22	1340(a)	2440(a)
...	20	...	...	6.06	2.19	730(a)	1350(a)
...	192	...	...	2.98	1.08	670(a)	1240(a)
2.222	56	...	...	3.20	1.16	740(a)	1360(a)
4.316	16	4.11	1.48	4.11	1.48	1580	2880
1.064	3	4.38	1.58	4.50	1.62	2790	5050
...	12	...	...	1.99	0.718	1100	2010
...	...	...	...	...	...	...	...
...	39	6.16	2.22	6.12	2.21	385(a)	725(a)
1.644	12	5.20	1.88	5.20	1.88	590	1090
...	184	2.80	1.01	2.86	1.03	...	...
...	26	...	...	2.92	1.05	<580	<1080
...	84	3.40	1.23	...	...	...	...
2.347	40	4.30	1.55	4.44	1.60	...	...
...	28	...	...	...	...	630(a)	1170(a)
...	...	...	...	...	...	...	...
1.885	...	...	...	...	...	...	...
...	...	...	...	...	...	...	...
...	16	...	...	3.55	1.28	~550(a)	~1020(a)
1.64	12	...	...	4.13	1.49	~950	~1740
...	162	...	...	2.69	0.971	~475(a)	~890(a)
...	96	3.02	1.09	...	...	~520(a)	~970(a)
...	39	4.94	1.78	4.90	1.77	~710(a)	~1310(a)
...	150	...	...	3.59	1.30	...	...
...	250	...	...	5.48	1.98	~820(a)	~1510(a)
...	...	...	...	...	...	...	...
...	...	...	...	...	...	~810(a)	~1490(a)
...	...	3.58	1.29	...	...	~860(a)	~1580(a)
...		...	...	...	...	...	...
91°	...	...	...	...	...	~700(a)	~1290(a)
1.54	...	3.00	1.08	...	...	~870(a)	~1600(a)
...	...	...	...	...	...	...	...
...	162	3.78	1.36	3.80	1.37	~530(a)	~990(a)
...	...	...	...	...	...	...	...
1.031	~26	3.74	1.35	...	...	...	...
0.392	...	2.79	1.01	...	...	...	...
...	...	...	...	...	...	...	...
1.20	18	2.82	1.02	2.82	1.02	...	...

Another instance is in the aluminum-iron-manganese-silicon quaternary system; here the stable phase $(FeMn)_3Si_2Al_{15}$ (body-centered cubic) can vary from $Mn_3Si_2Al_{15}$, a = 1.2652 nm (12.652 Å) to $\sim(Mn_{0.1}Fe_{0.9})_3Si_2Al_{15}$, a = 1.2548 nm (12.548 Å). The stable phase of the closest composition in aluminum-iron-silicon is Fe_2SiAl_8 (hexagonal); the hexagonal → cubic transition is also accomplished by small additions of vanadium, chromium, molybdenum, and tungsten, and larger additions of copper (Ref 7). Such chemical stabilization effects, coupled with the metastability introduced by casting, frequently cause complex alloy structure.

The origin of this vast range of structures has been the subject of considerable study (Ref 8). Some phases are normal valency compounds (ionic), with high melting points and low electrical conductivity, such as Al-Group V compounds like AlSb. For these, electron transfer occurs, and bonding is nondirectional; interionic spacing is less than is expected for metallic bond. Some phases are electron compounds with specific valency electron/atom ratios, for example, 3-to-2 for $AlCu_3$. No electron transfer occurs in this phase, and factors relating to the metallic bond predominate. These compounds have some ductility, reasonable electrical conductivity, and melting points that range between those of the alloying components.

The origin of aluminum-transition metal and silicon-phases is still being investigated. There is some evidence that the valency electrons are absorbed into the d-shell of the transition metals and are replaced by electrons from the aluminum shell. This leads to a reduction of some aluminum-transition metal spacings as for the ionic bond; these phases have high melting points. Some systemization has been attempted (Ref 9). The structures can be considered in terms of flattened, polyhedral groupings of aluminum atoms around the transition metal atoms, 8-, 9-, or 10-fold. The three-dimensional structures are controlled by the packing of these polyhedra. Crystal structures, lattice parameters, and density and melting point or peritectic decomposition temperature for the most important intermetallic phases of aluminum-rich alloys are given in Table 3.

EQUILIBRIUM AND NONEQUILIBRIUM SOLIDIFICATION

All commercial solidification processes involve some nonequilibrium effects. Although equilibrium solidification is not actually observed, it is of interest as a limiting case. In real casting processes, the extent of deviation from equilibrium conditions has a significant effect on the actual microstructure observed (Ref 10 and 11).

Equilibrium solidification is approached when $L^2 \ll D_s t$, where L is the length solidified, D_s is the diffusion coefficient of solute in the solid, and t is time. This situation is illustrated in Fig. 2. An alloy of overall composition, C_0, begins to freeze at T_L and is frozen at T_S. The initial solid to freeze has a solute concentration given by kC_0, where k is the equilibrium partition coefficient (C_S^*/C_L^*), the ratio of interfacial solid and liquid solute concentrations. Because diffusion in the solid is assumed to be complete, the bulk solid solute concentration (C_S) is equal to the interfacial solid solute concentration (C_S^*) on the solidus line. Diffusion

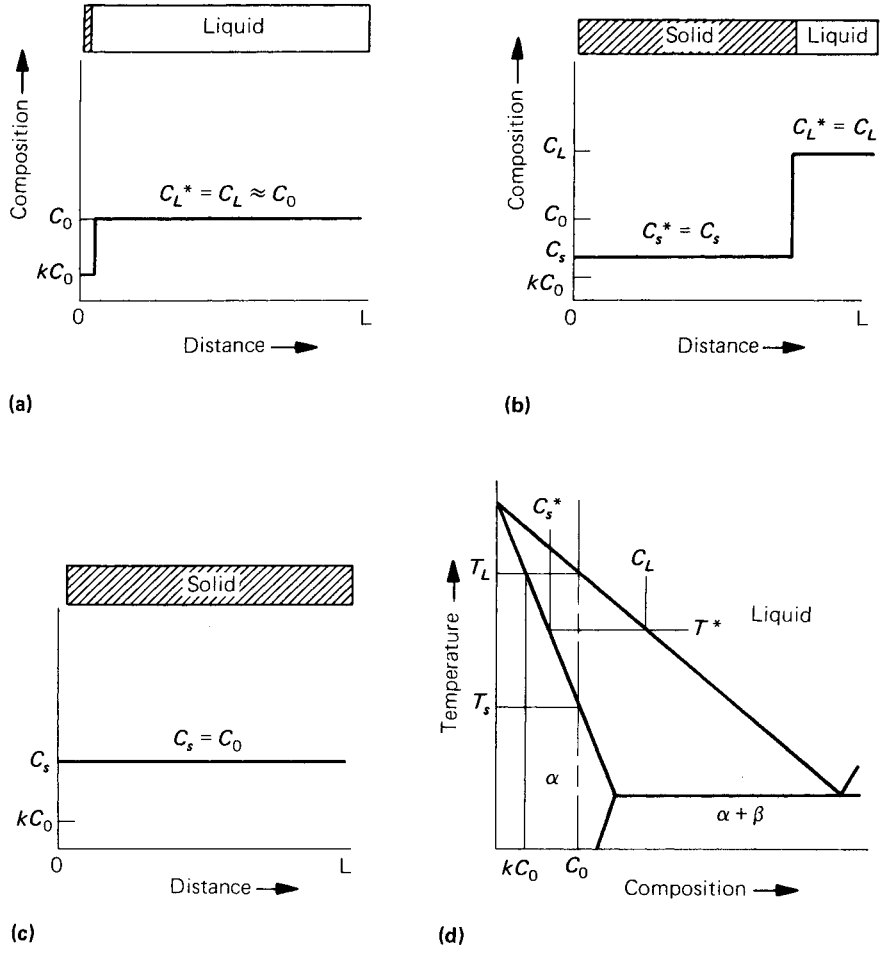

Fig. 2. Solute redistribution in equilibrium solidification of an alloy of composition C_0: (a) at start of solidification; (b) at temperature T; (c) after solidification; and (d) phase diagram (Ref 10).*

in the liquid is also assumed to be complete. After freezing, a uniform, single-phase solid with a solute concentration of C_0 is obtained.

Solidification with Local Equilibrium. Many commercial solidification processes, operating at moderate cooling rates (0.1 to 100 °C/s or 0.18 to 180 °F/s) can be approximated by the assumption that $D_S \simeq 0$ and local equilibrium at the interface is maintained ($k = C_S^*/C_L^*$) and $D_L \simeq \infty$. Solidification under these conditions is illustrated in Fig. 3. The first solid to freeze, at T_L, has a solute concentration of kC_0. At temperatures below the liquidus, the solid forming at the freezing interface is higher in solute than that previously frozen. To maintain a solute balance, additional solute is present in the liquid as a consequence of coring. This results in the formation of nonequilibrium eutectic in interdendritic re-

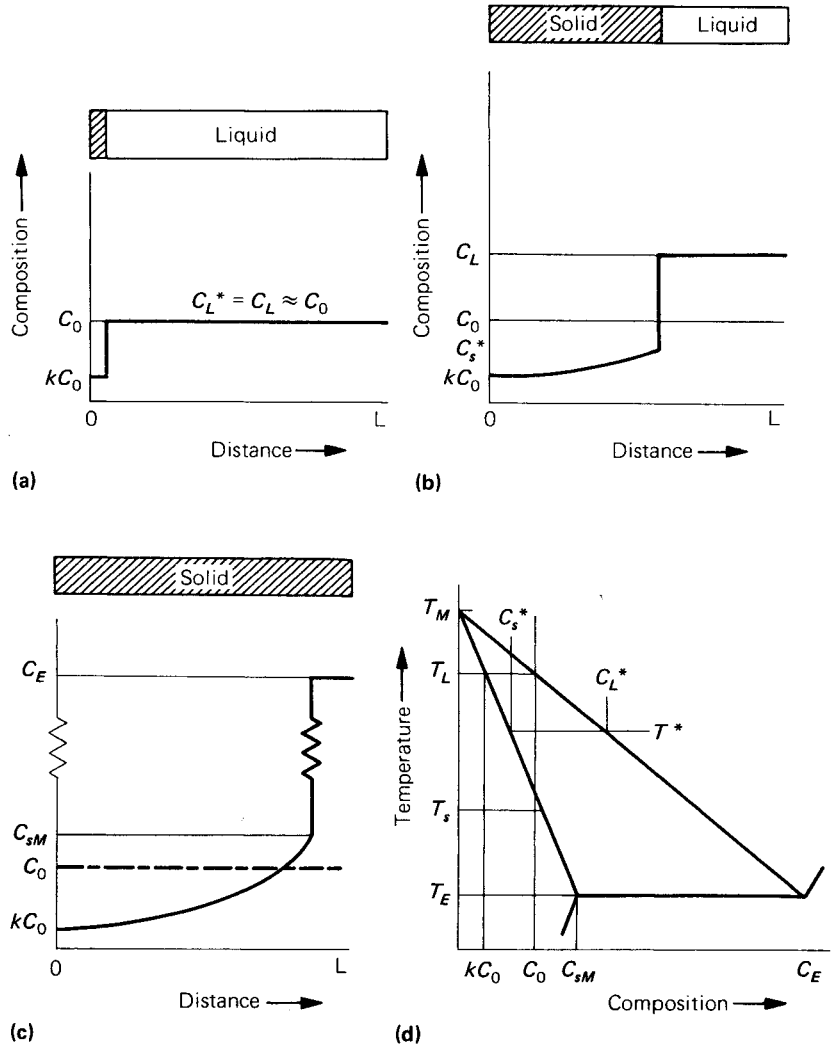

Fig. 3. Solute redistribution in solidification with no solid diffusion and complete diffusion in the liquid: (a) at start of solidification; (b) at temperature T; (c) after solidification; and (d) phase diagram (Ref 10).*

gions at the end of freezing. The amount of eutectic formed is to be given by:

$$f_E = \left(\frac{C_E}{C_0}\right)^{1/(k-1)} \qquad \text{(Eq 1)}$$

where f_E is the volume fraction eutectic and C_E is the eutectic solute concentration. The amount of eutectic actually observed is close to that predicted by Eq 1 for the cooling rate in the range of typical ingot casting processes (Ref 12). The dissolution of this nonequilibrium eutectic is achieved during ingot homogenization (Ref 13).

Rapid Solidification of Aluminum Alloys. In the search for improved properties for aluminum alloys, a variety of techniques that involve direct quenching from the liquid state have been investigated. These techniques, referred to as rapid solidification processing (RSP), are aimed at achieving a highly efficient dissipation of heat away from the liquid-solid interface so that a substantial increase in undercooling and the corresponding interface velocity can be obtained. This objective usually implies an improved heat transfer coefficient at the casting-quenchant surface and an increase in the surface area-to-volume ratio of the casting. The overall effect is the achievement of cooling rates estimated at from 10^3 to 10^{10} °C/s (1.8×10^3 to 1.8×10^{10} °F/s). A second guideline in RSP is to obtain a sufficient degree of supercooling before nucleation so that the liquid acts as the main sink for the heat of fusion. The solidification then proceeds in an essentially adiabatic manner. Solidification under the increasingly higher cooling rates, and conceivably, higher undercoolings typical of atomization, splat cooling, and other related techniques, usually results in progressive departure from the regular microstructures produced by conventional casting.

Microstructures of Rapidly Solidified Aluminum Alloys

Rapid solidification of aluminum alloys usually results in one or more of the following microstructural modifications:

- Microstructural refinement manifested as smaller grain size, as well as smaller dendrite arm and eutectic spacings
- Extension in terminal solid solubility of alloying elements in the primary α-aluminum phase and change in segregation patterns eventually leading to the reduction or elimination of the second phase
- Morphological changes of the eutectic or the primary phase
- Formation of metastable phases
- Coupled eutectic growth at off-eutectic compositions
- Vacancy supersaturation

Although all these effects have been observed in aluminum alloys, some even at the moderate cooling rates of 10 to 10^3 °C/s (18 to 1.8×10^3 °F/s) only the first four, which are important in terms of improving the properties of the final product, are well understood. A discussion of these effects follows.

Microstructural Refinement. In general, the fineness of microstructure during dendritic solidification of aluminum alloys, as in most other alloy systems, can be correlated to the average cooling rate during solidification, ϵ_{Avg}, or local solidification time (time available for coarsening), t_f, by:

$$DAS = a\epsilon_{Avg}^{-m} = bt_f^m \qquad \text{(Eq 2)}$$

and

$$\epsilon_{Avg} = \frac{(T_L - T_S)}{t_f} \qquad \text{(Eq 3)}$$

where $(T_L - T_S)$ is the solidification temperature range, DAS is the dendrite arm spacing, and a, b, and m are constants.

Experimental relationships between average cooling rate and dendrite arm spacing are available for several aluminum alloys (Ref 14 and 15). For example, dendrite arm spacings for an Al-10.5% Si alloy versus average cooling rates are reported for cooling rates of up to 10^5 °C/s (1.8×10^5 °F/s) (Ref 16). Dendritic spacings of 0.01 to 0.5 μm (0.0004 to 0.02 mil) (Ref 17–20), and eutectic spacings in the same order of magnitude (Ref 21), have been reported for electron-transparent areas of aluminum alloy gun splats on copper substrates. However, in most studies, experimental difficulties have limited the range of accurately measured cooling rates to less than ~10^3 °C/s (~1.8×10^3 °F/s).

Figure 4 illustrates the capabilities of various solidification techniques in terms of microstructural refinement expected from the estimated achievable cooling rates and a relationship of the type given by Eq 2 for aluminum alloys. Caution must be exercised when the exponential correlation in Eq 2 is used to estimate cooling rates in RSP from the dendrite spacings, because the reliability of extrapolating this relationship over many orders of magnitude is probably poor, especially if the microstructures examined do not exhibit typical dendritic morphologies. Furthermore, the constants in Eq 2 vary with alloy composition. Studies on the effect of alloy composition on structure at a fixed average cooling rate for aluminum binary alloys with copper, magnesium, silicon, or zinc have shown that increasing the solute content refines the dendrite arm spacing, especially at low solute concentrations (Ref 15 and 23). Refinement of secondary phases, including eutectic constituents, also occurs with an increasing cooling rate during solidification. Dispersion hardening associated with this effect has been reported in aluminum-silicon-based alloys (Ref 24–27).

Rapid solidification processing can also produce grain sizes of ~1 μm (~0.04 mil), significantly smaller than those developed in conventional casting. A quantitative analysis of the grain refinement resulting from solidification at high cooling rates (>10^5 °C/s or >1.8×10^5 °F/s) obtained by splat quenching has been made by Boswell and Chadwick (Ref 28), and good agreement was obtained between observed and predicted grain sizes for rapidly quenched aluminum.

Extension in Solid Solubility. Terminal solid solubility extension has been obtained at sufficiently high cooling rates in almost all aluminum alloy systems investigated, with the notable exception of aluminum-zinc (Ref 29). The increased solid solubility permits higher alloying levels, resulting in superior strength-ductility combinations in a number of systems. Table 4 shows the maximum reported solid solubilities for a number of binary aluminum alloys of practical interest.

There are indications that the extent of solute solubility increases with severity of the quench (Ref 30) and increased initial alloy composition (Ref 31) and that it is not necessarily bounded by the eutectic composition. Additions especially susceptible to solubility extension in binary alloys (for example, manganese) can be used in ternaries to increase the solubility limit of less susceptible elements such as iron, cobalt, and nickel (Ref 30).

Morphological Modifications. Both conventional dendritic (columnar and equiaxed) and modified dendritic morphologies have been reported

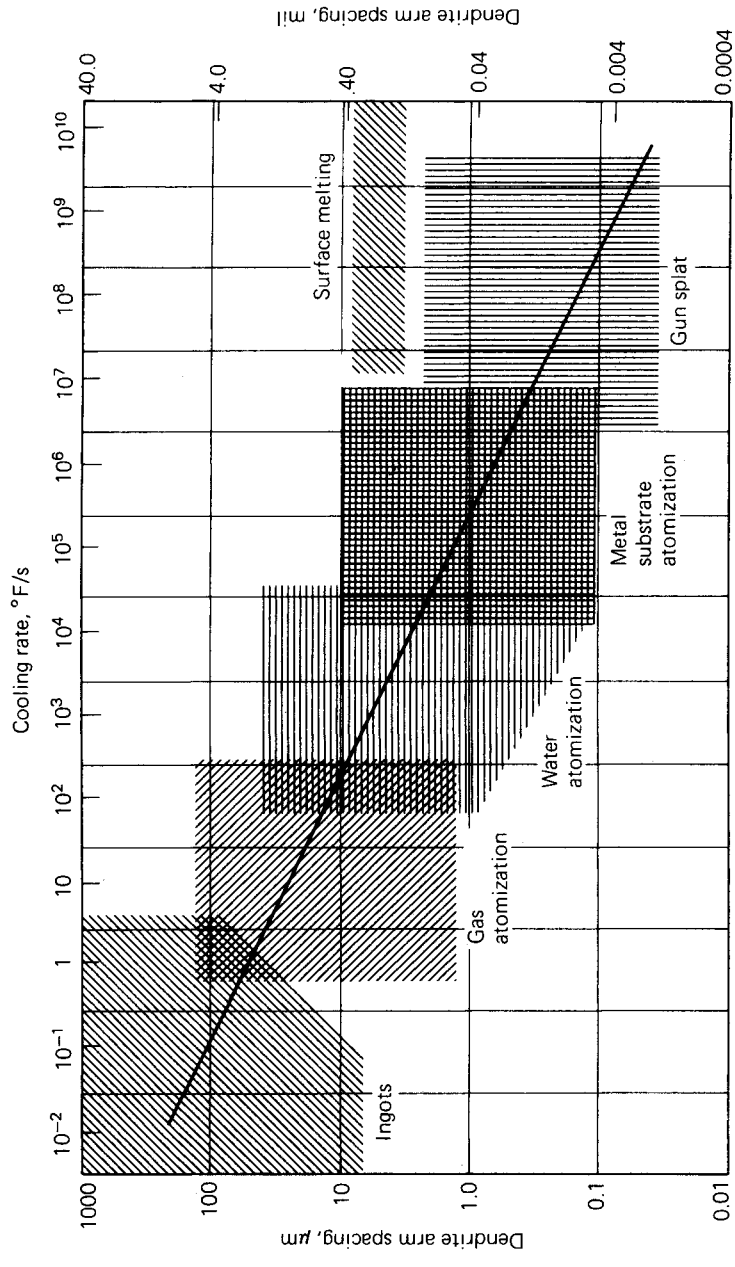

Fig. 4. Dendrite arm spacing as a function of cooling rate for aluminum and aluminum alloys (Ref 22).

Table 4. Extension of Solid Solubility in Binary Aluminum Alloys Quenched from the Melt

Element	Maximum at equilibrium Temperature at.%	K	°R	Reported maximum, at.%
Cr	0.44	935	1670	>5–6
Cu	2.5	820	1460	17–18
Fe	0.025	930	1660	4–6
Mg	18.9	725	1290	36.8–40
Mn	0.7	925	1650	>6–9
Ni	0.023	915	1600	1.2–7.7
Si	1.59	850	1520	10–16
Zn	66.5	655	1170	38–···

Source: H. Jones, *Aluminum*, Vol 54 (No. 4), 1978, p 274.

in alloys solidified at high cooling rates (Ref 32–34). The primary phase in the latter tends to assume a cellular or rod-like configuration with progressively faster cooling rates (Ref 18 and 34). Similar observations have been reported in bulk specimens of nickel- and iron-based alloys with increasing supercooling before nucleation of the solid phase (Ref 35). High cooling rates sometimes can suppress primary formation of an equilibrium phase from the melt. For example, formation of α-aluminum dendrites instead of equilibrium $FeAl_3$ phase in hypereutectic aluminum-iron alloys both in chill-cast (Ref 36) and splat-cooled specimens (Ref 37) has been reported.

Sufficiently rapid cooling rates during solidification can alter the composition range of cooperative eutectic growth, the eutectic constituents, and their morphologies. Relatively rapid solidification of aluminum-iron alloys in the range of 10 to 10^4 °C/s (18 to 1.8×10^4 °F/s) has resulted in eutectic morphologies changing from irregular Al—$FeAl_3$ to regular Al—$FeAl_6$, as well as coupled eutectic growth at noneutectic compositions (Ref 36). In addition, degenerate and radial eutectic structures in Al-17.3 at.% Cu and structural changes as a function of copper content have been studied via splat cooling (Ref 38).

Formation of Metastable Phases. Departure from the phase equilibria predicted by the phase diagram of aluminum alloys is not as common as the effects noted above. Nevertheless, a certain number of cases are reported in the literature and have been classified by Jones (Ref 30) as:

- Type I: phases present at equilibrium but not stable at the temperature and alloy compositions in which they were observed
- Type II: phases not formed from the melt but appearing, normally transiently, on further heat treatment or precipitated during quenching through the solid state
- Type III: phases present in the rapidly quenched specimen but not known to exist under equilibrium conditions at any composition within the alloy system

A summary of the reported observations in binary aluminum alloy systems is given in Table 5. The only report of a noncrystalline structure in an aluminum alloy (Ref 39), splat-cooled Al-17.3 at.% Cu alloy, has not been supported by further investigation (Ref 40).

Table 5. Nonequilibrium Phases Detected in Aluminum Binary Alloys Under Rapid Solidification

Alloying element	Concentration range, at.%	Nonequilibrium phase detected	Type	Corresponding equilibrium phases	
Cr	1.6–3	Al_4Cr	I	α-Al + Al_7Cr(a)	(Ref 1)
Cu	45	Al_3Cu_2 (trigonal)	III	O + η_2	(Ref 2)
	17.3	Noncrystalline	III	α-Al + O(a)	(Ref 3)
Fe	2–4	γ, γ′, γ″, o^{α}	II	Al_3Fe + α-Al	(Ref 4)
	4	Al_6Fe (orthorhombic)	II	...	(Ref 4)
	...	Al_6Fe	III	...	(Ref 5)
Mg	25	Le_2 superlattice	II	α-Al + β-Al_3Mg_2(a)	(Ref 5)
	40	(α-Mn)-like structure	III	α-Al + β-Al_3Mg_2(a)	(Ref 5)
	(b)	...	...	...	...
Mn	≤6	Al_4Mn	I	α-Al + Al_6Mn(a)	(Ref 6)
Ni	7.3–10.1	η (orthorhombic)	III	α-Al + β-Al_3Ni(a)	(Ref 7)

(a) Formed transiently during aging following a decomposition kinetics similar to the supersaturated aluminum-copper solid solutions. (b) Concentration range, ~10 wt%.
(Ref 1) Varich and Lyukevich, 1970. (Ref 2) Ramachandrarao and Lavidjoni, 1974. (Ref 3) Davies and Hull, 1974. (Ref 4) Jacobs, *et al.*, 1974. (Ref 5) Jones, 1978. (Ref 6) Varich and Kolesnichenko, 1961. (Ref 7) Toneje, *et al.*, 1971

Particular nonequilibrium effects do not happen above a critical thickness in splat cooling (below a given average cooling rate during solidification). For example, $FeAl_6$ can displace the equilibrium phase $FeAl_6$ at cooling rates as low as 3 °C/s (5 °F/s); however, cooling rates of the order of 10^4 °C/s (1.8×10^4 °F/s) are required to displace the equilibrium FCC Al_3Mg_2 phase in aluminum-magnesium alloys (Ref 30).

PHASE DIAGRAMS AND THERMODYNAMICS

Aluminum is alloyed with a large number of elements. Commercial alloys frequently contain more than one second phase, with the overall properties achieved by careful control of second-phase type, shape, size, and distribution. Consequently, the generation and understanding of phase diagrams has played an important part in aluminum technology.

Phase diagrams map phase stability in terms of important variables, usually temperature and composition. They are determined by fundamental thermodynamic factors. This section identifies these factors and discusses how they can be used to systemize alloying behavior, interpolate or extrapolate data, or predict unknown phase diagrams. The analytical treatment is limited and based on more specialized texts (Ref 41–43).

Background. Thermodynamics is concerned with the energy involved in the transfer of material from one phase to another, with the same or different composition. It does not by itself determine structural features such as crystallography, subdivision of a second phase, or rate of transfer. At constant temperature, T, and pressure this energy is the change in the Gibbs free energy of the system (ΔG) and is comprised of two factors, the enthalpy change (ΔH) and entropy change (ΔS), as shown below:

$$\Delta G = \Delta H - T\Delta S \qquad \text{(Eq 4)}$$

For the process to be spontaneous, ΔG must be negative, and for equilibrium, ΔG must be zero. ΔH represents the heat evolved or absorbed

during the reaction, negative for an exothermic reaction, and is determined by changes in bond energies or lattice strain because of atomic size difference. ΔS is determined primarily by changes in vibrational frequency, as is seen from its dependence on the change of heat capacity:

$$\Delta S = \int_0^T \frac{\Delta C_p}{T} dT$$

For solution reactions, ΔS is usually positive because of the complexity of vibrational spectrum of a mixture of atoms. It is also positive on liquation because of the breakdown of crystalline order.

Quantitative assessment of phase boundary position is determined through the concept of chemical potential, μ. This is the free energy/mole of a component of a solution at equilibrium and is the same everywhere within a system of phases. It is defined with respect to the free energy/mole of the pure component in the same physical state, μ_0:

$$\mu = \mu_0 + RT \ln a \qquad \text{(Eq 5)}$$

where R is the gas constant and a is the activity. A solution is termed ideal if activity equals mole fraction, X (atom fraction for metallic solutions). Physically, this means that bond energies and atom sizes are identical for solute and solvent, giving zero enthalpy and volume change on mixing. Most aluminum-based solutions are far from ideal except at very low concentration. However, the ideal solution model does give insight into some important characteristics of phase diagrams.

Liquidus and Solidus. Liquidus and solidus represent the variation with temperature of composition of liquid and solid solutions in equilibrium. Thus, for any component, $\mu^S = \mu^L$. This must be translated into a more usable form. For ideal solutions, atom fractions can be substituted in Eq 5 and equate:

$$RT \ln \frac{X^L}{X^S} = \mu_0^S - \mu_0^L \qquad \text{(Eq 6)}$$

From the definition of μ_0, $-(\mu_0^S - \mu_0^L)$ is the molar free energy of fusion of the pure component at temperature T displaced from T_f, the equilibrium fusion temperature. Hence, it is nonzero. If the fusion enthalpy ΔH_f (the latent heat of fusion) is assumed to be independent of temperature and composition, Eq 4 at T and T_f can be used to give $\Delta G_{f,T} = \Delta H_f(T_f - T)/TT_f$. Therefore:

$$\ln \frac{X^L}{X^S} \cong \frac{\Delta H_f}{RT_f} - \frac{\Delta H_f}{RT} = \frac{\Delta S_f}{R} - \frac{\Delta H_f}{RT} \qquad \text{(Eq 7)}$$

This relationship can be tested in two ways. The first is to use data for eutectic and peritectic invariant points which are relatively easy to establish (Table 1). When $1/T$ is plotted against log $(X^L/X^S)_{Al}$, the results should be close to the ideal solution line with slope $-2.303\ R/\Delta H_{f,Al}$. This is shown in Fig. 5; the data correlate well. The second method is to use data for individual solidus and liquidus curves of systems with higher solubilities as shown in Fig. 6. That closest to the ideal case is aluminum-gallium; gallium has similar atomic radius (Table 2) and, being in the same group of the periodic table, the same outer electronic structure. The unusual behavior of aluminum-zinc is probably associated with clustering in the solid solution.

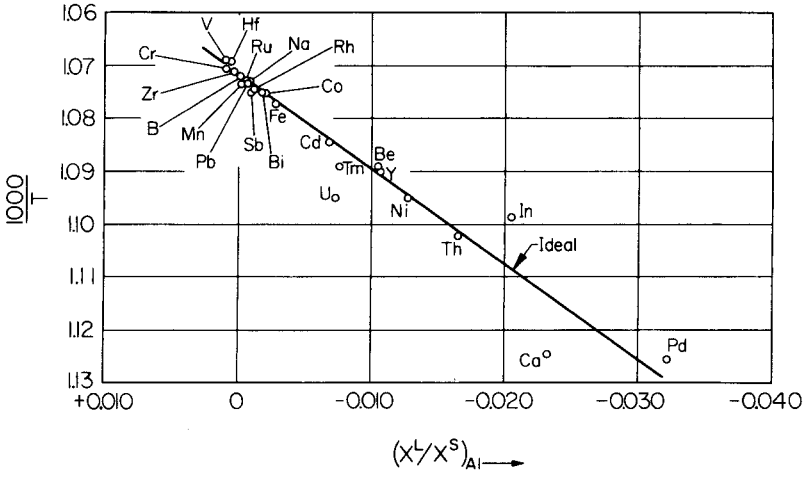

Fig. 5. Equilibrium eutectic and peritectic invariant point data for binary aluminum alloy systems plotted according to Eq 7 so as to show correlation with the ideal solution model (Ref 44).

The parameter that describes the heterogeneity of solute distribution in the primary phase after casting is the partition ratio, $k = (X^S/X^L)_{solute}$. When experimental values are not available, k can be calculated thermodynamically in two ways (Ref 42). For ideal aluminum + B solutions:

$$k = \exp\left[\frac{\Delta H_{f,B}(T_{f,Al} - T_{f,B})}{RT_{f,Al}T_{f,B}}\right] \qquad \text{(Eq 8)}$$

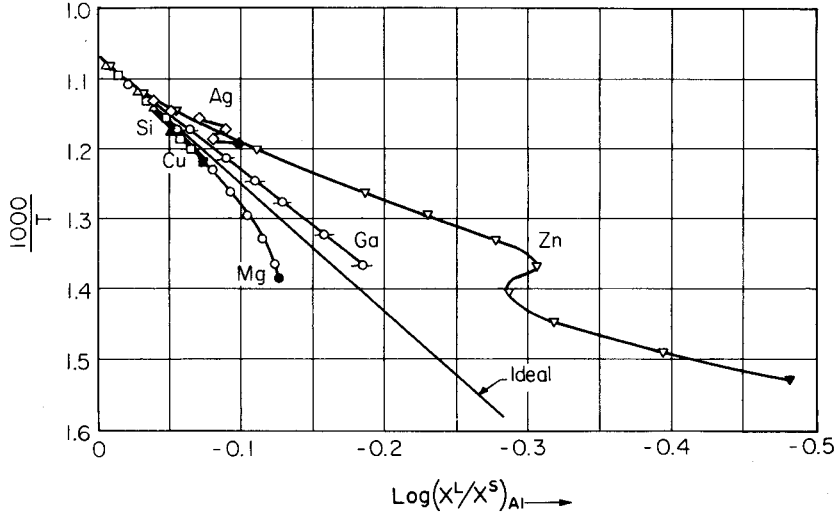

Fig. 6. Equilibrium solidus and liquidus data for binary aluminum alloy systems with extensive solid and liquid solubility plotted according to Eq 7 (Ref 44).

For ideal or real aluminum + B solutions:

$$k = 1 - \frac{m_L \Delta H_{f,Al}}{RT^2_{f,Al}} \qquad \text{(Eq 9)}$$

where m_L is the liquidus slope.

Figure 7 summarizes the effect of relative deviation from ideality on the general form of binary phase diagrams. Aluminum, being trivalent and reactive, forms multiple stable intermetallic compounds of the β-type in Fig. 7(e). This leads to complex phase diagrams and low solid solubility, the prerequisite for commercially useful age hardening.

Solvus. Thermodynamic analysis of the solvus curve, the locus of maximum solid solubility in the aluminum-rich phase, is more complex than for liquidus and solidus. Its very existence implies considerable deviation from ideality. Considering two-phase equilibrium between α and intermetallic compound β, the usual situation in age-hardening alloys, $\mu^B_\alpha = \mu^B_\beta$, $a^B_\alpha = a^B_\beta$. By making suitable assumptions ($a^B_\alpha = \gamma^B_\alpha X^B_\alpha$ where γ^B_α, the Henry's law activity coefficient, is independent of temperature

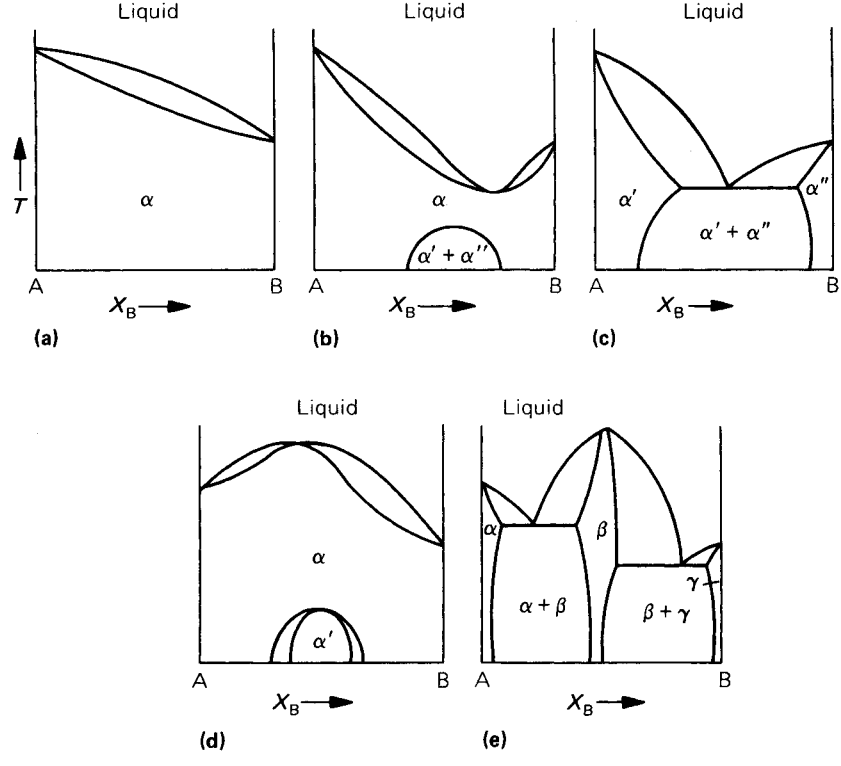

Fig. 7. The effect of relative deviation from ideality on the general form of binary phase diagrams: (a) phase diagram for ideal solutions; (b) phase diagram for case where $\Delta H^S_m > \Delta H^L_m > 0$ (m denotes mixing); (c) same as (b) except ΔH_m is more positive; (d) phase diagram for case where $\Delta H^S_m < \Delta H^L_m < 0$; (e) same as (b) except that ΔH_m is more negative (Ref 41).

and composition and $a_\beta^B = X_\beta^B$ in an ideal solution), Ref 41 shows that:

$$ln \frac{X_\alpha^B}{X_\beta^B} = \frac{\Delta \bar{S}_{v,\alpha}^B}{R} - \frac{\Delta \bar{H}_\alpha^B}{RT} \quad \text{(Eq 10)}$$

$\Delta \bar{S}_{v,\alpha}^B$ is the relative vibrational entropy change corresponding to the transfer of 1 mole of B from the pure state to α, $\Delta \bar{H}_\alpha^B$ is the relative partial molar enthalpy change of B in α; there is close similarity to Eq 7. Assuming that the β-phase is very stable and concentrated in B so that X_β^B is independent of temperature and close to unity, the relationship can be tested by plotting $1/T$ against log X_α^B; the result should be a straight line of slope $-2.303R/\Delta \bar{H}_\alpha^B$ and intercept on the concentration axis of $\Delta \bar{S}_{v,\alpha}^B/2.303R$. This is shown for a representative series of solutes in Fig. 8. There is reasonable agreement for the transition metals and at higher concentrations for silicon and copper. In general, the larger $\Delta \bar{H}_\alpha^B$, the higher is $\Delta \bar{S}_{v,\alpha}^B$. The most important contribution to solution enthalpy is strain energy; this is associated with a reduction in the local vibrational frequencies giving rise to increased solution entropy. Table 2 gives experimental values of $\Delta \bar{H}_\alpha^B$.

Strain energy is dependent on the difference of radius between solvent and solute. A measure of lattice strain is the variation of lattice parameter with concentration of solute; these data are also summarized in Table 2. In the absence of the formation of a stable compound, extensive solid solution is only achieved when there is $\lesssim$15% difference in atomic radii (Ref 8). Also summarized in Table 2 are resistivity increments and the atomic percents of solutes. These can vary widely and show period re-

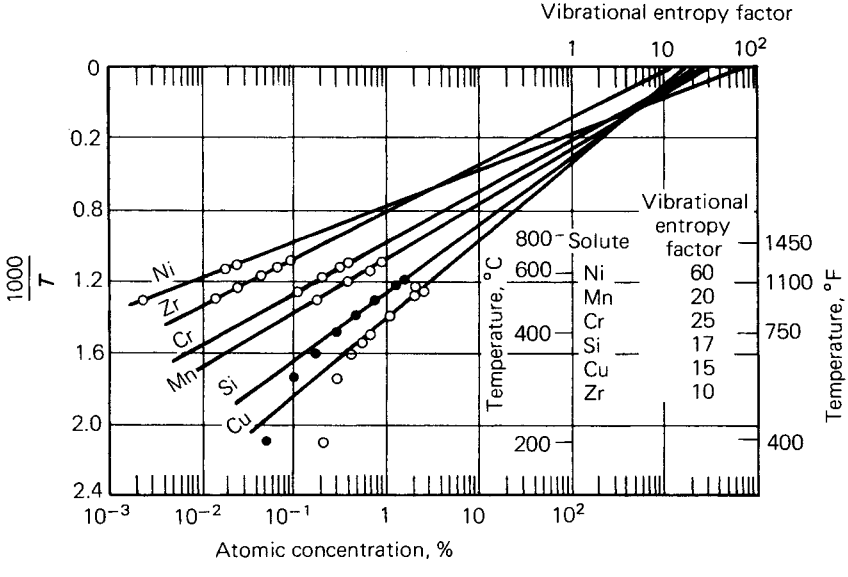

Fig.8. Equilibrium solvus data for selected binary aluminum alloy systems plotted according to Eq 10 so as to obtain relative partial molar solution enthalpy and entropy changes (Ref 50).

lationships associated with the variation of outer electronic structure of solvent and solute (Ref 44 and 45).

Ternary alloys with second phases of well-defined two- or three-component stoichiometry can be analyzed as pseudobinary through use of the equilibrium constant. In the general two-component case, $\beta = B_nC_n$, for example Mg_2Si and $MgZn_2$:

$$K = (a_\alpha^B)^n(a_\alpha^C)^m/(a_\beta^B)^n(a_\beta^C)^m$$

If activity coefficients in α are constant we can define $K' = (X_\alpha^B)^n(X_\alpha^C)^m$ and use Eq 10 to calculate:

$$lnK' = \frac{-\Delta\tilde{H}_\alpha^\beta}{RT} + \text{constant} \qquad \text{(Eq 11)}$$

$\Delta\tilde{H}_\alpha^\beta$ is the solution enthalpy of β in α.

Representative data are shown in Fig. 9 for alloys on the α-β tie line, and show reasonable agreement. This principle can be extended to off-stoichiometric alloy compositions because K' is constant for any particular temperature. From the definition of K', the following equation results:

$$\log X_\alpha^B = \log K' - \frac{m}{n}\log X_\alpha^C \qquad \text{(Eq 12)}$$

Thus, a logarithmic plot of X_α^B against X_α^C for any particular temperature should be linear with slope $-m/n$. An example is shown in Fig. 10 for the aluminum-magnesium-zinc system. The $\log X_\alpha^{Mg} - \log X_\alpha^{Zn}$ isotherms show a distinct change of slope as the stoichiometric composition of the equilibrium phase changes. Deviation from the expected slope of -2 for the $MgZn_2$ solvus is probably associated with systematic deviation from ideality with increased zinc concentration.

The Metastable Solvus. Age hardening is generally accomplished through the precipitation of a metastable variant of the equilibrium phase,

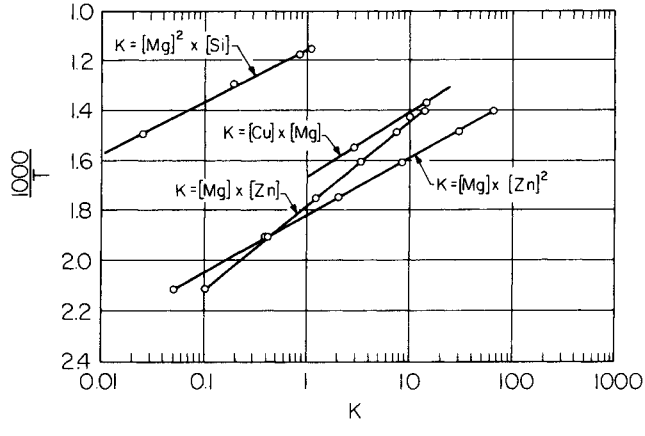

Fig. 9. Equilibrium pseudobinary solvus data for selected ternary aluminum alloy systems plotted according to Eq 11 to show how the equilibrium constant can be used to obtain the molar solution enthalpy of compound second phases (Ref 44).

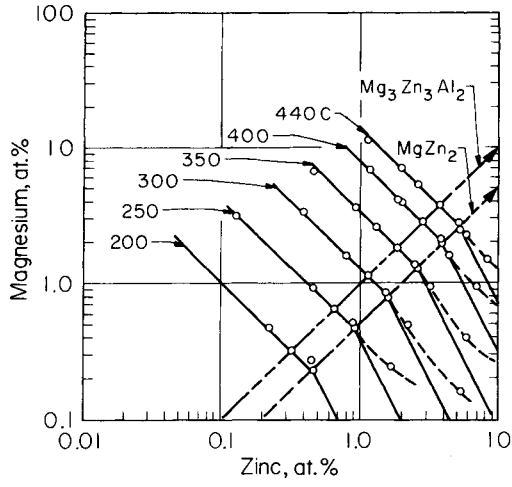

Fig. 10. Equilibrium solvus isotherms for the aluminum-rich corner of the aluminum-magnesium-zinc system plotted according to Eq 12 to show the effect of excess magnesium or zinc (Ref 44).

β' instead of β. The surface free energy change that accompanies the generation of new interfaces is minimized by structural rearrangement to give good precipitate and matrix lattice matching, but at the expense of volumetric free energy. By definition, ΔG for a metastable phase is less negative than that of the equilibrium phase. For metastable equilibrium $\alpha + \beta'$, $\mu_\alpha^B = \mu_{\beta'}^B > \mu_\beta^B$, the metastable solvus is shifted to higher concentration than the equilibrium solvus.

Because there can be more than one metastable variant, there can be more than one metastable solvus. Multiple structural rearrangement of this type is a feature of commercially useful, age-hardening alloy systems and often leads to difficulty in establishing the equilibrium phase relationship. Figure 11 shows metastable solvus curves in the aluminum-copper system.

Prediction of Phase Diagrams from Thermodynamic Data. In the past decade, considerable advances have been made in the thermodynamic evaluation of phase diagrams, particularly through the application of computer techniques (Ref 46). The available data and computational procedures have been systemized internationally since 1971 through the CALPHAD (Computer Coupling of Phase Diagrams and Thermochemistry) project (Ref 47) (Calculation of Phase Diagrams). Application for multicomponent aluminum alloy phase diagram prediction has some inherent problems, particularly regarding the unexpected occurrence of ternary intermetallic phases, but is rapidly becoming an effective procedure.

Prediction of the behavior of multicomponent systems requires explicit equations that describe the absolute free energy of all principal phases in the relevant binary systems as a function of composition and temperature. Solution phases are analyzed in terms of this deviation from ideality, and compound phases are analyzed as a function of stoichiometry. Critically

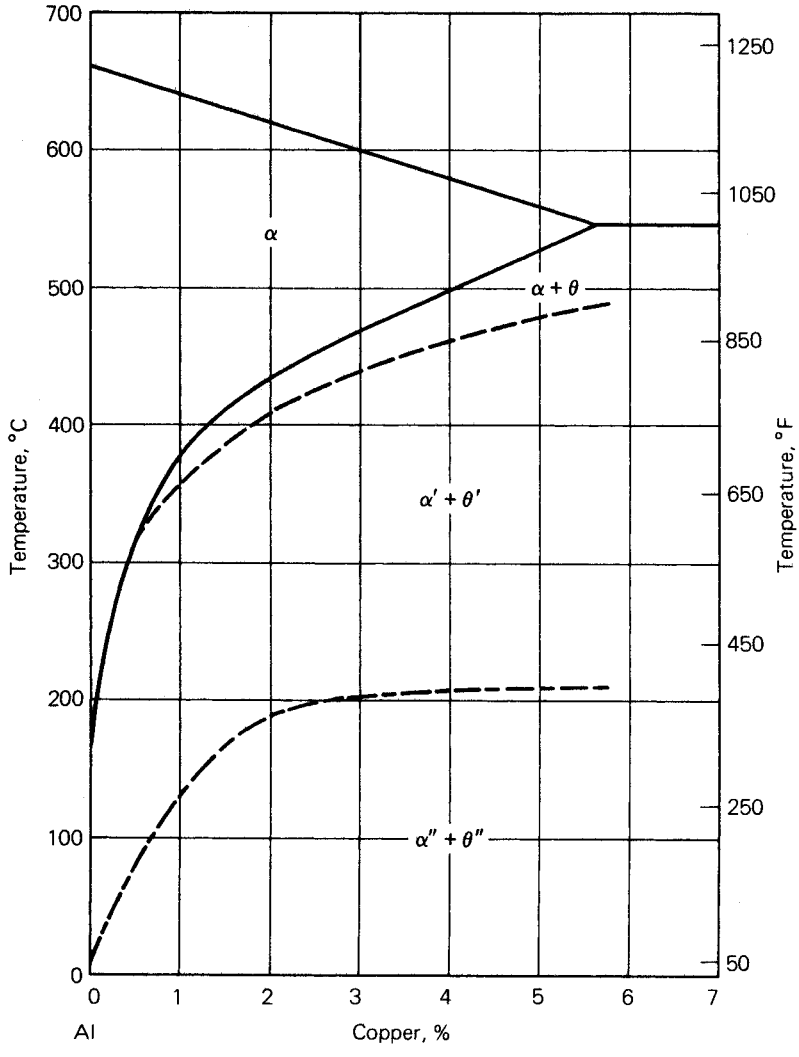

Fig. 11. Metastable equilibrium solvus curves for aluminum-rich aluminum-copper alloys (Ref 51).

assessed thermodynamic data are available in database form (ALLOYDATA) (Ref 48).

Ternary phase diagrams are calculated as isothermal sections by minimizing the Gibbs free energy of the system for progressive pair-wise combination of the available phases and by determining the most stable phase configuration. The calculated phase compositions show the positions of the phase boundaries. Once the generalized topographical form of the phase diagram is established, relatively few experiments are needed to test the validity. To date (1980), the following ternary aluminum-

containing systems have been examined: Al-Fe-Ti, Al-Ga-Ge, Al-Ga-In, Al-Ge-Sn, Al-Li-Mg, and Al-Ni-Ti.

As well as the 15 binaries required for these systems, phase diagrams of the following binary systems have also been examined: Al-Ca, Al-Ce, Al-Co, Al-Cr, Al-Cu, Al-Mn, Al-Mo, Al-Nb, Al-O, Al-P, and Al-Si (Ref 49). In principle, any ternary or quaternary combination of these binary systems can be analyzed.

MAJOR ALLOY SYSTEMS

Aluminum-Copper. Copper is one of the most important alloying elements for aluminum, because of its appreciable solubility and strengthening effect. Many commercial alloys contain copper, either as the major addition or among the principal alloying elements, in concentrations of 1 to 10%. It is used frequently in combination with magnesium.

The aluminum-copper system has been reviewed in detail (Ref 6). The aluminum-rich end of the phase diagram is eutectic Al-$CuAl_2$. The eutectic temperature is 548 °C (1018 °F), and the composition of the eutectic liquid is aluminum-33.2 wt% copper in equilibrium with an aluminum-solid solution containing 5.7 wt% copper (2.53 at.%). The $CuAl_2$ intermetallic phase has a range of composition from 52.5 to 53.7 wt% copper at the eutectic temperature, and from 53.2 to 53.9 wt% at 400 °C (750 °F), compositions slightly deficient in copper for the quoted stoichiometry.

The precipitation reactions are as follows (Ref 51): supersaturated solid solution → coherent platelike GP (Guinier-Preston) zones $/\!/\{001\}_{Al}$ → coherent platelike $\theta''/\!/\{001\}_{Al}$ → semicoherent platelike $\theta'/\!/\{001\}_{Al}$ → noncoherent θ. Structures of these phases are given in Table 3.

Aluminum-Lithium. Binary aluminum-lithium alloys offer interesting combinations of low-density and high-elastic modulus. In aluminum-rich alloys, the eutectic composition is 9.9% lithium and the eutectic temperature is 600 °C (1110 °F). Lithium has significant solubility in aluminum (5.2% max), and the binary alloys show appreciable precipitation hardening. The strengthening precipitate comes from Al_3Li, which is a metastable, ordered δ' phase.

Aluminum-Magnesium. Binary aluminum-magnesium alloys are the basis for an important class of non-heat treatable alloys (5XXX series alloys). Although magnesium has substantial solubility in solid aluminum, binary alloys do not show appreciable precipitation-hardening characteristics with concentrations below 7% magnesium. Magnesium, however, does provide substantial strengthening with good ductility as a result of cold work, in addition to excellent corrosion resistance and weldability.

In aluminum-rich alloys, the eutectic temperature is 450 °C (840 °F) and the concentration is 35% magnesium. The phase in equilibrium with aluminum is usually given as Mg_2Al_3 (37.3% magnesium), although this composition is outside the limits of existence (34.8 to 37.1%) (Ref 52). The formula Mg_5Al_8 (36% magnesium) fits the composition of the solid phase and most of the proposed structures. Equilibrium in solidification

is obtained only with cooling rates of less than 5×10^{-6} °C/h (9×10^{-6} °F/h) (Ref 53). Solidification under nonequilibrium conditions leads to coring, with the Mg_5Al_8 phase appearing at magnesium contents as low as 4 to 5% magnesium (Ref 54). Mg_5Al_8 is very brittle below 330 °C (630 °F), but shows some plasticity at higher temperatures (Ref 55).

Aluminum-Manganese. Non-heat treatable alloys containing slightly over 1% manganese, for example 3003 alloy, are of considerable commercial importance. Manganese is also widely used in lesser amounts as an alloying addition in heat treatable alloys such as 2024 alloy with 0.30 to 0.9% manganese, and non-heat treatable alloys such as 5182 alloy with 0.20 to 0.50% manganese. In general, manganese increases the strength of wrought alloys. However, manganese present as undissolved intermetallic compounds usually has the effect of decreasing ductility. Another important effect of manganese on aluminum and its alloys is to reduce the susceptibility to intergranular or stress corrosion.

In the binary system, manganese has only a slight effect in lowering the freezing point of aluminum. The eutectic temperature and concentration are 660 °C (1220 °F) and 1.9% manganese (Ref 56). The solid solubility limit of manganese in aluminum is 1.8% at the eutectic temperature. The intermetallic phase, which exists in equilibrium with the aluminum solid solution, has a composition closely corresponding to the formula $MnAl_6$. $MnAl_6$ separates as primary phase from liquid solution containing 1.9 to 4.1% manganese. From solutions of higher concentration, it is formed by peritectic reaction between $MnAl_4$ and liquid at 710 °C (1310 °F).

The only metastable phase that is definitely established for aluminum-manganese alloys has the composition of $MnAl_{12}$ with 14.5% manganese (Ref 57). Iron and silicon >0.2% suppress the formation of $MnAl_{12}$; chromium, on the other hand, stabilizes it (Ref 58). In the aluminum-manganese-chromium system, there is a ternary phase that forms only in the solid state by peritectoid reaction at 590 °C (1090 °F). This phase forms $(CrMn)Al_{12}$ with a range of composition from 2% chromium, 12% manganese to 4% chromium, 10% manganese (Ref 57). This ternary phase is isomorphous with the $MnAl_{12}$ phase.

Aluminum-Silicon. The commercial importance of aluminum-silicon alloys is based on their high fluidity and low shrinkage in casting, brazing, and welding applications. The hardness of silicon particles imparts wear resistance. Modification with sodium or strontium (<0.02%) results in a fine distribution of silicon particles in hypoeutectic alloys. Alternatively, phosphorous (<0.01%) can be added as a nucleating agent for hypereutectic alloys.

The aluminum-silicon system forms a simple eutectic with limited solid solubility at both ends. The eutectic occurs at 580 °C (1080 °F) and 12.5% silicon (Ref 6). At the eutectic temperature, the aluminum and silicon solid solutions contain 1.65% silicon and about 0.5% aluminum, respectively. Other intermetallics do not exist in the pure binary system.

Aluminum-Zinc. The aluminum-zinc binary alloys were among the first aluminum alloys commercially developed, but have been largely displaced by aluminum-copper and aluminum-silicon. Aluminum-zinc alloys are primarily used for electrolytic protection against corrosion. Super-

plasticity observed near the aluminum-zinc eutectoid (Ref 59, 60) offers the prospect for expanded commercial application. Currently, zinc is usually used with magnesium and copper in wrought products.

Zinc forms a eutectic-type system with aluminum. The eutectic reaction occurs at 380 °C (720 °F), with liquid containing 94.9% zinc reacting to form aluminum solid solution containing 82.8% zinc and zinc solid solution containing 1.1% aluminum.

A miscibility gap exists in the aluminum solid solution, resulting in a monotectoid reaction at 275 °C (530 °F) between aluminum solid solutions containing 78 and 31.6% zinc and zinc solid solution containing 0.6% aluminum. The solubility gap disappears at 60% zinc and 351.5 °C (664.7 °F), at 61.3% zinc. A eutectoid occurs at 78% zinc and 275 °C (530 °F).

Aluminum-Copper-Lithium. The addition of copper to aluminum-lithium binary alloys reduces the solubility significantly beyond about 1.5% lithium at 515 °C (960 °F). In the aluminum-rich end of the phase diagram, there are three compounds in equilibrium with aluminum: T_B, T_1, and T_2. The T_B phase is Cu_4LiAl_7, corresponding to 56.5% copper, 1.5% lithium. Its structure is similar to that of $\theta'(CuAl_2)$ phase formed in age-hardenable aluminum-copper alloys. The T_1 phase is $CuLiAl_2$ containing approximately 52.8% copper and 5.4% lithium. The T_2 phase has a composition close to $CuLi_3Al_6$ (26.9% copper, 8.8% lithium). Depending on the composition and temperature, the relative amounts of different phases of δ' and T-phases can be varied to obtain different mechanical properties.

Aluminum-Copper-Silicon (Ref 61). Several commercial aluminum-based casting alloys contain both copper and silicon as major alloying ingredients. Hot shortness in casting or welding aluminum-copper-silicon alloys is strongly dependent on composition. Hot shortness is maximum at the limit of solid solubility when the amount of eutectic present is at a minimum.

No ternary compounds are formed; the phases in equilibrium with aluminum are $CuAl_2$ and silicon. An alloy of eutectic composition contains 26 to 31% copper and 5 to 6.5% silicon and solidifies at 520 to 525 °C (970 to 975 °F). The solid solubility of silicon in $CuAl_2$, or of copper and aluminum jointly in silicon, is believed to be extremely small. In an aluminum solid solution, the presence of a second dissolved element usually reduces the solubility of the first, and vice versa. Nonequilibrium freezing, even by quenching from the liquid, has little effect on the structure of the alloys.

Aluminum-Copper-Magnesium (-Silicon). Commercial alloys containing both copper and magnesium as major additions also contain sufficient silicon to give them the characteristics of quaternary alloys rather than ternary alloys. The principal precipitation-hardening reactions, however, are those of the ternary aluminum-copper-magnesium system.

The commercially important alloys contain copper as major addition, and the phase reactions which occur are those between an aluminum solid solution and the intermetallic phases $CuAl_2$ and $CuMgAl_2$. At 510 °C (950 °F), a ternary eutectic reaction occurs between liquid containing 33.1% copper and 6.25% magnesium, $CuAl_2$, $CuMgAl_2$, and aluminum solid solution containing 4.28% copper and 1.35% magnesium. A quasibinary

section also exists with a eutectic at 520 °C (970 °F), at which a liquid phase with 24.5% copper and 10.5% magnesium reacts to form the solid phases $CuMgAl_2$ and aluminum solid solution containing 2.9% copper and 2.9% magnesium. Precipitation hardening at high ratios of copper to magnesium is achieved in the sequence GP zones through a coherent phase (θ′) to $CuAl_2$ (θ). Precipitation hardening at lower ratios of copper to magnesium is achieved in the sequence GP zones through a coherent phase to $CuMgAl_2$.

The addition of silicon to the system results in the appearance of three quaternary invariant reactions for compositions of commercial alloys. These are:

$$L \rightarrow (Al) + CuAl_2 + CuMgAl_2 + Mg_2Si \text{ at } 505\ °C\ (940\ °F)$$

$$L \rightarrow (Al) + CuAl_2 + Al_4CuMg_5Si_4 + Si \text{ at } 510\ °C\ (950\ °F)$$

$$L + Mg_2Si \rightleftharpoons (Al) + CuAl_2 + Al_4CuMg_5Si_4 \text{ at } 510\ °C\ (950\ °F)$$

As nonequilibrium eutectics after solidification, these reactions limit temperatures for ingot homogenization. In the higher strength alloys, these may be equilibrium reactions and may place an upper limit on temperatures for solution heat treatment.

Precipitation reactions involving silicon, Mg_2Si, or the Q-phase ($Al_4CuMg_5Si_4$) may occur at some compositions, but are not major contributors to hardening in the alloys with copper as major element. The iron and manganese in commercial aluminum-copper-magnesium-silicon alloys perform important functions in yielding constituents and dispersoids. By forming insoluble phases with copper and silicon, they reduce the amounts of copper and silicon available for the aluminum-copper-magnesium-silicon phase reactions.

Aluminum-Magnesium-Silicon. The aluminum-magnesium-silicon system is the basis of a major class of heat treatable alloys used for both wrought and cast products. These alloys combine many favorable characteristics, including moderately high strength, relatively low quench sensitivity, and good corrosion resistance. The more dilute alloys are used frequently for architectural applications, usually in the form of extruded sections which are given no separate solution heat treatment before artificial aging.

The equilibrium-phase diagram is relatively simple and well established. The system is pseudobinary Al—Mg_2Si at magnesium to silicon ratios of 1.73-to-1 (wt%). The pseudobinary eutectic horizontal is at 595 °C (1100 °F). The composition of the eutectic liquid is 8.15 wt% magnesium and 4.75 wt% silicon in equilibrium with aluminum solid solution containing 1.13 wt% magnesium and 0.67 wt% silicon (~1.85 wt% Mg_2Si). By dividing the system along this line, the aluminum-rich end can be considered as two simple ternary eutectic systems: Al—Mg_2Al_3—Mg_2Si at 450 °C (840 °F) and Al—Si—Mg_2Si at 555 °C (1030 °F). Solid solubility of Mg_2Si in aluminum is reduced slightly by excess silicon, much more so by excess magnesium. Wrought commercial alloys vary from aluminum ~0.6 wt% Mg_2Si to aluminum 1.5 wt% Mg_2Si with varying degrees of slight magnesium or silicon excess.

The precipitation reactions in this alloy system have been studied in detail (Ref 62–64). The following sequence takes place under normal cir-

cumstances: supersaturated solid solution → semicoherent β″ rods $/\!/\langle 001\rangle_{Al}$ → semicoherent β′ needles $/\!/\langle 001\rangle_{Al}$ → semicoherent β plates $/\!/\langle 001\rangle_{Al}$ → noncoherent βMg_2Si. It is thought that the β″ phase has the same structure as $\beta' Mg_2Si$ but there is some evidence that it contains ~20% Al. Details of the β′ and β structures are given in Table 3.

Aluminum-Magnesium-Lithium. The addition of magnesium to aluminum-lithium binary alloys further reduces density but has little effect on modulus. Magnesium additions reduce the solubility of lithium. Lithium additions restrict the field of existence of Mg_5Al_8 and of the E (AlMg) phase, and expand the $Mg_{17}Al_{12}$ phase field at 470 °C (880 °F). Thus, aluminum is in equilibrium with both Mg_5Al_8 and $Mg_{17}Al_{12}$, along with $LiMgAl_2$ and LiAl. $LiMgAl_2$ ternary phase is formed approximately at 8.5% lithium and 28.2% magnesium. Aging an alloy of 5% magnesium and 2% lithium in the range 130 to 180 °C (270 to 360 °F) gives rise to δ′ (Al_3Li) phase and $LiMgAl_2$. In aluminum-magnesium-lithium alloys, magnesium contributes to strength in two ways. It adds a component of solid solution strengthening and decreases the lithium solubility in aluminum, resulting in increased volume fraction of δ′.

Aluminum-Magnesium-Zinc and Aluminum-Copper-Magnesium-Zinc. Compositions within these systems form important classes of heat treatable alloys and, in the quaternary system, yield the highest strengths known for commercial aluminum alloys. In almost all cases, zinc is the major addition element.

The characteristics of ternary aluminum-zinc-magnesium alloys are influenced by the high solid solubility of both elements. In the ternary system, matrix compositions for invariant reactions are at such high zinc and magnesium levels that nonequilibrium melting is rarely encountered. For commercial compositions, solvus temperatures are generally low in comparison to those in other heat treatable alloy systems.

The phases in equilibrium with an aluminum matrix in commercial alloys are designated $MgZn_2$ (M-phase), $Mg_3Zn_3Al_2$ (T-phase), and Mg_5Al_3 (β-phase). The first phase ranges in composition from $MgZn_2$ to Mg_4Zn_7Al. The T-phase has a wide range of composition, from 74% zinc–16% magnesium to 20% zinc–31% magnesium. The β-phase appears only when the magnesium content is considerably greater than the zinc content. Such alloys are strengthened primarily by magnesium in solid solution.

Precipitation hardening of alloys with zinc in excess of magnesium occurs in the sequence zones through coherent precipitate to the M-phase. If the magnesium content is greater than the zinc content, the sequence is zones through coherent precipitate to the T-phase.

In quaternary alloys containing copper, zinc is the major addition in commercial wrought alloys, and magnesium is usually in excess of copper. The M-phase composition ranges in the quaternary system from $MgZn_2$ to CuMgAl, and may be described as $Mg(Al,Cu,Zn)_2$. The range of composition for the T-phase is from that of the aluminum-magnesium-zinc ternary to that of the phase designated $CuMg_4Al_6$, and may be described as $Mg_3(Al,Cu,Zn)_5$. A third phase in commercial alloys is $CuMgAl_2$ (S-phase), with a small range of composition. The $CuAl_2$ phase appears only if copper is considerably in excess of magnesium.

Several nonequilibrium invariant melting reactions are encountered in the high-strength quaternary alloys. A reaction at 475 °C (890 °F) involving the M-, T-, and S-phases is usually encountered, but as copper content increases, melting may be encountered down to about 460 °C (860 °F). Usually, the J-phase has the highest solvus temperature and is slow to disappear during ingot homogenization.

Precipitation hardening in high-strength alloys is by the sequence leading to M-phase. Zones and coherent precipitates are low in copper content, and precipitates increase in copper content in the overaging regime. Additions of iron, manganese, and silicon interact with one another and with copper and magnesium. Chromium reacts with aluminum and magnesium to form a dispersoid.

LOW LEVEL ALLOY SYSTEMS

Aluminum-Boron. Small amounts of boron (<0.1%) are added to aluminum alloys primarily to either refine the grain size, or increase the electrical conductivity by precipitating titanium and/or vanadium from liquid solution. There is a eutectic at 0.022% boron, 660 °C (1220 °F) between aluminum and B_2Al. The solid solubility of boron in aluminum is negligible. B_2Al forms by peritectic reaction at 980 °C (1800 °F) from $B_{12}Al$ (Ref 66).

Aluminum-Chromium. Chromium, in small amounts (<0.35%), is added to numerous commercial aluminum alloys. Chromium additions tend to raise the recrystallization temperature, and may also be used to produce a gold color upon anodizing. Above 0.4% chromium at the aluminum end of the aluminum-chromium equilibrium diagram, a constituent corresponding to the formula $CrAl_7$ reacts peritectically to form the aluminum-rich solid solution (Ref 67). The solid solubility of chromium in aluminum is quite low, decreasing from 0.8% at 660 °C (1220 °F) to 0.30% at 430 °C (810 °F). $CrAl_7$ reportedly ceases to be primary at about 2.5% chromium and 790 °C (1450 °F). It is replaced by a constituent having the formula Cr_2Al_{11} (Ref 68).

Aluminum-Iron (Ref 69). Iron is the dominant impurity in virtually all commercial aluminum alloys. Some iron may be added intentionally, although the total content is usually kept below 1.0%. There is a eutectic in aluminum-rich alloys at 655 °C (1210 °F) with a probable composition within the range 1.7 to 2.2% iron. The phase in equilibrium with aluminum is usually designated as $FeAl_3$ (40.7% iron), although some analysis of crystals extracted from alloys are close to Fe_2Al_7 (37.3% iron). The $FeAl_3$ compound forms directly from the liquid at 1150 °C (2100 °F) and not by peritectic reaction. In rapidly chilled alloy, the metastable compound $FeAl_6$ (22.6% iron) is produced.

Aluminum-Titanium. Titanium is a normal impurity in aluminum, originating from TiO_2, which is present in most bauxites. It is also a

common addition to most commercial alloys because it is a very effective grain refiner during casting. In aluminum-rich alloys, the eutectic temperature and concentration are 665 °C (1230 °F) and 0.12 to 0.15% titanium. The phase coexisting with aluminum corresponds to the formula $TiAl_3$ (37.2% titanium), which has a range of existence from 36.5 to 37.5% titanium and is formed by peritectic reaction (Ref 70).

Aluminum-Vanadium (Ref 71). Vanadium is a minor impurity in aluminum, originating in most cases from bauxite. Mechanical properties of aluminum and aluminum alloys are not increased substantially by vanadium or ferro-vanadium additions. The limited increase in strength resulting from small additions is largely because of the grain refining effect of vanadium, rather than any intrinsic strengthening.

VAl_{10} (15.8% vanadium), which has a range of existence from 15.1% vanadium (V_2Al_{21}) to 15.9% vanadium, forms by peritectic reaction at approximately 670 °C (1240 °F) from the liquid phase and a phase which can be designated as VAl_7 or V_7Al_{45}. V_7Al_{45} if formed by peritectic reaction at approximately 690 °C (1270 °F) from VAl_6. VAl_6, also given as V_4Al_{23}, is formed by peritectic reaction at 735 °C (1360 °F) from VAl_3.

Aluminum-Zirconium. Zirconium is a minor addition to certain aluminum-magnesium-zinc alloys such as 7005, in which it may reduce stress corrosion susceptibility. It also imparts a grain refining effect to many aluminum alloys, but is not commercially used for this purpose. The equilibrium diagram for aluminum-rich alloys of this system is of the peritectic type. The peritectic horizontal lies at 660 °C (1220 °F), the reactant being $ZrAl_3$ and the resultant an aluminum-rich solid solution containing a maximum of 0.28% zirconium. The break in the liquidus curve, at the end of the peritectic horizontal, lies at 0.11% zirconium. The solid solubility of zirconium in aluminum decreases with falling temperature and lies at about 0.05% at 500 °C (930 °F) (Ref 72).

Aluminum-Iron-Silicon (Ref 73). Iron and silicon are the most common impurities in both commercial wrought and cast aluminum alloys. Two ternary phases that can be in equilibrium with aluminum are Fe_2SiAl_8 (α) and $FeSiAl_5$ (β). Another phase, $FeSiAl_4$ (δ), is often present in high silicon alloys, and a fourth phase, $FeSiAl_3$ (γ), forms in high iron and high silicon alloys.

$FeSiAl_8$ (31.6% iron, 7.8% silicon) is the phase that appears as Chinese script (often reported as Fe_3SiAl_{12}). $FeSiAl_5$ (25.6% iron, 12.8% silicon) forms very thin platelets that in section appear as long needles. Most commercial alloys are not in equilibrium and often alloys in which $FeAl_6$, $FeAl_3$, Fe_2SiAl_8, $FeSiAl_6$, and $FeSi_2Al_4$ coexist with one another and with silicon are produced. In heat treated alloys, equilibrium may often be reached by diffusion in the solid state, and $FeSiAl_5$ may be found in the Chinese script shape characteristic of Fe_2SiAl_8 or in the platelet form characteristic of $FeSi_2Al_4$. Thus, identification of the phases by shape alone may be misleading.

REFERENCES

1. L.W. Eastwood, *Gases in Non-Ferrous Metals and Alloys,* American Society for Metals, 1953
2. L.P. Costas and R.P. Marshall, The Solubility of Lithium in Aluminum, *Transactions of AIME,* Vol 224, 1962, p 970–974
3. E.D. Levine and E.J. Rapperport, *The Aluminum-Lithium Phase Diagram,* U.S. Atomic Energy Commission, Division of Technical Information, 6 Feb 1962
4. W.R.D. Jones and P.P. Das, The Solid Solubility of Lithium in Aluminum, *Journal of the Institute of Metals,* Vol 87, 1958–1959, p 338–340
5. W.B. Pearson, *Handbook of Lattice Spacings and Structures of Metals and Alloys,* Vol 2, Oxford: Pergamon Press, 1967
6. L.F. Mondolfo, *Aluminum Alloys: Structure and Properties,* London: Butterworths, 1976
7. D. Munson, *Journal of the Institute of Metals,* Vol 95, 1967, p 217–219
8. W. Hume-Rothery and G.V. Raynor, *The Structure of Metals and Alloys,* London: The Institute of Metals, 1962
9. P.J. Black, *Acta Metallurgica,* Vol 4, 1956, p 172–178
10. M.C. Flemings, *Solidification Processing,* New York: McGraw-Hill, 1974
11. J.W. Cahn, S.R. Coriell, and W.J. Boettinger, Rapid Solidification, in *Laser and Electron Beam Processing of Material,* Edited by C.W. White and P.S. Peercy, New York: Academic Press, 1980
12. A.B. Michael and M.B. Bever, *Transactions of AIME,* Jan 1954, p 47
13. S.N. Singh and M.C. Flemings, *Transactions of AIME,* Jan 1969, p 1803
14. T.F. Bower, H.D. Brody, and M.C. Flemings, *Transactions of AIME,* Vol 236, 1966, p 624
15. R.E. Spear and G.R. Gardner, *Transactions of American Foundrymens Society,* Vol 71, 1963, p 209
16. G.R. Armstrong and H. Jones, *Solidification and Casting,* Proceeding of Conference at University of Sheffield, London: Metals Society, 1979
17. P. Ramachandrarao, M.G. Scott, and G.A. Chadwick, *Philosophical Magazine,* Vol 25, 1972, p 961
18. H. Matyja, B.C. Giessen, and N.J. Grant, *Journal of the Institute of Metals,* Vol 96, 1968, p 30
19. J.A. McComb, S. Nenno, and M. Meshii, *Journal of the Physical Society of Japan,* Vol 19, 1964, p 1691
20. C. Suryanarayana and T.R. Anantharaman, *Journal of Materials Science,* Vol 5, 1970, p 992
21. H.A. Davies and J.B. Hull, *Journal of Materials Science,* Vol 9, 1974, p 707
22. N.J. Grant, *Rapid Solidification Processing,* edited by R. Mehrabian, B.H. Kear, and M. Cohen, Baton Rouge, LA: Claitor Publishing Division, 1970, p 230

23. J.A. Horwath and L.F. Mondolfo, *Acta Metallurgica,* Vol 10, 1962, p 1037

24. C.F. Dixon and H.M. Skelly, *International Journal of Powder Metallurgy,* Vol 7 (No. 3), 1971, p 47

25. R.J. Town, *Metal Progress,* Vol 73 (No. 5), 1958, p 70

26. G. Thursfield and M.J. Stowell, *Journal of Materials Science,* Vol 6, 1971, p 1111

27. C. Panseri and M. Paganelli, *Alluminio,* Vol 36, 1967, p 179

28. P.G. Boswell and G.A. Chadwick, *Scripta Metallurgica,* Vol 11, 1977, p 11

29. T.R. Anatharaman and C. Suryanarayana, *Journal of Materials Science,* Vol 6, 1971, p 1111

30. H. Jones, *Aluminum,* Vol 54 (No. 4), 1978, p 274

31. K.O. Krishnanand and R.W. Cahn in *Rapidly Quenched Metals,* edited by N.J. Grant and B.C. Giessen, Cambridge, MA: MIT Press, 1976, p 67

32. R.K. Linde, *Transactions of AIME,* Vol 236, 1966, p 58

33. J.V. Wood and R.W.K. Honeycombe, *Journal of Materials Science,* Vol 9, 1974, p 1183

34. P.E. Brown and C.M. Adams, *Transactions of American Foundrymens Society,* Vol 69, 1961, p 879

35. T. Kattamis and R. Mehrabian, *Journal of Vacuum Science and Technology,* Vol 11 (No. 6), 1974, p 1118

36. H. Jones, *Metallography,* Vol 3 (No. 3), 1970, p 307

37. H. Jones, *Material Science and Engineering,* Vol 5, 1969–1970, p 1

38. D.B. Williams and J.W. Edington, High Resolution Microanalysis and Microstructural Characteristics of Splat Quenched Aluminum-Copper Alloys, in *Rapidly Quenched Metals,* edited by N.J. Grant and B.C. Giessen, Cambridge, MA: MIT Press, 1976, p 135

39. H.A. Davies and J.B. Hull, Some Aspects of Splat Quenching in an Inert Atmosphere and of the Formation of Non-Crystalline Phases in Al-17.3 at. percent Copper, Germanium and Tellurium, *Journal of Materials Science,* Vol 9, 1975, p 707

40. M.G. Scott and J.A. Leake, Formation and Decomposition of an A1-17.3 at. percent Cu Solid Solution, *Acta Metallurgica,* Vol 27, 1975, p 503

41. R.A. Swalin, *Thermodynamics of Solids,* New York: John Wiley & Sons, 1962

42. M.C. Flemings, *Solidification Processing,* New York: McGraw-Hill, 1974

43. K.S. Pitzer and L. Brewer, *Thermodynamics* (revision of Lewis and Randall), New York: McGraw-Hill, 1961

44. L.A. Willey, *Aluminum,* Vol 1, American Society for Metals, 1967

45. M. Mugahid and N.N. Engel, *Scripta Metallurgica,* Vol 13, 1979

46. F.L. Kaufman and H. Bernstein, *Computer Calculation of Phase Diagrams,* New York: Academic Press, 1970

47. L. Kaufman, Ed., CALPHAD: Computer Coupling of Phase Diagrams and Thermochemistry, Manlabs Inc., Cambridge, MA

48. ALLOYDATA: Division of Chemical Standards, National Physical Laboratory, Teddington, Middlesex, U.K.

49. Published in CALPHAD, New York: Pergamon Press, 1976–1980

50. C. Zener, *Thermodynamics in Physical Metallurgy,* American Society for Metals, 1950

51. E. Hornbogen, *Aluminium,* Vol 43, 1967, p 115

52. L.F. Mondolfo, *Aluminum Alloys: Structure and Properties,* London: Butterworths, 1976, p 312

53. J. Guillet, *et al,* Influence of Cooling Rate on the Condition of Solid Solutions After Annealing, *Memoire Scientifique de la Revue de Metallurgic,* Vol 67 (No. 9), June 1970, p 377 (French)

54. R.D. Vengrenovich, *et al,* Changes in Composition of Solid Solutions during Non-equilibrium Crystallization of Aluminum-Base Binary Alloys, *Zhurnal Fizicheskoi Khimii,* Vol 44 (No. 8), Aug 1970, p 1979 (Russian)

55. E.M. Savitsky, *et al, Journal of the Institute of Metals,* Vol 253 (No. 20.81), p 1002

56. L.F. Mondolfo, *Manganese in Aluminum Alloys,* the Manganese Center, 1978, p 4

57. L.F. Mondolfo, *Manganese in Aluminum Alloys,* the Manganese Center, 1978, p 29

58. L.F. Mondolfo, *Manganese in Aluminum Alloys,* the Manganese Center, 1978, p 326

59. W.A. Backofen, I.R. Turner, and D.H. Avery, *Transactions American Society for Metals,* Vol 57, 1964, p 980

60. S.D. Fields, Jr., *IBM J Res Develop,* Vol 9, 1964, p 134

61. L.F. Mondolfo, *Aluminum Alloys: Structure and Properties,* London: Butterworths, 1976, p 513

62. J.W. Pashley, J.W. Rhodes, and A. Sendorek, *Journal of the Institute of Metals,* Vol 94, 1966, p 41–48

63. M.H. Jacobs, *Philosophical Magazine,* Vol 26, 1972, p 1–13

64. H. Westengen and N. Ryum, *Zeitschrift fuer Metallkunde,* Vol 70, 1979, p 528–535

65. E.D. Boyes, *et al, Institute of Physics—Conference Series,* No. 36, 1977, p 343

66. L.F. Mondolfo, *Aluminum Alloys: Structure and Properties,* London: Butterworths, 1976, p 229

67. H.W.L. Phillips, *Annoted Equilibrium Diagrams of Some Aluminum Alloy Systems,* the Institute of Metals, 1959, p 6

68. L.F. Mondolfo, *Aluminum Alloys: Structure and Properties,* London: Butterworths, 1976, p 249–250

69. L.F. Mondolfo, *Aluminum Alloys: Structure and Properties,* London: Butterworths, 1976, p 283–285

70. L.F. Mondolfo, *Aluminum Alloys: Structure and Properties*, London: Butterworths, 1976, p 385

71. L.F. Mondolfo, *Aluminum Alloys: Structure and Properties*, London: Butterworths, 1976, p 392–393

72. H.W.L. Phillips, *Annotated Equilibrium Diagrams of Some Aluminum Alloy Systems*, The Institute of Metals, 1959, p 20

73. L.F. Mondolfo, *Aluminum Alloys: Structure and Properties*, London: Butterworths, 1976, p 534–536

Aluminum Properties and Physical Metallurgy
John E. Hatch editor, p 58-104
DOI: 10.1361/appm1984p058

CHAPTER 3

MICROSTRUCTURE OF ALLOYS*

The examination of microstructure is one of the principal means of evaluating alloys and products to determine the effects of various fabrication and thermal treatments, evaluate the effects of new procedures, and analyze the cause of failures. A compilation of typical and atypical micrographs is presented in Ref 1. Reference 2 discusses general preparation techniques for aluminum metallographic samples. Phase diagrams and identification of constituents, important to the interpretation of structures, are covered in Ref 2 and 3.

Many of the changes that become apparent with the examination of aluminum macrostructure and microstructure occur simultaneously with the freezing, homogenization, preheat, hot or cold reduction, annealing, or solution or precipitation heat treatment of the aluminum alloy. Good interpretation of microstructure relies on having a complete history of the sample for analysis. Although this is not always possible, the more information available, the more reliable the interpretation. Comparative samples with known histories are helpful in any given examination.

As a general rule, examination should start at normal vision level and proceed to higher magnification, according to the need for more detailed interpretation. This also permits better choice of sample location, for at higher magnification, the sample area becomes extremely small. Simplicity and cost make optical methods of macro- and micro-examination the most useful. Limited depth of field and magnification dictate the use of electron microscopy in areas where fine structure or depth of field are important. Electron techniques supplement and in some cases replace the selective use of etchants, and they enable the determination of microchemical analysis, which contributes to more conclusive answers.

Examination of fracture surfaces is essential to determine the mode and direction of crack propagation. Key fractographic features are usually not visible to the unaided eye and can be seen clearly only when magnified. Good analysis requires care in handling specimens to avoid contaminating the fracture surface before examination. Three techniques are commonly used to determine if a fracture occurred by fatigue, ultimate tensile rupture, or stress-corrosion cracking and other modes. These methods are (1) optical microscopy, (2) transmission electron microscopy replica methods (TEM), and (3) scanning electron microscopy (SEM).

Transmission electron microscopy replica methods are well established and widely used (Ref 4). The replica method involves making a thin,

*This chapter was revised by a team comprised of R.E. Hughes and S.A. Levy, Reynolds Metals Co.; A.T. Thomas and M.D. Ball, Alcan International Ltd.; P.R. Sperry, Consolidated Aluminum Corp.; A.G. Miller, W.H. Graham, and E.A. Ledbury, Boeing Commercial Airplane Co.; and F.M. Krill, Kaiser Aluminum & Chemical Corp. The original chapter was authored by M.S. Hunter, A.M. Montgomery, and G.W. Wilcox, Aluminum Company of America.

accurate replica of a portion of the fracture surface. Transmission electron microscopy is used to view the replica of the surface to determine fracture mode. Transmission electron microscopy replica methods offer a higher magnification range than optical microscopes with well-focused images at all magnifications. Typical TEM magnifications are 600 to 10,000 diameters. Handbooks of fracture surface appearances have been published for many alloy systems. Thus, a good database of information is available for analysis.

Some disadvantages of TEM replica methods include: (1) long specimen preparation time, (2) selective specimen sampling plan because typical replicas must fit onto a 3-mm (0.1-in.) grid, (3) artifacts in the replica that may occur during specimen preparation, and (4) unavailability of microchemical information for identification of chemical microheterogeneities. Thin foil techniques normally are used in TEM examination. Examples are given in the TEM section of this chapter.

Scanning electron microscopy of fracture surfaces is a newer process than both TEM and optical microscopy. The database of SEM fracture surfaces is much more limited than TEM methods. However, because of the flexibility of SEM, these techniques are expected to become the method of choice for most analyses.

LIGHT MICROSCOPY OF WROUGHT ALLOYS

Light microscopy is the major tool for microstructural determination of aluminum alloys and is recommended for use before electron optics. It is useful up to magnifications of about 1500× where features as small as 0.1 μm (0.004 mil) can be resolved. Light microscopy identifies most second-phase particles of sufficient size (>1 μm, or >0.04 mil), shows the size and distribution of resolvable particles, and shows the state of the grain or crystal structure of the aluminum or solid solution matrix. It can also show features such as cladding thickness and diffusion, type and depth of corrosive attack, partial melting because of overheating, and the presence of extraneous nonmetallic inclusions or unduly coarse intermetallic phases. Light microscopy does not reveal precipitate particles that are responsible for precipitation hardening, nor does it reveal dislocation arrangements; sometimes, etching or preparation effects can be used to infer conclusions about these conditions. Generally, analysis of these conditions is in the domain of electron microscopy.

The identification of elemental or intermetallic phases is an important part of a light microscopy examination. These phases are the consequence of equilibrium or nonequilibrium reactions and changes occurring within a given alloy because of casting conditions, mechanical working, and thermal treatment. The phases are related to the equilibrium or constitution diagrams for binary, ternary, quaternary, or even more complex systems (Ref 2 and 3). The crystal structure and compositional makeup of such phases have been determined, and means of identifying them by optical characteristics or etching behavior are known. See *Metals Handbook* for more information (Ref 2). For nonstandard specimens or where some ambiguity exists, optical examination can be supplemented or replaced by electron probe microanalysis or electron diffraction methods, which normally allow a precise identification to be made.

Conventionally produced wrought aluminum alloys originate from a cast ingot from which all subsequent mechanical and thermal processing represents varying degrees of change to the as-cast structure. Modifications are relatively minor for large wrought forms such as forgings, thick plate, and heavy extrusions that are hot worked. They become greater as the total amount of reduction in original cross-sectional area is increased by hot and cold working and as the frequency of thermal treatments, such as annealing and solution heat treating, is increased. The visible modifications consist of the following:

- Alteration of the composition and crystal structure of phases because of peritectic reactions that were suppressed during casting
- Solution of more soluble phases and spheroidization and coalescence to reduce their surface energy
- Elevated-temperature precipitation of elements that had supersaturated the as-cast solid solution
- Mechanical fragmentation of brittle intermetallic phases and alignment of these particles in the principal direction of working
- Deformation of the original cast grain matrix and subsequent recovery or recrystallization

For other processes such as powder metallurgy, the microstructure is dependent on the method of manufacturing the powders and compacting and sintering the finished pieces (Chapter 10 in this Volume).

Wrought alloys are divided into seven major classes according to their principal alloy elements. Each class represents a different type of microstructure because of these alloy differences. Typical microstructural features are described in this chapter for each class and show how microstructure progressively develops from the as-cast ingot to the final wrought form. Furthermore, alloy classes can be divided into two categories according to whether they are strengthened by work hardening only or by heat treatment (precipitation hardening). The former applies to 1XXX, 3XXX, 4XXX, and 5XXX alloys, while the latter applies to 2XXX, 6XXX, and 7XXX alloys.

1XXX or Commercially Pure Aluminum. Because iron and silicon are ever-present impurity elements and the solid solubility of iron in aluminum is very small, phases of aluminum-iron or aluminum-iron-silicon are seen in microstructures of all but refined, super-purity aluminum. In the as-cast condition, all of the phases that come into equilibrium with aluminum may be found—$FeAl_3$, Fe_3SiAl_{12}, or $Fe_2Si_2Al_9$. In addition, a number of metastable nonequilibrium phases may be formed when solidification is rapid. $FeAl_6$, a phase that has the same crystal structure as $MnAl_6$, is one example (Ref 5 and 6). Minor impurity or addition elements such as copper and manganese that are not in sufficient quantity to form their own phases influence the type and quantity of less stable phases. High resolution and sophisticated identification techniques are required to identify these phases. Subsequent thermal processes generally revert these phases back to the equilibrium types.

1100 Alloy. Figure 1 shows the typical constituent in as-cast 1100 aluminum; Fig. 2 shows the effect of a high-temperature treatment before working; and Fig. 3 shows redistributed constituent in a typical worked

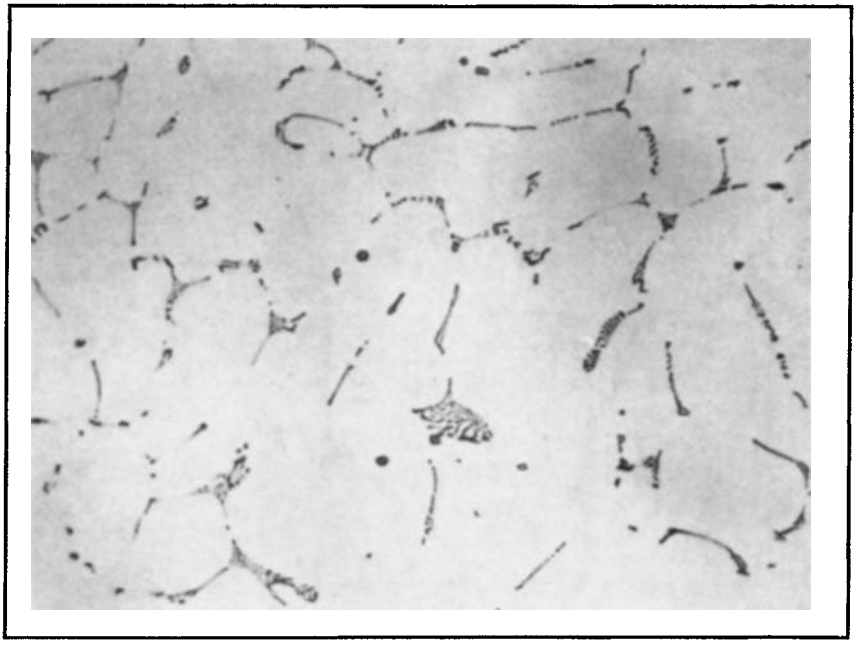

Fig. 1. 1100 as-cast ingot showing the typical constituent, predominantly Fe_3SiAl_{12}, in the dendrite interstices. 0.5% hydrofluoric acid, 455×. (Courtesy of Kaiser Aluminum & Chemical Corp.)

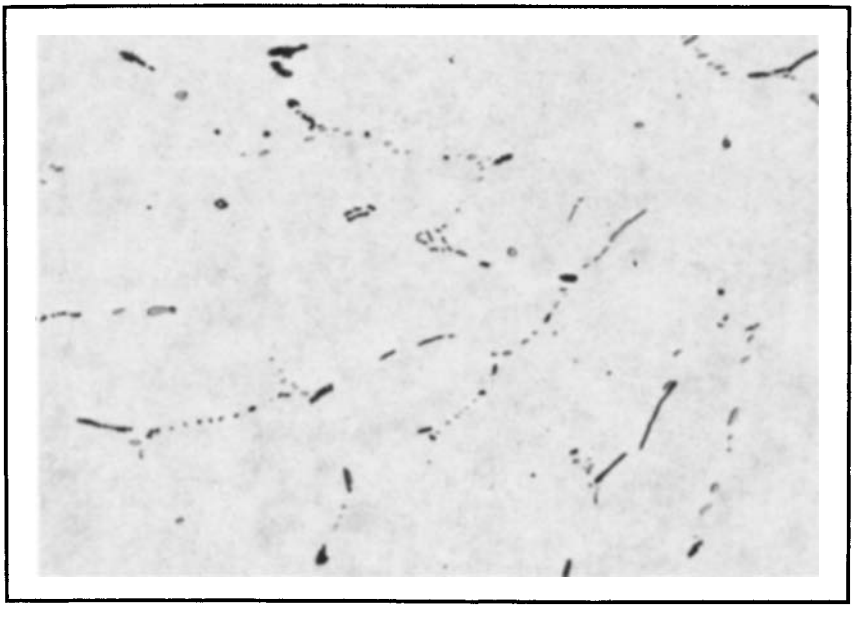

Fig. 2. 1100 homogenized ingot showing the effect of heating on the microstructure. A portion of the Fe_3SiAl_{12}, (light) has reverted to $FeAl_3$ (dark). 20% sulfuric acid, 455×. (Courtesy of Kaiser Aluminum & Chemical Corp.)

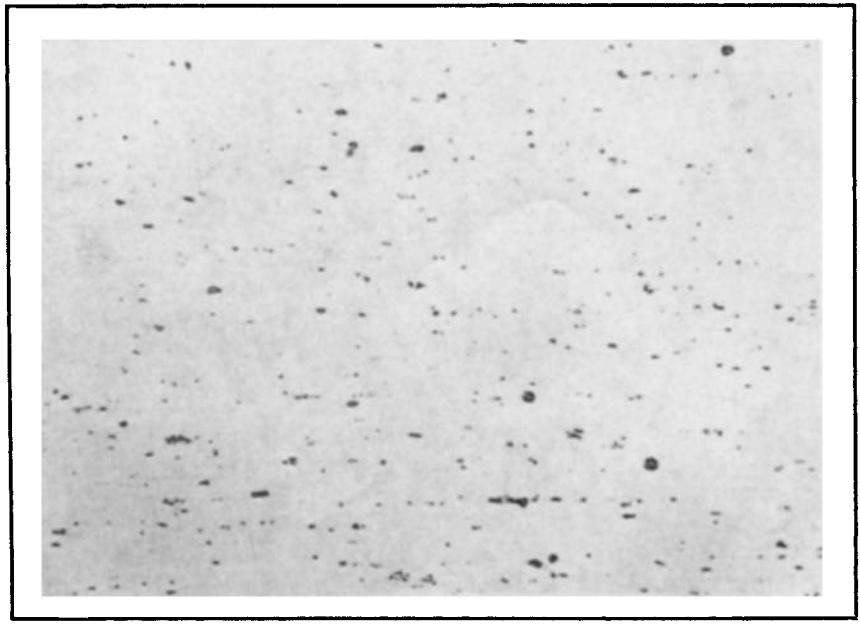

Fig. 3. 1100 sheet showing fragmented and redistributed constituent as a result of mechanical working. 0.5% hydrofluoric acid, 455×. (Courtesy of Kaiser Aluminum & Chemical Corp.)

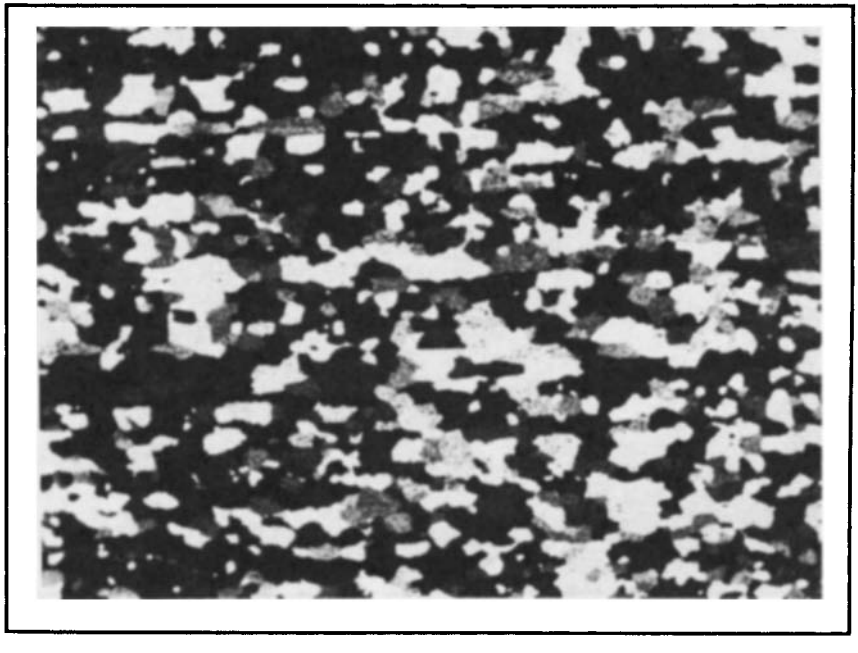

Fig. 4. 1100 sheet showing slightly elongated annealed grain structure. Barker's electrolytic etch, 90×. (Courtesy of Kaiser Aluminum & Chemical Corp.)

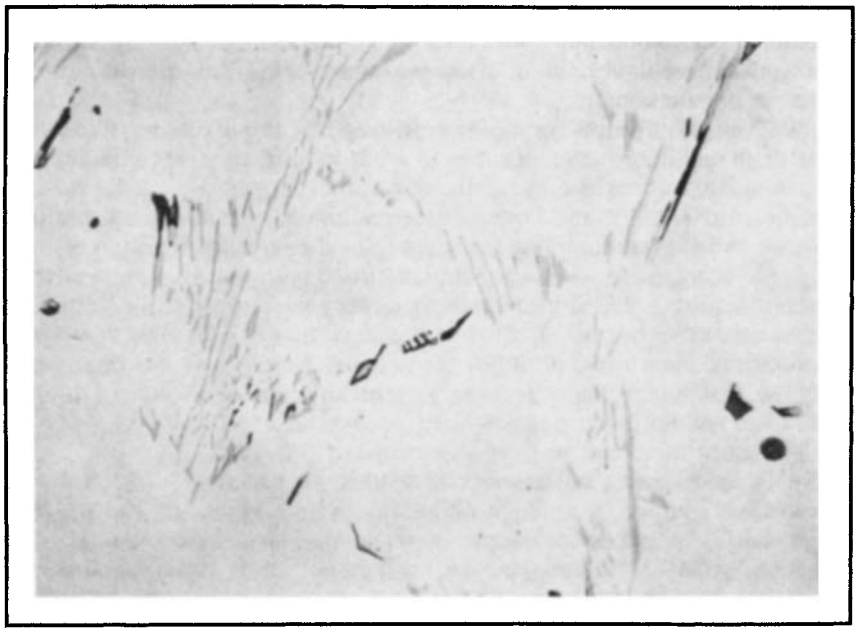

Fig. 5. 3003 as-cast ingot showing the distribution of predominantly $(Mn,Fe)Al_6$ (light) and $(Fe,Mn)_3SiAl_{12}$ (dark) at dendrite interstices. 10% phosphoric acid, 455×. (Courtesy of Kaiser Aluminum & Chemical Corp.)

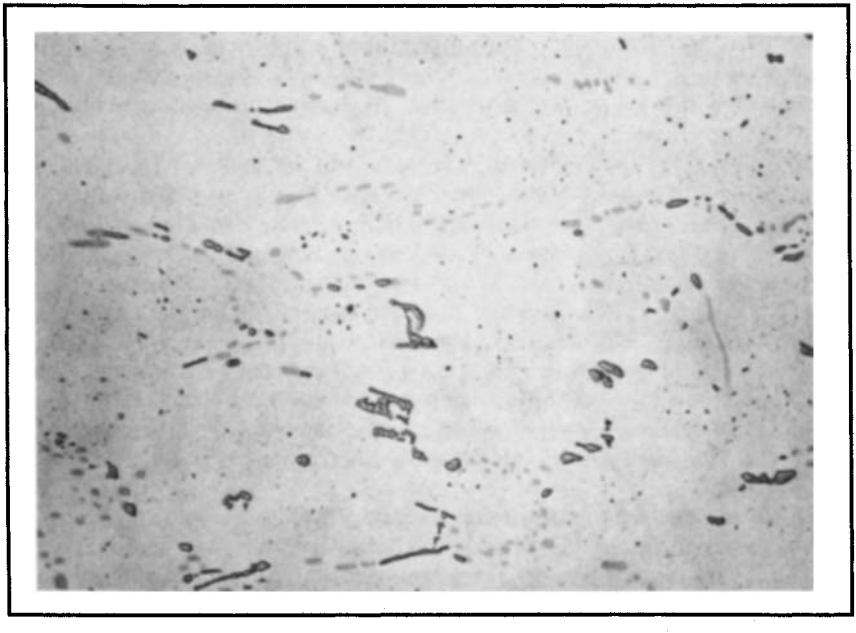

Fig. 6. 3003 homogenized ingot showing transformation to the predominantly $(Fe,Mn)_3SiAl_{12}$ phase by a delayed peritectic reaction. 10% phosphoric acid, 455×. (Courtesy of Kaiser Aluminum & Chemical Corp.)

structure. The grain structure of annealed sheet (Fig. 4) shows a slight departure from equiaxiality because of alignment of iron-rich particles. The apparent volume fraction of second-phase particles is almost a direct function of iron content.

3XXX or Aluminum-Manganese Alloys. The popular alloy 3003 consists of the addition of manganese to what is basically 1100 aluminum. The dominant phases become $(Mn,Fe)Al_6$ and $(Fe,Mn)_3SiAl_{12}$. In the as-cast structure (Fig. 5), the former phase predominates; subsequent heating causes a transformation to the latter phase by a delayed peritectic reaction (Fig. 6). Manganese also supersaturates the cored solid solution of the primary dendrites and subsequently precipitates as a dispersoid (Fig. 7). Grains formed by annealing of work-hardened material are more flattened or elongated than those of 1100, principally because of the dispersoid (Fig. 8). Some manganese remains in solid solution. A few alloys in this class also contain magnesium which, because of its affinity for silicon, tends to shift the phase proportioning toward $(Mn,Fe)Al_6$.

5XXX or Aluminum-Magnesium Alloys. Magnesium is largely present in solid solution in wrought alloys, but it appears as eutectic Mg_2Al_3 in increasing amounts in as-cast ingots as the magnesium content increases (Fig. 9). In the same manner, magnesium forms increasing amounts of Mg_2Si, but the solubility of this phase is reduced so that a certain amount may remain out of solution and visible in wrought products (Fig. 10). When magnesium content exceeds about 3.5%, Mg_2Al_3 or metastable Mg_2Al_3' may precipitate in grain boundaries or within grains, resulting from low-temperature thermal operations (Fig. 11). Chromium is a frequent additive and may appear as a fine dispersoid of $Cr_2Mg_3Al_{18}$. When manganese also is present, iron-rich phases become quite complex, and $MnAl_6$, probably containing some chromium, appears as a dispersoid. Cold working of aluminum-magnesium alloys produces prominent deformation bands that are decorated by magnesium-rich precipitates (Fig. 12).

4XXX or Aluminum-Silicon Alloys. Except for some architectural applications and forged pistons, most wrought 4XXX alloys are used for welding and brazing filler materials where they are remelted. However, good joining characteristics may depend on having a uniform and fine initial wrought structure. The as-cast phases are usually elemental silicon and $Fe_2Si_2Al_9$ (Fig. 13). Thermal treatment causes silicon to coalesce and spheroidize (Fig. 14), while the insoluble iron-rich phase is not altered. Figure 15 shows a 4343 clad layer on a 3003 core used for brazing sheet, and Fig. 16 shows a bare 3003 fin brazed to this clad sheet. Because of interalloying between the two alloys, needle-like $Fe_2Si_2Al_9$ is replaced by polygonal $(Fe,Mn)_3SiAl_{12}$. Interalloying also changes the constitution of weld beads.

6XXX or aluminum-magnesium-silicon alloys are formulated to make use of the solubility of Mg_2Si and thereby utilize precipitation hardening. If there is no manganese or chromium present, the iron-rich phases are Fe_3SiAl_{12}, $Fe_2Si_2Al_9$, or a mixture of the two, depending on the proportions of magnesium, silicon, and iron. Manganese and chromium stabilize $(Fe,Mn,Cr)_3SiAl_{12}$. In dilute alloys such as 6063, heating the cast structure (Fig. 17) to moderate temperatures dissolves all Mg_2Si (Fig. 18).

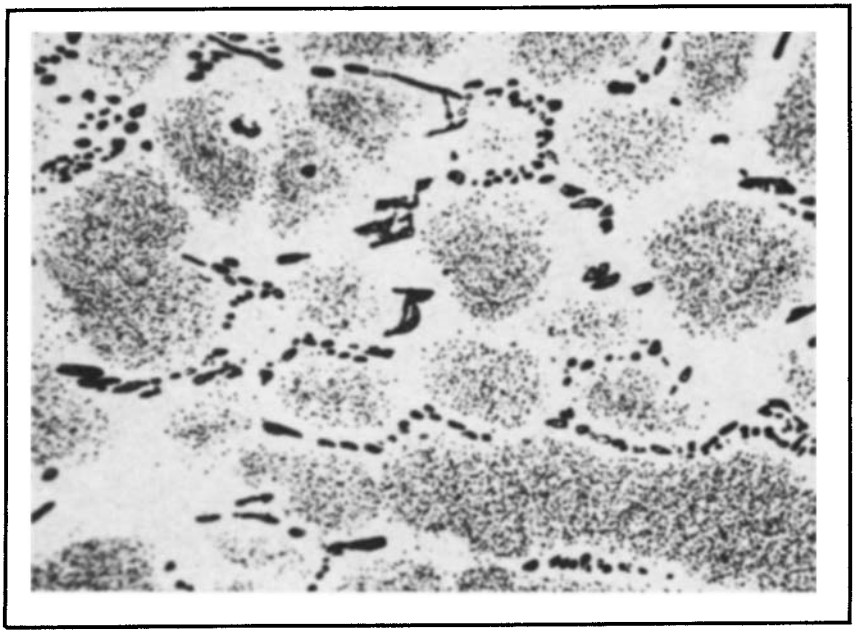

Fig. 7. 3003 homogenized ingot, similar to Fig. 6 but etched to reveal dispersoid precipitate in the primary aluminum dendrite matrix. 0.5% hydrofluoric acid, 455×. (Courtesy of Kaiser Aluminum & Chemical Corp.)

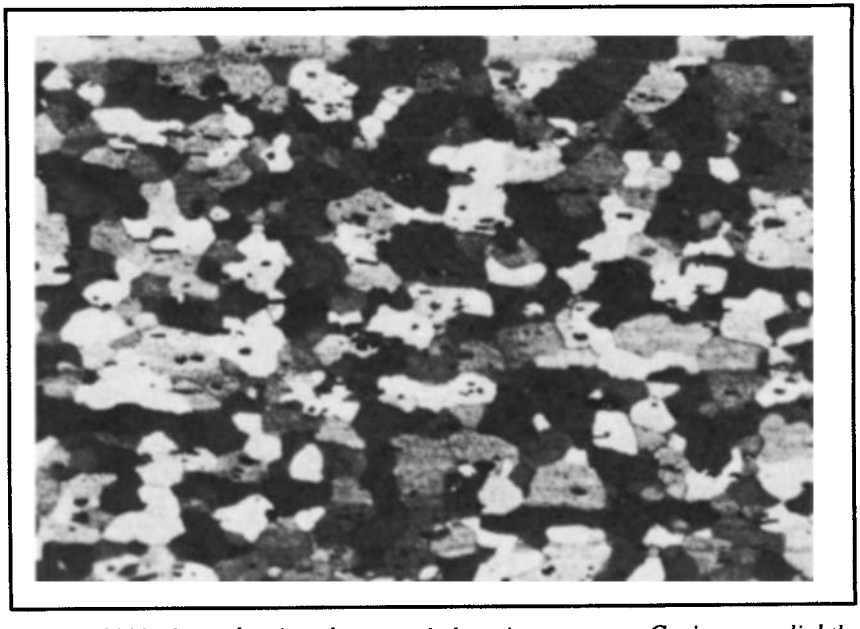

Fig. 8. 3003 sheet showing the annealed grain structure. Grains are slightly elongated because of the dispersoid. Barker's electrolytic etch, 260×. (Courtesy of Kaiser Aluminum & Chemical Corp.)

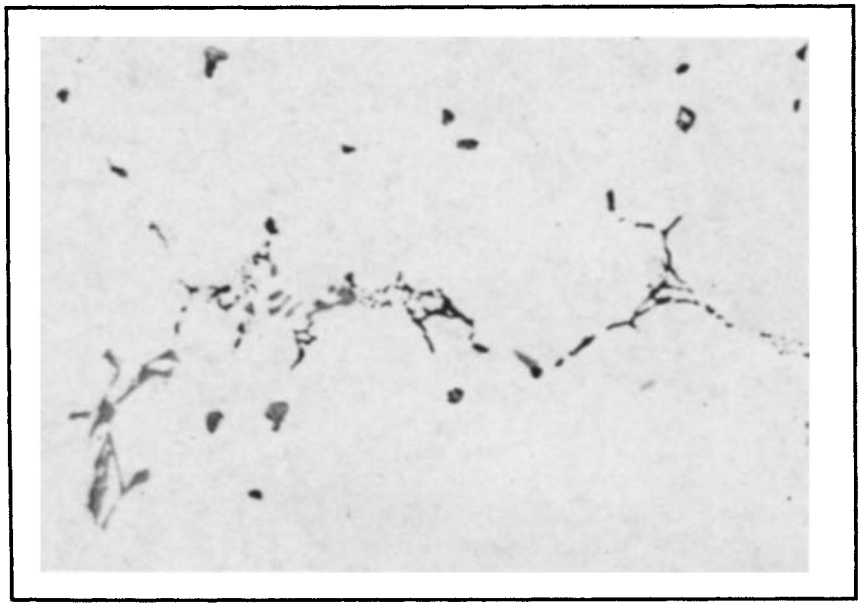

Fig. 9. 5056 as-cast ingot showing $(Fe,Cr)_3SiAl_{12}$ (gray), Mg_2Si (dark), and Mg_2Al_3 (mottled, outlined) in dendrite interstices. 0.5% hydrofluoric acid, 435×. (Courtesy of Kaiser Aluminum & Chemical Corp.)

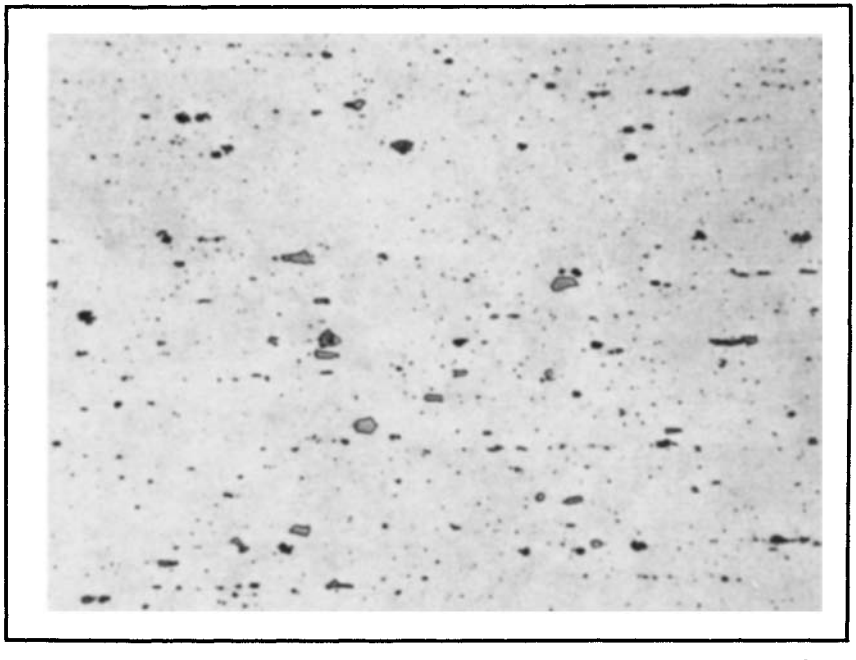

Fig. 10. 5052 sheet showing the fragmented, more uniform distribution of the constituent particles consisting of $(Fe,Cr)_3SiAl_{12}$ (light) and Mg_2Si (dark). 0.5% hydrofluoric acid, 455×. (Courtesy of Kaiser Aluminum & Chemical Corp.)

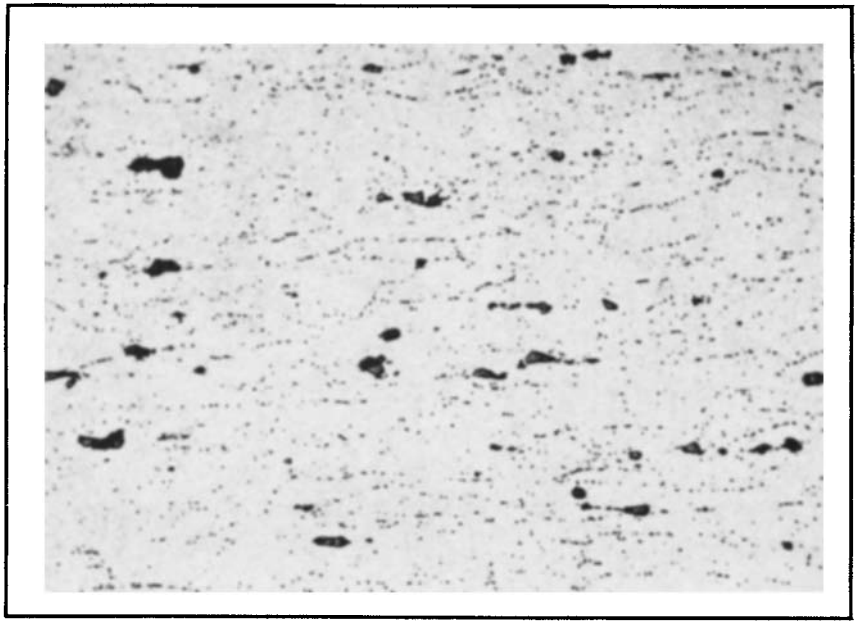

Fig. 11. 5086-H34 cold rolled and stabilized sheet showing the constituent distribution and discontinuous Mg_2Al_3 grain boundary precipitate. 10% phosphoric acid, 455×. (Courtesy of Kaiser Aluminum & Chemical Corp.)

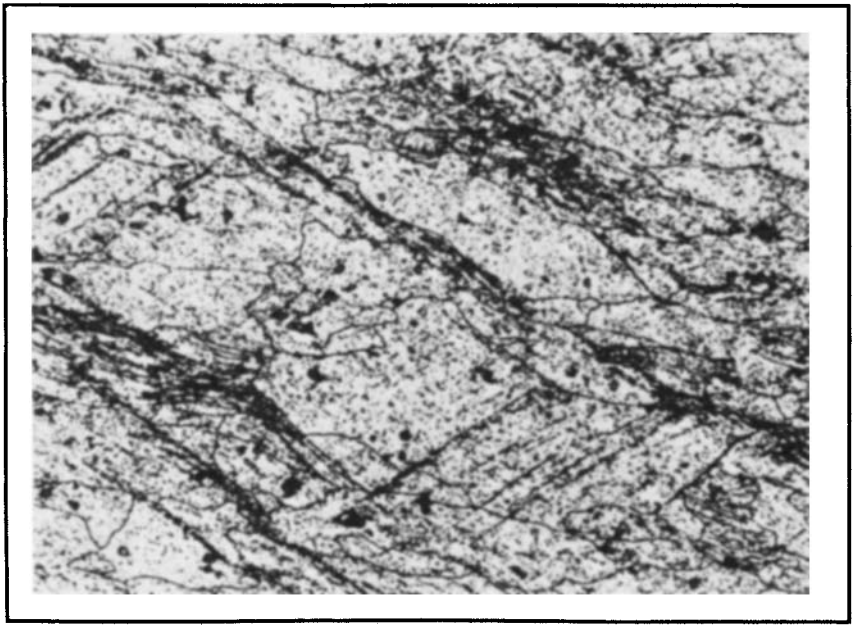

Fig. 12. 5083 cold forged stock, heated 24 h at 120 °C (250 °F), showing Mg_2Al_3 precipitate on deformation bands. 10% phosphoric acid, 445×. (Courtesy of Kaiser Aluminum & Chemical Corp.)

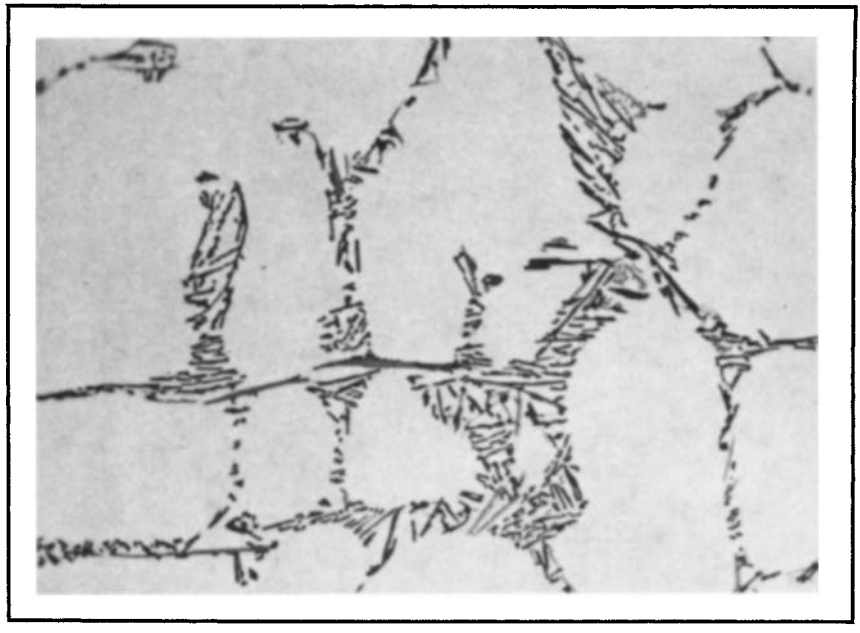

Fig. 13. 4043 as-cast ingot with $Fe_2Si_2Al_9$ (light) and silicon (dark) in dendrite interstices. 0.5% hydrofluoric acid, 455×. (Courtesy of Kaiser Aluminum & Chemical Corp.)

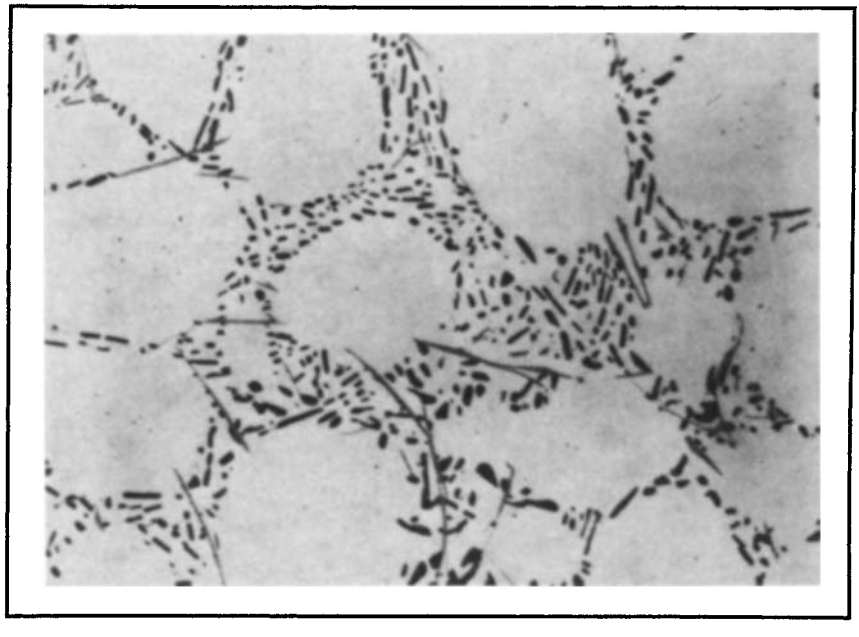

Fig. 14. 4043 homogenized ingot showing rounding and coalescence of the silicon constituent with the insoluble iron-rich phase remaining unchanged. 0.5% hydrofluoric acid, 445×. (Courtesy of Kaiser Aluminum & Chemical Corp.)

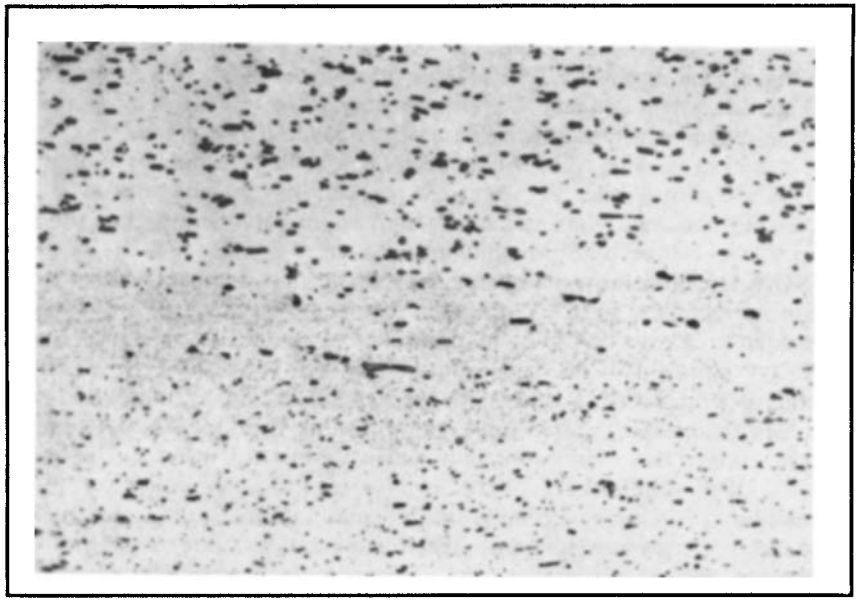

Fig. 15. No. 12 brazing sheet—4343 clad on 3003 core, showing the spheroidized silicon particles in the cladding (upper portion). 0.5% hydrofluoric acid, 225×. (Courtesy of Kaiser Aluminum & Chemical Corp.)

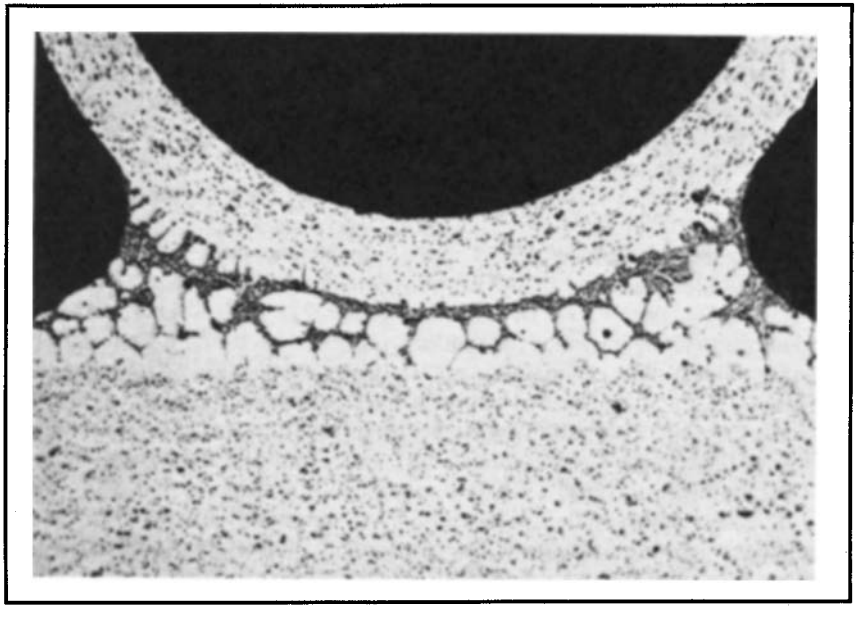

Fig. 16. 3003 bare fin brazed to a No. 12 brazing sheet showing that the 4343 has reverted to a cast dendritic structure, with some interalloying. 0.5% hydrofluoric acid, 90×. (Courtesy of Kaiser Aluminum & Chemical Corp.)

More highly alloyed 6061 generally has an excess of Mg_2Si at the solutionizing temperature and, if slowly cooled, precipitates in a Widmænstatten form (Fig. 19). Solution heat treated 6061 appears as shown in Fig. 20, where T4 and T6 tempers cannot be readily distinguished. Special etching techniques can be used to make a distinction (Fig. 21), but it is best to have a known standard to use for comparison. Some of the 6XXX alloys used for electrical conductivity are put into an overaged condition and, when etched, exhibit a light band along grain boundaries that is caused by a precipitate-free zone (Fig. 22).

2XXX or aluminum-copper alloys are usually complex because of the many additives used for strength, corrosion resistance, or grain structure control. Alloy 2024, with aluminum + copper + magnesium + manganese + iron + silicon, has a multiphase ingot structure (Fig. 23) consisting of $(Mn,Fe)_3SiAl_{12}$, Mg_2Si, $CuAl_2$, and Al_2CuMg, and occasional $(Fe,Mn)Al_3$ or $(Mn,Fe)Al_6$. Subsequent heating (Fig. 24) dissolves much of the copper and magnesium but leaves some Al_2CuMg and perhaps $CuAl_2$ out of solution. All of the iron-containing phases undergo transformation to Al_7Cu_2Fe, possibly accompanied by other minor phases. Simultaneously, manganese is precipitated from solid solution as $Cu_2Mn_3Al_{20}$ dispersoid. Slow cooling causes Al_2CuMg to precipitate in a Widmænstatten pattern.

The normal wrought 2024-T4 product shows rounded Al_2CuMg as an undissolved excess phase, irregularly shaped particles of unreacted $(Mn,Fe)_3SiAl_{12}$ and reaction product Al_7Cu_2Fe, along with fine dispersoid of $Cu_2Mn_3Al_{20}$ (Fig. 25). The latter causes grains formed during solution heat treatment to be moderately elongated or flattened. Grain contrast in copper-rich alloys is obtained by a combination of etch pitting and redeposition of copper on the more rapidly dissolved grain orientations (Fig. 26). This etching characteristic is useful to indicate when there has been excessive diffusion of copper into the pure aluminum cladding on sheet. Magnesium is also diffused, although this diffusion is not as readily revealed by light microscopy.

Alloy 2014 differs from 2024 in that the magnesium content is less and the silicon content is higher. The high silicon stabilizes $(Mn,Fe)_3SiAl_{12}$ as the only iron-rich phase. $CuAl_2$ and a quaternary phase, $Cu_2Mg_8Si_6Al_5$, are the soluble phases and $Cu_2Mn_3Al_{20}$ dispersoid is probably augmented by Mn_3SiAl_{12} coming out of solution (Fig. 27). The higher dispersoid concentration and pronounced banding inherited from the cast structure may result in highly elongated, recrystallized grains (Fig. 28).

Alloy 2011 is simpler in composition (aluminum + copper + iron + silicon), except for the addition of lead and bismuth to improve machinability. The phases after solidification and after thermal treatment are Al_7Cu_2Fe (insoluble) and $CuAl_2$ (usually some in excess of solid solubility). The lead-bismuth liquid phase first separates out in the dendrite interstices while solidification is in progress, then completes its solidification at a very low temperature. It spheroidizes during solution heat treatment and has a complex structure when resolidified during quenching (Fig. 29).

Because solution heat treatment temperatures are close to the equilibrium solidus in 2XXX alloys, overheating is a hazard that requires mi-

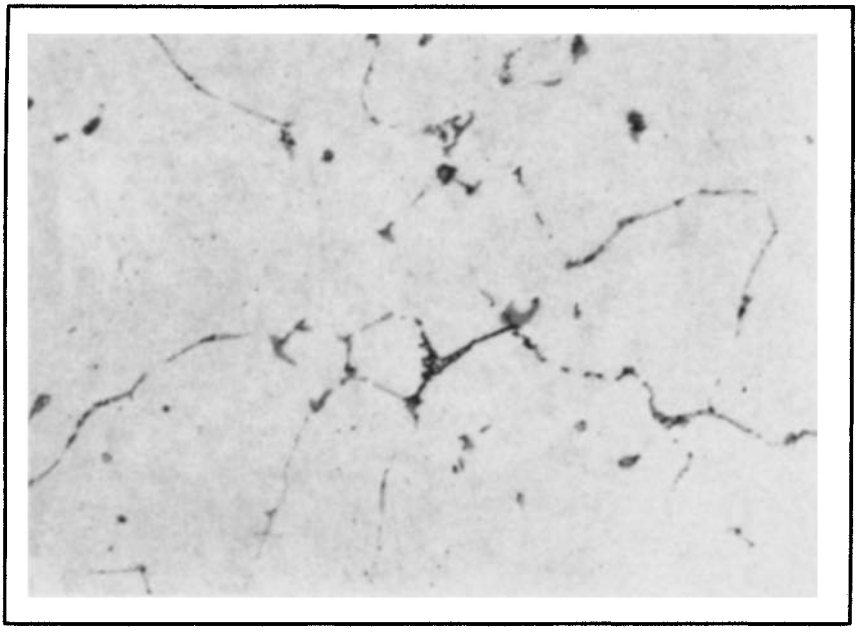

Fig. 17. 6063 as-cast ingot showing iron-rich phases (light) and Mg_2Si (dark) in dendrite interstices. 0.5% hydrofluoric acid, 445×. (Courtesy of Kaiser Aluminum & Chemical Corp.)

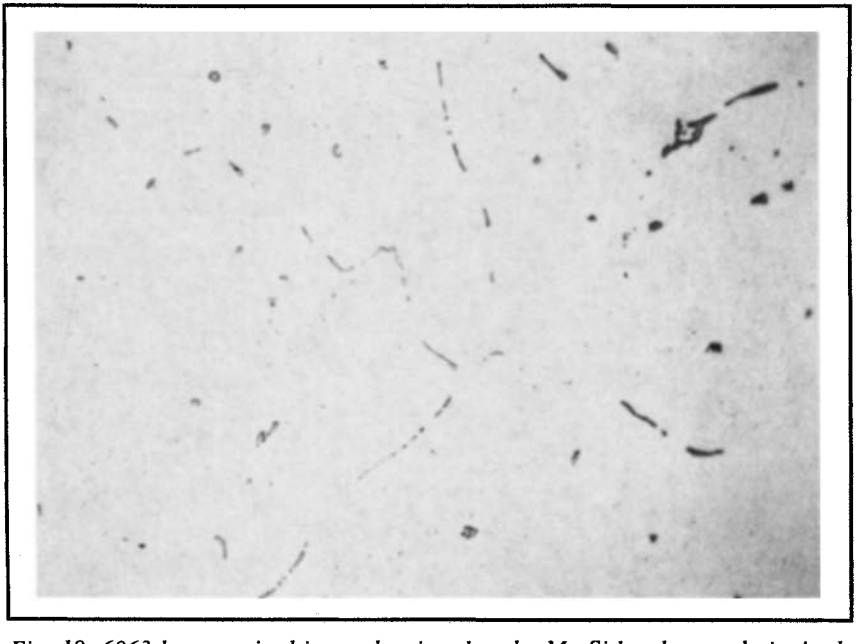

Fig. 18. 6063 homogenized ingot showing that the Mg_2Si has been solutionized, leaving only slightly spheroidized iron-rich phases. 0.5% hydrofluoric acid, 445×. (Courtesy of Kaiser Aluminum & Chemical Corp.)

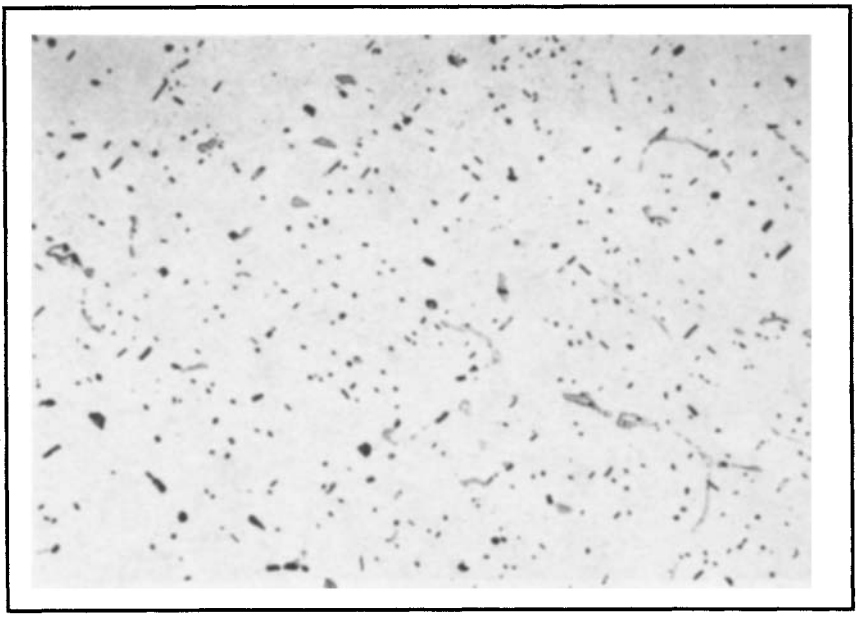

Fig. 19. 6061 homogenized ingot showing some undissolved Mg_2Si and some Mg_2Si reprecipitation during cooling in a Widmænstatten pattern. 0.5% hydrofluoric acid, 455×. (Courtesy of Kaiser Aluminum & Chemical Corp.)

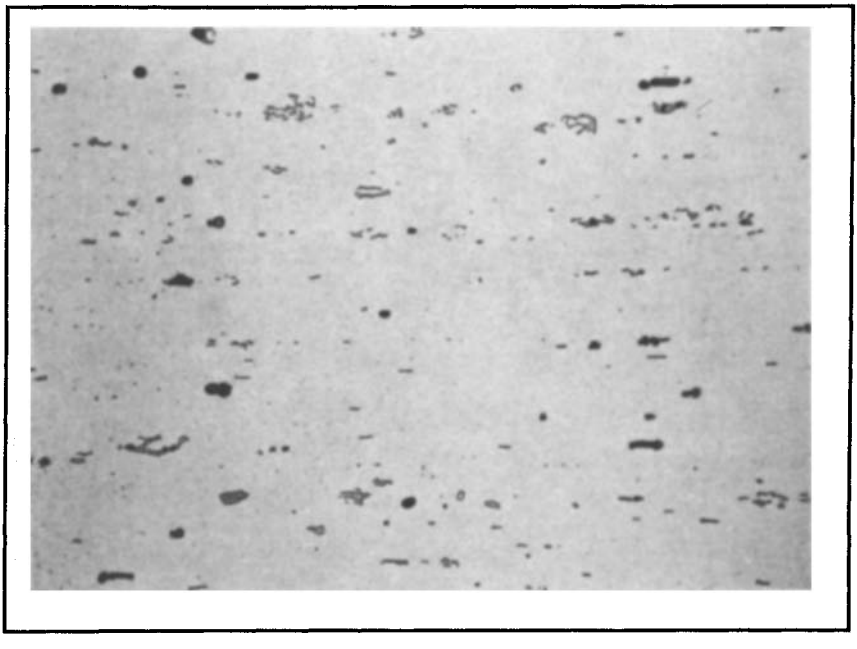

Fig. 20. 6061-T6 sheet showing insoluble $(Fe,Cr)_3SiAl_{12}$ and excess soluble Mg_2Si particles (dark) as redistributed by mechanical working. 0.5% hydrofluoric acid, 455×. (Courtesy of Kaiser Aluminum & Chemical Corp.)

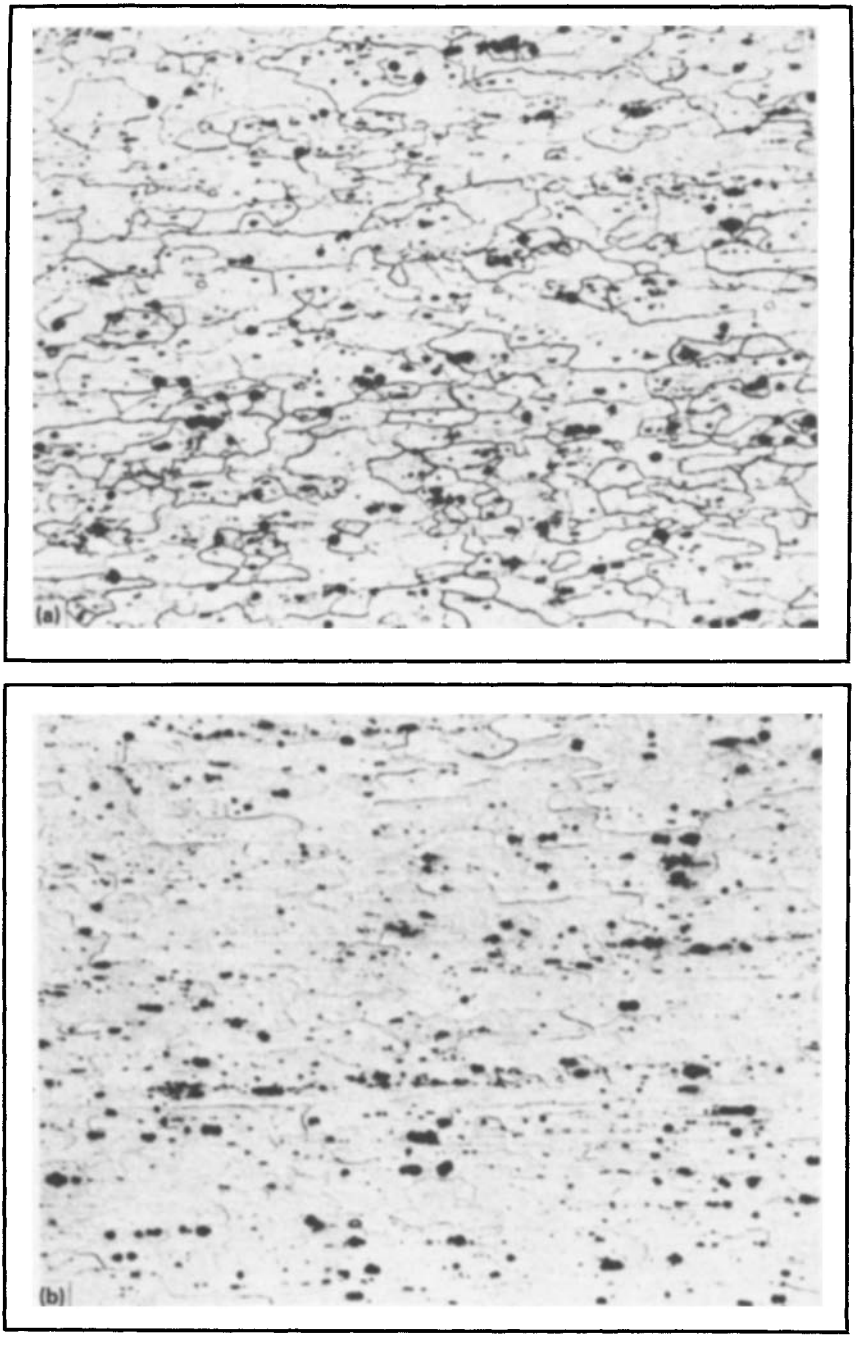

Fig. 21. 6061-T4(a) and T6(b) sheet showing the typical constituent distribution and loss of clear grain delineation caused by Mg_2Si precipitation from artificial aging. Hydrofluoric acid and sulfuric acid, 230×. (Courtesy of Kaiser Aluminum & Chemical Corp.)

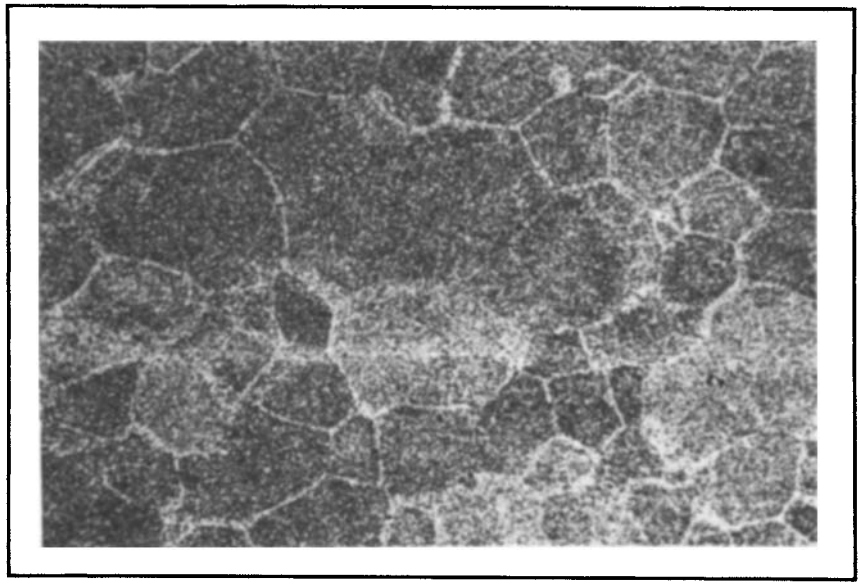

Fig. 22. 6063 extrusion in an overaged condition, showing a dense Mg_2Si matrix precipitate and a precipitate-free zone at the grain boundaries. 25% nitric acid at 70 °C (170 °F), 235×. (Courtesy of Reynolds Metals Co.)

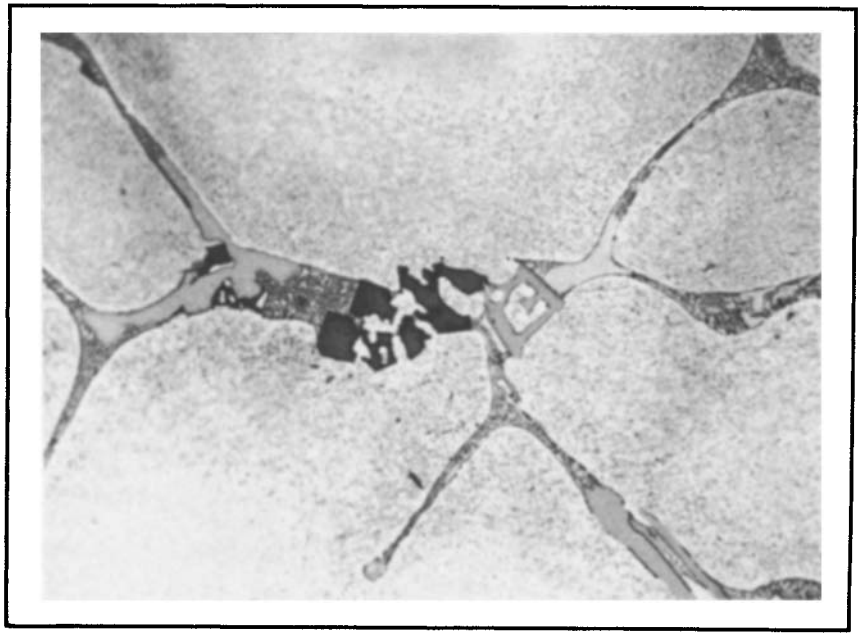

Fig. 23. 2024 as-cast ingot showing the complex multiphase structure. The fine precipitate in the aluminum matrix is formed during subsequent slow cooling of the ingot. 10% phosphoric acid, 455×. (Courtesy of Kaiser Aluminum & Chemical Corp.)

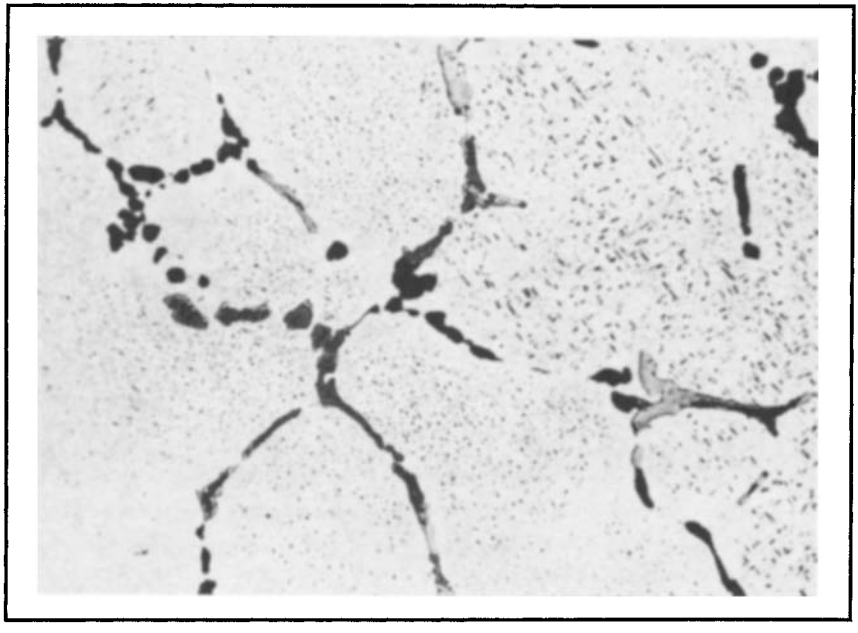

Fig. 24. 2024 heated ingot showing that the as-cast multiphase structure has been reduced to two principal iron-rich phases and soluble Al_2CuMg. The latter phase also forms Widmænstatten precipitate during subsequent slow cooling. 10% phosphoric acid, 460×. (Courtesy of Kaiser Aluminum & Chemical Corp.)

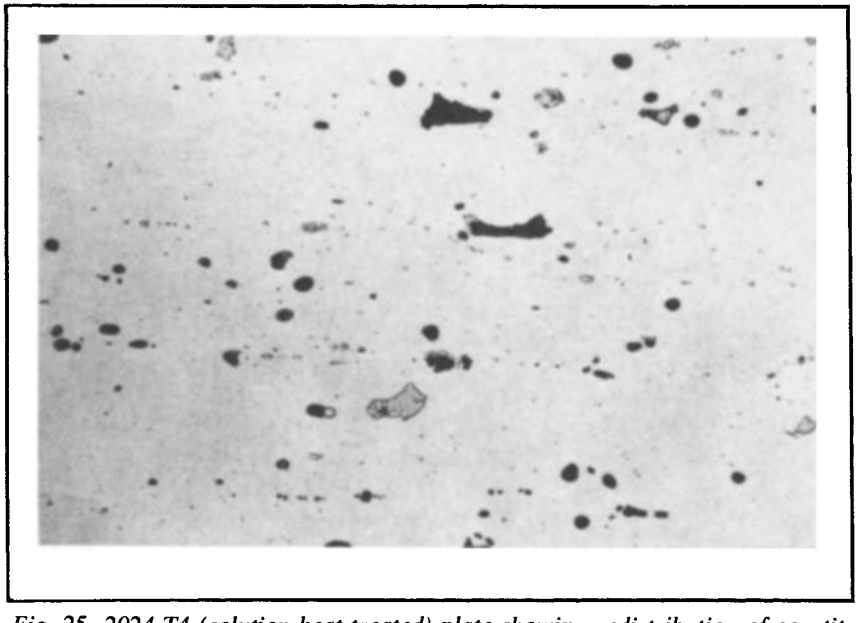

Fig. 25. 2024-T4 (solution heat treated) plate showing redistribution of constituent because of mechanical working. 10% phosphoric acid, 455×. (Courtesy of Kaiser Aluminum & Chemical Corp.)

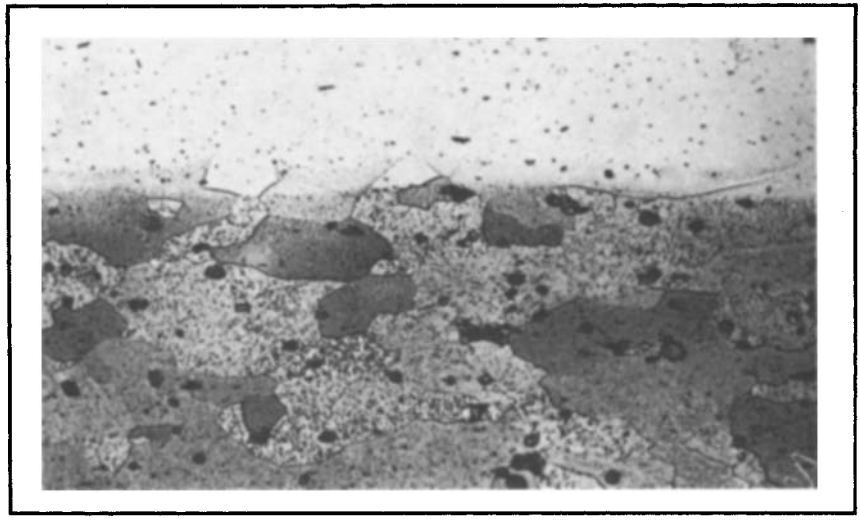

Fig. 26. Alclad 2024-T3 sheet showing some diffusion of copper into the commercial-purity aluminum cladding. Keller's etch, 460×. (Courtesy of Kaiser Aluminum & Chemical Corp.)

Fig. 27. 2014-F forged billet showing constituent differing from 2024. 10% phosphoric acid, 460×. (Courtesy of Kaiser Aluminum & Chemical Corp.)

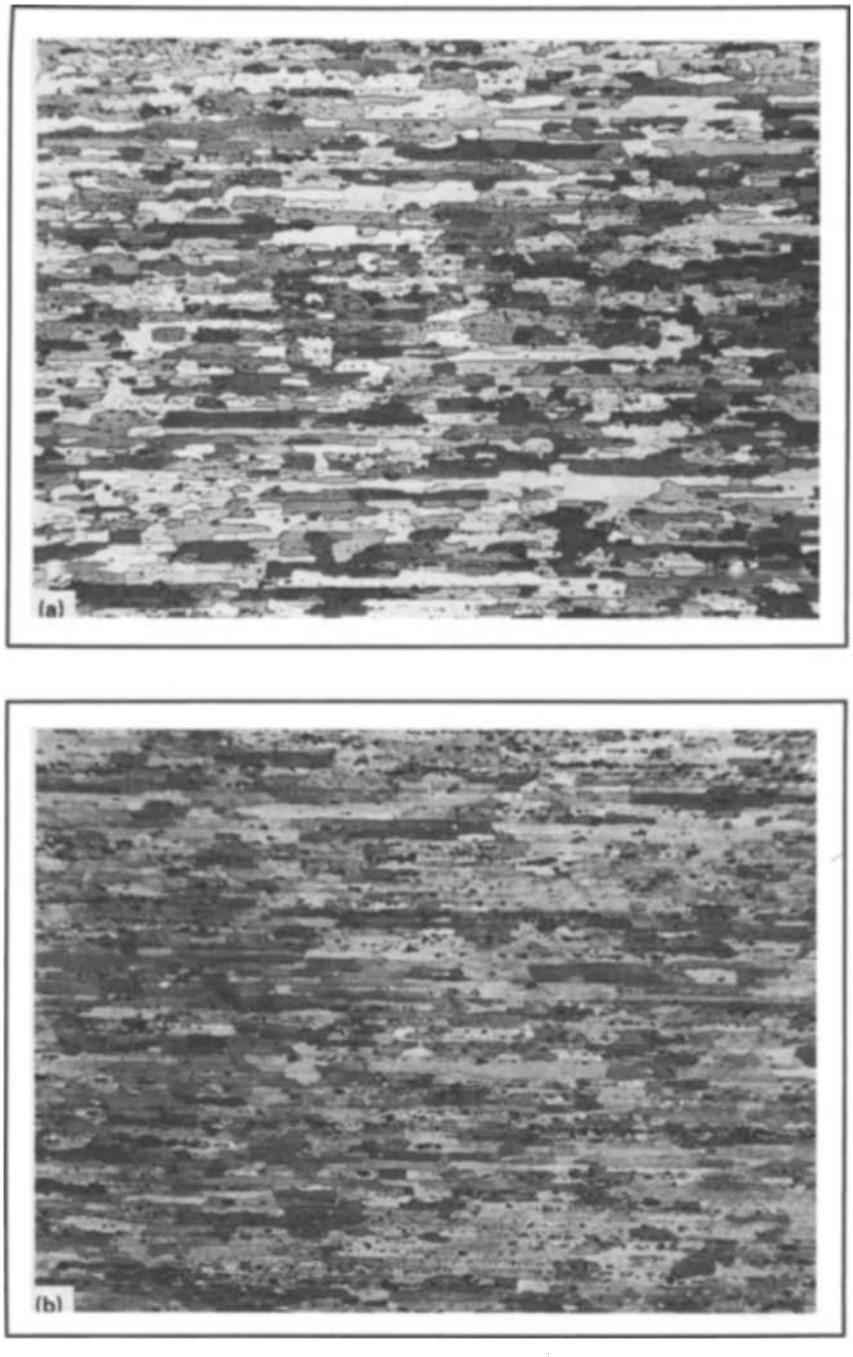

Fig. 28. 2014-T4(a) and T6(b) sheet showing reduction in etch grain contrast in the artifically aged T6 material. Keller's etch, 90×. (Courtesy of Kaiser Aluminum & Chemical Corp.)

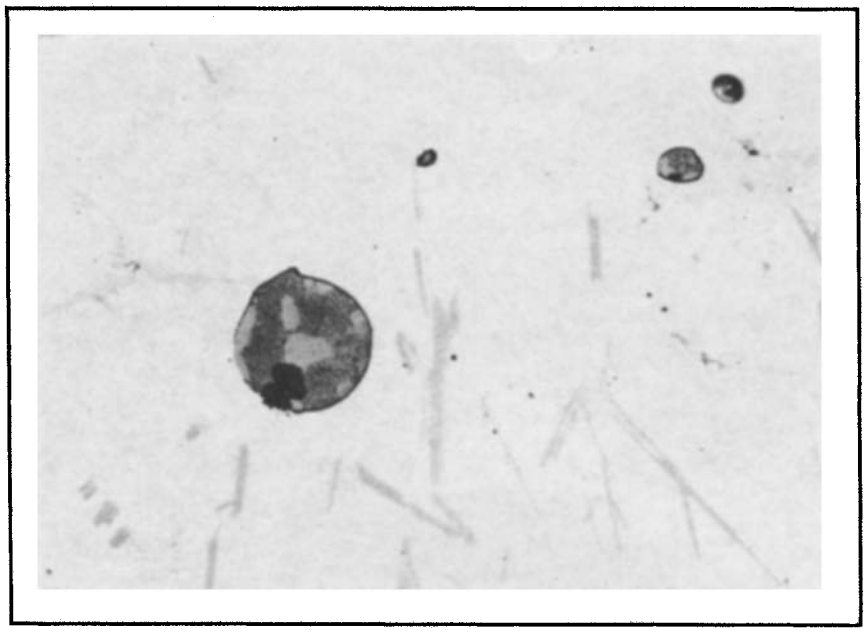

Fig. 29. 2011 as-cast ingot showing eutectic structure within the lead-bismuth globule. Unetched, 455×. (Courtesy of Kaiser Aluminum & Chemical Corp.)

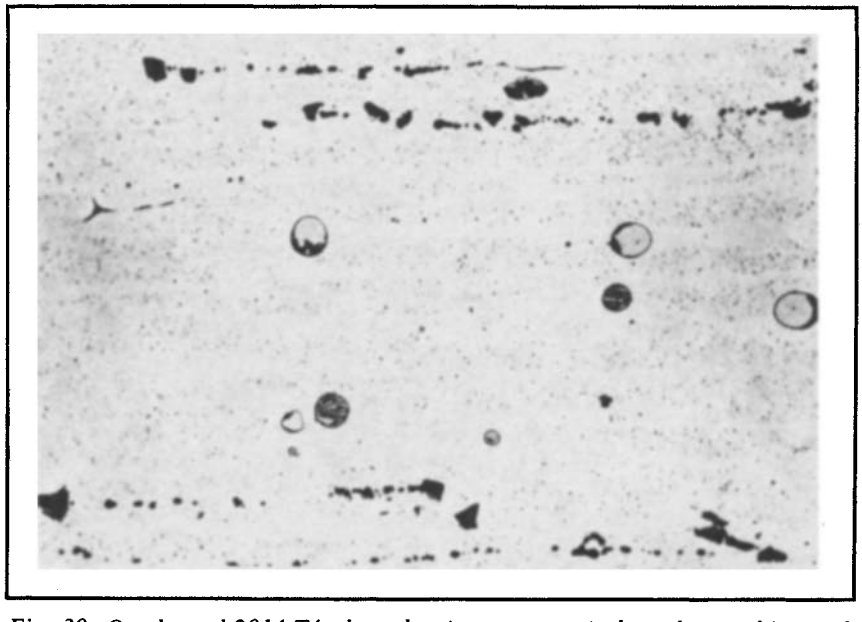

Fig. 30. Overheated 2014-T4 plate showing some grain boundary melting and formation of the liquid phase at the interface of the aluminum matrix and the $CuAl_2$ particles. Rosette structure is formed by rapid resolidification during quenching. 10% phosphoric acid, 460×. (Courtesy of Kaiser Aluminum & Chemical Corp.)

croscopic evaluation. Rosettes appear as the first stage of overheating. This is melting of undissolved eutectic (Fig. 30). Quenching while liquid is still present causes the appearance of rosettes. More extensive overheating causes grain boundary melting, particularly at triple intersections. This signals the onset of solid solution melting.

7XXX or Aluminum-Zinc Alloys. Zinc, by itself, is highly soluble in aluminum and exerts no appreciable influence on the microstructure of a simple alloy such as 7072. However, the class of alloy most frequently encountered contains magnesium and copper, as well as additives such as chromium, manganese, or zirconium, and the ever-present iron and silicon. In cast ingot form, alloy 7075 forms one or more variants of $(Fe,Cr)_3SiAl_{12}$, Mg_2Si, and a pseudobinary eutectic made up of aluminum and $MgZn_2$ (Fig. 31). The latter phase contains aluminum + copper as substitutes for zinc and can be written $Mg(Zn,Cu,Al)_2$. Subsequent heating (Fig. 32) causes the iron-rich phases to transform to Al_7Cu_2Fe. Mg_2Si is relatively insoluble and tends to spheroidize somewhat; $Mg(Zn,Cu,Al)_2$ rapidly begins to dissolve, and at the same time some Al_2CuMg precipitates, which then requires high temperatures and lengthy soaking to become completely dissolved. Chromium is precipitated from supersaturated solution as $Cr_2Mg_3Al_{18}$ dispersoid, concentrated heavily in the primary dendrite regions (Fig. 33). A well-solutionized wrought alloy contains only Al_7Cu_2Fe, $(Fe,Cr)_3SiAl_{12}$, and Mg_2Si, along with the dispersoid. Recrystallized grains are extremely elongated or flattened because of dispersoid banding, and unrecrystallized regions are not unusual even in sheet (Fig. 34). The unrecrystallized regions are made up of very fine subgrains in which boundaries are decorated by hardening precipitate. This is more obvious in hot worked structures (Fig. 35), especially in the more highly worked regions near the surface, where critical deformation has caused coarse recrystallized grains to form (Chapter 4 in this Volume). The dispersoids inhibit recrystallization and foster formation of the fine subgrain structures. $ZrAl_3$ is coherent with the matrix, and it has similar effects.

Annealing in the heat treatable alloys has a two-fold purpose: (1) the removal of residual equivalent cold work, and (2) the precipitation of solute from solid solution. The latter is accomplished by a controlled slow cooling (Chapter 5 in this Volume) and results in a random distribution of precipitate (Fig. 36). The presence of this dense precipitation makes the grain structure of such O-temper (Ref 2) alloys difficult to reveal.

Other high- and moderate-strength 7XXX alloys represent variants from 7075. Alloy 7050, with higher copper and zinc, has more Al_2CuMg to be dissolved at the solutionizing temperature. More dilute alloys can readily dissolve all of the zinc-rich phases. Signs of overheating in 7XXX alloys are usually related to segregated regions with unusual concentrations of Al_2CuMg. The homogeneous alloy has an equilibrium solidus that is well above the solution heat treating temperature range. If Al_2CuMg is present, however, very rapid heating rates can result in the appearance of rosettes, because of the inadequate time for diffusion and particle dissolution before exceeding the nonequilibrium eutectic temperature.

A given alloy cannot be characterized by a single microstructural aspect. The initial size of second-phase particles formed during solidification depends on the rate of heat removal. The degree of comminution

Fig. 31. 7075 as-cast ingot showing the multiphase structure. The fine precipitate in the aluminum matrix is formed during slow cooling from the initial ingot solidification. Dilute Keller's etch, 445×. (Courtesy of Kaiser Aluminum & Chemical Corp.)

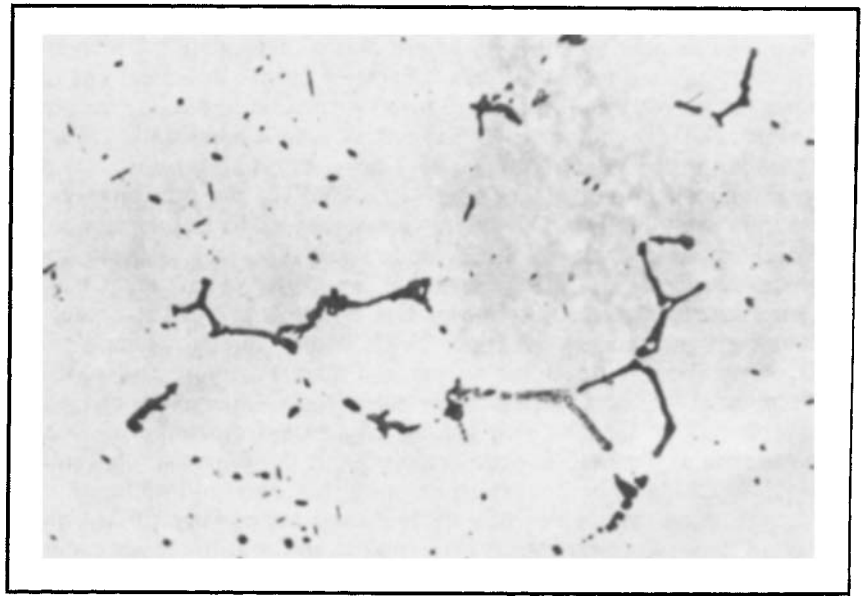

Fig. 32. 7075 homogenized ingot showing iron-rich phases, nearly insoluble Mg_2Si and soluble Al_2CuMg formed by transformation from $Mg(Zn,Al,Cu)_2$ as the latter enters solid solution. Dilute Keller's etch, 445×. (Courtesy of Kaiser Aluminum & Chemical Corp.)

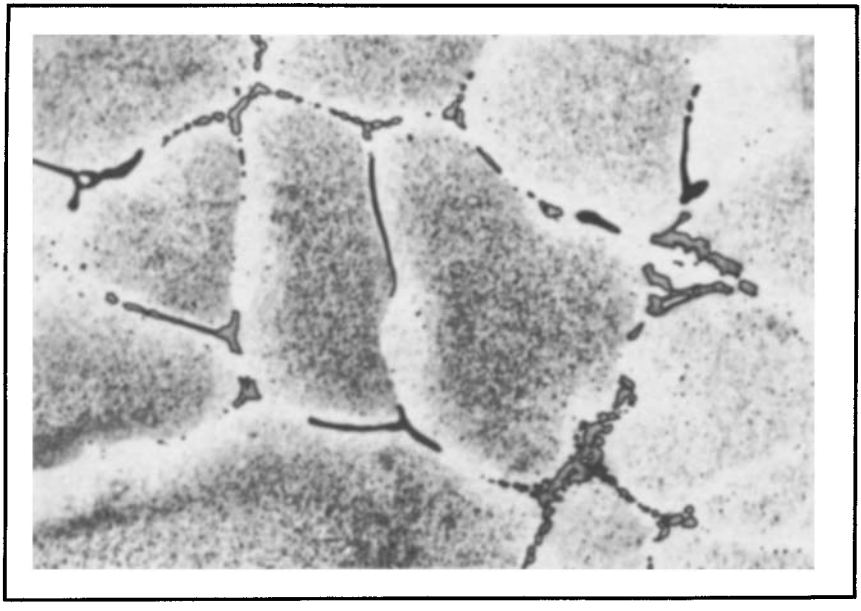

Fig. 33. 7075 heated ingot etched to reveal the fine dispersoid of the chromium-rich phase that precipitated at elevated temperatures and reflects the original distribution of chromium in the as-cast supersaturated solid solution. 0.5% hydrofluoric acid, 460×. (Courtesy of Kaiser Aluminum & Chemical Corp.)

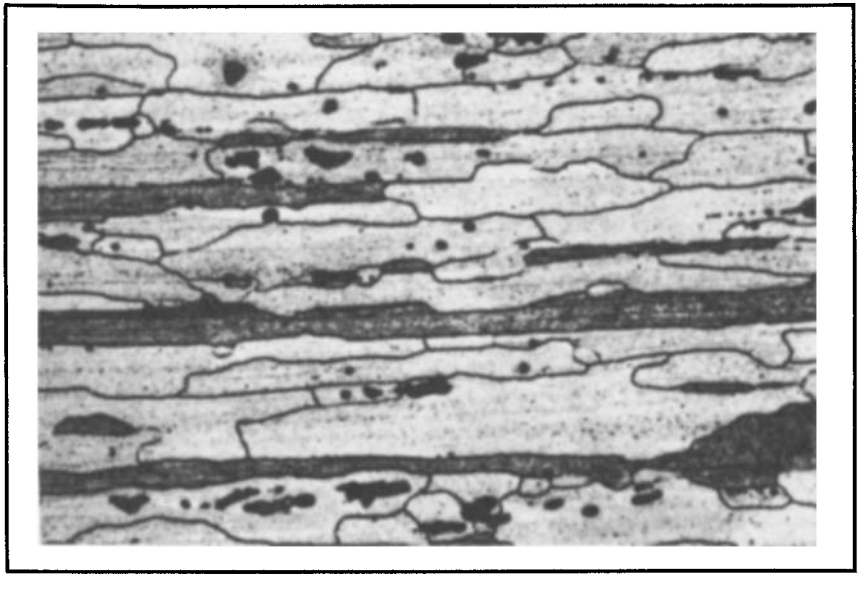

Fig. 34. 7075-T6 sheet etched to distinguish between recrystallized grains (clear) and unrecrystallized grain fragments that appear dark as a result of precipitation at boundaries of fine subgrains. 10% phosphoric acid, 455×. (Courtesy of Kaiser Aluminum & Chemical Corp.)

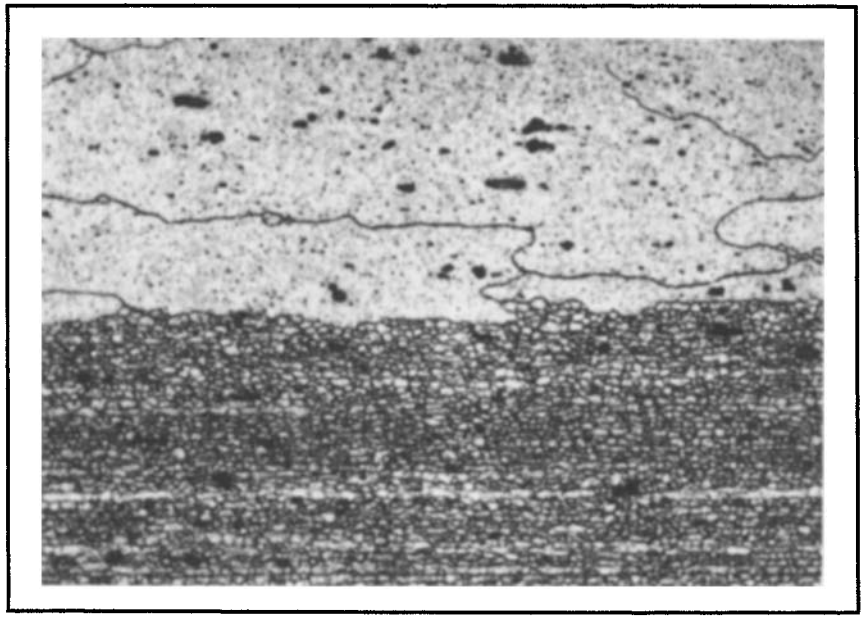

Fig. 35. 7075-T6 large extrusion with the section near the surface showing a layer of coarse recrystallized grains overlying fine subgrain structure that reflects recovery during or subsequent to hot working. 10% phosphoric acid, 455× (Courtesy of Kaiser Aluminum & Chemical Corp.)

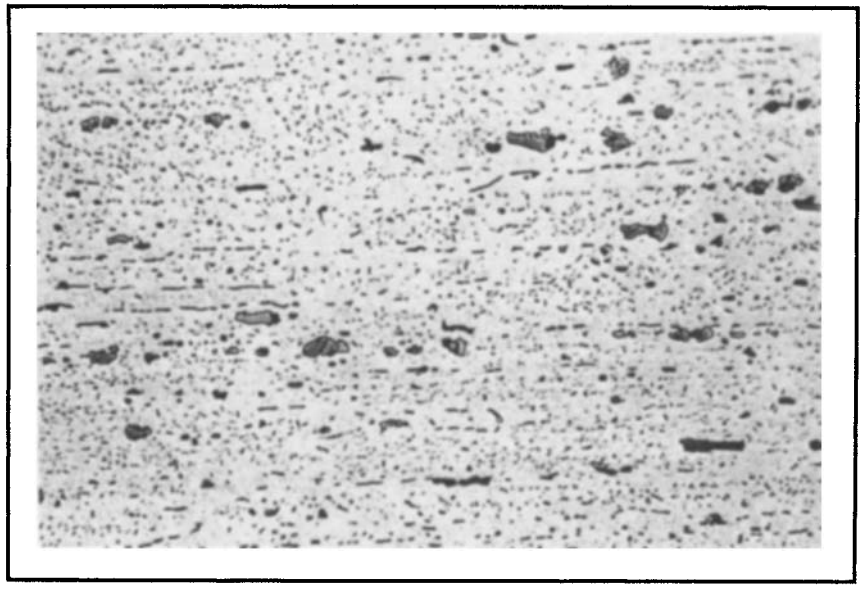

Fig. 36. 7075-O annealed sheet showing the random distribution of insoluble phases interspersed with precipitate particles of $Mg(Zn,Al,Cu)_2$ that precipitate from solid solution during controlled slow cooling from annealing. Dilute Keller's etch, 445×. (Courtesy of Kaiser Aluminum & Chemical Corp.)

and randomization of less soluble second-phase particles depends upon the total accumulation of mechanical working. The amount of excess soluble phase depends on the individual alloy composition, within specification limits, and upon the thermal treatment. The quantity and size of the dispersoid depends on the individual composition and the total thermal history, supplemented by severity of mechanical deformation. The degree of recovery and recrystallization and the size and shape of recrystallized grains depend in large measure on all of the above, as well as on factors such as rate of heating. An understanding of these interactions is important for correct interpretation of microstructural features.

QUANTITATIVE METALLOGRAPHY

The use of quantitative metallography to relate properties to microstructure is used more widely because of the introduction of automated devices. Reference 7 provides a review of techniques and theory in this field.

Microstructural features that are relevant include: (1) porosity, (2) inclusions, (3) constituent particles (insoluble phase formed during solidification, e.g., Al_6 (FeMn) or $FeAl_3$), (4) dispersoids (fine precipitate that forms during high-temperature thermal operations, e.g., $ZrAl_3$, $Al_{12}(FeMn)_3Si$, and $Al_{12}Mg_2Cr$), and (5) fine age hardening precipitates (fine, usually coherent precipitates that form at low temperature, generally as a consequence of high solute supersaturation resulting from a solution heat treatment and quench, e.g., $MgZn_2$, $CuAl_2$ (θ'), and GP zones). All of the above-mentioned features can influence the behavior of a material, and most are amenable to quantitative description.

Constituent particles, porosity, and inclusions are generally large enough to be measured optically. Features of this scale have strong effects on the fracture behavior of aluminum, especially fracture toughness, fatigue, and elongation. Constituent particles are large enough to be analyzed chemically using EMPA or scanning electron microscopy—energy dispersive x-ray (SEM-EDX) methods (for example, LeMont analysis) and hence, in multiconstituent alloys these constituents are differentiable chemically. Vruggink (Ref 8) used this approach to correlate short transverse elongations in 2×24 alloys with type and volume percent of constituent. Blau (Ref 9), Thompson (Ref 10), and Hahn and Rosenfeld (Ref 11) analyzed constituent size, spacing, and volume fraction and correlated these measurements with the fracture toughness of high-strength aircraft alloys.

Features of finer scale than the constituent (the dispersoid) are not generally measurable optically and must be measured using higher resolution techniques (TEM or SEM). These particles affect the recrystallization behavior of aluminum alloys and also can either directly or indirectly affect tensile properties. The high magnifications required and the consequent small areas that are analyzed make this random sampling difficult. If these particles are analyzed by EDX-equipped STEM, they can also be classified chemically. Features of the finest scale, the age hardening precipitates, can only be analyzed by TEM. Their effect is primarily to increase yield and tensile strength.

Staley (Ref 12) related fatigue behavior of aluminum high-strength 7x75 alloys to constituent content. At high levels of stress intensity, the growth

rates of fatigue cracks were lower for a lower constitutent alloy (7475) than for the higher constituent content of 7075. At low-stress intensity, constituent particles may beneficially pin dislocations.

SCANNING ELECTRON MICROSCOPY (SEM)

A good description of how SEM works and some of its applications to fracture surface studies can be found in *Practical Scanning Electron Microscopy* by Goldstein *et al* (Ref 13). The chief advantages of SEM analysis are:

- Easy specimen preparation
- Widest range of magnification available (commonly from 15 to 50,000 diameters)
- Ability to observe large areas of specimen surface, including origin and propagation zones, because 645 mm^2 (1 $in.^2$) or more of the fracture surface can be directly placed into the microscope
- Excellent depth of field for focusing on surfaces with large topography variation
- Ability to view the fracture face and simultaneously perform microchemical analysis if the microscope is so equipped

Disadvantages of SEM analysis have related to uncertain specimen tilt or orientation in the microscope that can alter the apparent size of fracture features, such as fatigue striation spacings, or influence quantitative microchemical analysis (actual takeoff angle of x-ray from specimen surface). The use of stereo pair SEM images offsets this disadvantage, for they can precisely define surface topography. In addition, uncertain fracture surface topographies may be encountered because of the lack of well-documented literature of SEM fracture surfaces.

Scanning electron microscopy micrographs of fracture surfaces are performed by two types of emitted electrons. Secondary electrons are most commonly used because of their fidelity in showing topographical features. Higher energy, back-scattered electrons can be used to show average compositional variations across a fracture surface, usually with only a slight degradation of surface detail. Actual microchemical identification of the elements on a fracture surface usually involves examination of the characteristic x-rays emitted from the surface because of ionization processes caused by an incident electron beam. Characteristic x-rays fingerprint the identity of elements present and are detected by either a solid-state detector that is sensitive to the x-ray energy, or by a wavelength dispersive detector that is sensitive to the x-ray wavelength.

Examples of SEM imaging and microchemical analysis, contrasted against TEM imaging of replicas, follow. Figure 37 is an SEM secondary electron image clearly showing fatigue cracking in 2024 aluminum. Note the resulting great depth of field, despite large topographic differences. Measurements of fatigue striation spacing cannot generally be made without detailed knowledge of local specimen surface tilt relative to the electron beam and secondary electron detector or by the use of stereo pairs. Figure 38 is a TEM image of a replica of the same fatigue fracture. Here, striations are clearly visible and can be measured to determine fatigue crack growth rate. However, a pitfall similar to that of SEM is encoun-

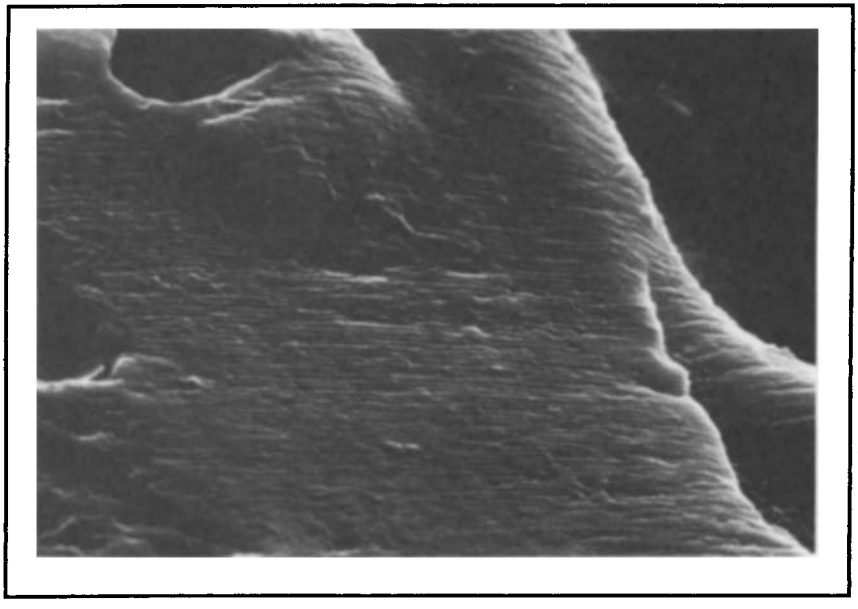

Fig. 37. SEM secondary electron image showing fatigue fracture in 2024 aluminum (4600×). (Courtesy of Boeing Commercial Airplane Co.)

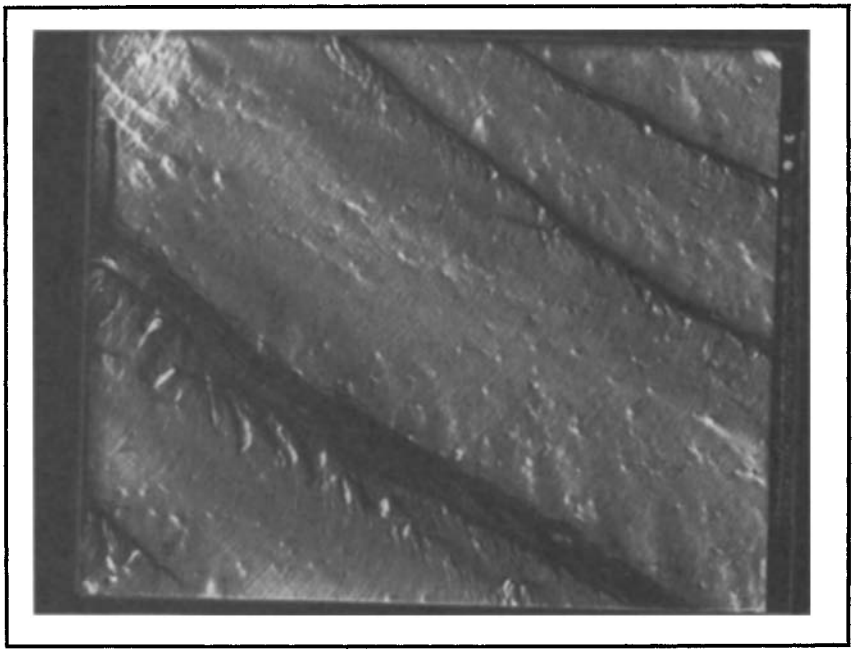

Fig. 38. TEM replica showing fatigue fracture in 2024 aluminum (4075×). (Courtesy of Boeing Commercial Airplane Co.)

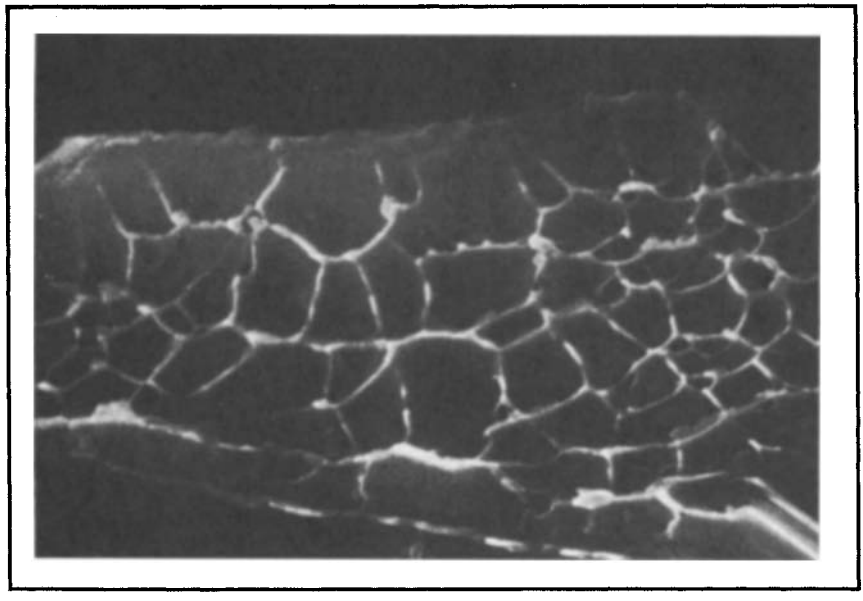

Fig. 39. SEM imaging of tensile fracture in A357 casting (18,400×). (Courtesy of Boeing Commercial Airplane Co.)

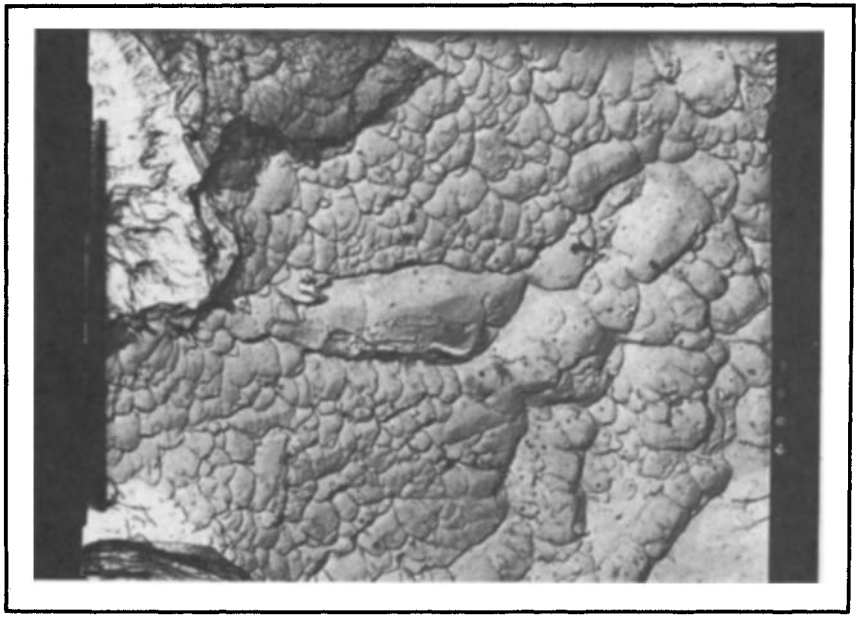

Fig. 40. TEM replica imaging of tensile fracture in A357 casting (6550×). (Courtesy of Boeing Commercial Airplane Co.)

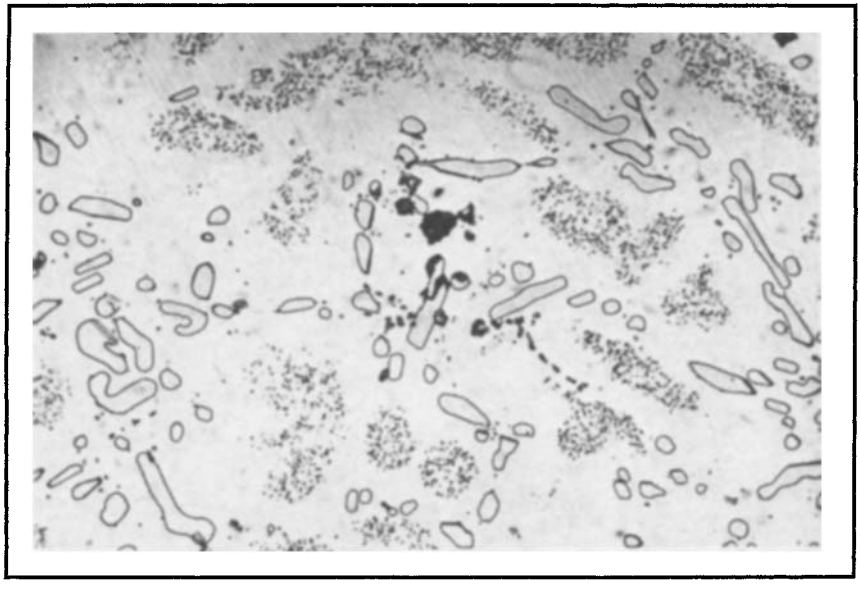

Fig. 41. Light optical image of a polished section of A357 casting (380×). (Courtesy of Boeing Commercial Airplane Co.)

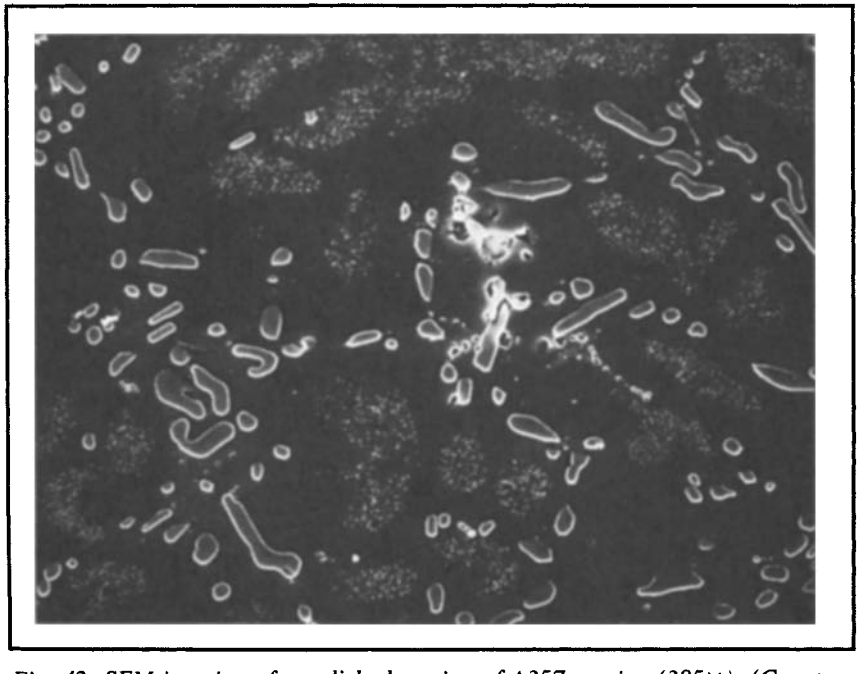

Fig. 42. SEM imaging of a polished section of A357 casting (385×). (Courtesy of Boeing Commercial Airplane Co.)

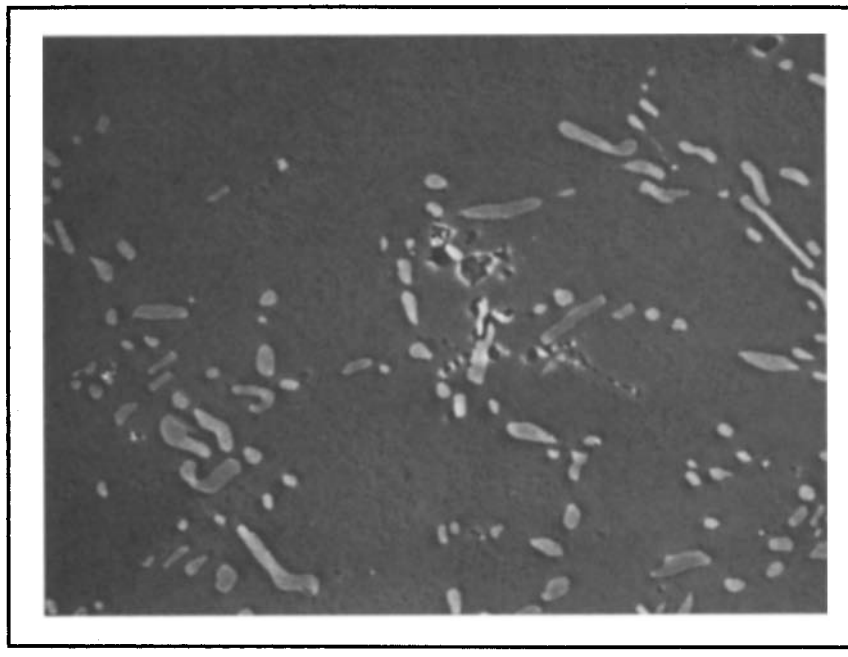

Fig. 43. Back-scattered electron imaging of a polished section of A357 casting (385×). (Courtesy of Boeing Commercial Airplane Co.)

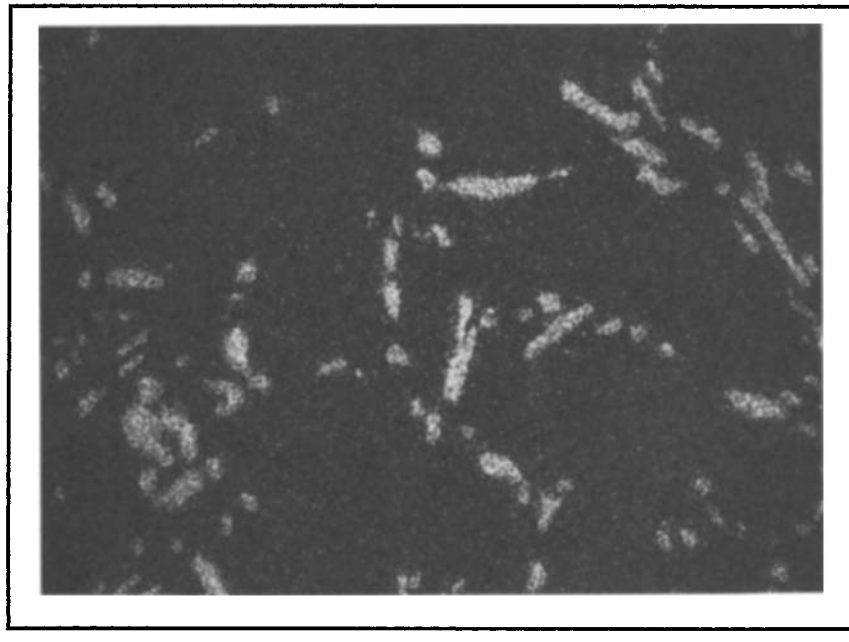

Fig. 44. Silicon x-ray map of a polished section of A357 casting (385×). (Courtesy of Boeing Commercial Airplane Co.)

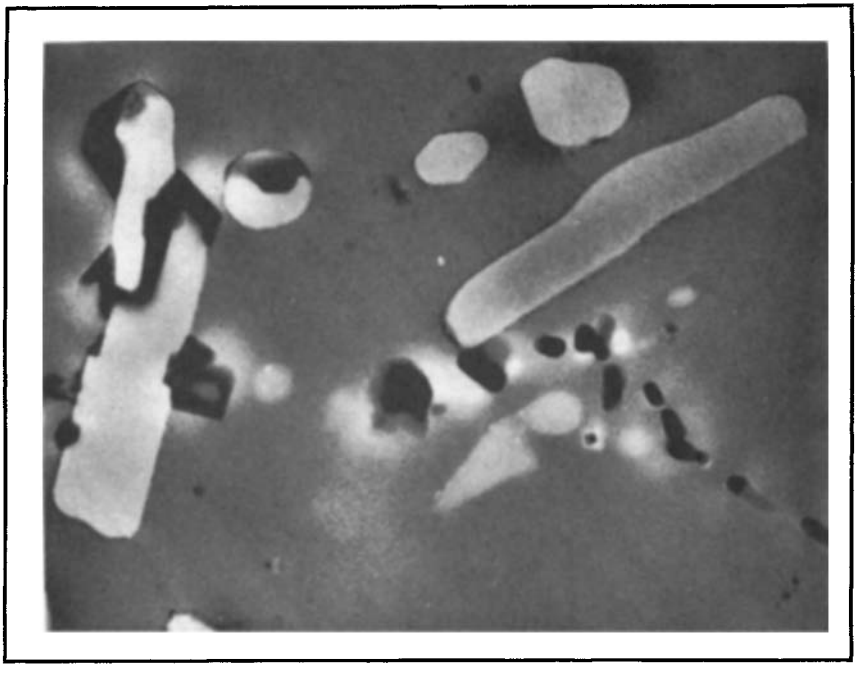

Fig. 45. Back-scattered electron imaging of a polished section of A357 casting (2300×). (Courtesy of Boeing Commercial Airplane Co.)

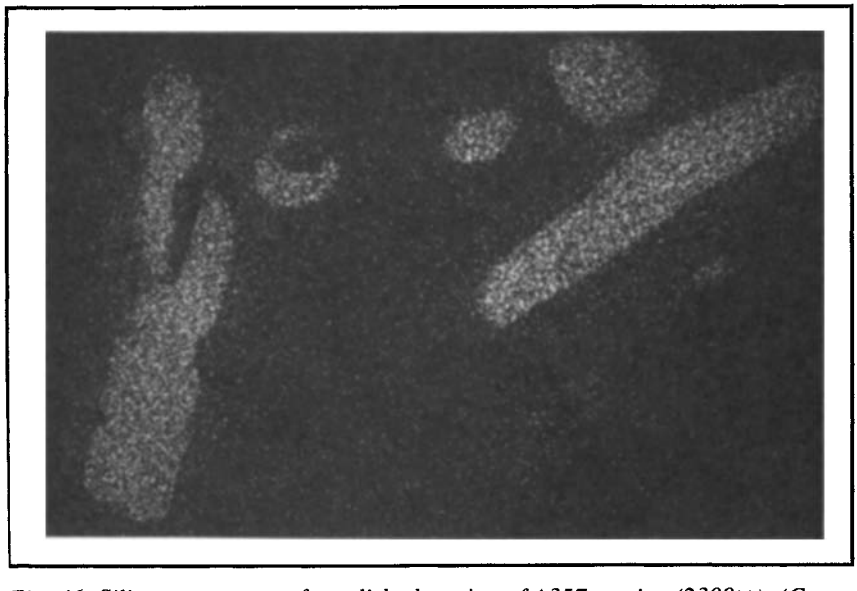

Fig. 46. Silicon x-ray map of a polished section of A357 casting (2300×). (Courtesy of Boeing Commercial Airplane Co.)

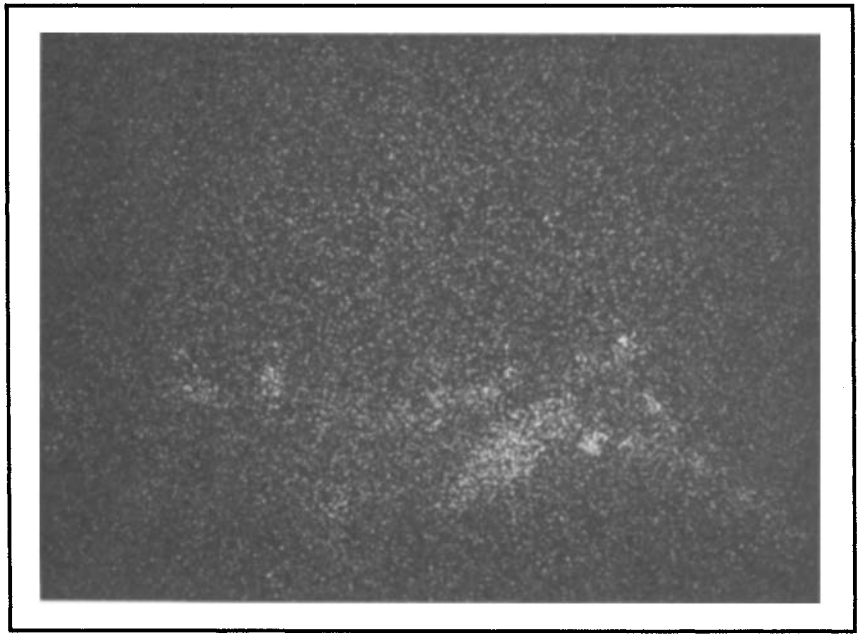

Fig. 47. Iron x-ray map of a polished section of A357 casting (2300×). (Courtesy of Boeing Commercial Airplane Co.)

tered. The striation spacing observed must be representative of the principal crack front. This is not always clear, because the act of replicating fracture surfaces presents the probability that despite their planar appearance, the striations observed can derive from local out-of-plane crack front geometry.

Dimple topography characteristic of microvoid coalescence in tensile and shear mode fractures is exhibited by SEM and TEM imaging in Fig. 39 and 40, respectively, for A357 casting alloy. An example of the microchemical analysis advantage afforded by SEM is demonstrated on a polished section of A357 as shown in Fig. 41 through 47. Figures 41 and 42 are light optical and SEM secondary electron images, respectively, showing identical fields of view. Phases dissolved by the etchant are clearly shown as holes in the SEM image. When imaged using back-scattered electrons, as in Fig. 43, this same field contains small patches of micropitting, appearing as white in color by secondary electron imaging, and black in color by light optical methods. The use of back-scattered electron imaging permits qualitative knowledge of the relative average atomic number of differing phases; silicon-containing particles (see x-ray map in Fig. 44) absorb fewer electrons, and silicon has a higher back-scattered coefficient than the aluminum matrix and appears light in Fig. 43. A detailed examination of the center region of Fig. 41 through 43 shows the presence of both silicon-rich and iron-rich phases (Fig. 45 through 47) by back-scattered electron imaging.

Intergranular primary and secondary cracking in 7075 alloy are shown in Fig. 48 and 49, SEM and TEM images, respectively. Corroded areas

on this fracture face, including elements of the corrosion product, are shown by SEM secondary electron and TEM imaging, Fig. 50 and 51, respectively. The light rectangle of Fig. 50 defines a region of SEM-EDX analysis, which showed the corrosion product to contain sodium and chlorine, in addition to alloying elements. Both SEM and TEM imaging of fracture faces are generally far superior to light optical methods. The specific advantages of SEM techniques, allowing microchemical analysis *in situ,* as well as superior imaging, continues to become more important as the number and scope of documented fracture topographies grows.

TRANSMISSION ELECTRON MICROSCOPY (TEM)

Developments in instrumentation and techniques during recent years have enabled electron microscopy to play an increasingly important role in advancing the understanding of aluminum alloy microstructure. The high magnification, resolving power, and excellent depth of focus enable the ultrafine details of the microstructure to be imaged in these instruments. When ultrafine detail is needed, TEM methods are preferable to optical microscopy. Magnifications of up to 300,000× and resolutions better than 0.5 nm (5 Å) are routinely available.

Transmission electron microscopy is usually carried out using thin foil specimens that have been carefully prepared from the sample of interest, although for some investigations, replicas of the specimen surface can be used. In standard 100-kV TEM, aluminum alloy specimens must be prepared so that the area of interest is less than about 0.5 μm (0.02 mil) thick and preferably as thin as 0.2 μm (0.008 mil). Elaborate techniques including jet electropolishing and ion beam erosion have been developed to prepare such specimens. The contrast in electron microscope images arises as the result of differences in the diffraction and absorption of the electrons by different features in the specimen.

Localized changes in orientation that occur at grain and subgrain boundaries and in the strain fields associated with dislocations and coherent precipitates cause contrast variations. Similarly, the different crystal structure factors and absorption coefficients of second-phase particles also produce image contrast. Although the specimens are thin, the image is a projection of a three-dimensional structure, and the orientation and distribution of features can be established three-dimensionally.

In addition to excellent imaging capabilities, TEM can also be used for electron diffraction. In this mode of operation, areas of the image as small as 1 μm (0.04 mil) can be selected, and diffraction patterns can be obtained. These selected area diffraction patterns are used extensively to identify second-phase particles and to establish crystallographic orientations of an area or particle of interest.

Scanning transmission electron microscopy (STEM) offers an even more impressive range of capabilities. In these instruments, the incident electron beam is demagnified to produce a very small spot size, typically between 0.1 and 50 nm (1 and 500 Å) at the specimen, and this is scanned in a raster over the area of interest. With appropriate detectors, a number of different imaging modes can be selected. Thus, in addition to the scanning transmission image (similar to TEM), secondary electron images

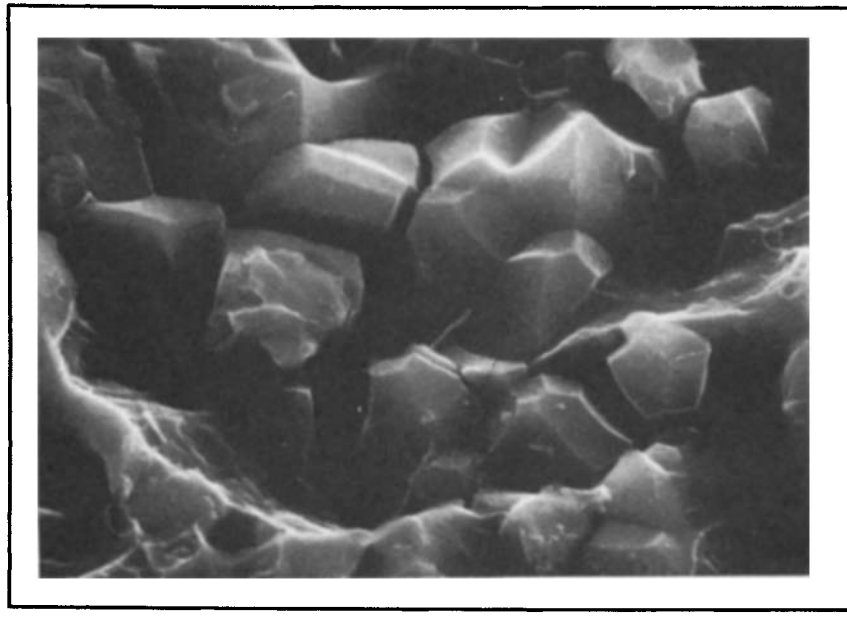

Fig. 48. Intergranular stress-corrosion cracking in 7075 alloy with SEM imaging (9200×). (Courtesy of Boeing Commercial Airplane Co.)

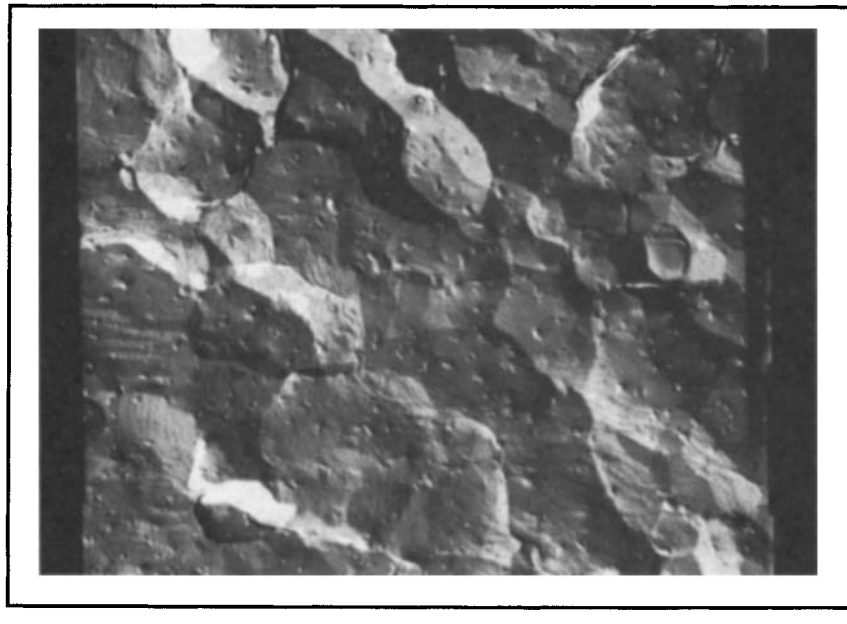

Fig. 49. Intergranular stress-corrosion cracking in 7075 alloy with TEM imaging (5830×). (Courtesy of Boeing Commercial Airplane Co.)

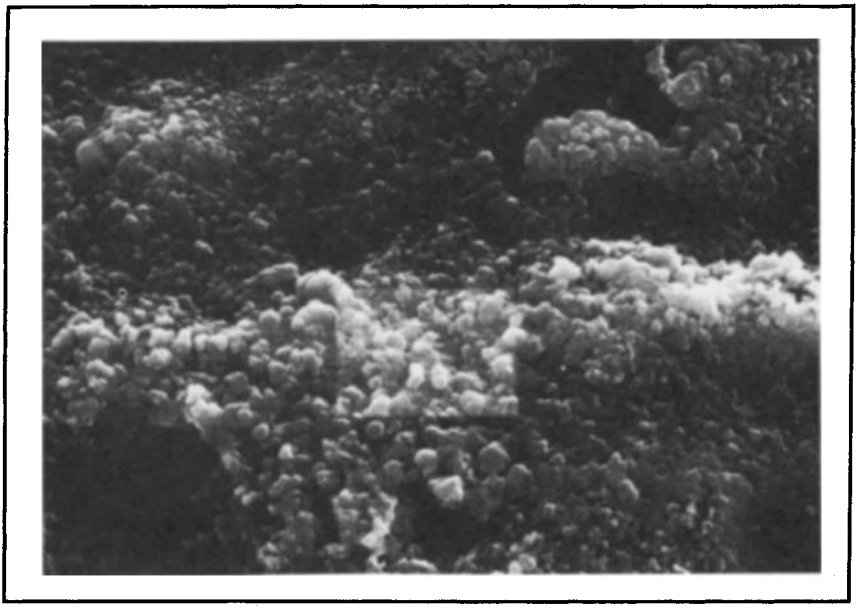

Fig. 50. Stress-corrosion product of 7075 alloy with SEM imaging (4325×). (Courtesy of Boeing Commercial Airplane Co.)

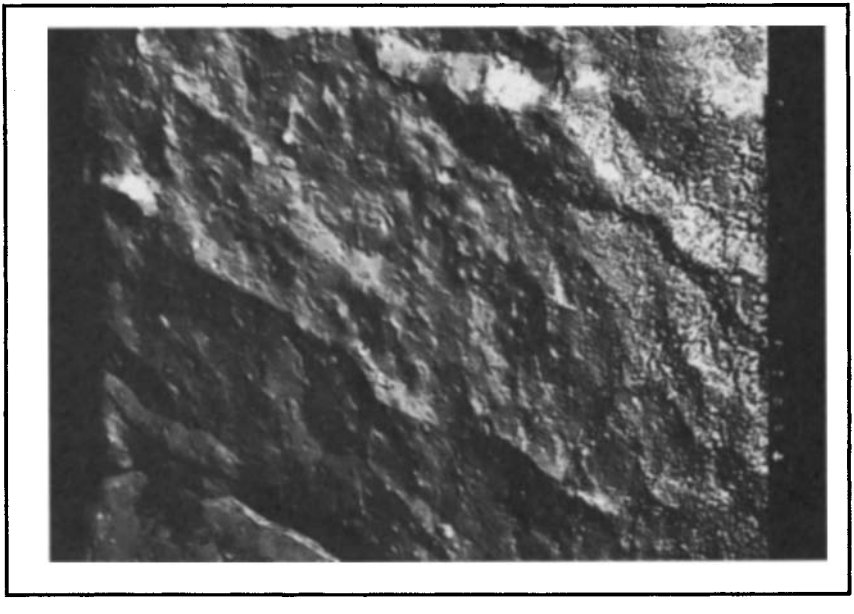

Fig. 51. Stress-corrosion cracking and product of 7075 alloy with TEM imaging (4075×). (Courtesy of Boeing Commercial Airplane Co.)

(surface), back-scattered electron images (atomic number contrast), and x-ray images (composition maps) can be selected.

In addition to excellent imaging facilities, STEM has the capability to generate and accurately position a fine electron beam on a small area of a specimen. This ability is of particular value for microdiffraction and microanalysis. Microdiffraction patterns provide crystallographic information from very small features, and by using an energy-dispersive x-ray detector, quantitative microanalysis from regions of thin specimens less than 100 nm (1000 Å) in diameter are readily obtainable in many cases.

High-voltage electron microscopy (HVEM), using instruments that operate at up to 1 million V, enable thicker specimens to be studied in transmission. This method is used for *in situ* experiments involving observations during heat treatment or straining. Expense and specialization have limited use of HVEM to a few research centers.

Even more sophisticated imaging and microanalytical techniques are being developed that offer opportunities to study aluminum microstructure in greater detail. High-resolution TEM is capable of directly imaging the lattice structure of aluminum and has contributed to the understanding of lattice defects and the early stages of zone formation in some alloy systems. The ultimate high-resolution imaging and analytical devices, however, are the field ion microscopes and atom probes that, with suitable specimens, can image and identify individual atoms. Using these instruments, investigations of segregation of alloying elements to grain boundaries or other defects may be possible in the near future.

Structural Features. Many of the structures observed by light microscopy can be studied in more detail in the electron microscope. Furthermore, a great deal of information that cannot be obtained by light microscopy is available. Thus, in addition to the familiar grain structure of the material, subgrains and dislocation substructures can be observed, and if required, crystallographic orientations can be measured using electron diffraction patterns.

Grain boundaries generally appear as bands that have widths corresponding to their magnified projections. This boundary image width is determined by the inclination of the boundary with respect to the location beam direction and the thickness of the specimen. These grain boundary images have distinct fringes running along their lengths. The fringe contrast is the result of electron diffraction effects, and the number and contrast of the fringes vary if the diffraction conditions are changed by specimen tilting.

The electron microscope can also reveal dislocation networks that are introduced during deformation processes and subsequent changes that occur during recovery and recrystallization. The lattice strain associated with a dislocation causes a change in the local diffraction conditions, causing dislocation contrast. Dislocations normally appear as lines that terminate at the specimen surface, although helices and loops can be present in certain cases. The best dislocation images are obtained by a technique known as weak beam dark field imaging. Using this method, only regions of highest lattice distortion (near the dislocation cores) appear in the image.

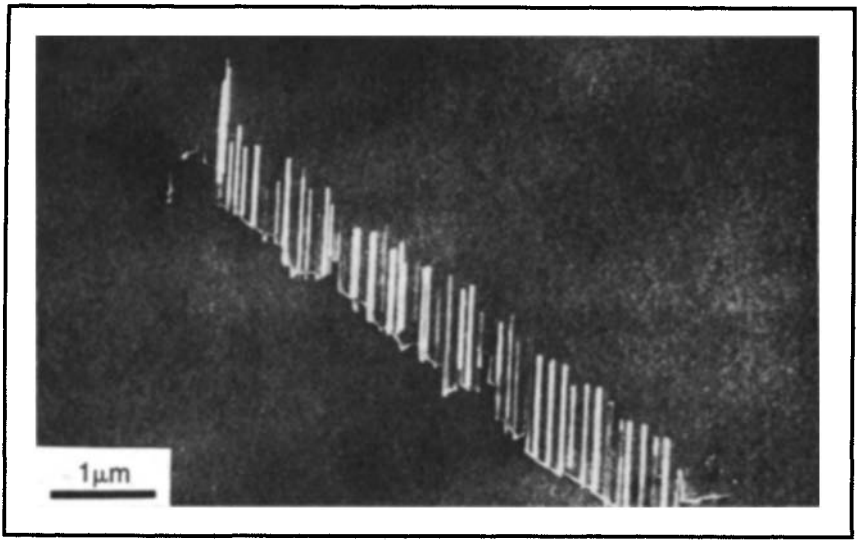

Fig. 52. Weak beam dark field imaging. β-Mg_2Si needle-like precipitates that have nucleated and grown in association with a dislocation in a sample that was solution treated and cooled directly to 270 °C (515 °F). (Courtesy of Alcan International Ltd.)

The weak beam technique is also useful for studying the strain fields associated with Guinier-Preston (GP) zones and fine coherent precipitates (Fig. 52). These zones are extremely small clusters of solute atoms in the solid-solution matrix and are the precursors of precipitate particles. Examinations of fine precipitates and dispersoids are frequently carried out using TEM. Size distributions and the spatial distribution of particles within the substructure can be obtained by standard imaging techniques. The dispersoid particles frequently occur at grain or subgrain boundaries, on dislocations, or at the interface with other particles. Some types of particles develop at apparently random sites within the matrix, although the nucleation may be associated with point defects such as vacancies.

Certain precipitate particles grow with characteristic shapes and can often be tentatively identified in this way. In cases where this is not possible or where a more positive identification is required, electron diffraction and thin foil microanalysis can be used to characterize the crystallographic structure, orientation, and composition of particles (Fig. 53). Thin foil microanalysis can also be used in some cases to determine the concentrations of elements in solid solution in the aluminum matrix. The high spatial resolution of ≤50 nm (≤500 Å) for microanalysis, which is available in a STEM system, enables the establishment of matrix compositions between dispersoid particles. Studies of concentration profiles of elements in the vicinity of grain boundaries have also been made.

Electron Microstructure of Wrought Alloys. A wide range of aluminum alloys has been studied by electron microscopy, and characteristic microstructures of the more common alloy systems after various fabrication and thermal treatments have been described. In general, plastic

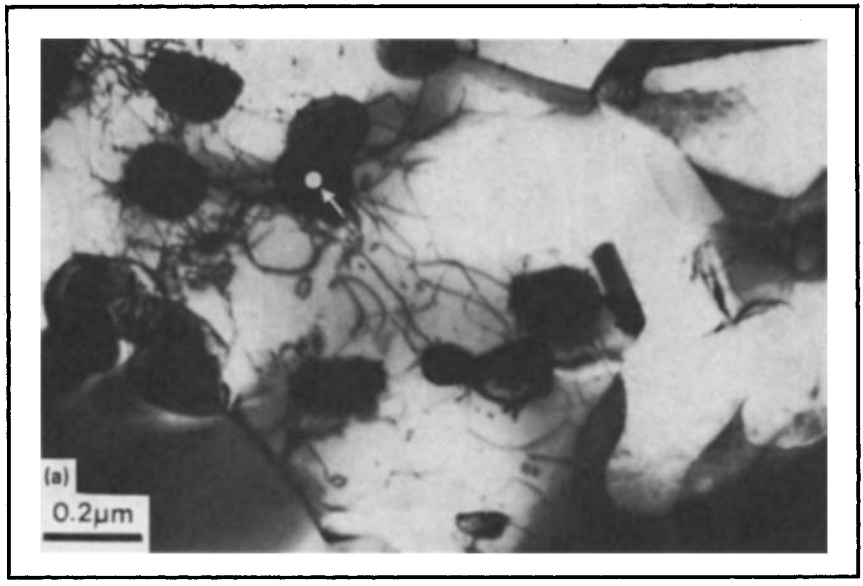

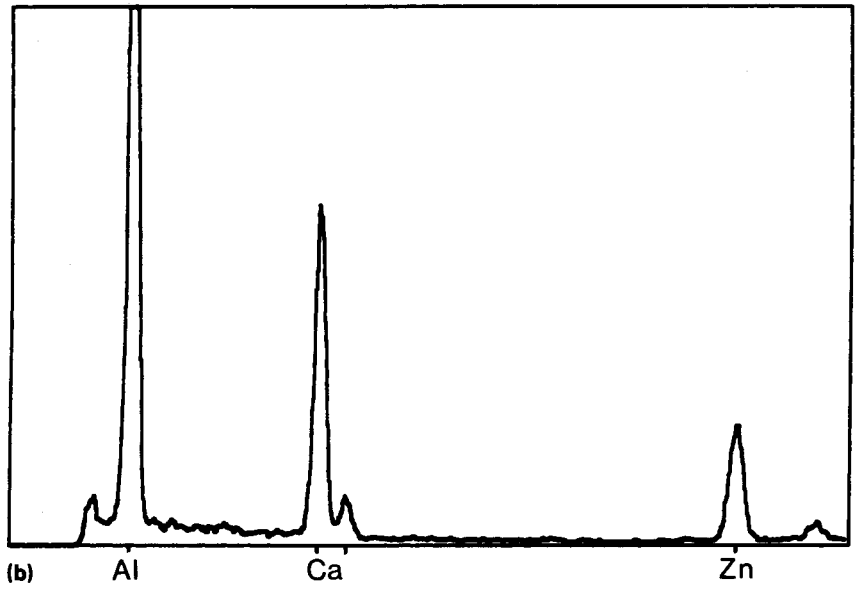

Fig. 53. (a) Energy dispersive microanalysis of a small particle in STEM. (b) The spectrum from the arrowed particle in a sample of an aluminum-calcium-zinc superplastic alloy. (Courtesy of Alcan International Ltd.)

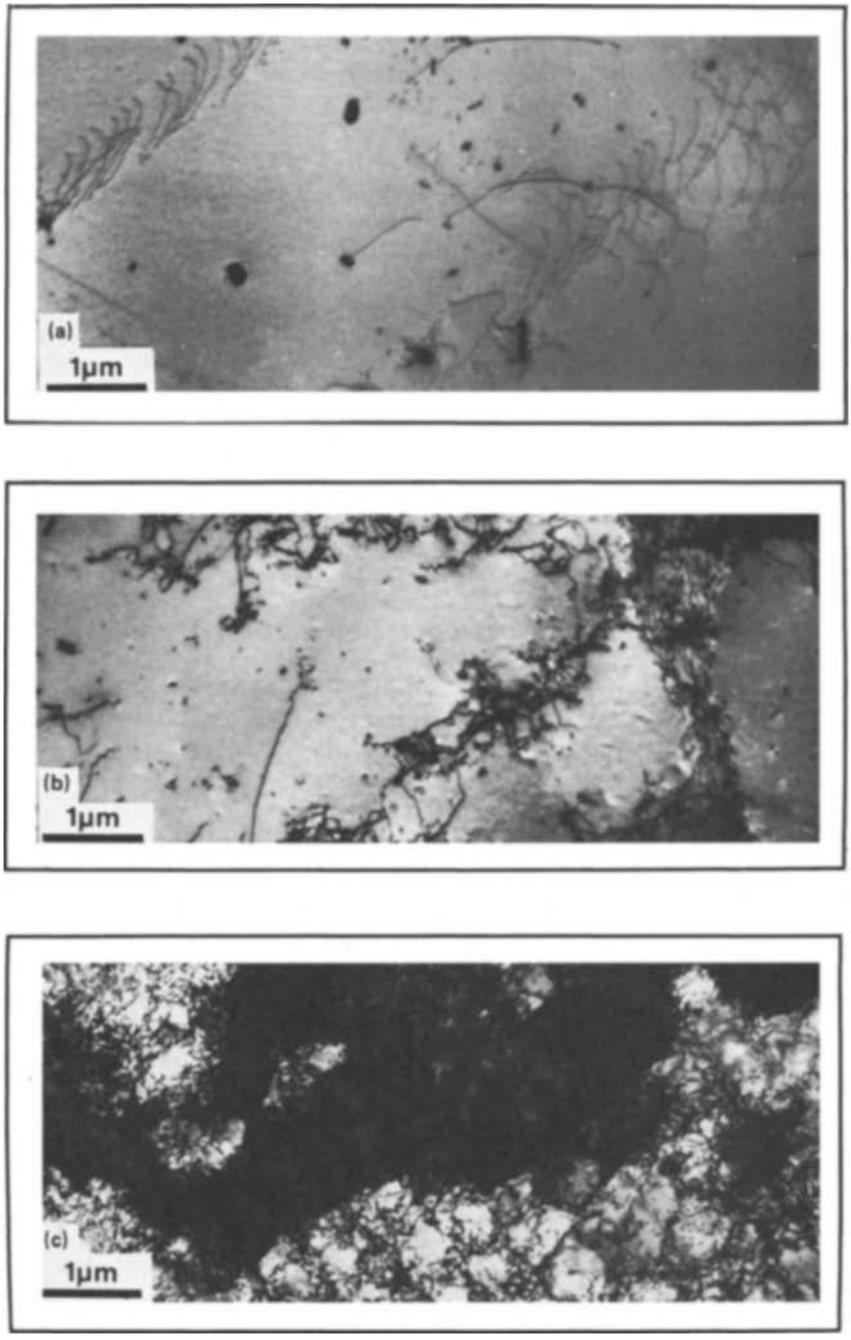

Fig. 54. A sequence of micrographs showing substructure development during cold rolling. (a) 2% reduction; isolated dislocations and slip bands. (b) 5% reduction; early stages of the development of cellular dislocation networks. (c) 60% reduction; well-developed cellular structure. (Courtesy of Alcan International Ltd.)

deformation of an aluminum alloy is usually associated with an increase in dislocation content. The nature and distribution of the resulting substructures depends on the extent, temperature, and rate of deformation, and also on other microstructural conditions such as grain size, particle size, and distribution.

In commercially pure aluminum (1XXX), a small amount of cold deformation generates a low density of essentially isolated dislocations (Fig. 54). As the deformation increases, dislocations increase in number and become concentrated in tangles along slip bands. With still further deformation, tangles increase in number and density, and a cellular network is developed, with tangles of dislocations surrounding relatively dislocation-free areas. In other alloy systems, similar changes in the dislocation substructure are observed, although they are modified by the presence of the alloying elements. Where coarse, hard particles ($\gtrsim$1 μm or $\gtrsim$0.04 mil) are present in an alloy before cold working, a high density of dislocations develops in their vicinity (Fig. 55). In alloys with a dense dispersion of finer particles ($\lesssim$0.1 μm or $\lesssim$0.004 mil), development of slip bands tends to be inhibited and a more homogeneous dislocation distribution is generated. If elements such as magnesium are present in solid solution during deformation, the dislocation mobility is reduced by interaction with the solute atoms. This results in a more rapid buildup of dislocations and is responsible for the more rapid work hardening observed in alloys such as 5182.

During the heat treatment of aluminum alloys, changes in properties create corresponding changes in microstructure. The detailed microstructural changes that occur depend on the particular alloy, its fabrication

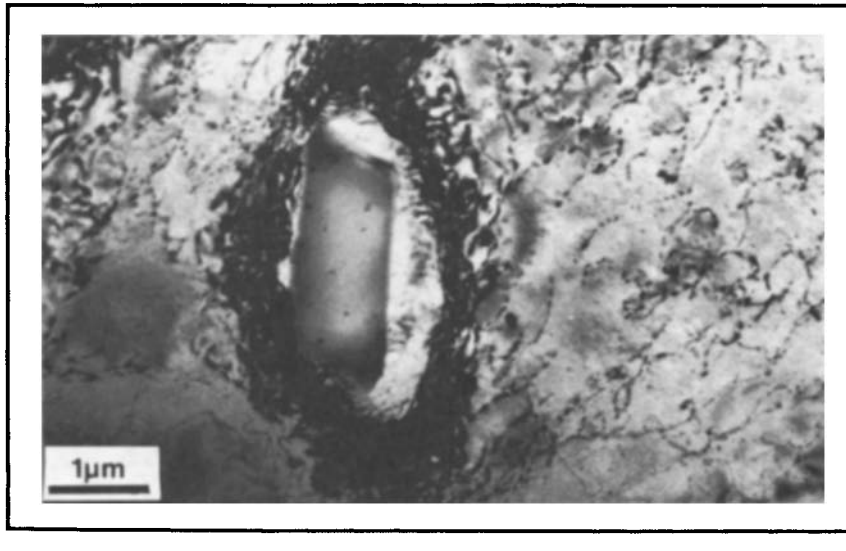

Fig. 55. Region of high local deformation in the vicinity of a coarse $FeAl_3$ particle in a cold rolled sample (20% reduction). (Courtesy of Alcan International Ltd.)

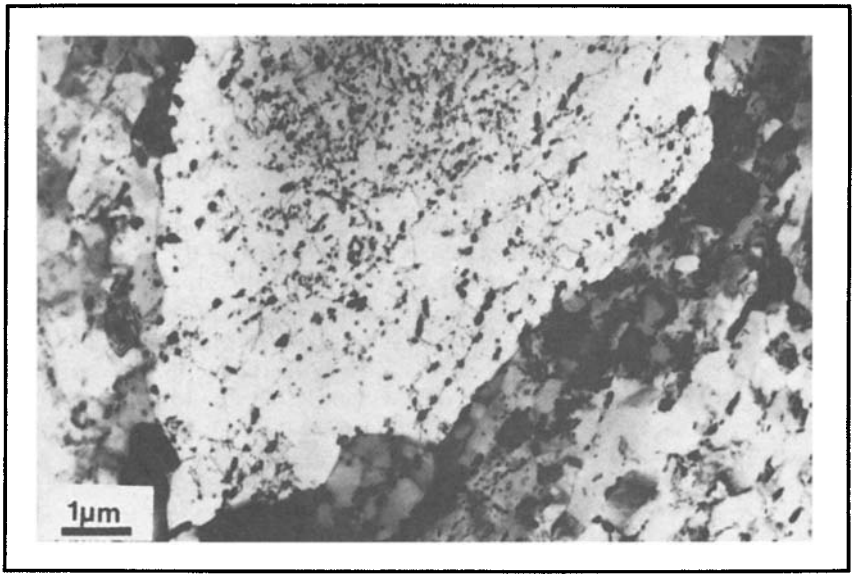

Fig. 56. An early stage of recrystallization of AA3003, showing a new grain growing into the substructure. The manganese-bearing precipitates interact strongly with the moving boundary and retard its progress. (Courtesy of Alcan International Ltd.)

history, and the temperature and duration of heat treatment. Commercial heat treatments can produce a number of microstructural changes including particle dissolution, particle coarsening, precipitation, changes in dislocation distribution and density, and the development and migration of subgrain and grain boundaries. In many cases, several of these phenomena occur simultaneously and often interact so that, for example, a precipitation process may significantly inhibit subgrain boundary migration.

In a number of alloy systems, the most important microstructural changes that occur involve changes in the dislocation and subgrain structures. As an example of the sort of change that can occur in this type of alloy, heat treatment of cold rolled (1XXX) alloy can be considered. At low temperatures ($\lesssim$100 °C or $\lesssim$212 °F), changes in dislocation density that occur are insignificant. At higher temperatures, dislocations become more mobile, rearranging themselves into lower energy configurations, and decrease in density by mutual annihilation or escape. As this recovery process proceeds, cellular dislocation tangles develop into subgrains with well-defined, low-misorientation boundaries. If the heat treatment temperature is sufficiently high, discontinuous recrystallization occurs, and new grains nucleate at favorable sites and grow rapidly to consume the dislocation and subgrain structures.

The recovery and recrystallization phenomena described here can occur in most aluminum alloys under the appropriate conditions. However, the kinetics and temperatures at which the microstructural changes are observed vary depending on the particular alloy and its condition. The sizes

and distribution of particles and the presence of elements in solid solution can significantly modify behavior during annealing.

A number of commercial alloys are supplied in the fully recrystallized condition (O temper) to be used in forming applications (1XXX, 3XXX, and 5XXX). For many applications of these alloys, a fine grain size is desirable, because a coarse-grained material causes surface roughening during forming (orange peel effect). Achieving a fine grain size often requires rigorous compositional and processing control. The number of potential recrystallization nuclei can often be related to the size and distribution of coarser particles in the alloy and can therefore be modified to some extent by homogenization. The growth of these potential nuclei into new grains is markedly affected by the size and distribution of finer dispersoid particles and, to a lesser extent, by the concentrations of elements in solid solution. Additions of manganese, chromium, and zirconium are made to a wide variety of alloys because the dispersions of particles that can be developed are useful for inhibiting the development and growth of new grains during recrystallization (Fig. 56). Inhibiting the growth of new grains can, under appropriate conditions, allow a fine grain size to develop; by delaying the growth of the first few grains that nucleate, other nuclei are afforded the time to develop.

If a sufficiently high volume fraction of suitable dispersoid particles can be generated, discontinuous recrystallization can be strongly inhibited. Alloys with such a microstructure have been developed and have a useful combination of formability and strength (Fig. 57). In the aluminum-calcium-zinc alloy of this type, a high volume fraction of fine particles can be achieved. This alloy has excellent superplastic particles.

In several important alloy systems, including aluminum-copper (2XXX), aluminum-magnesium-silicon (6XXX), and aluminum-zinc-magnesium

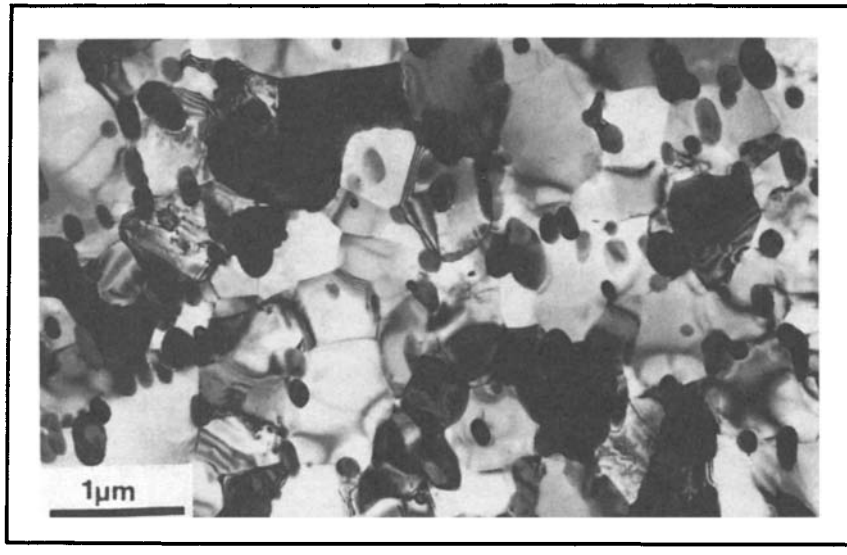

Fig. 57. An ultrafine grain size, particle-stabilized microstructure (×7125). (Courtesy of Alcan International Ltd.)

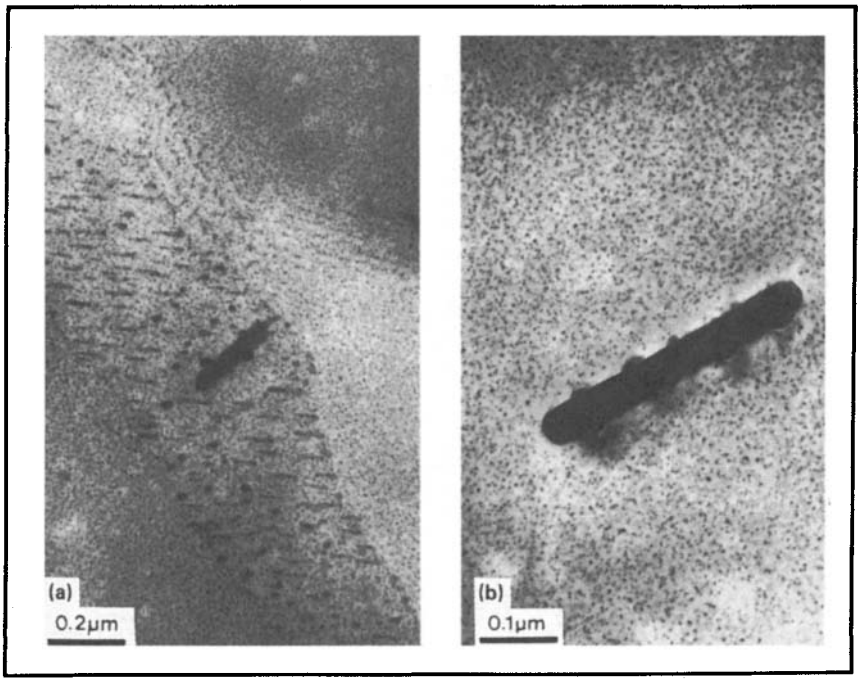

Fig. 58. Precipitation of $MgZn_2$ at heterogeneous sites: (a) on subgrain boundaries; and (b) on a manganese-bearing dispersoid particle. (Courtesy of Alcan International Ltd.)

(7XXX), the heat treatments that are normally used are designed to produce a very high density of fine GP zones or precipitates that strongly interact with dislocations and thereby increase the yield strength of the alloy. A typical heat treatment program for these alloy systems consists of an initial solution heat treatment, which dissolves particular alloying elements. This is followed by quenching, which is designed to retain a high level of the dissolved elements in supersaturated solid solution. In this condition, the alloy can be given an aging heat treatment to achieve the required temper, although for some alloys, particularly the aluminum-zinc-magnesium (7XXX) series, significant improvements in properties occur during a period of natural (room temperature) aging.

Microstructural changes that occur during quenching and aging treatments of these alloy systems have been extensively studied using TEM. During quenching of the solution treated alloy, dislocations and precipitates can develop. These dislocations generally appear as helices, loops, or tangles generated as a result of quenching strains and the condensation of excess vacancies. Dislocation density depends on the solution treatment temperature and the levels of elements in solution, as these factors affect vacancy concentration. Quench rate also is important, because this determines the temperatures and times during which the vacancies are

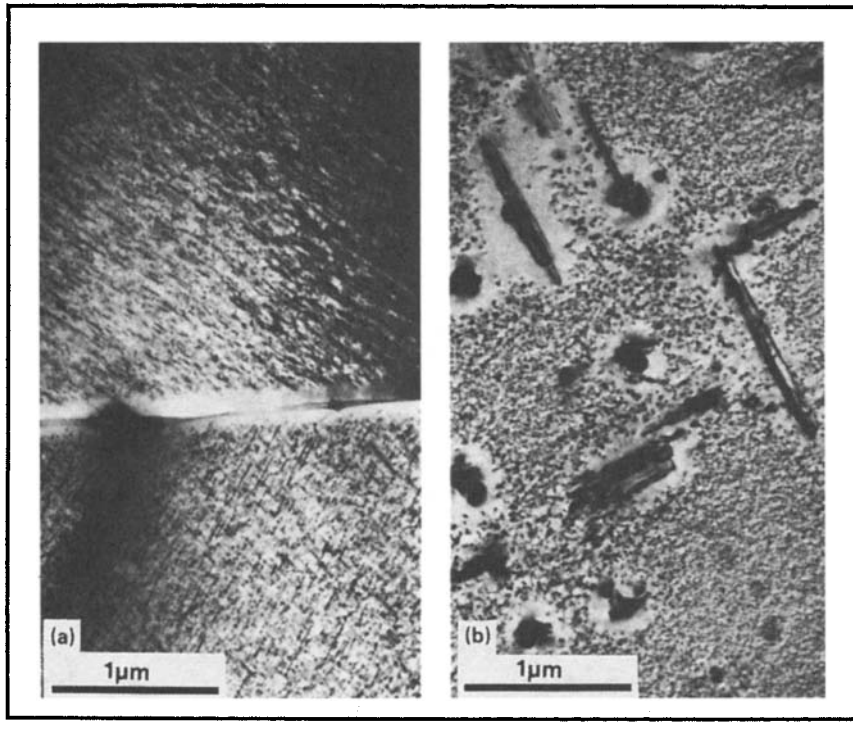

Fig. 59. Precipitate-free zones in samples that have been solution treated, slowly quenched, and then aged. (a) At a grain boundary in a 6XXX alloy. (b) Around manganese-bearing dispersoid particles in a 7XXX alloy. (Courtesy of Alcan International Ltd.)

mobile. Dislocations are also generated at constituent or dispersoid particles. These dislocations are produced by the differential contraction that occurs during the quench.

Ideally, to obtain maximum age hardening, all the dissolved elements should be retained in solid solution during the quench. This can be achieved by very rapid quenching, but in many commercial situations this is not possible, and lower cooling rates are used. As the cooling rate decreases, precipitate particles are found in increasing numbers. These precipitates nucleate at heterogeneous sites such as grain boundaries, dislocations, or on dispersoid particles. The most advantageous sites are populated first (Fig. 58). Thus, some grain boundaries, because of their misorientation, offer more favorable precipitate nucleation sites than others, and similarly some dislocations are preferred because of their edge or screw character. As well as acting as favorable nucleation sites for precipitation during quenching, subsequent aging reveals precipitate-free zones having widths related to the rate of quenching (Fig. 59a).

The presence of dispersoid particles in an alloy can substantially affect this quench-sensitive precipitation, partly because they modify the dis-

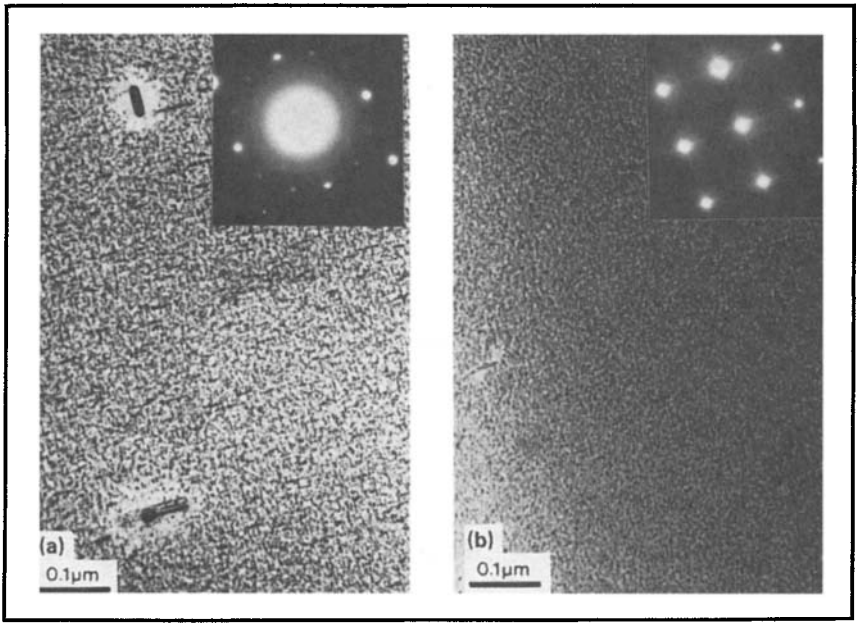

Fig. 60. Examples of heat treatable alloys that have been overaged to show the precipitates. (a) 6XXX alloy; needle-like β-Mg_2Si precipitates growing in $[100]_{Al}$ directions. The extra spots and streaks in the diffraction pattern are because of the precipitates and the associated strain fields. (b) An Al-4% Cu alloy; platelike θ′ precipitates arranged on $\{200\}_{Al}$ planes. The precipitates and strain fields again result in streaking in the diffraction pattern. (Courtesy of Alcan International Ltd.)

location structure of the quenched material. Also, dispersoid particles act as nucleation sites for precipitation in their own right (Fig. 59b). Manganese- and chromium-bearing phases are particularly potent dispersoids and readily nucleate precipitates during quenching, whereas coherent $ZrAl_3$ particles are less active nucleation sites.

During artificial aging, the elements in supersaturated solution begin to precipitate, and the strength of the material increases as the number and size of the precipitates increases. Eventually, the strength reaches a maximum value (the peak aged condition), and any further overaging leads to coarsening of the precipitates and a reduction in properties.

During age hardening, the precipitation phenomena that are observed can be quite complicated, and often several intermediate phases are involved. For example, in an aluminum-copper (2XXX) alloy, aging normally starts with the development of very fine plate-like GP zones in the matrix, on {001} planes. At this stage, GP zones are about 10 nm (100 Å) in diameter and consist of single planes of copper atoms. As aging proceeds, the GP zones transform to a coherent θ″ phase. Further aging results in successive transformation to semicoherent θ′ and eventually to plate-like particles of θ-$CuAl_2$. The aging kinetics and to some extent the precipitation sequence depend on the diffusion of copper atoms and is

influenced by the levels of vacancies and also the presence of traces of certain elements such as cadmium, indium, or tin that interact with the vacancies.

During the aging of aluminum-zinc-magnesium (7XXX) alloys, small spherical zones develop. As particles coarsen, they grow in preferred crystallographic orientations, and an overaged structure consists of elongated precipitates. Crystallographically distinct phases have been detected in these alloys including η', x, t, and η phases. The aging kinetics and the types of precipitate that are preferred are again influenced by the presence of trace elements. For example, a very low level of silver (<0.1 at.%) significantly accelerates the aging process. Aging of aluminum-magnesium-silicon (6XXX) alloys involves the nucleation and growth of rods of Mg_2Si that grow in [002], as shown in Fig. 60.

REFERENCES

1. Microstructure of Aluminum Alloys, *Metals Handbook, Atlas of Microstructures of Industrial Alloys,* 8th ed., Vol 7, American Society for Metals, 1972, p 242-272
2. Metallographic Technique for Aluminum Alloys, *Metals Handbook, Metallography, Structures and Phase Diagrams,* 8th ed., Vol 8, American Society for Metals, 1972, p 120-129
3. L.F. Mondolfo, *Aluminum Alloys—Structure & Properties,* Boston: Butterworths, 1976
4. R.W. Hertzberg, *Deformation and Fracture Mechanics of Engineering Material,* New York: John Wiley & Sons, 1976
5. J. Iglessis, C. Frantz, and M. Gantois, *Memoires Scientifique de la Revue de Metallurgie,* Vol 73, 1977, p 237
6. J. Iglessis, C. Frantz, and M. Gantois, *Memoires Scientifique de la Revue de Metallurgie,* Vol 74, 1978, p 93
7. H. Elias, Ed., *Stereology,* New York: Springer-Verlag, 1967
8. J.E. Vruggink, *Metals Engineering Quarterly,* Vol 49 (No. 9), Aug 1974, p 3-8
9. P.V. Blau, *Metallography,* Vol 9, 1976, p 257-271
10. D.S. Thompson, Metallurgical Factors Affecting High Strength Aluminum Alloy Production, *Metallurgical Transactions A,* Vol 6A, 1975, p 671
11. G.T. Hahn and A.R. Rosenfeld, Metallurgical Factors Affecting Toughness of Aluminum Alloys, 5th annual AIME meeting, May 1973
12. J.T. Staley, How Microstructure Affects Fatigue and Fracture of Aluminum Alloys, *Fracture Mechanics,* 1979, p 671-684
13. J.I. Goldstein and H. Yakowitz, Eds., *Practical Scanning Electron Microscopy,* New York: Plenum Press, 1975

SELECTED REFERENCES

- J.W. Edington, *Practical Electron Microscopy in Materials Science* (series of five monographs), London: Macmillan, 1976
- P.B. Hirsch, *et al, Electron Microscopy of Thin Crystals,* London: Butterworths, 1971
- J.W. Martin and R.D. Doherty, *Stability of Microstructure in Metallic Systems,* London: Cambridge University Press, 1976

Aluminum Properties and Physical Metallurgy
John E. Hatch editor, p 105-133
DOI: 10.1361/appm1984p105

CHAPTER 4

WORK HARDENING, RECOVERY, RECRYSTALLIZATION, AND GRAIN GROWTH*

Work, or strain hardening, is a natural consequence of most working and forming operations on aluminum and its alloys. Work increases the strengths achieved through solid solution and dispersion hardening. In heat treatable alloys, strain hardening not only supplements the strengths achieved by precipitation, but may also increase the rate of precipitation hardening (Chapter 5 in this Volume).

Products hardened by cold working can be restored to a fully soft, ductile condition by annealing. Annealing eliminates strain hardening, as well as the microstructural features that develop as a result of cold working. Some of the structural changes and the corresponding variation in properties that result from both strain hardening and annealing are the subjects of this chapter.

WORK HARDENING

Work hardening is used extensively to produce strain-hardened tempers of the non-heat treatable alloys (Table 1). The severely cold worked or full-hard condition (H18 temper) is usually obtained with cold work equal to about a 75% reduction in area. The H19 temper identifies products with substantially higher strengths because of greater reduction. The H16, H14, and H12 tempers are obtained with lesser amounts of cold working, and they represent three-quarter-hard, half-hard, and quarter-hard conditions, respectively. A combination of strain hardening and partial annealing is used to produce the H28, H26, H24, and H22 series of tempers; the products are strain hardened more than is required to achieve the desired properties and then are reduced in strength by partial annealing. A series of strain-hardened and stabilized tempers—H38, H36, H34, and H32—are used for aluminum-magnesium alloys. In the strain-hardened condition, these alloys tend to age soften at room temperature. Therefore, they are usually heated at a low temperature to complete the age-softening process and to provide stable mechanical properties and improved working characteristics.

Structural Changes. The deformation of aluminum and its alloys proceeds by normal crystallographic slip processes. Evidence of such slip can be seen in single crystals and in coarse-grained materials if surfaces are polished metallographically before deformation. The presence of slip

*This chapter was revised by a team comprised of B.A. Riggs, Kaiser Aluminum & Chemical Corp.; W.W. Berkey, Reynolds Metals Co.; D.B. Kulp, Anaconda Aluminum Co.; J.K. McBride, Alcoa Technical Center; and P.R. Sperry, Consolidated Aluminum Corp. The original chapter was authored by W.A. Anderson, Alcoa Research Labortories.

Table 1. Temper Designations for Strain-Hardened Alloys

Temper	Description
F	**As-fabricated.** No control over the amount of strain hardening; no mechanical property limits.
O	**Annealed, recrystallized.** Temper with the lowest strength and greatest ductility.
H1	**Strain hardened.** H12, H14, H16, H18. The degree of strain hardening is indicated by the second digit and varies from quarter-hard (H12) to full-hard (H18), which is produced with approximately 75% reduction in area. H19. An extra-hard temper for products with substantially higher strengths and greater strain hardening than obtained with the H18 temper.
H2	**Strain hardened and partially annealed.** H22, H24, H26, H28. Tempers ranging from quarter-hard to full-hard obtained by partial annealing of cold worked materials with strengths initially greater than desired.
H3	**Strain hardened and stabilized.** H32, H34, H36, H38. Tempers for age-softening aluminum-magnesium alloys that are strain hardened and then heated at a low temperature to increase ductility and stabilize mechanical properties.
H112	**Strain hardened during fabrication.** No special control over amount of strain hardening but requires mechanical testing and meets minimum mechanical properties.
H321	**Strain hardened during fabrication.** Amount of strain hardening controlled during hot and cold working.
H116	Special strain hardened, corrosion-resistant temper for aluminum-magnesium alloys.

bands and deformation bands in some alloys can also be demonstrated by heating or aging practices that induce precipitation along these bands. Figure 1 shows examples of this and of the changes in grain shape that accompany rolling deformation.

On a still finer scale, deformation produces a defect structure that can be detected by transmission electron microscopy (Chapter 3 in this Volume). The effects of varying amounts of cold work on the fine structure of 99.99% aluminum are shown in Fig. 2. These electron micrographs show the accumulation of dislocations that combine to form the boundaries of a cellular substructure. More severe cold working produces even higher dislocation densities and a further reduction in the size of the dislocation cell structure. Lattice distortions associated with dislocations and interaction stresses between dislocations are the principal sources of strain hardening resulting from cold work.

Mechanical Properties. The internal structural changes described previously produce substantial changes in the mechanical properties of aluminum and its alloys. Tensile properties are among those most affected. Work-hardening curves for several non-heat treatable alloys (Fig. 3) illustrate the increase in strength that accompanies cold work. This increase is obtained at the expense of ductility, as measured by the percentage of elongation in the tensile test and by reduced formability in operations such as bending and drawing. For this reason, the strain-hardened tempers are not usually used where high ductility and formability are required. Aluminum alloy beverage cans, readily formed by a unique drawing and ironing process using 3004-H19 as the starting material, are an exception.

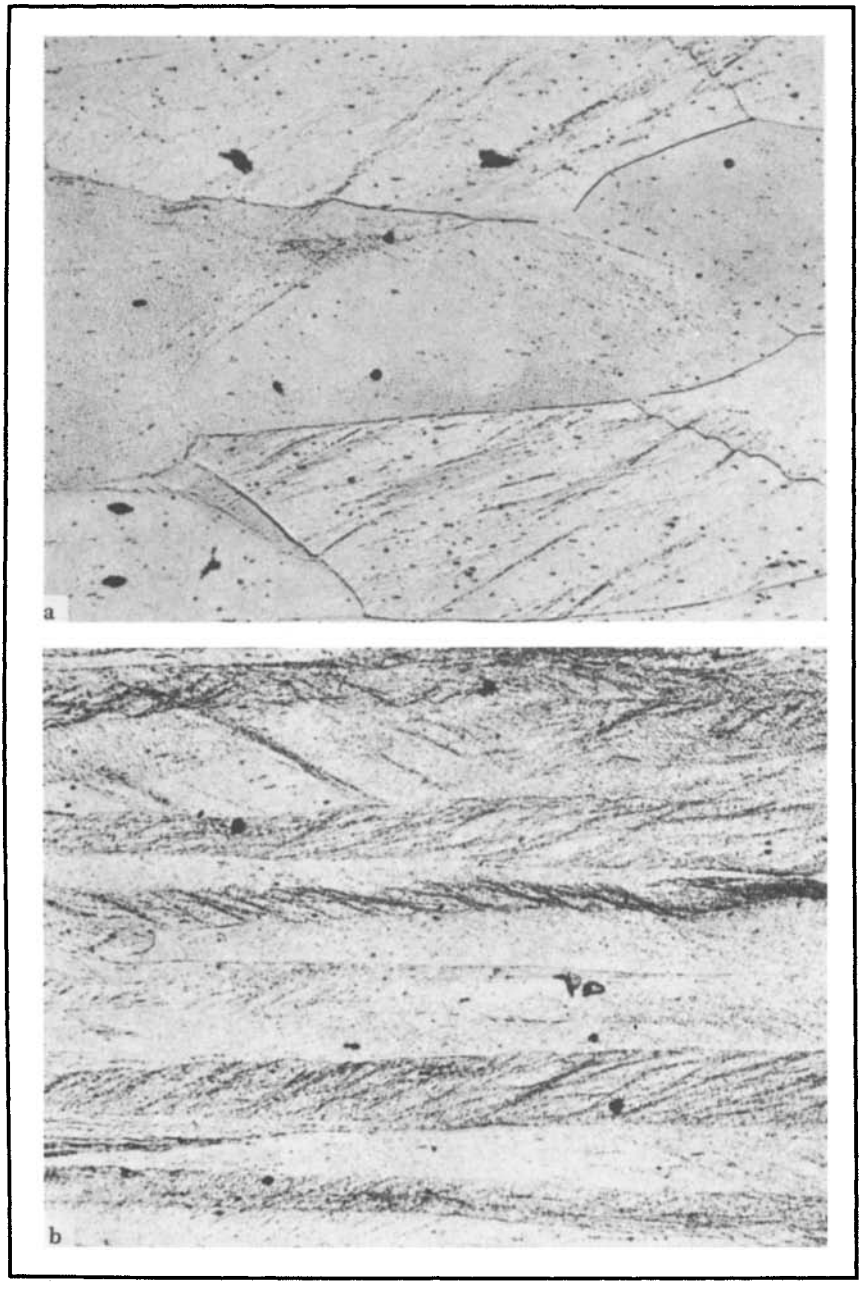

Fig. 1. Deformation bands in Al-2% Cu alloy. (a) 40% reduction; (b) 80% reduction. (100×)

The effects of increasing alloy content on the tensile properties and work-hardening characteristics of aluminum are also illustrated in Fig. 3. The two principal types of non-heat treatable alloys represented are (1)

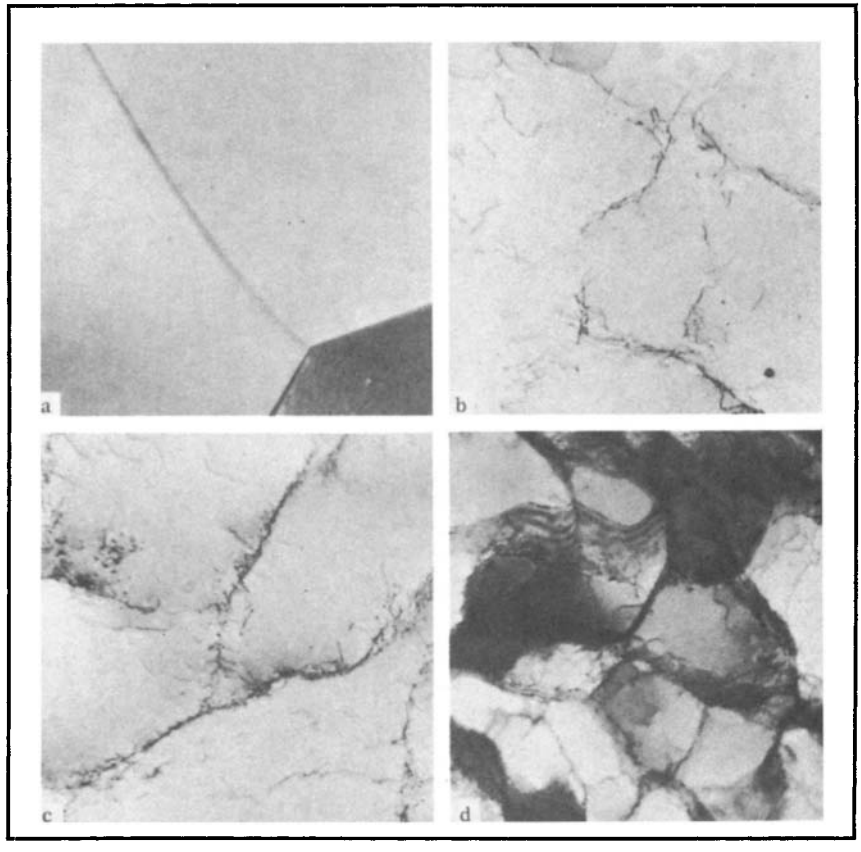

Fig. 2. Transmission electron micrographs showing the effects of cold work on the dislocation structure of 99.99% aluminum sheet. (a) Annealed; (b) 2% reduction by cold rolling; (c) 7% reduction by cold rolling; (d) 30% reduction by cold rolling. 14,560×. (Courtesy of Aluminum Company of America)

alloys containing magnesium, which is largely in solid solution in aluminum, and (2) an alloy containing manganese that is largely out of solution and distributed as a finely divided, dispersed aluminum-manganese constituent. Figure 3 shows that magnesium in solid solution hardens aluminum more effectively than an equal percentage of manganese as a dispersed second phase. Also, alloying with magnesium or manganese increases strain hardening. Electron micrographic studies suggest that the greater strain hardening of alloyed aluminum is related to an increase in the density of dislocations.

Cold working also increases shear strength, creep strength at low temperatures, and smooth-specimen fatigue strength. It has little effect on notch fatigue strength, but increases notch tensile strength in about the same proportion as smooth-specimen tensile strength.

The work-hardening characteristics of the annealed and T4 tempers of the heat treatable alloys (Chapter 5 in this Volume) are similar to those

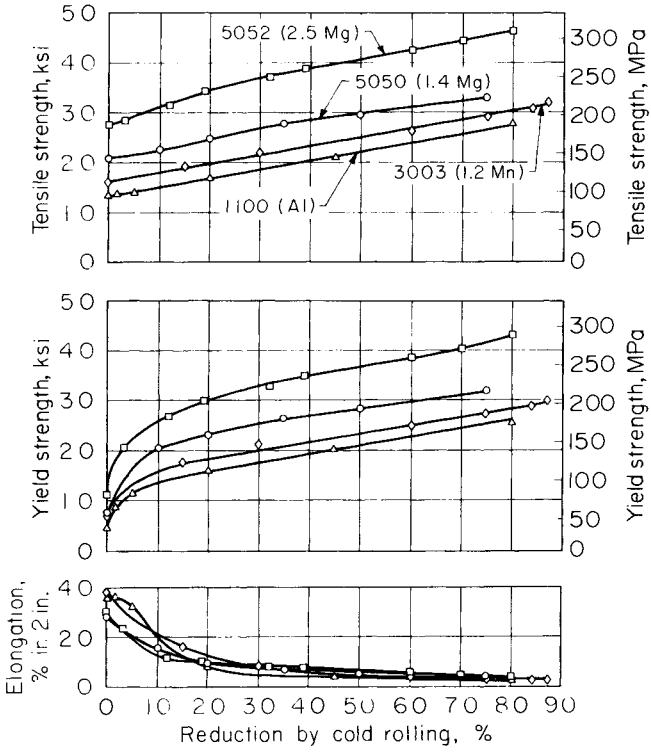

Fig. 3. Work-hardening curves for alloys 1100, 3003, 5050, and 5052. (Courtesy of Aluminum Company of America)

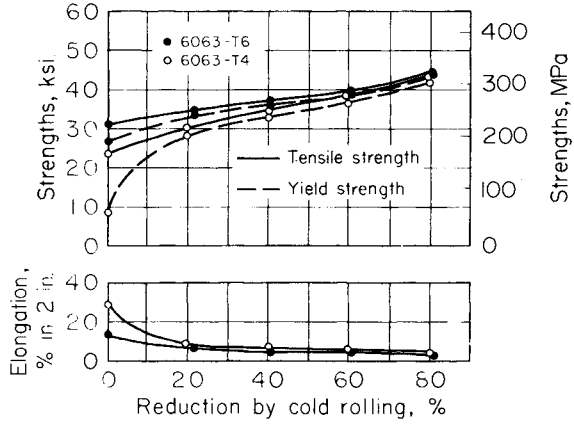

Fig. 4. Work-hardening curves for 6063-T4 and 6063-T6 sheet. (Courtesy of Aluminum Company of America)

of the non-heat treatable alloys. The work-hardening curve for the T4 temper of an aluminum-magnesium-silicon alloy (Fig. 4) is characterized by the same rapid, initial increase in yield strength shown by non-heat treatable alloys (Fig. 3), followed by a more gradual increase in yield strength, roughly paralleling the change in tensile strength. In the artificially aged T6 temper (Fig. 4), the increase in yield strength and tensile strength with cold working is less than that for the T4 temper, except at very high strains.

Limited use is made of strain hardening to increase the strength of heat treatable alloys. The principal applications are in extruded and drawn products such as wire, rod, and tube. Heat treated aluminum-magnesium-silicon alloys are used extensively in such products, which are sometimes drawn after heat treatment to increase strength and improve surface finish. The low ductility and poor workability of other artificially aged, heat treatable alloys have restricted cold working as a procedure for obtaining higher strengths. In the aluminum-copper alloys, however, small amounts of cold work are used after solution heat treatment to obtain increased response during artificial aging (Chapter 5 in this Volume).

Work-hardening curves for annealed, recrystallized aluminum alloys, when plotted as a function of true stress and true strain, are approximately parabolic and usually can be described by:

$$\sigma = k\epsilon^n \qquad \text{(Eq 1)}$$

where σ is the true stress, k is the stress at unit strain, ϵ is the true or logarithmic strain,* and n is the strain-hardening exponent. A plot of this relationship is shown in Fig. 5 for several annealed aluminum alloys.

As a close approximation, all of the alloys obey Eq 1 over the range of strains used here. The slopes of the lines may decrease as the initial strengths of the alloys increase, indicating a decrease in the value of n. At the same time, there is an increase in k. Measurements for the curves shown in Fig. 5 indicate that n decreases from 0.24 to 0.17 as k increases from 146 to 479 MPa (21 to 69 ksi). Strain hardening parameters are shown in the table below:

Alloy	Strain hardening exponent (n)	Stress at unit strain (k) MPa	ksi
1100-0	0.242	146	21.1
3003-0	0.242	188	27.2
6061-0	0.209	224	32.5
5052-0	0.198	281	40.7
5454-0	0.189	340	49.3
5086-0	0.193	368	53.3
5456-0	0.178	479	69.4

Source: Aluminum Company of America.

*The true or logarithmic strain is usually defined as $\ln A_0/A_f$, where A_0 and A_f are initial and final cross-sectional areas of the sample. In sheet rolling without widening, the logarithmic strain simplifies to $\ln T_0/T_f$, where T_0 and T_f are the initial and final sheet thicknesses.

Rates of strain hardening can be obtained from the first derivative of Eq 1:

$$\frac{d\sigma}{d\epsilon} = nk\epsilon^{n-1} \qquad \text{(Eq 2)}$$

Non-heat treatable alloys initially in a cold worked or hot worked condition have rates of strain hardening substantially below those of material in the annealed temper. For the cold worked tempers, this difference is caused by the strain necessary to produce the temper. If this strain equals ϵ_0, then the equation for strain hardening becomes:

$$\sigma = k(\epsilon_0 + \epsilon)^n \qquad \text{(Eq 3)}$$

A similar situation exists for products initially in the hot worked condition. The strain hardening resulting from hot working or forming is assumed to be equivalent to that achieved by a certain amount of cold work. From the tensile properties of the hot worked product, the amount of equivalent cold work can be estimated, using the work-hardening curve for the annealed temper. By such procedures, it is usually possible to calculate work-hardening curves for hot worked products that are in reasonable agreement with those for annealed products.

The work-hardening characteristics of aluminum alloys vary considerably with temperature. At cryogenic temperatures, strain hardening is greater than it is at room temperature. Figure 6 shows the work-hardening characteristics of alloy 1100 rolled at room temperature and at −195 °C (−320 °F). The gain in strength by working at −195 °C (−320 °F) is about 40%, but is accompanied by a significant reduction in ductility.

Studies have shown that the yield strength of aluminum alloys increases as strain rates increase. These effects are not large at room temperature; rate changes of several orders of magnitude are required to produce an appreciable increase in yield strength (Ref 1). At elevated temperatures,

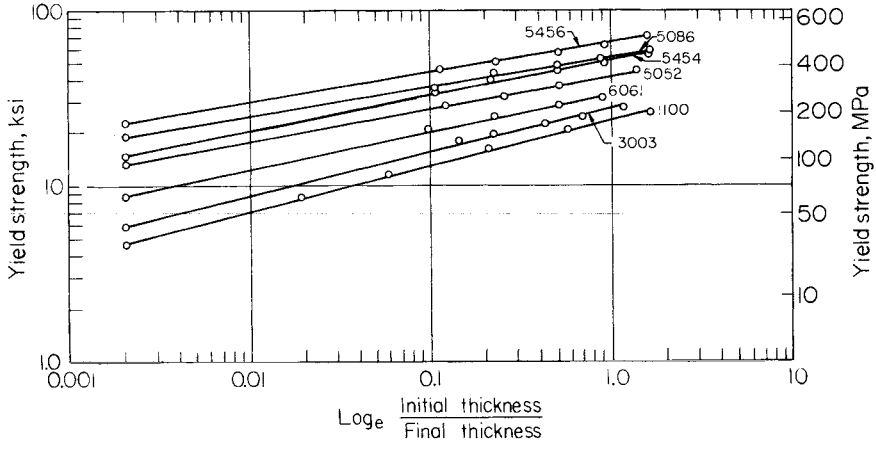

Fig. 5. Strain-hardening curves for annealed aluminum alloys plotted according to the relation in Eq 1, and substituting yield strength for true stress. (Courtesy of Aluminum Company of America)

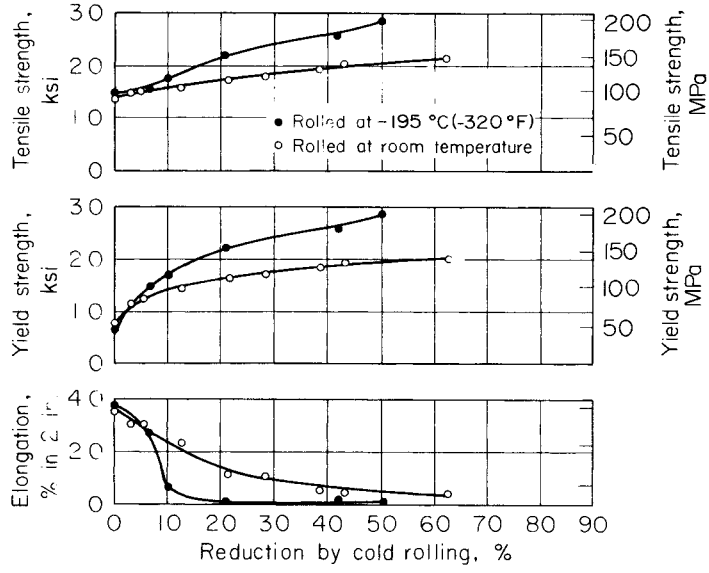

Fig. 6. Work-hardening curves for 1100-0 sheet rolled at room temperature and at −195 °C (−320 °F). (Courtesy of Aluminum Company of America)

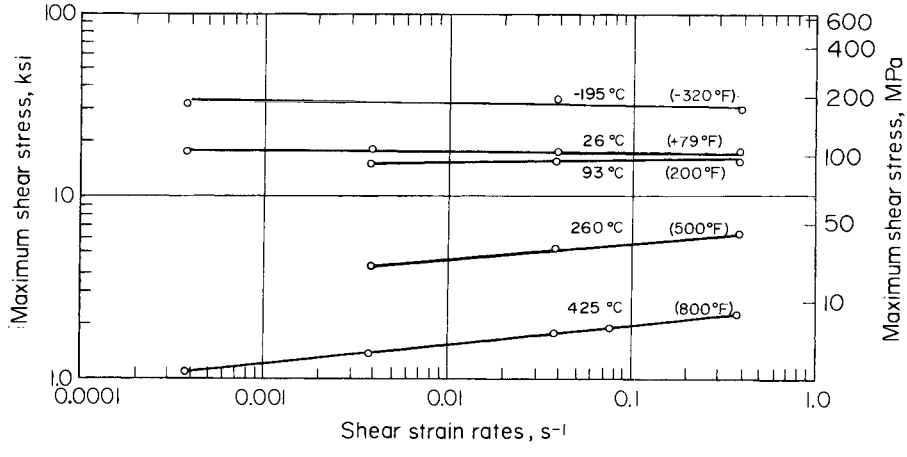

Fig. 7. Effects of strain rate and temperature on the maximum shear stress for 3003-0. (Courtesy of J.M. Waller of the Aluminum Company of America)

the relative increase in yield strength is much larger. This is illustrated in Fig. 7, where the maximum shear stress in torsion is plotted against strain rate for the aluminum-manganese alloy 3003 at various temperatures. Although the yield strength of aluminum increases as strain rates increase, this should not be interpreted as a substantial, or necessarily permanent, increase in strain hardening. Except for shock loading, the effects are small and may be offset by recovery phenomena resulting from the heat generated by rapid plastic deformation.

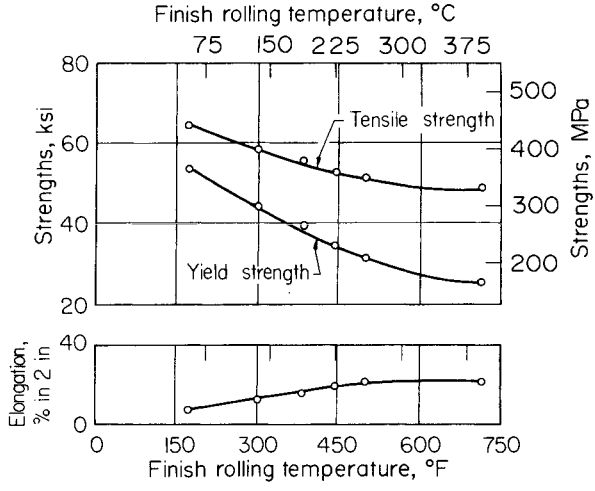

Fig. 8. Effects of hot rolling temperature on the tensile properties of 5456 alloy plate rolled from 19 to 13 mm (0.75 to 0.50 in.) thickness.

Deformation at Elevated Temperature. The work-hardening characteristics of aluminum alloys at elevated temperatures vary both with temperature and with strain rate (Ref 2). Figure 8 shows the strengths achieved by rolling an Al-5% Mg alloy at various temperatures. Strain hardening decreases progressively as rolling temperature increases, until at 370 °C (700 °F) and above no effective strain hardening occurs. These results are similar to those observed in many commercial operations, although the exact strength-temperature relationship varies with the method and amount of deformation, time at temperature, and other factors. Forgings, extrusions, and some tempers of plate are important product forms that receive their final shaping at elevated temperatures.

The mechanism of plastic deformation of aluminum and some aluminum alloys during elevated-temperature working has been extensively studied (Ref 3 and 4). Strain hardening diminishes at elevated temperatures because softening, via thermally activated recovery, occurs rapidly during and immediately succeeding deformation. Studies have shown that such dynamic recovery results in the formation of a subgrain structure that is similar to the structure resulting from heating a previously cold worked aluminum (Fig. 9b and 9c). Deformation at constant temperature and strain rate (steady state) results in a subgrain size that is related to the rate and temperature of working. The resistance to elevated-temperature deformation is inversely related to the size of the subgrains that form. Smaller subgrain sizes, and hence, greater elevated-temperature flow stresses, result from lower working temperatures or faster deformation rates (Ref 3).

Rapid cooling after elevated-temperature working may forestall recrystallization and thereby preserve the previously formed subgrain structure. When this occurs, the subsequent room temperature strength of the hot worked aluminum is a function of subgrain size. Figure 10 illustrates

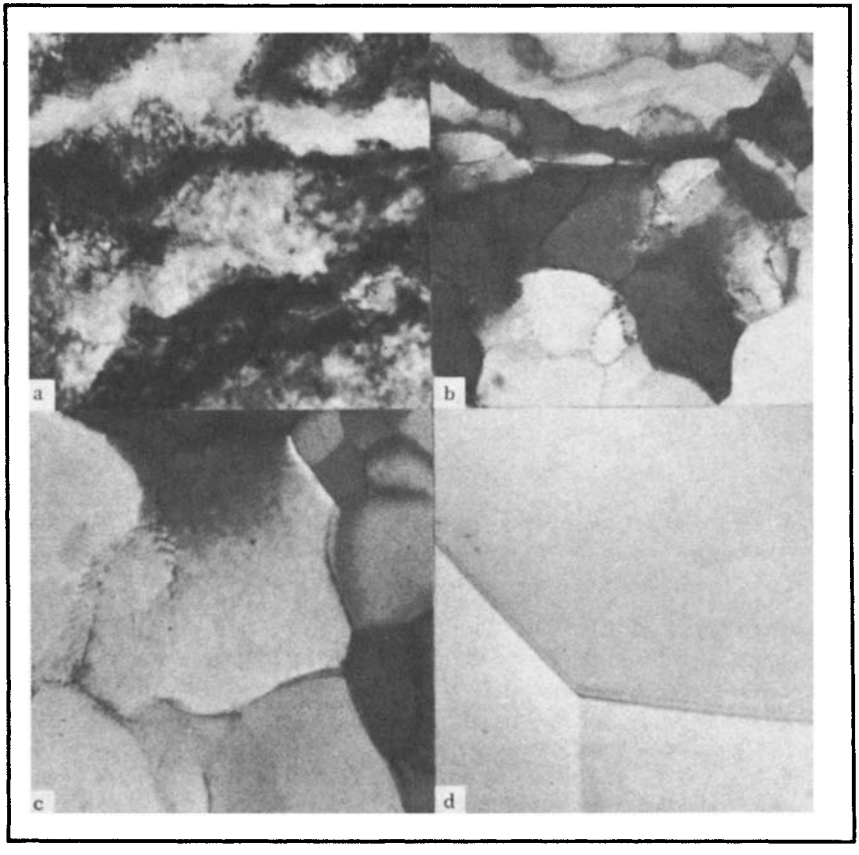

Fig. 9. Transmission electron micrographs of Al-5% Mg alloy sheet cold rolled 75% and annealed for various times at 345 °C (650 °F). (a) As-rolled; (b) 1 min; (c) 5 min; (d) 1 h. (21,420×)

this in terms of hardness for aluminum and some aluminum-magnesium binary alloys. Subgrain, or substructure, hardening of this sort can add an increment of strength in excess of that of the same alloy in a completely recrystallized condition.

Physical and chemical properties of aluminum and its alloys are affected by strain hardening. Usually, however, the changes are small and of academic interest only. In some instances, notably the resistance to stress corrosion of certain alloys and alloy types (Chapter 7 in this Volume), the effects of strain hardening are of commercial importance.

The effect of strain hardening on the electrical conductivity of aluminum is small and generally less than that of alloy in solid solution or of the heat treatments used for many aluminum alloys. The electrical conductivity of conductor-grade aluminum is decreased from a typical value of 63% IACS in the annealed condition to 62.5% in the strain-hardened H19 temper.

Density is also decreased slightly by cold working. This change may

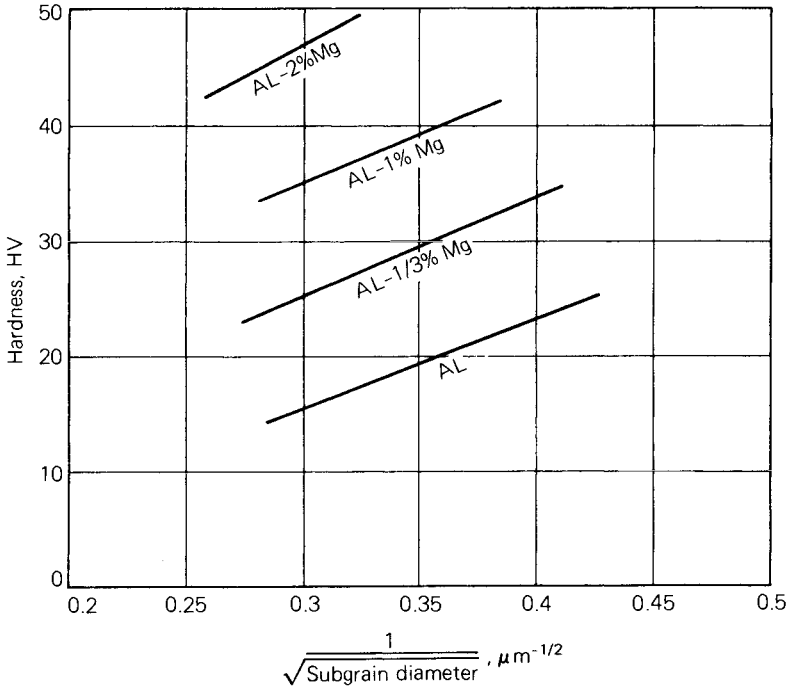

Fig. 10. Relationship between room temperature hardness and subgrain size for aluminum and aluminum-magnesium alloys. (Ref 4)

amount to 0.2% with severe cold working of aluminum (Ref 5). Little is known about the density changes of various alloys through cold working. The data in Table 2 show that the change in density of cold worked aluminum-magnesium alloys is greater than that of unalloyed aluminum. This suggests that magnesium increases the number of dislocations and point defects produced by the cold working of aluminum.

The dislocations and point defects remaining after cold working increase the internal strain energy. This stored energy, which provides the driving force for the structural changes that occur during annealing, can be measured by calorimetric techniques. Measurements indicate that the stored energy increases progressively with cold working and is about 13 or 16 kJ/kg-atom (3 or 4 cal/g-atom) for moderately to severely deformed aluminum (Ref 6).

The elastic moduli of aluminum and its alloys are affected only slightly by cold working. These slight changes result principally from variations in texture and crystal anisotropy. As a result, elastic constants such as shear modulus and modulus of elasticity have the same engineering value in both annealed and cold worked tempers.

Anelastic properties, such as internal friction and damping, are influenced by strain hardening. Damping usually is greater in annealed aluminum alloys than in strain-hardened alloys. Results vary, however, with the conditions of testing and the applied stress. Where the applied stress is large and mechanical hysteresis is observed, annealed alloys damp bet-

Table 2. Densities of Cold Worked Aluminum-Magnesium Alloys

Alloy	Density, Annealed, g/cm³	Density, Annealed, lb/in.³	Density, Cold rolled, 80%, g/cm³	Density, Cold rolled, 80%, lb/in.³	Change, %
Al	2.7011	0.97583	2.7006	0.97565	−0.018
Al-1 Mg	2.6883	0.97121	2.6877	0.97099	−0.022
Al-2.4 Mg	2.6696	0.96445	2.6687	0.96413	−0.034
Al-4.4 Mg	2.6450	0.95556	2.6430	0.95484	−0.076

Source: Courtesy of Aluminum Company of America.

ter than strain-hardened alloys. But when applied stresses are very small and mechanical hysteresis is not a factor, strain hardening may increase damping.

The effects of strain hardening on the chemical properties of aluminum are usually quite small. Substantial effects can often be traced to secondary reactions from the effects of strain hardening on the metallurgical structure of the alloy. Aluminum alloys are expected to react with specific environments at an increased rate, because of the greater strain energy stored in the metals by deformation. But, evidence shows that cold work has little effect on the corrosion resistance of most aluminum alloys in a variety of exposure conditions.

In some special situations, the corrosion resistance of certain aluminum alloys may be decreased by cold working (Chapter 7 in this Volume). Cold working can cause residual tensile stresses and consequent stress-corrosion cracking of some heat treatable alloys exposed to corrosive environments. Cold work also may induce or accelerate grain boundary precipitation in the non-heat treatable aluminum-magnesium alloys; alloys containing more than 4% magnesium may thereby become susceptible to stress-corrosion cracking. Generally, only long aging at room temperature or heating at elevated temperatures produces sufficient grain boundary precipitation to induce susceptibility to stress-corrosion cracking. However, in most commercial aluminum-magnesium alloys, the amount of cold work is intentionally limited; special corrosion-resistant tempers are recommended.

ANNEALING

The dislocation structure resulting from cold working of aluminum is less stable than the strain-free, annealed state to which it tends to revert. In zone-refined aluminum, this reversion may take place at room temperature. Lower purity aluminum and commercial aluminum alloys undergo detectable structural changes only with annealing at elevated temperatures. Accompanying the structural reversion are changes in the various properties affected by cold working. These changes occur in several stages, according to temperature or time, and have led to the concept of different annealing mechanisms or processes. The first of these, occurring at the lowest temperatures and shortest times of annealing, is known as the recovery process.

Recovery. Structural changes occurring during the early stages of the recovery process usually cannot be detected by ordinary metallographic

techniques. Evidence obtained by x-ray diffraction and with the transmission electron microscope shows that during recovery, dislocations are greatly reduced in number and often rearranged into a cellular subgrain structure. Figure 9 shows this sequence of recovery in an Al-5% Mg alloy. This process of recovery is sometimes referred to as polygonization. With increasing time and temperature of heating, polygonization becomes more nearly complete and the subgrain size gradually increases. In this stage, many of the subgrains have boundaries that are completely free of dislocation tangles.

The decrease in dislocation density caused by recovery-type annealing produces a decrease in strength and other property changes. The effects on the tensile properties of 1100 alloy are shown in Fig. 11. At temperatures through about 230 °C (450 °F), softening is accomplished by a recovery mechanism. The process is characterized by an initial rapid decrease in strength and a slow, asymptotic approach to a lower strength, the higher the temperature. Other aluminum alloys behave similarly, although the response to recovery annealing varies with composition. The aluminum-magnesium alloys show a particularly marked response.

Recovery annealing is also accompanied by changes in other properties

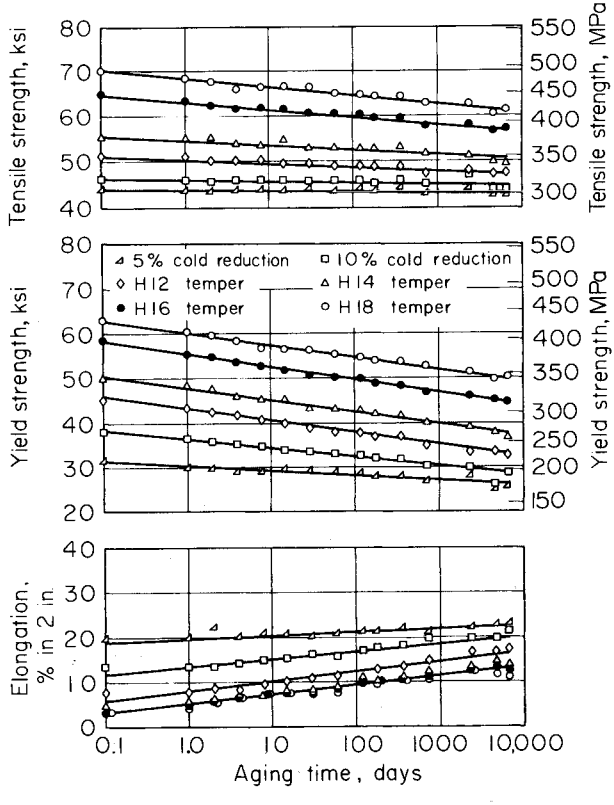

Fig. 11. Isothermal annealing curves for 1100-H18 sheet. (Courtesy of Aluminum Company of America)

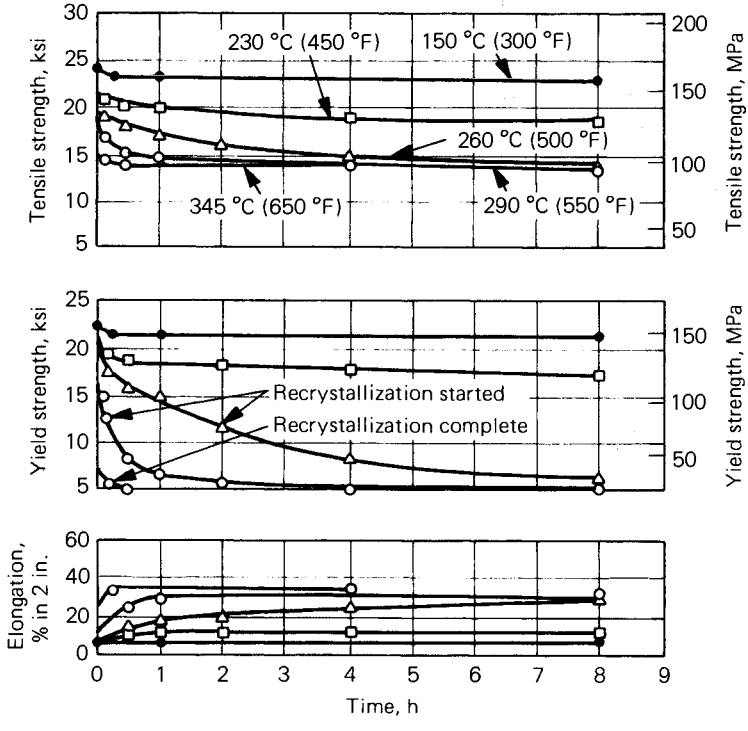

Fig. 12. Age softening of strain-hardened Al-6% Mg sheet. (Courtesy of Aluminum Company of America)

of cold worked aluminum. Electrical conductivity increases, while x-ray line broadening, internal stresses, and stored energy decrease. The relative change is not the same for each property. Generally, some property change can be detected at temperatures as low as 93 to 120 °C (200 to 250 °F). The change increases in magnitude with increasing temperature. Complete recovery from the effects of cold working is obtained only with recrystallization.

Strain-hardened aluminum-magnesium alloys are a special commercial problem, because they tend to age soften at room temperature. Figure 12 shows this effect for an Al-6% Mg alloy. Age softening increases with increasing cold work and magnesium content.

Electron micrographic studies of highly strained aluminum-magnesium alloys reveal no change in dislocation density during age softening. Apparently, strain energy is released through the interaction and relaxation of tangled dislocations without causing an obvious decrease in their numbers.

Because age softening complicates the guaranteeing of minimum properties for strain-hardened aluminum-magnesium alloys, industry practice is to accelerate age softening and increase ductility by heating the alloy briefly from 120 to 175 °C (250 to 350 °F). The properties achieved are quite stable. These strain-hardened tempers are identified by H3*x* (Table 1).

Recrystallization is characterized by the gradual formation and appearance of a microscopically resolvable grain structure (Fig. 13). The new structure is largely strain free, with few if any dislocations within the grains and no concentrations at the grain boundaries. Recrystallization occurs with longer times or higher heating temperatures than do the recovery effects described in the preceding section, although some overlapping of the two processes is usual. Metallographic studies indicate that the recrystallized grains are formed by the growth of selected subgrains in the deformed and recovered structure (Ref 7).

Recrystallization depends upon time and temperature (Ref 8). Times for the beginning and end of recrystallization in 1100 sheet are shown in

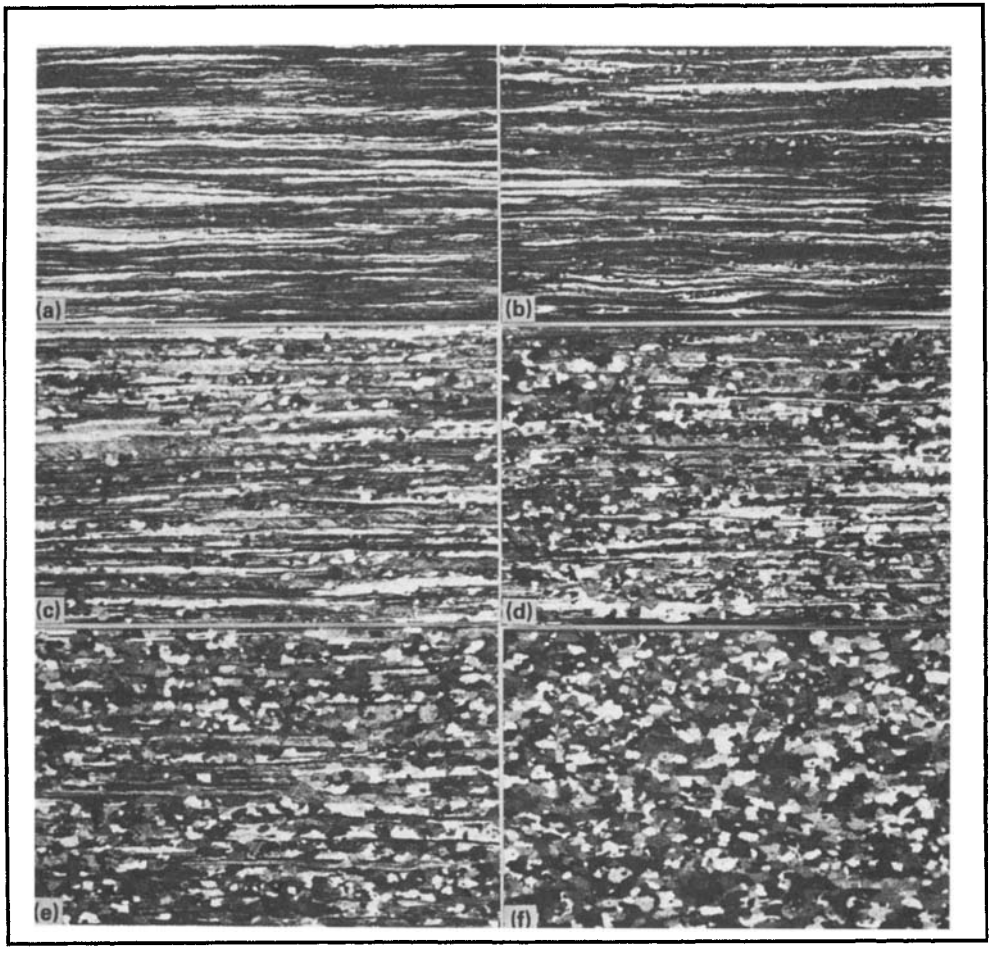

Fig. 13. Polarized light micrographs showing the progress of recrystallization in 5182-H19 sheet annealed at 245 °C (470 °F); (a) As-rolled; (b) after 1 h at 245 °C (470 °F); (c) after 2 h; (d) after 3 h; (e) after 4 h; and (f) after 7 h. Barkers etch, 120×. (Courtesy of B.A. Riggs, Kaiser Aluminum & Chemical Corp.)

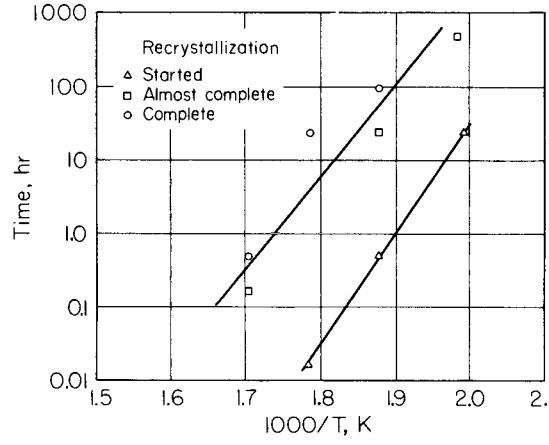

Fig. 14. Time-temperature relations for the recrystallization of 1100-H18 sheet. (Courtesy of Aluminum Company of America)

Fig. 14 as a function of annealing temperature. This relationship can be expressed by a rate equation of the type:

$$\frac{1}{t} = ke^{-a/T} \qquad \text{(Eq 4)}$$

where t is time, T is the absolute temperature, e is the base of natural logarithms, and k and a are material-dependent variables unique to each alloy and its condition. The term a may be replaced by Q/R, where R is the gas constant and Q is an energy term, similar to an activation energy. The magnitude of Q has been reported to be about 214 kJ/mol for commercially pure aluminum (Ref 9). Aluminum alloys generally show good agreement with Eq 4, except when secondary reactions, such as the solution or precipitation of intermetallic phases at annealing temperatures, interfere.

The amount and temperature of working also affect recrystallization. Generally, a greater amount of cold work reduces the time and the temperature for recrystallization. Information on the effects of working temperatures is not precise, but recrystallization becomes more difficult as the working temperature is raised. Alloys worked at temperatures above about 400 °C (750 °F) are usually very difficult to recrystallize.

Composition also influences the recrystallization process. This is particularly true when various elements are added to extreme-purity aluminum; almost any added impurity or alloying element in solid solution raises the recrystallization temperature substantially. When the solubility limit of the added element in aluminum is exceeded, however, the effects on recrystallization can be complex. Dispersed phases in aluminum may act to accelerate or retard the recrystallization process depending on their size, interparticle spacing, and stability at the annealing temperature (Ref 10).

Figure 15 illustrates the change in recrystallization behavior resulting from increasing iron additions to high-purity aluminum. For the most di-

lute alloys, all the iron is retained in solid solution, and a progressive increase in the recrystallization temperature range occurs with increasing iron. This trend is reversed as further iron additions exceed the solubility limit, and a dispersed ($FeAl_3$) phase appears in the matrix. Further iron additions increase the volume fraction of the dispersed $FeAl_3$ particles, and a corresponding progressive reduction in the recrystallization temperature range is exhibited. The narrowing range of recrystallization temperature can be attributed to enhanced rates of nucleation resulting from the increasing numbers of dispersed $FeAl_3$ particles of 0.6 to 2.2 μm (0.02 to 0.09 mil) diameter (Ref 11).

A regime of particle size (≤0.1 μm or ≤0.004 mil) and interparticle spacing (≤1.5 μm or ≤0.06 mil) exists, in which recrystallization can be inhibited because the dislocation cell structure in the deformed metal becomes anchored and stabilized by the particles (Ref 12). In extreme cases, the recrystallization temperature can be raised to 500 °C (930 °F) or higher (Ref 13). This situation may result in a generally larger recrystallized grain size than usual. However, the ultrafine dispersions required to achieve such high recrystallization temperatures do not normally occur in aluminum alloys fabricated by conventional practices. Extraordinary processing, for example, an extremely fast ingot solidification rate, is necessary to significantly raise recrystallization temperatures above the 340 to 410 °C (645 to 770 °F) range that is typical for commercial aluminum alloys.

The grain size obtained by recrystallization is an important structural feature and is subject to some measure of control. In a given alloy, one of the most important variables affecting grain size is the amount of cold work (Fig. 16). With small amounts of cold work, the grain size obtained on recrystallization is relatively large. As cold work increases, the grain size decreases asymptotically at a rate determined by composition, the fabrication history of the metal, and annealing conditions. For a given history and annealing condition, recrystallization does not occur below a

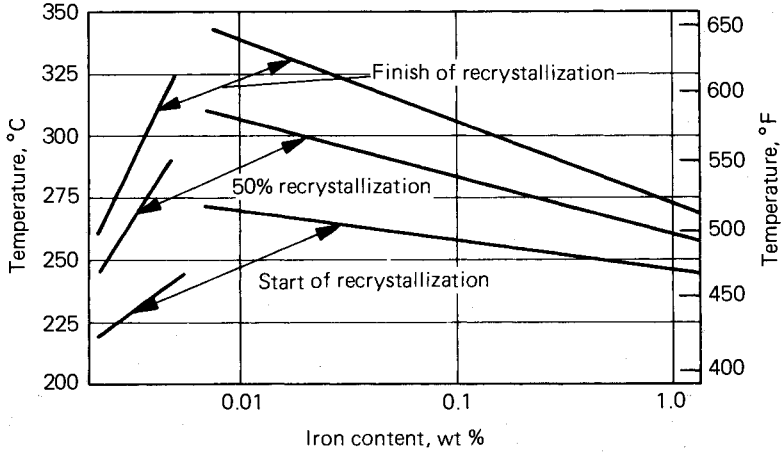

Fig. 15. Isochronal (1-h) recrystallization temperature versus iron content for high-purity aluminum-iron alloys cold-rolled 60%.(Ref 11)

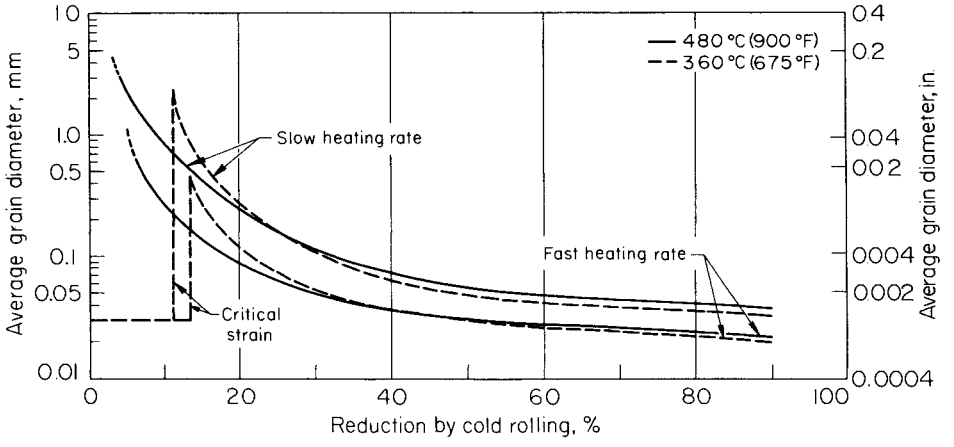

Fig. 16. Grain size of 1100 sheet after annealing at 375 or 400 °C (675 or 900 °F). (Courtesy of Aluminum Company of America)

specific minimum strain. This critical strain produces the largest recrystallized grains under the specified heating conditions.

The rate of heating to the annealing temperature also has a considerable effect on the grain size of aluminum alloys. Figure 16 shows that slow heating produces a much larger grain size than rapid heating. The effects of annealing temperature are also illustrated in Fig. 16. A higher annealing temperature decreases the critical strain at which recrystallization occurs, but it does not significantly change the relationship between grain size and the degree of deformation, or the heating rate.

Many hot worked alloy products, especially those from the higher strength alloys, may resist recrystallization, even when subjected to solution heat treating temperatures. However, large recrystallized grains may be found at a shallow depth below the outer surfaces. One explanation for this is that the working processes are such that deformation is more severe at the outer surface than toward the center (Fig. 17). Thus, an effective strain hardening gradient exists at the completion of working. This effective strain hardening may straddle the critical strain required to produce recrystallization under a given combination of time and temperature. Holding at temperature after hot working or subsequent reheating can produce recrystallization in the surface region that exceeds the critical strain. Under such conditions, the recrystallized grains are very large.

Grain size is also strongly affected by composition. Generally, common alloying elements and impurities such as copper, iron, magnesium, and manganese decrease grain size. The effects of elements of limited solubility, such as chromium, iron, and manganese, are influenced by the compounds they form with each other and with other elements, and by their distribution in the structure. Manganese is particularly notable in this regard (Ref 14). The distribution of such solute elements is determined by ingot casting conditions, by ingot preheating (Chapter 5 in this Volume), and by other fabricating variables. These operations are con-

trolled commercially to produce a distribution favorable to the formation of a fine grain size.

The recrystallized grain shape in wrought aluminum alloys varies considerably, from nearly equiaxial in commercially pure or low alloyed materials, to very elongated or flattened in highly alloyed materials. The grain shape is influenced mainly by elements such as manganese, chromium, and zirconium. These elements are inhomogeneously distributed in the original cast material and form very fine precipitate (dispersoid) particles, generally in the order of 0.1 μm (0.004 mil), or less. The wrought structure consists of alternating bands or layers of dense or sparse dispersoid. Recrystallizing grains tend to have their growth obstructed by such bands and, therefore, produce the elongated grain shape common to most higher strength alloys.

Recrystallization produces further changes in the properties of the deformed and recovered metal. These continue until annealing and recrystallization are complete. The properties then are those of the original, unstrained metal, except as they are changed by differences in grain size and preferred orientation. In heat treatable alloys, annealing also may be accompanied by precipitation and changes in solute concentration (Chapter 5 in this Volume).

Tensile property changes during isothermal annealing are illustrated in Fig. 11, and the time for the beginning of recrystallization is indicated.

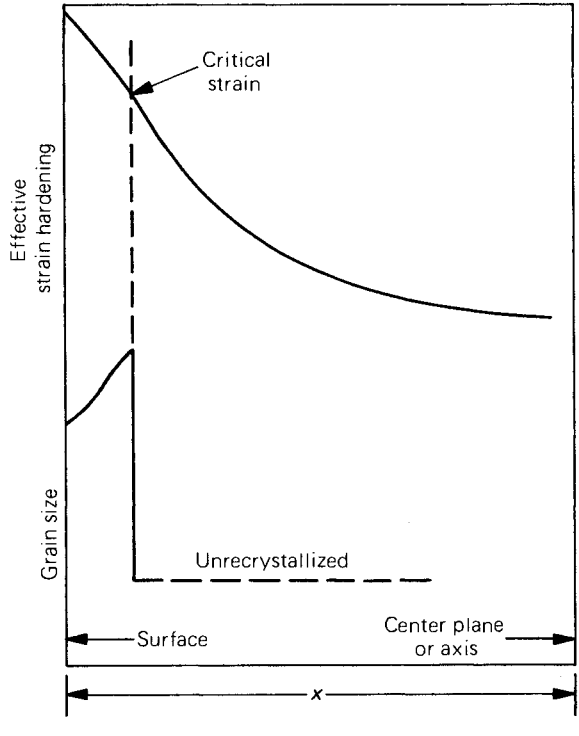

Fig. 17. Partial recrystallization because of hot working. (Courtesy of P.R. Sperry)

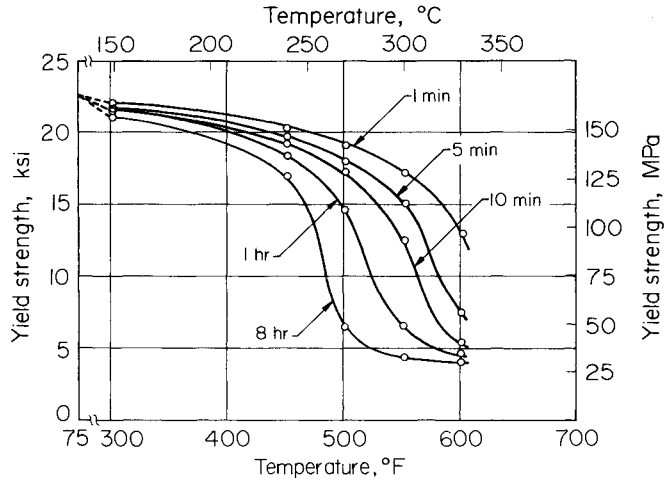

Fig. 18. Annealing curves for 1100-H18 sheet. (Courtesy of Aluminum Company of America)

The relationship between recrystallization and softening is better shown in the isochronal plots of Fig. 18. Here, recrystallization changes the slope of the softening curve and increases the annealing rate. The annealing rate increases approximately exponentially as temperature increases. Annealing occurs at lower temperatures with greater amounts of prior cold work. Recrystallization is also accompanied by a further decrease in stored energy, as measured calorimetrically (Ref 6), as well as by complete elimination of residual stresses.

Grain Growth After Recrystallization. Heating after recrystallization may produce grain coarsening, which can take one of several forms. The grain size may increase by a gradual and uniform coarsening of the microstructure, usually identified as normal grain growth. The process proceeds by the gradual elimination of small grains with unfavorable shapes or orientations relative to their immediate neighbors. This occurs readily in high-purity aluminum and its solid solution alloys and can lead to relatively large average grain sizes. Such grain growth is promoted by small recrystallized grains, high temperatures, and extensive heating. Some grain coarsening of this type also occurs in commercial aluminum alloys, but is greatly restricted by finely divided impurity phases and by intermetallic compounds of elements, such as manganese and chromium, that slow down the process, pin the grain boundaries, and prevent further movement. Figure 19 shows grain growth in recrystallized 1100 aluminum. Some grain growth does occur in very fine-grained sheet, but not to any appreciable extent in sheet with initial grain counts of 200 to 700 grains per square millimeter. Grain counts of this magnitude are typical of most commercially produced 1100-0 alloy sheet.

Aluminum alloys subject to some form of pinning or growth restraint occasionally undergo a different kind of grain growth. This exaggerated grain growth, or secondary recrystallization, proceeds by the growth of a very few grains in recrystallized metals. Generally, these grains grow

only at very high temperatures and may attain diameters of several millimeters. Apparently, the normal growth-inhibiting effects of elements such as iron, manganese, and chromium are lost or modified at high temperatures, through solution, or through changes in particle size and shape (Ref 15). Because of the high temperatures, the few grains that first lose or overcome these restraints grow rapidly and consume other potential growth centers, and in this manner, a few grains of very large size are formed. In most alloys, high temperatures alone are not the only cause for giant grains. Small primary grain size and well-developed annealing texture are other factors that promote this form of grain growth.

CRYSTALLOGRAPHIC TEXTURE

Rolling Texture. Cast aluminum tends to have a random distribution of grain orientations, except where columnar grains are formed. The random character of the cast structure is rapidly lost during hot or cold working and is replaced by crystallographic textures in which considerable numbers of the deformed grains assume, or approach, certain orientations. Such textures occur because deformation, or slip, in aluminum is confined to certain crystallographic planes and directions. At room temperature, slip occurs on the {111} planes in the ⟨110⟩ directions (Ref 16). Deformation on sets of such planes produces a gradual crystallographic alignment (rotation) of deformed grains into specific orientations with respect to the surface of the workpiece and the direction of working.

The crystallographic texture of sheet can be accurately described by means of x-ray pole figures that are stereographic projections of poles of the {111} slip planes (Ref 16). Figure 20 illustrates such pole figures obtained on two heavily cold rolled aluminum sheet alloys. The relative number of poles is indicated by the shading, which gives the concentrations in terms of R, the number of poles to be expected in an ideal metal sample of random grain orientation (Ref 17).

The final textures achieved with large amounts of deformation vary with the nature of the working process, with the changes in shape of the workpiece and, to a lesser extent, with the composition of the alloy.

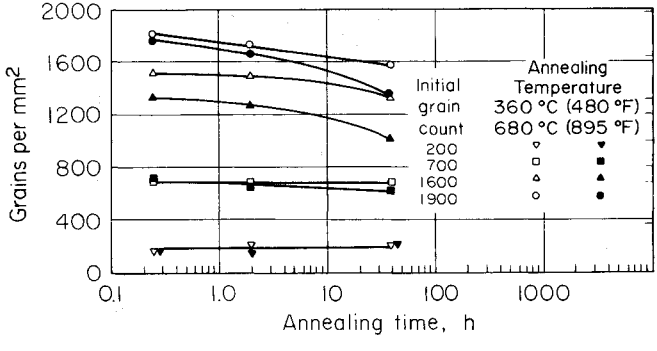

Fig. 19. Effects of annealing time and temperature on grain growth in 1100-0 sheet with different initial grain sizes. (Courtesy of Aluminum Company of America)

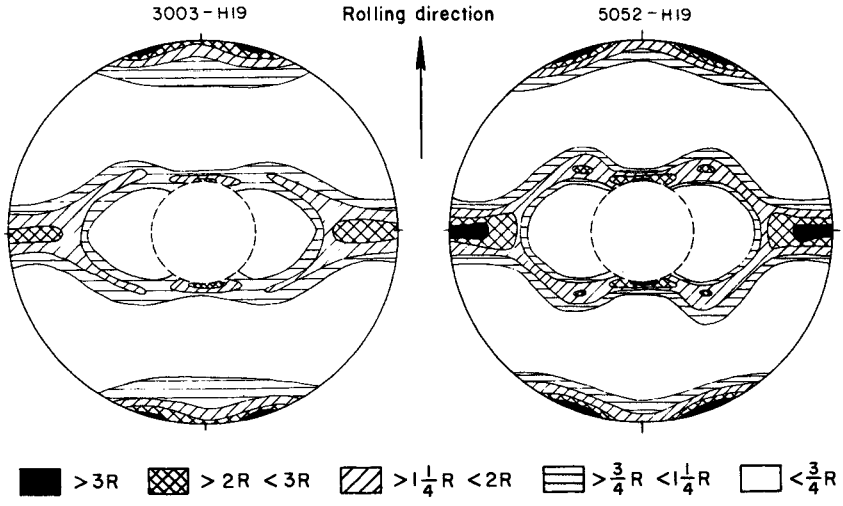

Fig. 20 {111} pole figures showing rolling textures in 3003-H19 and 5052-H19 sheet. Densities of poles are in multiples of random concentration, R. (Courtesy of Aluminum Company of America)

In rolled sheet, the deformation texture (Fig. 20) may be described as a mixture of the three ideal textures (110)[$\bar{1}$12], (112)[11$\bar{1}$], and (123)[1$\bar{2}$1]. A practical consequence of the textures developed by various working practices is the production of some directionality in properties. Generally, this directionality is much less than that observed in hexagonal metals and in some other cubic metals. The principal problem associated with directionality in aluminum alloys is the formation of ears during deep drawing of sheet (Fig. 21). The height and location of the ears on the drawn article vary with the texture of the sheet. In sheet with rolling texture, four ears are located 45° to the rolling direction. The height of the ears increases roughly in proportion to the strength and intensity of the rolling texture.

Recrystallization Texture. When new grains are formed by recrystallization,* they frequently develop in orientations that differ from the principal components of the deformation texture. This reorientation has been extensively studied in rolled sheet and varies considerably with the fabrication history and the composition of the alloy. There is a strong tendency for the new grains to form with a cube plane {100} parallel to the surface of the sheet and a cube edge parallel to the rolling direction. In contrast to rolling texture, which produces 45° earing during deep drawing, this (100)[001] (cube) texture produces four ears at the 0° and 90° position around the drawn cup (Fig. 21). The height of the ears increases with the percentage of cubically aligned grains.

Another component of some annealing textures is one near {123}⟨211⟩. This appears in cold rolling textures as well, which suggests that recrystallized grains of this orientation may grow from polygonized substruc-

*The recovery process is not accompanied by any significant change in preferred orientation or texture of the deformed metal.

tures of the same orientation in deformed metal. Furthermore, a ⟨111⟩ direction of the four components of the texture near (123)[12̄1] closely approaches a ⟨111⟩ direction of the cube texture. A rotation of approximately 40° around ⟨111⟩ is sufficient to superimpose these components of the rolling and recrystallization textures. This has been interpreted as evidence of the selective growth of grains of the cube component into the related component of the deformation texture.

Although ideal orientations, such as (100)[001], are useful in describing the principal components of recrystallization texture, a considerable spread in orientations around the pole positions for this and other textures encountered in deformed and recrystallized metals exists. The series of pole figures in Fig. 22 show the spread of orientations that can be encountered in cold worked and in annealed 1100 aluminum. These pole figures also show changes in texture encountered during the progress of recrystallization. Generally, the first component of the rolling texture to disappear is the (110)[1̄12] orientation. This cannot be related to the (100)[001] or (123)[12̄1] components of the recrystallization texture through rotations of the type described previously; however, rotations of 30 to 40° around (110)[1̄12] can produce a (235)[23̄1] texture, which accounts for some of the observed changes during annealing.

From a practical standpoint, it is usually desirable that preferred orientation be at a low level, because there is a lower probability of directional properties. This is especially important in the deep drawing of sheet into cylindrical shapes, where minimal earing is frequently necessary. Practical controls over earing are exercised through manipulation of the primary fabricating and annealing schedules. Deep drawing conditions also influence earing (Ref 18).

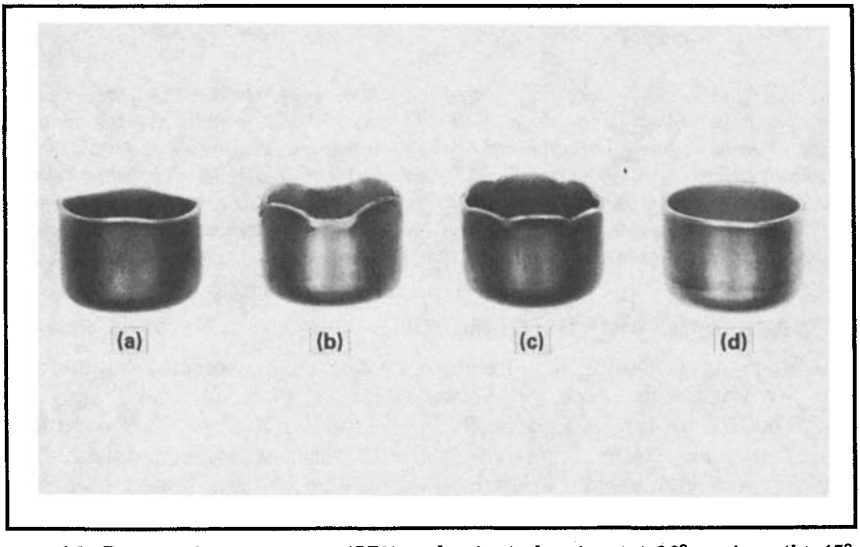

Fig. 21. Drawn aluminum cups (57% reduction) showing (a) 90° earing; (b) 45° earing; (c) mixed 90° and 45° earing; and (d) no earing; with respect to rolling direction. (Courtesy of W.W. Berkey of the Reynolds Metals Co.)

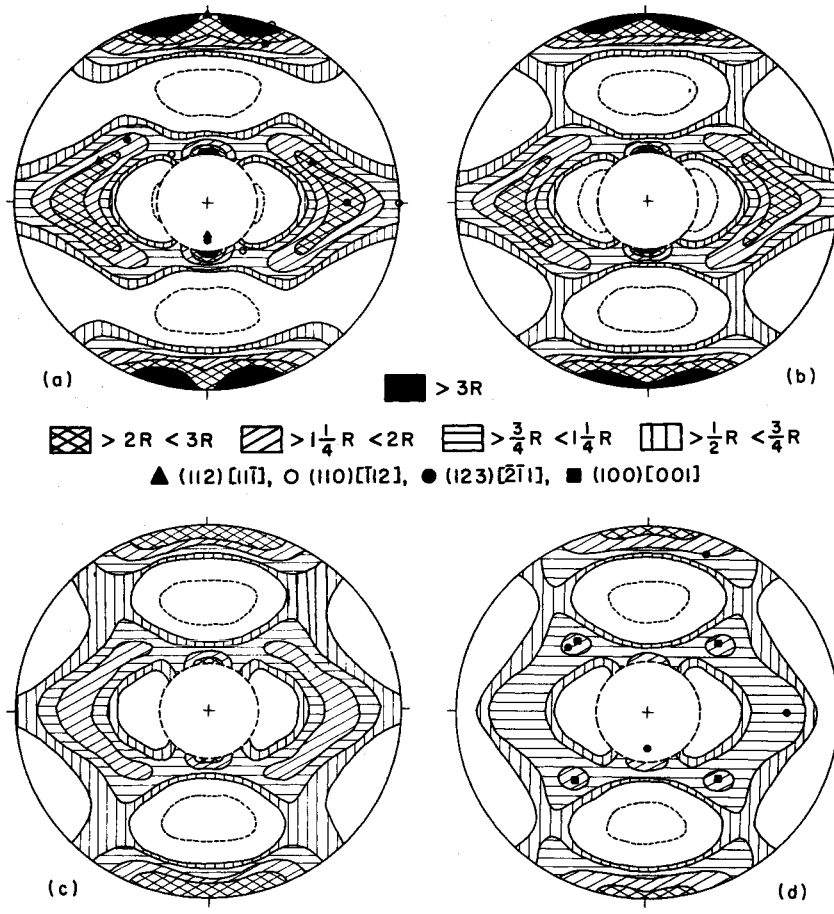

Fig. 22. {111} pole figures for cold rolled 1100 sheet, showing change in preferred orientations on annealing at 290 °C (550 °F). Recrystallization is started after 15 min, is partially complete after 40 min, and is complete after 70 min. (a) Cold rolled 95%. (b) Annealed 15 min at 290 °C (550 °F). (c) Annealed 40 min at 290 °C (550 °F). (d) Annealed 70 min at 290 °C (550 °F). In the pole figure, the rolling direction is parallel to the vertical dimension of the figure. (Courtesy of Aluminum Company of America)

SURFACE EFFECTS OF DEFORMATION

Lüder Lines. During the stretching or forming of some aluminum alloys, two distinctive types of surface markings, or Lüder lines, may occur. The first, or type A Lüders (Ref 19), is shown in Fig. 23. Sometimes called stretcher strains, this type of Lüder lines is associated with the yielding and yield point elongation of annealed or heat treated solid solution alloys, such as aluminum-magnesium. This type of Lüder line is very similar to that observed in some types of sheet steel and is generally associated with stretch-forming operations. Although there is no impairment of properties in parts with Lüders markings, the markings may prove

esthetically objectionable. For this reason, special tempers (H11X) are produced that preclude the formation of type A Lüders during forming. Forming at temperatures above about 150 °C (300 °F) also prevents Lüder lines in alloys susceptible to this phenomenon.

The second, or type B, Lüder line formation is sometimes called the Portevin-LeChatelier phenomenon. It is observed during the stretching of sheet beyond the yield point. In contrast to type A Lüders, type B Lüder lines can occur in the strain-hardened as well as annealed tempers of some alloys. These Lüder lines appear as diagonal bands oriented approximately 50° to the tension axis. The bands form along the axis during stretching and increase in number as stretching progresses. On a stress-strain curve, the nonuniform deformation associated with these bands appears as a series of steps or serrations that continue until necking of the specimen. Failure is usually through a Lüder band. This type of Lüder band is rarely observed in commercial forming operations but may be encountered in strain-hardened sheet or plate stretched to produce flatness. Aluminum-magnesium alloy sheet is especially susceptible to Lüder-line formation, which increases in severity with increasing solute content. Heat treatable aluminum alloys are also susceptible to Lüder-line formation, but usually only in the freshly quenched condition.

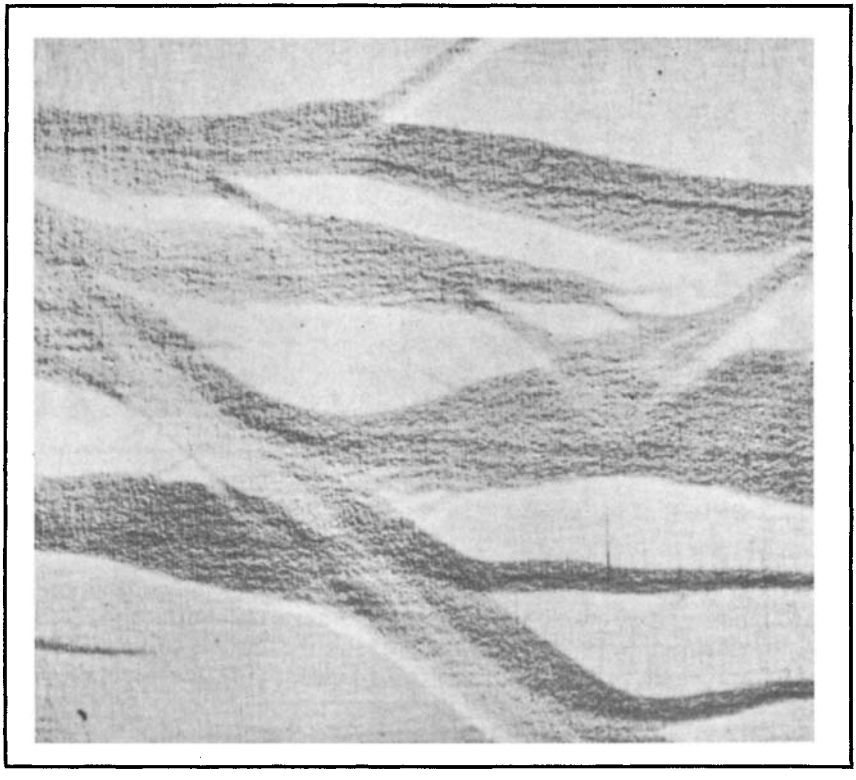

Fig. 23. Lüder lines in aluminum-magnesium alloy sheet, 8×. (Courtesy of Aluminum Company of America)

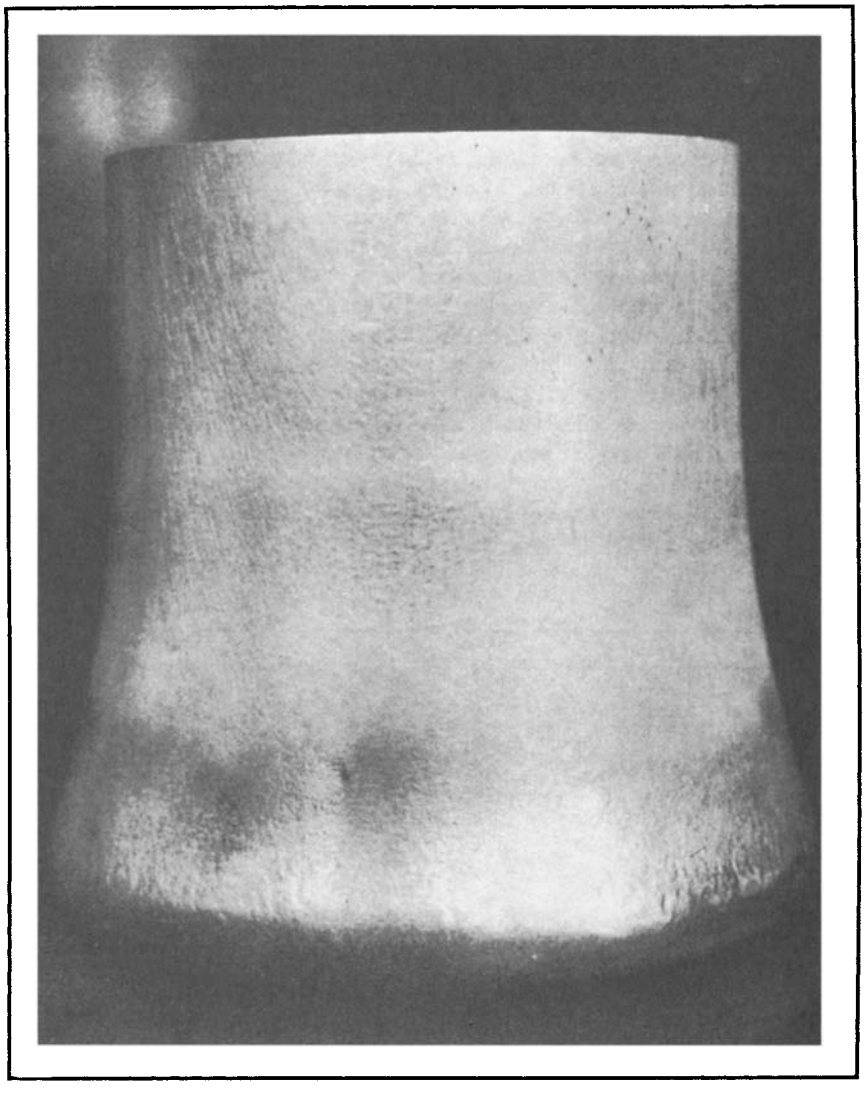

Fig. 24. Orange peel surface on a drawn and expanded aluminum alloy shell (129% reduction). (Courtesy of J.T. Hobbs of the Aluminum Company of America)

Orange Peel. Aluminum products formed by stretching, bending, or drawing sometimes develop a roughened, orange peel surface (Fig. 24). This roughness is related to the grain size at the surface of the product. A fine grain size produces little or no roughening; a coarse grain size produces surface roughening and the orange peel condition. Orange peel is produced because grains at a free surface are not constrained to deform as do those in the interior, but may deform more freely, according to basic crystallographic slip mechanisms. These mechanisms produce varying amounts of deformation, depending on the orientation of the grain in

relation to its neighbors and to the imposed strains. Nonuniform deformation from grain to grain produces the rough, orange peel condition.

The grain size that produces visible orange peel varies with the product, the amount of deformation, and the structure of the alloy. Sometimes, clusters of small grains with about the same orientation deform, as do coarse-grained metals, and produce a similar orange peel condition. Coarse surface grains with little depth or thickness produce less orange peel than similar grains of greater thickness. Hot worked products usually show less orange peel than cold worked products.

Looper Lines. Looper-line formation, or roping, is another form of surface roughening sometimes encountered during the deep drawing of aluminum sheet. The name derives from the characteristic form of this roughening on drawn shapes, such as that shown in Fig. 25.

Looper lines are a form of nonuniform deformation that results from irregularities in the structure of the metal. One of the most common causes

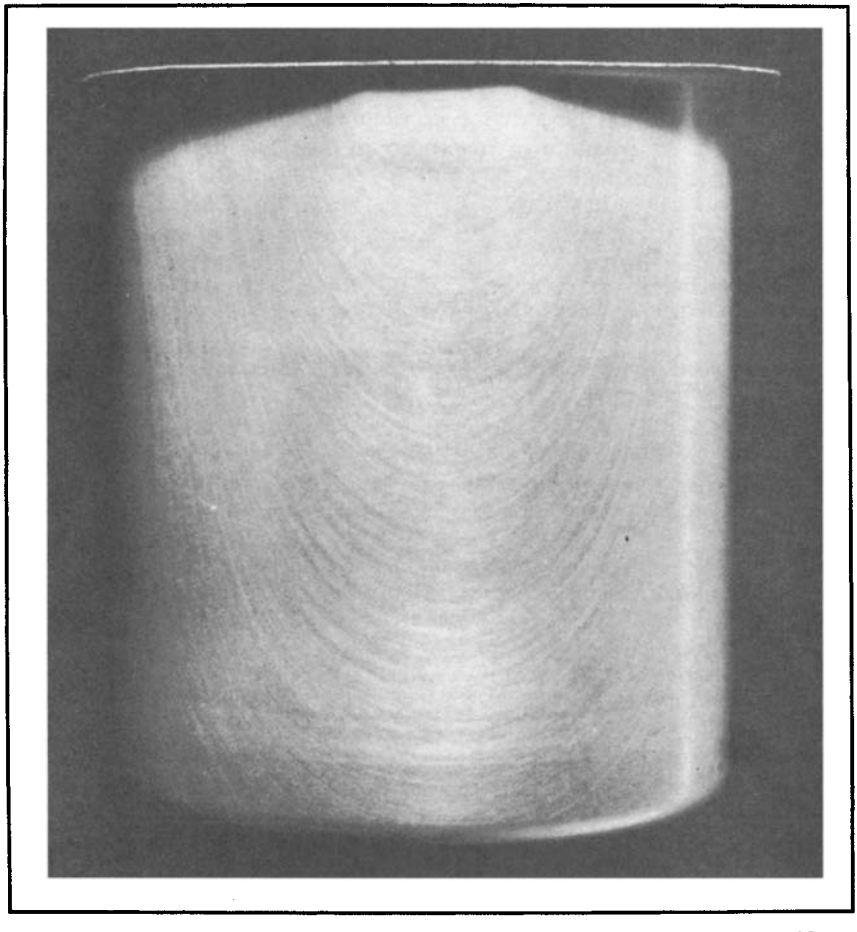

Fig. 25. Deep drawn aluminum sheet showing looper lines (roping) (127% reduction).

of looper lines in strain-hardened sheet is a striated grain structure. These structures usually have their origin in coarse grains formed during hot rolling or intermediate annealing and drawn out into fibers during temper rolling. These same fibers can produce looper lines in annealed sheet if they fail to recrystallize, or if they recrystallize to a fine grain structure in which the grains originating from a given fiber have approximately the same orientations and tend to deform as a single fibrous grain. The term "ghost grains" is sometimes applied to structures containing such colonies of fine grains outlining portions of an earlier, larger grain structure.

Looper lines may also form because of segregated constituent or solute. Coarse dendritic segregation that persists through ingot preheating and reheating can produce a striated structure and looper lines. The principal elements producing such segregation and structural conditions are chromium, iron, and manganese. This results from their limited solubility in aluminum and their slow diffusion rates, which make homogenization difficult.

Commercially, looper lines are only an occasional problem. They are controlled through ingot casting, homogenization, and fabricating practices selected to minimize segregation and to prevent formation of coarse grains.

Residual Stresses. One of the consequences of cold working is the establishment of a pattern of macroscopic residual stresses that can be relieved through annealing.

REFERENCES

1. U.S. Lindholm, R.L. Bessey, and G.V. Smith, Effect of Strain Rate on Yield Strength, and Elongation of Three Aluminum Alloys, *Journal of Materials Science*, Vol 6, 1971, p 119-133
2. J.E. Hockett, On Relating the Flow Stress of Aluminum to Strain, Strain Rate, and Temperature, *Transactions of AIME*, Vol 239, 1967, p 969-976
3. J.J. Jonas, C.M. Sellars, and W.J. McG. Tegart, Strength and Structure Under Hot Working Conditions, *Metallurgical Reviews*, Review 130, 1969
4. J.R. Cotner and W.J. McG. Tegart, High Temperature Deformation of Aluminum-Magnesium Alloys at High Strain Rates, *Journal of the Institute of Metals*, Vol 97, 1969, p 73-76
5. R.L. Templin, Relation of Cold Working to the Physical Properties of Aluminum, in *The Aluminum Industry*, New York: McGraw-Hill, 1930, p 396-417
6. L.M. Clarebrough, M.E. Hargreaves, and M.H. Loretto, Changes in Internal Energy Associated with Recovery and Recrystallization, in *Recovery and Recrystallization of Metals*, New York: Interscience Publishers, 1963, p 63-121
7. R.D. Doherty and R.W. Cahn, Nucleation of New Grains in Recrystallization of Cold Worked Metals, *Journal of the Less-Common Metals*, Vol 28, 1972, p 279-296
8. W.A. Anderson and R.F. Mehl, Recrystallization of Aluminum in Terms of the Rate of Nucleation and the Rate of Growth, *Transactions of AIME*, Vol 161, 1945, p 140-167
9. P.C. Varley, The Recovery and Recrystallization of Rolled Aluminum of Commercial Purity, *Journal of the Institute of Metals*, Vol 75, 1948, p 185-202

10. U. Köster, Recrystallization Involving a Second Phase, *Metal Science*, Vol 8, 1974, p 151-160

11. P.R. Mould and P. Cotterill, The Effect of Particle Content and Matrix Grain Size on the Recrystallization of Two-Phase Aluminum-Iron Alloys, *Journal of Materials Science*, Vol 2, 1967, p 241-255

12. R.D. Doherty and J.W. Martin, The Effect of Dispersed Second Phase on the Recrystallization of Aluminum-Copper Alloys, *Journal of the Institute of Metals*, Vol 91, 1962-63, p 332-338, and Vol 57, p 874

13. N. Ryum, Precipitation and Recrystallization in an Al-0.5 wt. % Zr Alloy, *Acta Metallurgica*, Vol 17, 1969, p 269-278

14. P. Furrer and G. Hausch, Recrystallization Behavior of Commercial Al-1% Mn Alloy, *Metal Science*, Vol 13, 1979, p 155-162

15. P.A. Beck, M.L. Holzworth, and P.R. Sperry, Effect of a Dispersed Phase on Grain Growth in Al-Mn Alloys, *Transactions of AIME*, Vol 180, 1949, p 163

16. R.W.K. Honeycombe, The Deformation of Metal Crystals—General Aspects, *The Plastic Deformation of Metals*, London: Edward Arnold Publishing Co., 1968, p 5-32

17. Method for Preparing Quantitative Pole Figures of Metals, ASTM Designation E81-77, ASTM Standards, 1977

18. J.C. Wright, Influence of Deep-Drawing Conditions on the Earing of Aluminum Sheet, *Journal of the Institute of Metals*, Vol 93, 1964-65, p 289-296

19. V.A. Phillips, A.J. Swain, and R. Eborall, Yield Point Phenomena and Stretcher-Strain Markings in Aluminum-Magnesium Alloys, *Journal of the Institute of Metals*, Vol 81, 1952-53, p 625-647

Aluminum Properties and Physical Metallurgy
John E. Hatch editor, p 134-199
DOI: 10.1361/appm1984p134

CHAPTER 5

METALLURGY OF HEAT TREATMENT AND GENERAL PRINCIPLES OF PRECIPITATION HARDENING*

The heat treatable alloys contain amounts of soluble alloying elements that exceed the equilibrium solid solubility limit at room and moderately higher temperatures. The amount present may be less or more than the maximum that is soluble at the eutectic temperature. Figure 1, which shows a portion of the aluminum-copper equilibrium diagram, illustrates these two conditions and the fundamental solution-precipitation relationships involved. Two alloys containing 4.5 and 6.3% copper are represented by the vertical dashed lines (a) and (b). The solubility relationships and heat treating behavior of these compositions approximate those of commercial alloys 2025 and 2219, and the principles apply to the other heat treatable alloys.

The diagram in Fig. 1 shows that, regardless of the initial structure, holding the 4.5% copper alloy at 515 to 550 °C (960 to 1020 °F) until equilibrium is attained causes the copper to go completely into solid solution. This operation is generally known as "solution heat treating." If the temperature is then reduced to below 515 °C (960 °F), the solid solution becomes supersaturated, and there is a tendency for the excess solute over the amount actually soluble at the lower temperature to precipitate. The driving force for precipitation increases with the degree of supersaturation and, consequently, with decreasing temperature; the rate also depends on atom mobility, which is reduced as temperature decreases. Although the solution-precipitation reaction is fundamentally reversible with temperature change, in many alloys transition structures form during precipitation but not during solution. Mechanical and physical properties depend not only on whether the solute is in or out of solution but also on specific atomic arrangements, as well as on size and dispersion of any precipitated phases.

Referring again to Fig. 1, the alloy with 6.3% copper, which exceeds the maximum content soluble at the eutectic temperature, consists of a solid solution plus additional undissolved $CuAl_2$ when heated to slightly below the eutectic temperature. The solid solution has a higher copper concentration than that of the 4.5% copper alloy if the temperature exceeds 515 °C (960 °F). The increased copper in solid solution provides greater driving force for precipitation at lower temperatures and increases

*This chapter was revised by a team comprised of J.T. Staley, Alcoa Technical Center; R.F. Ashton, Reynolds Metals Co.; I. Broverman, Kaiser Aluminum & Chemical Corp.; and P.R. Sperry, Consolidated Aluminum Corp. The original chapter was authored by H.Y. Hunsicker, Alcoa Research Laboratories.

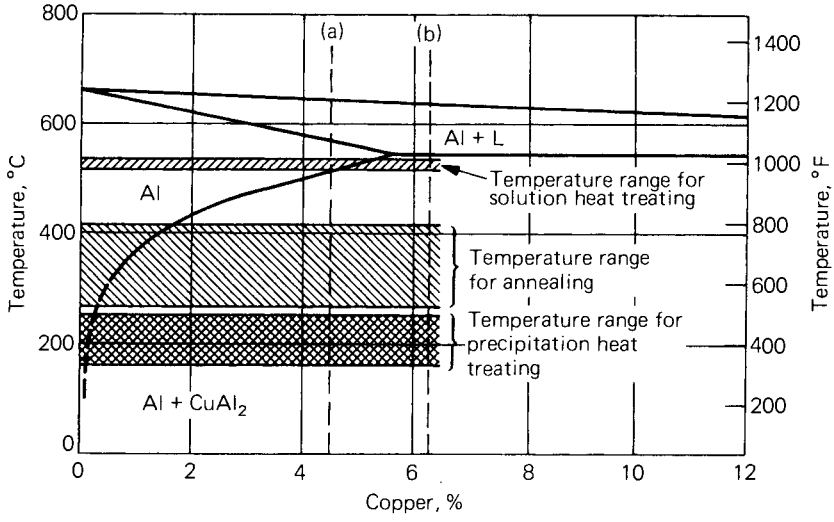

Fig. 1. Partial equilibrium diagram for aluminum-copper alloys, with temperature ranges for heat treating operations.

the magnitude of property changes that may occur. The $CuAl_2$ that is not dissolved at the high temperature, while remaining essentially unaltered through heating and cooling, perceptibly raises the overall strength level.

Although the simple aluminum-copper binary phase diagram is convenient for illustrating principles, the presence of an impurity or other alloying element alters the real values of solid solubility limits and the equilibrium or nonequilibrium solidus temperatures. Familiarity with ternary and more complex phase diagrams is essential for a deeper understanding of heat treatment phenomena. The additional degrees of freedom resulting from each component added to a binary system produce phase compositions and transition temperatures that cannot be depicted readily by the two-dimensional binary diagram.

The solid solution formed at a high temperature may be retained in a supersaturated state by cooling with sufficient rapidity to minimize precipitation of the solute atoms as coarse, incoherent particles. Controlled precipitation of fine particles at room or elevated temperatures after the quenching operation is used to develop the mechanical properties of the heat treated alloys.

Most alloys exhibit property changes at room temperature after quenching. This is called "natural aging" and may start immediately after quenching, or after an incubation period. The rates vary from one alloy to another over a wide range, so that the approach to a stable condition may require only a few days or several years. Precipitation can be accelerated in these alloys, and their strengths further increased, by heating above room temperature; this operation is referred to as "artificial aging" or "precipitation heat treating."

Alloys with slow precipitation reactions at room temperature must be precipitation heat treated to attain the high strengths of which they are capable. In certain alloys, considerable additional increase in strength can

be obtained by imposing controlled amounts of cold work on the product after quenching. A portion of the increase in strength obtained by this practice is attributed to strain hardening, but when cold working is followed by precipitation heat treating, the precipitation effects are greatly accentuated. As is apparent from the descriptions of the Aluminum Association temper designations applicable to heat treatable alloys below, other combinations and sequences of cold working and precipitation heat treatments are used; these are discussed subsequently in more detail. The basic temper designations are as follows:

F **As fabricated:** Applies to the products of shaping processes in which no special control over thermal conditions or strain-hardening is used. For wrought products, there are no mechanical property limits

O **Annealed:** Applies to wrought products that are annealed to obtain the lowest strength temper and to cast products that are annealed to improve ductility and dimensional stability. The O may be followed by a digit other than zero

W **Solution heat treated:** An unstable temper applicable only to alloys which spontaneously age at room temperature after solution heat treatment. This designation is specific only when the period of natural aging is indicated; for example: W $^1/_2$h

T **Thermally treated to produce stable tempers other than F, O, or H:** Applies to products which are thermally treated, with or without supplementary strain hardening, to produce stable tempers

The T is always followed by one or more digits. A period of natural aging at room temperature may occur between or after the operations listed for the T tempers. Control of this period is exercised when it is metallurgically important. Numerals 1 through 10 indicate specific sequences of treatments:

T1 **Cooled from an elevated-temperature shaping process and naturally aged to a substantially stable condition:** Applies to products that are not cold worked after cooling from an elevated-temperature shaping process, or in which the effect of cold work in flattening or straightening may not be recognized in mechanical property limits

T2 **Cooled from an elevated-temperature shaping process, cold worked, and naturally aged to a substantially stable condition:** Applies to products that are cold worked to improve strength after cooling from an elevated-temperature shaping process, or in which the effect of cold work in flattening or straightening is recognized in mechanical property limits

T3 **Solution heat treated, cold worked, and naturally aged to a substantially stable condition:** Applies to products that are cold worked to improve strength after solution heat treatment, or in which the effect of cold work in flattening or straightening is recognized in mechanical property limits

T4 **Solution heat treated and naturally aged to a substantially stable condition:** Applies to products that are not cold worked after solution heat treatment, or in which the effect of cold work in flattening or straightening may not be recognized in mechanical property limits

T5 **Cooled from an elevated-temperature shaping process and then artificially aged:** Applies to products that are not cold worked after cooling from an elevated-temperature shaping process, or in which the effect of cold work in flattening or straightening may not be recognized in mechanical property limits

T6 **Solution heat treated and then artificially aged:** Applies to products that are not cold worked after solution heat treatment, or in which the effect of cold work in flattening or straightening may not be recognized in mechanical property limits

T7 **Solution heat treated and stabilized:** Applies to products that are stabilized after solution heat treatment to carry them beyond the point of maximum strength to provide control of some special characteristic

T8 **Solution heat treated, cold worked, and then artificially aged:** Applies to products that are cold worked to improve strength, or in which the effect of cold work in flattening or straightening is recognized in mechanical property limits

T9 **Solution heat treated, artificially aged, and then cold worked:** Applies to products that are cold worked to improve strength

T10 **Cooled from an elevated-temperature shaping process, cold worked, and then artificially aged:** Applies to products that are cold worked to improve strength, or in which the effect of cold work in flattening or straightening is recognized in mechanical property limits

Solution heat treatment is achieved by heating cast or wrought products to a suitable temperature, holding at that temperature long enough to allow constituents to enter into solid solution, and cooling rapidly enough to hold the constituents in solution. Some 6000 series alloys attain the same specified mechanical properties whether furnace solution heat treated or cooled from an elevated-temperature shaping process at a rate rapid enough to hold constituents in solution. In such cases the temper designations T3, T4, T6, T7, T8, and T9 are used to apply to either process and are appropriate designations.

The following designations involving additional digits are assigned to stress-relieved tempers of wrought products:

T—51 **Stress relieved by stretching:** Applies to the following products when stretched the indicated amounts after solution heat treatment or cooling from an elevated-temperature shaping process:

Plate ..... $1\frac{1}{2}$ to 3% permanent set
Rod, bar, shapes,
extruded tube ..... 1 to 3% permanent set
Drawn tube ..... $\frac{1}{2}$ to 3%

Applies directly to plate and rolled or cold finished rod and bar. These products receive no further straightening after stretching

Applies to extruded rod, bar, shapes, and tube and to drawn tube when designated as follows:

T—510: Products that receive no further straightening after stretching

T—511: Products that may receive minor straightening after stretching to comply with standard tolerances

T—52 **Stress-relieved by compressing:** Applies to products that are stress-relieved by compressing after solution heat treatment or cooling from an elevated-temperature shaping process to produce a permanent set of 1 to 5%

T—54 **Stress-relieved by combined stretching and compressing:** Applies to die forgings that are stress relieved by restriking cold in the finish die

The same digits (51, 52, 54) may be added to the designation W to indicate unstable solution heat treated and stress-relieved tempers. The following temper designations have been assigned for wrought products heat treated from O or F temper to demonstrate response to heat treatment:

T42 Solution heat treated from the O or F temper to demonstrate response to heat treatment, and naturally aged to a substantially stable condition

T62 Solution heat treated from the O or F temper to demonstrate response to heat treatment, and artificially aged

Temper designations T42 and T62 may also be applied to wrought products heat treated from any temper by the user when such heat treatment results in the mechanical properties applicable to these tempers.

The increases in strength of the alloys that exhibit natural aging either continue indefinitely at room temperature or stabilize. Aging at elevated temperatures is characterized by a different behavior in which strength and hardness increase to a maximum and subsequently decrease. The softening effects, observed as more complete precipitation, occur during extended aging at elevated temperatures and are referred to as "overaging." They are as significant as the strengthening effects associated with the preceding stages of precipitation. Softening results from changes in both the type and size of precipitated particles and from dilution of the solid solution. The softest, lowest strength condition of the heat treatable alloys is obtained by annealing treatments that precipitate the maximum amount of solute as relatively large, widely spaced, incoherent particles.

Alloy hardening and softening attributable to precipitation are illustrated by the isothermal aging curves in Fig. 2. These curves show typical effects of time and temperature that are basic to the heat treating process and influence the selection of conditions to achieve various mechanical properties. Some of the important features illustrated are:

- Hardening can be greatly retarded or suppressed indefinitely by lowering the temperature
- The rates of hardening and subsequent softening increase with increasing temperature
- Over the temperature range in which a maximum strength can be observed, the level of the maximum generally decreases with increasing temperature

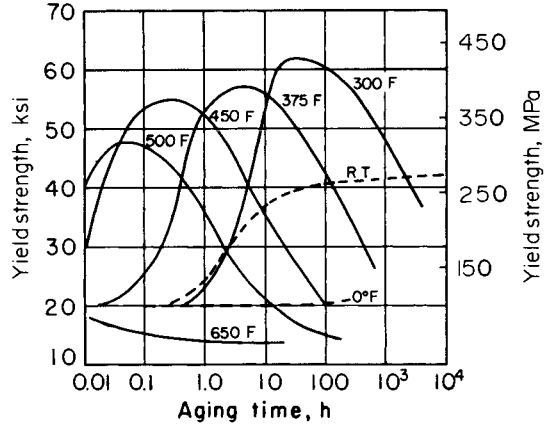

Fig. 2. Representative isothermal aging curves for alloy 2014-T4.

- At sufficiently high temperatures no hardening is observed, and precipitation causes an initial and continued softening

In selecting combinations of time and temperature for commercial processing to achieve maximum strength and hardness, the features given above are considered, together with certain limitations imposed by economic factors. Adequate control favors avoiding short-time, high-temperature combinations, which are on steeply sloping portions of the aging curves, and leads to a preference for temperatures that provide a broad maximum. The variations in aging behavior shown in Fig. 2 can now be related to Fig. 1, which indicates the temperature ranges for the different basic heat treating operations. Thus, the temperature range for annealing produces effects of the type illustrated by the 345 °C (650 °F) curve in Fig. 2, whereas the range for precipitation heat treating is associated with aging characteristics of the type shown by the curves for 150 to 260 °C (300 to 500 °F).

NATURE OF PRECIPITATES AND SOURCES OF HARDENING

Intensive research over many decades has resulted in a progressive accumulation of knowledge concerning the atomic and crystallographic structural changes that occur in supersaturated solid solutions during precipitation and the mechanisms through which the structures form and alter alloy properties. In most precipitation-hardenable systems, a complex sequence of time- and temperature-dependent changes is involved. At relatively low temperatures and during initial periods of artificial aging at moderately elevated temperatures, the principal change is a redistribution of solute atoms within the solid-solution lattice to form clusters or GP (Guinier-Preston) zones that are considerably enriched in solute. This local segregation of solute atoms produces a distortion of the lattice planes, both within the zones and extending for several atom layers into the matrix. With an increase in the number or density of zones, the degree of disturbance of the regularity and periodicity of the lattice increases. The strengthening effect of the zones results from the additional interference with the motion of dislocations when they cut the GP zones. This may be because of chemical strengthening (the production of a new particle-matrix interface) and the increase in stress required to move a dislocation through a region distorted by coherency stresses. The progressive strength increase with natural aging time has been attributed to an increase in the size of the GP zones in some systems and to an increase in their number in others.

In most systems, as aging temperatures or time are increased, the zones are either converted into or replaced by particles having a crystal structure distinct from that of the solid solution and also different from the structure of the equilibrium phase. These are referred to as transition precipitates. In most alloys, they have specific crystallographic orientation relationships with the solid solution, such that the two phases remain coherent on certain planes by adaptation of the matrix through local elastic strain. The strengthening effects of these semicoherent transition structures are related to the impedance to dislocation motion provided by the presence of lattice strains and precipitate particles. Strength continues to increase

as the size of these precipitates increases, as long as the dislocations continue to cut the precipitates.

Further progress of the precipitation reaction produces growth of transition phase particles, with an accompanying increase in coherency strains, until the strength of the interfacial bond is exceeded and coherency disappears. This frequently coincides with a change in the structure of the precipitate from transition to equilibrium form. With the loss of coherency strain, strengthening effects are caused by the stress required to cause dislocations to loop around rather than cut the precipitates. Strength progressively decreases with growth of equilibrium phase particles and an increase in interparticle spacing.

Kinetics of Solution and Precipitation. The relative rates at which solution and precipitation reactions occur with different solutes depend on the respective diffusion rates, in addition to solubilities and alloying contents. Bulk diffusion coefficients for several of the commercially important alloying elements in aluminum were determined by various experimental methods, including activation and electron microprobe analyses. A summary of these data, including those for self-diffusion, is shown in Fig. 3. Copper, magnesium, silicon, and zinc, which are the principal solutes involved in precipitation-hardening reactions, have relatively high rates of diffusion in aluminum.

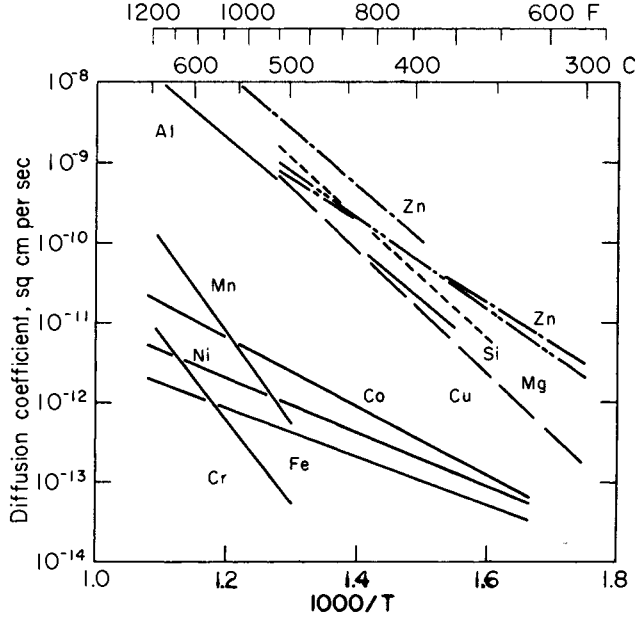

Fig. 3. Diffusion coefficients for various elements in aluminum. Letters in parentheses refer to sources of data. (a) K. Hirano, R.P. Agarwala, and M. Cohen, Acta Metallurgica, *Vol 10, 1962, p 857-863. (b) W.G. Fricke, Jr., Alcoa Research Laboratories. (c) T.S. Lundy and J.F. Murdock,* Journal of Applied Physics, *Vol 33, 1962, p 1671-1673. (d) J.E. Hilliard, B.L. Averbach, and M. Cohen,* Acta Metallurgica, *Vol 1, 1959, p 86-92*

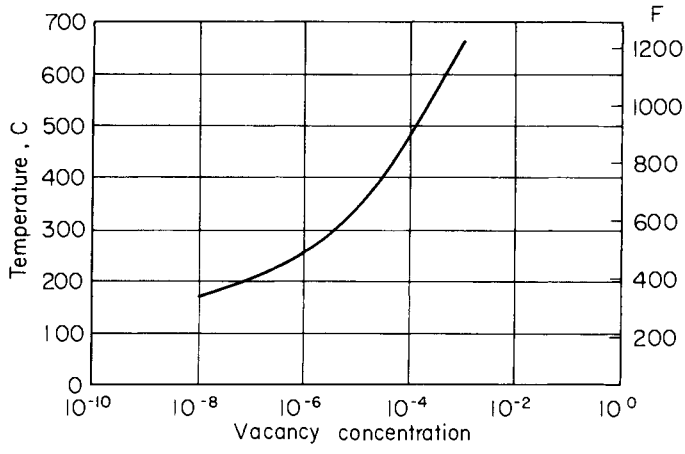

Fig. 4. Equilibrium concentration of vacancies in pure aluminum as a function of temperature. (D. Altenpohl, Aluminium, *Vol 37, 1961, p 401-411)*

Vacancies. Considerable experimental evidence accumulated during the past 20 years strongly indicates that significant numbers of the lattice positions in most crystalline solids are not occupied by atoms. These vacant lattice sites are called "vacancies" (Ref 1). Diffusion of the substitutional solid-solution-forming elements, as well as self-diffusion, is believed to occur primarily by a vacancy exchange mechanism. Vacancies have a particularly significant role in the formation of GP zones. In order to explain the rates of zone formation that are observed at relatively low temperatures, diffusion rates several orders of magnitude greater than those obtained by extrapolating rates measured at higher temperatures are required (Ref 2). Precise measurements of electrical resistivities and relative changes in density and lattice conditions with temperature have been used to ascertain an equilibrium concentration of vacancies in aluminum that varies with temperature, approximately as illustrated in Fig. 4.

The increased low-temperature solute mobility required to account for the high rates of zone formation was explained by a vacancy-assisted diffusion mechanism, made possible by the retention of a nonequilibrium high vacancy concentration at the low temperature (Ref 3). In addition to this fundamental role of vacancies, several specific interactions between vacancies and various solute atoms influence aging kinetics and make the effects of trace elements important. Magnesium appears to play a special role in this process. Because of its large atomic diameter, magnesium-vacancy complexes are readily formed and make retention of excess vacancies during quenching easier. The availability of these vacancies has a marked effect on precipitation kinetics and strengthening potential.

Nucleation. The formation of zones can occur in an essentially continuous crystal lattice by a process of homogeneous nucleation. Several investigations provide evidence that critical vacancy concentration is required for this process and that a nucleation model involving vacancy-solute atom clusters is consistent with certain effects of solution temperature and quenching rate (Ref 4-10).

The nucleation of a new phase is greatly influenced by discontinuities in the lattice such as grain boundaries, subgrain boundaries, dislocations, and interphase boundaries. Because these sites are locations of greater disorder and higher energy than the solid-solution matrix, they nucleate either transition or equilibrium precipitates. The solute that precipitates in this uncontrolled manner during the quench is unavailable for subsequent precipitation either at room or elevated temperatures, so precipitation during the quench can affect the development of properties. The effect on strength of precipitating during the quench onto grain boundaries, subgrain boundaries, and scattered particles on the order of 0.5 μm (0.02 mil) or larger is generally negligible. The effects of precipitating onto the fine dispersoid particles (<0.1 μm or <0.004 mil) formed by high temperature precipitation at an earlier stage in the processing, however, can be large when the rate of cooling is not rapid enough. Figure 5 illustrates precipitate formed on one such particle with an accompanying deficiency of precipitate adjacent to the particle. This phenomenon of a

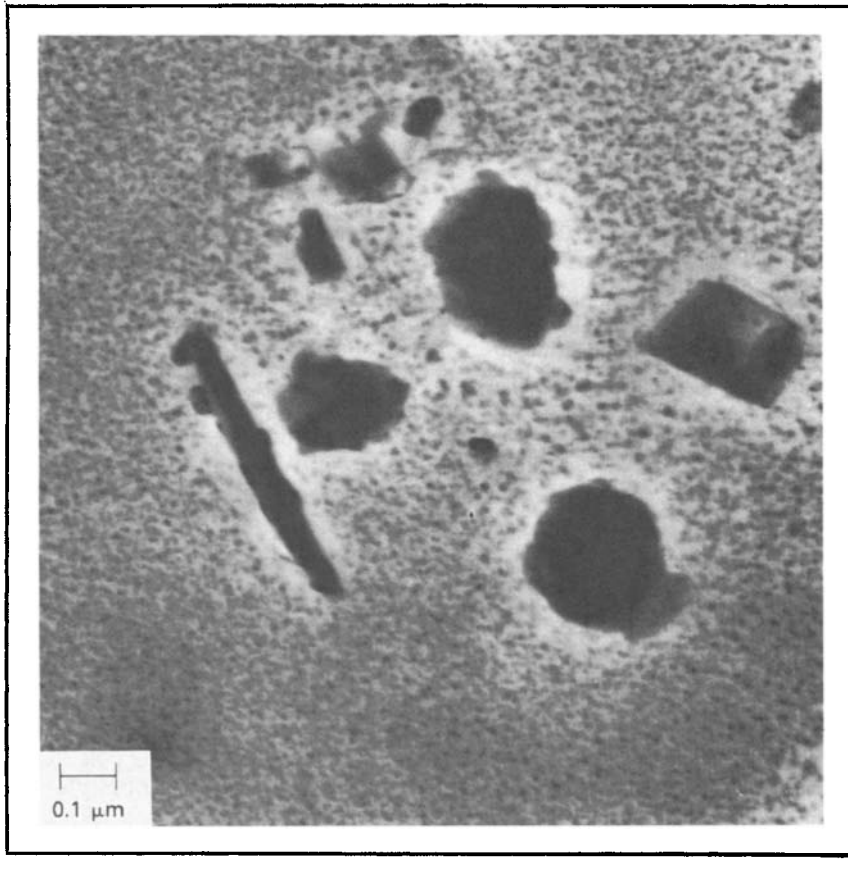

Fig. 5. Transmission electron micrograph of 75-mm (3-in.) thick 7039-T63 plate. Note the precipitate on the dispersoids and the resultant precipitate-free-zone surrounding each dispersoid particle.

precipitate-free zone (PFZ) after slow quenching and aging is attributed to the depletion of solute atoms near the particles and to the scarcity of nucleation sites caused by the migration of vacancies to the particle-matrix boundaries during the quench.

Although precipitates at grain boundaries do not have a large effect on attainable strength, they can have a harmful effect on the corrosion resistance of the material and increase the tendency toward intergranular fracturing. Grain boundary precipitation is frequently accompanied by the development of precipitate-free zones similar to those seen adjacent to dispersoid particles. Electrochemical potential relations between intergranular precipitate particles, precipitate-depleted or GP zone-depleted layers, and grain interiors are fundamental to the electrochemical theory of intergranular stress-corrosion cracking.

Investigations of precipitated structures by transmission electron microscopy have demonstrated that dislocations formed by condensation of vacancies or by introduction of plastic strain are also very active nucleation sites for precipitation (Ref 11). Variations in dislocation density resulting from different quenching rates, as well as the degree of vacancy and solute retention achieved during the quench, are factors in determining the effects of quenching rates on strengthening. The introduction of dislocations by cold working after quenching accelerates precipitation in 2XXX alloys and increases the strength developed during artificial aging. In other alloys, the effects of cold working are either negligible or detrimental, as subsequently discussed in this chapter.

PRECIPITATION IN SPECIFIC ALLOY SYSTEMS

Several commercially important aluminum alloy systems have been subjected to careful investigation of the structures existing at various stages of the precipitation process, and these are briefly described below.

Aluminum-Copper. In these alloys, the hardening observed at room temperature is attributed to localized concentrations of copper atoms forming Guinier-Preston zones, designated GP (1). These consist of two-dimensional copper-rich regions of disk-like shape, oriented parallel to {100} planes. The diameter of the zones is estimated to be 3 to 5 nm (30 to 50 Å) and does not change with aging time at room temperature. The number, however, increases with time, until in the fully aged condition, the average distance between zones is about 100 nm (1000 Å).

At temperatures of 100 °C (212 °F) and higher, the GP (1) zones disappear and are replaced by a structure designated GP (2) or θ″ which, although only a few atom layers in thickness, is considered to be three-dimensional and to have an ordered atomic arrangement. The transition phase, θ′, having the same composition as the stable phase and exhibiting coherency with the solid solution lattice, forms after GP (2), but coexists with it over a range of time and temperature. The final stage in the sequence is the transformation of θ′ into noncoherent equilibrium θ ($CuAl_2$). The structure sequence in aluminum-copper alloys may be diagrammed:

$$SS \rightarrow GP\,(1) \rightarrow GP\,(2) \rightarrow \theta' \rightarrow \theta'' \qquad \text{Eq 1}$$

The correlation of these structures with hardness is illustrated in Fig. 6 for a 4% copper alloy aged at two temperatures. At some temperatures,

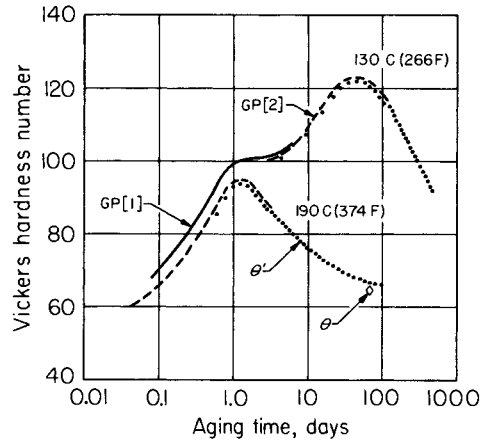

Fig. 6. Correlation of structure and hardness of Al-4% Cu alloy aged at two temperatures. (J.M. Silcock, T.J. Heal, and H.K. Hardy, Journal of the Institute of Metals, *1953-1954, p 82239-82248)*

for example 130 °C (265 °F), the initial hardening from formation of GP (1) is distinguishable from a second stage attributable to GP (2). Maximum hardness and strength occur when the amount of GP (2) is essentially at a maximum, although some contribution may also be provided by θ′. As the amount of θ′ increases, particle growth eventually decreases the coherency strains. This loss in coherency, together with the simultaneous decrease in GP (2), causes overaging. When the noncoherent θ appears, the alloy is softened far beyond the maximum-strength condition.

Aluminum-Copper-Magnesium Alloys. Additions of magnesium to aluminum-copper alloys accelerate and intensify natural age hardening. These were the first heat treatable high-strength aluminum alloys, and they have continued through the years to be among the most popular and useful. Despite their early origin and large-volume production, details of the precipitation mechanisms and structures of aluminum-copper-magnesium alloys are less well developed than for aluminum-copper alloys. Although evidence is strong for the formation of zones during natural aging, it has not been possible to ascertain their form or size. They are believed to consist of groups of magnesium and copper atoms that collect on {110} matrix planes. The apparent acceleration of this process by the addition of magnesium may result from complex interactions between vacancies and the two solutes. Some preparatory pairing of copper and magnesium atoms also has been suggested, and the pairing may contribute to hardening by a mechanism of dislocation pinning.

Aging of 2024-T4 alloy at elevated temperatures produces the transition phase S' (Al_2CuMg), which is coherent on {021} matrix planes, whereas overaging is associated with formation of the equilibrium S phase (Al_2CuMg) and loss of coherency. The precipitation structure sequence may be represented as follows:

$$SS \rightarrow GP \rightarrow S' (Al_2CuMg) \rightarrow S (Al_2CuMg) \qquad \text{Eq 2}$$

Small additions of magnesium significantly strengthen aluminum-copper alloys even though no evidence of S' has been detected after precipitation heat treatments.

Aluminum-Magnesium-Silicon Alloys. Appreciable strengthening in these alloys occurs over an extended period at room temperature. This strengthening probably entails the formation of zones, although they have not been positively detected in the naturally aged state. Short aging times at temperatures up to 200 °C (390 °F) produce x-ray and electron diffraction effects indicating the presence of very fine, needle-shaped zones oriented in the ⟨001⟩ direction of the matrix. Electron microscopy indicated the zones to be approximately 6 nm (60 Å) in diameter and 20 to 100 nm (200 to 1000 Å) in length. Another investigation indicates that the zones are initially of spherical shape and convert to needlelike forms near the maximum strength inflections of the aging curves. Further aging causes apparent three-dimensional growth of the zones to rod-shaped particles with a structure corresponding to a highly ordered Mg_2Si. At higher temperatures, this transition phase, designated β', undergoes diffusionless transformation to the equilibrium Mg_2Si.

No direct evidence of coherency strain is found in either the zone or transition precipitate stages. It has been suggested that the increased resistance to dislocation motion accompanying the presence of these structures arises from the increased energy required to break magnesium-silicon bonds in the zones as dislocations pass through them. Grain boundary precipitate particles of silicon are found at very early stages of aging in alloys having an excess of silicon over the Mg_2Si ratio. The normal precipitation sequence may be diagrammed as follows:

$$SS \rightarrow GP \rightarrow \beta' (Mg_2Si) \rightarrow \beta (Mg_2Si) \qquad \text{Eq 3}$$

Aluminum-Zinc-Magnesium and Aluminum-Zinc-Magnesium-Copper Alloys. The aging of rapidly quenched aluminum-zinc-magnesium alloys from room temperature to relatively low aging temperatures is accompanied by the generation of GP zones having an approximately spherical shape. With increasing aging time, GP zones increase in size, and the strength of the alloy increases. Figure 7 shows GP zones in alloy 7075 that attained a diameter of 1.2 nm (12 Å) after 25 years at room temperature. After that time, the yield strength was about 95% of the value after standard T6 aging. Extended aging at temperatures above room temperature transforms the GP zones in alloys with relatively high zinc-magnesium ratios into the transition precipitate known as η' or M′, the precursor of the equilibrium $MgZn_2$, η, or M phase precipitate. The basal planes of the hexagonal η' precipitates are partially coherent with the {111} matrix planes but the interface between the matrix and the c direction of the precipitate is incoherent. Aging times and temperatures that develop the highest strengths, characteristic of the T6 temper, produce zones having an average diameter of 2 to 3.5 nm (20 to 35 Å) along with some amount of η'. The nature of the zones is still uncertain, although they undoubtedly have high concentrations of zinc atoms and probably magnesium atoms as well. Some variation in x-ray and electron diffraction effects indicative of zone structure variations were noted, depending on relative zinc and magnesium contents of the alloys.

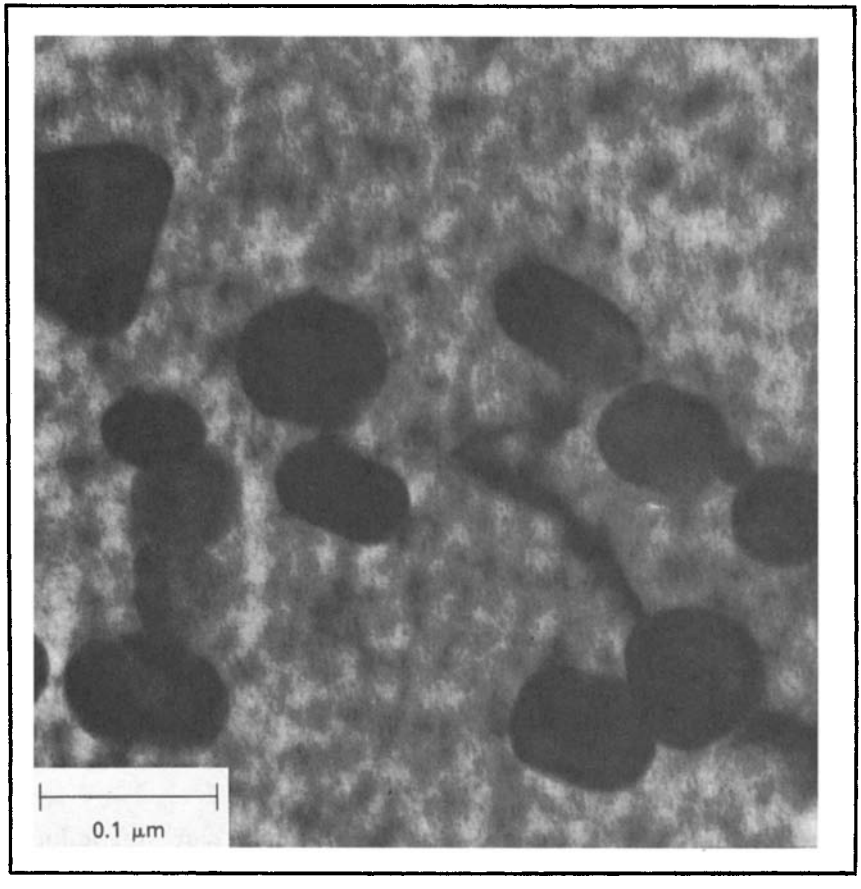

Fig. 7. Transmission electron micrograph of 7075-W aged 25 years at room temperature. The large particles are $Al_{12}Mg_2Cr$ dispersoid. The GP zones throughout the structure have an average diameter of 1.2 nm (12 Å), and an approximate density of 4×10^{18} zones per cm^{-3}. The yield strength of the as-quenched 7075-W was 150 MPa (22 ksi). After 25 years, yield strength had increased to 465 MPa (67 ksi).

Several investigators have observed that the transition phase η' forms over a considerable range of compositions that are in the Al + T field, as well as those in the Al + η field under equilibrium conditions (Fig. 8). With increased time or higher temperature, the η' converts to ($MgZn_2$) or, in cases where T is the equilibrium phase, is replaced by T ($Mg_3Zn_3Al_2$). Evidence exists for a transition form of T in alloys with lower zinc-magnesium ratios, at times and temperatures that produce overaging. The precipitation sequence depends on composition, but that of rapidly quenched material aged at elevated temperatures may be represented as:

$$\text{SS} \rightarrow \text{GP zones [spherical]} \begin{cases} \nearrow \eta' \rightarrow \eta \\ \searrow T' \rightarrow T \end{cases} \qquad \text{Eq 4}$$

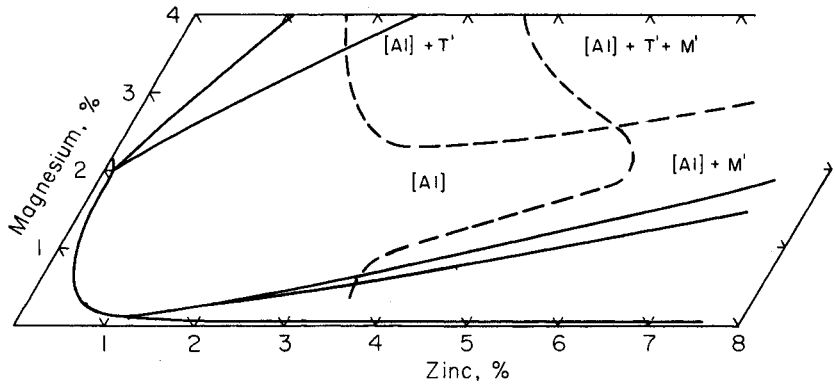

Fig. 8. Comparison of phases present in aluminum-magnesium-zinc alloys. Fields separated by dashed lines identify phases present after alloys were solution heat treated, quenched, and aged 24 h at 120 °C (250 °F) ([Al] = GP zone structure). Fields separated by solid lines are phases in equilibrium at 175 °C (350 °F). (H.C. Stumpf, Alcoa)

In this schematic, GP zones nucleate homogeneously, and the various precipitates develop sequentially within the matrix. However, the presence of high-angle grain boundaries, subgrain boundaries, and lattice dislocations alters the free energy such that significant heterogeneous nucleation may occur either during quenching or aging above a temperature known as the GP zone solvus temperature. Above this temperature, the semicoherent transition precipitates nucleate and grow directly on dislocations and subgrain boundaries, and the incoherent equilibrium precipitates nucleate and grow directly on high-angle boundaries. These heterogeneously nucleated precipitates do not contribute to strength and, hence, decrease attainable strength by decreasing the amount of solute available for homogeneous nucleation.

Decreasing the quench rate has another consequence besides allowing solute atoms an opportunity to nucleate heterogeneously. Slow quenching permits vacancies to migrate to free surfaces and become annihilated. Decreasing the number of vacancies decreases the temperature at which GP zones nucleate homogeneously. Therefore, a particular aging temperature may allow only homogeneous nucleation to occur in rapidly quenched materials, but may allow heterogeneous nucleation to predominate in slowly quenched material. Under the latter conditions, the precipitate distribution is extremely coarse, so strength developed is particularly low. Some of the loss in strength from slow quenching in this case can be minimized by decreasing the aging temperature to maximize homogeneous nucleation.

When an aged aluminum-zinc-magnesium alloy is exposed to a temperature higher than that to which it has previously been exposed, some GP zones dissolve while others grow. Whether a GP zone dissolves or grows depends on its size and on the exposure temperature. When the zone size is large enough, most of the zones transform to transition precipitates even above the GP zone solvus temperature. This phenomenon

is the basis for the two-step aging treatments to be discussed in a later section of this chapter.

The addition of up to 1% copper to the aluminum-zinc-magnesium alloys does not appear to alter the basic precipitation mechanism. In this range, the strengthening effects of copper are modest and attributed primarily to solid solution. Higher copper contents afford greater precipitation hardening, with some contribution of copper atoms to zone formation, as indicated by an increased temperature range of zone stability. Crystallographic arguments indicate that copper and aluminum atoms substitute for zinc in the $MgZn_2$ transition and equilibrium precipitates. In the quaternary aluminum-zinc-magnesium-copper system, the phases $MgZn_2$ and MgAlCu form an isomorphous series in which an aluminum atom and a copper atom substitute for two zinc atoms. Moreover, electropotential measurements and x-ray analyses indicate that copper atoms enter into the η' phase during aging temperatures above about 150 °C (300 °F). These observations are significant because aging aluminum-zinc-magnesium-copper alloys containing above about 1% copper above this temperature substantially increases their resistance to stress-corrosion cracking. Little effect is shown on the stress corrosion of alloys containing lower amounts of copper.

INGOT PREHEATING TREATMENTS

The initial thermal operation applied to ingots prior to hot working is referred to as "ingot preheating" or "homogenizing" and has one or more purposes depending on the alloy, product, and fabricating process involved. One of the principal objectives is improved workability. As described in Chapter 2 of this Volume, the microstructure of most alloys in the as-cast condition is quite heterogeneous. This is true for alloys that form solid solutions under equilibrium conditions and even for relatively dilute alloys. The cast microstructure is a cored dendritic structure with solute content increasing progressively from center to edge with an interdendritic distribution of second-phase particles or eutectic.

Because of the relatively low ductility of the intergranular and interdendritic networks of these second-phase particles, as-cast structures generally have inferior workability. The thermal treatments used to homogenize cast structures for improved workability were developed chiefly by empirical methods, correlated with optical metallographic examinations, to determine the time and temperature required to minimize coring and dissolve particles of the second phase. More recently, methods have become available to determine quantitatively the degree of microsegregation existing in cast structures and the rates of solution and homogenization. Figure 9 shows the microsegregation measured by an electron microprobe across the same dendrite cell in the as-cast condition and after the cell was homogenized by preheating. Rapid solidification, because it is quite different from equilibrium, produces maximum microsegregation across dendrite walls, and these cells are relatively small. The situation is complex, however, and in typical commercial ingots, large cells are more segregated than fine cells and, because diffusion distances are longer, large cells are more difficult to homogenize (Ref 12 and 13). For example, electron microprobe analyses of unidirectionally solidified cast-

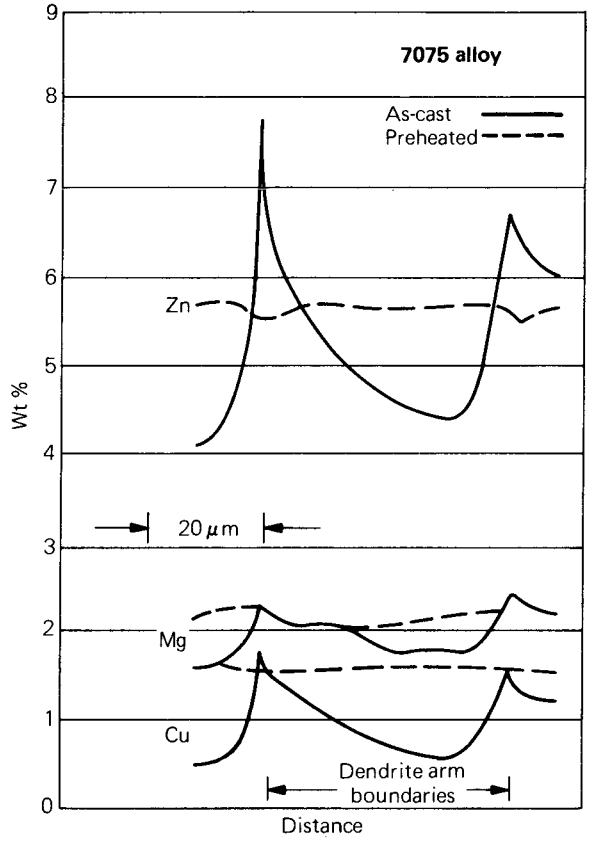

Fig. 9. Effect of preheating on ingot microsegregation.

ings of an Al-2.5% Mg alloy indicated that the degree of microsegregation was greater in the coarser, more slowly solidified structure, and that the approach to uniform solute distribution during heating at 425 °C (800 °F) was more rapid for the finer structure, as shown in Fig. 10.

Solution of the intermetallic phases rejected interdendritically during solidification, effected by the homogenizing operation, is only one step toward providing maximum workability. Because most of the solute is in solid solution after this heating, further softening and improvement in workability can be obtained by slow cooling, to re-precipitate and coalesce the solute in an intradendritic distribution of fairly large particles.

In aluminum-magnesium-silicon alloys, redistribution of magnesium and silicon occurs very rapidly, in as little as 30 min at 585 °C (1090 °F). However, greatly extended homogenizing periods result in a higher rate of extrusion and in an improved surface appearance of extruded products. The mechanism consists of spheroidizing the nearly insoluble iron-rich phases; the lower the solubility and diffusion rate of the elements involved, the slower the rate of spheroidization. Secondary effects are also achieved by precipitation of additional transition elements from solid so-

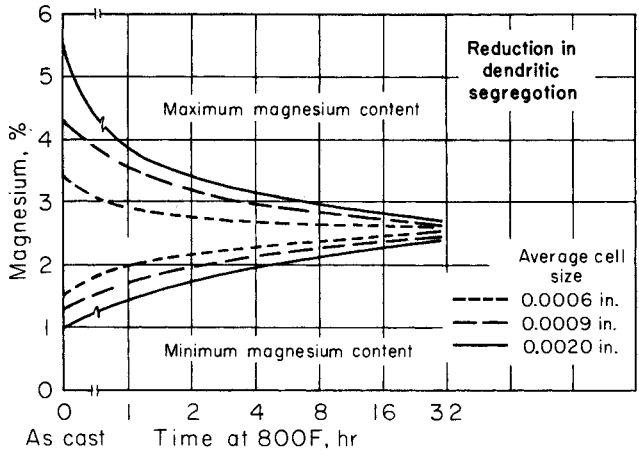

Fig. 10. Effect of time at 425 °C (800 °F) on maximum and minimum magnesium contents within dendrites of cast Al-2.5% Mg alloy. (W.G. Fricke, Jr., Alcoa Research Laboratories)

lution and by delayed peritectic transformations that could not go to completion during solidification.

Elements such as chromium and zirconium, which separate by a peritectic reaction during solidification, segregate in a manner just the reverse of that previously described. The first portion of the dendrite to solidify is richer in solute than the subsequently solidified portions. Consequently, the alloy content is maximum to the center of the dendrites and diminishes progressively toward the edges. The solid solutions formed by these elements and by manganese during rapid solidification are supersaturated with respect to their equilibrium solid solubilities. This is thought to result from the relatively low diffusion rates of the elements in the solid state.

Ingot preheating treatments for some of the alloys containing these elements are designed to induce precipitation, resulting in the formation of particles of equilibrium phases such as $Al_{20}Cu_2Mn_3$ and $Al_{12}Mg_2Cr$ with dimensions of 10 to 100 nm (1 to 10 Å). These high-temperature precipitates are frequently called dispersoids. They occur within the original dendrites, with a distribution essentially the same as that established during solidification, because the diffusion rates are too low to permit any substantial redistribution. In aluminum-magnesium-manganese alloys, the preheating operation increases the heterogeneity of manganese because of localized precipitation of manganese-bearing dispersoids near the dendrite arms. Nonuniform distribution persists in some wrought products, leading to microstructural patterns called banding. Ingot preheating treatments for certain alloys containing manganese, such as 3003, are designed to induce precipitation under controlled conditions; this lowers the recrystallization temperature and favors the development of fine, recrystallized grains during later process and final anneals (Ref 14).

Equilibrium Versus Nonequilibrium Melting. Figure 11 illustrates some of the restrictions that must apply to ingot preheating because of the phase diagram. The same principles apply to more complex systems,

but the details differ because different phases have different solvus temperatures and the eutectic may be a trough instead of a point.

Different compositions on the diagram represent different types of commercial alloys. Alloy X represents an alloy in which the alloy content does not exceed the maximum solubility. This is typified by relatively dilute alloys such as 2117, 6063, and 7029, but it is also true of alloys 7075 and 6061. Cursory examination of the phase diagram indicates that the ingot preheating range can be located anywhere between the solvus and solidus temperatures. However, to avoid the possibility of nonequilibrium melting, as explained below, either the upper limit should be below the eutectic temperature or the time below the eutectic temperature should be of sufficient duration to produce complete solution of the elements comprising the eutectic. Alloy Y represents an alloy in which an excess of soluble phase always remains undissolved. The upper end of the preheat temperature range must lie below the equilibrium eutectic temperature if melting is to be avoided. This case is typified by alloys 2219, 2011, and 7178. Alloys such as 2024 may respond like either alloy

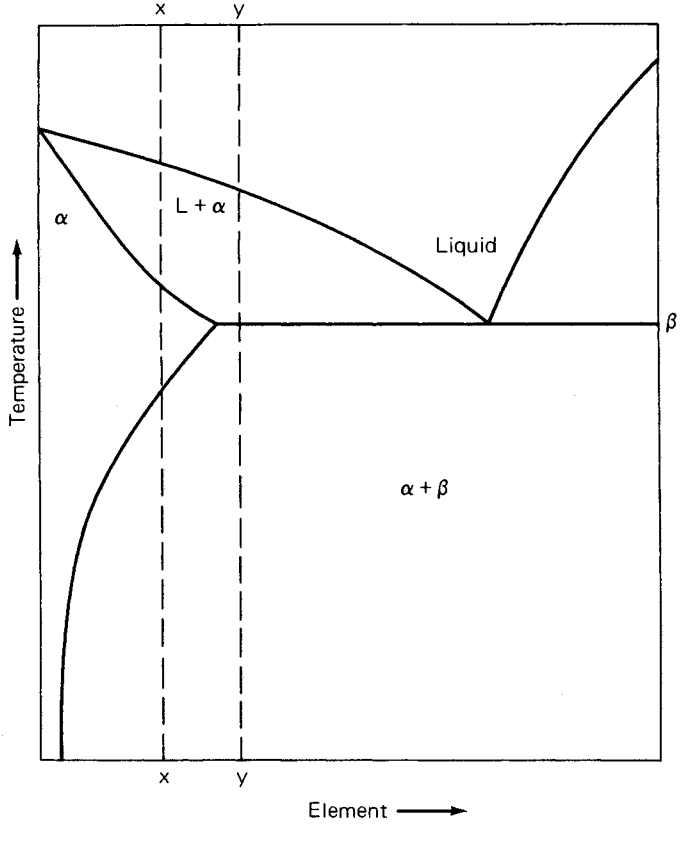

Fig. 11. Schematic phase diagram. Alloy X melts at the eutectic temperature if B is not dissolved below this temperature. Alloy Y always melts at the eutectic temperature.

X or alloy Y, depending on the amounts and proportions of the alloying and impurity elements.

Incipient melting, or the beginnings of liquid phase formation, can occur under either equilibrium or nonequilibrium conditions. Alloy Y in Fig. 11 obviously produces melting whenever its temperature is at or above the eutectic temperature. However, it is not as obvious that the same reaction occurs for alloy X, which has a higher equilibrium solidus temperature than alloy Y. When alloy X is in the as-cast condition, it contains a nonequilibrium eutectic structure. If reheating to the eutectic temperature is done at a rapid enough rate so that the soluble intermetallic cannot dissolve, the eutectic melts. Holding alloys like alloy X for sufficient time between the eutectic temperature and the true solidus causes the liquid phase to disappear as the soluble element passes into solution. The solution of the elements in the liquid phase leaves evidence in the form of microporosity at the previous sites of eutectic if the hydrogen content is above some critical level. The size of the micropores is smaller than the shrinkage porosity in good quality as-cast ingot. The principles expounded above apply to non-heat-treatable alloys as well as to heat treatable ones.

The real test of the harmfulness of overheating is whether there is microstructural damage of a type that cannot subsequently be repaired. Damage consists of excessive void formation, segregation, blistering, cracking, or severe external oxidation. Rosettes, the spherical structural feature that occurs when eutectic liquid solidifies during cooling after overheating, are very hard and persistent. They have been detected in thin sheet fabricated from thick, overheated ingot, despite extensive thermal-mechanical treatments used during the fabrication.

ANNEALING

Annealing may be required before forming or cold working heat treatable alloys, when they have been strain hardened by previous forming or are in heat treated tempers. The principles outlined in Chapter 4 of this Volume governing recovery, recrystallization, and grain size control for non-heat-treatable alloys apply also to the annealing of heat treatable alloys. However, the maximum temperature and cooling rate used must be more carefully controlled to avoid precipitation hardening either during or subsequent to annealing.

The type of annealing treatment required depends on the previous thermal and mechanical history, and the structure resulting from these prior operations. Alloys that are initially in the F temper may require annealing; O-temper material may require re-annealing after partial forming. Under these conditions, the operations that preceded forming already have caused the extensive precipitation and coalescence of precipitates that is desired, so that the objective of the annealing treatment is only to remove the strain hardening. This can be accomplished by heating to about 345 °C (650 °F) and holding long enough to ensure attainment of uniform temperature. The rates of heating and cooling are not critical in this operation, although a rapid heating rate is preferred to provide a fine grain size.

The annealing of alloys that have previously been heat treated to tem-

pers such as W, T3, T4, T6, or T8 requires use of treatments that first cause the precipitates to reach their equilibrium crystal structure and then cause them to coarsen. This can be accomplished by heating for 2 to 3 h at about 355 to 410 °C (675 to 775 °F) or slightly higher, followed by cooling to about 260 °C (500 °F) at rates of about 25 to 40 °C/h (45 to 72 °F/h). A too-slow cooling rate results in platelets of precipitate and poor formability in 7XXX alloy sheet. In the case of 2XXX series alloys, this treatment should precipitate most of the copper, leaving only 0.4 to 0.5% in solution. For 7XXX series alloys, even slow cooling does not provide sufficiently complete precipitation to remove solid solution effects and prevent natural aging; a period of additional heating at 230 °C (450 °F) for 2 to 6 h may be used to attain maximum stability and formability. Despite this more extensive procedure, the alloy annealed from the heat treated tempers usually has slightly poorer formability than annealed material not previously heat treated. In annealing thin-gage clad products, the heating time at the maximum temperature must be limited to avoid excessive diffusion from core to cladding. Annealing treatments are applied to castings only when the most exacting requirements for dimensional stability must be met, or when some unusual forming operation is specified.

SOLUTION HEAT TREATING

The purpose of solution heat treatment is to put the maximum practical amount of hardening solutes such as copper, magnesium, silicon, or zinc into solid solution in the aluminum matrix. For some alloys, the temperature at which the maximum amount is soluble corresponds to a eutectic temperature. Consequently, temperatures must be limited to a safe level below the maximum to avoid consequences of overheating and partial melting. Alloy 2014 exhibits this characteristic. Figure 12 illustrates

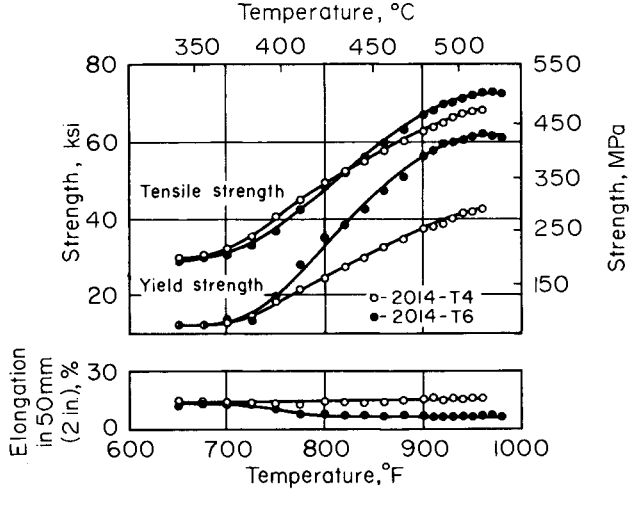

Fig. 12. Effects of solution heat treating temperature on the tensile properties of 2014-T4 and 2014-T6 sheet.

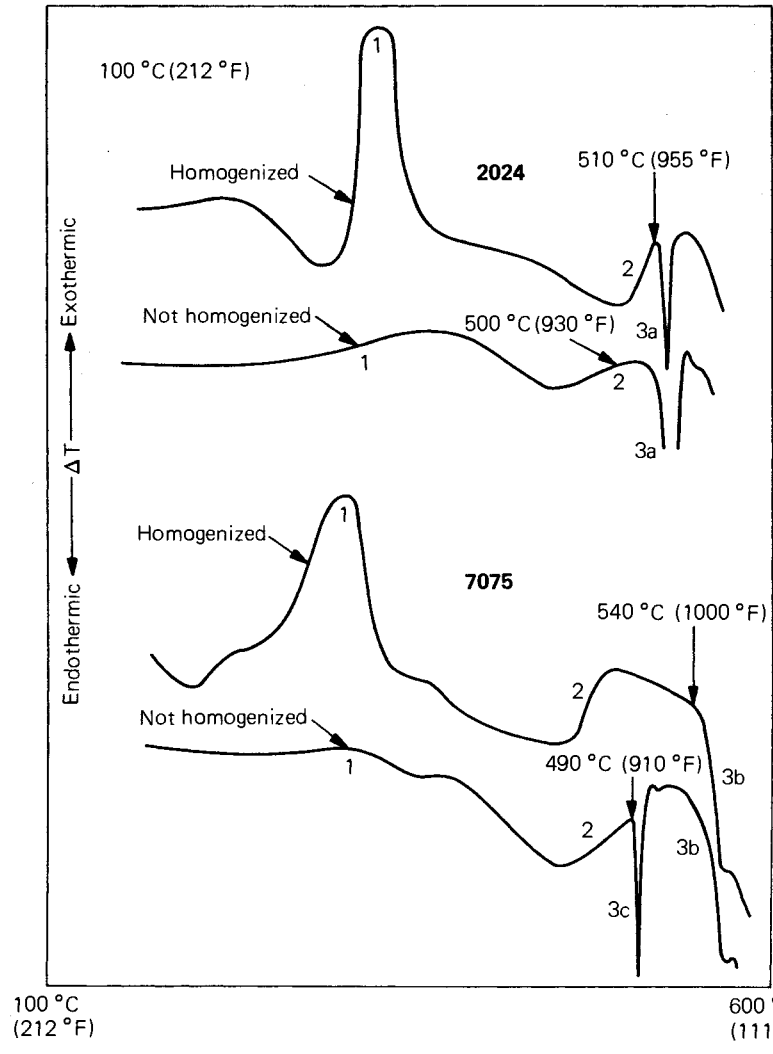

Fig. 13. DTA curves at 20 °C/min (36 °F/min) heating, indicating temperatures for easily identified beginning of melting (shown by arrows). Significant curve inflections are (1) precipitation from saturated solid solution, (2) re-solution of precipitated phase(s), and (3) melting. Equilibrium eutectic melting for 2024 is indicated by (3a); equilibrium solidus melting for 7075 by (3b), and nonequilibrium eutectic melting for 7075 by (3c).

the effect of solution temperature on the tensile properties of 2014-T4 and 2014-T6. Other alloys such as 7029 are more dilute with respect to their maximum solubility, and greater temperature tolerances are allowable. Nevertheless, the upper limit must be set with a regard to grain growth, surface effects, and economy of operation.

Some alloys, such as 7075 and 7050, which should allow much leeway in selection of solution temperature, based on the equilibrium solvus and

solidus temperature, can exhibit incipient melting at temperatures much below the latter under certain circumstances. Chapter 3 in this Volume shows that alloy 7075 has two soluble phases—$MgZn_2$ (with aluminum and copper substituting for some zinc) and Al_2CuMg. The latter phase is very slow to dissolve. Local concentrations of this phase can produce a nonequilibrium melting between 485 and 490 °C (905 and 910 °F) if brought to this or a higher temperature too rapidly. Figure 13 shows this by means of differential thermal analysis curves. A sample of nominal composition alloy 7075 that had been well homogenized and quenched began to melt somewhere in excess of 540 °C (1000 °F), while one not homogenized showed an endothermic spike indicating incipient melting at 490 °C (910 °F). Nominal composition 2024 cannot be homogenized to remove the S phase, and melting occurs near 510 °C (955 °F) in products that are homogenized and not homogenized. The curves indicate that only the quantity of liquid phase formed differed.

The grain size of heat treated aluminum alloys is greatly influenced by the amount of cold work introduced before the solution heat treatment. In general, grain size decreases as the amount of cold work prior to solution increases. With small amounts of cold work, usually less than 15%, grains may develop that are so coarse that relatively few are contained in the cross section of a standard tension test coupon. Although mechanical properties of heat treated aluminum alloys are generally insensitive to grain size, the properties are affected under these conditions. This phenomenon is illustrated in Fig. 14 for alloy 7475 sheet. Because of this effect of critical strain, care must be taken that parts formed from an

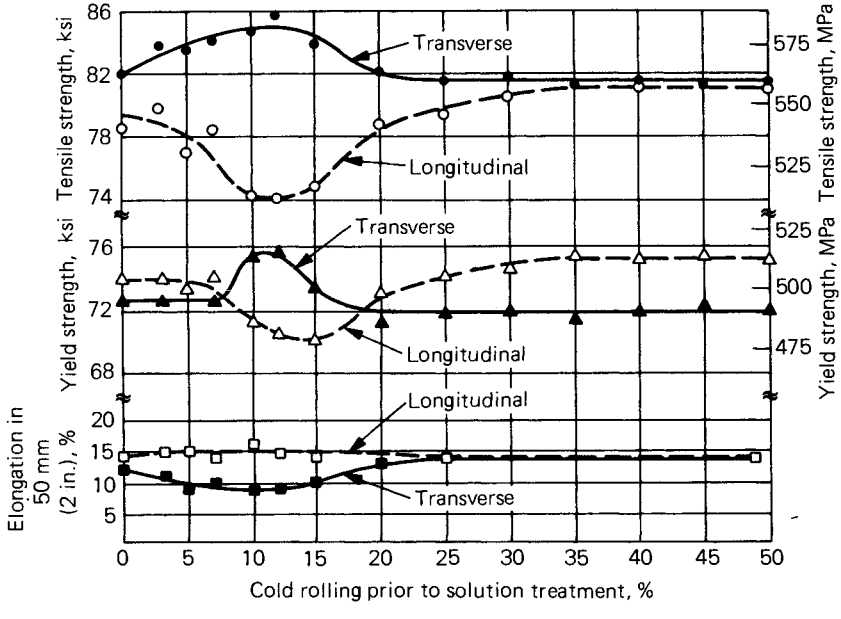

Fig. 14. Effect of cold work prior to solution treatment on tensile properties of 7475-T6 sheet.

annealed temper and subsequently heat treated have sufficient strain hardening at all locations.

For products that are annealed and cold worked prior to heat treatment, the annealing practice and the rate of heating to the solution heat treating temperature also affect grain size. Fine grain sizes are favored by annealing practices that give a copious distribution of coarse precipitates and by high heating rates. The coarse precipitates serve as nucleation sites for recrystallization, and the high heating rates ensure that nucleation begins before the precipitates dissolve. Air is the usual heating medium, but molten salt baths or fluidized beds are advantageous in providing more rapid heating.

The time required for solution heat treating depends on the type of product, alloy, casting or fabricating procedure used and thickness insofar as it influences preexisting microstructure. These factors establish the proportions of the solutes that are in or out of solution and the size and distribution of precipitated phases. Sand castings are usually held at the solution temperature for about 12 h; permanent mold castings, because of their finer structure, may require only 8 h. Thick-section wrought products are generally heated longer, the greater the section thickness. Once the product is at temperature, the rate of dissolution is the same for a given size of particle, regardless of section thickness. The main consideration is the coarseness of microstructure and the diffusion distances required to bring about a satisfactory degree of homogeneity. Thin products such as sheet may require only a few minutes. To avoid excessive diffusion, the time of solution heat treatment for clad sheet products must be limited to the minimum required to develop the specified mechanical properties. For the same reason, limitations are placed on reheat treatment of thin clad products where the correspondingly thin clad layer changes composition rapidly and loses its effectiveness in protecting against corrosion.

Reheat treating of previously heat treated products is subject to other hazards. When cold working has been applied after the previous heat treatment to develop T3 or T8 tempers, the residual strain may be of the critical amount to cause excessively large recrystallized grains. In reheat treating 2XXX series alloys, the temperature must not be lower than that of the original treatment, and heating time should be prolonged. Otherwise, corrosion resistance may be impaired and formability is seriously decreased by the development of continuous, heavy precipitate at grain boundaries.

A condition called "high-temperature oxidation" (HTO) or "high-temperature deterioration" results when metal is heated to solution heat treatment temperatures in a furnace that has too much moisture in the atmosphere. It is aggravated when the moist atmosphere is contaminated with gases containing sulfur. This condition manifests itself by formation of rounded voids or crevices within the metal and by surface blisters. It occurs when atomic hydrogen, formed when moisture reacts with the aluminum surfaces, diffuses through the aluminum lattice and recombines to form molecular hydrogen at locations of lattice discontinuity and disregistry. Such reactions may be alleviated by using moisture-free atmos-

pheres, or by use of volatile fluoride-containing salts or boron-trifluoride gas injected into the furnace atmosphere.

Severe void formation and blistering may also be a consequence of severe but temporary overheating. It may have the same aspect as high-temperature oxidation if, during the heat treatment cycle, the temperature is brought back down to the normal range and held before the metal is quenched. In this instance, the solute-enriched liquid phase disappears through resolidification and dissolution. Hydrogen undoubtedly plays a role, but the primary problem is partial melting. This phenomenon can be distinguished from high-temperature oxidation by the distribution of the voids; with HTO, the number of voids progressively decreases as distance from the surface increases. With this phenomenon, the voids are scattered throughout the workpiece.

Another phenomenon may also cause microvoid formation. The soluble phases containing magnesium have a tendency to leave behind microvoids when they dissolve, especially when the particles are large and the heating rate is very rapid. This has been attributed to a density difference between particle and matrix and insufficient time for aluminum atoms to back-diffuse into the volume formerly occupied by the particle. No known detrimental effect of these voids exists, unless they are combined with high-temperature oxidation.

QUENCHING

Quenching is in many ways the most critical step in the sequence of heat treating operations. The objective of quenching is to preserve the solid solution formed at the solution heat treating temperature, by rapidly cooling to some lower temperature, usually near room temperature. From the preceding general discussion, this statement applies not only to retaining solute atoms in solution, but also to maintaining a certain minumum number of vacant lattice sites to assist in promoting the low-temperature diffusion required for zone formation. The solute atoms that precipitate either on grain boundaries, dispersoids, or other particles, as well as the vacancies that migrate (with extreme rapidity) to disordered regions, are irretrievably lost for practical purposes and fail to contribute to the subsequent strengthening.

As a broad generalization, the highest strengths attainable and the best combinations of strength and toughness are those associated with the most rapid quenching rates. Resistance to corrosion and to stress-corrosion cracking are other characteristics that are generally improved by maximum rapidity of quenching. Some of the alloys used in artificially aged tempers and in particular the copper-free 7XXX alloys are exceptions to this rule. The argument for maximum quenching rate also is not entirely one-sided, because both the degree of warpage or distortion that occurs during quenching and the magnitude of residual stress that develops in the products tend to increase with the rate of cooling. In addition, the maximum attainable quench rate decreases as the thickness of the product increases. Because of these effects, much work has been done over the years to understand and predict how quenching conditions and product form influence properties.

Critical Temperature Range. The fundamentals involved in quenching precipitation-hardenable alloys are based on nucleation theory applied to diffusion-controlled solid-state reactions. The effects of temperature on the kinetics of isothermal precipitation depend principally upon the degree of supersaturation and the rate of diffusion. These factors vary oppositely with temperature, as illustrated in Fig. 15 for an alloy having a composition C_1 in a system with a solvus curve C_S. The degree of supersaturation after solution heat treating (C_1 - C_S) is represented by the curve S and the rate of diffusion by curve D. When either S or D is low, the rate of precipitation, represented by curve P, is low. At intermediate temperatures, both of the rate-controlling factors are favorable, and a high rate of precipitation may be expected.

Fink and Willey pioneered attempts to describe the effects of quenching on properties of aluminum alloys (Ref 15). Using isothermal quenching techniques, they developed C-curves for strength of 7075-T6 and corrosion behavior of 2024-T4. The C-curves were plots of the time required at different temperatures to precipitate a sufficient amount of solute to either reduce strength by a certain amount or cause a change in the corrosion behavior from pitting to intergranular. Inspection of the curves revealed the temperature range that gave the highest precipitation rates. Fink and Willey called this the critical temperature range.

Investigators used critical temperature ranges in conjunction with properties of samples quenched continuously from the solution temperature to compare relative sensitivities of alloys to quenching condition. Strength, as a function of quenching rate, was determined for a number of the commercial heat treatable aluminum alloys by quenching sheet and plate panels of various thicknesses in different media to produce a wide range of cooling rates through the critical temperature range. Representative tensile strength data for several alloys are presented in Fig. 16. The reduction in strength for a specific decrease in cooling rate differs from one

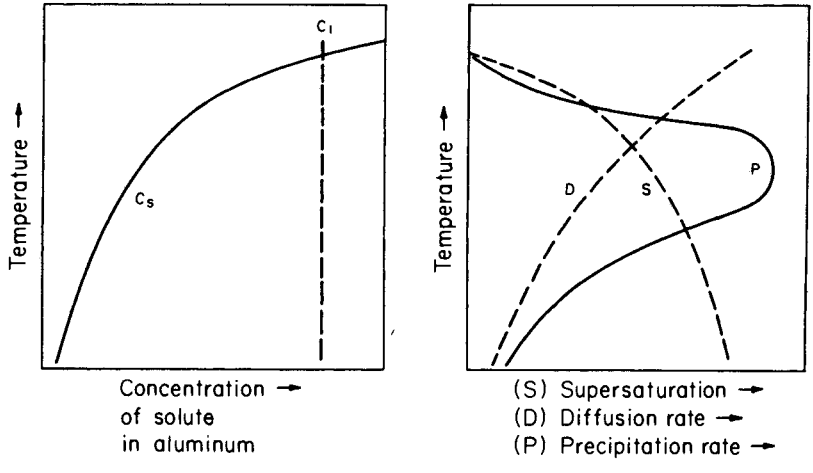

Fig. 15. Schematic representation of temperature effects on factors that determine precipitation rate.

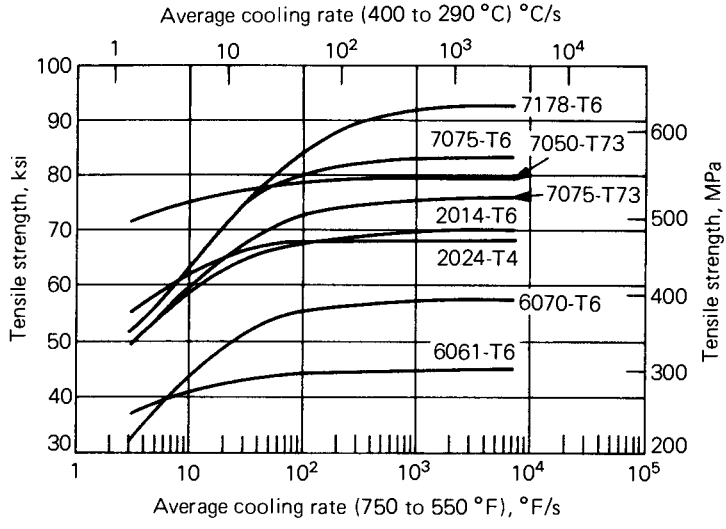

Fig. 16. Tensile strengths of eight alloys as a function of average cooling rate during quenching.

alloy composition to another. In comparing two alloys, the one having the higher strength in the form of sheet or a thin-walled extrusion may exhibit the lower strength when produced as a thick plate, extruded section, or forging. The relative strength rating of the alloys at a given cooling rate may also shift with temper. These factors may significantly influence the selection of alloy and temper for a specific application.

Quench Factor Analysis. Although useful as a first approximation, average quenching rates and critical temperature ranges are too qualitative to permit accurate prediction of the effects of quench rates when the rate of cooling does not change smoothly (Ref 16). To handle such instances, a procedure known as quench factor analysis has been developed. This procedure uses the information in the entire *C*-curve. Precipitation kinetics for continuous cooling are defined by the equation:

$$\xi = 1 - \exp(k\tau) \qquad \text{Eq 5}$$

where ξ is the fraction transformed and k is a constant, and:

$$\tau \int = \frac{dt}{C_t} \qquad \text{Eq 6}$$

where t is time and C_t is the critical time as a function of temperature (the loci of critical times is the *C*-curve.)

When $\tau = 1$, the fraction transformed, ξ, equals the fraction transformed designated by the *C*-curve. The solution of the integral, τ, has been designated the quench factor, and the method of using the *C*-curve and the quench curve to predict properties has been termed quench factor analysis. To perform quench factor analysis, the integral above is graphically evaluated to the required accuracy using the method shown in Fig. 17. Examples of ways to use quench factor analysis to predict corrosion resistance and yield strength are presented later in this chapter.

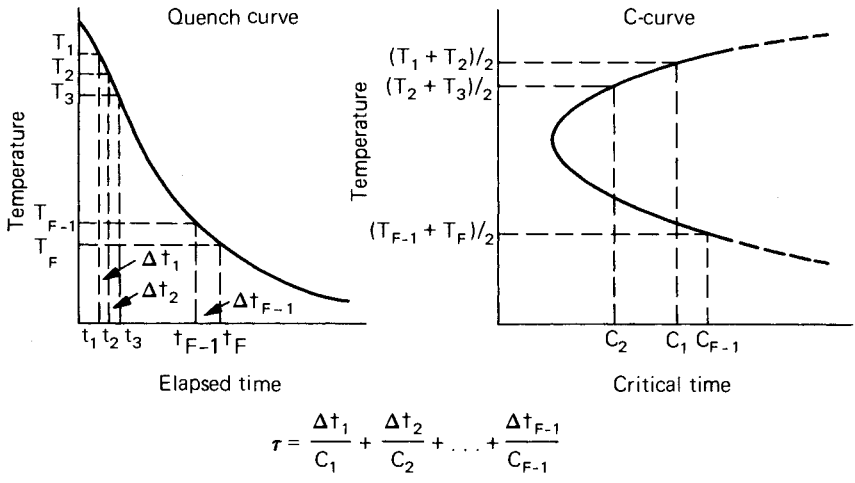

Fig. 17. Method of evaluating τ from the **C***-curve and a quench curve.*

Predicting Corrosion. Alloy 2024-T4 is susceptible to intergranular corrosion when a critical amount of solute precipitates during the quench, but corrodes in the less severe pitting mode when lesser amounts precipitate. To predict effects of proposed quenching conditions on corrosion characteristics of 2024-T4, the postulated quench curve is drawn, and the quench factor is calculated using the *C*-curve in Fig. 18. Corrosion characteristics are predicted from the plot in Fig. 19. When the quench factor, τ, is less than 1.0, the corrosion mode of continuously quenched 2024-T4 is pitting.

One application of these relationships is in studies of effects of proposed changes in quench practice on design of new quenching systems. For example, consider that a goal of a proposed quenching system for

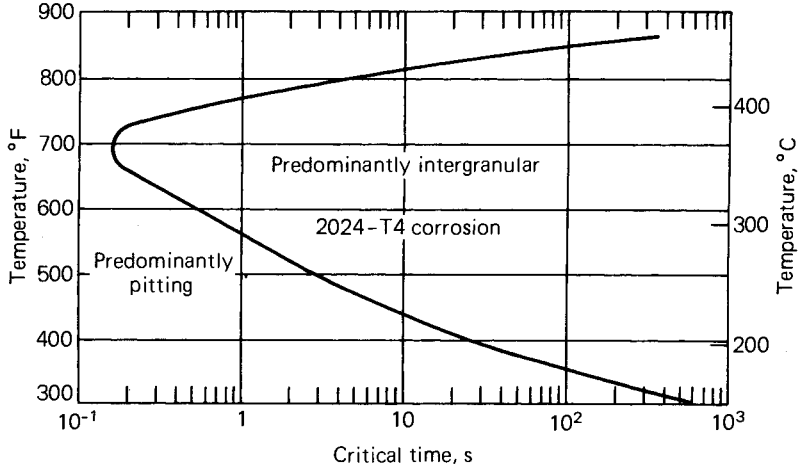

Fig. 18. **C***-curve for intergranular corrosion of 2024-T4.*

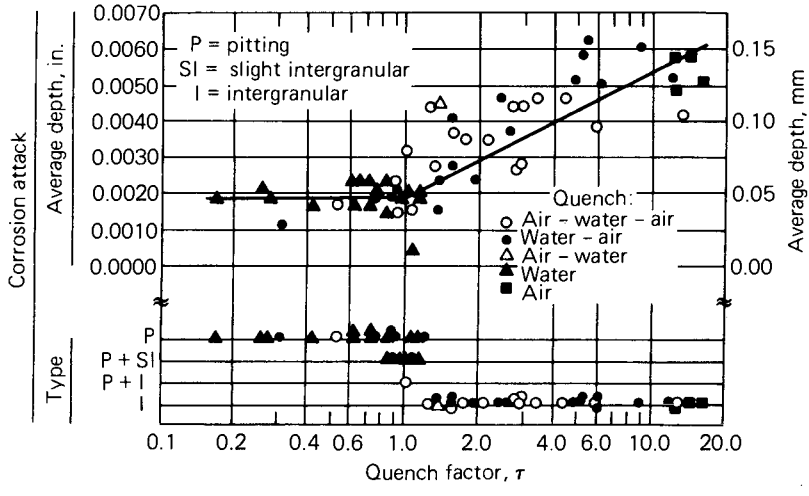

Fig. 19. Effect of quench factor on corrosion characteristics of 2024-T4.

alloy 2024-T4 sheet products is to minimize warping while preventing susceptibility to intergranular corrosion in sheet up to 3.2 mm (0.13 in.) thick. Warping occurs when stresses imposed by temperature differences across the sheet exceed the flow stress. These differences decrease as quench rate decreases, but the tendency toward intergranular corrosion increases. Quench factor analysis allows one to predict the effects on the corrosion mode of stepped quench practices to minimize warping.

As an example, one-step, two-step, and three-step quench curves that can provide acceptable corrosion characteristics in 3.2 mm (0.13 in.) 2024-T4 sheet (quench factor = 0.99) were calculated. Some of these are plotted in Fig. 20, which illustrates that 2024 can be quenched at a linear rate of 475 °C/s (855 °F/s), or higher. A quench rate below 150 °C (300 °F) was irrelevant. If the sheet is air-blast quenched with a rate of heat extraction of 5.68 W/m^2 per degree centigrade to 395 °C (740 °F), however, the quench rate from 395 to 150 °C (740 to 300 °F) must be at least 945 °C/s (1700 °F/s) to maintain the acceptable corrosion behavior. The sheet may also be quenched by a three-step practice of air blasting to 395 °C (740 °F), spray quenching at 3300 °C/s (6000 °F/s) to 245 °C (480 °F). The sheet is then air-blast quenched to 150 °C (300 °F). Other curves could be drawn, but the important points are that air-blast quenching cannot be continued more than a few degrees below 395 °C (740 °F), nor can it be initiated more than a few degrees above 270 °C (520 °F), even if infinite quench rates are attained from 395 to 270 °C.

Experimental quenching methods using continuous and various stepped quenching procedures were applied to verify that quench factor analysis could predict corrosion characteristics of 2024-T4. Figure 19 summarizes effects on type of corrosion attack observed with 2024-T4 sheet specimens quenched by these techniques. The results confirm that the method is valid for all types of quench paths evaluated and shows that corrosion depth increases progressively with increasing the quench factor above a value of 1.0.

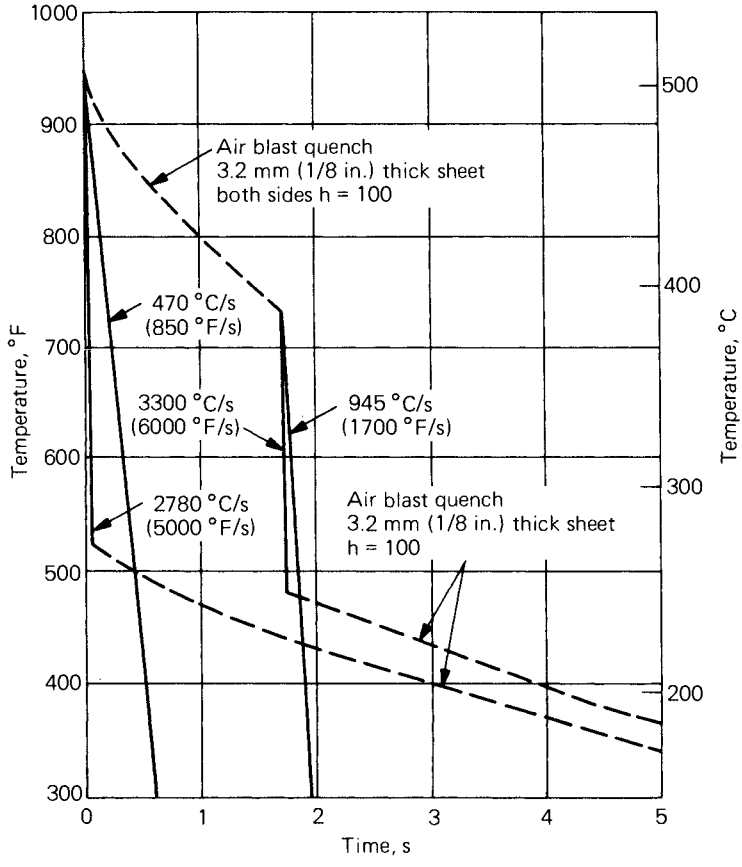

Fig. 20. Hypothetical cooling curves.

Predicting yield strength is more complex because knowledge of the relationship between the extent of precipitation and the ability to develop yield strength after aging is required. Attainable strength of 7XXX alloys is a function of the amount of solute remaining in solid solution after the quench, as long as aging is conducted so that GP zones nucleate prior to the appearance of η'. Under these conditions, relationships between the strength attainable after continuous cooling, σ, and quench factor, τ, can be represented by the following:

$$\sigma = \sigma_{max}\, \tau^{\exp(K)} \qquad \text{Eq 7}$$

where σ_{max} is the strength attainable with infinite quench rate and K is 0.005013 (natural log of 0.995) and

$$\tau = \int \frac{dt}{C_{99.5}} \qquad \text{Eq 8}$$

where t is time and $C_{99.5}$ is the C-curve for $\sigma_{99.5}$; critical time as a function of temperature to reduce attainable strength to 99.5% of σ_{max}.

The advantage of predicting yield strength from the quench factor instead of from the average quench rate is illustrated in the following com-

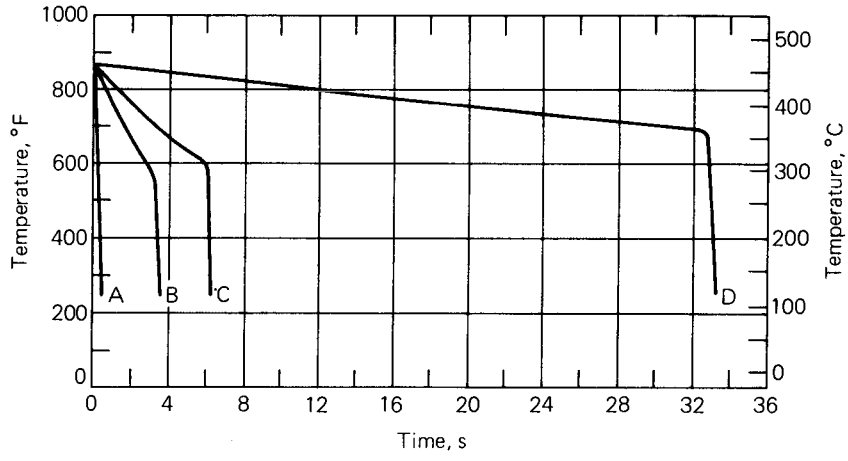

Quench	Average quench rate at 400-290 °C (750-550 °F) °C/s	°F/s	Quench factor, *f*	Measured yield strength MPa	ksi	Yield strength predicted from average quench rate MPa	ksi	Yield strength predicted from quench factor MPa	ksi
A, cold water	930	1680	0.464	506	73.4	499	72.4	498	72.3
B, denatured alcohol to 290 °C (550 °F), then cold water	49	88	8.539	476	69.1	463	67.2	478	69.4
C, boiling water to 315 °C (600 °F), then cold water	29	53	15.327	458	66.4	443	64.2	463	67.1
D, still air to 370 °C (700 °F), then cold water	5	9	21.334	468	67.9	242	35.1	449	65.1

Fig. 21. Cooling curves for 1.6-mm (0.06-in.) thick 7075 sheet.

parison. Four samples of 7075 quenched by various means (Fig. 21) were aged by the standard T6 practice of 24 h at 120 °C (250 °F). Yield strengths were predicted from both the average quench rate from 340 to 290 °C (750 to 550 °F) and from the quench factor. The quench factor was calculated using the *C*-curve for 99.5% maximum strength for 7075-T6 (Fig. 22), and yield strength was estimated from Eq 3 (graphically presented in Fig. 23).

A comparison of predicted yield strengths with actual yield strength is given in the table that accompanies Fig. 21. Yield strengths predicted from quench factors agree very well with measured yield strengths for all of the samples, the maximum error being 19.3 MPa (2.8 ksi). Yield strengths predicted from average quench rates, however, differ from the measured yield strength by as much as 226 MPa (32.8 ksi).

The advantage of using the quench factor for predicting yield strength from cooling curves is apparent. Average quench rate is not a predictor for cooling curves, which have long holding times either above or below the critical temperature range of 340 to 290 °C (645 to 555 °F), such as curve *D* of Fig. 21. For such cases, yield strength prediction using the quench factor is particularly advantageous.

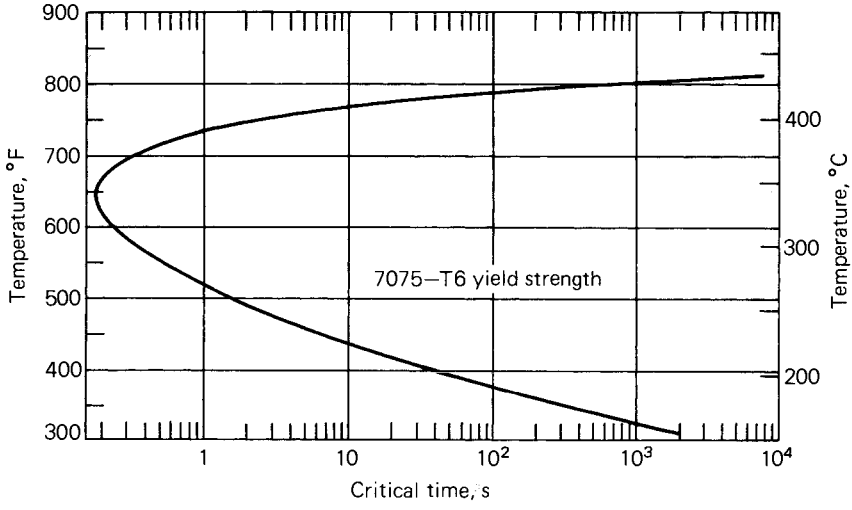

Fig. 22. **C-curve for 7075-T6 yield strength.**

Product Size and Shape. In commercial heat treating, the shape or dimensions of the product cannot be varied arbitrarily. Because heat transfer during quenching basically is limited by resistance at the surface in contact with the quenching medium, the rate of cooling is a function of the ratio of surface area to volume. This ratio may vary considerably, depending upon the shape of the product. For sheet and plate, as well as other products of similar shape, average cooling rates (through the critical temperature range measured at a center or midplane location) vary with thickness in a relatively simple manner. The relation can be approximated by the equation:

$$\text{Log } r_1 = \log r_2 - k \log t \qquad \text{Eq 9}$$

where r_1 is the average cooling rate at thickness t, r_2 is the average cooling rate at 1 cm (0.4 in.) thickness, and k is a constant.

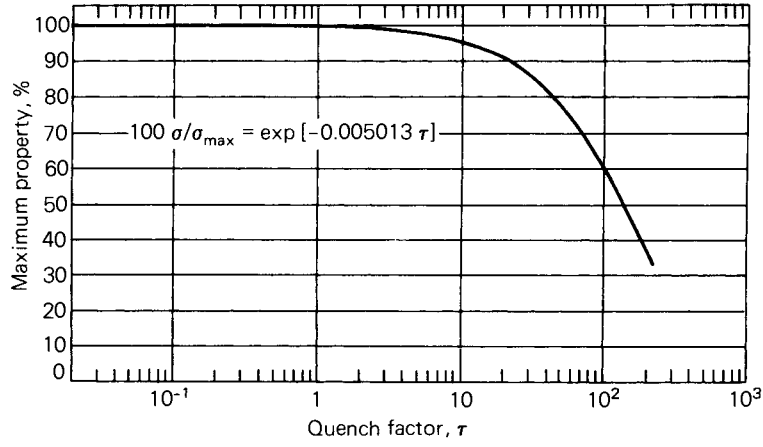

Fig. 23. Curve relating attainable strength to quench factor.

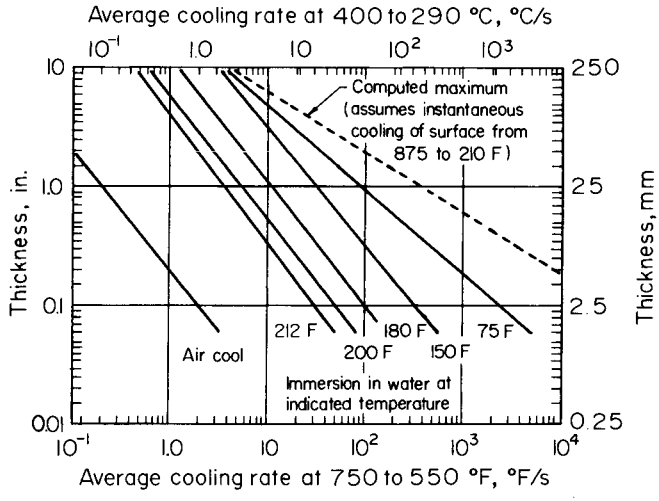

Fig. 24. Effects of thickness and quenching medium on average cooling rates at midplane of aluminum alloy sheet and plate quenched from solution temperatures.

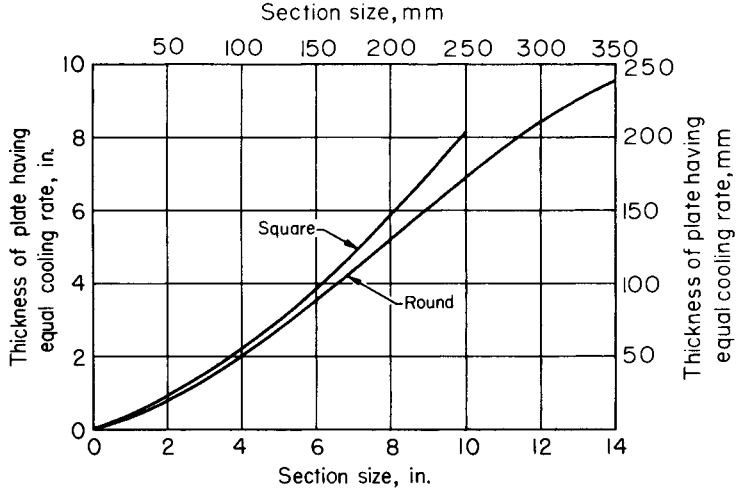

Fig. 25. Experimentally determined correlation between average cooling rates of 400 to 290 °C (750 to 550 °F) of rod and square bars to plates. Rates were measured at centers of sections.

Cooling rates determined experimentally for 1.6-mm (0.06-in.) to 20-cm (8-in.) thick sections that were quenched by immersion in water at five different temperatures and by cooling in still air are shown in Fig. 24. Experimentally determined relationships between the thickness of plates and either the diameter of rounds or the dimensions of square bars having equal cooling rates are shown in Fig. 25.

The dashed line at the extreme right in Fig. 24 delineates the maximum cooling rates theoretically obtainable at the midplane of plate, assuming an infinite surface heat transfer coefficient and a diffusivity factor of 1400

cm^2/s (Ref 17). No rates higher than those defined by this line have been observed, although rates approaching them were measured with impinging spray quenches. Because the rates indicated in Fig. 24 are for locations most distant from the surfaces, they are the lowest to be expected in sheet or plate. In plate, slightly higher rates should exist at the quarter-planes, and portions closer to the surface should cool at appreciably higher rates.

Quenching Medium. Water is the most widely used and most effective quenching medium. As Fig. 24 indicates, in immersion quenching, cooling rates can be reduced by increasing water temperature. Conditions that increase the stability of a vapor film around the part decrease the cooling rate; various additions to water that lower surface tension have the same effect. Slower cooling also results from the use of additions such as polyalkylene glycol that form film coatings on the hot metal. Organic quenching media provide lower cooling rates than water. Molten salt and low-melting eutectic baths have been used for experimental investigation of quench-aging treatments; these may have some advantage for continuous heat treatment of alloys that are adversely affected by a delay between quenching and aging (Ref 18). Moving air is sufficient for less quench-sensitive dilute alloys, such as 6063, when they are extruded in thin-walled sections.

Other Factors. Quenching rates are very sensitive to the surface condition of the parts. Lowest rates are observed with products having freshly machined or bright-etched, clean surfaces, or products that have been coated with materials that decrease heat transfer. The presence of oxide films or stains increases cooling rates. Further marked changes can be effected through the application of nonreflective coatings, which also accelerate heating, as shown in Fig. 26. Surface roughness exerts a similar effect; this appears related to vapor film stability. The manner in which complex products, such as engineered castings and die forgings, enter the quenching medium can significantly alter the relative cooling rates at various points, thereby affecting mechanical properties and residual stresses established during quenching. Similarly, quenching complex extruded

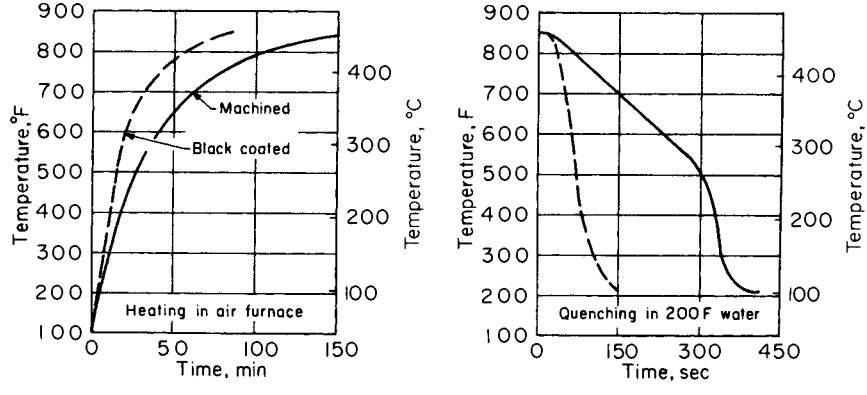

Fig. 26. Effect of surface condition on heating and cooling of 165-mm (6.5-in.) diam by 216-mm (8.5-in.) long aluminum alloy cylinder. Temperatures were measured at the center.

shapes whose wall thicknesses differ widely poses special problems if distortion and stresses are to be minimized. In batch heat treating operations, placement and spacing of parts on the racks can be a major factor in determining the quenching rates. In immersion quenching, adequate volumes of the quenching medium must be provided to prevent an excessive temperature rise in the medium. When jet agitation is used to induce water flow between parts, jets should not impinge directly and cause rapid localized cooling.

Reheating During Quenching. Recent information indicates that neither the average quenching rate through a critical temperature range nor quench factor analysis can predict strength when the temperature increases during quenching after it is cooled below some critical temperature (Ref 19 and 20). Under this condition, strength in the affected areas can be significantly lower than in other areas of the material. The most likely way for this phenomenon to occur is during spray quenching, when the surface cools rapidly by the impinging spray, but reheats by heat flow from the hotter interior when the spray is interrupted. Recent work may have explained the mechanism for the severe loss of strength in areas of alloy 2024 extrusions that were reheated under laboratory conditions (Ref 21). Nucleation is difficult during quenching, so few *S* or *S'* precipitates formed. It is postulated that, during reheating, many precipitates grew from the GP zones that nucleated homogeneously when the temperature fell below the GP zone solvus during the quench.

Predicting Strengths of Thick Products. Effects of the quenching rate on alloy strengths can be represented on a generalized graph of the type shown in Fig. 16, and the expected quenching rates of products having various shapes and dimensions can be determined from Fig. 24 and 25. Nevertheless, combining these two kinds of information to predict mechanical properties must be done with caution. Inconsistencies were encountered, for example, in correlating properties of thick sections quenched in high-cooling-rate media with properties of thinner sections quenched in media affording milder quenching action. One of the reasons for the inconsistencies is believed to be the different shapes of the cooling curves. This difficulty can be overcome by using quench factor analysis. The other reason is that the degree of recrystallization and texture of the thick and thin sections may be different.

Careful analyses were made of data from a large number of production-control tensile tests of bulk-quenched rolled, forged, and extruded products that varied in section thickness to a maximum of about 20 cm (8 in.). The tensile and yield strengths decreased with increasing section thickness over 2.5 cm (1 in.) in a simple linear relationship. This is illustrated by the average properties for 7075-T651 plate in Fig. 27. The reversal in curve direction at thicknesses lower than 2.5 cm (1 in.) is accounted for by a change in structure, from completely unrecrystallized to partially recrystallized. When test specimens of uniform size (2.5 cm^2 or 0.4 $in.^2$, or less) cut from products thicker than 2.5 cm (1 in.) were reheat treated, the tensile properties showed no consistent variation with product thickness. This indicates that the quenching rate is the major factor establishing the property differences of sections thicker than about 2.5 cm (1 in.).

Corrosion Resistance. Rates of cooling from the solution temperature

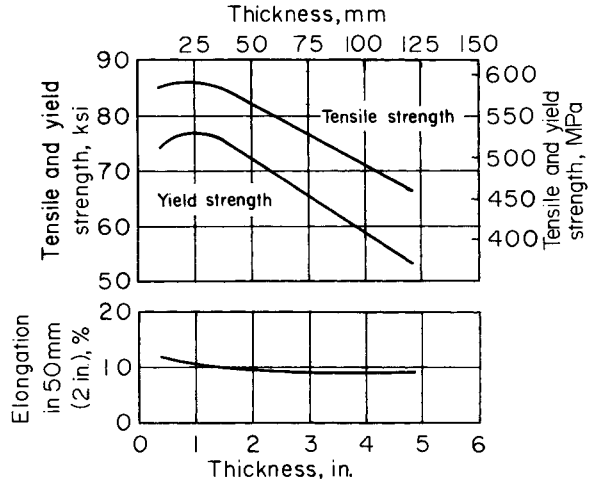

Fig. 27. Average tensile properties of 7075-T651 plate as a function of thickness.

markedly influence both the resistance of heat treatable alloys to corrosion and the characteristics of the corrosion attack. Extensive research with 7075-T6 sheet has shown that the material is subject only to pitting attack and has a high degree of resistance to stress corrosion and exfoliation if sufficiently rapid cooling is achieved during quenching. Conversely, when the cooling rate is relatively low, this alloy becomes prone to intergranular attack and may be susceptible to stress-corrosion cracking and exfoliation.

Experimental quenching methods, of the same type used to determine the critical temperature range that is important in developing strength, were applied to define the range in which the corrosion characteristics of 7075-T6 are established. The most critical changes occur in a similar temperature range for both corrosion characteristics and tensile properties. In Fig. 28, tensile strengths, losses in tensile strength after 12 weeks of alternate immersion in 3.5% NaCl solution, and the type and maximum depth of corrosion in NaCl-H_2O_2 solution (MIL-H-6088) are correlated with the average cooling rates through the critical temperature range. The most rapid decrease in tensile properties occurs at cooling rates somewhat higher than those that have the greatest effects on corrosion. To avoid completely the intergranular type of attack, rates in excess of about 165 °C/s (300 °F/s) are needed. Such rates are not attainable with thick sections. Therefore, when thick-section parts are required to endure service conditions conducive to stress corrosion in the short-transverse direction, the stress corrosion-resistance T73 temper of 7075 is preferred (Ref 22). When stresses in the short-transverse direction are low, but a resistance to exfoliation corrosion is required, 7075-T76 with strength intermediate to that of 7075-T6 and 7075-T73 is often specified. Newer alloys such as 7049-T73 and 7050-T74 develop superior combinations of strength and resistance to stress-corrosion cracking, particularly in thicker sections.

Delay in Quenching. The effects of delay in the transfer of parts from the solution heat treating furnace to the quenching medium are similar to those indicated for a reduction in the average cooling rate. Because the

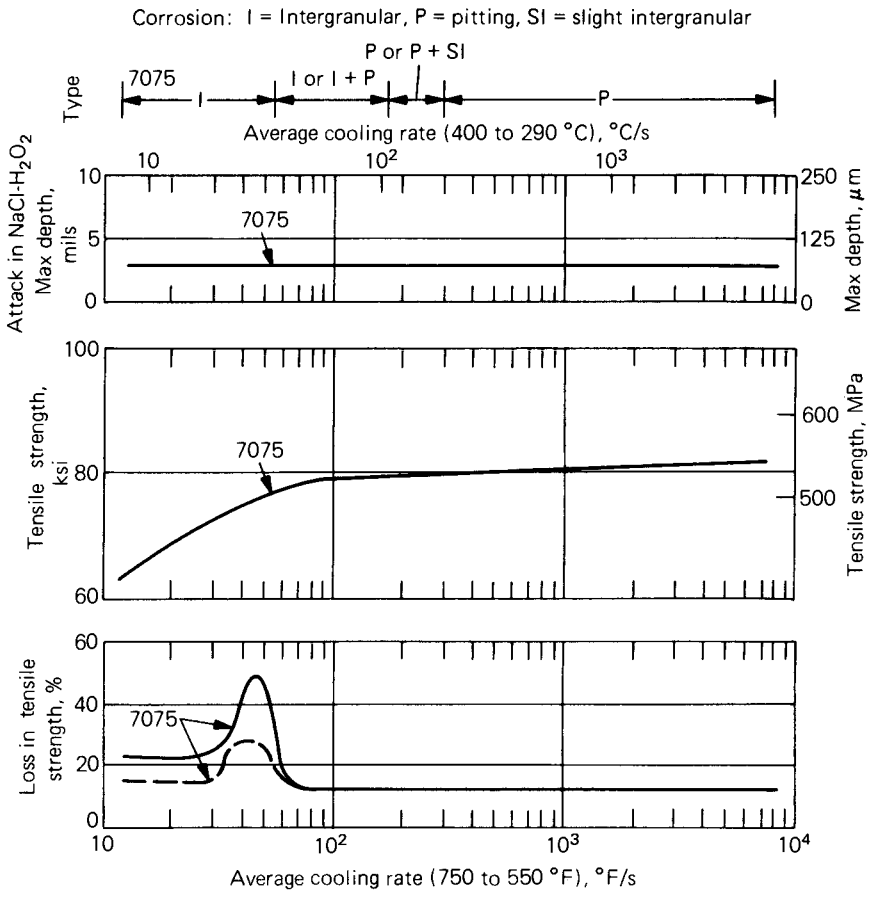

Fig. 28. Effects of quenching rate on tensile properties and corrosion resistance of 7075-T6 sheet. (B.W. Lifka and D.O. Sprowls, Alcoa Research Laboratories)

rate of cooling in air during the transfer is highly dependent upon the mass, section thickness, and spacing of the parts—and to a smaller extent upon air temperature, velocity, and emissivity—the allowable transfer time, or quench delay, varies with these factors. Certain specifications stipulate maximum delay periods ranging from 5 to 15 s for sheet under 0.4 mm (0.02 in.) to over 2.0 mm (0.08 in.) thick. Quench factor analysis indicates that the maximum allowable delay is also a function of the subsequent quenching conditions. Shorter times are required when the quench is less drastic than that obtained by a quench into cold water.

Fracture Toughness. As indicated previously, precipitation during the quench occurs initially on sites such as high-angle grain boundaries. The grain boundary precipitates and the associated precipitate-free zone that appears after aging provide a preferential fracture path. Consequently, decreasing the quench rate usually increases the proportion of intergranular fracture and decreases the fracture toughness of high-solute alloys, particularly those in T6-type tempers. The phenomenon cannot be reliably detected by the usual quality control tensile test because yield, ultimate,

and elongation values are usually not affected despite the low-energy, intergranular fracture mode. Tests of a specimen containing either a sharp notch or a crack must be used. The results of tear tests of alloy 7075-T6 sheet quenched in either cold or hot water, illustrated in Fig. 29, show how toughness can decrease significantly with an insignificant loss in strength. With extended precipitation within the grains, either as a result of a further decrease in the quench rate or overaging, strength begins to suffer. When the strength decrease gets large enough, toughness begins to increase (Fig. 30). The combination of strength and toughness, however, is highest in rapidly quenched material aged to peak strength.

Aluminum-magnesium-silicon alloys, although generally not considered for critical applications with fracture toughness requirements, can also suffer a loss in toughness and ductility in T6 and T5 tempers when the quench rate is low enough to permit substantial grain boundary precipitation. This is especially true when the silicon content is in excess of that required to form Mg_2Si and when elements that inhibit recrystallization are not present. In extreme cases, tensile fractures are completely intergranular.

Residual stresses originate from the temperature gradient produced by quenching. The gradient induces plastic deformation from differential contraction or expansion in the part (Ref 23 and 24). Because the surface of the part cools first, it tends to contract, thereby imposing a state of compressive stress on the interior. The reaction places the surface in tension. The surface layer deforms plastically when the tensile stress exceeds

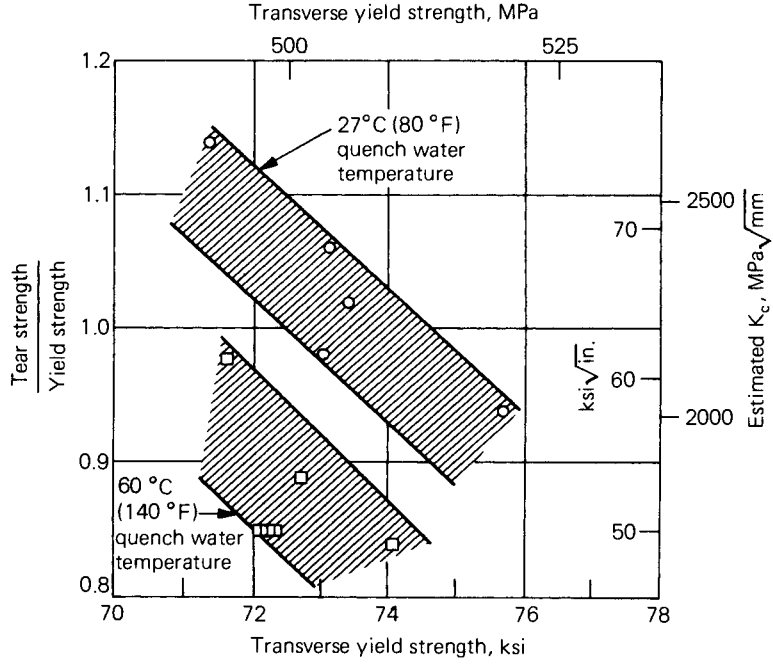

Fig. 29. Effects of quench water temperature on the tear strength and yield strength ratio of 7075 sheet.

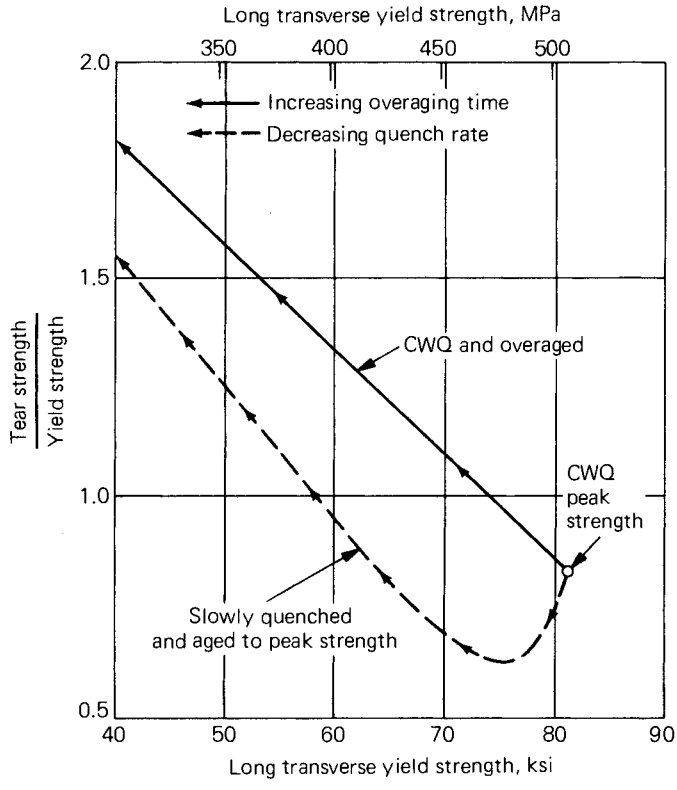

Fig. 30. Effects of quenching and aging condition on the tear strength and yield strength ratio of 7050 sheet.

the flow stress of the material. Then, as the interior of the part cools, it is restrained from contracting by the cold surface material. The resulting reaction places the surface in a state of compressive stress and the center in a state of tensile stress. When the part is completely cooled, it remains in a state of equilibrium, with the surface under high compression stresses balanced by tensile stresses in the interior. Generally, the compressive stresses in the surface layers of a solid cylinder are two-dimensional (longitudinal and tangential), and the tensile stresses in the core are triaxial (longitudinal, tangential, and radial), as illustrated in Fig. 31.

The magnitude of the residual stresses is directly related to the temperature gradients generated during quenching. Conditions that decrease the temperature gradient reduce the residual stress ranges (Ref 25). Quenching variables that affect the temperature gradient include the temperature at which quenching begins, cooling rate, section size, and variation in section size for nonflat products. For a part of a specific shape or thickness, lowering the temperature from which the part is quenched or decreasing the cooling rate reduces the magnitude of residual stress by reducing the temperature gradient. Figures 32 and 33 illustrate the effect of quenching temperature and cooling rate, respectively. With a specific

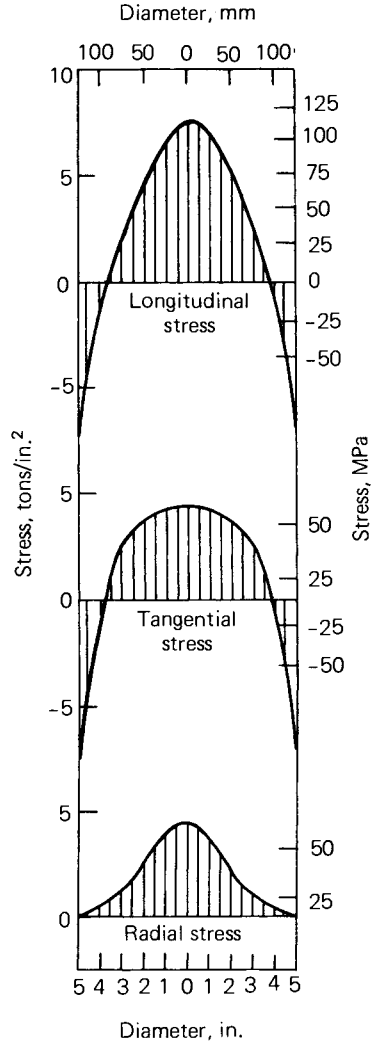

Fig. 31. Residual stress diagram for 2014 alloy quenched in cold water from 500 °C (935 °F).

cooling rate, the temperature gradient is greater in a section of large diameter or thickness than it is in a smaller section. Therefore, the residual stresses in the larger section are higher (Fig. 34). In products having differences in cross section, large temperature gradients can be minimized by covering or coating the thinner sections with a material that decreases the quench rate, so that it more closely matches that of the thicker sections.

The range of residual stresses generated during quenching varies considerably for different alloys. Those properties related to alloy composition that specifically affect the thermal gradient and the degree of plastic deformation that occur during quenching are involved. High residual stresses are promoted by high values of properties such as Young's modulus of

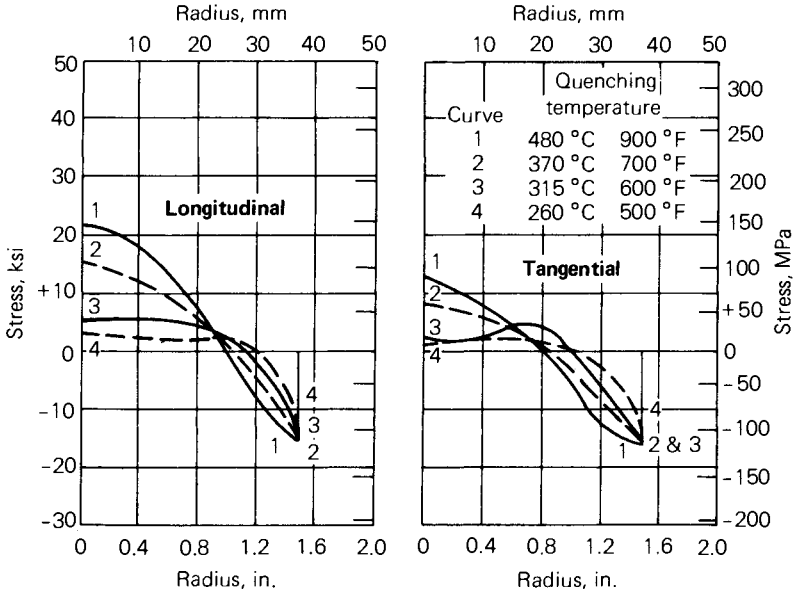

Fig. 32. Effect of quenching temperature on residual stresses in 5056 alloy cylinders of 76 by 229 mm (3 by 9 in.) quenched in water at 24 °C (76 °F).

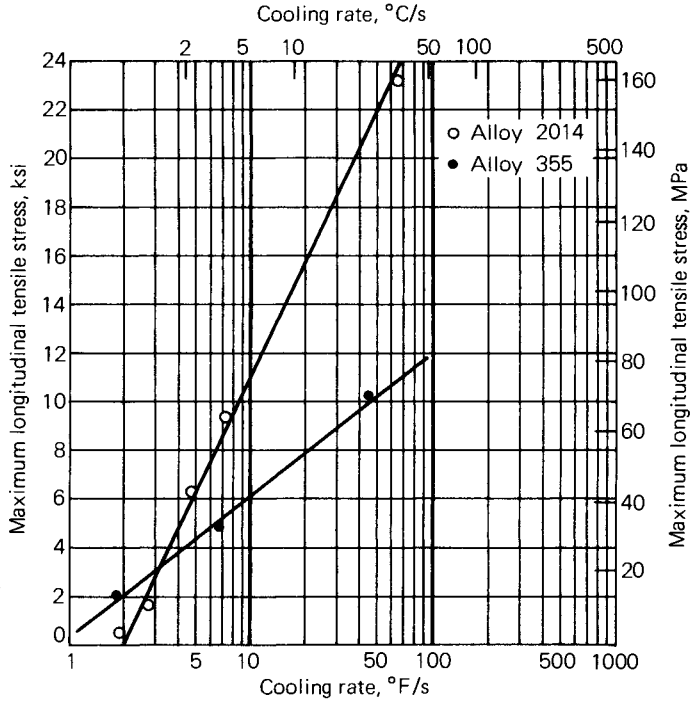

Fig. 33. Effect of quenching rate on residual stresses in 2014 and 355 alloy cylinders of 76 by 229 mm (3 by 9 in.) quenched from 500 °C (935 °F) and 525 °C (980 °F), respectively.

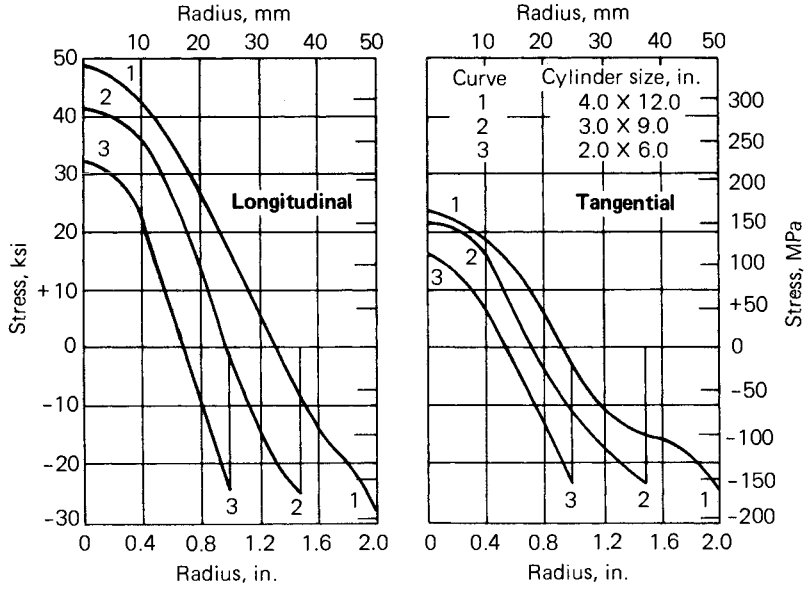

Fig. 34. Effect of section size on residual stresses in 2014 alloy cylinders quenched from 505 °C (940 °F) in water at 20 °C (70 °F).

elasticity, proportional limit at room and elevated temperature, and coefficient of thermal expansion; and by a low value of thermal diffusivity. These property factors affect the magnitude of residual stresses to different degrees. The influences of the coefficient of thermal expansion and elevated-temperature yield strength are especially significant. For example, a low coefficient of thermal expansion can counteract a high proportional limit. The net effect is a low residual stress level. Or, an alloy such as 2014 can develop a high residual stress range because of its very high elevated-temperature strength, despite average values for coefficient of thermal expansion, modulus of elasticity, and thermal diffusivity.

The effects of residual stresses from quenching require consideration in the application of heat treated parts. Where the parts are not machined, the residual compressive stresses at the surface may be favorable by lessening the possibility of stress corrosion or initiation of fatigue. However, heat treated parts are most often machined. Where the quenching stresses are unrelieved, they can result in undesirable distortion or dimensional change during machining. Metal removal upsets the balance of the residual stresses and the new system of stresses that restore balance generally results in warpage of the part. Further, in the final balance stress system, the machined surfaces of the finished part can be under tensile stress with attendant higher risk of stress corrosion or fatigue.

Because of the practical significance of residual stress in the application of heat treated parts, various methods have been developed either to minimize the residual stresses generated during quenching or to relieve them after quenching. The methods commonly used for stress relieving heat treated parts include mechanical and thermal methods. The methods used

to avert the development of high residual stresses during quenching rely on a reduced cooling rate to minimize the temperature gradients. Using quenching media that provide less rapid cooling in quenching irregularly shaped parts that cannot readily be stress relieved by subsequnt cold deformation is common practice. For this reason, the quenching of die forgings and castings in hot (60 to 80 °C or 140 to 180 °F) or boiling water is standard practice. In some cases, though, quench-rate sensitive alloys may suffer a loss in mechanical properties, particularly strength and fracture toughness. Intergranular corrosion resistance may also be impaired with such reduced cooling rates. Liquid organic polymer, such as polyalkylene glycol (10 to 40 vol% in water), is effective as a quenchant for minimizing residual stresses and distortion with lesser loss in properties (Ref 26-28). Owing to inverse solubility, a film of the liquid organic polymer is immediately deposited on the surface of the hot part when it is immersed in the quenchant. By reducing the rate of heat transfer, the deposited film reduces thermal gradients. Other additions to water, including suspensions of mineral powders, have been proposed. Extruded or rolled shapes may be cooled in an air blast, fog, or water spray. Production economics frequently favors the use of these milder quenches to decrease the need for straightening operations or to simplify machining operations because of the lower stresses. In other cases, the reduction in tension stress at machined surfaces of the finished part is most advantageous. In the manufacture of large, complex parts from die or hand forgings, an established practice is to heat treat after rough machining, thus averting the higher stresses that are associated with heat treating before metal removal.

Because of the trade-offs of tensile properties with residual stress, researchers have been developing methods of analysis that combine prediction of properties by quench factor analysis and prediction of stresses from heat transfer analyses and other considerations. One of these methods predicts that a cooling rate that is slow at the beginning, but continuously accelerates, can significantly reduce residual stresses while maintaining the same mechanical properties as those obtained by quenching in cold water (Ref 29). Another method, to eliminate warping of parts that have variations in section thickness without sacrificing mechanical properties, has been patented (Ref 30).

AGING AT ROOM TEMPERATURE (NATURAL AGING)

Most of the heat treatable alloys exhibit age hardening at room temperature after quenching. The rate and extent of such hardening varies from one alloy to another. Microstructural changes accompanying room temperature aging, except for long-time aging of 7XXX alloys, are undetectable because the hardening effects are attributable solely to the formation of zone structure within the solid solution. The changes in tensile properties for three representative commercial alloys aged at room temperature, 0 °C (32 °F), and −18 °C (0 °F) are shown in Fig. 35. In alloys 2024 and 2036, most of the strengthening occurs within a day at room temperature; the mechanical properties are essentally stable after four days. These alloys are widely used in the naturally aged tempers: T4, T3, and T361 for 2024 and T4 for 2036. Alloys 6061, 6009, and 6010 age more

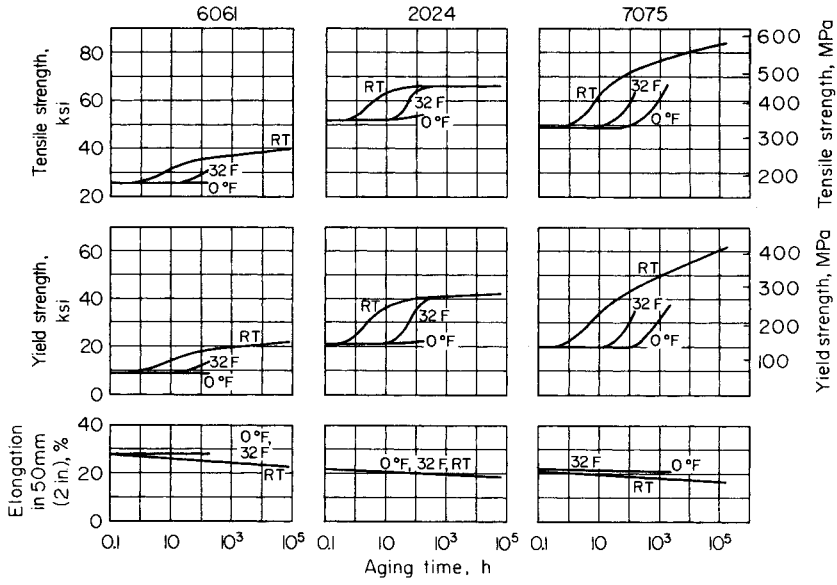

Fig. 35. Aging characteristics of aluminum sheet alloys at room temperature, 0 °C (32 °F), and −18 °C (0 °F). (J.A. Nock, Jr., Alcoa Research Laboratories)

slowly. Alloy 6061 may be used in the T4 temper; however, it is more frequently given a precipitation heat treatment to the T6 temper. Alloys 6009 and 6010, on the other hand, are commonly used in the T4 temper. However, these alloys are commonly used in automotive application, where paint baking is typically used. Consequently, they realize significant increases in strength during this thermal cycle, which is equivalent to an artificial aging treatment. Alloy 7075 and other 7XXX series alloys continue to age harden indefinitely at room temperature; because of this instability, they are very seldom used in the W temper.

Because heat treatable alloys are softer and more ductile immediately after quenching than after aging, straightening or forming operations may be performed more readily in the freshly quenched condition. For many alloys, production schedules must permit these operations before appreciable natural aging occurs. As alternatives, the parts may be stored under refrigeration to retard aging (Fig. 35), or they may be restored to near-freshly quenched condition by reversion treatments that dissolve the GP zones. The newer automotive body sheet alloys, however, remain highly formable even after extended natural aging. The introduction of localized strain hardening and residual stresses in parts by forming after quenching may have an adverse effect on fatigue, or on resistance to stress corrosion. In critical applications, forming prior to heat treatment is the procedure preferred to avoid these effects. In some cases, forming is permissible in the freshly quenched condition, but not after aging has occurred.

The electrical and thermal conductivities of most heat treatable alloys decrease with the progress of natural aging. This is in sharp contrast to the changes that occur during elevated-temperature aging. Electrical con-

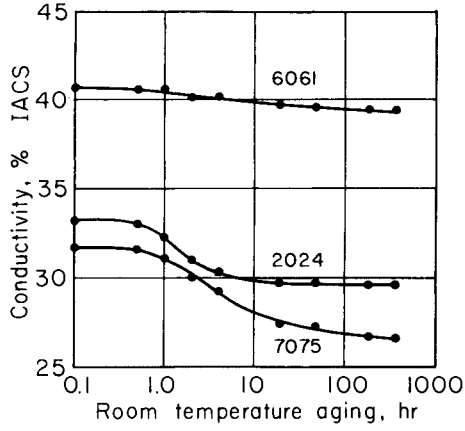

Fig. 36. Effects of room temperature aging on the electrical conductivity of as-quenched aluminum alloy sheet.

ductivity data for three alloys representing the major alloy types are presented in Fig. 36. Because a reduction of solid solution solute content normally increases electrical and thermal conductivities, the observed decreases are regarded as significant evidence that natural aging is a process of zone formation, not true precipitation. Decreased conductivity has been attributed to impairment of the periodicity of the lattice.

Castings are used in the naturally aged T4 temper in a relatively few instances where the higher ductility of this temper is of value. Hardening occurs with time after quenching, the rates varying considerably with alloy composition. The aluminum-magnesium alloy 220, normally used in the T4 temper, shows very gradual increases in strength over a period of years. The aluminum-zinc-magnesium casting alloys, which are used without heat treatment, exhibit a relatively rapid change in mechanical properties during the first three or four weeks at room temperature and subsequent additional aging at progressively reduced rates. In these alloys, a sufficient concentration of solute is retained in solution by the rate of cooling in the mold after solidification to permit substantial increases in strength.

PRECIPITATION HEAT TREATING (ARTIFICIAL AGING)

The effect of precipitation on mechanical properties is greatly accelerated, and usually accentuated, by reheating the quenched material to about 95 to 205 °C (200 to 400 °F). The effects are not attributable solely to a changed reaction rate; as mentioned previously, the structural changes occurring at the elevated temperatures differ in fundamental ways from those occurring at room temperature. These differences are reflected in the mechanical characteristics and some physical properties. A characteristic feature of elevated-temperature aging effects on tensile properties is that the increase in yield strength is more pronounced than the increase in tensile strength. Also, ductility and toughness decrease. Thus, an alloy in the T6 temper has higher strength but lower ductility than the same

alloy in the T4 temper. Overaging decreases both the tensile and yield strengths, but ductility generally is not recovered in proportion to the reduction in strengths, so that the combinations of these properties developed by overaging are considered inferior to those prevalent in the T6 temper or underaged conditions. Other factors, however, may greatly favor the use of an overaged temper. In certain applications, for example, strength factors are outweighed as criteria for temper selection by the resistance to stress-corrosion cracking, which improves markedly with overaging for some alloys, or by the greater dimensional stability for elevated-temperature service that is provided by overaging. In corrosive environments, resistance to the growth of fatigue cracks under constant amplitude and under various spectrum loading conditions increases with an increasing degree of overaging of 7XXX alloys. This improvement was a major factor influencing the decision to use 7475-T73 in a recent application in a fighter aircraft.

Precipitation-hardening curves (isothermal-aging curves) showing changes in tensile properties with time at constant temperature have been established for most of the commercial alloys at several temperatures and over extended periods of aging. To illustrate basic relationships, such data are summarized for alloys 2014 (aluminum-copper-magnesium-silicon) and 6061 (aluminum-magnesium-silicon) in Fig. 37. With both alloys, the curves reflect the influence of reversion, as shown by initial losses in strength. This initial softening is caused by partial destruction of the zone hardening prior to rehardening by precipitation. As mentioned previously, a special treatment based on the reversion phenomenon is occasionally

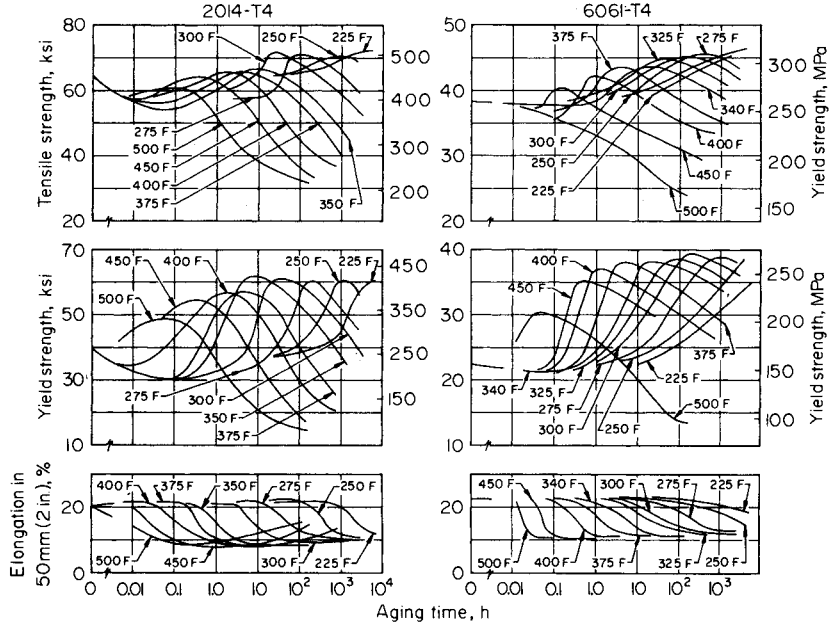

Fig. 37. Aging characteristics of two aluminum sheet alloys at elevated temperatures. (J.A. Nock, Jr., Alcoa Research Laboratories)

used to assist in forming alloys in the W or T4 temper. By heating the naturally aged alloy for a few minutes at temperatures in the artificial-aging range, the workability characteristic of the freshly quenched condition is restored. The effects are temporary, and the alloy re-ages at room temperature. Because such treatments decrease the corrosion resistance of series 2XXX alloys, they should be followed by artificial aging to obtain satisfactory corrosion characteristics.

The precipitation-hardening temperature range is similar for alloys 2014 and 6061, although aging is more rapid in 2014 at specific temperatures. Recommended commercial treatments for the T6 temper have been selected on the basis of experience with many production lots, representing an optimum compromise for high strengths, good production control, and operating economy. These consist of 8 to 12 h at 170 °C (340 °F) for 2014, and 16 to 20 h at 160 °C (320 °F) or 6 to 10 h at 175 °C (350 °F) for 6061, depending on product form.

Some paint bake operations are in the temperature range commonly used to artificially age. Consequently, auto body sheet can be formed in the T4 temper where formability is high, and then it can be aged to higher strengths during the paint bake cycle. Alloy 6010 was developed to maximize the response to aging in the temperature range used for paint baking. The differing behavior of alloys 6010 and 2036 in this respect are illustrated by the isostrength curves in Fig. 38 and 39.

Aging practice and cold work after quenching affect the combinations of strength and ductility or toughness that are developed. The curves of Fig. 37 illustrate the fact that recovery of ductility in the overaged condition is not appreciable until severe reduction in strength is encountered. The relationship between strength and toughness of notched specimens of two alloys is illustrated in Fig. 40. The unit energy to propagate a crack in notched tear specimens, which is a measure of toughness, was determined for several stages of precipitation heat treatment, from the T4 or naturally aged temper to the T6 and for overaged tempers. For a spe-

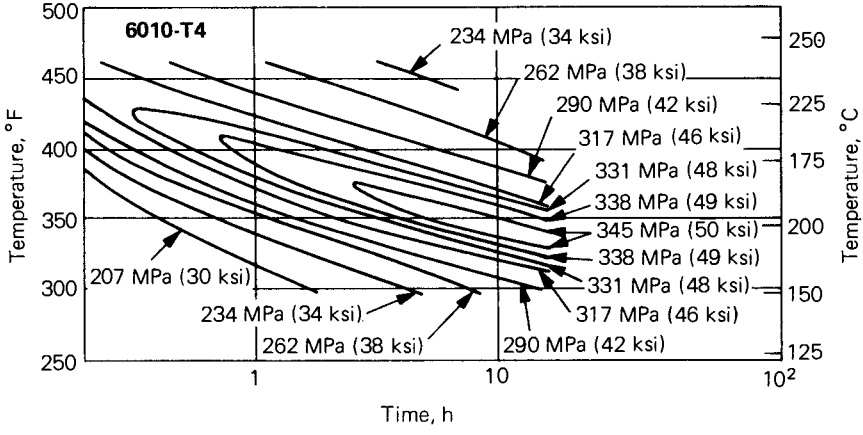

Fig. 38. Effect of aging time and temperature on longitudinal yield strength of 6010-T4.

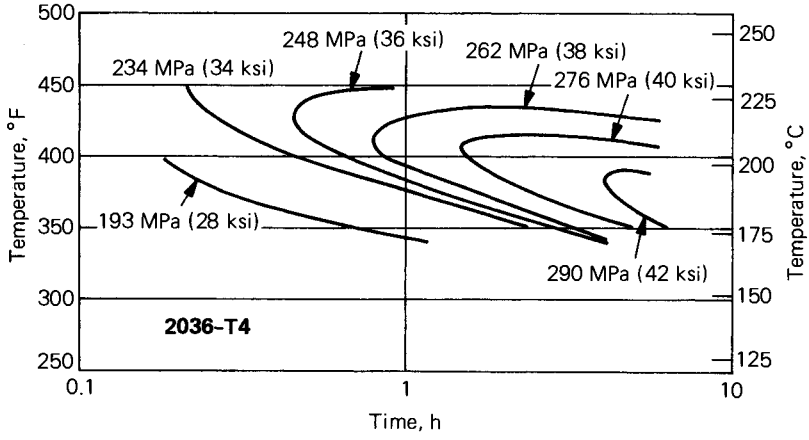

Fig. 39. Effect of aging time and temperature on longitudinal yield strength of 2036-T4.

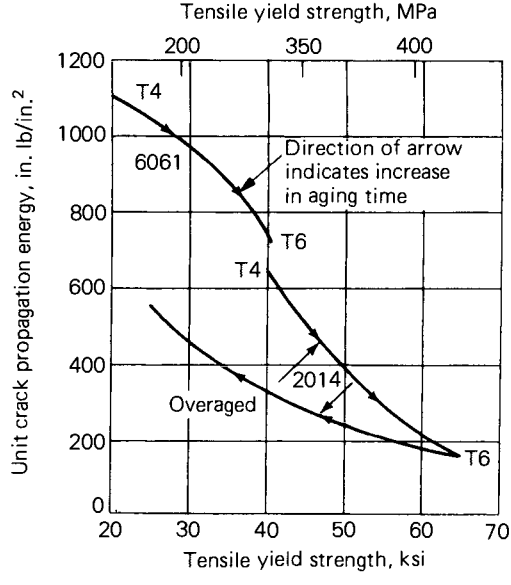

Fig. 40. Effects of precipitation heat treatment on unit crack propagation energy and yield strength of 2014 and 6061 alloys. (J.A. Nock, Jr. and H.Y Hunsicker, Journal of Metals, *Vol 15, 1963, p 216-224)*

cific yield strength, 2014 exhibited higher toughness in the underaged conditions than in the overaged condition. Different investigators found different effects of aging on the toughness of alloy 7075. In one investigation, the toughness of overaged 7075 was found to be lower than when it was underaged to the same yield strength (Ref 31). In another investigation of several lots of 7075, the toughness of material in underaged and overaged tempers was virtually identical, and toughness of a

high-purity variant of 7075 was superior in the overaged condition (Ref 32). In the instances where toughness was different at the same yield strength, the materials having the lower toughness exhibited a higher proportion of intergranular fracture. The reasons for the different results are tentatively attributed to differences in heating rate to the overaging temperature affecting the width of the precipitate-free zone at grain boundaries. Effects of cold work after solution heat treatment are opposite in 2XXX and 7XXX alloys (Ref 32). Cold work improves the combination of strength and toughness in 2024 (Fig. 41) and decreases it in overaged tempers of 7050 (Fig. 42). The improvement in 2024 is attributed to the refinement of the S' precipitate. This refinement in microstructure provided a simultaneous increase in strength and toughness. The negative effect of cold work in 7050 is attributed to the nucleation of coarse η' precipitates on dislocations, thereby decreasing strength without correspondingly improving toughness.

Because all heat treatable alloys overage with extended heating, the decrease in strength with time must be considered in selecting alloys and tempers for parts subjected to elevated-temperature service. Heat treatable alloys used as electrical conductors, such as 6101 or 6201, are frequently used in overaged tempers because of the higher electrical conductivity associated with more advanced decomposition of the solid solution.

Corrosion Resistance. The extent of precipitation during elevated-temperature aging of alloys 2014, 2219, and 2024 markedly influences

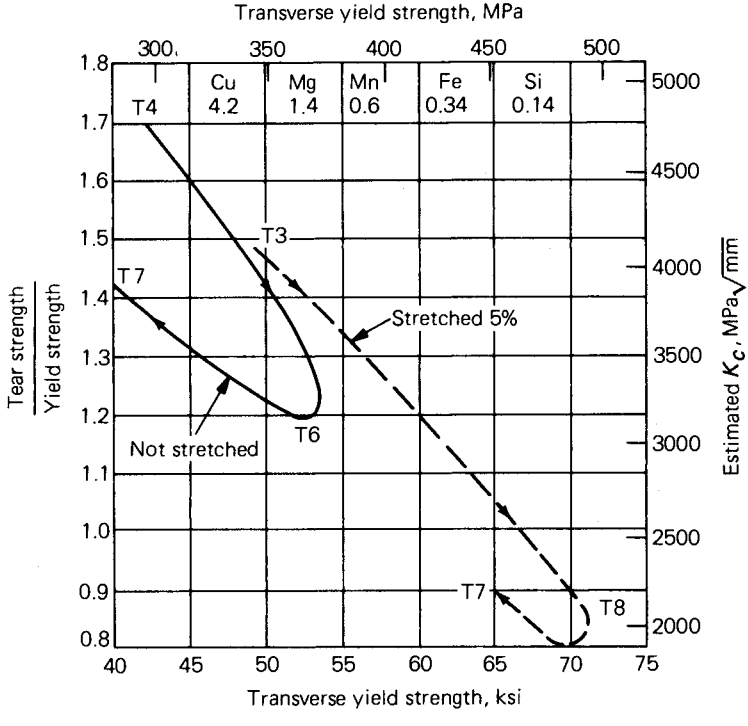

Fig. 41. Effect of stretching and aging on the toughness of 2024 sheet.

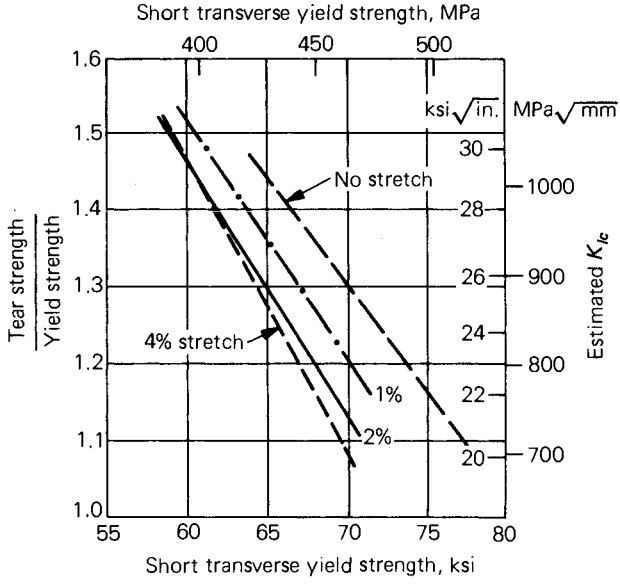

Fig. 42. Effects of stretching on the relationship between strength and notch toughness of alloy 7050 plate.

the type of corrosion attack and the corrosion resistance. With thin-section products quenched at rates sufficiently rapid to prevent precipitation in the grain boundaries during the quench, short periods of precipitation heat treating produce localized grain boundary precipitates adjacent to the depleted areas, producing susceptibility to intergranular corrosion. Additional heating, however, induces extensive general precipitation within the grains, lowering the corrosion potential differences between the grains and the boundary areas, thus removing the cause of the selective corrosion. To illustrate, changes in corrosion potential and corrosion resistance of 2024-T3 sheet with time and temperature of aging are charted in Fig. 43.

Fortunately, the extent of precipitation required to restore good corrosion resistance essentially coincides with that needed to develop maximum strength in some alloys. For products of thicker section, such as plate, extrusions, and forgings that cannot be quenched with sufficient rapidity to achieve the most favorable structures, commercial precipitation treatments also improve corrosion resistance.

Effect of Precipitation on Directional Properties of Extrusions. Extruded products that remain unrecrystallized after solution heat treating exhibit greater directional differences in mechanical properties than are shown by most other wrought products. These extrusions have a highly developed preferred orientation, with ⟨111⟩ and ⟨001⟩ axes parallel to the direction of extrusion. The directional variation in tensile properties correlates with the relative degree of alignment between planes of maximum shear stress and crystallographic slip planes (Ref 33). In extrusions of alloy 2024 that are straightened by stretching, the variation in preferred

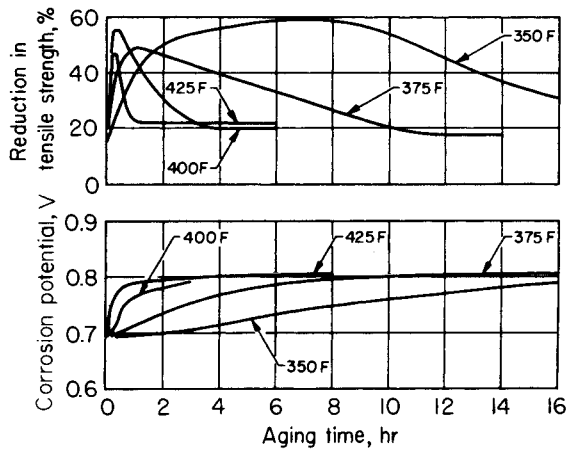

Fig. 43. Effect of precipitation heat treating on corrosion potential and corrosion resistance of alloy 2024-T3 sheet. Corrosion potential is measured in 53 g/L (7 oz/gal) NaCl and 9 mL/L (1.2 fluid oz/gal) of 30% H_2O_2 against a 0.1N calomel electrode.

orientation effect with section thickness tends to outweigh the influence of thickness on quenching rate, so that in naturally aged tempers the strength increases with increasing section thickness to about 3.75 cm (1.5 in.). When precipitation heat treatments are applied, the changes in tensile properties in the longitudinal and transverse directions are different, as indicated in Fig. 44. The anisotropy is reduced during precipitation by a decrease in high longitudinal tensile strength, coincidental with an improvement in tensile strength in the transverse direction. Precipitation heat treated tempers are used for extrusions of these alloys when higher transverse strengths and better corrosion resistance are advantageous.

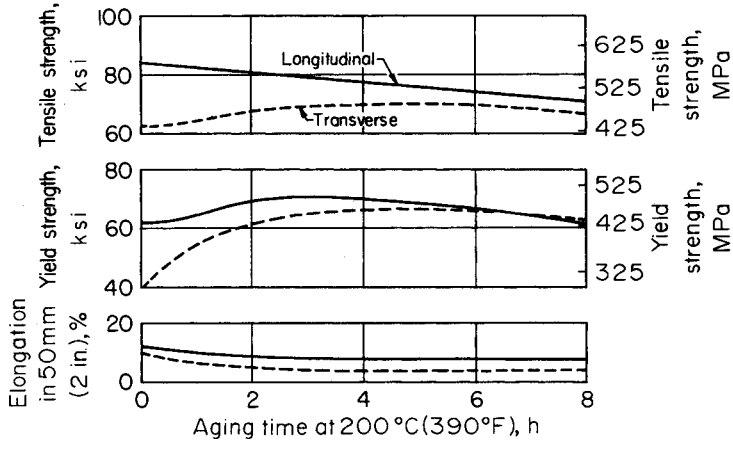

Fig. 44. Effect of precipitation heat treating at 200 °C (390 °F) on directional tensile properties of 32-mm (1 1/4-in.) thick 2024-T3 extruded shape.

ARTIFICIAL AGING OF 7XXX ALLOYS

Peak Strength. As illustrated by Fig. 35, aluminum-zinc-magnesium and aluminum-zinc-magnesium-copper alloys do not exhibit a stable W temper. Strengths increase over a period of many years by the growth of GP zones. Stable properties, higher strengths, improved corrosion resistance, and a lower rate of growth of fatigue cracks are obtained by the use of elevated-temperature aging. In contrast to the 2XXX and 6XXX series, which are aged at 170 to 190 °C (340 to 375 °F), temperatures of 115 to 130 °C (240 to 260 °F) are usually used for obtaining T6 properties with the 7XXX alloys. The reason is that in most cases, they provide high strength in reasonably short aging cycles. Aging curves are shown in Fig. 45 for rapidly quenched sheet of alloy 7075 that was brought slowly to the aging temperatures of 120 to 150 °C (250 to 300 °F). Under these conditions, peak strength was developed at 120 °C (250 °F).

Because of the nature of hardening precipitates, many variables are important to consider when aging 7XXX alloys. One variable that must be recognized is the time interval at room temperature between quenching and the start of the precipitation treatment. As shown in Fig. 46, the influence of this variable is specific for a given alloy composition. For 7178, the highest strengths are obtained with a minimum delay between quenching and aging. This is also true of 7075, but delays of 4 to 30 h are more detrimental than longer delays. The reasons for these effects are not completely understood, but there is an apparent relation to the degree of supersaturation existing in the quenched state and to reversion of GP zones during artificial aging (Ref 6 and 7). The effects of a natural aging interval for 7075-T6 sheet are eliminated by use of the two-step treatments, such as 4 h at 100 °C (212 °F) plus 8 h at 160 °C (315 °F). This treatment develops the same strength in 7075 sheet as that provided by 24 h at 120 °C (250 °F), despite the fact that isothermal aging above 250 °F usually provides much lower strength. The reason is that the treatment at 100 °C (212 °F) develops a distribution of GP zones that is stable when

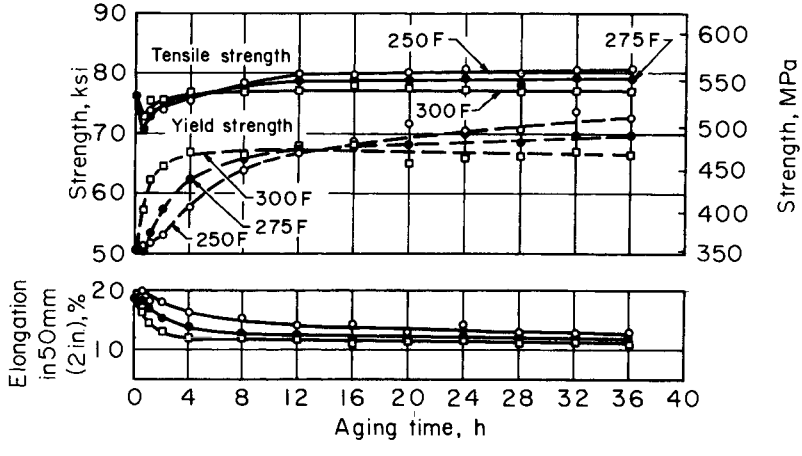

Fig. 45. Aging of 7075 sheet at 120 to 150 °C (250 to 300 °F). (J.A. Nock, Jr., Alcoa Research Laboratories)

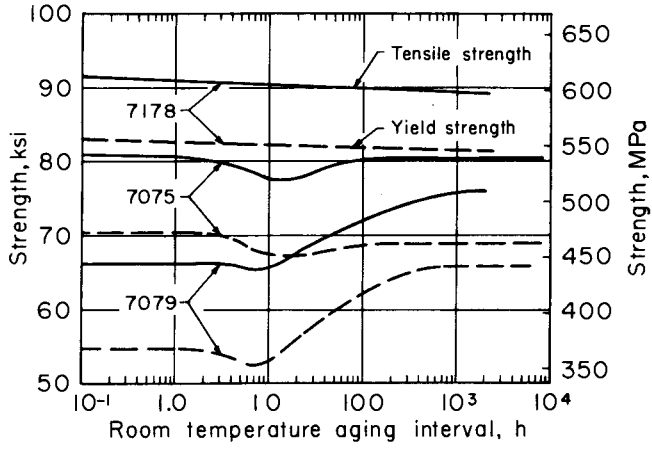

Fig. 46. Effect of time interval at room temperature between quenching and precipitation heat treating on tensile and yield strengths of 7178-T6, 7075-T6, and 7079-T6 alloy sheet. (J.A. Nock, Jr., Alcoa Research Laboratories)

the temperature is raised (Ref 34). When the quench rate is lowered, as in quenching thick forgings in hot water, homogeneous nucleation becomes difficult even at temperatures as low as 120 °C (250 °F), or even lower. Under these conditions, a preage near 100 °C (212 °F) before the age near 120 °C (250 °F) increases strength (Ref 35). Another variable to be considered, then, is quench rate and first-step aging conditions. The copper-free 7XXX alloys such as 7005 also use two-step aging practices to provide high strength. A standard treatment for 7005 extrusions is 8 h at 110 °C (225 °F), followed by 16 h at 150 °C (300 °F). Slow heating to the aging temperature acts like a first step in that it permits GP zones to grow to a size that does not dissolve at higher temperatures. Consequently, heating rate is an important factor. One standard treatment for 7039 calls for a controlled rate of heating.

Overaged Tempers. During the early 1960's, T7X-type practices were developed to improve the corrosion resistance of the 7XXX alloys containing more than 1% copper. The T73 temper was developed to improve the short-transverse stress-corrosion cracking resistance of 7075 thick section products (Ref 22). The T76 temper was applied to 7075 and 7178 for improved resistance to exfoliation corrosion (see Chapter 7 of this Volume). Since that time, T7 tempers have been developed for later generation 7XXX alloys such as 7475, 7049, and 7050. These tempers are based on the fact that selective corrosion at grain boundaries is reduced with increased overaging. Aging temperatures in the range 160 to 175 °C (325 to 350 °F) are used following a controlled exposure at lower temperatures to allow the formation of large numbers of GP zones that are stable at the higher temperatures. The zones transform to the intermediate η' precipitate and finally to the equilibrium η ($MgZn_2$) phase during overaging. Eliminating the first step and rapidly heating to the final aging temperature results in low strength, because of reversion of the GP zones and insufficient nuclei for the formation of a fine dispersion of η. As

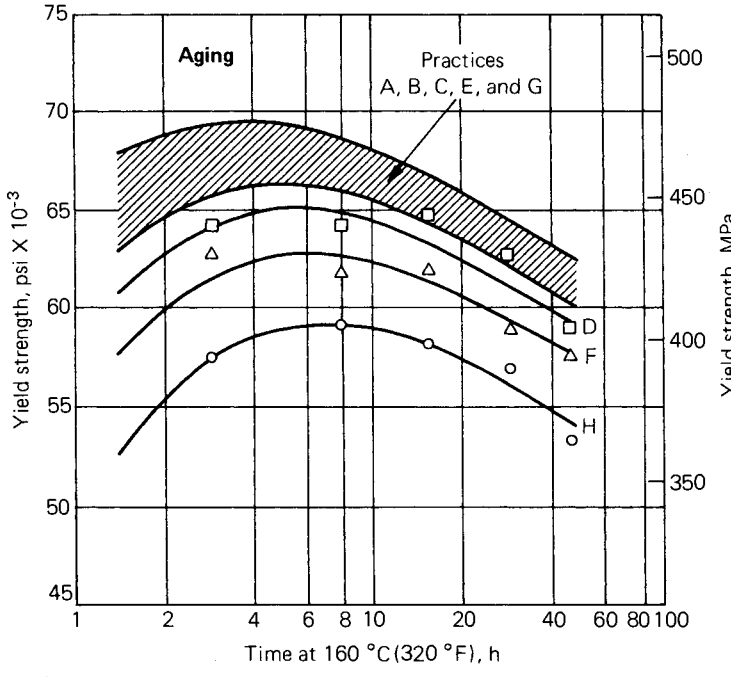

Two-step aging	Single-step aging	Heating method	Heating rate °C/min	Heating rate °F/min
A	B	Programmed air oven	0.23 ± 0.01	0.4 ± 0.02
C	D	Programmed air oven	0.93 ± 0.03	1.7 ± 0
E	F	Air oven at 160 °C (320 °F)	~10	~18
G	H	Oil bath at 160 °C (320 °F)	~100	~180

Fig. 47. The influence of processing variables on 7075 aging curves.

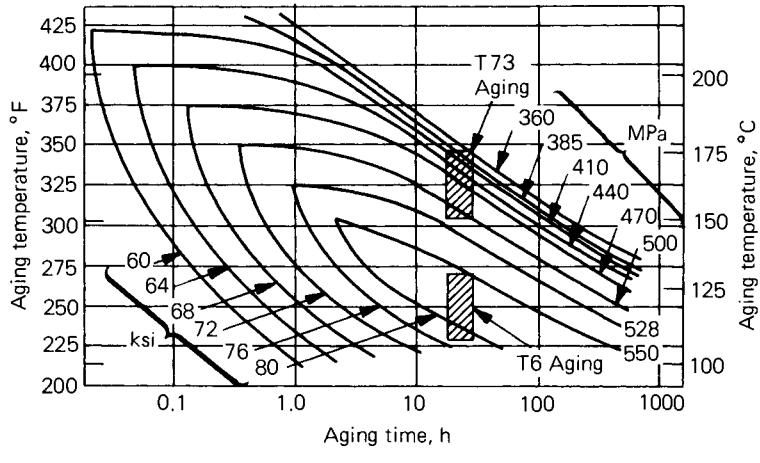

Fig. 48. ISO yield strength curves for 7075.

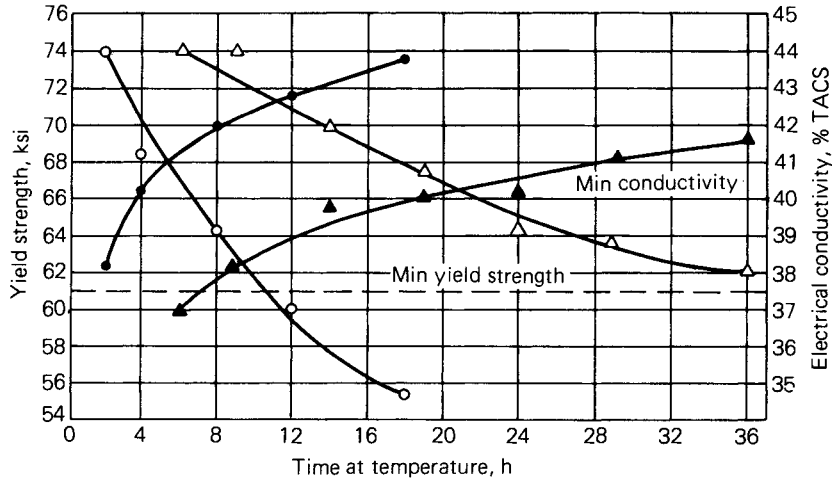

Fig. 49. Second-step aging curves for 100-mm (4-in.) 7050 plate.

shown in Fig. 47, the use of either a slow heating rate or a two-step aging practice overcomes this problem (Ref 36). Greatly extending the natural aging interval also permits GP zones to grow to a size that resists reversion, even with rapid heating, but this extended time at room temperature is not practical (Ref 34). Consequently, suggested commercial practices normally involve heating to the temperature range of 100 to 120 °C (210 to 250 °F) and soaking 1 to 24 h before exposure at the higher temperature. Numerous combinations of time and temperature are possible during the second-step age, as shown in Fig. 48. In any case, overaging can occur rather rapidly, as shown in Fig. 49. Therefore, extraordinary process control is required.

To assist with the control problem, a new method has been developed that gives a quantitative description of effects of precipitation during overaging (Ref 37). The method is based on the observation that the overaging reaction is isokinetic (Fig. 50) (Ref 38). These effects can be described by the following equation:

$$S = Y \exp - \left(\frac{t_s}{F} + \phi\right) \qquad \text{Eq 10}$$

where S is yield strength; Y is a term having units of strength and that is alloy, fabrication practice, and test direction dependent; t_s is the time at soak temperature; F is a temperature-dependent term; and

$$\phi = \int \frac{dt}{F} \qquad \text{Eq 11}$$

where t is time during heating. These relationships provide the furnace operator with a method of compensating for heating rate and for differ-

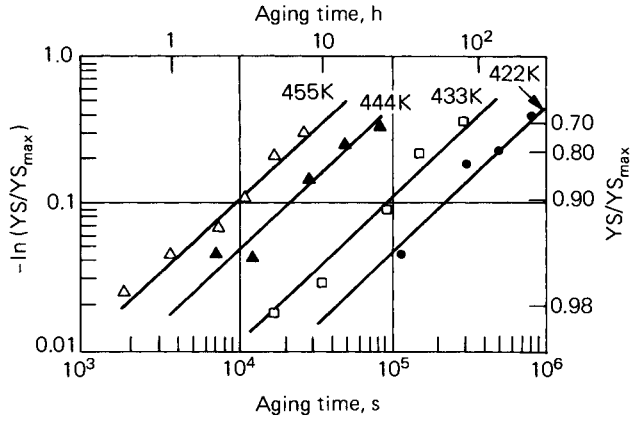

Fig. 50. Overaging kinetics of alloy 7050.

ences in soak temperature between that desired and that attained. The information provided by solving these equations can be used in a variety of ways. One way is to transfer the solutions to a series of graphs and read the answers off the graphs. Other ways are to program and use a pocket calculator or to use a patented process (Ref 39).

High temperature aging practices also are used with the lower copper or copper-free 7XXX alloys such as 7004, 7005, 7021, and 7039. In general, these practices are used to obtain the best combination of strength, corrosion resistance, and toughness. While stress-corrosion performance in the longitudinal and long-transverse directions is relatively high, resistance to stress-corrosion cracking in the short-transverse direction is less than that obtained by aging the 7XXX alloys containing higher copper by T7X-type practices.

Thermomechanical aging (TMA) involves deformation after solution heat treatment. The deformation step may be warm or cold and before, after, or during aging. The simplest TMA practices are those of the conventional T3, T8, or T9 tempers. The rate and extent of strengthening during precipitation heat treatment are distinctly increased in some alloys by cold working after quenching, whereas other alloys show little or no added strengthening when treated by this sequence of operations (Ref 40). Alloys of the 2XXX series such as 2024, 2124, and 2219 are particularly responsive to cold work between quenching and aging, and this characteristic is the basis for the higher strength T8 tempers. The strength improvement accruing from the combination of cold working and precipitation heat treating is a result of nucleation of additional precipitate particles by the increased strain. The effect on the precipitate shape of artificially aging 2024 from three initial conditions is given in Fig. 51: that of aging of 2024-T4, which is not cold worked; that of 2024-T3, cold worked equivalent to a 1 to 2% reduction; and that of 2024-T361, cold worked 5 to 6%. The *S'* precipitate platelets in Fig. 51(a), which shows the structure of 2024-T6 having a nominal yield strength of 400 MPa (58 ksi), were nucleated exclusively by dislocation loops resulting from condensation of vacancies about dispersoid particles during quenching. The much

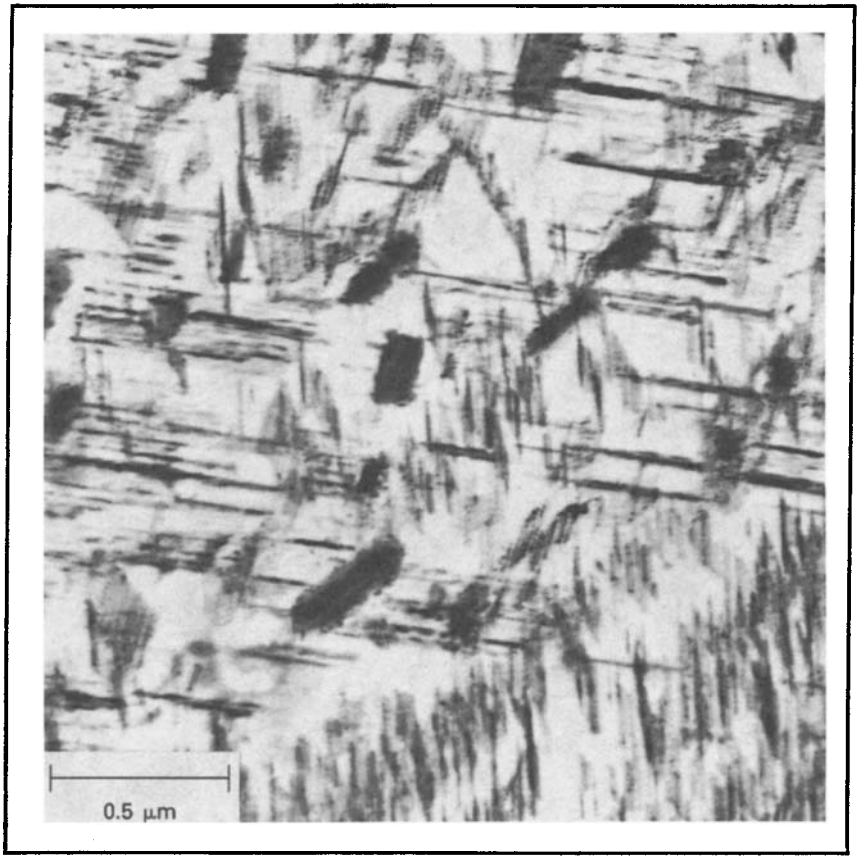

Fig. 51a. Electron transmission micrograph of 2024-T6, solution heat treated, quenched, aged 12 h at 190 °C (375 °F). (50,000×).

finer, more numerous, precipitate particles apparent in Fig. 51(b), representing 2024-T81 with a yield strength of 455 MPa (66 ksi), and Fig. 51(c), the structure of 2024-T861 having a yield strength of 500 MPa (73 ksi), were nucleated by the extensive network of additional dislocations introduced by cold working after quenching.

Normally, cold work is introduced by stretching; however, other methods such as cold rolling can be used. Recently, 2324-T39 was developed. The T39 temper is obtained by cold rolling approximately 10% after quenching followed by stretching to stress relieve. This type of approach results in strengths similar to those obtained with T8 processing but with the better toughness and fatigue characteristics of T3 products.

Various combinations of cold working or warm working after quenching, followed by natural or artificial aging, have been tried with 2XXX alloys (Ref 41). Regardless of the working practice, artificial aging progressively decreases toughness and fatigue performance but improves the corrosion resistance of 2XXX alloys. Therefore, the choice of practice depends on application design conditions.

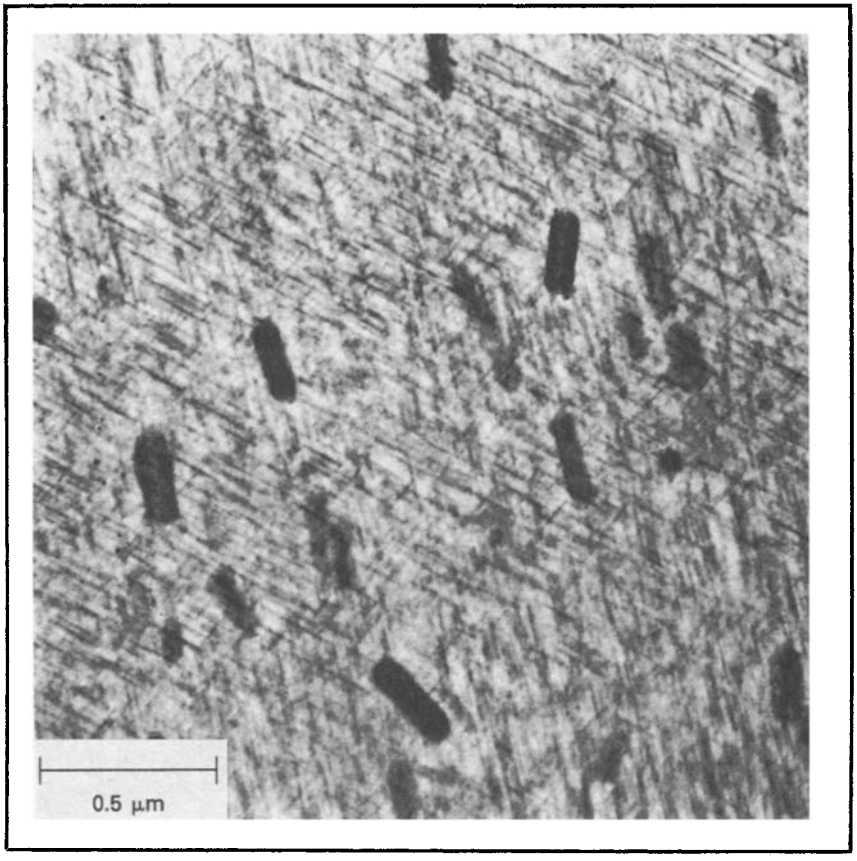

Fig. 51b. Electron transmission micrograph of 2024-T81, solution heat treated, quenched, stretched 1.5%, aged 12 h at 190 °C (375 °F). Precipitate platelets are smaller and more numerous than in (a). (50,000×).

Cold work after solution heat treatment affects the aging response of 7XXX alloys. Because amounts of cold work are usually introduced for mechanical stress relieval, the effect on properties obtained by aging for a T6 treatment of 24 h at 120 °C (250 °F) is minimal (Fig. 52). The same amount of cold work, however, significantly reduces the strength obtainable by T7-type aging. The data in Fig. 52 reveal that the effect is not because of a change in the rate of overaging. Rather, cold work decreases the maximum attainable strength. The attainable strength decreases progressively with increasing cold work up to at least 5%. This effect is attributed to the effect of dislocations on heterogeneously nucleating η' precipitate. Cold working by cold rolling to levels higher than those used for stress relief purposes can provide hardness levels surpassing those provided by precipitation hardening effects (Fig. 53), but these treatments are not used commercially.

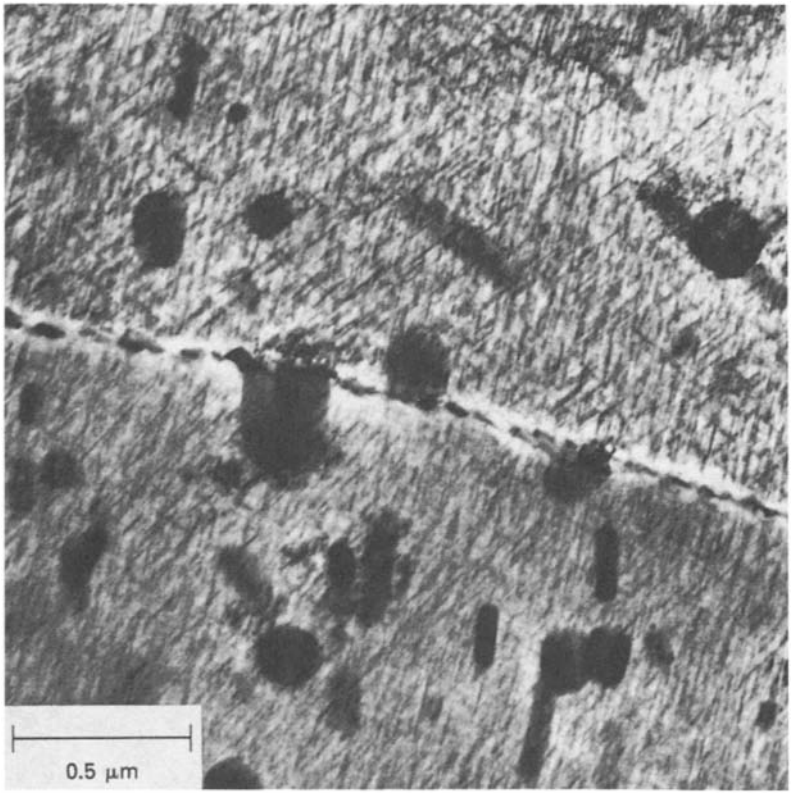

Fig. 51c. Electron transmission micrograph of 2024-T86, solution heat treated, quenched, cold rolled 6%, aged 12 h at 190 °C (375 °F). Precipitate platelets are smaller and more numerous than in (b). (50,000×).

Considerable experimentation has been conducted on the effects of final thermomechanical treatments (FTMT) on the performance of 7XXX alloys, in an attempt to provide more attractive combinations of strength, toughness, and resistances to fatigue and stress-corrosion cracking (Ref 42-44). This type of processing involves a preage after quenching and cold or warm working followed by a final age. No consensus exists as to the value of such processing at this time, nor has the use of FTMT been accepted commercially.

Precipitation Heat Treating Without Prior Solution Heat Treatment. Certain alloys that are relatively insensitive to cooling rate during quenching can be either air cooled or water quenched directly from a final hot working operation. In either condition, these alloys respond strongly to precipitation heat treatment. This practice is widely used in producing thin extruded shapes of alloys 6061, 6063, 6463, and 7005. Upon precipitation heat treating after quenching at the extrusion press, these alloys

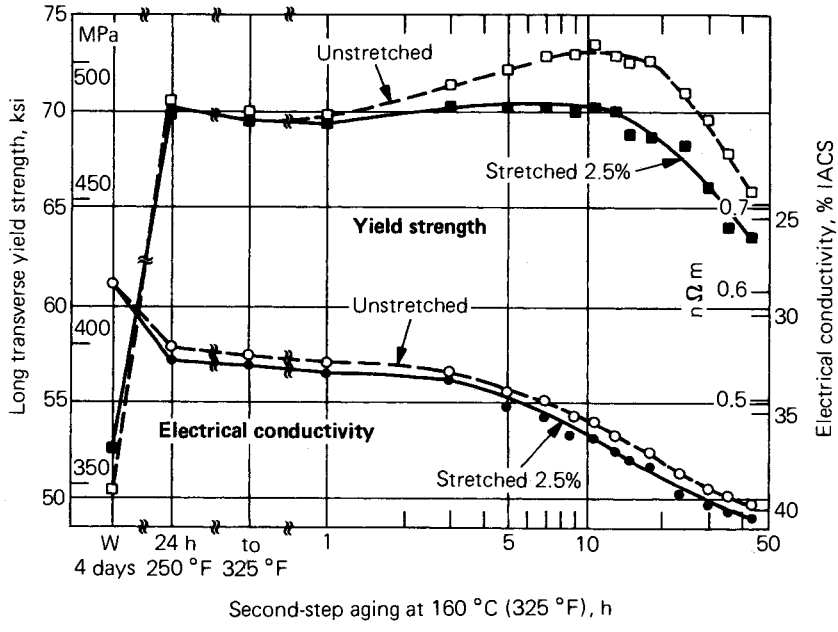

Fig. 52. Effect of stretching on aging response of 10-mm ($^3/_8$-in.) thick 7475 plate.

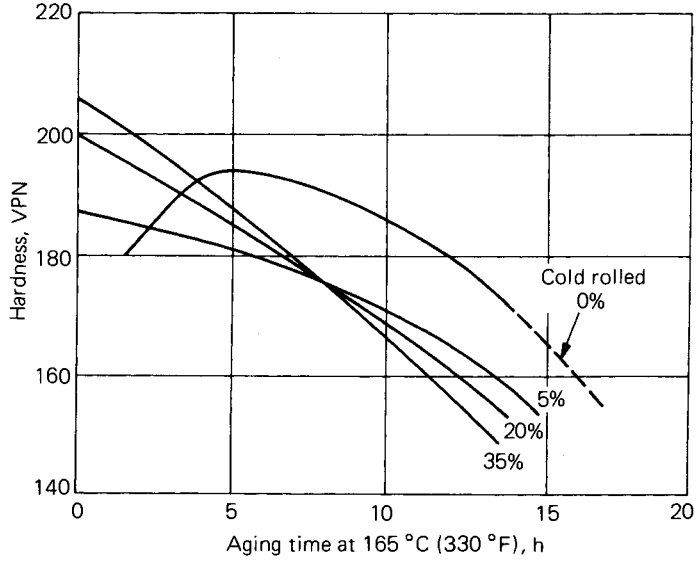

Fig. 53. The effect of cold work on the aging kinetics of a 7075-type alloy.

develop strengths nearly equal to those obtained by adding a separate solution heat treating operation. Changes in properties occurring during the precipitation treatment follow the principles outlined in the discussion of solution heat treated alloys.

Precipitation Heat Treating Cast Products. The mechanical properties of permanent mold, sand, and plaster castings of most alloys are greatly improved by solution heat treating, quenching, and precipitation heat treating, using practices analogous to those used for wrought products. In addition to this sequence of operations, used to establish tempers of the T6 and T7 types, precipitation heat treatment can be used without prior solution heat treating to produce T5-type tempers. The effects of precipitation treatment on mechanical properties have the same characteristic features cited for wrought products. The use of either T5 or T7 overaging treatments is more prevalent for cast than for wrought products. These treatments, which result in lower strength and hardness than are obtained in the T6 temper, are used to minimize dimensional changes during elevated-temperature service. Thermal treatments are not generally beneficial to the mechanical properties of die castings, and therefore usually are not applied to them.

Representative effects of precipitation heat treating on the tensile properties of the widely used aluminum-silicon-magnesium alloy 356 are illustrated in Fig. 54. Higher strengths and superior ductility are obtained by solution heat treating before precipitation heat treating than by precipitation heat treating directly from the as-cast condition (F temper). Because of the finer cast structure of the more rapidly solidified permanent mold castings, their tensile properties are superior to those of sand castings similarly heat treated.

Effect of Precipitation Heat Treating on Residual Stress. The stresses developed during quenching from solution heat treatment are reduced during subsequent precipitation heat treatment. The degree of relaxation of stresses is highly dependent upon the time and temperature of the precipitation treatment and the alloy composition. In general, the precipi-

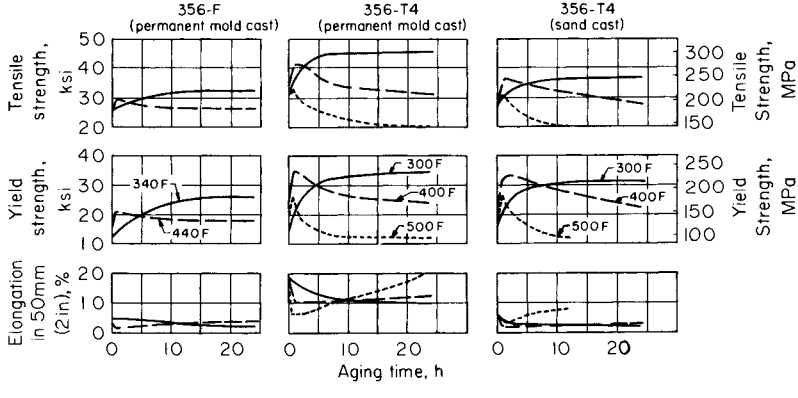

Fig. 54. Elevated-temperature aging characteristics of cast 356. Temper designations given apply before aging.

tation treatments used to obtain the T6 tempers provide only modest reduction in stresses, ranging from about 10 to 35%. To achieve a substantial lowering of quenching stresses by thermal stress relaxation, higher temperature treatments of the T7 type are required. These treatments are used when the lower strengths resulting from overaging are acceptable. Specific methods for reducing the residual stresses in heat treated products by both mechanical and thermal treatment are described in Volume III in Chapter 10 of *Aluminum* published by ASM in 1967.

The relaxation of stress under constant strain is essentially the conversion of elastic to plastic strain, by the same mechanisms involved in creep. The deformation accomplished by this means is used to establish precise final dimensions in large welded tanks. Primary forming of alloy 2219 tank segments is accomplished in the solution heat treated and cold worked T37 temper, followed by assembly welding. The achievement of final contours and dimensions of the welded assembly is facilitated by performing the precipitation heat treatment of 24 h at 165 °C (325 °F) to the T87 temper while the assembly is clamped in a contour-restraining fixture. In the restrained condition, the alloy yields, assuming the shape imposed by the fixture.

DIMENSIONAL CHANGES IN HEAT TREATING

In addition to the completely reversible changes in dimensions that are a simple function of temperature change and the thermal expansion coefficients, expansions and contractions of a more permanent character are encountered during heat treatment (Ref 45). These changes are of a metallurgical nature, arising from the introduction and relaxation of stresses, recrystallization, and solution or precipitation of alloying elements. Elements that decrease the lattice spacing when in solid solution generally cause a decrease in dimensions, because solution is affected during solution heat treating. During subsequent precipitation at elevated temperatures, a reversal of this change is expected. Because certain elements expand the lattice and others contract it, these effects vary considerably with the proportions of different elements used in commercial alloys. These solution and precipitation effects are primarily nondirectional in nature.

Other important effects that may be highly directional are those associated with relief of residual stresses introduced during fabrication, or with development of residual stresses during quenching. The degree of directionality is dependent to a major extent upon the type, shape, and section thickness of the product, the nature of the quenching medium, and the manner in which quenching is performed. The dimensional changes associated with recrystallization vary with the type and extent of prior working, and the degree of anisotropy varies with preferred orientation. These factors are subject to so much variation that there is no valid generalization regarding specific changes that may be expected in different products.

Results obtained in laboratory experiments are summarized in Fig. 55. A sequence of thermal treatments was applied to sheet and extruded rod of four alloys, and the unit dimensional changes were determined after each step. These data demonstrate certain characteristic differences among compositions. In addition, directional effects result from stresses present

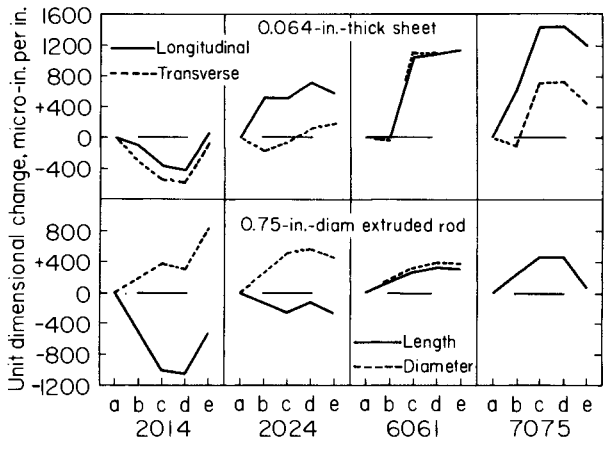

Fig. 55. Effects of heat treatments on dimensional changes in sheet and extruded rod. (a) As fabricated. (b) Annealed. (c) Solution heat treated and quenched in cold water. (d) Naturally aged, T4. (e) Precipitation heat treated, T6. (L.A. Willey, Alcoa Research Laboratories)

in the as-fabricated condition, as well as those introduced by quenching, which vary with the shape and type of product.

Dimensional changes occurring during room temperature aging of cold water quenched sheet are illustrated in Fig. 56 for four alloys. The direction of initial change is, in some cases, opposite to that consistent with a reduction in solute concentration of the solid solution. The existence of such changes and of the subsequent reversal was verified, however, by careful dilatometric measurements. The changes are small, but of sufficient magnitude so that tempers more stable dimensionally are sometimes preferred for parts used in instruments or apparatus requiring maximum dimensional stability.

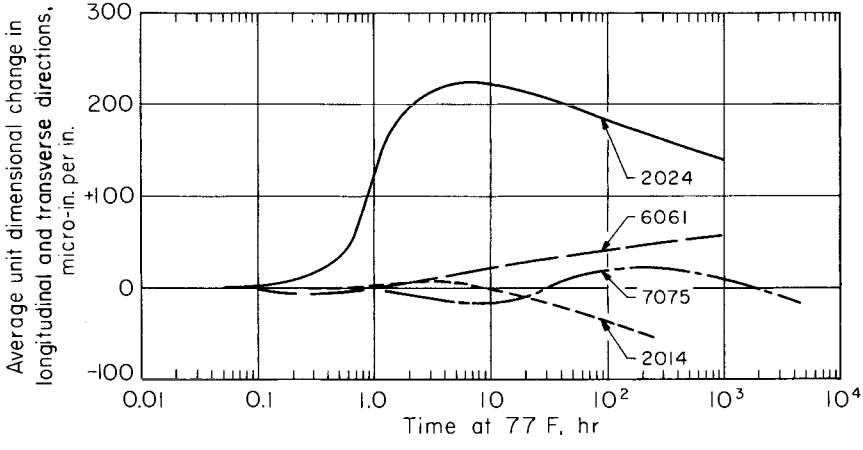

Fig. 56. Average unit dimensional changes during room temperature aging of cold water quenched sheet. (L.A. Willey, Alcoa Research Laboratories)

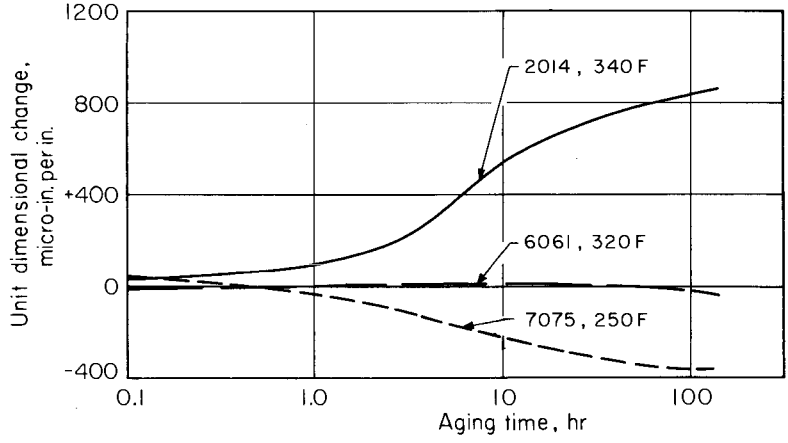

Fig. 57. Effects of unit dimensional changes of time at precipitation heat treating temperatures used to produce the T6 temper of three alloys. (L.A. Willey, Alcoa Research Laboratories)

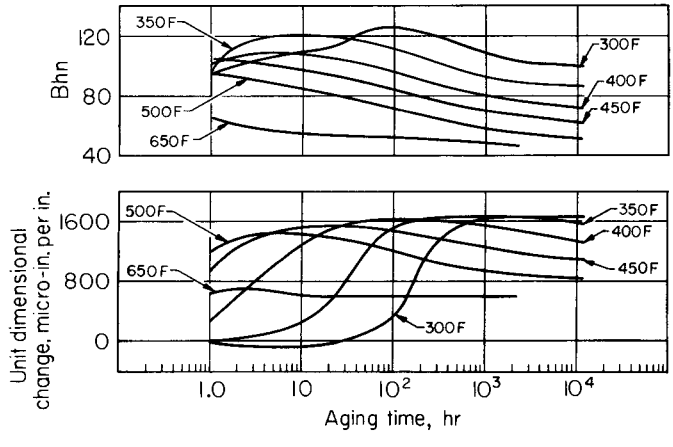

Fig. 58. Unit dimensional changes and hardness of aluminum-copper-manganese-silicon alloy 2025-T4, precipitation heat treated at six temperatures. (M.W. Daugherty, Alcoa Research Laboratories)

Unit dimensional changes that accompany precipitation heat treating three alloys at the temperature used for producing the T6 temper in each alloy are charted in Fig. 57. These effects are normally not directional, although evidence was found that some anisotropy may be encountered in products having a high degree of preferred orientation. Growth in dimensions as a result of precipitation is greatest for alloys containing substantial amounts of copper, but is reduced progressively with increasing magnesium content in such aluminum-copper-magnesium alloys as 2014 and 2024. The aluminum-magnesium-silicon alloy 6061 shows little dimensional change during precipitation heat treatment, whereas aluminum-

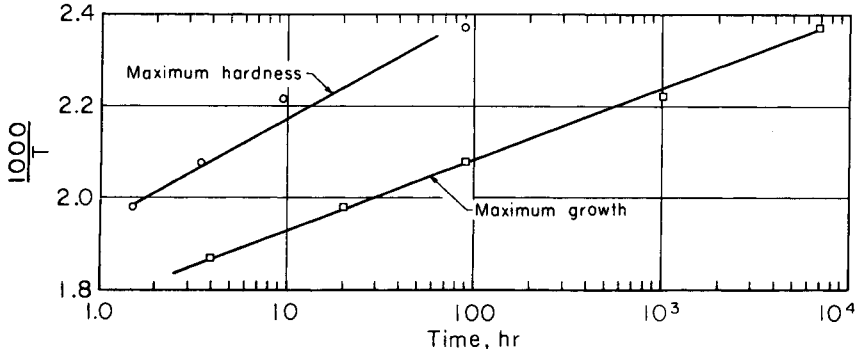

Fig. 59. Variation in time to produce maximum hardness and maximum growth during precipitation heat treating of 2025-T4, as a function of the reciprocal of absolute temperature.

zinc-magnesium-copper alloy 7075 actually contracts.

These effects assume considerable importance for parts that must maintain a precision fit over long periods of operation at elevated temperature, such as engine pistons. The thermal treatments used for such parts are designed to promote growth during the heat treating operation, avoiding this change during service. To accomplish this, the precipitation treatment must be at a temperature high enough so that the hardness and strength of the product are lower than if dimensional stability were not the critical objective.

The effects of time and temperature for precipitation heat treatment on the unit dimensional change and Brinell hardness of the aluminum-copper-manganese-silicon alloy 2025-T4 are demonstrated in Fig. 58. The extent of aging required to produce maximum hardness or strength at a specific temperature is much shorter than that needed to develop the maximum dimensional change. This is also illustrated by reciprocal temperature plots of the data (Fig. 59). The contraction that follows the attainment of maximum growth at temperatures of 175 °C (350 °F) or higher is attributed to transformation of the transition precipitate to the equilibrium structure. It also may be influenced by changes in coherency with growth and coalescence of the precipitate particles.

REFERENCES

1. "Vacancies and Other Point Defects in Metals and Alloys", Institute of Metals Monograph and Report Series No. 23, 1958
2. H. Jagodzinski and F. Laves, Uber Die Deutung der Entmischungsvorgange in Mischkristallen unter besonder Berucksichtigung der Systeme Aluminium-Kupfer und Aluminium-Silber, *Zeitschrift fur Metallkunde*, Vol 40, 1949, p 296-305
3. F. Seitz, in *L'Etat Solide*, Stoopes, Brussels, 1952, p 401
4. R.B. Nicholson, G. Thomas, and J. Nutting, Electron Microscopic Studies of Precipitation in Aluminum Alloys, *Journal of the Institute of Metals*, Vol 87, 1958-1959, p 429-488
5. J.D. Embury and R.B. Nicholson, The Nucleation of Precipitates: The System Al-Zn-Mg, *Acta Metallurgica*, Vol 13, 1965, p 403-417
6. D.W. Pashley and M.H. Jacobs, The Mechanism of Phase Transformation

in Crystalline Solids, London, Institute of Metals, Monograph 33, 1969
7. J.D. Embury and R.B. Nicholson, The Mechanism of Phase Transformation in Crystalline Solids, London, Institute of Metals, Monograph 33, 1969
8. A. Kelly and R.B. Nicholson, Precipitation Hardening in *Progress in Materials Science,* Vol 10, Edited by B. Chalmers, New York: Macmillan, 1963
9. E.A. Starke, Jr., The Causes and Effects of Denuded or Precipitate-Free Zones at Grain Boundaries in Aluminum-Base Alloys, *Journal of Metals,* Jan 1970
10. N. Ryum, Precipitation Kinetics in an Al-Zn-Mg Alloy, *Zeitschrift fur Metallkunde,* Vol 64, Feb 1975, p 338-343
11. G. Thomas and J. Nutting, Electron Microscopic Studies of Precipitation in Aluminum Alloys, in "The Mechanisms of Phase Transformations in Metals", Institute of Metals Monograph and Report Series No. 18, 1956, p 57-66
12. T.F. Bower, H.D. Brody, and M.C. Flemings, Effects of Solidification Variables on the Structure of Aluminum Base Ingots, Army Materials Research Agency Contract DA-19-020-ORD-5706A, Frankford Arsenal, Philadelphia, 1964
13. D. Altenpohl, Detailed Investigation on the Cast Microstructure of Aluminum and Aluminum Alloys, *Zeitschrift fur Metallkunde,* Vol 56, 1965, p 653-663
14. P.R. Sperry, The Relation Between Constitution and Ultimate Grain Size in Aluminum-1.25% Manganese Alloy 3003, *Transactions of ASM,* Vol 50, 1958, p 589-610
15. W.L. Fink and L.A. Willey, Quenching of 75S Aluminum Alloy, *Transactions of AIME,* Vol 175, 1948, p 414-427
16. J.W. Evancho and J.T. Staley, Kinetics of Precipitation in Aluminum Alloys During Continuous Cooling, *Metallurgical Transactions A,* Vol 5, Jan 1974, p 43-47
17. J.B. Austin, The Flow of Heat in Metals, American Society for Metals, 1942, p 91-138
18. J. Katz, A New Heat Treatment for Precipitation Hardening Aluminum Alloys, *Metal Progress,* Feb 1966, p 70-72
19. S.E. Axter, Effects of Interrupted Quenches on the Properties of Aluminum, Tech Paper CM80-409 Society of Manufacturing Engineers, 1980
20. L. Swartzendruber *et al,* Nondestructive Evaluation of Nonuniformities in 2219 Aluminum Alloy Plate—Relationship to Processing, National Bureau of Standards Report NBSIR 80-2069, Dec 1980
21. R.E. Sanders, Jr. and J.T. Staley, Relationships Between Microstructure, Conductivity, and Mechanical Properties of Alloy 2024-T4, *Aluminium,* Parts I and II, Dec 1982/Jan 1983/Feb 1983
22. United States Patent 3198676, Aug 1965
23. L.W. Kempf, H.L. Hopkins, and E.V. Ivanso, Internal Stress in Quenched Aluminum and Some Aluminum Alloys, *Transactions of AIME,* Vol 3, 1934, p 150-180
24. G. Forrest, Internal or Residual Stresses in Wrought Aluminum Alloys and Their Structural Significance, *Journal of the Royal Aeronautical Society,* Vol 58, April 1954, p 261-276
25. K.R. Van Horn, Residual Stresses Introduced During Metal Fabrication, *Journal of Metals,* March 1953, p 405-422
26. R.T. Torgerson and C.J. Kropp, Improved Heat Treat Processing of 7050 Aluminum Alloy Forgings Using Synthetic Quenchants, General Dynamics Convair Division Report, 1977
27. E.A. Lauchner, Glycol Quenching 7075 Forgings 2.5 Inches Thick, Aerospace Heat Treatment Committee Report R-3, Dec 1973
28. J.F. Collins and C.E. Maduell, Polyalkylene Glycol Quenching of Aluminum Alloys, Paper No. 28, Corrosion/77, March 1977, p 14-18
29. P. Archambault *et al,* Optimum Quenching Conditions for Aluminum Alloy Castings, Heat Treatment 1976—Proceedings of 16th International Heat Treatment Conference, Metals Society (London) Book 181, 1976, p 105-109, 219-220

30. United States Patent 3996075, Dec 1976
31. I. Kirman, *Metallurgical Transactions A*, Vol 2, 1971, p 1761-1770
32. J.T. Staley, Microstructure and Toughness of High-Strength Aluminum Alloys, "Properties Related to Fracture Toughness", ASTM STP 605, American Society for Testing and Materials, 1976, p 71-103
33. K.R. Van Horn, Factors Affecting Directional Properties in Aluminum Wrought Products, *Transactions of ASM*, Vol 35, 1944, p 130-155
34. J.T. Staley, R.H. Brown, and R. Schmidt, Heat Treating Characteristics of Al-Zn-Mg-Cu Alloys With and Without Silver, *Metallurgical Transactions A*, Vol 3, Jan 1972, p 191-199
35. S. DesPortes, E. Sanko, and K. Wolfe, "Effect of Quench Rate on Precipitate Nucleation in Aluminum Alloy 7075", Purdue University School of Materials Engineering, May 1980
36. R.F. Ashton and D.S. Thompson, Effect of Heating Rate on the Aging Behavior of 7075 Alloy, *Metallurgical Transactions A*, Vol 245, 1969, p 2101
37. J.T. Staley, Kinetics for Predicting Effects of Heat Treating Precipitation-Hardenable Aluminum Alloys, *Industrial Heating XLIV*, Oct 1977, p 6-9
38. J.T. Staley, Aging Kinetics of Aluminum Alloy 7050, *Metallurgical Transactions 5*, April 1974, p 929-932
39. United States Patent 3645804, 1972
40. E.H. Dix, Jr., New Developments in High Strength Aluminum Wrought Products, *Transactions of ASM*, Vol 35, 1944, p 130-155
41. D.S. Thompson, S.A. Levy, and G.E. Spangler, Thermomechanical Aging of Aluminum Alloys I and II, *Aluminium*, Jan 1974, p 647-649, 719-723
42. R.R. Sawtell, Effects of FTMT Versus Alloying on Fatigue and Fracture of 7XXX Alloy Sheet, Thermomechanical Processing of Aluminum Alloys, AIME Conference Proceedings, 1979
43. A.W. Sommer, N.E. Paton, and D.G. Folgner, Effects of Thermomechanical Treatments on Aluminum Alloys, Technical Report AFML-TR-72-5, Feb 1972
44. E. DiRusso *et al*, Thermomechanical Treatments on High Strength Al-Zn-Mg(Cu) Alloys, *Metallurgical Transactions 4*, April 1973, p 1133-1144
45. H.Y. Hunsicker, Dimensional Changes in Heat Treating Aluminum Alloys, *Metallurgical Transactions A*, May 1980, p 759-773

Aluminum Properties and Physical Metallurgy
John E. Hatch editor, p 200-241
DOI: 10.1361/appm1984p200

CHAPTER 6

EFFECTS OF ALLOYING ELEMENTS AND IMPURITIES ON PROPERTIES*

With over 100 possible alloying elements, even leaving out the elements that are very rare or very poisonous, millions of useful alloy combinations would seem possible. The possibilities are quite limited if small alloy variations are ignored. Alloying elements are usually added to aluminum to increase its strength, although improvements in other properties are very important. The two most commonly used methods of increasing the strength of aluminum alloys are to:

- Disperse alloying elements or elements in solid solution and cold work the alloy (work-hardening alloys)
- Dissolve the alloying elements into solid solution and precipitate them as coherent submicroscopic particles (precipitation-hardening alloys)

The solid solubility in aluminum of the elements is given in Table 1, Chapter 2 in this Volume. Note that only nine elements have a maximum solid solubility greater than 1 wt% and have substantially lower solubilities at lower temperatures. Of these nine elements, silver, gallium, and germanium are expensive and lithium, because of processing difficulties, is presently used only in special alloys. This leaves five elements: zinc, magnesium, copper, manganese, and silicon, which form the basis for the principal commercial aluminum alloys. These are used in various combinations, as shown in Fig. 1.

All age-hardening alloys contain alloying elements that can be dissolved at elevated temperatures (solution heat treated) and precipitated at lower temperatures (aged) to produce significant increases in strength. Most casting alloys have silicon as the major alloying addition because aluminum-silicon alloys are able to fill the mold completely and are not sensitive to hot cracking. The silicon in shape casting produces a modest increase in strength because of the large volume fraction of hard silicon particles or fibers formed during solidification. The work-hardening alloys are of two basic types: the aluminum-manganese based alloys, which form a fine dispersion of intermetallic phase particles giving a modest increase in strength, and the aluminum-magnesium based alloys in which the magnesium remains in solid solution and produces a larger increase in strength, particularly after cold working. A combination of aluminum-

*This chapter was revised by a team comprised of L. Morris and G. Marchand, Alcan International, Kingston Laboratories; R.E. Sanders, Jr. and R.A. Kelsey, Alcoa Technical Center; and J.E. Hatch, consultant. The original chapter was authored by W.A. Dean, Alcoa Research Laboratories.

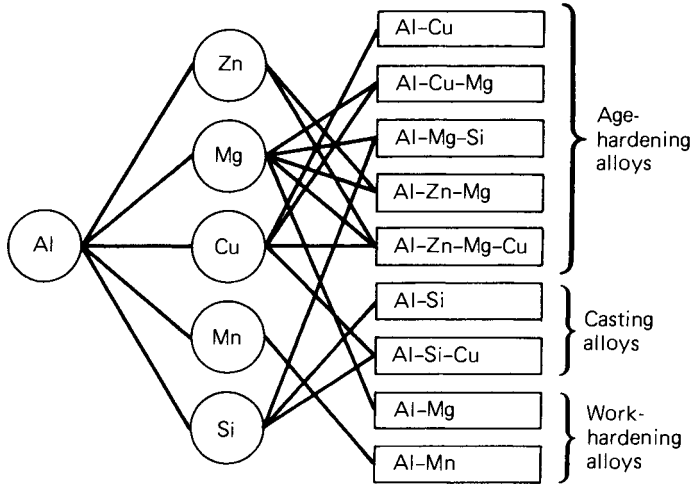

Fig. 1. Principal aluminum alloys. (Ref 1)

magnesium-manganese is widely used in aluminum alloy beverage containers. All alloying elements will increase work hardening, but the above two systems are extensively used because they both remain stable during processing and have excellent corrosion resistance.

Transition metals with moderate solid solubilities, such as manganese, chromium, and zirconium are added to aluminum alloys because they can be precipitated as a dispersion of fine intermetallic phase particles, less than 1 μm (0.04 mil) in diameter, which do not dissolve during hot working or annealing. This fine, stable dispersion of particles can be used to pin grain or subgrain boundaries and improve strength, toughness, and improve resistance to stress-corrosion cracking.

Most elements have a very low solid solubility in aluminum and are segregated to the dendrite cell boundaries during casting. If the concentration of these elements is high enough, they form second-phase particles, usually in the order of 10 μm (0.4 mil) in cross section, which remain as particles in the alloy during subsequent processing. The most commonly encountered of these particles are the iron-rich intermetallic phases that result from iron, which is always present as an impurity in commercial metal. These relatively large particles add only a small increment to the strength of the alloy and can decrease toughness and corrosion resistance. Elements with low solid solubilities can also be useful, for example, lead and bismuth are added to some alloys to improve machinability.

PHYSICAL PROPERTIES

Density. The relative lightness of aluminum is one of its outstanding characteristics. Of the common alloying elements, magnesium, lithium, and silicon decrease the density of aluminum and chromium, copper, iron, manganese, nickel, titanium, and zinc increase it (Ref 2).

The relationship between the density of an alloy and its composition usually approaches linearity closely enough to justify calculating density

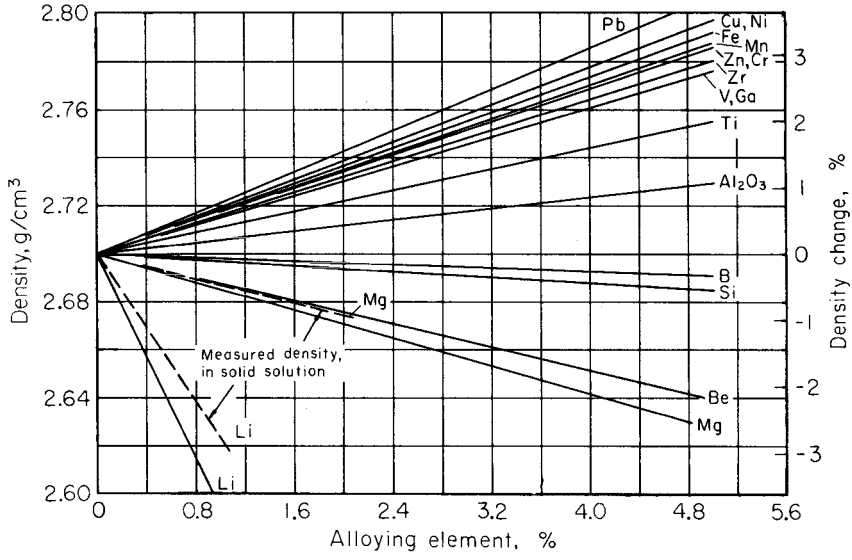

Fig. 2. Density of binary aluminum alloys (calculated). (Courtesy of D.E. Kunkle, Alcoa)

as the sum of the density contributions of each element present. The departure from a linear relation between density and composition is influenced by many factors: porosity, macrosegregation of constituents, degree of solid solution, specific volumes of constituents that differ from those of the added elements, as well as phenomena associated with quenching from elevated temperatures, cold work, and growth. The conditions under which the density of an alloy is determined should be specified. Because the effects of many of the above factors are minimized when the alloy is annealed, the densities of alloys in this condition are more readily comparable. The effects of several common additions to aluminum on its density (calculated values) are shown in Fig. 2.

Metals soluble in the aluminum lattice affect density in a more complex manner than when an alloy is composed of two or more phases, where the density can be predicted by the law of mixtures. The effects of several elements on the lattice parameter of aluminum are shown in Table 1, Volume I, Appendix 2 of *Aluminum*, American Society for Metals, 1967. Generally, if an element goes into solid solution and contracts the lattice, it increases the density. On precipitation of such an element, the lattice expands and the density decreases, unless there is a decrease in the specific volume of the precipitating phase, which may cause the density to increase.

The changes in density brought about by the presence of silicon in aluminum are an example of the complex effect of an added element on this property. If up to 1.65% silicon is added to aluminum (its maximum solid solubility) and if the silicon is out of solution, a reduction in density occurs by the rule of mixtures. A solution heat treatment and quench brings all of the silicon into solid solution and because the silicon decreases the lattice parameter of aluminum, the density of the alloy in-

creases. Thus, the net effect of silicon on the density of the alloy is the sum of the individual effects of these two phenomena: the solid solubility of silicon in aluminum, and its presence in a heterogeneous mixture.

Similar effects resulting from multiple influences on density occur in aluminum-magnesium alloys, except that in this system the situation is complicated by precipitation of the Mg_2Al_3 constituent, which is appreciably less dense than the solid solution. Another example is lithium, which contracts the aluminum lattice but decreases density. The dotted curves of Fig. 2 show measured densities of alloys containing lithium or magnesium when these elements are in solid solution in aluminum.

In addition to the influence on density of composition and heat treatment, changes in density occur during fabrication. For example, rolling an ingot may increase its density by eliminating porosity. Cold work decreases density by developing dislocations; these are subsequently removed by annealing, with an accompanying increase in density. The changes are on the order of 0.1%.

Thermal expansion is the reversible dimensional change resulting solely from a change in temperature; irreversible dimensional changes resulting from metallurgical causes, such as residual stresses or behavior of soluble phases, are excluded.

The expansion of an aluminum-based alloy is a constant fraction of the expansion of 99.996% aluminum when the materials are tested in the annealed state (the condition of maximum dimensional stability). Expansion characteristics of 99.996% aluminum are discussed in Chapter 1 in this Volume.

Table 1 shows the change in alloy constant for various alloy additions to aluminum per weight percentage of addition, including a group (chromium, manganese, titanium, vanadium, and zirconium) for which only limited data are available. More detailed information is given in Ref 3.

Additions of Al_2O_3, copper, iron, magnesium, nickel, silicon, or zinc to aluminum change its expansion coefficient in approximately a linear manner. As shown in Fig. 3, magnesium or zinc increase the expansion, whereas the other additions decrease it.

The effects of alloying additions, with some exceptions, are additive, following the rule of mixtures. However, elements that were in solid solution may combine to form phases of greatly reduced solubilities, such

Table 1. Effect of Alloying Elements on the Thermal Expansion of Aluminum

Alloying element	Change in alloy constant per wt% addition (annealed temper)(a)	Alloying element	Change in alloy constant per wt% addition (annealed temper)(a)
Aluminum oxide (Al_2O_3)	−0.0105	Zinc	+0.0032
Copper	−0.0033	Chromium	−0.010(b)
Iron	−0.0125	Manganese	−0.010(b)
Magnesium	+0.0055	Titanium	−0.010(b)
Nickel	−0.0150	Vanadium	−0.010(b)
Silicon	−0.0107	Zirconium	−0.010(b)

(a) Constant is 1.0000 for high-purity aluminum. (b) Estimated.
Source: L.A. Willey, Alcoa Research Laboratories.

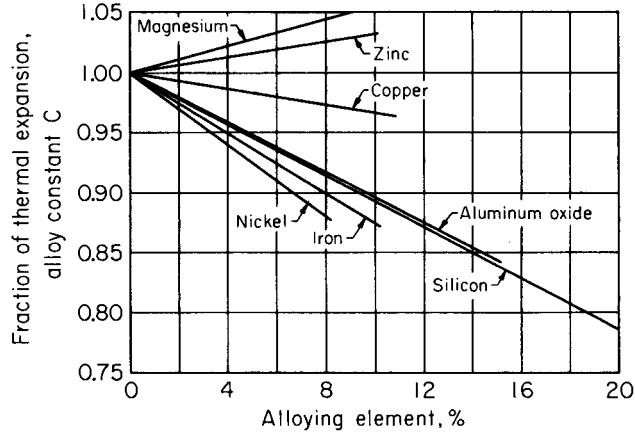

Fig. 3. Effects of alloying elements on the thermal expansion of aluminum. Fraction is based on a value of 1.00 for 99.996% aluminum. (Courtesy of L.A. Willey, Alcoa)

as Mg_2Si or $MgZn_2$; these phases will be largely out of solution in the annealed state. The phases will, therefore, remove from solution the magnesium and zinc that would still remain in solution in annealed binary alloys. From limited data, the observed expansions of alloys containing Mg_2Si or $MgZn_2$ are lower than those expected from a calculation based on individual metal additions.

The temper of an alloy has an influence on its thermal expansivity. Measurements indicate that the thermal expansivity constants of alloys in the heat treated condition (T4 or T6 tempers) are higher by about 0.015 than those for alloys in the annealed condition.

Thermal Conductivity. Because thermal conductivity can be calculated from electrical resistivity measurements, this approach is generally used to arrive at the values quoted in the literature. Kempf, Smith, and Taylor (Ref 4) found the relationship between thermal and electrical conductivities for annealed aluminum alloys between 0 and 400 °C (32 and 750 °F) to be largely independent of composition, with the exception of an effect of silicon. This relationship was expressed by the equation:

$$K = 5.02\lambda T \times 10^{-9} + 0.03$$

where K is thermal conductivity, λ the electrical conductivity, and T the absolute temperature in degrees Kelvin.

The effect of silicon is anomalous, in that the K/T ratio (Lorenz factor) for the aluminum-silicon alloys is greater than for other aluminum alloys by about 0.05 per weight percent of silicon up to the eutectic concentration of 12.6%. The effects of composition on electrical and thermal conductivities are similar (Ref 5).

Electrical Conductivity and Resistivity. Electrical conductivity, which is the reciprocal of resistivity, is one of the most sensitive properties of aluminum, being particularly responsive to changes in composition and thermal condition. Fortunately, conductivity is readily measured with high precision (Ref 6).

Table 2. Effect of Elements In and Out of Solid Solution on the Resistivity of Aluminum

Element	Maximum solubility in Al, %	Average increase in resistivity per wt%, μΩ·cm	
		In solution	Out of solution(a)
Chromium	0.77	4.00	0.18
Copper	5.65	0.344	0.030
Iron	0.052	2.56	0.058
Lithium	4.0	3.31	0.68
Magnesium	14.9	0.54(b)	0.22(b)
Manganese	1.82	2.94	0.34
Nickel	0.05	0.81	0.061
Silicon	1.65	1.02	0.088
Titanium	1.0	2.88	0.12
Vanadium	0.5	3.58	0.28
Zinc	82.8	0.094(c)	0.023(c)
Zirconium	0.28	1.74	0.044

Note: Add above increase to the base resistivity for high-purity aluminum, 2.65 μΩ·cm at 20 °C (68 °F) or 2.71 μΩ·cm at 25 °C (77 °F).
(a) Limited to about twice the concentration given for the maximum solid solubility, except as noted. (b) Limited to approximately 10%. (c) Limited to approximately 20%.
Source: L.A. Willey, Alcoa Research Laboratories.

All known metallic additions to aluminum reduce its electrical conductivity. Metals in solid solution depress the conductivity to a greater extent than when out of solution. Manganese is an example of the importance of the condition in which the added element appears in aluminum. As the amount of manganese in solid solution increases, the resulting rapid increase in resistivity is in marked contrast to the much slower increase in resistivity as manganese concentration exceeds its solid-solubility limit.

A summary of the maximum solubilities of various elements in aluminum is shown in Table 2, together with the average increase in resistivity per 1% of the element in solution and out of solution. For example, if the alloy contains 1.0% chromium and the maximum amount of it is in solid solution, the increase in resistivity of high-purity aluminum (2.65 μΩ·cm at 20 °C) is $0.77 \times 4.00 + 0.23 \times 0.18 = 3.13$ μΩ·cm. The potent effects on resistivity of chromium, iron, lithium, manganese, titanium, and vanadium are apparent.

The effect of two or more additions on the resistivity of aluminum depends on the relationship between the elements. In general, if the elements individually go into solid solution in aluminum, their effects on resistivity are additive. If a compound is formed, the solid solubility of one or both elements may be reduced, or the compound may have a solubility of its own. In the aluminum-magnesium-zinc system, the effect of the combined presence of magnesium and zinc on the resistivity of aluminum falls between the values of each alone. The resistivities are approximately additive on an atomic basis, even when magnesium and zinc are present in the ratio to form $MgZn_2$.

Quenching an alloy after a solution heat treatment generally results in the lowest electrical conductivity, because a large part of the constituents present are retained in solid solution. However, in systems that age at

room temperature, there may be a subsequent decrease in conductivity occurring during the initial stages of aging, attributed to Guinier-Preston zone formation and related phenomena. By removing constituents from solid solution, aging (particularly at elevated temperatures) and, to a greater degree, annealing increase the electrical conductivity.

The change in resistivity with temperature of 99.996% aluminum is approximately constant at 0.0115 $\mu\Omega \cdot$ cm per °C over the range of −160 to 300 °C (−260 to 570 °F). Because the resistivity-temperature relations for different alloys form a family of lines parallel to that of aluminum, the change in resistivity with temperature is essentially independent of composition. As a consequence, the 0.0115 $\mu\Omega \cdot$ cm per °C value is useful for calculating the resistivity of an aluminum alloy at any temperature from its known resistivity at another temperature, provided no metallurgical change takes place.

Electrical conductor grade metal (EC metal, 99.60% aluminum minimum) deserves special consideration. The effect of small concentrations of impurities is a factor of considerable economic importance in this application. Common impurities in EC metal are copper, iron, silicon, titanium, and small amounts of several other elements. Conductivity is reduced by 0.8% IACS for each 0.01% total of titanium plus vanadium present. Boron in amounts equal to half the weight of titanium-plus-vanadium content will form the compounds TiB_2 and VB_2, which are insoluble in liquid and solid aluminum. The greater amounts of these compounds settle out of the liquid melt, and the small amounts that remain exert essentially no effect on conductivity.

Magnetic susceptibility depends upon the magnetic characteristics and amount of the addition element, and the form the addition takes. For example, the addition of Al_2O_3 forms a simple mechanical mixture; iron as $FeAl_3$ is paramagnetic to about the same extent as aluminum and hence the effects of small iron additions are indistinguishable; vanadium decreases the paramagnetic susceptibility from 0.628×10^{-6} cgs at 0% vanadium to 0.582 at 0.36% vanadium. Manganese and chromium increase the property beyond that predicted by the law of mixtures—that is, to 0.959 at 1.38% manganese and to 0.669 at 0.63% chromium.

Magnetic susceptibility changes as solid solutions decompose, because it is sensitive to whether the added metal is in solid solution (as-quenched) or is in a precipitated phase (annealed condition), as in the aluminum-copper binary system shown in Fig. 4. In this system, the magnetic susceptibility of the quenched material depends on the amount of solute remaining in the solid solution during aging and is insensitive to the different phases that form as decomposition products.

Magnetic susceptibility is a quench-sensitive property. For example, the aging of 3 to 5% copper alloys at different temperatures, as followed by magnetic susceptibility measurements, is linear with respect to the logarithm of time for cold water quenched material, but proceeds as a two-step aging process following a boiling water quench.

Magnetic susceptibility is not sensitive to strain hardening, to small deviations in metallurgical structure such as vacancies, dislocations, or new grain boundaries, to residual or applied stresses, or to whether the alloy is wrought or cast.

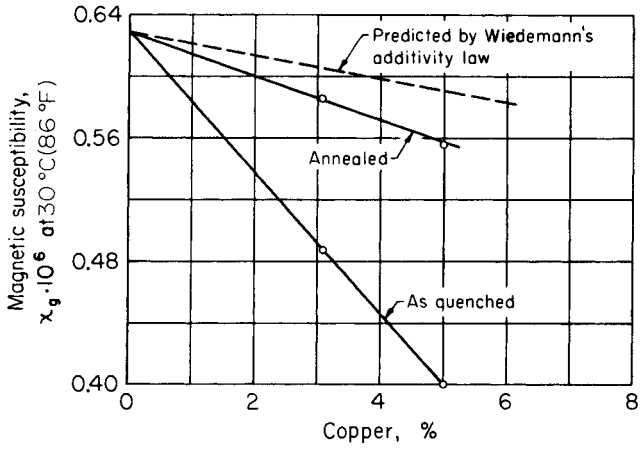

Fig. 4. Variations in magnetic susceptibility of aluminum-copper alloys with composition. (Courtesy of W.C. Sleppy, Alcoa)

Reflectance and Emissivity. Because total reflectance for white light (visible reflectance) and emissivity of aluminum are surface phenomena characteristics of the metal (Chapter 1 in this Volume), they are only indirectly influenced by the presence of alloying additions. The presence of films or coatings on aluminum alters the total reflectance for white light and emissivity, depending on their composition and opacity, from values representing the metal surface to those representing the film or coating itself. Anodic films on polished aluminum have a reflectance for visible radiation approaching that of bare aluminum; on diffuse surfaces, the reflectance decreases significantly with increases in film thickness (Fig. 5).

Although alloying additions do not appreciably affect either visible reflectance or emissivity, they can influence formation of surface films during fabrication, thermal treatment, or service, which usually decrease visible reflectance and increase emissivity.

With certain fabricating practices, the presence of magnesium or Mg_2Si in aluminum will reduce the reflectance in the visible range from 85 to 90% to approximately 70%. Under similar fabricating conditions, the emissivity of aluminum also is not affected by the presence of 1.25% manganese, but additions of 3.5% magnesium or 1.6% Mg_2Si increase this value from 3 to 6%.

A correlation has been noted between the increase in emissivity and the presence of MgO in the surface film with additions of magnesium or Mg_2Si to aluminum. Furthermore, the emissivity of aluminum increases to about 10% with additions of magnesium or Mg_2Si when it is heat treated at temperatures of 260 to 510 °C (500 to 950 °F), in wet or dry air or helium.

The specular (mirrorlike) reflectance for visible radiation, as distinguished from total reflectance for white light, can be increased by polishing and decreased by roughening treatments. The particular alloying addition will determine the type of polishing required to provide a high

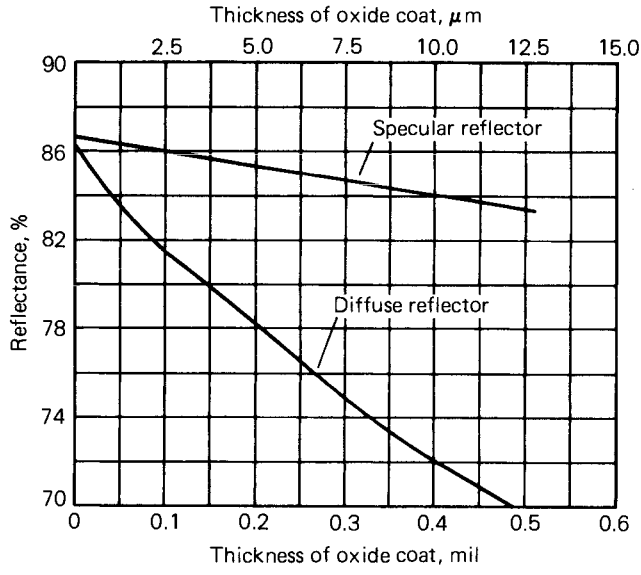

Fig. 5. Reflectance for light of aluminum surfaces with anodic coatings of different thicknesses. (C.S. Taylor and J.D. Edwards, Heating, Piping, Air Conditioning, ASHVE Journal Section, *Vol 11, 1939, p 59-63)*

specular reflectance of about 90%. All alloys can be mechanically polished, but chemical and electrochemical polishing are restricted to those alloys that will not pit with such treatments. Magnesium in solid solution strengthens aluminum while not impairing its high specular reflectance (90%) on polishing. Thus, this alloying element widens the range of commercial use of aluminum as a reflector.

The commercial interest is in the specular reflectance of bright etched and sulfuric acid anodized aluminum and aluminum alloy products. Softness, large grain size, and cost limit the commercial applications of superpurity aluminum. Magnesium or magnesium and zinc are frequently used to improve hardness and strength, because they have a minor effect on specularity in the range up to 2 or 3%. Iron has the most harmful effect (Ref 7). Loss of specularity is proportional to iron contents above 0.008%. Commercial minimums are in the range of 0.10 to 0.12% iron, depending on cost and availability. Manganese has little effect up to 0.30%, but above 0.30% the loss in brightness is progressive. Magnesium and silicon in 6063 extrusions can adversely affect brightness if the Mg_2Si is permitted to agglomerate. Proper air quench at the press and lower aging temperatures produce good specularity.

Surface Tension. The true surface tension of molten aluminum is difficult to measure, because of the error introduced by the very thin oxide film that forms on the surface of aluminum, even under carefully controlled conditions involving the use of high vacuum or inert atmosphere (Ref 8). The oxide film and liquid-solid interfacial tension cause high results with the dipping cylinder, capillary, and sessile drop methods. Because of the problems of measurement, it is difficult to compare the

values obtained by one investigator with those of another, as wide discrepancies in results may occur when different methods or techniques are used.

Alloying additions to aluminum may decrease, increase, or have virtually no influence on the results of tests intended to measure surface tension. Figure 6 shows data obtained by the capillary method at 700 to 740 °C (1290 to 1360 °F) in argon that indicate that bismuth, calcium, lithium, magnesium, lead, antimony, and tin substantially reduce the surface tension of 99.99% aluminum, whereas silver, copper, iron, germanium, manganese, silicon, and zinc have little effect. Surface tension decreases as the temperature increases.

Viscosity. Internal friction measurements in molten metal have been used to predict the formation of solid-state phases. Maxima reportedly (Ref 9) occur at limits of solid solubility, and minima are found at eutectic compositions in aluminum-copper, aluminum-magnesium, aluminum-nickel, and aluminum-silicon systems.

Viscosity is also a measure of the effect of alloying additions on the fluidity of aluminum. Figure 7 shows that at 700 °C (1290 °F), copper, iron, and titanium increase viscosity. Additions of zinc have little influence, whereas magnesium and silicon reduce internal friction of aluminum. In all cases, the viscosity drops with an increase in temperature, and the curves for various alloy compositions are essentially parallel.

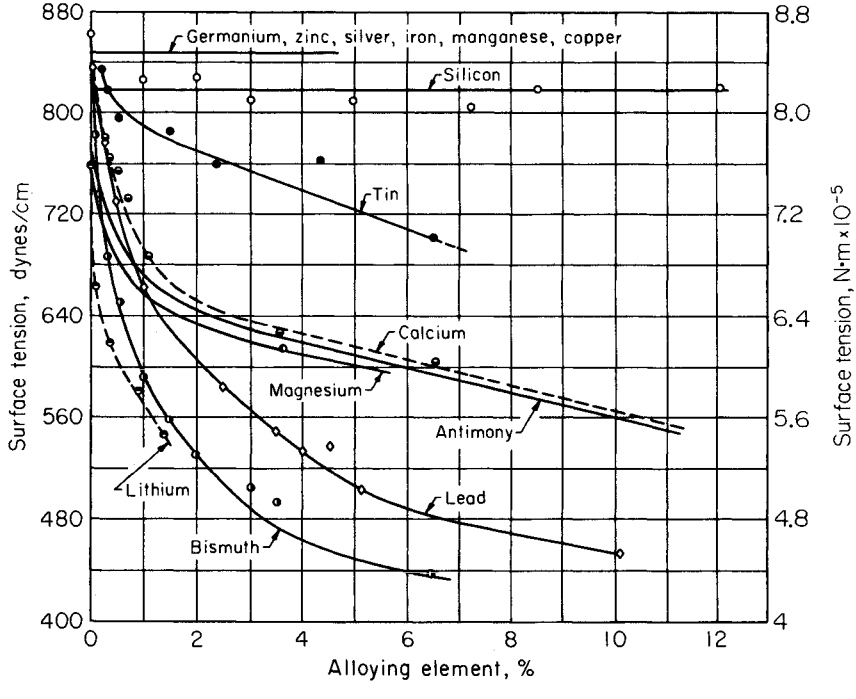

Fig. 6. Effect of added elements on the surface tension of 99.99% aluminum at 700 to 740 °C (1290 to 1360 °F) in argon. (A.M. Korol'kov, Otdelenie Tekhnicheskik Nauk, Vol 2, 1956, p 35-42)

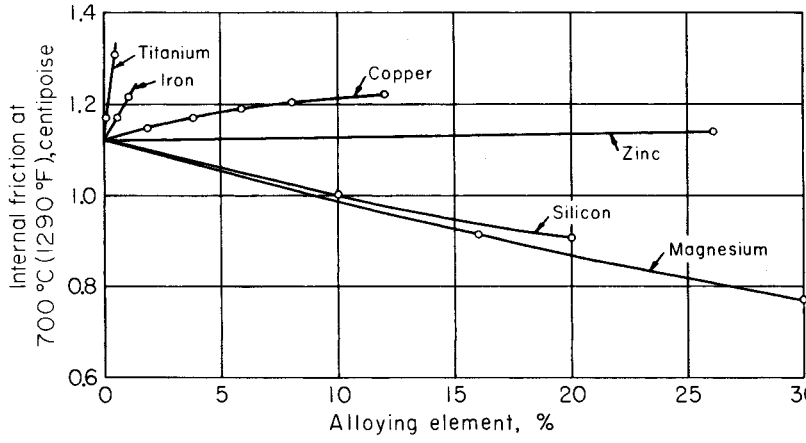

Fig. 7. Effect of alloying additions on the viscosity of aluminum. (E. Gebhardt, M. Becker, and S. Dorner, Aluminium, *Vol 31, 1955, p 315-321; E. Gebhardt and K. Detering,* Z. Metallk., *Vol 50, 1959, p 379-385)*

Specific Heat. Aluminum has a relatively high specific heat when compared with other metals on a weight basis. The differences between metals are small on a volume basis, consequently, the measured effects of small-to-moderate concentrations of other metals are not much different from values calculated on the basis of the specific heats of the weight fractions of atomic species present. Because the measurement of specific heat is difficult, the values for alloys are often calculated, and the specific heat of the alloy in the annealed condition is assumed to vary with composition in a linear manner.

Specific heat of aluminum increases approximately linearly from room temperature to its melting point (Chapter 1 in this Volume). Although supporting data are limited, it appears that the effect of other elements added to aluminum is to form a family of parallel curves, from which the specific heat at any temperature may be calculated from the known value for aluminum at that temperature (Ref 3).

The specific heat of aluminum containing additions that form insoluble constituents would not be expected to be influenced appreciably by thermal condition. The apparent specific heats (which would include heats of precipitation and solution of constituents) of solid solution aluminum alloys, in particular those of aluminum-copper and Al–Mg_2Si, depend upon the thermal condition in a nonlinear manner.

Modulus of Elasticity. Young's modulus of elasticity of aluminum alloys, determined under static conditions, is dependent upon composition to the extent that, in dilute alloys, the modulus can be calculated approximately from the individual contributions of the metals present, on a volume basis (with the exceptions of lithium and magnesium). If a second phase is formed and it is essentially the terminal member of the equilibrium system, as is the case with silicon and beryllium, the rule of mixtures is still generally applicable at higher alloy contents. If the addition to aluminum forms intermetallic compounds or other phases with alu-

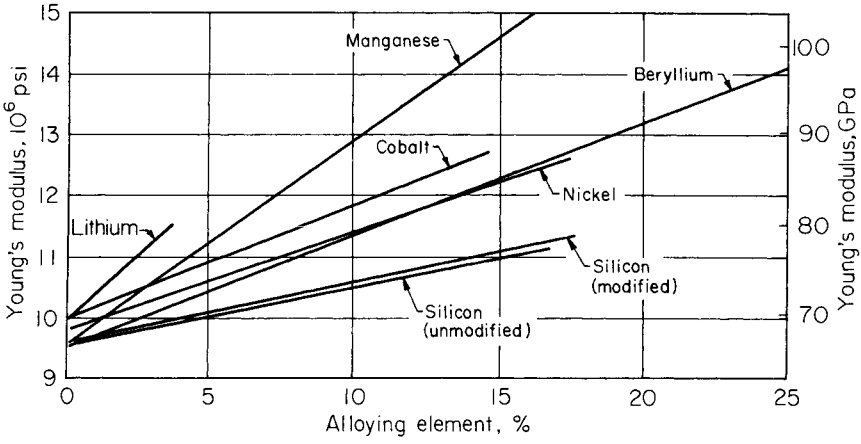

Fig. 8. Influence of several additions to aluminum on Young's modulus. (N. Dudzinski, et al., J. Inst. Metals, Vol 74, 1947-1948, p 291-314

minum, the elastic properties of these phases exert their own influence on the modulus of the alloy.

Figure 8 shows the increase in Young's modulus caused by additions of beryllium, cobalt, manganese, nickel, silicon, and lithium (Ref 10).

Powder metallurgy techniques permit alloying aluminum with other metals in higher concentrations than are obtainable by conventional means. The modulus values for several powder metal alloys are shown in Table 3.

Modulus of elasticity is determined not only under static conditions but also under dynamic conditions. Results from static and dynamic measurements do not always coincide. It is reported (Ref 11) that magnesium, zinc, silicon, and copper lower the dynamically determined elastic modulus of aluminum decreasingly in the order listed, on an atomic percent basis. Another source (Ref 12) reports that under dynamic conditions pure aluminum retains a higher modulus to 370 °C (700 °F) than do aluminum-copper, aluminum-magnesium, and aluminum-zinc alloys. Furthermore, the higher concentrations of magnesium or zinc cause a slightly greater reduction in modulus as temperature increases, compared to the more dilute alloys of the same elements.

Table 3. Modulus of Elasticity of Some Aluminum Powder Metallurgy Alloy Extrusions (APM)

Alloying constituent, %	Modulus GPa	Modulus 10^6 psi	Alloying elements(a), %	Modulus GPa	Modulus 10^6 psi
6 Al_2O_3	73	10.6	10 Cr	93	13.5
11 Al_2O_3	77	11.1	13 Fe	88	12.7
14 Al_2O_3	79	11.5	16 Mn	110	15.9
			5.9 Fe, 6.2 Ni	88	12.8
			12.6 Mn, 2.9 Si	96	13.9

(a) These alloys contain about 0.5% Al_2O_3.
Source: J.P. Lyle and H.G. Paris, Alcoa Laboratories.

MECHANICAL PROPERTIES AND PROCESSING

Forming. The formability of a material is the extent to which it can be deformed in a particular process before the onset of failure. Aluminum sheet or aluminum shapes usually fail by localized necking or by ductile fracture. Necking is governed largely by bulk material properties such as work hardening and strain-rate hardening and depends critically on the strain path followed by the forming process. In dilute alloys, the extent of necking or limit strain is reduced by cold work, age hardening, gross defects, a large grain size, and the presence of alloying elements in solid solution. Ductile fracture occurs as a result of the nucleation and linking of microscopic voids at particles and the concentration of strain in narrow shear bands. Fracture usually occurs at larger strains than does localized necking and therefore is usually important only when necking is suppressed. Common examples where fracture is encountered are at small radius bends and at severe drawing, ironing, and stretching near notches or sheared edges (Ref 13-15).

Considerable advances have been made in developing alloys with good formability but, in general, an alloy cannot be optimized on this basis alone. The function of the formed part must also be considered and improvements in functional characteristics, such as strength and ease of machining, often tend to reduce the formability of the alloy.

The principal alloys that are strengthened by alloying elements in solid solution (often coupled with cold work) are those in the aluminum-magnesium (5XXX) series, ranging from 0.5 to 6 wt% magnesium. These alloys often contain small additions of transition elements such as chromium or manganese, and less frequently zirconium to control the grain or subgrain structure and iron and silicon impurities that usually are present in the form of intermetallic particles. Figure 9 illustrates the effect of magnesium in solid solution on the yield strength and tensile elongation for most of the common aluminum-magnesium commercial alloys. Note the large initial reduction in the tensile elongation with the addition of small amounts of magnesium.

The reductions in the forming limit produced by additions of magnesium and copper appear to be related to the tendency of the solute atoms to migrate to dislocations (strain age). This tends to increase work hardening at low strains, where dislocations are pinned by solute atoms, but produces a decrease in work hardening at large strains. Small amounts of magnesium or copper also reduce the strain-rate hardening, which will reduce the amount of useful diffuse necking that occurs after the uniform elongation. Zinc in dilute alloys has little effect on work hardening or necking, and it does not cause strain aging.

Elements that have low solid solubilities at typical processing temperatures, such as iron, silicon, and manganese, are present in the form of second-phase particles and have little influence on either strain hardening or strain-rate hardening and thus a relatively minor influence on necking behavior. Second-phase particles do, however, have a large influence on fracture, as is shown in Fig. 10 and 11. In these examples an increase in the iron, nickel, or manganese content produces an increase in the number of microscopic particles that promote fracture. The addition of

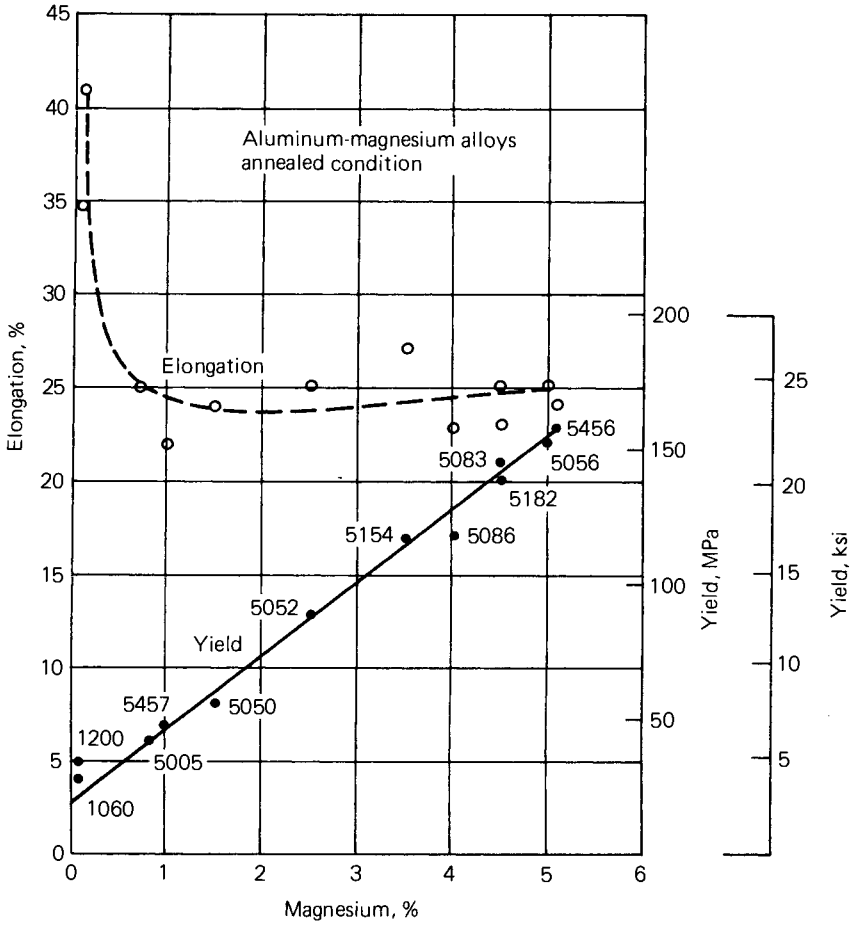

Fig. 9. Correlation between tensile yield, elongation, and magnesium content for some commercial alloys. (Ref 14)

magnesium promotes an additional reduction in fracture strain, because the higher flow stresses aid in the formation and growth of voids at the intermetallic particles. Magnesium in solid solution also promotes the localization of strain into shear bands, which concentrates the voids in a thin plane of highly localized strain.

Precipitation-strengthened alloys are usually formed in the naturally aged (T4) condition or in the annealed (O) condition but only very rarely in the peak strength (T6) condition where both the necking and fracture limits are low. In Fig. 12 the effect of a wide range of precipitate structures on some of the forming properties is illustrated for alloy 2036 (2.5% copper-0.5% magnesium). Curves similar in shape can be drawn for most of the precipitation strengthened alloys in the 2XXX and 6XXX series.

The properties in Fig. 12 were obtained from sheet tensile specimens first solution heat treated, then aged at temperatures ranging from room

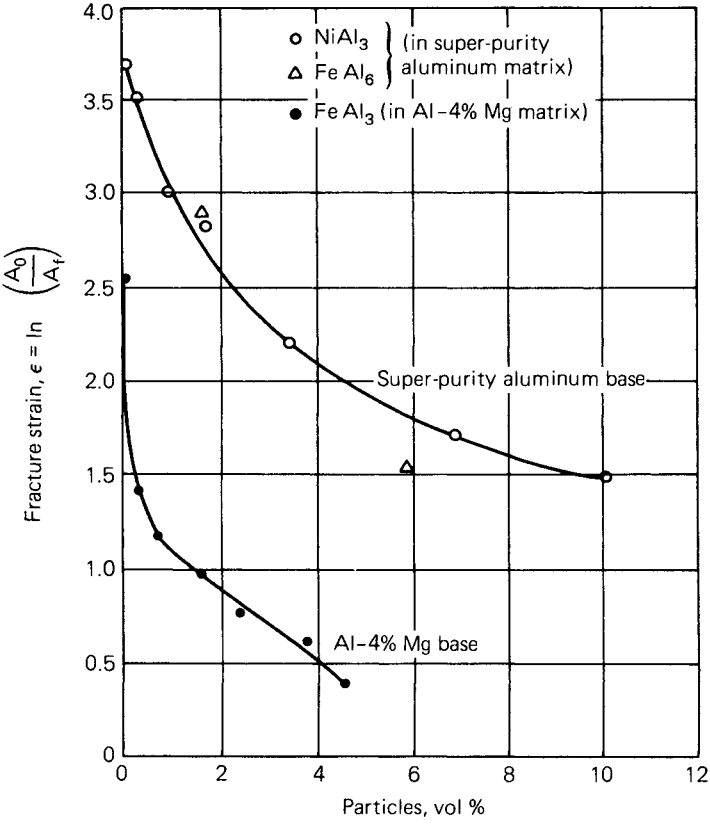

Fig. 10. Effect of volume percent fraction of micron size intermetallic particles and composition of the matrix on the fracture strain of 6-mm (0.2-in.) diam tensile specimens. A_0 is initial cross-sectional area; A_f is area of fracture. (Ref 14)

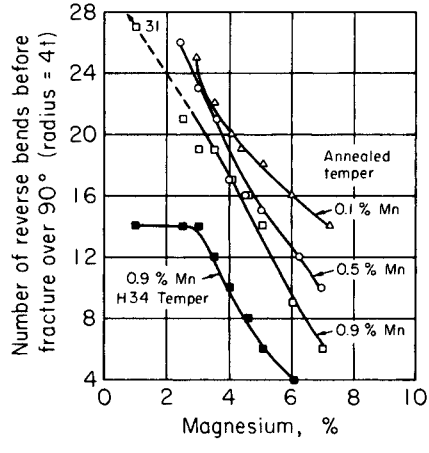

Fig. 11. Effect of magnesium and manganese on the formability of aluminum alloys in the annealed and H34 tempers; 1.6-mm (0.064-in.) thick sheet. (Courtesy of W.A. Anderson, Alcoa)

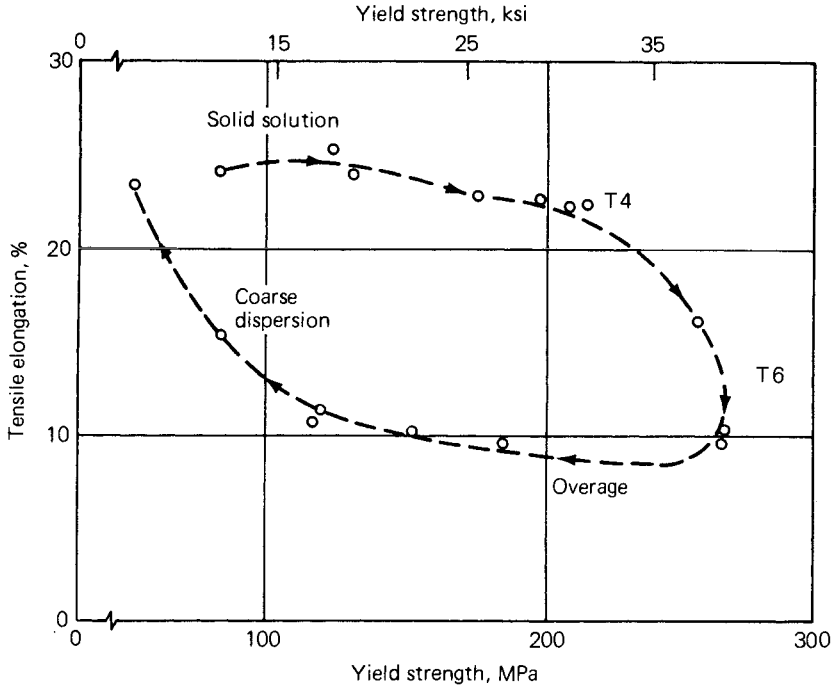

Fig. 12. Effect of precipitation on yield strength and elongation in alloy 2036. (Ref 14)

temperature to 350 °C (660 °F). This produced a full range of structures from solid solution (as-quenched) through T4 and T6 tempers to various degrees of overaging and precipitate agglomeration.

Fracture Toughness and Fatigue Behavior. The application of high-strength aluminum alloys in the aerospace industry has resulted in increased performance requirements in the areas of fatigue and fracture. In the development of aluminum alloys for these applications, it is necessary to control the alloy composition to produce specific microstructures tailored for resistance to specific failure mechanisms.

The design of damage-tolerant aluminum alloys such as 7475, 7050, or 2124 has been primarily based upon the control, through composition and fabrication practice, of the alloy microstructure (Ref 16 and 17). Three types of second-phase particles are known to influence fracture and fatigue behavior in high-strength aluminum alloys:

Type	Size, μm	Size, mil	Typical examples
Constituent particles	2–50	0.08–2	Cu_2FeAl_7, $CuAl_2$, $FeAl_6$
Dispersoid particles	0.01–0.5	0.0004–0.02	$ZrAl_3$, $CrMg_2Al_{12}$
Strengthening precipitates	0.001–0.5	0.00004–0.02	Guinier-Preston zones

The effect of these particles on the fracture and fatigue behavior is discussed below.

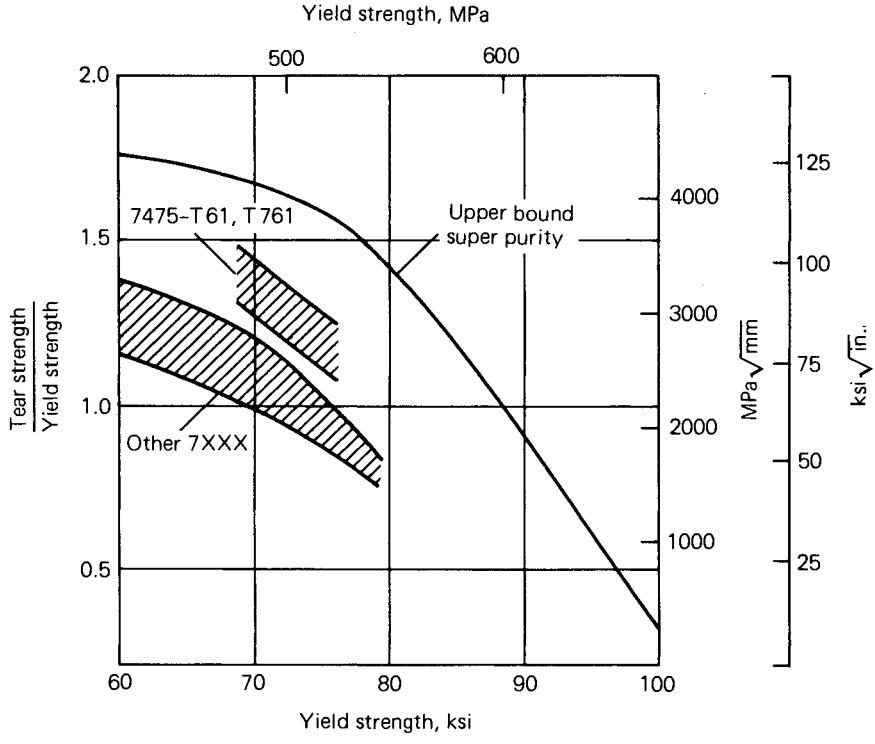

Fig. 13. Tear strength and yield strength ratio of alloy 7475 sheet.

Fracture Toughness. It is generally accepted that the fracture of brittle constituent particles leads to preferential paths for crack advance and reduced fracture toughness (Ref 18). Consequently, an often-used approach to improve the toughness of high-strength aluminum alloys has been the reduction of iron and silicon levels. The recent development of improved alloys such as 7475, 7050, and 2124 has hinged, in large part, upon the use of higher purity base metal than 7075 or 2024. Figure 13 illustrates the influence of base metal purity on the fracture resistance of alloy 7050 sheet. The partially soluble constituents exert a similar effect on the fracture behavior of high-strength alloys. Figure 14 shows the reduction in toughness experienced as the volume fraction of Al_2CuMg is increased in alloy 2024 plate.

For superior toughness, the amount of dispersoid-forming element should be held to the minimum required for control of grain structure, mechanical properties, or resistance to stress-corrosion cracking. Results for 7XXX alloy sheet (Fig. 15) show the marked decrease in unit propagation energy as chromium is increased. Substitution of other elements, such as zirconium or manganese, for chromium can also influence fracture toughness. However, the observed effects of the different dispersoids on fracture toughness can quite possibly be related to the particular toughness parameter chosen and the influence of the dispersoid on the grain structure of the wrought product.

The primary effect of hardening precipitates on fracture toughness of high-strength aluminum alloys is through the increase in yield strength and depends upon the particular working and heat treatment practices applied to the wrought products. However, composition changes, particularly magnesium level, can produce significant effects on toughness of 7XXX alloys. These variations in composition do not alter the basic character of the hardening precipitates, but exert a subtle influence on the overall precipitate structure.

Fatigue and Fatigue Crack Growth. Aluminum does not exhibit the sharply defined fatigue limit typically shown by low-carbon steel in *S-N* tests. For smooth or notched coupon tests, where lifetime is governed primarily by crack initiation, the fatigue resistance is expressed as a fatigue strength (stress) for a given number of cycles. In tests where fatigue crack growth is of interest, the performance of aluminum is measured by recording the crack growth rate (*da/dN*) as a function of stress intensity range (ΔK). This type of fatigue crack growth (FCG) test is currently of prime importance for alloys used in aerospace applications.

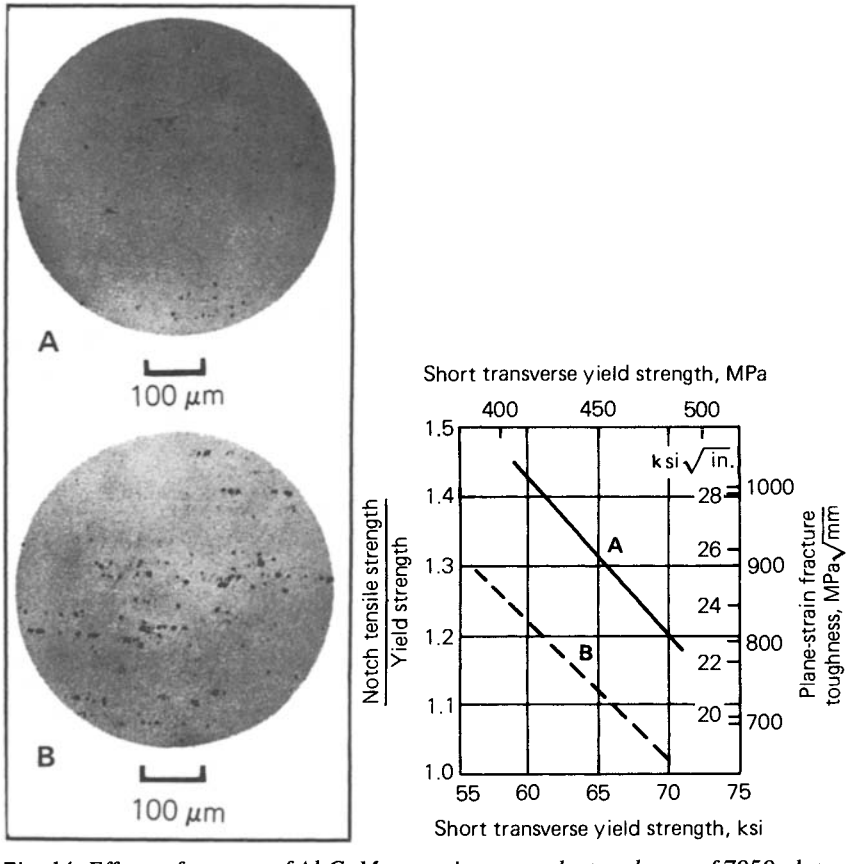

Fig. 14. Effects of amount of Al_2CuMg constituent on the toughness of 7050 plate.

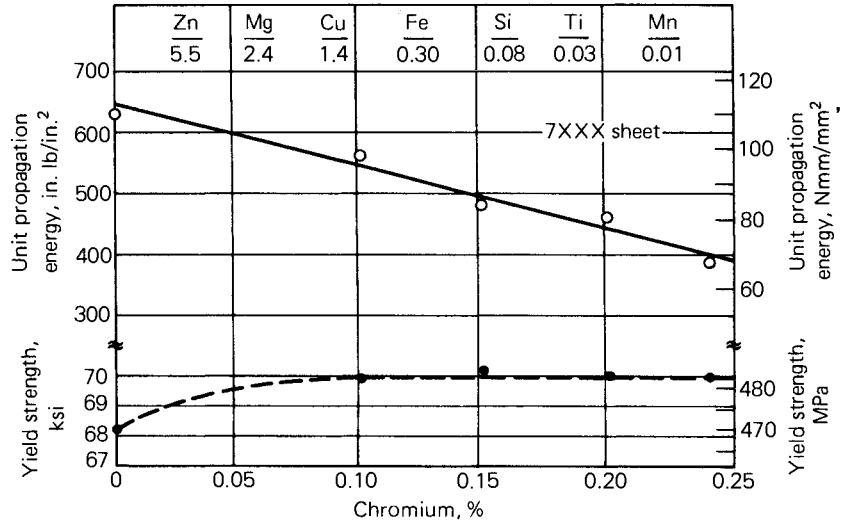

Fig. 15. Effect of chromium content on unit crack propagation energy and yield strength.

It is generally known that alloying, processing, or heat treatment that improve tensile strength tend to increase the fatigue strength of aluminum. However, the design of aluminum alloys to resist failure by fatigue mechanisms has not proceeded to the same extent as for fracture toughness.

The effect of large constituent particles on the fatigue behavior of high-strength aluminum alloys is highly dependent upon the type of fatigue test or stress regime chosen for the evaluation. Reduced iron and silicon contents do not always result in improved fatigue resistance commensurate with the previously described improvements in fracture toughness. Increased purity level does not, for instance, produce any appreciable improvement in notched or smooth *S-N* fatigue strength (Ref 19 and 20). No consistent differences in FCG rates have been observed for low- and high-purity 7XXX alloy variants at low to intermediate ΔK levels. However, at high stress-intensity ranges, FCG rates are notably reduced for low iron and silicon alloys (Ref 20 and 21). The reason for the observed improvement is undoubtedly related to the higher fracture toughness of high-purity materials. At high stress-intensity ranges, where crack growth per cycle (da/dN) values are large, localized fracture and void nucleation at constituent particles become the dominant FCG mechanism. For samples subjected to periodic spike overloads, low-purity alloys were shown to exhibit slower overall FCG rates than higher purity materials. This effect was attributed to localized crack deviation induced by the insoluble constituents. Secondary cracks at these particles acted to lower crack tip stress-intensity values and reduce measured FCG rates.

No clear-cut influence of dispersoid particles on the fatigue behavior of aluminum alloys has emerged. Two separate studies have concluded that dispersoid type has little effect on either FCG resistance (Ref 19) or notched fatigue resistance (Ref 21) of 7XXX alloys. The only expected

effect of dispersoid type on fatigue performance should occur for high ΔK fatigue crack growth, where mechanisms similar to those for fracture toughness predominate.

Within a given alloy system, slight changes in composition that influence hardening precipitates have not been shown to influence the *S-N* fatigue resistance of aluminum alloys. However, significant differences have been observed in comparison of alloys of different systems. For instance, 2024-T3 is known to outperform 7075-T6 at stresses where fatigue lives are short ($\sim 10^5$ cycles). The superior fatigue performance of alloy 2024-T3 in the 10^5 cycle range has led most aircraft designers to specify it in preference to 7075-T6 in applications where tension-tension loads are predominant.

Alloy 2024-T3 shows a similar advantage over 7075-T6 and other 7XXX alloys in fatigue crack growth. The superior performance for 2024-T3 plate versus 7075-T6 extends over the entire da/dN-ΔK range, as shown in Fig. 16. Within the 7XXX alloy system, increasing copper content improves FCG performance in high humidity. This result was attributed to an increased resistance of the high-copper alloy to corrosion in the moist environment (Ref 21).

Fatigue designers are currently beginning to use increasingly complex "spectrum" FCG tests to predict the performance of materials in service.

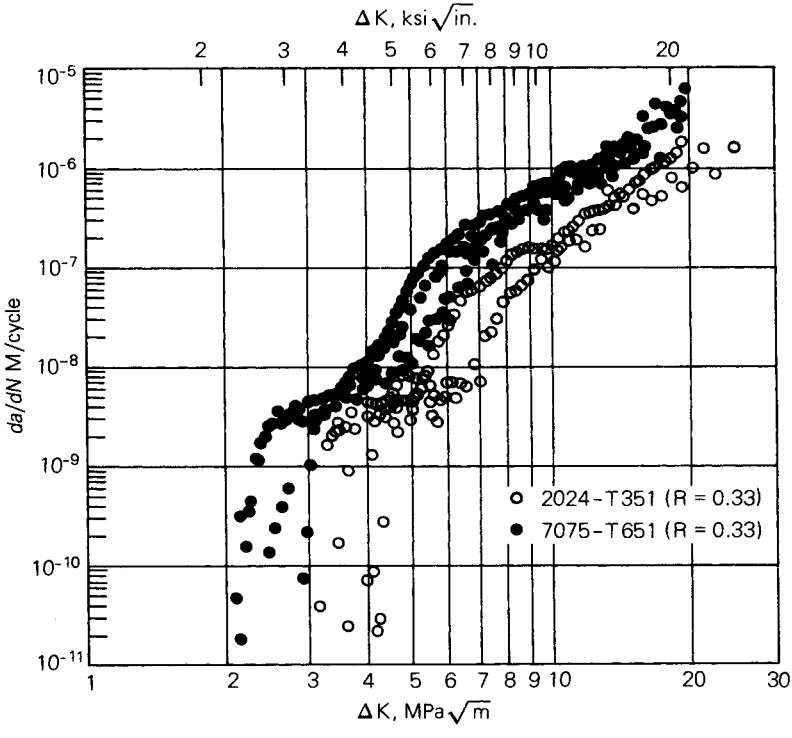

Fig. 16. Fatigue crack growth of 2024-T3 versus 7075-T6 plate over entire da/dN-ΔK range.

Early work in the area of spectrum fatigue showed that high-toughness alloy 7475-T76 performed better than either 2024-T3 or 7075-T6 (Ref 22).

Forging. Aluminum of commercial and higher purity is readily forgeable into intricate shapes over a wide range of temperatures. While many aluminum alloys are also readily forgeable, difficulty tends to increase because the addition of alloying elements increases flow strength. The formation of discrete phases that interrupt continuity of the structure also adversely affects forgeability. The higher deformation strength increases pressure requirements, while the discrete phases make flow less uniform and increase the likelihood of cracking. Alloying additions that significantly increase solid solution strength are copper, magnesium, and silicon. Chromium, manganese, titanium, vanadium, and zirconium form insoluble phases. The presence of these elements strengthens the aluminum at elevated temperature, but they have less effect than the higher solid solubility elements. If the low-solubility elements are present in sufficient quantity, massive primary particles may form. These particles can promote local cracking during forging or other hot working operations. Figure 17 shows the effect of several common additions on forgeability in the range of 370 to 455 °C (700 to 850 °F).

This figure indicates that forgeability, as measured by deformation resistance, is nearly linear for the temperature and alloy range shown. Forgeability as measured by freedom from cracking falls off abruptly near or at the temperature where initial melting occurs in an alloy.

Sound aluminum direct chilled (D.C.) ingot with a low alloy content can be forged as-cast. Where the alloying content is higher, it is usually advantageous to homogenize the ingots before forging and, in the case of some high-content alloys, heavy sections and intricate finished shapes, it may be desirable to hot roll, extrude or preforge the stock to obtain a uniform structure more suitable for forging. Thermal treatments should be used to maximize solid solution and to spheroidize the remaining constituents.

Machining. Pure, unalloyed aluminum is relatively soft and ductile and tends to adhere to a cutting tool, forming a built-up edge and long chips. It requires special machining techniques to avoid producing rough surfaces and heavy burrs. Alloying aluminum improves its machinability. Elements in solid solution that make an alloy heat treatable or work-hardenable increase the hardness of the aluminum matrix and thereby reduce the built-up edge on the cutting tool, formation of burrs, roughness, and tearing of the machined surface, and the length of chips.

Elements out of solution can act as chip breakers, thereby reducing the length of chips. Elements such as lead or bismuth form small insoluble globules and are effective chip breakers. If present in sufficient quantity (generally about 0.5% each), lead and bismuth permit increased machining speeds and reduce the need for cutting fluids. Intermetallic constituents such as $CuAl_2$ or $FeAl_3$ similarly act as chip breakers without significantly reducing the life of cutting tools. However, the very hard constituents, such as silicon or the complex intermetallics that contain chromium or manganese, while effectively acting as chip breakers, noticeably decrease tool life. The presence of primary silicon in hypereu-

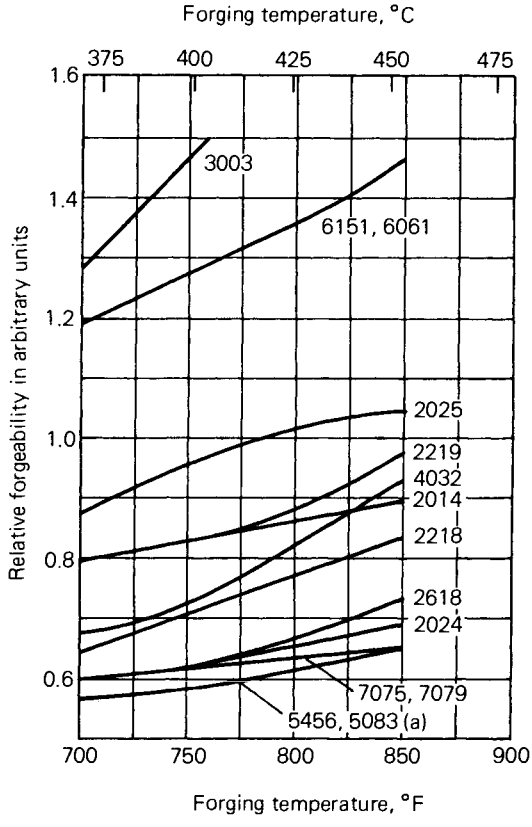

Fig. 17. Effect of temperature on relative forgeability of various aluminum alloys. Vertical scale is based on deformation per unit of energy absorbed. (a) Estimated from production experience.

tectic aluminum-silicon cast alloys is especially harmful in terms of tool life, but at the same time, it produces very short chips, minimum tool edge buildup and excellent machined surface finish. The elements sodium, strontium, antimony, and phosphorus also affect machinability because they affect the cast microstructure. Sodium, strontium, or antimony modify the eutectic silicon morphology, changing it from acicular or needle-like to a very fine, lacy or spheroidized structure. Phosphorus refines primary silicon in hypereutectic alloys, reducing its size by a factor of approximately 10 to 1. Modification and refinement both tend to increase tool life significantly.

In summary, the alloys having the poorest machining characteristics are of low alloy content and are in the softest condition. Cold working, increasing alloy concentration, and/or heat treatment all harden an alloy and tend to reduce adherence to the cutting tool, improve surface finish, reduce burrs, and reduce the built-up edge on the tool. Elements and constituents out of solution promote chip breaking. Hard constituents, especially if large and unrefined, can significantly reduce tool life.

Recycling. One of the major problems in recycling is the buildup of impurities. These impurities originate from four main sources:

1. Mixed alloys due to poor scrap segregation, recovery of metal from furnace dross, remelting of multialloy products such as used beverage cans and clad sheet
2. Contamination of the scrap by extraneous materials such as banding iron, sand, painted sheet, and coatings on cans
3. Incorporation of nonmetallic inclusions, such as oxide films and aluminum-magnesium spinel, into the metal during melting and casting
4. Contamination from furnace tools, refractories, and hydrogen from furnace atmospheres

The mixing of alloys presents the most obvious problem, due to an inability to meet alloy specifications such as those published by the Aluminum Association (AA). An important example of this is the mixing of can body material (3004) and can end material (5182) to produce a mixed recycled alloy that has to be diluted or otherwise modified to meet the alloy specification of one of the original alloys.

Most of the AA specifications permit the presence of 0.05% each (0.15% total) of impurity elements. These general impurity limits are lower in some alloys but are set higher for some specified elements, particularly iron and silicon, in most alloys. Molten aluminum can reduce most oxides and rapidly dissolves most elements so that it is quite common for recycled metal to pick up impurities, particularly iron and silicon, and while these do not necessarily exceed the specified limits, they can produce detectable changes in mechanical and physical properties.

The effect of a wide range of elements is summarized later in this chapter and the physical metallurgy of recycled aluminum alloys has been covered in more detail by J.B. Hess (Ref 23). The following comments on tolerances for various impurities and additions are abstracted from this paper to illustrate the variety of problems that can be encountered in recycling.

Melting and casting

- *Explosion hazards*: A major safety problem when the furnace charge contains water, rust, or certain chemicals.
- *Increased melt loss*: An increase in melting dross results from organic or anodic coatings on the scrap and from the presence of alloying or impurity elements such as lithium, sodium, calcium, magnesium, bismuth, and zinc.
- *Inclusions*: Potential inclusions include: aluminum oxide, $MgAl_2O_4$ spinel, titanium and vanadium diboride, aluminum carbide, as well as miscellaneous materials such as pieces of furnace refractory, flakes from tool washes, and fragments of filter media. In alloys containing relatively large amounts of magnesium or zinc, primary intermetallic particles can crystallize from the melt if the level of transition metal impurities is too high.
- *Gas porosity*: Hydrogen that is readily picked up by molten aluminum from water vapor and from hydrogen-containing compounds such as

in paints, can lead to gas porosity in ingots and castings if the melt is not properly fluxed.

Fabrication

- *Hot-shortness and embrittlement*: In aluminum-magnesium (manganese) alloys such as 5182, a few ppm of sodium or calcium can lead to cracking during hot rolling. Small amounts of low melting point metals such as indium, tin, bismuth, cadmium, and lead can lead to hot cracking in some alloys.
- *Recovery and recrystallization*: Small amounts of zirconium and chromium, and to a lesser extent vanadium and manganese, can reduce the rate of recovery during annealing and increase the recrystallization temperature and final grain size.
- *Heat treatment*: Increased amounts of chromium and manganese increase the quench sensitivity of precipitation-strengthened alloys. Small amounts of cadmium, indium, or tin change the precipitation kinetics of aluminum-copper alloys.

Physical and mechanical properties

- *Reduced ductility, strength, and fracture toughness*: Increasing amounts of iron and silicon increase the volume fraction of insoluble intermetallic phases, which in turn decrease the strain to fracture. Other elements that can form intermetallic particles such as nickel, cobalt, or combinations of iron with manganese or copper have similar detrimental effects.
- *Reduced electrical conductivity*: All elements in solution will reduce conductivity, but vanadium, chromium, titanium, and manganese are particularly deleterious.
- *Weld arc instability*: As little as 10 ppm calcium or lithium in 5XXX welding wire causes the weld arc to be unstable.
- *Reduced vacuum brazeability*: As little as 10 ppm lithium or calcium in the cladding layer of brazing sheet can interfere with vacuum brazing process.

Secondary fabrication

- *Tool wear*: Hard inclusions such as oxides, diborides, and some intermetallic phases cause excessive tool wear.
- *Crystallographic textures*: The iron and silicon content and their ratio affect both the rolling and recrystallization textures of aluminum sheet. In the more dilute alloys, impurities such as copper, manganese, and chromium also can be detrimental.

Chemical properties

- *Toxicities*: Welding wire and alloys to be welded should not contain more than a few ppm beryllium to avoid exposure to toxic beryllium oxide fumes. In alloys intended for food containment, the concentration of toxic metals such as lead, arsenic, cadmium, and thallium are also restricted to avoid possible contamination.

- *Corrosion*: When 1145 foil contains more than about 3 ppm lithium, the foil becomes susceptible to so-called "blue haze" corrosion, which can limit storage life. Small amounts of nickel and most impurity elements that form second-phase particles usually reduce corrosion resistance. Small amounts of gallium and mercury affect the corrosion rate in seawater.
- *Cladding*: Small amounts of copper change the anodic potential of 7072 cladding alloy.
- *Finishing*: 6063 alloy extrusions that contain more than about 0.02% zinc can develop an uneven "spangled" appearance during caustic etching.

SPECIFIC ALLOYING ELEMENTS AND IMPURITIES

The important alloying elements and impurities are listed here alphabetically as a concise review of major effects. Some of the effects, particularly with respect to impurities, are not well documented and are specific to particular alloys or conditions. More detailed information on commercial alloys is given in other chapters.

Antimony is present in trace amounts (0.01 to 0.1 ppm) in primary commercial-grade aluminum. Antimony has a very small solid solubility in aluminum (<0.01%). It has been added to aluminum-magnesium alloys because it was claimed that by forming a protective film of antimony oxychloride, it enhances corrosion resistance in salt water. Some bearing alloys contain up to 4 to 6% antimony. Antimony can be used instead of bismuth to counteract hot cracking in aluminum-magnesium alloys. In hypereutectic aluminum-silicon casting alloys, antimony impedes the nucleation of the primary silicon. Antimony, in the range 0.05 to 0.2%, is used to refine the eutectic silicon in casting alloys. The silicon modification is not as pronounced as with sodium or strontium additions, but antimony is not "burned off" during holding or remelting (see Chapter 8 in this Volume).

Arsenic. The compound AsAl is a semiconductor. Arsenic is very toxic (as AsO_3) and must be controlled to very low limits where aluminum is used as foil for food packaging.

Beryllium is used in aluminum alloys containing magnesium to reduce oxidation at elevated temperatures. Oxidation and mold reaction are prevented by a beryllium content of 5 to 50 ppm, enabling the use of green sand molds for casting aluminum-magnesium alloys. Beryllium is used in small quantities (0.01 to 0.05%) in aluminum casting alloys to improve fluidity and castability in production of engine parts such as pistons and cylinder heads. In modified eutectic aluminum-silicon casting alloys, beryllium additions help retain sodium, the modifying agent.

Up to 0.1% beryllium is used in aluminizing baths for steel to improve adhesion of the aluminum film and restrict the formation of the deleterious iron-aluminum complex. The mechanism of protection is attributed to beryllium diffusion to the surface and the formation of a protective layer.

Oxidation and discoloration of wrought aluminum-magnesium products are greatly reduced by small amounts of beryllium, because of the dif-

fusion of beryllium to the surface and the formation of an oxide of high volume ratio. Beryllium does not affect the corrosion resistance of aluminum. Beryllium is generally held to <8 ppm in welding filler metal, and its content should be limited in wrought alloys that may be welded.

Beryllium poisoning is an allergic disease, a problem of individual hypersensitivity that is related to intensity and duration of exposure. Inhalation of dust containing beryllium compounds may lead to acute poisoning. Beryllium is not used in aluminum alloys that may contact food or beverages.

Bismuth. The low melting point metals such as bismuth, lead, tin, and cadmium are added to aluminum to make free-machining alloys. These elements have a restricted solubility in solid aluminum and form a soft, low melting phase that promotes chip breaking and helps to lubricate the cutting tool. An advantage of bismuth is that its expansion on solidification compensates for the shrinkage of lead. A 1-to-1 lead-bismuth ratio is used in the aluminum-copper alloy, 2011, and in the aluminum-Mg_2Si alloy, 6262. Small additions of bismuth (20 to 200 ppm) can be added to aluminum-magnesium alloys to counteract the detrimental effect of sodium on hot cracking.

Boron is used in aluminum and its alloys as a grain refiner and to improve conductivity by precipitating vanadium, titanium, chromium, and molybdenum (all of which are harmful to electrical conductivity at their usual impurity level in commercial-grade aluminum). Boron can be used alone (at levels of 0.005 to 0.1%) as a grain refiner during solidification, but becomes more effective when used with an excess of titanium. Commercial grain refiners commonly contain titanium and boron in a 5-to-1 ratio. Boron has a high neutron capture cross section and is used in aluminum alloys for certain atomic energy applications, but its content has to be limited to very low levels in alloys used in reactor areas, where this property is undesirable.

Cadmium is a relatively low melting element that finds limited use in aluminum. Up to 0.3% cadmium may be added to aluminum-copper alloys to accelerate the rate of age hardening, increase strength, and increase corrosion resistance. At levels of 0.005 to 0.5%, it has been used to reduce the time of aging of aluminum-zinc-magnesium alloys. It has been reported that traces of cadmium lower the corrosion resistance of unalloyed aluminum. In excess of 0.1%, cadmium causes hot shortness in some alloys. Because of its high neutron absorption, cadmium has to be kept very low for atomic energy use. Cadmium has been used to confer free-cutting characteristics, particularly to aluminum-zinc-magnesium alloys; it was preferred to bismuth and lead because of its higher melting point. As little as 0.1% provides an improvement in machinability. Cadmium is used in bearing alloys along with silicon. The oral toxicity of cadmium compounds is high. In melting, casting, and fluxing operations, cadmium oxide fume can present hazards.

Calcium has very low solubility in aluminum and forms the intermetallic $CaAl_4$. An interesting group of alloys containing about 5% calcium and 5% zinc have superplastic properties. Calcium combines with silicon to form $CaSi_2$, which is almost insoluble in aluminum and therefore will increase the conductivity of commercial-grade metal slightly. In alumi-

num-magnesium-silicon alloys, calcium will decrease age hardening. Its effect on aluminum-silicon alloys is to increase strength and decrease elongation, but it does not make these alloys heat treatable. At the 0.2% level, calcium alters the recrystallization characteristics of 3003. Very small amounts of calcium (10 ppm) increase the tendency of molten aluminum alloys to pick up hydrogen.

Carbon may occur infrequently as an impurity in aluminum in the form of oxycarbides and carbides, of which the most common is Al_4C_3, but carbide formation with other impurities such as titanium is possible. Al_4C_3 decomposes in the presence of water and water vapor, and this may lead to surface pitting. Normal metal transfer and fluxing operations usually reduce carbon to the ppm level.

Cerium, mostly in the form of mischmetal (rare earths with 50 to 60% cerium), has been added experimentally to casting alloys to increase fluidity and reduce die sticking. In alloys containing high iron (>0.7%), it is reported to transform acicular $FeAl_3$ into a nonacicular compound.

Chromium occurs as a minor impurity in commercial-purity aluminum (5 to 50 ppm). It has a large effect on electrical resistivity (Table 2). Chromium is a common addition to many alloys of the aluminum-magnesium, aluminum-magnesium-silicon, and aluminum-magnesium-zinc groups, in which it is added in amounts generally not exceeding 0.35%. In excess of these limits, it tends to form very coarse constituents with other impurities or additions such as manganese, iron, and titanium. This limit is decreased as the content of transition metals increases. In casting alloys, excess chromium will produce a sludge by peritectic precipitation on holding.

Chromium has a slow diffusion rate and forms fine dispersed phases in wrought products. These dispersed phases inhibit nucleation and grain growth. Chromium is used to control grain structure, to prevent grain growth in aluminum-magnesium alloys, and to prevent recrystallization in aluminum-magnesium-silicon or aluminum-magnesium-zinc alloys during hot working or heat treatment. The fibrous structures that develop reduce stress corrosion susceptibility and/or improve toughness. Chromium in solid solution and as a finely dispersed phase increases the strength of alloys slightly. The main drawback of chromium in heat treatable alloys is the increase in quench sensitivity when the hardening phase tends to precipitate on the pre-existing chromium phase particles. Chromium imparts a yellow color to the anodic film.

Cobalt is not a common addition to aluminum alloys. It has been added to some aluminum-silicon alloys containing iron, where it transforms the acicular β (aluminum-iron-silicon) into a more rounded aluminum-cobalt-iron phase, thereby improving strength and elongation. Aluminum-zinc-magnesium-copper alloys containing 0.2 to 1.9% cobalt are produced by powder metallurgy.

Copper. Aluminum-copper alloys containing 2 to 10% copper, generally with other additions, form important families of alloys (Chapters 8 and 9 in this Volume). Both cast and wrought aluminum-copper alloys respond to solution heat treatment and subsequent aging with an increase in strength and hardness and a decrease in elongation. The strengthening is maximum between 4 and 6% copper, depending upon the influence of other constituents present.

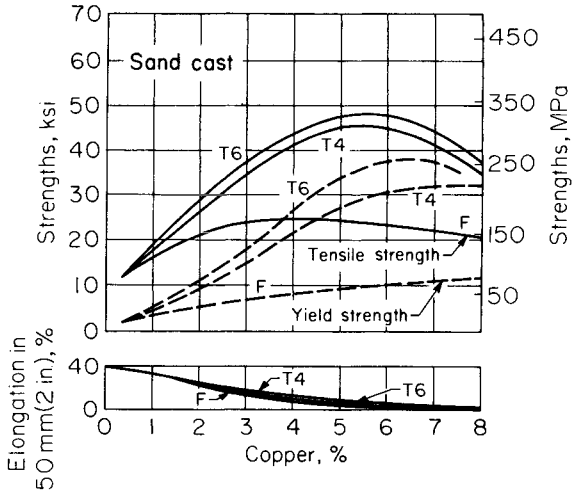

Fig. 18. Tensile properties of sand cast, high-purity, aluminum-copper alloys. Specimens cast to size, 13 mm (0.5 in.) in diameter. F, as cast; T4, quenched in water after solution treatment at high temperature; T6, precipitation hardened after solution treatment. (E.H. Dix, Jr. and J.J. Bowman, in Metals Handbook, *American Society for Metals, 1948, p 804)*

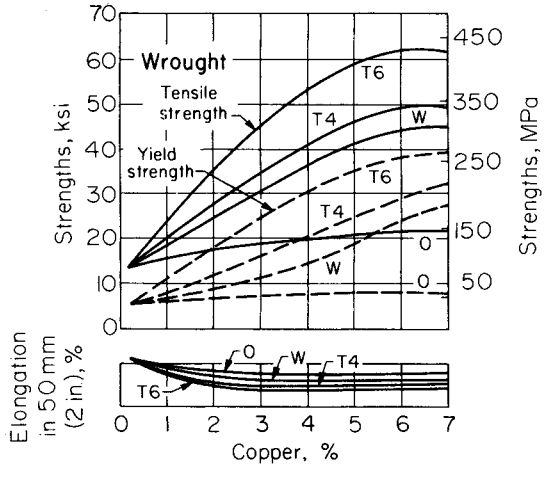

Fig. 19. Tensile properties of high-purity, wrought aluminum-copper alloys. Sheet specimen was 13 mm (0.5 in.) wide and 1.59 mm (0.0625 in.) thick. O, annealed; W, tested immediately after water quenching from a solution heat treatment; T4, as in W, but aged at room temperature; T6, as in T4, followed by precipitation treatment at elevated temperature.

The extent to which copper increases strength while lowering elongation of sand cast aluminum is shown in Fig. 18. The properties of aluminum-copper alloy sheet in a number of thermal conditions are assembled in Fig. 19. The aging characteristics of binary aluminum-copper alloys have been studied in greater detail than any other system, but there

are actually very few commercial binary aluminum-copper alloys. Most commercial alloys contain other alloying elements.

Copper-Magnesium. The main benefit of adding magnesium to aluminum-copper alloys is the increased strength possible following solution heat treatment and quenching. In wrought material of certain alloys of this type, an increase in strength accompanied by high ductility occurs on aging at room temperature. On artificial aging, a further increase in strength, especially in yield strength, can be obtained, but at a substantial sacrifice in tensile elongation. In castings, magnesium increases strength but decreases ductility of aluminum-copper alloys. On both cast and wrought aluminum-copper alloys, as little as about 0.05% magnesium is effective in changing aging characteristics. The effect of magnesium on the corrosion resistance of aluminum-copper alloys depends on the type of product and the thermal treatment (Chapter 7 in this Volume).

Copper-Magnesium Plus Other Elements. The cast aluminum-copper-magnesium alloys containing iron are characterized by dimensional stability and improved bearing characteristics, as well as by high strength and hardness at elevated temperatures. However, in a wrought Al-4%Cu-0.5%Mg alloy, iron in concentrations as low as 0.5% lowers the tensile properties in the heat treated condition, if the silicon content is less than that required to tie up the iron as the αFeSi constituent. In this event, the excess iron unites with copper to form the Cu_2FeAl_7 constituent, thereby reducing the amount of copper available for heat treating effects. When sufficient silicon is present to combine with the iron, the properties are unaffected. Silicon also combines with magnesium to form Mg_2Si precipitate and contributes in the age-hardening process.

Silver substantially increases the strength of heat treated and aged aluminum-copper-magnesium alloys. Nickel improves the strength and hardness of cast and wrought aluminum-copper-magnesium alloys at elevated temperatures. Addition of about 0.5% nickel lowers the tensile properties of the heat treated, wrought Al-4%Cu-0.5%Mg alloy at room temperature.

The alloys containing manganese form the most important and versatile system of commercial high-strength wrought aluminum-copper-magnesium alloys; the properties and characteristics of these alloys are discussed in Chapter 9 in this Volume. The substantial effect exerted by manganese on the tensile properties of aluminum-copper alloys containing 0.5% magnesium is shown in Fig. 20. It is apparent that no one composition offers both maximum strength and ductility. In general, tensile strength increases with separate or simultaneous increases in magnesium and manganese, and the yield strength also increases, but to a lesser extent. Further increases in tensile and particularly yield strength occur on cold working after heat treatment. Additions of manganese and magnesium decrease the fabricating characteristics of the aluminum-copper alloys, and manganese also causes a loss in ductility; hence, the concentration of this element does not exceed about 1% in commercial alloys. Additions of cobalt, chromium, or molybdenum to the wrought Al-4%Cu-0.5%Mg type of alloy increase the tensile properties on heat treatment, but none offers a distinct advantage over manganese.

Alloys with lower copper content than the conventional 2024 and 2014

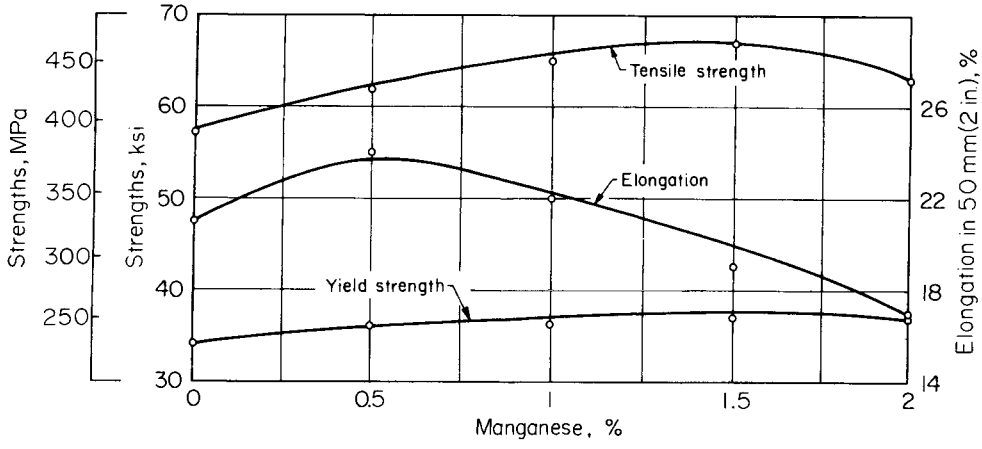

Fig. 20. Relationship between tensile properties and manganese content of an Al-4%Cu-0.5%Mg alloy, heat treated at 525 °C (980 °F).

type alloys were necessary to provide the formability required by the automobile industry. Copper-magnesium alloys developed for this purpose are 2002, AU2G, and 2036 variations. These have acceptable formability, good spot weldability, reasonable fusion weldability, good corrosion resistance, and freedom from Lüder lines. The paint baking cycle serves as a precipitation treatment to give final mechanical properties.

Copper and Minor Additions. Casting alloys of this type are discussed in Chapter 8 in this Volume. In the wrought form, an alloy family of interest is the one containing small amounts of several metals known to raise the recrystallization temperature of aluminum and its alloys, specifically manganese, titanium, vanadium, or zirconium. An alloy of this nature retains its properties well at elevated temperatures, fabricates readily, and has good casting and welding characteristics. Figure 21 illustrates the effect of 3 to 8% copper on an alloy of Al-0.3%Mn-0.2%Zr-0.1%V at room temperature and after exposure at 315 °C (600 °F) for two different periods of time. The stability of the properties, as reflected in the small reduction in strength with time at this temperature, should be noted.

Gallium is an impurity in aluminum and is usually present at levels of 0.001 to 0.02%. At these levels its effect on mechanical properties is quite small. At the 0.2% level, gallium has been found to affect the corrosion characteristics and the response to etching and brightening of some alloys. Liquid gallium metal penetrates very rapidly at aluminum grain boundaries and can produce complete grain separation. In sacrificial anodes, an addition of gallium (0.01 to 0.1%) keeps the anode from passivating.

Hydrogen has a higher solubility in the liquid state at the melting point than in the solid at the same temperature (Chapter 1 in this Volume). Because of this, gas porosity can form during solidification. Hydrogen is produced by the reduction of water vapor in the atmosphere by aluminum and by the decomposition of hydrocarbons. Hydrogen pickup in both solid and liquid aluminum is enhanced by the presence of certain impurities,

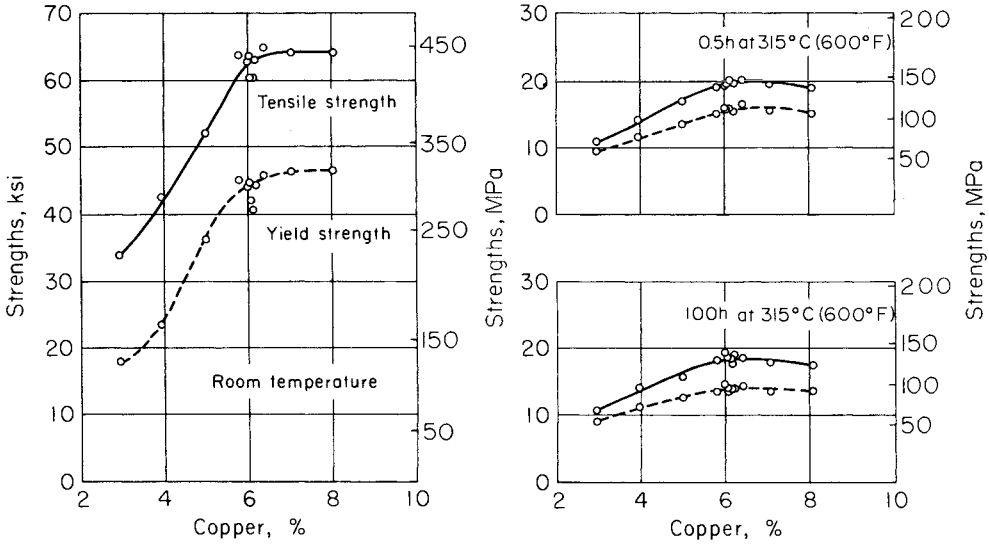

Fig. 21. Variation of tensile properties with copper content in Al-0.3%Mn-0.2%Zr-0.1%V alloy in the T6 temper. (Courtesy of J.A. Nock, Jr., Alcoa)

such as sulfur compounds, on the surface and in the atmosphere. Hydride-forming elements in the metal increase the pickup of hydrogen in the liquid. Other elements such as beryllium, copper, tin, and silicon decrease hydrogen pickup.

In addition to causing primary porosity in casting, hydrogen causes secondary porosity, blistering, and high-temperature deterioration (advanced internal gas precipitation) during heat treating. It probably plays a role in grain boundary decohesion during stress-corrosion cracking. Its level in melts is controlled by fluxing with hydrogen-free gases or by vacuum degassing.

Indium. Small amounts (0.05 to 0.2%) of indium have a marked influence on the age hardening of aluminum-copper alloys, particularly at low copper contents (2 to 3% copper). In this respect, indium acts very much like cadmium in that it reduces room temperature aging but increases artificial aging. The addition of magnesium decreases the effect of indium. Small amounts of indium (0.03 to 0.5%) are claimed to be beneficial in aluminum-cadmium bearing alloys.

Iron is the most common impurity found in aluminum. It has a high solubility in molten aluminum and is therefore easily dissolved at all molten stages of production. The solubility of iron in the solid state is very low (~0.04%) and therefore, most of the iron present in aluminum over this amount appears as an intermetallic second phase in combination with aluminum and often other elements. Because of its limited solubility, it is used in electrical conductors in which it provides a slight increase in strength (Fig. 22) and better creep characteristics at moderately elevated temperatures. Although small amounts of iron in aluminum may reduce soldering during die casting, its presence in aluminum-silicon casting al-

loys is generally undesirable because it forms coarse iron-rich phases that reduce ductility.

Iron reduces the grain size in wrought products. Alloys of iron and manganese near the ternary eutectic content, such as 8006, can have useful combinations of strength and ductility at room temperature and retain strength at elevated temperatures. The properties are due to the fine grain size that is stabilized by the finely dispersed iron-rich second phase. Iron is added to the aluminum-copper-nickel group of alloys to increase strength at elevated temperatures.

Lead. Normally present only as a trace element in commercial-purity aluminum, lead is added at about the 0.5% level with the same amount of bismuth in some alloys (2011 and 6262) to improve machinability. Additions of lead may be troublesome to the fabricator as it will tend to segregate during casting and cause hot shortness in aluminum-copper-magnesium alloys. Lead compounds are toxic.

Lithium. The impurity level of lithium in aluminum is of the order of a few ppm, but at a level of less than 5 ppm it can promote the discoloration (blue corrosion) of aluminum foil under humid conditions. Traces of lithium greatly increase the oxidation rate of molten aluminum and alter the surface characteristics of wrought products. Binary aluminum-lithium alloys age harden but are not used commercially. Present interest is in the aluminum-magnesium-lithium alloys, which can be heat treated to strengths comparable to present aircraft alloys. In addition, the density is decreased and the modulus is increased. This type of alloy has a high volume fraction of coherent, ordered $LiAl_3$ precipitate. In addition to increasing the elastic modulus, the fatigue crack growth resistance is increased at intermediate levels of stress intensity.

Magnesium is the major alloying element in the 5XXX series of alloys. Its maximum solid solubility in aluminum is 17.4%, but the magnesium content in current wrought alloys does not exceed 5.5%. Casting alloys range from 4 to 10% magnesium. Precipitation of magnesium will

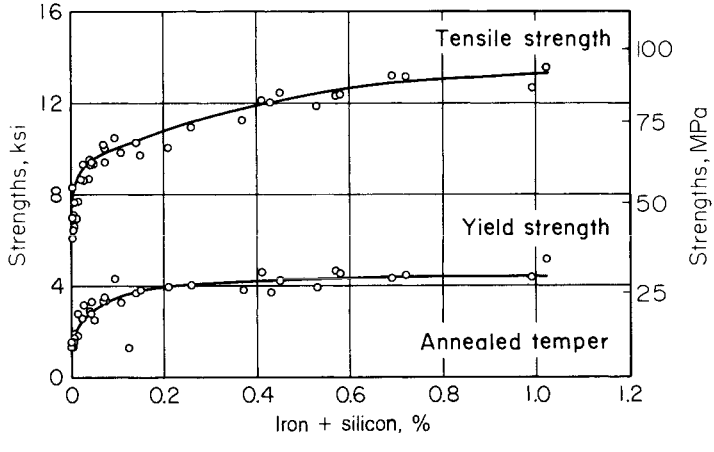

Fig. 22. Effect of iron plus silicon impurities on tensile strength and yield strength of aluminum. (Courtesy of J.A. Nock, Jr., Alcoa)

occur even at room temperature in Al-10% Mg casting alloys. Alloys containing less than about 7% magnesium are substantially stable at room temperature, but not at temperatures above ambient. Magnesium precipitates preferentially at grain boundaries as a highly anodic phase (Mg_5Al_3 or Mg_5Al_8), which produces susceptibility to intergranular cracking and to stress corrosion (see Chapter 7 in this Volume). Wrought alloys containing up to 5% magnesium properly fabricated are stable under normal usage. The addition of magnesium markedly increases the strength of aluminum without unduly decreasing the ductility. Corrosion resistance and weldability are good. In the annealed condition, magnesium alloys form Lüders lines during deformation.

Magnesium-Manganese. Additions of up to 0.75% manganese to aluminum-magnesium casting alloys increases hardness, decreases ductility, and has little effect on corrosion resistance. In wrought alloys this system has high strength in the work-hardened condition, high resistance to corrosion, and good welding characteristics. Increasing amounts of either magnesium or manganese intensify the difficulty of fabrication and increase the tendency toward cracking during hot rolling, particularly if traces of sodium are present. The two main advantages of manganese additions are that the precipitation of the magnesium phase is more general throughout the structure, and that for a given increase in strength, manganese allows a lower magnesium content and ensures a greater degree of stability to the alloy.

The tensile properties of 13 mm (0.5 in.) plate at various magnesium and manganese concentrations are shown in Fig. 23 for the O temper and

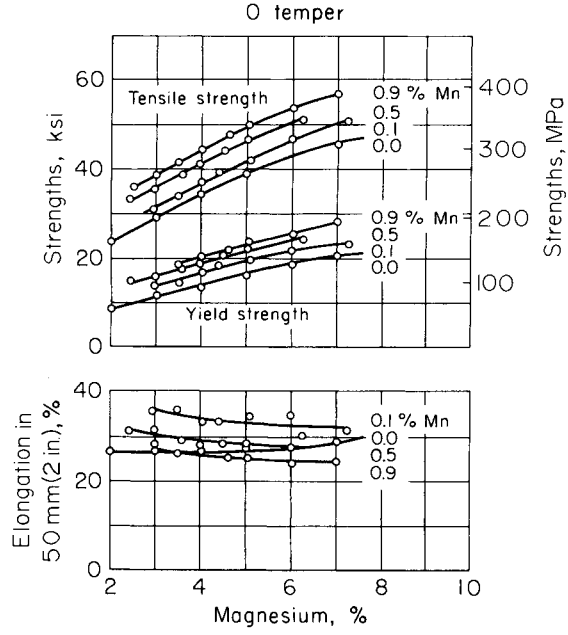

Fig. 23. Tensile properties of 13-mm (0.5-in.) aluminum-magnesium-manganese plate in O temper. (Courtesy of W.A. Anderson, Alcoa)

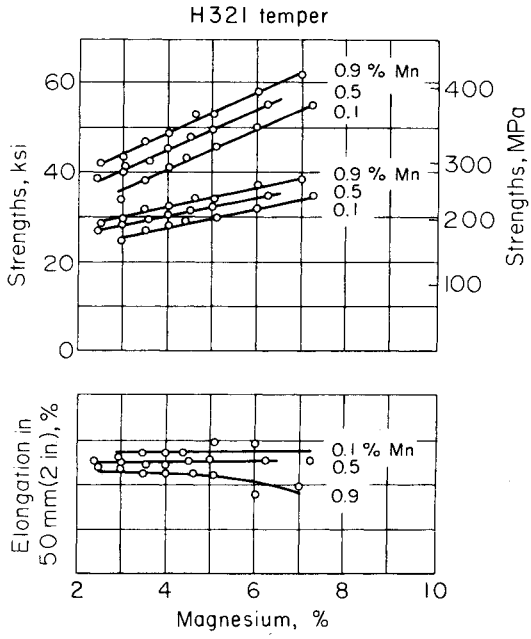

Fig. 24. Tensile properties of 13-mm (0.5-in.) aluminum-magnesium-manganese plate in H321 temper. (Courtesy of W.A. Anderson, Alcoa)

in Fig. 24 for a work-hardened temper. Increasing magnesium raises the tensile strength by about 34 MPa (5 ksi) for each 1% increment; manganese is about twice as effective as magnesium.

Magnesium-Silicide. Wrought alloys of the 6XXX group contain up to 1.5% each of magnesium and silicon in the approximate ratio to form Mg_2Si, i.e., 1.73:1. The maximum solubility of Mg_2Si is 1.85%, and this decreases with temperature. Precipitation upon age hardening occurs by formation of Guinier-Preston zones and a very fine precipitate. Both confer an increase in strength to these alloys, though not as great as in the case of the 2XXX or the 7XXX alloys (see Chapter 2 in this Volume).

Al-Mg_2Si alloys can be divided into three groups. In the first group, the total amount of magnesium and silicon does not exceed 1.5%. These elements are in a nearly balanced ratio or with a slight excess of silicon. Typical of this group is 6063, widely used for extruded architectural sections. This easily extrudable alloy nominally contains 1.1% Mg_2Si. Its solution heat treating temperature of just over 500 °C (930 °F) and its low quench sensitivity are such that this alloy does not need a separate solution treatment after extrusion but may be air quenched at the press and artificially aged to achieve moderate strength, good ductility, and excellent corrosion resistance.

The second group nominally contains 1.5% or more of magnesium + silicon and other additions such as 0.3% copper, which increases strength in the T6 temper. Elements such as manganese, chromium, and zirconium are used for controlling grain structure. Alloys of this group, such as the structural alloy 6061, achieve strengths about 70 MPa (10 ksi) higher than

the first group in the T6 temper. Alloys of the second group require a higher solution treating temperature than the first and are quench sensitive. For these reasons, they generally require a separate solution treatment followed by rapid quenching and artificial aging.

The third group contains an amount of Mg_2Si overlapping the first two but with a substantial excess silicon. An excess of 0.2% silicon increases the strength of an alloy containing 0.8% Mg_2Si by about 70 MPa (10 ksi). Larger amounts of excess silicon are less beneficial. Excess magnesium, however, is of benefit only at low Mg_2Si contents because magnesium lowers the solubility of Mg_2Si. In excess silicon alloys, segregation of silicon to the boundary causes grain boundary fracture in recrystallized structures. Additions of manganese, chromium, or zirconium counteract the effect of silicon by preventing recrystallization during heat treatment. Common alloys of this group are 6351 and the more recently introduced alloys 6009 and 6010. Additions of lead and bismuth to an alloy of this series (6262) improves machinability. This alloy has a better corrosion resistance than 2011, which also is used as a free-machining alloy.

The addition of small amounts of magnesium to aluminum-silicon casting alloys such as 356.0 (7% silicon, 0.3% magnesium) makes them heat treatable and allows a substantial increase in strength without reducing corrosion resistance.

Manganese is a common impurity in primary aluminum, in which its concentration normally ranges from 5 to 50 ppm. It decreases resistivity (Table 2). Manganese increases strength either in solid solution or as a finely precipitated intermetallic phase. It has no adverse effect on corrosion resistance. Manganese has a very limited solid solubility in aluminum in the presence of normal impurities, but remains in solution when chill cast so that most of the manganese added is substantially retained in solution, even in large ingots. As an addition, it is used to increase strength and to control the grain structure (Fig. 25). The effect of manganese is to increase the recrystallization temperature and to promote the formation of fibrous structure upon hot working. As a dispersed precipitate it is effective in slowing recovery and in preventing grain growth.

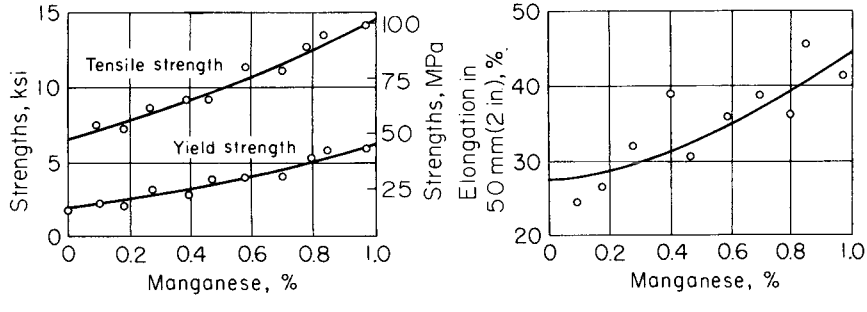

Fig. 25. Effect of manganese on tensile properties of wrought 99.95% aluminum, 1.6-mm (0.064-in.) thick specimens, quenched in cold water from 565 °C (1050 °F). (Courtesy of Alcoa Research Laboratories)

The manganese precipitate increases the quench sensitivity of heat treatable alloys.

Manganese is also used to correct the shape of acicular or of platelike iron constituents and decrease their embrittling effect. Up to the 1.25% level, manganese is the main alloying addition of the 3XXX series of alloys, in which it is added alone or with magnesium. This series of alloys is used in large tonnages for beverage containers and general utility sheet. Even after high degrees of work hardening, these alloys are used to produce severely formed can bodies.

The combined content of manganese, iron, chromium and other transition metals must be limited, otherwise large primary intermetallic crystals precipitate from the melt in the transfer system or in the ingot sump during casting. In alloys 3003 and 3004 the iron plus manganese content should be kept below about 2.0 and 1.7%, respectively, to prevent the formation of primary $(Fe,Mn)Al_6$ during casting.

Mercury has been used at the level of 0.05% in sacrificial anodes used to protect steel structures. Other than for this use, mercury in aluminum or in contact with it as a metal or a salt will cause rapid corrosion of most aluminum alloys. The toxic properties of mercury must be kept in mind when adding it to aluminum alloys.

Molybdenum is a very low level (0.1 to 1.0 ppm) impurity in aluminum. It has been used at a concentration of 0.3% as a grain refiner, because the aluminum end of the equilibrium diagram is peritectic, and also as a modifier for the iron constituents, but it is not in current use for these purposes.

Nickel. The solid solubility of nickel in aluminum does not exceed 0.04%. Over this amount, it is present as an insoluble intermetallic, usually in combination with iron. Nickel (up to 2%) increases the strength of high-purity aluminum but reduces ductility. Binary aluminum-nickel alloys are no longer in use, but nickel is added to aluminum-copper and to aluminum-silicon alloys to improve hardness and strength at elevated temperatures and to reduce the coefficient of expansion. Nickel promotes pitting corrosion in dilute alloys such as 1100. It is limited in alloys for atomic reactor use, due to its high neutron absorption, but in other areas it is a desirable addition along with iron to improve corrosion resistance to high-pressure steam.

Niobium (Columbium). As with other elements forming a peritectic reaction, niobium would be expected to have a grain refining effect on casting. It has been used for this purpose, but the effect is not marked.

Phosphorus is a minor impurity (1 to 10 ppm) in commercial-grade aluminum. Its solubility in molten aluminum is very low (~0.01% at 660 °C or 1120 °F) and considerably smaller in the solid. Phosphorus is used as a modifier for hypereutectic aluminum-silicon alloys where aluminum-phosphide acts as nucleus for primary silicon, thus refining silicon and improving machinability (Chapter 8 in this Volume). Phosphorus in trace amounts prevents modification by sodium in hypoeutectic aluminum-silicon casting alloys. The aluminum-phosphorus compound reacts with water vapor to give phosphine (PH_3), but the level of phosphorus in aluminum is sufficiently low that this does not constitute a health hazard if adequate ventilation is used when machining phosphorus-nucleated cast-

ings. Phosphine can be a problem in furnace teardowns where phosphate-bonded refractories are used.

Silicon, after iron, is the highest impurity level in electrolytic commercial aluminum (0.01 to 0.15%). It is also the most common addition in casting alloys (see Chapter 8 in this Volume). In wrought alloys, silicon is used with magnesium at levels up to 1.5% to produce Mg_2Si in the 6XXX series of heat treatable alloys.

High-purity aluminum-silicon alloys are hot short up to 3% silicon, the most critical range being 0.17 to 0.8% silicon, but additions of silicon (0.5 to 4.0%) reduce the cracking tendency of aluminum-copper-magnesium alloys. A whole series of aluminum casting alloys containing silicon with copper and/or magnesium are in commercial use. Small amounts of magnesium added to any silicon-containing alloy will render it heat treatable, but the converse is not true as excess magnesium over that required to form Mg_2Si sharply reduces the solid solubility of this compound. The mechanical properties of aluminum-silicon casting alloys benefit by modification as shown in Fig. 26. Chill casting achieves the same result of refining the silicon eutectic (Fig. 27). Modification of the silicon can be achieved through the addition of sodium in eutectic and hypoeutectic alloys and by phosphorus in hypereutectic alloys. Up to 12% silicon is added in wrought alloys used as cladding for brazing sheet. Alloys containing about 5% silicon acquire a black color when anodized and are used for ornamental purposes.

Silver has an extremely high solid solubility in aluminum (up to 55%). Because of cost, no binary aluminum-silver alloys are in use, but small additions (0.1 to 0.6% silver) are effective in improving the strength and stress corrosion resistance of aluminum-zinc-magnesium alloys.

Strontium. Traces of strontium (0.01 to 0.1 ppm) are found in commercial grade aluminum. Strontium is used with sodium for modifying aluminum-silicon casting alloys (see Chapter 8 in this Volume).

Sulfur. As much as 0.2 to 20 ppm sulfur are present in commercial grade aluminum. It has been reported that sulfur can be used to modify both hypo- and hypereutectic aluminum-silicon alloys.

Tin is used as an alloying addition to aluminum—from concentrations of 0.03 to several percent in wrought alloys, to concentrations of about 25% in casting alloys. Small amounts of tin (0.05%) greatly increase the response of aluminum-copper alloys to artificial aging following a solution heat treatment. The result is an increase in strength and an improvement in corrosion resistance. Higher concentrations of tin cause hot cracking in aluminum-copper alloys. If small amounts of magnesium are present, the artificial aging characteristics are markedly reduced, probably because magnesium and tin form a noncoherent second phase.

Tin improves the machinability of aluminum and its alloys, and it is used for this purpose in aluminum-copper, aluminum-copper-silicon, and aluminum-zinc casting alloys, in concentrations under 1% tin.

The aluminum-tin bearing alloys, with additions of other metals such as copper, nickel, and silicon are used where bearings are required to withstand high speeds, loads, and temperatures. The copper, nickel, and silicon additions improve load-carrying capacity and wear resistance, and the soft tin phase provides antiscoring properties.

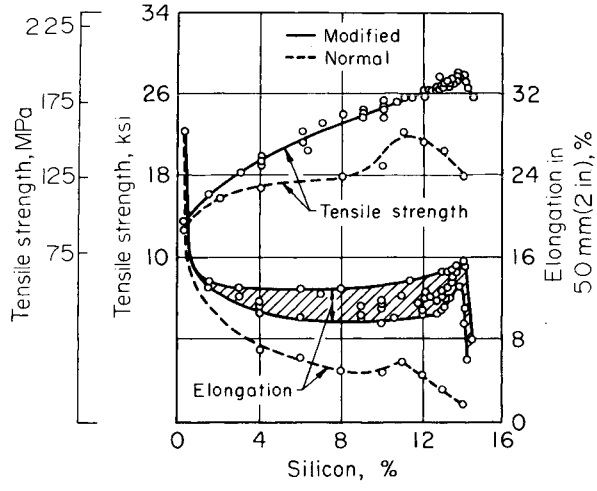

Fig. 26. Tensile properties of aluminum-silicon alloy sand cast 13-mm (0.5-in.) diam test bars in as-cast condition. (L.W. Kempf, in Metals Handbook, *American Society for Metals, 1948, p 805)*

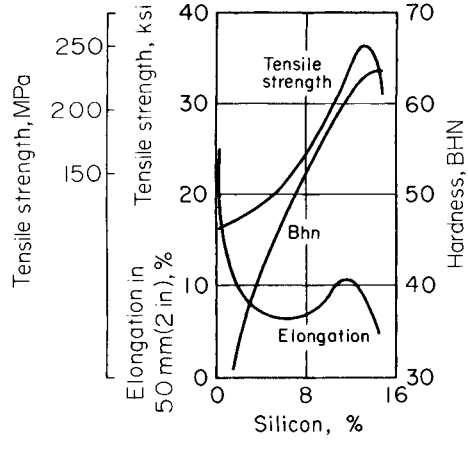

Fig. 27. Tensile properties of chill cast test bars of aluminum-silicon alloy in as-cast condition. (L.W. Kempf, in Metals Handbook, *American Society for Metals, 1948, p 805)*

As little as 0.01% tin in commercial grade aluminum will cause surface darkening on annealing and increase the susceptibility to corrosion, which appears to be due to migration of tin to the surface. This effect may be reduced by small additions (0.2%) of copper. Aluminum-zinc alloys with small additions of tin are used as sacrificial anodes in salt water.

Titanium. Amounts of 10 to 100 ppm titanium are found in commercial-purity aluminum. Titanium depresses the electrical conductivity of aluminum, but its level can be reduced by the addition of boron to the melt to form insoluble TiB_2. Titanium is used primarily as a grain refiner

of aluminum alloy castings and ingots. When used alone, the effect of titanium decreases with time of holding in the molten state and with repeated remelting. The grain-refining effect is enhanced if boron is present in the melt or if it is added as a master alloy containing boron largely combined as TiB_2. Titanium is a common addition to weld filler wire; it refines the weld structure and prevents weld cracking. It is usually added alone or with TiB_2 during the casting of sheet or extrusion ingots to refine the as-cast grain structure and to prevent cracking.

Vanadium. There is usually 10 to 200 ppm vanadium in commercial-grade aluminum, and because it lowers conductivity, it generally is precipitated from electrical conductor alloys with boron. The aluminum end of the equilibrium diagram is peritectic and therefore, the intermetallic VAl_{11} would be expected to have a grain-refining effect upon solidification, but it is less efficient than titanium and zirconium. The recrystallization temperature is raised by vanadium.

Zinc. The aluminum-zinc alloys have been known for many years, but hot cracking of the casting alloys and the susceptibility to stress-corrosion cracking of the wrought alloys curtailed their use. The addition of zinc alone to aluminum does not result in improved cast alloys. In the wrought condition, the improvement in strength is modest, as shown in Fig. 28. On the other hand, the aluminum-zinc alloys containing other elements offer outstanding advantages in strength as-cast, and the highest combination of tensile properties in wrought aluminum alloys. Efforts to overcome the aforementioned limitations have been successful, and these aluminum-zinc based alloys, cast and wrought, are being used commercially to an increasing extent. The presence of zinc in aluminum increases its solution potential, hence its use in protective cladding (7072) and in sacrificial anodes.

Zinc-Magnesium. The addition of magnesium to the aluminum-zinc alloys develops the strength potential of this alloy system, especially in the range of 3 to 7.5% zinc. Magnesium and zinc form $MgZn_2$, which

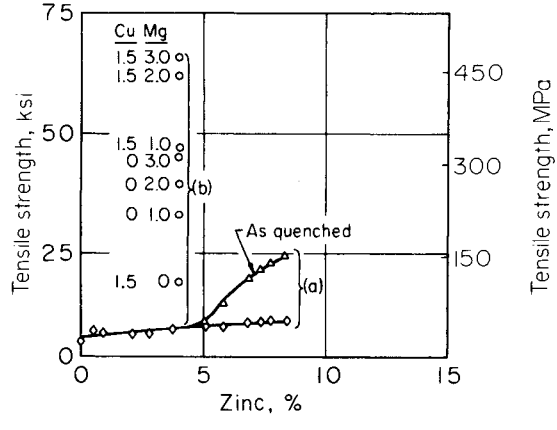

Fig. 28. (a) Effect on tensile strength of zinc in 99.95% aluminum that was heat treated and aged at 135 °C (275 °F). (b) Effect on tensile strength of alloy additions to Al-4%Zn alloy heat treated and aged at 135 °C (275 °F).

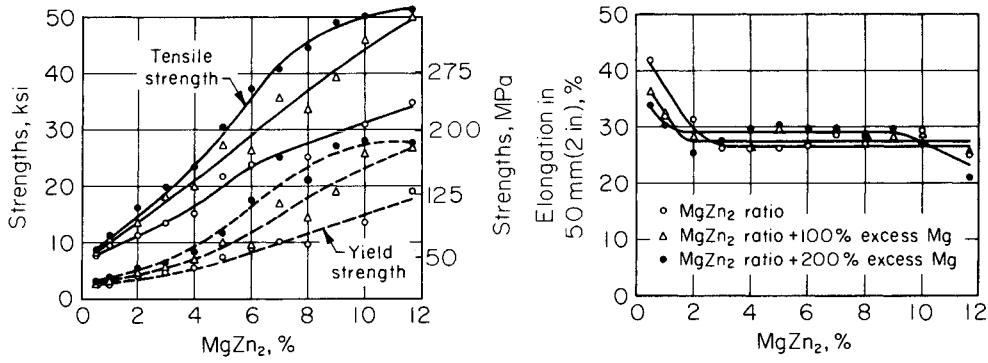

Fig. 29. Effect of $MgZn_2$ and $MgZn_2$ with excess magnesium on tensile properties of wrought 99.95% aluminum; 1.59-mm (0.0625-in.) specimens, quenched in cold water from 470 °C (875 °F). (Courtesy of Alcoa Research Laboratories)

produces a far greater response to heat treatment than occurs in the binary aluminum-zinc system. Although aluminum-zinc-magnesium alloys have casting characteristics inferior to those of the aluminum-silicon alloys, their tensile properties in the as-cast condition are high, and several are used commercially (Chapter 8 in this Volume).

The strength of the wrought aluminum-zinc alloys also are substantially improved by the addition of magnesium. Increasing the $MgZn_2$ concentration from 0.5 to 12% in cold water quenched 1.6-mm (0.062-in.) sheet continuously increases the tensile and yield strengths. The addition of magnesium in excess (100 and 200%) of that required to form $MgZn_2$ further increases tensile strength, as shown in Fig. 29.

On the negative side, increasing additions of both zinc and magnesium decreases the overall corrosion resistance of aluminum to the extent that close control over the microstructure, heat treatment, and composition are often necessary to maintain adequate resistance to stress corrosion and to exfoliatory attack. For example, depending upon the alloy, stress corrosion is controlled by some or all of the following:

- Overaging
- Cooling rate after solution treatment
- Maintaining a nonrecrystallized structure through the use of additions such as zirconium
- Copper or chromium additions (see zinc-magnesium-copper alloys)
- Adjusting the zinc-magnesium ratio closer to 3:1

Zinc-Magnesium-Copper. The addition of copper to the aluminum-zinc-magnesium system, together with small but important amounts of chromium and manganese, results in the highest strength aluminum-based alloys commercially available. The properties of a representative group of these compositions, after one of several solution and aging treatments to which they respond, are shown in Fig. 30.

In this alloy system, zinc and magnesium control the aging process. The effect of copper is to increase the aging rate by increasing the degree of supersaturation and perhaps through nucleation of the $CuMgAl_2$ phase.

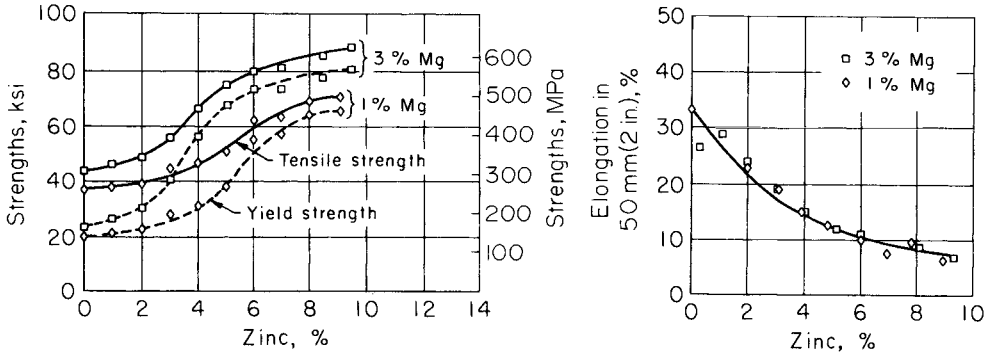

Fig. 30. Effect of zinc on aluminum alloy containing 1.5% copper and 1 and 3% magnesium; 1.6-mm (0.064-in.) thick sheet. Alloy with 1% magnesium heat treated at 495 °C (920 °F); that with 3% magnesium heat treated at 460 °C (860 °F); all specimens quenched in cold water, aged 12 h at 135 °C (275 °F).

Copper also increases quench sensitivity upon heat treatment. In general, copper reduces the resistance to general corrosion of aluminum-zinc-magnesium alloys, but increases the resistance to stress corrosion. The minor alloy additions, such as chromium and zirconium, have a marked effect on mechanical properties and corrosion resistance (see Chapters 5 and 7 in this Volume).

Zirconium additions in the range 0.1 to 0.3% are used to form a fine precipitate of intermetallic particles that inhibit recovery and recrystallization. An increasing number of alloys, particularly in the aluminum-zinc-magnesium family, use zirconium additions to increase the recrystallization temperature and to control the grain structure in wrought products. Zirconium additions leave this family of alloys less quench sensitive than similar chromium additions. Higher levels of zirconium are employed in some superplastic alloys to retain the required fine substructure during elevated-temperature forming. Zirconium additions have been used to reduce the as-cast grain size, but its effect is less than that of titanium. In addition, zirconium tends to reduce the grain-refining effect of titanium plus boron additions so that it is necessary to use more titanium and boron to grain refine zirconium-containing alloys.

REFERENCES

1. D. Altenpohl, Aluminum Viewed From Within, *Aluminium-Verlag*, Dusseldorf, 1982
2. F. Kutner and G. Lang, The Influence of Alloying Elements on the Density of Super-Purity Aluminum, *Aluminium*, Vol 46 (No. 10), 1970, p 691-694
3. Properties of Aluminum and Aluminum Alloys, Report No. 21, Thermophysical Properties Research Centre, Y.S. Touloukian and C.Y. Ho, Ed., Purdue University, 1973
4. L.W. Kempf, C.S. Smith, and C.S. Taylor, Thermal and Electrical Conductivities of Aluminum Alloys, *Trans AIME*, Vol 124, 1937, p 287-298
5. C.Y. Ho, *et al.*, Thermal Conductivity of Ten Selected Binary Alloy Systems, *Journal Physical Chemistry Reference Data*, Vol 7, 1978
6. J.R. Milck and S.J. Welles, Chemical Composition and Electrical Resistivity of Aluminum Alloys, Report AD-687-145, National Bureau of Standards, 1969

7. W.E. Cooke and R.C. Spooner, The Effect of Alloying and Impurity Elements on the Bright-Anodizing Characteristics of Aluminum - 1% Magnesium Sheet Alloy, *Australian Institute of Metals Journal*, Vol 9, 1964, p 80
8. L. Goumiri, *et al.*, Surface Tension of Binary Al Alloys, *Surface Science*, Vol 83, 1979, p 471
9. W.R.D. Jones and W.L. Bartlett, The Viscosity of Aluminum and Binary Aluminum Alloys, *Journal Institute of Metals*, Vol 81, 1952-53, p 145-152
10. T.H. Sanders and E.A. Starke, Ed., The Aluminum-Lithium Alloys, *The Metallurgical Society of AIME*, New York, 1981, p 106
11. W. Koster and W. Rauscher, Relation Between Modulus of Elasticity of Binary Alloys and Their Structure, *Z. Metallk.*, Vol 39, 1948, p 111-120
12. R.F. Wilde and N.J. Grant, Dynamic Elastic Modulus Values at High Temperatures for Nickel-Base, Aluminum-Base and Metal-Metal Oxide Alloys, *ASTM Proc.*, Vol 57, 1957, p 917-928
13. S.S. Hecker, Forming Limit Diagrams, *Metals Engineering Quarterly*, Vol 14, 1974, p 30-36
14. L.R. Morris, *et al.*, Formability of Aluminum Sheet Alloys, Aluminum Transformation Technology and Applications, C.A. Pampillo, *et al.*, Ed., American Society for Metals, 1982, p 549-582
15. I.J. Polmear, *Light Alloys*, London: Edward Arnold, 1981
16. T.H. Sanders, Jr. and J.T. Staley, Review of Fatigue and Fracture Research on High-Strength Aluminum Alloys, in *Fatigue and Microstructure*, American Society for Metals, St. Louis, 1979, p 467-522
17. J.T. Staley, Microstructure and Toughness of High-Strength Aluminum Alloys, *Properties Related to Fracture Toughness, ASTM STP 605*, American Society for Testing and Materials, 1976, p 71-103
18. G.T. Hahn and A.R. Rosenfield, Metallurgical Factors Affecting Fracture Toughness of Aluminum Alloys, *Metallurgical Transactions A*, Vol 6A, April 1975, p 653-670
19. J.S. Santner and D. Eylon, Fatigue Behavior and Failure Mechanisms of Modified 7075 Aluminum Alloys, *Metallurgical Transactions A*, Vol 10A, July 1979, p 841-848
20. J.M. VanOrden, W.E. Krupp, E. Walden, and J.T. Ryder, Effects of Purity on Fatigue and Fracture of 7XXX-T76511 Aluminum Extrusion, *J. Aircraft*, Vol 16, May 1979, p 327-335
21. W.G. Truckner, J.T. Staley, R.J. Bucci, and A.B. Thakker, Effects of Microstructure on Fatigue Crack Growth of High-Strength Aluminum Alloys, AFML-TR-76-169, Oct 1976
22. R.J.H. Wanhill, Manoeuvre Spectrum Fatigue Crack Propagation in Aluminium Alloy Sheet Materials, *Aluminium*, Vol 55, May 1979, p 340-343
23. J.B. Hess, Physical Metallurgy of Recycling Wrought Aluminum Alloys, *Metallurgical Transactions A*, Vol 14A, 1983, p 323-327

Aluminum Properties and Physical Metallurgy
John E. Hatch editor, p 242-319
DOI: 10.1361/appm1984p242

CHAPTER 7

CORROSION BEHAVIOR*

Most aluminum alloys have good corrosion resistance in natural atmospheres, fresh waters, seawater, many soils and chemicals, and most foods, although thin-walled aluminum food containers are coated to resist perforation (Ref 1 and 2). A distinction must be made between durability and aesthetics. An aluminum surface may become unattractive through roughening by shallow pitting and may become dull or even black by dirt retention, but this mild surface attack has no effect on durability of the product, for example, roofing or siding.

While this chapter is devoted almost exclusively to wrought aluminum alloys, some information has been included on aluminum casting alloys. There is a paucity of published information on the corrosion of aluminum castings, and the authors of this chapter have only limited data. This is probably because the corrosion of aluminum castings is usually less of a problem than with the wrought products because their cross section is thicker, and more surface corrosion can be tolerated without loss of function. Further, aesthetics are less of a consideration in the applications of aluminum castings. Alloy composition and temper influence corrosion behavior. Differences in casting practice have only a minor influence on corrosion.

Surface Oxide Film on Aluminum. According to thermodynamics, aluminum should be a reactive metal, with low corrosion resistance. The resistance of aluminum to many environments depends on the presence of a thin, compact film of adherent aluminum oxide on the surface. Whenever a fresh aluminum surface is created and exposed to either air or water, a surface film of aluminum oxide forms at once and grows rapidly. The normal surface film present in air is about 5 nm (50 Å) thick. The film thickness increases at elevated temperature. Protective film growth is much more rapid in water, with much thicker films formed in the absence of oxygen.

Aluminum oxide dissolves in some chemicals, notably strong acids and alkalis. When the film is removed, the metal corrodes rapidly by uniform dissolution. Generally, the oxide film is stable over a pH range of about 4.0 to 9.0, but there are exceptions, such as stability in concentrated nitric acid (pH 1) and concentrated ammonium hydroxide (pH 13). The effect of pH is discussed in greater detail later in this chapter.

Complexity of the Corrosion Process. The definition of corrosion involves both the environment and the metal. Accordingly, the corrosion

*This chapter was revised by a team comprised of H.P. Godard, Alcan International, Ltd.; W.H. Anthony, Anaconda Aluminum Co.; J.A.S. Green, Martin Marietta Laboratories; E.T. Englehart, Alcoa Technical Center; J.S. Snodgrass, Reynolds Metals Co.; T.J. Summerson and J. Moskovitz, Kaiser Aluminum & Chemical Corp.; and M. Zamin, Alcan International, Kingston Laboratories. The original chapter was authored by W.W. Binger, E.H. Hollingsworth, and D.O. Sprowls, Alcoa Research Laboratories.

resistance of an aluminum alloy depends on the environment as well as the alloy. Both chemical and physical environmental variables affect corrosion. The chemical influence of the environment depends on its composition and the presence of impurities, such as heavy metal ions. Physical variables are temperature, degree of movement and agitation, and pressure. Another physical variable that can cause corrosion of aluminum is the presence of stray electrical currents (ac or dc).

Alloy variables that affect corrosion are composition and fabrication practice. These determine the microstructure, which decides whether localized corrosion occurs and the method of attack. The design of an aluminum structure can also have an important influence on its corrosion behavior. The design of the joints and the presence of other metals are important factors.

Because of the many variables that influence corrosion, the suitability of aluminum cannot be considered solely on the basis of a specific product or environment. A detailed knowledge of traces of impurities, conditions of operation, design of a piece of equipment, and alloy microstructure is essential. Experience gained from previously successful service applications is most valuable. The remainder of this chapter deals with the following specific aspects of the corrosion behavior of aluminum:

- Behavior in specific environments
- Types of corrosion
- Influence of microstructure on corrosion
- Influence of environmental factors on corrosion
- Means of corrosion prevention

GENERAL CORROSION BEHAVIOR

Atmospheres

Relative Corrosivity of Natural Atmospheres. Atmospheres are usually classified as rural, industrial, marine, or industrial-marine, although these are generic types only, and there are wide variations in corrosivity within any one kind. From atmospheric tests on aluminum in various locations around the world, weight loss corrosion rates of 0.03 to 4.1 μm/yr (0.001 to 0.16 mil/yr), a variation of 160-to-1, have been reported (Ref 3). The relative corrosivity of an atmosphere is greatly dependent on the metal being considered. In a 5-year test of five metals (aluminum, copper, lead, zinc, and iron) at 21 locations, Lagos, Nigeria was the most corrosive site to steel, but was only one-eighth as corrosive to aluminum as Stratford, a suburb of London.

The relative corrosivity of atmospheres also varies from one aluminum alloy to another. The spread is greater for the less resistant alloys, as shown by the data of Dix and Mears (Ref 4) for three marine atmospheres:

Location	Alloy 1200	Alloy 3003	Alloy 2017-T6
Key West, FL	1	1	1
Sandy Hook, NJ	2	1	11
La Jolla, CA	4	27	59

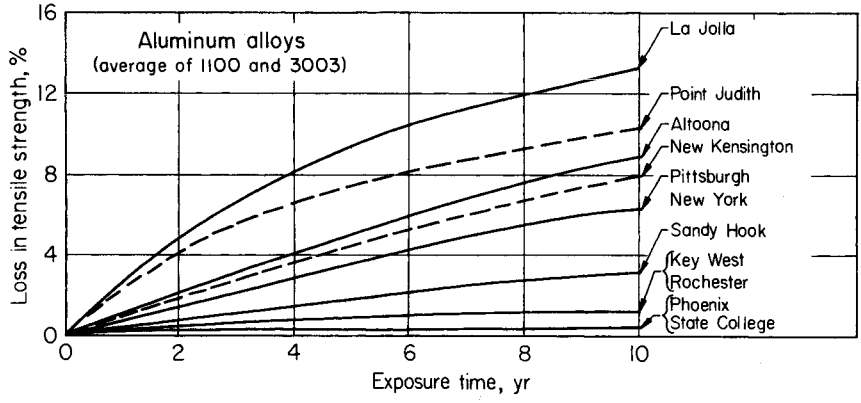

Fig. 1. Relative severity of atmospheric conditions at exposure stations at New Kensington (industrial), Point Judith (seacoast), and nine ASTM stations. Different thicknesses of material were used at the Alcoa (1.6 mm or 0.064 in.) and ASTM (0.9 mm or 0.035 in.) stations, but comparison was made possible by conversion of the percentage losses in tensile strength for 1.6 mm (0.064 in.) thickness to the equivalent percentage loss for 0.9 (0.035 in.) thickness. Curves representing Point Judith and New Kensington are shown as broken lines to indicate that these were calculated from data obtained on the 1.6 mm (0.064 in.) specimens.

The corrosivity of a marine atmosphere at a particular location depends on the amount of air-borne salt, the period of wetness of the exposed metal surface, and the temperature. The distance air-borne salt is carried inland depends on the direction, velocity, and frequency of the prevailing wind, the topography of the coast, and the expanse of sea over which the wind has come. At all locations, the salt content drops rapidly with distance from the sea (Ref 5 and 6), and at most of them it is negligible only a few miles inland.

Nature of Weathering of Aluminum Surfaces. Aluminum alloys corrode in weather by mild roughening of the surface as a result of shallow pitting. No general thinning of the metal occurs. Thus, the maximum pit depth at a given time is a more meaningful measure of the extent of corrosion than weight loss. However, weight loss is a measure of the amount of roughening.

Rate of Atmospheric Corrosion. Typical corrosion rate curves for aluminum in weather are shown in Fig. 1. The shape of the curve is similar, whether the amount of corrosion is measured by weight loss, depth of pitting, or loss of mechanical strength. The steepness of the initial portion of the curve and the time needed for leveling off depend on the corrosivity of the atmosphere. Leveling off usually occurs in 6 months to 2 years, after which the rate is approximately linear, with a very flat slope. In rural atmospheres, the weight loss rate is less than 0.03 μm/yr (0.001 mil/yr). In a number of industrial locations, the rate is in the order of 0.8 to 2.8 μm/yr (0.03 to 0.11 mil/yr) (Ref 7). In a few especially polluted industrial atmospheres, somewhat higher rates of up to 13 μm/yr (0.5 mil/yr) have been encountered, based on maximum pit

depth. Other atmospheric data on aluminum have been published (Ref 8 and 9).

Typical aluminum-magnesium casting alloys are 514.0 and 520.0-T4. Both suffer negligible weight loss corrosion on exposure to all types of atmospheres, but 520.0-T4 is subject to stress-corrosion cracking (SCC) in marine environments, especially after aging. Small cast specimens of 76 by 102 by 8 mm (3 by 4 by $^5/_{16}$ in.) of 514 alloy lost only 0.1 g (0.004 oz) after 20 years of exposure to an urban atmosphere in Kingston, Ontario, and to a marine atmosphere at Kure Beach, NC (240 m or 800 ft).

Aluminum-silicon casting alloys such as B443.0, 356.0-T6, and 413.0 have good resistance to atmospheric corrosion. Small specimens of 76 by 102 by 8 mm (3 by 4 by $^5/_{16}$ in.) lost only 0.2 g (0.007 oz) after 20 years of atmospheric exposure at Kingston, Ontario, and Kure Beach, NC (240 m or 800 ft.). A large, painted, cast steam whistle installed on a minesweeper was examined after 30 years of service. After removal of the paint, the casting was found to be unaffected and was suitable for re-use on another vessel.

Aluminum-copper casting alloys such as 295.0-T6 and 333.0-F require surface protection in corrosive marine and industrial atmospheres. Small specimens of 76 by 102 by 8 mm (3 by 4 by $^5/_{16}$ in.) of a 10% Cu-2% Si casting alloy lost 0.8 g (0.03 oz) after 20 years in the atmosphere in Kingston, Ontario, and 13 g (0.5 oz, or 8% of original weight) at Kure Beach, NC. The underside of the Kure Beach specimen (exposed at 30° to the horizontal) had large, crater-like pits with a maximum depth of 508 μm (20 mils). Harper (Ref 10) has reported 10-year weight loss data on 12 aluminum casting alloys exposed to an English marine atmosphere 90 m (100 yd) from the ocean. Aluminum-silicon-copper casting alloys such as 355.0-T6 and 380.0-F also require protection under corrosive conditions because of their copper content.

Some aluminum-zinc-magnesium casting alloys are subject to SCC in the atmosphere. In one case, an appreciable number of A712.0-type alloy cast awning clamps (7.5% Zn-0.5% Mg) that were stressed in service failed by SCC. An investigation showed that a 6.5% Zn-0.7% Mg-0.4% Cu alloy, which has equivalent strength, was appreciably more resistant to SCC. Lowering the zinc content from 6.5 to 6.0% caused only a small drop in mechanical properties and was found to triple the SCC life in a laboratory test.

Influence of Type of Atmosphere

Rural. In rural atmospheres, the corrosion of aluminum sheet is hardly detectable. In time, the surface becomes gray in color.

Marine. In marine atmospheres, the original shiny surface dulls to a non-aluminum-looking gray color. Commercial purity aluminum-manganese, aluminum-magnesium, and aluminum-magnesium-silicon alloys exhibit good corrosion resistance, and some have been widely used for ship superstructures. The aluminum-copper and aluminum-zinc-magnesium alloys have poorer resistance to marine atmospheres and should be protected by painting or cladding.

Industrial. In industrial atmospheres, the aluminum surface darkens rapidly and may become jet black in only 1 year. Vertical surfaces discolor at a slower rate than inclined surfaces. Sheltered surfaces not washed by rain discolor more rapidly. Over very long periods (25 to 50 years), surface roughening is pronounced and a gradual loss of strength of thin sheet, for example 0.8 mm (0.032 in.), occurs. A commercial-purity aluminum sheet flashing on a building in downtown Montreal pitted to a depth of only 152 μm (6 mils) after 52 years. In severe locations, such as tunnels and stations that accommodate steam locomotives, the rate of corrosion can become appreciable.

Fresh Waters

Aluminum alloys have good resistance to most natural fresh waters. If corrosion does occur, it takes the form of pitting, which follows a decreasing rate curve.

Influence of Water Composition. Soft waters have the least pitting tendency to aluminum, and the lowest rates of penetration, in contrast to their effect on black iron, galvanized iron, and copper. Soft waters, especially if acidic, tend to dissolve copper, which causes deposition corrosion of aluminum. Distilled and deionized water and steam condensate are handled in aluminum equipment (Ref 11).

The main components of natural waters that cause pitting of aluminum are copper, bicarbonate, chloride, sulfate, and oxygen. Harder waters (more bicarbonate) have a higher pitting tendency. Studies on the influence of water composition on pitting have been published by Porter and Hadden (Ref 12), Sverepa (Ref 13), Davies (Ref 14), and Rowe and Walker (Ref 15). Pathak and Godard (Ref 16) have published an equation to predict the pitting tendency of a natural water from its composition, but it must be regarded only as an approximate first step.

Extreme Value Pitting Statistics. The most practical aspect of pitting of aluminum in fresh waters is the maximum pit depth. Aziz (Ref 17) showed that the pit depths can be treated by extreme value statistics. A pitted surface (the larger the better) is divided into 10 to 20 equal portions for examination purposes, and the deepest pit is found on each portion. These are plotted on extreme value graph paper and fall on a straight line that can be extrapolated to predict the true maximum pit depth somewhere on the total area of interest.

An extreme value plot has a further advantage of revealing spurious data. The deepest pit found on a given sample may have had an abnormal special cause (for example, adjacent to a speck of rolled-in copper) and not be typical of the main population of pits. Such a pit would probably fall well above the straight line plot and thus be revealed as not part of the general pit population. The deepest pit found may possibly be shallower than that typical for the rest of the pit population.

Pitting Rate Curves. Godard (Ref 18) has shown that the pitting of aluminum in fresh waters (several hundred waters tested) follows a cube root curve. Thus:

$$d_1 = Kt_1^{1/3} \qquad \text{Eq 1}$$

where d_1 is the maximum pit depth at time t_1. The time to perforation (t_2) can be calculated if the wall thickness is d_2. It follows that:

$$t_2 = t_1 \left(\frac{d_2}{d_1}\right)^3 \qquad \text{Eq 2}$$

A rather obvious consequence of the cube root rate curve is that doubling the wall thickness increases the time to perforation by a factor of 8.

Seawater

Aluminum alloy structures are frequently used in seawater. Navigation buoys, life boats, motor launches, cabin cruisers, patrol boats, barges, and larger vessels have been built since 1930. Today, aluminum-hulled craft up to 61 m (200 ft) in length are built. The hulls are painted to prevent fouling by marine growth, and the superstructures are painted for aesthetic reasons. The painted aluminum superstructure on an ocean-going ship requires repainting only half as frequently as the painted steel portions of the same ship. By providing a marked contrast, the painted aluminum superstructures often induce repainting of the steel section of the ship more frequently than would otherwise occur.

Early Experience With Aluminum Marine Craft. An account of the early history of marine applications of aluminum has been provided by MacIntyre (Ref 19). In 1960, Rogers (Ref 20) summarized the extensive marine corrosion experience of the Canadian Navy in part as follows:

> "It cannot be emphasized too strongly that aluminum as a new shipbuilding material needs treating as such. It has its own design problems, its own maintenance problems, and its own repair problems.It cannot be used everywhere as a substitute for steel or any other alloy, but if the constructors, naval architects, shipwrights and shipbuilders, and of course the suppliers will treat it as something that requires a new approach they will find they have a very fine metal for use in seawater and marine atmospheres."

In 1964, Leveau (Ref 21) described a number of American-built, all-aluminum craft from the 17-m (55-ft) tug Sumter (1958, still in service) to a 59-m (195-ft) tank barge (1963) and a new class of U.S. Navy 50-m (165-ft) gunboats. More recently, Holtyn *et al* (Ref 22 and 23) described the performance of a 91-m (300-ft) aluminum trailer ship and a 17-year-old 30-m (100-ft) aluminum barge.

Pitting Rate Curves. If corrosion occurs, it takes the form of pitting, which follows a cube root curve as for fresh waters. Wright, Godard, and Jenks (Ref 24) published such a curve for 6061-T6 sheet in seawater for 14 months. In a later test program, a cube root curve was also found for 6061-T6 sheet over a 5-year immersion period. Southwell, Hummer, and Alexander (Ref 25) published 16-year pitting data on 1100 and 6061-T6 aluminum sheet immersed in Canal Zone Pacific seawater. For each alloy, the maximum pit depths followed a cube root plot. An exception is the pitting of alclad aluminum, in which the maximum pit depth does not exceed the thickness of cladding until a large area of cladding is removed.

Published Corrosion Data. In 1944, Mears and Brown (Ref 26) reported seawater immersion data on aluminum alloys, including the 8-year performance of a 1724-kg (3800-lb) aluminum ship section model christened the Alumette. In 1949, Walton and Englehart (Ref 27) extended the description of Alcoa's marine experience. In 1952, Wanderer and Sprowls (Ref 28) described the performance of a 37-km (23-mile) bare aluminum submarine pipeline immersed in the Gulf of Mexico. In 1956, Summerson *et al* (Ref 29) published a statistical treatment of pitting data obtained on four aluminum alloys immersed in seawater for 2 years. In 1961, Sutton (Ref 30) reported the results of 7-year seawater immersion tests on four commercial and eight experimental aluminum-magnesium alloys. From 1952 to 1963, Guildhaulis (Ref 31) published several papers (in French) on aluminum specimens immersed in the sea (up to 10 years). In 1964, Ailor and Reinhart (Ref 32) presented the results of 3-year seawater tests on several aluminum alloys. In 1965, Godard and Booth (Ref 33) presented both English and Canadian marine immersion test data on aluminum plate and extrusion alloys for periods up to 10 years. In 1974, Ailor (Ref 34) reported 10-year seawater test results for eight aluminum alloys.

Aluminum-magnesium cast alloy placques of 102 by 127 by 8 mm (4 by 5 by $^5/_{16}$ in.) of Al-4% Mg and Al-7% Mg lost only 0.2 g (0.007 oz) after 10 years of immersion in seawater. Similar specimens of aluminum-silicon casting alloys containing 5 to 12% silicon lost about 5 g (0.2 oz) after 20 years of immersion in seawater, compared to 0.3 g (0.01 oz) for pure cast aluminum, and 0.2 g (0.007 oz) for an Al-4% Mg alloy. Alloy 413.0 pits extensively in seawater. Specimens of 6 mm ($^1/_4$ in.) in thickness lost 10% of their original weight and perforated in only 2 years. The 710.0 aluminum-zinc casting alloy suffers appreciable corrosion in salt-peroxide solution (and probably also in seawater). For example, 13-mm ($^1/_2$-in.) diam test bars were reduced to 6 mm ($^1/_4$ in.) in only 40 to 60 days.

Aluminum-magnesium wrought alloys are the most resistant to seawater. A pit depth of 1270 μm (50 mils) is rarely found, even after 10 years of immersion. Aluminum-magnesium-silicon alloys are somewhat less resistant, although structural members can be used in seawater without protection. These alloys also suffer pitting and may undergo some intergranular corrosion.

Aluminum-copper and high-strength aluminum-zinc-magnesium-copper alloys are less resistant and should not be immersed in seawater unless protected or clad.

Soils

Published information on the corrosion of aluminum alloys in soil is limited. However, the test results available suggest that with the exception of the aluminum-copper (and probably also the aluminum-zinc-magnesium-copper family), aluminum alloys are resistant to many soils. No general thinning of the metal occurs unless the soil is contaminated by cinders or corrosive chemicals, including some aggressive oilfield brines. If corrosion does occur, it takes the form of pitting, and the rate of penetration decreases with time. Not enough pitting data has been established

for soils to prove that a cube root pitting curve holds for unclad aluminum in soil as it does for fresh waters and seawater, although it seems logical to expect it will occur in soils as well.

Experience. In 1951, a 2.9 km (1.8 mile) 6061-T6 aluminum pipe buried for 30 years near Listerhill, AL in sandy soil showed no corrosion in unprotected or cathodically protected sections of the pipeline (Ref 35). In 1957, 29 km (18 miles) of unprotected 3003 alloy pipe were laid in the Pembina oilfield near Edmonton, Alberta with a minimum wall thickness of 4.78 mm (0.188 in.) (Ref 36). The system was later extended to 48 km (30 miles). No leaks have been reported to 1981 (24 years).

In 1961, Whiting and Wright (Ref 37) described the perforation and subsequent cathodic protection of a 10-km (6-mile) pipeline of 3003 alloy near Cantaur, Saskatchewan. The same authors reviewed Canadian experience with buried aluminum pipe (Ref 38). Short specimens from bare aluminum pipelines buried in Canadian soils for periods of 5 to 11 years have been examined (Ref 39). Four of these were 6063 alloy and the fifth was 3003. The maximum pit depth found was on the aluminum-manganese alloy (2032 μm or 80 mils) after 10 years. Dalrymple (Ref 40 and 41) has reported on American experience.

Some 20,000 alclad 3004 alloy culverts were installed throughout the United States over the period of 1959 to 1963 (Ref 42). When 500 of these were inspected after 1 to 3 years, only slight pitting was found, and this was confined to the cladding layer. Subsequent examinations have been made by several state highway authorities since that time. Performance has been good and most states now specify alclad aluminum culvert and drainage pipe for a 50-year design life criterion. More recently, the Federal Highway Administration (FHWA) has reported on these tests (Ref 43).

Soil Burial Test Data. In 1965, Godard (Ref 44) reviewed the available published data on aluminum soil corrosion tests. After tests lasting up to 5 years in which aluminum specimens were buried in 26 soils (6 American, 12 Canadian, and 8 British), the corrosion of those alloys that are considered for use underground (aluminum-manganese, aluminum-magnesium, and aluminum-magnesium-silicon) was appreciable in only three cases. One was a salt marsh recovered from the sea, another a cinder embankment, and the third an acid New Orleans muck that had previously been found to be the most corrosive to steel, of 47 American soils tested by the National Bureau of Standards (NBS).

A special problem in soil, seawater, and concrete is the possible presence of stray currents that may leak onto some points of a buried aluminum metallic structure and go into the ground at other points. If buried aluminum is in electrical contact with other metals, the possibility of galvanic corrosion exists. This decreases as the resistivity of the soil increases. Connecting to copper ground mats has caused appreciable corrosion of buried aluminum.

Foods

Aluminum is resistant to most foods, and as a result commands a substantial share of the domestic cooking utensil market. Items such as corn and potatoes tend to produce a superficial dark stain on aluminum pots

that can be removed by an abrasive scouring pad. Rhubarb, which contains oxalic acid, has a brightening action on aluminum utensils and dissolves anodic films if present. Much information on the performance of aluminum with specific foods has been presented by Bryan (Ref 45). For more recent information, see the Aluminum Association publication entitled *Guidelines for use of Aluminum with Food and Chemicals* (Ref 46). Aluminum containers are used for many foods, usually with a protective film to prevent pitting. Coated aluminum foil domestic food packages and coated aluminum beverage cans are produced in great numbers.

Chemicals

Aluminum is completely resistant to many chemicals, while in others it dissolves uniformly and rapidly. In some chemicals, such as methanol or phenol, a trace of water (0.1%) prevents corrosion, especially at high temperatures. In others, such as liquid SO_2, a trace of water promotes corrosion. Much information is available on aluminum in the chemical industry (Ref 47-50). Applications of aluminum in the chemical process industries are described in *Aluminum,* Vol II, published by the American Society for Metals, 1967. In addition, aluminum suppliers have much accumulated experience. While the dictionaries cited are of considerable value because they describe actual experience, many essential details are usually lacking. For example, complicating factors such as may be caused by dissimilar metals may be a factor, either in direct contact with aluminum, or as a contaminant from prior contact of the product with other metals. For example, glacial acetic acid is innocuous to aluminum, but traces of mercury may cause deposition corrosion of aluminum upon dilution. Temperature and degree of agitation may have an influence. For a major application of aluminum with a new product, a corrosion test in the actual product should be run. The testing of metals for corrosion resistance has been discussed at length by LaQue (Ref 51), Champion (Ref 52), and Ailor (Ref 53). A listing of chemicals that have been handled in aluminum, along with the conditions of these applications, can be found in Ref 46.

Halogenated Hydrocarbons

Aluminum alloys usually are resistant to pure halogenated hydrocarbons and other organic chemicals containing halogens under most conditions, particularly at and below room temperature. Some hydrocarbons may produce a rapid rate of aluminum corrosion or a violent reaction. Service conditions to ensure safety should be recognized or established before aluminum alloys are used with any halogenated hydrocarbon.

Halogenated hydrocarbons may decompose by hydrolysis if water is present, or by other processes, to yield mineral acids such as hydrochloric acid. These acids corrode aluminum alloys by destroying the natural protective surface oxide film that provides inherent corrosion resistance. Corrosion of aluminum alloys by these acids may also promote reactions of the hydrocarbons themselves, because aluminum halides formed by corrosion are catalysts for reactions such as $AlCl_3$ for a Friedel-Crafts re-

action. In some instances, aluminum alkyls may be produced. Because of the rapid heating rate, corrosion of aluminum and reaction of a halogenated hydrocarbon, once initiated, may tend to become autocatalytic.

The reactivity of aluminum alloys with halogenated hydrocarbons generally decreases in the order of increasing chemical stability of these hydrocarbons, which may be established precisely by thermodynamic data or qualitatively by the structural formulas of the hydrocarbons and by the halogens they contain. Thus, aluminum is most resistant to hydrocarbons halogenated with fluorine, followed in order of decreasing resistance to those with chlorine, bromine, and iodine. Aluminum also is resistant to highly polymerized halogenated hydrocarbons, reflecting the high degree of chemical stability of these materials.

The behavior of aluminum alloys in a mixture of halogenated hydrocarbons, or mixtures of these hydrocarbons with other organic compounds, cannot be predicted from their behavior with each of the components. Methyl alcohol and carbon tetrachloride mixtures, for example, produce rapid corrosion of some aluminum alloys at ambient temperature even though the components alone do not.

The resistance of aluminum alloys to halogenated hydrocarbons tends to decrease as the temperature is raised. The rate of corrosion in many liquid halogenated hydrocarbons remains low until the boiling point is reached; in some, it is low or nonexistent even at this temperature. Other factors that affect resistance include the presence of an inhibitor and the purity of a halogenated hydrocarbon; amines or various heterocyclic compounds have been effectively used as inhibitors in certain cases.

Aluminum in a finely divided form, such as in a powder, should not be exposed to a halogenated hydrocarbon. The possibility of creating a violent reaction that may lead to an explosion is increased when aluminum with a large surface area is exposed to a small volume of a halogenated hydrocarbon, and even more so when this operation is carried out under pressure. Specific sources (Ref 46) that discuss fluorinated hydrocarbons, such as Freons, and inhibited halogenated hydrocarbons, such as solvents for degreasing, illustrate applications with halogenated hydrocarbons.

Aluminum tubing is used to handle Freon refrigerants. Trichloroethylene degreasing baths are used for cleaning wrought aluminum products. These baths have proven satisfactory, providing that a stabilized solvent is used, the accumulation of aluminum fines and water is prevented, and the bath is discarded when acid is detected.

Building Materials

A large amount of aluminum is used in commercial buildings in the form of facades, doors, windows, and electrical conduits, and in private dwellings in the form of windows, screen doors, siding, gutters, and soffits. The performance of aluminum embedded in, or in contact with, building materials such as concrete, plaster, brick mortar, and wood is important in these applications.

Contrary to popular belief, aluminum alloys are not seriously corroded by long-time embedment in portland cement concrete, standard brick mortar,

lime brick mortar, hardwall plaster, or stucco (Ref 55-59). Slight superficial etching of the aluminum takes place while these products are setting, but unless there is frequent intermittent wetting and drying, no appreciable corrosion takes place. Aluminum can corrode when embedded in chloride-containing concrete and in contact with dissimilar metal, such as reinforcing steel.

Absorbent material such as paper, asbestos, or wood refuse wall board that is in contact with aluminum under conditions where it may become wet, because of condensation or water from another source, tends to corrode aluminum. Composite-bonded insulated aluminum panels are made with a moisture barrier on the inside to prevent the insulation from becoming wet. Some insulating materials such as magnesia are alkaline and quite aggressive to aluminum. Magnesium oxychloride, a flooring compound sometimes used for subway cars, passenger cars, and ship decks, is very corrosive to aluminum and should not be used with it, regardless what preventive measures are provided.

While few woods cause appreciable corrosion of aluminum in contact with them (Ref 60), a risk of corrosion develops if the moisture content of the wood exceeds 18 to 20%, a condition reached when the relative humidity of the environment exceeds 85% (Ref 61). If the wood may become moist in service, aluminum in contact with it should be protected by an impermeable membrane or a bituminous paint coating.

Farmer (Ref 62) has called attention to a possible cause of corrosion of metals by wood—absorbed salt from logs having floated in seawater. The British Forest Products Laboratory (Ref 63) has proposed general recommendations to prevent the corrosion of metals (including aluminum) by wood.

Little published information exists on the corrosion behavior of aluminum embedded in or in contact with wood that has been impregnated with a wood preservative. Coal tar creosote, a common wood preservative, has an inhibitive effect on the corrosion of aluminum. Certain chromate-containing preservatives are innocuous to aluminum, as is pentachlorophenol, another common preservative. In general, preservatives containing copper have a detrimental effect on aluminum corrosion behavior. Those containing mercury should definitely not be used where aluminum is involved.

TYPES OF CORROSION

Uniform Surface Attack. If the surface oxide film is soluble in the environment, as in phosphoric acid or sodium hydroxide, aluminum dissolves uniformly at a steady rate. If heat is evolved, as with dissolution in sodium hydroxide, the temperature of the solution and the rate of attack increases. Depending on the specific ions present, and their concentration and temperature, the attack may range from superficial etching to rapid dissolution. Uniform attack can be assessed by measurement of weight loss or loss of thickness.

Localized Corrosion. In environments in which the surface film is insoluble, corrosion is localized at weak spots in the oxide film, and takes one of the forms described in the following sections, if it occurs at all. Localized corrosion has an electrochemical mechanism and is caused by

a difference in corrosion potential in a local cell formed by differences in or on the metal surface. The difference is usually in the surface layer because of the presence of cathodic microconstituents that can be insoluble intermetallic compounds or single elements. Most common are $CuAl_2$, $FeAl_3$, and silicon. However, the difference may be on the surface because of local differences in the environment. A common example of the latter is a differential aeration cell. Another is particles of heavy metal plated out on the surface. Less frequent is the presence of a tramp impurity such as iron or copper embedded in the surface. Other causes of local cell formation have been listed by Mears and Brown (Ref 64). The severity of local cell corrosion tends to increase with the conductivity of the environment.

Another electrochemical cause of localized corrosion is the result of a stray electric current leaving the surface of aluminum to enter the environment. The only type of localized corrosion that does not have an electrochemical mechanism is fretting corrosion, which is a form of dry oxidation. In almost all cases of localized corrosion, the process is a reaction with water:

$$2Al + 6H_2O \rightarrow Al_2O_3 \cdot 3H_2O + 3H_2 \qquad \text{Eq 3}$$

The corrosion product is almost always aluminum oxide trihydrate (Bayerite). Localized corrosion does not usually occur in extremely pure water at ambient temperature or in the absence of oxygen, but may occur in more conductive solutions because of the presence of ions such as chloride or sulfate. An examination of the corrosion product may identify the offending ion and thus the cause of corrosion (Ref 65 and 66). Localized corrosion frequently can be controlled or prevented, as the following sections show.

Pitting Corrosion. Pitting is the removal of metal at localized sites on the surface, resulting in the development of cavities. For pitting to occur, an electrolyte must be present. This may be a bulk liquid, a moist solid, a film of condensed moisture, or droplets of water standing on the surface. Oxygen must also be present for pit initiation.

While the shape of pits in aluminum can vary from shallow, saucer-like depressions to cylindrical holes, the mouth is usually more or less round, and the pit cavity is roughly hemispherical. This distinguishes pitting from intergranular corrosion, in which attack is confined to subsurface tunnels along grain boundaries, usually visible only on metallographic examination of cross sections. Intergranular corrosion may occur along with pitting, in which case intergranular fissures advance into the metal laterally and inwardly from the pit cavity. The primary cause of pitting in aluminum is the presence of local cells at the metal surface, as described in the previous section on localized corrosion.

In the early stages of pit growth, the rate is autocatalytic (Ref 67 and 68). Initiation occurs by breaking down a spot in the surface oxide film adjacent to a cathodic particle. If a copper ion is present, it plates out on the cathodic site and increases the driving potential. As the pit cavity (anode) develops, the environment in it becomes acidic (pH 3 to 4), and the environment over the cathode surface becomes slightly alkaline. These local environmental changes increase the driving potential of the local cell, and also the pit current. Once a steady state is reached, the pit cur-

rent remains steady and is controlled by the external cathode, the area of which is influenced by the conductivity of the electrolyte. Nearby pits interact by competing for available cathode area. Generally, the greater the number of pits, the shallower the deepest pit. In deep pits that have become capped with corrosion product, the role of the external cathode area is probably less, and the pH of the liquid in the pit cavity is probably more important.

The composition of the electrolyte has a strong influence on the initiation and growth rate of pits in aluminum. The influence of the many anions and cations possible is complex and not fully understood. The work of Sotovdeh *et al* is relevant (Ref 69).

In all cases, the rate of penetration slows appreciably with time. This aspect was discussed previously under individual environments. The various stages of pitting—initiation, propagation, termination, and reinitiation—have been discussed by Godard (Ref 70).

Doubly refined, very high-purity aluminum (1099) has excellent resistance to pitting and is much superior to any of the commercial alloys. Alloy 3003, made with a very high-purity base for experimental cooking utensils, was also found to be very resistant to pitting. Of the commercial alloys, the aluminum-magnesium family (5XXX) have the lowest pitting probability and penetration rates. With a low ($\leq$0.04%) copper content, aluminum-manganese (3XXX) alloys have comparable pitting behavior, but at 0.15% copper, they pit more extensively, especially in seawater. In commercial-purity aluminum (1XXX), pitting behavior improves with purity and is better at low iron and copper contents. In aluminum-magnesium-silicon alloys (6XXX), pitting is combined with intergranular corrosion. For example, 6351 extrusions may develop mild surface blistering in severe industrial atmospheres and in seawater. In sheet form, the aluminum-copper (2XXX) and aluminum-zinc-magnesium-copper (7XXX) alloys are normally clad to protect against pitting.

Crevice Corrosion

If an electrolyte is present in a crevice formed between two faying aluminum surfaces, or between an aluminum surface and a nonmetallic material such as a gasket, localized corrosion in the form of pits or etch patches may occur. The oxygen content of the liquid in the crevice is consumed by the film formation reaction with the aluminum surface, and corrosion stops because the replenishment of oxygen by diffusion into the crevice is slow. At the mouth of the crevice, whether it is submerged or exposed to air, oxygen is more plentiful. This creates a local cell: water with oxygen versus water without oxygen, and the corrosion potentials are such that localized corrosion occurs in the oxygen-depleted zone (anode) immediately adjacent to the oxygen-rich (cathode) near the mouth of the crevice. This is sometimes called a concentration cell or a differential aeration cell. Once the crevice attack has initiated, the anode area becomes acidic and the cathode area becomes alkaline. These changes further enhance local cell action.

An important variable in crevice corrosion is the width of the crevice opening, because this determines the ease of oxygen diffusion into the

crevice, and also affects the resistivity of the liquid in the crevice. Crevice corrosion of aluminum is negligible in fresh waters.

Submerged Crevices. Rosenfeld (Ref 71) has shown that with submerged crevices, another important variable is the ratio of the actively corroding surface area in the crevice to the effective external cathode area. The rate of aluminum crevice corrosion increases as the crevice mouth narrows and as the external cathode area increases.

Rosenfeld also studied the influence of aluminum alloy on the rate of crevice corrosion and obtained the results plotted in Fig. 2. Aluminum-copper and aluminum-zinc-magnesium-copper alloys corroded many times faster than 1100, 3XXX, or 5XXX alloys. Again, crevice width is important, because corrosion rates are low for crevice openings greater than 254 μm (10 mils).

Atmospheric Crevices. In the design of aluminum structures for marine service, no provision need be made for crevice corrosion to obtain a service life of 5 years, except where the cross section is less than 1016 μm (40 mils) (Ref 72). For longer life, the faying surfaces should be

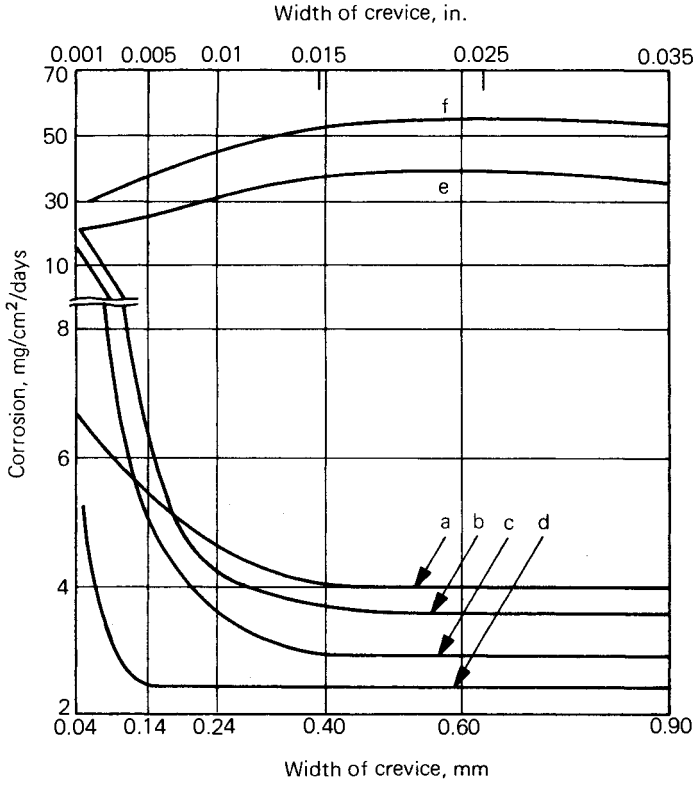

Fig. 2. Dependence of crevice corrosion of aluminum alloys on the width of the crevice in 0.5N NaCl. Duration of experiment 54 days. No outside contact. (a) Aluminum. (b) Clad Duralumin (D16). (c) Aluminum-manganese (AMc). (d) Aluminum-magnesium. (e) Aluminum-zinc-magnesium-copper unclad. (f) Duralumin (D16) unclad. (Ref 71)

coated with an inhibitive paint system, and where possible the crevice should be filled with a resilient, moisture-excluding sealant. On thicker sections no provision need be made.

Crevices in Waters. In most fresh waters crevice corrosion of aluminum is negligible. In seawater, crevice corrosion takes the form of pitting, and the rate is low. Resistance to crevice corrosion has been found to parallel resistance to pitting corrosion in seawater, and is higher for aluminum-magnesium alloys than for aluminum-magnesium-silicon alloys (Ref 73).

Water Staining. The most common case of aluminum crevice corrosion occurs when water is present in the restricted space between layers of aluminum in close contact, as in packages of sheet or circles, or wraps of coil or foil. This may occur during storage or transit because of inadequate protection from the ingress of rain, or be caused by condensation within the crevice when the metal surface temperature falls below the dew point. Matching irregular stain patterns of corrosion product are produced on the contacting surfaces, which can vary from gray to brown to black. In severe cases, the corrosion product cements the two surfaces together and makes separation difficult.

In some cases, the stain pattern shows a series of irregular rings, like the lines on a contour map. These are believed to represent the outlines of a receding water pool at various stages of evaporation. The stain patches mar the shiny surface and impair the use of the sheet where surface appearance is important, though corrosion is shallow, and perforation rarely occurs, even on thin sheet. The stained areas are not more susceptible to subsequent corrosion; they are more resistant, because they are covered with a thickened oxide film. Water staining can be prevented by avoiding the ingress of rain and condensation conditions. The metal temperature must be maintained above the dew point, either by providing a low relative humidity or preventing cooling of the metal.

Filiform corrosion is another special case of crevice corrosion that may occur on an aluminum surface under an organic coating. It takes the form of randomly distributed thread-like filaments, and is sometimes called vermiform or worm track corrosion. The corrosion products formed raise a bulge in the surface coating, much like molehills in a lawn. The tracks proceed from one or several points where the coating is breached. The surface film itself is not involved in the process, except in the role of providing inadequate zones of poor adhesion that form the crevices in which the corrosion occurs, upon access of moisture with restricted access of oxygen. Filiform corrosion has occurred on lacquered aluminum surfaces in aircraft exposed to marine and other high-humidity environments. This has been controlled by the use of chemical conversion coatings, anodizing, and the use of chromate-inhibited primers prior to painting.

The amount of aluminum consumed by crevice corrosion is small, and is of practical importance only when the metal is of thin cross section, or in cases where surface appearance is important. More serious is the disruptive force of corrosion products produced in a confined space. These are about five times as bulky as the metal from which they were produced (about twice as bulky as rust on steel) and can distort even heavy sections of metal.

Galvanic Corrosion. Accelerated corrosion of a metal because of electrical contact with a more noble metal or a nonmetallic conductor such as graphite in a conductive environment is called galvanic corrosion (Ref 74). The most common examples of galvanic corrosion of aluminum alloys in service occur when they are joined to steel or copper and exposed to a wet saline environment. The aluminum alloy corrodes more rapidly than it does in the absence of the contacting dissimilar metal.

For each environment, a galvanic series can be constructed in which metals are arranged in order of their corrosion potential, with the most active metals at the top, and the most inactive metals at the bottom. These series usually are similar to, but are not exactly the same, as the well-known electromotive series. The best defined, and the most commonly used galvanic series is that based on corrosion potentials in salt solution (Ref 75), which is reproduced in Table 1. The corrosion potentials of the most common aluminum casting alloys are given in Table 2.

The rate of attack depends on (1) the difference in corrosion potentials between the two metals, (2) the electrical resistance between the two metals, (3) the conductivity of the electrolyte, (4) the cathode-anode area ratio, and (5) the polarization characteristics of the two metals. Although Table 1 can be used to predict which metal suffers galvanic attack when compared with another, the extent of attack cannot be predicted because of polarization. For example, the potential difference between aluminum and stainless steel is greater than that between aluminum and copper, yet the galvanic influence of stainless steel on aluminum is much less because of polarization, while the aluminum-copper couple shows little polarization. In the common case, the two metals are in direct physical contact, as in a riveted joint. Galvanic corrosion can also occur if the metals are

Table 1. Corrosion Potentials of Various Metals in Salt Solution (Galvanic Series)

Metal	Corrosion potential, V(a)
Magnesium	−1.65
Zinc	−1.02
Aluminum alloys 7072	−0.88
Aluminum alloys 5XXX	−0.77 to −0.79
Aluminum alloy 7075-T3	−0.76
Aluminum alloys 1XXX, 3XXX, 6XXX	−0.72 to −0.75
Cadmium	−0.74
Aluminum alloys 2024-T6	−0.73
Low-carbon steel, cast and wrought iron	−0.50
Lead	−0.47
Tin	−0.41
Lead-tin solder (60-40)	−0.37
Brass (60-40)	−0.20
Copper	−0.12
Inconel	−0.04
Stainless steel (18-8, passive)	−0.01
Bronze (95-5)	+0.00
Nickel	+0.01
Monel	+0.02

(a) With reference to a saturated calomel electrode, values calculated from those measured in 53 g/L (6 oz/gal) NaCl plus 3 g/L (0.3 oz/gal) H_2O_2 at 25 °C (77 °F), using a 0.1N calomel electrode. (*Metals Handbook*, Vol 2, 9th ed., American Society for Metals)

Table 2. Corrosion Potentials of Aluminum Casting Alloys in Salt Solution

AA designation	Old designation	Corrosion potential, V(a)
710.0	A712.0	−0.91
520.0-T4	220-T4	−0.84
514.0	214	−0.79
518.0	218	−0.79
413.0	13	−0.74
B443.0	43	−0.74
356.0-T6	356-T6	−0.73
360.0	360	−0.73
355.0-T6	355-T6	−0.71
850.0-T4	750-T4	−0.70
208.0-F	108-F	−0.69
380.0-F	380-F	−0.67
319.0-F	319-F	−0.67
333.0-F	333-F	−0.67
295.0-T6	195-T6	−0.65
296.0-T6	B295.0-T6	−0.64

(a) With reference to a saturated calomel electrode, values calculated from those measured in 53 g/L (6 oz/gal) NaCl plus 3 g/L (0.3 oz/gal) H_2O_2 at 25 °C (77 °F), using a 0.1N calomel electrode. (Alcoa Laboratories)

separated, but both are exposed to a common electrolyte and joined by an external electrical connection.

The galvanic corrosion of aluminum is usually mild, except in highly conductive media such as seawater, wind-blown sea spray, and salted slush from road de-icing salts, when corrosion can be appreciable. In natural surface waters and nonsaline atmospheres, the galvanic corrosion of aluminum is rarely significant, although rain runoff from copper and its alloys pit aluminum appreciably.

In natural environments, including saline conditions, zinc is anodic to aluminum and corrodes preferentially, giving protection to aluminum. Magnesium is similarly protective, although in severe marine environments it causes cathodic corrosion of aluminum because of an alkaline condition produced on the aluminum surface. Cadmium is neutral to aluminum and can safely be used in contact with it. The other structural metals are cathodic to and promote galvanic corrosion of aluminum. Of the metals, copper (and its alloys: brass, bronze, and Monel) are the most aggressive to aluminum, followed closely by steel (in saline environments only). In normal atmospheres and natural waters, stainless steels can be safely coupled with aluminum. Nickel is less aggressive than copper, approaching stainless steel in its action on aluminum. In severe marine atmospheres, stainless steel corrodes aluminum. In seawater, the action depends on the cathode-anode area ratio. Chromium electroplate has about the same action as stainless steel. Lead may be used with aluminum except in severe marine atmospheres. For example, lead washers can be used on aluminum nails to secure aluminum sheet in all but the most corrosive atmospheres.

In unusual environments aluminum is anodic to zinc, while in others it is cathodic to steel (Ref 75 and 76). The galvanic behavior of aluminum

has been described by several authors (Ref 77–81). The galvanic corrosion performance of the different aluminum alloys is quite similar, so that a problem cannot be solved by changing alloys.

In structural applications, especially where salt may be encountered, the crevice between the metal pair should be filled with a high-quality, resilient, nonhardening sealant. For more complete instructions for the prevention of galvanic corrosion of aluminum, see the section on prevention of galvanic corrosion in this chapter.

Deposition corrosion is a special case of galvanic corrosion that takes the form of pitting. It occurs when particles of a more cathodic metal in solution plate out on an aluminum surface to set up local galvanic cells. The ions aggressive to aluminum are copper, lead, mercury, nickel, and tin, often referred to as heavy metals. The effect of heavy metals is greater in acidic solutions. In alkaline solutions, their solubility is much lower, resulting in less severe effects (Ref 82).

Copper ion is the most common cause of this type of corrosion in applications for aluminum. A common example is rain runoff from copper roof flashing, causing corrosion of aluminum gutters. Very small amounts of copper can be detrimental (as low as 0.05 ppm), depending upon other conditions of exposure (Ref 82 and 83). For example, copper presents a much greater problem in aerated halide solutions than in aerated nonhalide solutions.

Mercury is the most aggressive ion to aluminum, and even traces can be serious (Ref 84). Fortunately, mercury is rarely present in natural waters or commercial aqueous solutions, but occasionally it is found in unexpected places, such as from a broken thermometer, or where tramp mercury has contaminated the structure.

Liquid mercury does not wet an aluminum surface, and mercury has been handled in anodized aluminum bottles. However, if the natural oxide film on the aluminum surface is broken (the presence of halides greatly assists this), aluminum dissolves in the mercury to form an amalgam and the corrosion reaction becomes catastrophic. The dissolved aluminum oxidizes immediately in the presence of moisture, and further aluminum dissolves to form an aggressive cycle. Very high corrosion rates ensue (up to 1270 mm/yr or 50 in./yr). The safe level of mercury that can be tolerated in a solution or environment is difficult to determine, because of the uncertainty of initiation of amalgamation. However, in corrosive solutions any concentration of >0.01 ppm should be cause for concern, and in an environment where attack is initiated less readily, any concentration exceeding that permitted by EPA regulations is suspect.

Stray Current Corrosion. Whenever an electric current (ac or dc), leaves an aluminum surface to enter an environment such as water, soil, or concrete, aluminum is corroded at the area of current passage in proportion to the amount of current passed. This is known as stray current corrosion or electrolysis (a poorly chosen, ambiguous term, but one firmly entrenched in pipeline and shipping technology).

At low current densities corrosion may take the form of pitting, while at higher current densities considerable destruction of the metal can occur. The rate does not diminish with time. Other than uniform dissolution in

an active chemical, this is one of the two main causes of unexpected, very rapid corrosion of aluminum (an uncommon event). The other is the presence of mercury ions in the environment.

Since the aluminum surface from which the current leaves functions as an anode, oxidation (corrosion) occurs, and the area becomes acidic. The presence of acidity on the surface often provides the clue that reveals unexpected stray current activity. Local acidity can develop even in an alkaline environment such as concrete.

Stray currents encountered in practice are usually direct current (for example, from a welding generator), but may also be alternating current. For most metals, ac corrosion is negligible, but with aluminum it can be appreciable (Ref 85). Below a critical small ac current density, no corrosion of aluminum occurs. This value has been reported variously at 0.5, 1.0 (Ref 86), and 5.7 mA/cm^2 (Ref 87) or 0.003, 0.006 (Ref 86), and 0.04 $mA/in.^2$ (Ref 87). See also Williams (Ref 88), and French (Ref 89).

Examples of stray current corrosion of aluminum have been reported in concrete (electrical conduit), in seawater (boat hulls), and in soils (pipelines and drainage systems). Usually, stray current corrosion can be prevented by appropriate design and protection measures. For example, corrosion of aluminum conduit in concrete is prevented by not allowing the conduit to serve as a neutral ground under any circumstances, especially during welding. Chloride content of concrete and avoidance of contact with reinforcing bars also is important in avoiding corrosion. The welding generator must be provided with a separate ground.

A special case of stray current corrosion can develop when an aluminum-hulled boat is moored to a steel dock, and the electrical system of the boat is plugged into 110 V ac power on the dock to save the boat batteries. The aluminum hull can become coupled to the steel dock through the shore electrical grounding system. Currents as high as 160 mA have been measured on a 13-m (44-ft) aluminum hull. The galvanic current concentrates at breaks in the paint, and perforation of the hull can be rapid. The external aluminum drive unit of an inboard-outboard motor in a nonaluminum hull can become coupled to the steel dock in the same way, and galvanic currents of 18 mA have been measured. To interrupt the galvanic couple yet permit passage of the shore ac, a capacitor is placed in the boat ground wire leading to the plug that receives the shore power supply (Ref 90).

In soils, stray current corrosion can be caused by close proximity to other buried metal systems that are being protected by an impressed current cathodic protection system. These stray currents may leak onto a buried aluminum structure at one point, then off at another (where corrosion occurs), taking a low-resistance path between the driven buried anode and the nearby structure being protected. Common bonding of all buried metal systems in close proximity is the usual way to avoid such attack (Ref 91 and 92).

Intergranular corrosion is selective attack of the grain boundary zone, with no appreciable attack of the grain body or matrix (Fig. 3). The mechanism is electrochemical and is the result of local cell action in the grain boundaries. Cells are formed between second-phase microconstituents and the depleted aluminum solid solution from which the constituents formed.

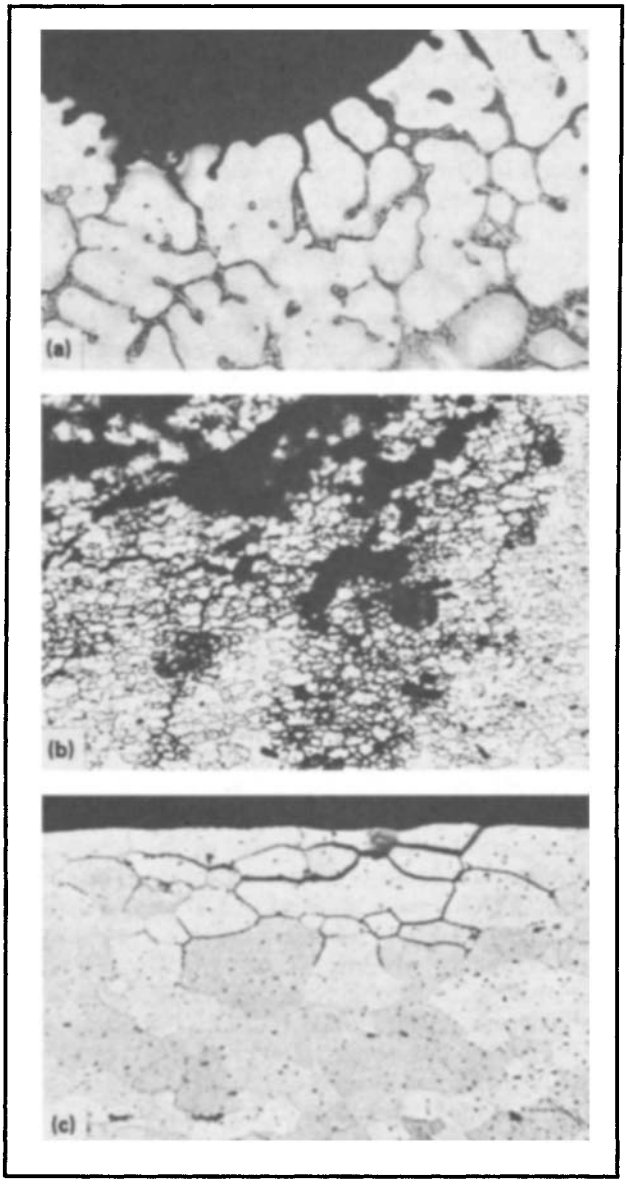

Fig. 3. Various types of intergranular corrosion attack. (a) Interdendritic (ID) corrosion in a cast structure. (b) Interfragmentary (IF) corrosion in a wrought structure, unrecrystallized. (c) Intergranular (I or IG) corrosion in a recrystallized wrought structure. Keller's etch. (500×)

These constituents have a different corrosion potential than the adjacent depleted solid solution. In some alloys, such as the aluminum-magnesium and aluminum-zinc-magnesium-copper families, the precipitates (Mg_2Al_3, $MgZn_2$, and Al_x-Zn_x-Mg) are more anodic than the adjacent solid solu-

tion. In other alloys, such as aluminum-copper, the precipitates ($CuAl_2$ and Al_xCu_xMg) are cathodic to the depleted solid solution. In either case, selective attack of the grain boundary region occurs.

The degree of intergranular susceptibility is controlled by fabrication practices that can affect the amount, size, and distribution of second-phase intermetallic precipitates. Discussion of precipitation and heat treatment can be found in Chapter 5 in this Volume. Resistance to intergranular corrosion is obtained by use of heat treatments that cause precipitation to be more general throughout the grain structure, or by restricting the amount of alloying elements that cause the problem.

Alloys that do not form second-phase microconstituents at grain boundaries, or those in which the constituents have corrosion potentials similar to the matrix ($MnAl_6$), are not susceptible to intergranular corrosion. Examples of alloys of this type are 1100, 3003, and 3004.

Aluminum-magnesium alloys (5XXX) containing less than 3% magnesium are quite resistant to intergranular corrosion. In unusual instances, intergranular attack has occurred in the heat-affected zone of weldments after months or years of exposure at moderately elevated temperatures of ≈100 °C (≈212 °F), in hot, acidified ammonium nitrate solutions of ≈150 °C (≈300 °F), or hot, potable water at 80 °C (175 °F). At higher magnesium concentrations, intergranular corrosion does not occur when these alloys are properly fabricated and used at ambient temperatures. Alloys can become susceptible to intergranular corrosion, however, after prolonged exposure to elevated temperatures above 27 °C (80 °F). This is commonly referred to as sensitization. The degree of susceptibility increases with magnesium content, time at temperature, and amount of cold work.

Aluminum-magnesium-silicon wrought alloys (6XXX) usually show some susceptibility to intergranular corrosion. With a balanced magnesium-silicon composition that results in the formation of Mg_2Si constituent, intergranular attack is minor, and less than that observed with aluminum-copper (2XXX) and aluminum-zinc-magnesium-copper (7XXX) alloys. When the 6XXX alloy contains an excessive amount of silicon (more than that needed to form Mg_2Si), intergranular corrosion increases because of the strong cathodic nature of the insoluble silicon constituent.

In aluminum-copper-magnesium alloys (2XXX), thermal treatments that cause selective grain boundary precipitation lead to intergranular corrosion susceptibility. Many studies have shown fast cooling on quenching during heat treatment, and subsequent aging to peak or slightly overaged strength, results in high resistance to intergranular corrosion. Conversely, slow cooling results in intergranular susceptibility.

Intergranular corrosion in aluminum-zinc-magnesium-copper (7XXX) alloys can also be affected by thermal treatments. Heat treatment, sometimes in combination with strain hardening, is used to provide good resistance to intergranular corrosion. Testing for intergranular susceptibility varies with the alloy family. Metallographic examination after exposure to an $NaCl\text{-}H_2O_2$ corrosive solution (see MIL-H-6088F) is used primarily for aluminum-copper-magnesium (2XXX) alloys. It has also been used with aluminum-magnesium-silicon (6XXX) and aluminum-zinc-magnesium-copper (7XXX) alloys. For aluminum-magnesium alloys, a

weight loss test method (NAWLT) has recently been established (ASTM G69-80). With aluminum-copper-magnesium (2XXX) and aluminum-zinc-magnesium-copper (7XXX) alloys, limited use has been made of electrochemical methods (corrosion potential, potentiostatic, and galvanostatic) for predicting intergranular corrosion susceptibility. However, confirmation by metallographic examination is still considered necessary.

Exfoliation Corrosion. Exfoliation, also called layer corrosion or lamellar corrosion, is a type of selective subsurface attack that proceeds along multiple narrow paths parallel to the surface of the metal. The attack is usually along grain boundaries (intergranular corrosion), but it has also been observed along striations of insoluble constituents that have strung out in parallel planes in the direction of working. Exfoliation occurs predominantly in relatively thin products with highly worked, elongated grain structures. The intensity of exfoliation increases in slightly acidic environments and when the aluminum is coupled to a cathodic dissimilar metal.

Exfoliation is characterized by leafing, or alternate layers of thin, relatively uncorroded metal and thicker layers of corrosion product that are more bulky than the metal from which they came. The layers of corrosion products cause the metal to swell. In an extreme case, a 1.3-mm (0.050-in.) thick sheet was observed to swell to a 25-mm (1-in.) thickness—an amazing 20 times!

Exfoliation usually proceeds inwards laterally from a sheared edge, rather than inward from a rolled or extruded surface. In mild cases, it takes the form of blisters that resemble volcanoes, with corrosion product welling up in the center. In this case, pits occur first and proceed inward until the susceptible layer is encountered. The attack then changes to lateral penetration with generation of bulky corrosion products that cause the blisters to develop. Exfoliation is not accelerated by stress and does not lead to stress-corrosion cracking.

The commercial-purity (1XXX) and aluminum-manganese (3XXX) alloys are quite resistant to exfoliation corrosion in all tempers. Exfoliation has been encountered in some highly cold worked aluminum-magnesium (5XXX) materials such as 5456-H321 boat hull plates. These developed a highly elongated grain structure and selective grain boundary precipitation. This exfoliation problem led to the establishment of a special boat hull plate temper (H116) that has high resistance to exfoliation corrosion.

In the heat treatable aluminum-copper-magnesium (2XXX) and aluminum-zinc-magnesium-copper (7XXX) alloys, exfoliation corrosion has usually been confined to relatively thin sections of highly worked products with an elongated grain structure. In 2124-T351 plate, for example, 13-mm (0.5-in.) plate was quite susceptible in laboratory and atmospheric tests, while 50-mm (2-in.) and 100-mm (4-in.) plate, with less directional structures, did not exfoliate. In extrusions, the surface is often quite resistant to exfoliation because of its recrystallized grain structure. Subsurface grains are unrecrystallized, elongated, and vulnerable to exfoliation. In aluminum-zinc-magnesium alloys containing copper, such as 7075, resistance to exfoliation can be improved markedly by overaging. This is designated by the temper designations of T7XXX for wrought products. While a 5 to 10% loss in strength occurs, improved resistance

to exfoliation is provided. In copper-free or low-copper 7XXX alloys, exfoliation corrosion resistance can be controlled by overaging or by recrystallizing heat treatments and can also be controlled to some extent by changes in alloying elements. In aluminum-copper-magnesium (2XXX) alloys, artificial aging to the T6 or T8 condition provides improved resistance.

Several laboratory methods have been developed to test for exfoliation corrosion susceptibility in aluminum alloys. These include metallographic examination, visual rating, and weight loss measurements after exposure to corrosive environments (solutions and sprays) at ambient and elevated temperatures. Some of the methods and tests are described in ASTM Standards G34 (EXCO), G43 (SWAAT), and G66 (ASSET).

Stress-Corrosion Cracking

Under the combined action of a continuous tensile stress and a specific corrosive environment, rupture of some aluminum alloy members may occur by stress-corrosion cracking (SCC). In cases of extreme susceptibility, the rupture of thick sections of 13 mm (0.5 in.) can occur in a short time (days). Stress-corrosion cracking is limited to aluminum-copper-magnesium alloys (2XXX) and aluminum-magnesium alloys (5XXX) that contain more than 3% magnesium, and aluminum-zinc-magnesium-copper alloys (7XXX series). On very rare occasions, SCC occurs in the aluminum-magnesium-silicon alloys (6XXX). It does not occur in commercial-purity alloys (1XXX), aluminum-manganese alloys (3XXX), or aluminum-magnesium alloys (5XXX) containing less than 3% magnesium. Table 3 presents a summary of SCC ratings of the different alloy families.

When stressed in the longitudinal or transverse directions, SCC may occur when stresses in the order of the yield stress are present. However, when stressed in the short transverse direction, for example across the flash line of a forging, SCC can occur at low stresses. Usually a chloride-containing aggressive environment must be present, but in cases of extreme susceptibility, SCC can occur in humid air.

The susceptibility of aluminum alloys to SCC depends on microstructure, and the resistance of susceptible alloys can be greatly influenced by metallurgical treatment. The attack is usually intergranular and involves the presence of an active constituent in the grain boundaries. Recently, hydrogen embrittlement caused by grain boundary local cell corrosion reactions has been shown to play an important role, especially for aluminum-zinc-magnesium-copper and aluminum-magnesium alloys.

Historical. The first failures of aluminum alloys by SCC were noted in the early 1930's (Ref 93)*. Most of these early failures occurred in aluminum-copper-magnesium (2XXX) aircraft alloys. A number of papers have discussed these failures over the years. These alloys were generally susceptible to intergranular corrosion in the peak strength tempers,

*For the pre-1970 period, only review articles have been referenced. These reviews contain extensive citations, to which the reader should refer if more specific or detailed information is desired.

Table 3. Ratings of Resistance to Stress Corrosion Cracking (SCC) of Wrought Commercial Aluminum Alloys (Ref 121)

Alloy series	Type of alloy	Strengthening method	Tensile strength MPa	Tensile strength ksi	SCC rating
1XXX	Al	Cold working	69–172	10–25	(a)
2XXX	Al-Cu-Mg-Si (3–6% Cu)	Heat treatment	379–517	55–75	(b)
3XXX	Al-Mn-Mg	Cold working	138–276	20–40	(a)
5XXX	Al-Mg (1–2.5% Mg)	Cold working	138–290	20–42	(a)
5XXX	Al-Mg-Mn (3–6% Mg)	Cold working	290–379	42–55	(b)
6XXX	Al-Mg-Si	Heat treatment	152–379	22–55	(a)
7XXX	Al-Zn-Mg	Heat treatment	379–503	55–73	(b)
7XXX	Al-Zn-Mg-Cu	Heat treatment	517–621	75–90	(b)

(a) No known instance of SCC in service or in laboratory tests. (b) SCC has occurred in service with certain alloys and tempers; service failures can be avoided by careful design and assembly and proper selection of alloy and temper.

and were quite susceptible to SCC as well. Generally, they have been replaced by more resistant alloys such as 2014, 2024, and 2124.

Today, the most widely used high-strength aluminum alloys are generally resistant to SCC in service when in the proper temper, but can still be made susceptible under highly specific circumstances. In particular, applied stresses in the short transverse direction should be minimized. However, these circumstances can usually be avoided, so that SCC failures of aluminum alloys can be prevented by design of the structure. A number of books and review articles have been published in recent years that outline in detail the required design principles (Ref 94-99). The following paragraphs describe the most important metallurgical and engineering principles that determine the SCC susceptibility of aluminum alloys.

Mechanism of Stress-Corrosion Cracking. Because SCC failures in aluminum alloys are generally intergranular, the microstructure along the grain boundaries plays a primary role in determining SCC susceptibility. In heat treatable alloys, selective grain boundary precipitation can result from a too-slow quench or from inadequate artificial aging. In non-heat-treatable aluminum-magnesium alloys, grain boundary precipitation can occur at modestly elevated temperatures. In all wrought alloys, SCC susceptibility is greatest in the plane where the most continuous grain boundary path is available. Figure 4 shows such an intergranular stress corrosion crack following the directional grain structure. For flat rolled products (sheet and plate), this situation occurs when stress is applied in the short transverse direction (normal to the rolling plane) and crack growth occurs in the rolling plane. For forgings and extrusions, the grain patterns are more complex, but maximum susceptibility occurs when stress is applied normal to the two principal grain flow directions, with crack growth occurring in the plane of metal flow.

Because of the orientation dependence of SCC in aluminum alloys, stresses in the most susceptible direction must be avoided. In addition to operating stresses, SCC can result from residual forming stresses, stresses introduced by machining operations, and stresses from misfit of parts being assembled. It is these residual stresses, rather than operating stresses, that are most often responsible for SCC failure, because they may be overlooked during the design process. Reducing stresses in the short trans-

Fig. 4. Typical intergranular stress corrosion crack in 6.4-mm (0.25-in.) 7075-T651 plate stressed in short transverse direction. (Courtesy of Alcoa Laboratories)

verse direction to a minimum greatly reduces the likelihood of SCC failure in susceptible alloys.

For years, the mechanism of SCC in aluminum alloys was believed to be mainly electrochemical (Ref 93-95). In the 1960's, hydrogen embrittlement (HE) of grain boundaries was found to play a major role in the SCC of high-strength steels and titanium. As late as 1969, no such mechanism appeared to play a role in the SCC of aluminum alloys (Ref 94). However, in 1974, reports (Ref 100 and 101) showed that while hydrogen is unable to enter 7075 alloy cathodically protected at −1.5 V saturated calomel electrode (SCE) at a sufficient rate to cause HE, at −2.0 V SCE the hydrogen permeation rate rises substantially, and at such a potential

SCC occurred. Later, it was found that atomic hydrogen is absorbed by aluminum and causes embrittlement of certain aluminum alloys (Ref 102). Others (Ref 103 and 104) have confirmed the role of hydrogen in the SCC of aluminum-zinc-magnesium-copper alloys. In 1980, it was found (Ref 105) that magnesium hydride formation can occur in an aluminum-magnesium alloy during exposure to moist air. Others (Ref 106) have shown that the change in SCC susceptibility of aluminum-zinc-magnesium alloys may be related to the magnesium content of the surface oxide film, which can affect the ease of hydrogen entry into the metal. While the SCC of aluminum-copper-magnesium alloys is believed to proceed by simple stress-assisted grain boundary local cell dissolution, recent research suggests that cracking in aluminum-magnesium and aluminum-zinc-magnesium-copper alloys may in fact be because of hydrogen embrittlement, as a result of hydrogen generated at the crack tip.

Aluminum-Copper-Magnesium Alloys (2XXX). The 2XXX series alloys are strengthened primarily by solution heat treatment and age hardening, with silicon and manganese often added for increased strength. Maximum strengthening is obtained when the copper content is between 4 and 6%, depending on the influence of other elements present. After solution heat treatment and quenching, these alloys can be strengthened either by natural aging (at room temperature) to the T3 or T4 tempers, or by artificial aging (at elevated temperature) to the T6 or T8 tempers. The strengthening sequence involves the formation of transition precipitates in the grain bodies. During this sequence, the equilibrium $CuAl_2$ or Al_2CuMg precipitates also form at the grain boundaries, creating a copper-depleted zone at the boundaries. The susceptibility of the alloy to

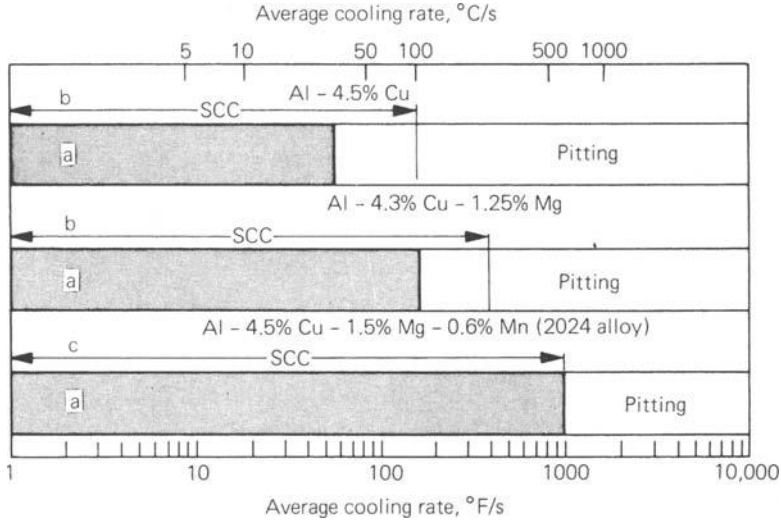

Fig. 5. Effect of cooling rate during quenching between 400 to 315 °C (750 to 600 °F) on susceptibility to intergranular corrosion and stress corrosion cracking. (a) Darkened area is susceptible to intergranular corrosion in NaCl—H_2O_2 solution. SCC tests in 3.5% NaCl alternate immersion (10/50 min cycle). (b) Ketcham—C-rings from 32-mm (1.25-in.) forged bar. (c) Lifka-Preformed sheet specimens.

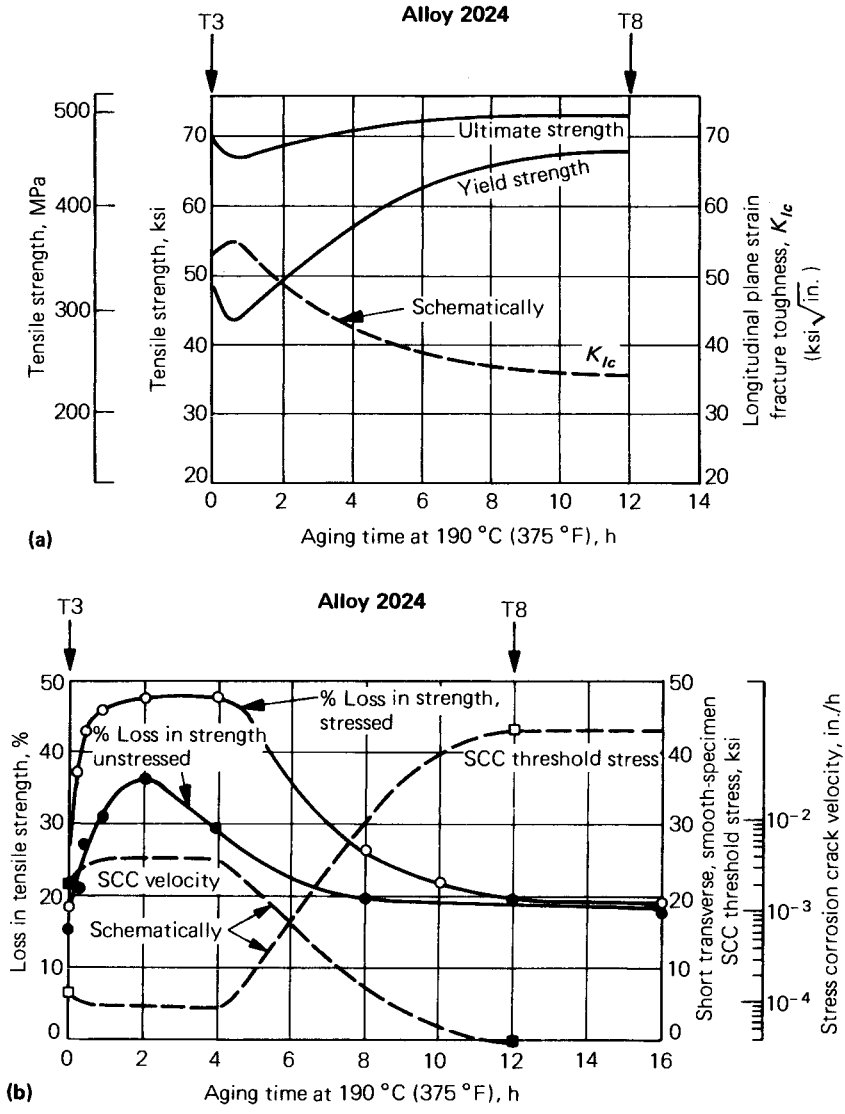

Fig. 6. (a) Effects of artificial aging on the mechanical and fracture properties of alloy 2024. The T3 and T8 tempers are indicated by arrows. (b) Effects of artificial aging on the corrosion and stress-corrosion properties of alloy 2024 in NaCl solution. The T3 and T8 tempers are indicated by arrows.

both intergranular corrosion and SCC depends on the magnitude of the corrosion potential differences between the grain boundary precipitates, the depleted zone, and the grain matrix.

The most commonly used aluminum-copper-magnesium alloys are 2014 and 2024. Both alloys contain both magnesium and manganese, with silicon added to 2014 to enhance aging response. Other widely used alloys include 2011, an aluminum-copper-bismuth-lead alloy noted for its machinability, and 2219, an aluminum-copper-manganese-zirconium-vana-

dium alloy with good weldability. In all these alloys in naturally aged tempers, SCC resistance shows a strong dependence on quenching rate. Figure 5 shows how both SCC and intergranular corrosion resistance of the as-quenched tempers increase with quenching rate (Ref 94). Although in naturally aged material, moderate intergranular corrosion susceptibility does indicate SCC susceptibility, in artificially aged material intergranular corrosion can occur in aged material possessing good SCC resistance. In the naturally aged condition, aluminum-copper-magnesium alloys have moderate SCC resistance. They are often used in this condition because of their relatively high ductility and fracture toughness. While SCC resistance initially decreases substantially with short artificial aging times, it increases to a level equal to or better than naturally aged material, as full aging is approached (Fig. 6). This effect occurs as precipitation in the grain bodies become more complete, and the amount of copper in solid solution diminishes, reducing the corrosion potential difference between the grain bodies and the copper-depleted zone at the grain boundaries.

Aluminum-Magnesium Alloys (5XXX). Unlike aluminum-copper-magnesium alloys, aluminum-magnesium alloys do not gain significant strength because of precipitation hardening. These alloys are used in strain-hardened (H) tempers. However, in the work-hardened condition, selective grain boundary precipitation may occur during long-term ambient temperature or short-term elevated temperature exposure and cause SCC susceptibility. Normally, this effect is restricted to alloys 5182, 5083, 5086, 5154, 5356, and 5456, which contain more than about 3% magnesium. The precipitation reaction is slow at room temperature, but prior cold work or exposure to elevated temperatures accelerates precipitation significantly. The beta-phase (Mg_2Al_3) precipitate that forms is highly anodic to the aluminum-magnesium matrix, and the formation of a continuous grain boundary network of beta-phase precipitate produces susceptibility to SCC.

In general, the most detrimental precipitate structures form at room temperature in heavily cold worked material over a number of years, or after prolonged exposure to slightly elevated temperatures of 66 to 180 °C (150 to 350 °F), as shown in Fig. 7. Exposure to higher temperatures results in a coarsening of the precipitates, producing a discontinuous grain boundary precipitate structure and reducing or eliminating SCC susceptibility.

Aluminum-magnesium-silicon alloys (6XXX) are medium-strength, heat treatable alloys that generally possess excellent SCC resistance. They are strengthened primarily by the aging precipitate Mg_2Si. The most commonly used alloy, 6061, contains a stoichiometric balance of magnesium and silicon to form Mg_2Si. Excess silicon is added to other alloys for increased strength, but the excess silicon alloys can be rendered more susceptible to SCC by improper heat treatments. Confirmed service SCC failures of 6XXX-series alloys are rare, despite the fact that these alloys may be susceptible to intergranular corrosion in the T4 and T6 tempers. However, laboratory SCC tests on naturally aged 6061-T4 samples that had been exposed to abnormally high solution heat treat temperatures, followed by a slow quench, did produce failure. This sensitivity can be eliminated by aging to T6 temper. As a rule, SCC can be prevented by

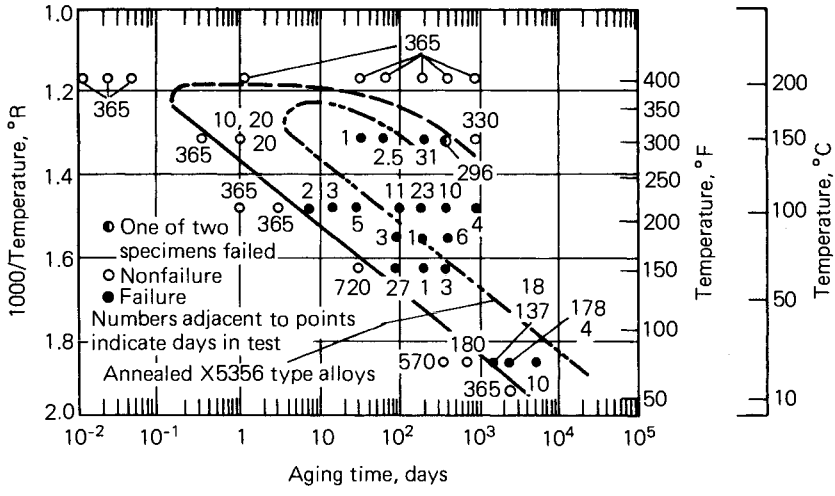

Fig. 7. Approximate time required to sensitize strain hardened X5356-type alloys to stress corrosion cracking. Composition: 5.15% magnesium, 0.03% copper, 0.22% iron, 0.11% silicon, 0.11% manganese, 0.10% chromium, and 0.10% titanium.

avoiding both higher-than-recommended solution heat treat temperatures and slow quenches.

Aluminum-Zinc-Magnesium and Aluminum-Zinc-Magnesium-Copper Alloys (7XXX). The three classes of 7XXX series alloys are the binary aluminum-zinc cladding alloys, the medium-strength aluminum-zinc-magnesium alloys that contain less than 1% copper, and the high-strength aluminum-zinc-magnesium-copper alloys that are used in the aerospace industry. The medium- and high-strength 7XXX series alloys gain strength by solution heat treatment, quenching, and artificial aging through a complex sequence of reactions that finally produce the stable precipitates $MgZn_2$ and $Mg_3Zn_3Al_2$ (Ref 94 and 107-109). Up to 3% copper is added in some alloys for higher strength, however, such additions of copper must be limited if weldability and general corrosion resistance are desired. Small amounts of manganese, chromium, and zirconium are usually added to control recrystallization and preserve the highly directional wrought grain structure in wrought alloys. This effect is highly desirable for SCC resistance, because it is extremely difficult to propagate intergranular SCC cracks perpendicular to a highly elongated grain structure.

The higher strength, copper-containing alloys (such as 7049, 7050, 7178, and 7075) are quite susceptible to short transverse SCC in the underaged (W) and peak-aged (T6) temper. This generally limits the application of T6 temper alloys to structures in which there is no conceivable source of short transverse stress. To minimize SCC susceptibility, overaging treatments are utilized at some sacrifice of tensile strength. Various overaged (T7) tempers are available that offer a range of combinations of SCC resistance and tensile strength, as shown in Fig. 8. For alloys in the peak aged temper, a rapid quench following solution heat treatment provides

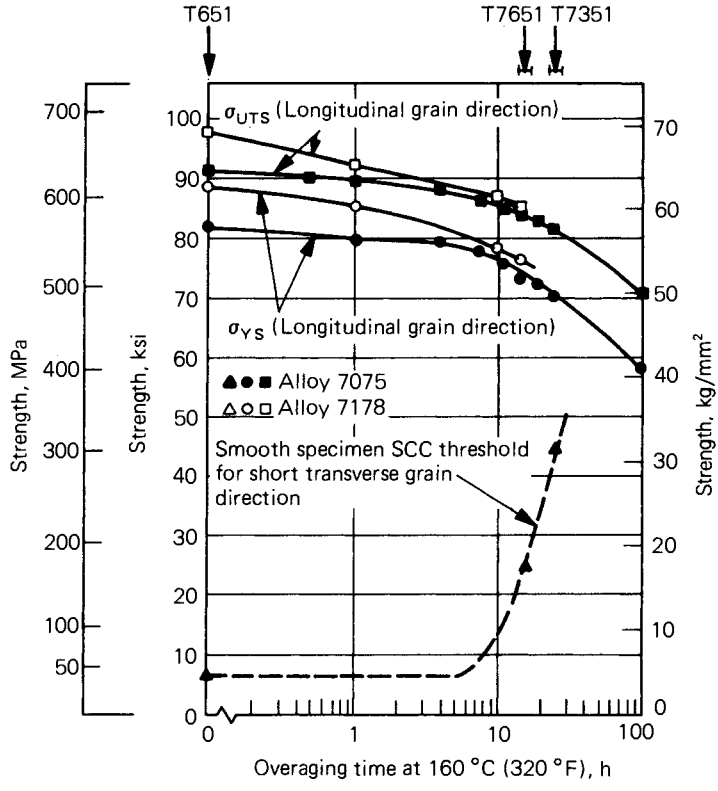

Fig. 8. Effect of artificial aging at 160 °C (320 °F) on the strength and smooth-specimen SCC threshold of 7075-T651 and 7178-T651. The T651, T7651, and T7351 tempers are indicated with arrows.

increased SCC resistance. Among these alloys, SCC resistance varies with copper content and zinc-magnesium ratio, and also with the zirconium, chromium, and manganese content. Slow quenching 7075, the most widely used alloy, causes poor resistance to SCC. Improvements in thick-section SCC have been realized with alloys 7049 and 7050, through increased zinc-magnesium ratio and through zirconium additions to reduce susceptibility of 7050 to SCC caused by slow quenching. However, increasing the zinc-magnesium ratio above 3 can be detrimental to SCC resistance (Ref 110).

Medium-strength, low-copper, and copper-free 7XXX alloys have been developed for a variety of engineering properties. Armor plate alloy 7039, a higher strength copper-free weldable alloy, suffers from poor SCC resistance in the short transverse direction. Its successful use is predicated on controlling short transverse stresses and through the use of weld overlays. Alloy 7021 (with <0.25% copper), offers improved SCC resistance in sheet form, because zirconium additions prevent recrystallization. For these medium-strength 7XXX alloys, a zinc-magnesium ratio of around 2.7 provides maximum SCC resistance (Ref 110). Alloys 7016 and 7029, with a higher copper content (≈0.5 to 1.0%), have good formability and

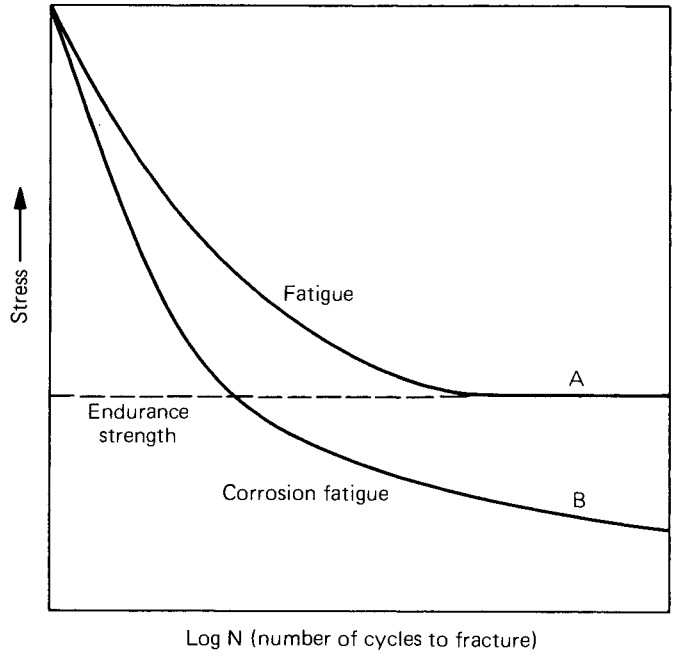

Fig. 9. Typical fatigue and corrosion fatigue curves.

finishing properties in extruded forms for automotive applications. Maximum SCC resistance is obtained by forming in the freshly quenched (W) temper followed by a two-step aging treatment, but because these alloys recrystallize during extrusion, they may be still susceptible to SCC.

Aluminum alloys are commonly tested for resistance to SCC by standard laboratory tests (Ref 111). The literature contains the results of many studies (Ref 96, 112, and 113). Recently, a new rapid testing method has been proposed (Ref 114).

Corrosion Fatigue. To explain corrosion fatigue, the fatigue failure of metals must first be introduced. Fatigue is the rupture of metal by a purely physical mechanism, as a result of the repeated application of a cyclic stress. As the magnitude of the stress increases, the time to failure is reduced. A stress life curve (S/N) is conventionally plotted for a metal such as that shown in curve A of Fig. 9, with stress plotted against the logarithm of the number of cycles of stress (Ref 115). The curve levels off and the stress level below which failure does not occur for a specified large number of cycles is called the fatigue endurance strength.

In the presence of a corrosive environment, the S/N curve (now called a corrosion fatigue curve) is lowered. Thus, corrosion fatigue is defined as failure of metal under the combined action of cyclic stress and a corrosive environment. In this case, the slope of the S/N curve lessens, but does not level off, as shown in curve B of Fig. 9. A maximum stress that a metal can withstand without failure for a specific number of stress cycles of defined frequency and amplitude in a specific corrosive environment must be determined. The damage caused is greater than might occur from the separate actions of fatigue and corrosion (Ref 116).

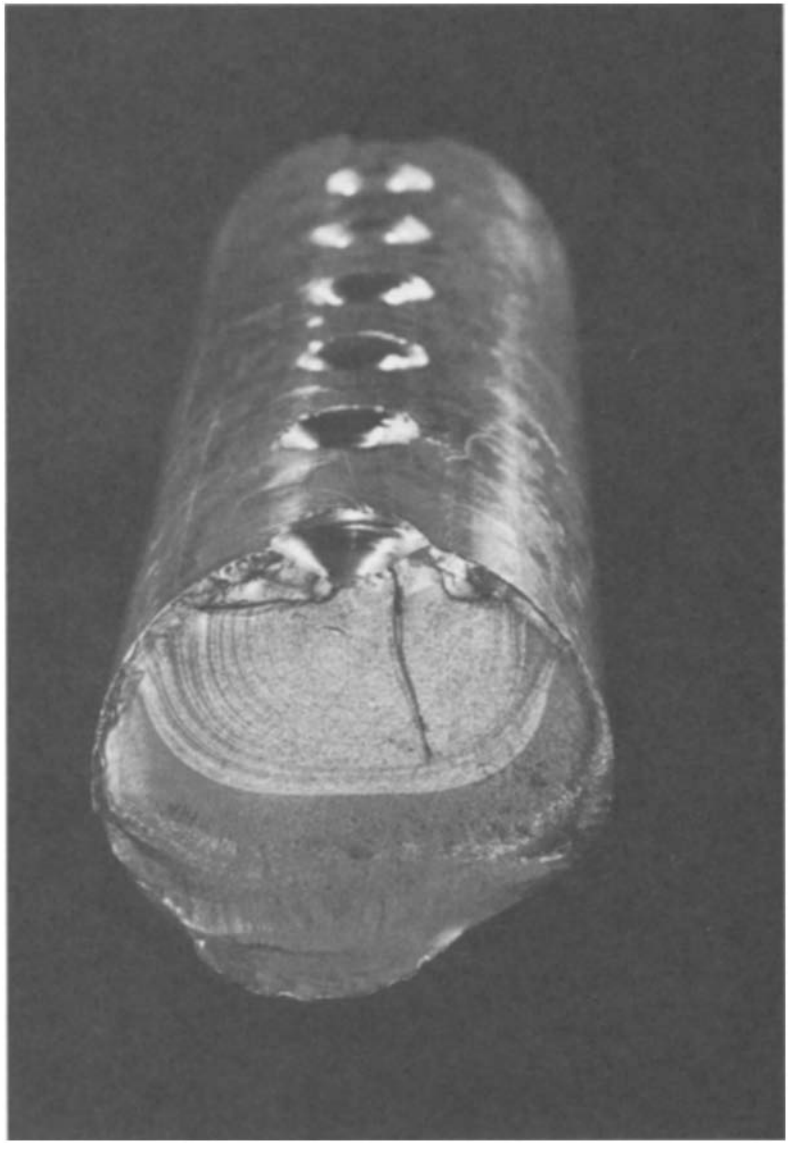

Fig. 10. Oyster shell markings on fatigue failure fractured surface from a 2024 alloy shaft, from a spool used to coil papers. Fatigue checks initiated from each of the shallow reference holes used to position flanges on the shaft. (Courtesy of Alcan International, Kingston Laboratory)

Fatigue (and corrosion fatigue) failures can be recognized by a characteristic oyster shell pattern on the fractured surfaces (Fig. 10) and by evidence of brittle fracture (lack of metal flow adjacent to the fracture). It is usually not possible to distinguish between corrosion fatigue and normal fatigue by examination of the fractured surfaces.

Fatigue tests are carried out in ambient air with laboratory apparatus that subjects a selected shape of metal specimen to cyclic stress. The cyclic stress may be axial, torsional, or reverse bending. When testing polished cylindrical specimens rotating under flex in a Moore machine, the stress that just does not cause failure at 500×10^6 cycles is taken. For sheet specimens subjected to reverse bending in a Krouse machine, the value is usually taken for survival at 50×10^6 cycles.

Corrosion fatigue tests are carried out with the same apparatus, with provisions made to subject the specimen to a corrosive environment by spraying or dripping a solution onto the specimen, creating a mist in an enclosure about the specimen, or immersing the specimen in a solution. The corrosive environments used most frequently are distilled or demineralized water, tap water, and brines (including natural or synthetic seawater). Because of the complexity of service environments, a good correlation of normal laboratory corrosion fatigue data with actual service performance is difficult (Ref 116). When fail-safe service is desired, corrosion fatigue tests should be made under cyclic loading conditions that replicate service (spectrum loading), in a corrosive environment that is representative of service conditions before the alloys are placed into service.

Aluminum alloys, like many steels, have relatively low corrosion fatigue strengths—about half the fatigue strength in air and a quarter of the original ultimate strength of the material. Surprisingly, the corrosion fatigue strength of an alloy is not greatly affected by variations in heat treatment, even in the case of aluminum-copper-magnesium (2XXX), aluminum-magnesium-silicon (6XXX), and aluminum-zinc-magnesium-copper (7XXX) alloys. Corrosion fatigue failures of aluminum alloys are characteristically transgranular, and thus differ from SCC failures, which are normally intergranular. Localized corrosion of an aluminum surface, such as pitting or intergranular corrosion, provides stress risers and greatly lowers fatigue life (Ref 117-119).

In air, relative humidity has a small effect on the corrosion fatigue life of aluminum alloys. At very low values (<5% relative humidity), however, fatigue life increases modestly. Laboratory corrosion fatigue tests indicate that the presence of water on the cycling specimen surface markedly lowers the fatigue life obtained. The fatigue strength obtained in demineralized water, hard tap water, or brine solutions show little real difference. This is surprising because the normal corrosivity of these waters to aluminum varies considerably.

Little work has been done on the role of metallurgical variables on corrosion fatigue resistance. It cannot be assumed that alloys and tempers with good SCC resistance show good resistance to corrosion fatigue. However, the beneficial effect of copper in SCC of 7XXX series alloys is known, and increased copper content in these alloys also increases corrosion fatigue resistance (Ref 120). Also, although 7075-T6 has longer fatigue lifetimes in air than 7075-T73, lifetimes are almost identical in 0.5N NaCl solution (Ref 121). This result indicates a slightly greater environmental sensitivity in the T6 temper; however, the environmental contribution is quite large in either case.

Peening the metal surface increases fatigue life (Ref 122 and 123) and probably increases corrosion fatigue life as well. Care must be taken not to overpeen the surface to the extent where excessive plastic deformation

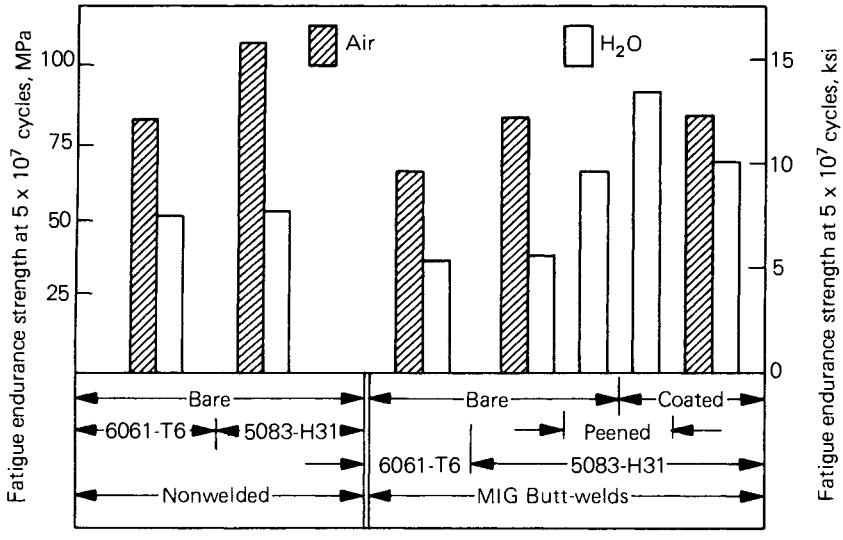

Coated ..... Chromate etch primer plus a two-component aluminum-pigmented epoxy top coat
Peened ..... Brush shot-peened to Almen 6 level, as described in Ref 123
Air ..... Tests done in normal room environment
Water ..... Tests done with the surface of the test piece wet. Results are similar regardless of whether wetting was with demineralized water, hard (tap) water, or a 3% brine solution

Fig. 11. Krouse reversed bending fatigue tests. (Courtesy of Alcan International, Kingston Laboratory)

may cause susceptibility to exfoliation or SCC. Protective surface coatings are also beneficial (Ref 118 and 124). Welding lowers both fatigue and corrosion fatigue life, but peening after welding increases the corrosion fatigue life. Paint coating also increases the corrosion fatigue life, and the highest corrosion fatigue life for welded specimens is achieved by peening followed by coating. These relationships are shown in Fig. 11.

Corrosion fatigue data have been reported by Takeuchi (Ref 119 and 125) on aluminum-magnesium, aluminum-magnesium-silicon, and 7075-T6 alloys. Other reports have been made by Cole and Payne (Ref 124), Lorkovic *et al* (Ref 126) on 2XXX and 7XXX, Biefer (Ref 127) on 6061-T6 alloy, and Stoltz and Pelloux (Ref 128) on aluminum-zinc-magnesium-copper alloy. Stoltz and Pelloux (Ref 128) and LeBeau (Ref 129) have studied the influence of cathodic protection on corrosion fatigue life. Khobaib *et al* (Ref 130) have reported on the development of an inhibitor for corrosion fatigue of high-strength aluminum alloys. Some guidelines for selecting aluminum alloys to minimize failure problems have been outlined by Bucci (Ref 131).

Cavitation, Impingement, and Erosion-Corrosion

Cavitation damage to aluminum can occur in the presence of a turbulent liquid. It takes the form of pitting, which can be sufficiently dense to cause roughening of the surface. During turbulence, voids form and

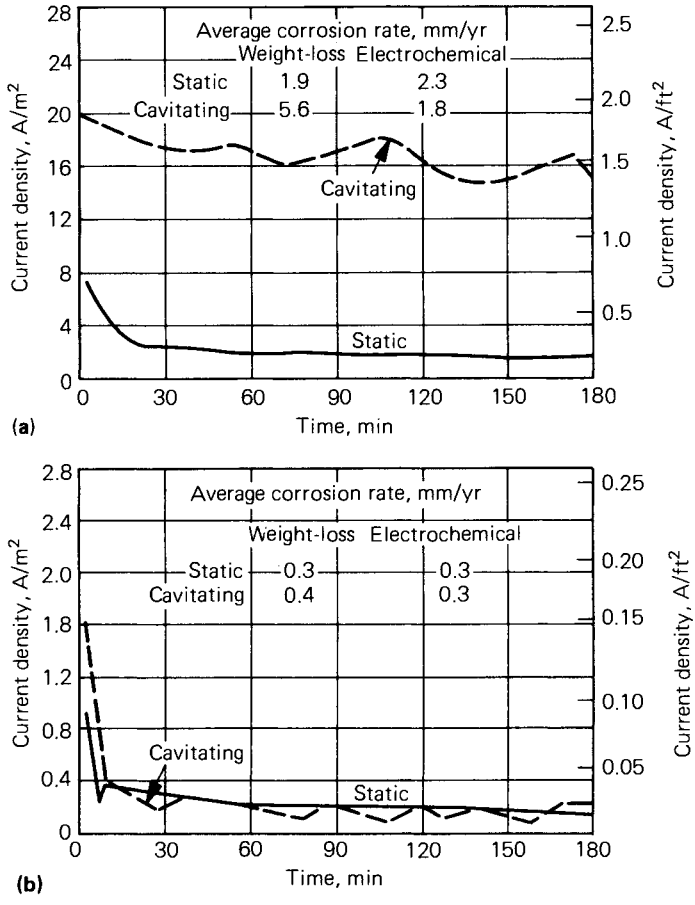

Fig. 12. Corrosion current versus time curves under potentiostatic control at −0.60 V relative to a calomel electrode. (a) Poorly-inhibited coolant. (b) Well-inhibited coolant. (Ref 135)

collapse, releasing bursts of energy. If these are released at the metal surface, they may break the protective surface oxide film and initiate a pit. In time, the bursts of energy may work harden the surface to the point where corrosion fatigue occurs, and bits of metal may be knocked from the surface by mechanical action. Thus, cavitation damage may be the result of corrosion or of mechanical action, or the two acting together. In mild cases of cavitation, chemical action probably predominates and can be prevented by cathodic protection. In more severe cases, mechanical action probably predominates and cannot be prevented by cathodic protection. When mechanical action predominates, damage can be prevented only by eliminating the cavitation condition through altering the design of the equipment. A review of the subject has been published by Wheeler (Ref 132). Mousson (Ref 133) has reported a limited amount of data on the cavitation of aluminum alloys.

An ASTM test (Ref 134) measures the combined effects of cavitation and erosion on automotive water pumps. This test can be used either to

evaluate pump materials, or the ability of a coolant formulation to prevent metal loss. Chance (Ref 135) has studied cavitation of 319 cast aluminum alloy in both inhibited and noninhibited coolants. In a poorly-inhibited coolant (Fig. 12), the metal loss was three times that calculated from the measured current output, which suggests mechanical removal of metal. In contrast, in a well-inhibited coolant the weight loss and metal loss calculated from the measured current output agreed fairly closely.

Impingement attack, which is related to cavitation damage and may occur with it, takes the form of pitting and is caused by a stream of moving liquid striking a metal surface at an angle. The impinging stream may exist submerged in a liquid system. Entrained air bubbles accelerate this action. There are few data in the literature on the impingement resistance of aluminum, but it is probably low compared to that of other metals.

A stream of high-pressure steam striking an aluminum surface, for example at a "tee" in an aluminum piping system, erodes a hole at the point of impingement. Impinging streams of liquids in heat exchangers have been known to erode holes in aluminum baffle plates and heat exchange tubing.

Brazed aluminum automobile radiators can fail by impingement, because of high coolant velocity in the passages. Figure 13 shows erosion-corrosion channeling in a brazed 6951 aluminum radiator tube that perforated after 19,312 km (12,000 miles) of service. Anthony and Popplewell (Ref 136) have studied impingement corrosion of aluminum radiator alloys at velocities up to 40 m/s (130 ft/s). After the test, the area of impingement was shiny and surrounded by a black filmed area con-

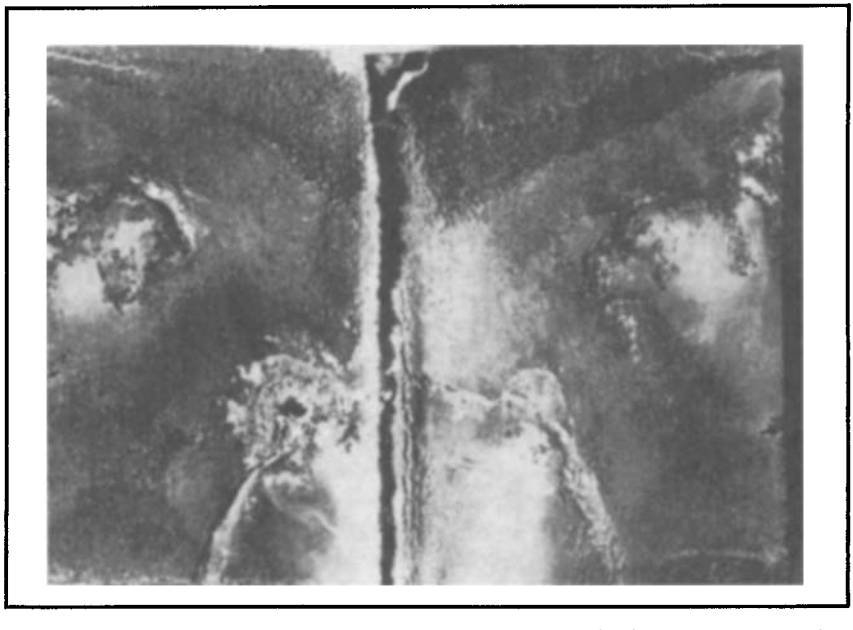

Fig. 13. Failure of a 6951 alloy automotive radiator tube by erosion corrosion channeling. (Ref 135)

taining particles of metallic copper. A local cell was created that deposited metallic copper (from traces in the coolant) at the cathode, around the impinged area that acted as the anode.

The damage to aluminum surfaces caused by the impingement of high-velocity water droplets has been studied (Ref 137 and 138), as a result of damage to military aircraft in rain squalls. At velocities of 90 to 148 m/s (295 to 486 ft/s); or 322 to 530 km/h (200 to 330 mph), failure can occur by ductile rupture of small particles or by removal of whole grains by intergranular fracture. Aircraft skin surfaces, vulnerable to rain impingement damage, are coated with protective coatings.

Erosion-Corrosion. When a liquid passing over an aluminum surface exceeds a certain velocity, grooves may be worn in the surface, the probable result of mechanical and chemical action. This phenomena does not usually occur on aluminum at velocities below 3 m/s (10 ft/s).

Gehring (Ref 139) studied attack on aluminum by high-velocity seawater, using the polarization resistance technique to estimate metal removal as well as weight loss. Typical data for 5456 alloy show that following a plateau of calculated, constant metal removal rate from 3 to 10 m/s (10 to 33 ft/s), the removal rate climbed rapidly at higher velocities. Weight losses were an order of magnitude higher than those calculated from the polarization resistance measurements, suggesting a mechanical influence, as found by Chance (Ref 135) in poorly-inhibited automotive coolant.

The foregoing paragraphs indicate that all three forms of attack are similar and may occur together. They have a common mechanism—damage to the surface oxide film by mechanical action, followed by localized corrosion. The loss of metal by corrosion may be accompanied by mechanical property loss by either fatigue or erosion.

The adverse effects of cavitation, impingement, and erosion-corrosion can be minimized in various ways. Cavitation in automotive water pumps is minimized if the coolant contains an adequate inhibitor system. Scale lodgement in aluminum radiators that causes perforation by corrosion channeling can be minimized by improved radiator design and an adequate inhibitor system. For example, circular cross-sectional tubes are not subject to scale lodgement. Aluminum hulls of high-speed surface effect ships require cathodic protection. Impressed current systems that avoid overprotection have been developed by the U.S. Navy (Ref 140 and 141) and others.

Fretting corrosion is a wear process that produces small abraded spots on mating aluminum surfaces in pressure contact that slip relative to one another under the influence of vibratory motion. Fretting can develop even in the complete absence of foreign matter or grit. The mating surfaces show a matching pattern of abraded spots with similar contours. The spots resemble shallow pits that contain a black powder and resemble cinders embedded in the surface. The black powder is finely divided aluminum oxide, such as corundum, which is produced only at very high temperatures (Ref 142) by dry oxidation during the rubbing.

Fretting corrosion occurs most frequently during shipment of packages of sheet or circles by truck, and is sometimes called traffic damage or traffic marking. Fretting corrosion has also been observed on loosely packed

tubing after shipment. Susceptibility increases with the degree of polish of the surface. The damage is minimized by pressure packaging, which prevents relative movement within the package. Oiling and paper interleaving are also beneficial. Anodizing the aluminum also greatly reduces fretting damage.

Fretting corrosion has been observed on heat exchanger tubes at tube supports and at bolted or riveted joints in structures such as truck bodies. The condition appears to be more likely to develop when aluminum contacts aluminum rather than when aluminum contacts a dissimilar metal. In service, this type of damage has been controlled by changes in design. For example, in heat exchangers, the baffle supports can be relocated, the hole size enlarged, the baffles increased in thickness, or the tube bent or sprung into position to prevent or minimize vibration. In riveted lap joints, precautions should be taken to ensure that the pressure between the components is sufficient to prevent slippage. In pinned connections, an effort should be made to displace the fretted area away from the region of maximum stress. The abraded spots reduce the fatigue properties of the affected parts.

Measurement of fretting corrosion can be carried out by a push-pull type of fatigue machine to which a device is attached to produce simultaneous fretting wear. An excellent treatise of this subject has been provided by Waterhouse (Ref 143).

INFLUENCE OF MICROSTRUCTURE ON CORROSION

The microstructure of an aluminum product determines whether localized corrosion will occur because of metallurgical causes (as opposed to environmental causes). Microstructure is affected by alloy composition, the practices used in the plant to produce the alloy, and also by subsequent mechanical and thermal treatments used to fabricate the final product. The following paragraphs point out the more important metallurgical factors that influence microstructure and susceptiblity to localized corrosion.

Alloy Constituents. The composition of microconstituents, their size, quantity, location, continuity, and corrosion potential relative to that of the adjacent aluminum solid solution matrix, are the important aspects of microstructure that affect corrosion behavior (Ref 144).

Iron and silicon are present as normal impurities in aluminum alloys. They form constituents ($FeAl_3$, $\alpha AlMnSi$, silicon, and others) that are cathodic to the aluminum matrix. When these are present in the surface, the oxide film over them is thin or nonexistent. The local cells produced by these impurities promote pitting attack of the surface in a conductive liquid. The fact that high-purity aluminum (1095) contains only a small number of these consitutents, and that they are small in size, explains in part the high resistance to localized corrosion of high-purity metal (Ref 144 and 145). The effects of alloying elements on the corrosion resistance of commercial alloys are varied, depending on whether they are in solid solution, or present as second-phase precipitates distributed throughout the matrix, or segregated at grain boundaries.

Copper reduces the corrosion resistance of aluminum to a greater extent than any other alloying element. The influence of copper is highly dependent upon its amount, form, and distribution throughout the micro-

structure. In solid solution, copper shifts the corrosion potential of aluminum in the cathodic direction, the value depending on the amount present. The corrosion potential is independent of the heat treating temperature if all the copper is in solid solution at the heat treating temperature. The amount of copper in an aluminum-copper solid solution can be determined by standard electrode potential measurements.

Manganese and aluminum form a compound ($MnAl_6$) that has almost the same electrode potential as aluminum; the aluminum-manganese alloys have good corrosion resistance and were the earliest to be used for cooking utensils, chemical equipment, and architectural products requiring high resistance to corrosion. Chromium in solid solution has little effect on the corrosion potential of aluminum. Although used only as a minor alloying element, chromium is particularly valuable in improving the resistance to SCC of several types of aluminum alloys. Aluminum-silicon alloys are corrosion resistant. Silicon in solid solution has little effect on the corrosion potential of aluminum. However, the elemental silicon constituent is cathodic to aluminum.

In aluminum-magnesium alloys, the solid solution is more anodic than aluminum. The magnesium in excess of that in solid solution forms a constituent (Mg_2Al_3) that is anodic to the aluminum-magnesium solid solution. Under some conditions, this constituent may precipitate in generally continuous zones either at grain boundaries or along slip planes caused by plastic deformation. In a corrosive environment, the anodic constituent corrodes electrochemically, producing a highly selective attack that can be predicted qualitatively by potential measurements (Ref 146) and by weight loss (ASTM-G-67). Extensive, random precipitation throughout the grain body, achieved by metallurgical control, decreases the rate of localized attack on the constituents at grain boundaries and slip planes. As a result, alloys in this condition are generally as resistant as commercially pure aluminum and even more resistant to salt water and some alkaline solutions, such as sodium carbonates and amines.

In aluminum alloys, magnesium in solid solution tends to make the corrosion potential more anodic, while silicon in solid solution is more cathodic. When both are in solid solution in the ratio of Mg_2Si, the corrosion potential is essentially the same as that of aluminum. In solid solution, zinc shifts the corrosion potential of aluminum in the anodic direction. As a result, aluminum-zinc alloys are widely used as alclad coatings on aluminum alloys and as galvanic anodes in seawater for cathodic protection of steel ship hulls, ballast tanks, and off-shore oilfield structures.

Nickel and aluminum form a strongly cathodic constituent ($NiAl_3$) that usually has an adverse effect on the corrosion resistance of aluminum alloys. Nickel is used mainly in alloys that require high strength and hardness at elevated temperatures; in these applications, for example, pistons, corrosion resistance is of minor importance.

Titanium forms a constituent $TiAl_3$, that although cathodic to aluminum, does not have a detrimental effect on corrosion resistance in the small amounts used in aluminum alloys. Tin, bismuth, and lead do not form intermetallic compounds, but are cathodic in aluminum alloys. Bismuth and lead are used in free-cutting alloys such as the aluminum-copper and magnesium-silicide types. Tin is an important element in aluminum

bearing alloys; these alloys resist the action of the breakdown products of lubricating oils.

Grain Size and Orientation. Variations in grain structure, such as differences in grain size and orientation, have only minor effects upon the corrosion resistance of aluminum, except in relatively thick sections, when grain orientation is a major factor in resistance to SCC. However, experiments on single crystals have shown that the difference in corrosion potential among faces of widely different orientation is extremely small.

In certain products, such as extrusions and die forgings of high-strength aluminum alloys, potential differences can exist between recrystallized and unrecrystallized portions of the grain structure. The large recrystallized grains forming the skin (surface layer) on these products usually are slightly cathodic (5 to 20 mV) to the underlying fragmented (unrecrystallized) grain stucture. Thus, evidence of preferential attack of the more anodic layer may be observed on machined surfaces and on edges.

The SCC susceptibility of wrought aluminum alloy products with highly directional grain structures is dependent on the orientation of the stress (Ref 147). These directional differences are most apparent in the more susceptible tempers, but are usually much lower in tempers produced by extended precipitation treatments (Ref 146, 148, and 149). Highly directional grain structures may be susceptible to exfoliation.

Metallurgical and Thermal Treatments. Metallurgical treatment of aluminum alloys to develop desired mechanical properties can also influence corrosion resistance. Thermal treatment and cold work determine the quantity and distribution of the constituents and the magnitude of residual stresses and are important influences on the type and rate of corrosion. The effect of commercial tempering procedures is described subsequently.

Variations in thermal treatments such as heat treating, quenching, and aging can have a marked effect on the localized corrosion resistance of aluminum alloys, particularly the higher strength alloys. Variations in thermal treatment from one portion of an alloy surface to another can result in differences in corrosion potentials between these areas and affect corrosion behavior. For example, fusion welding not only introduces a region of metal with a cast grain structure, but also creates a number of metallurgical and mechanical property changes in the parent metal in the heat-affected zone. Thermal treatments may produce residual stresses in a product. In some alloys and tempers, these stresses can cause SCC (Ref 150). In practice, most high-strength alloy products are stress-relieved to avoid such problems.

Effect of Cold Work. Cold work can influence the distribution of alloy constituents and the magnitude of residual stresses in some alloys. As a result, the type and rate of localized corrosion of an alloy can be greatly affected by the degree of cold work. The residual stress produced by cold working can lead to SCC of some strong alloys, as illustrated in Fig. 14. As another example, the resistance to SCC of aluminum-magnesium alloys (5XXX) can be changed significantly by the effect of cold work, in combination with natural aging, on the microstructure. Aluminum-magnesium alloy rivets should contain less than 3.0% magnesium, otherwise the heavily cold worked heads suffer SCC (Ref 150–152).

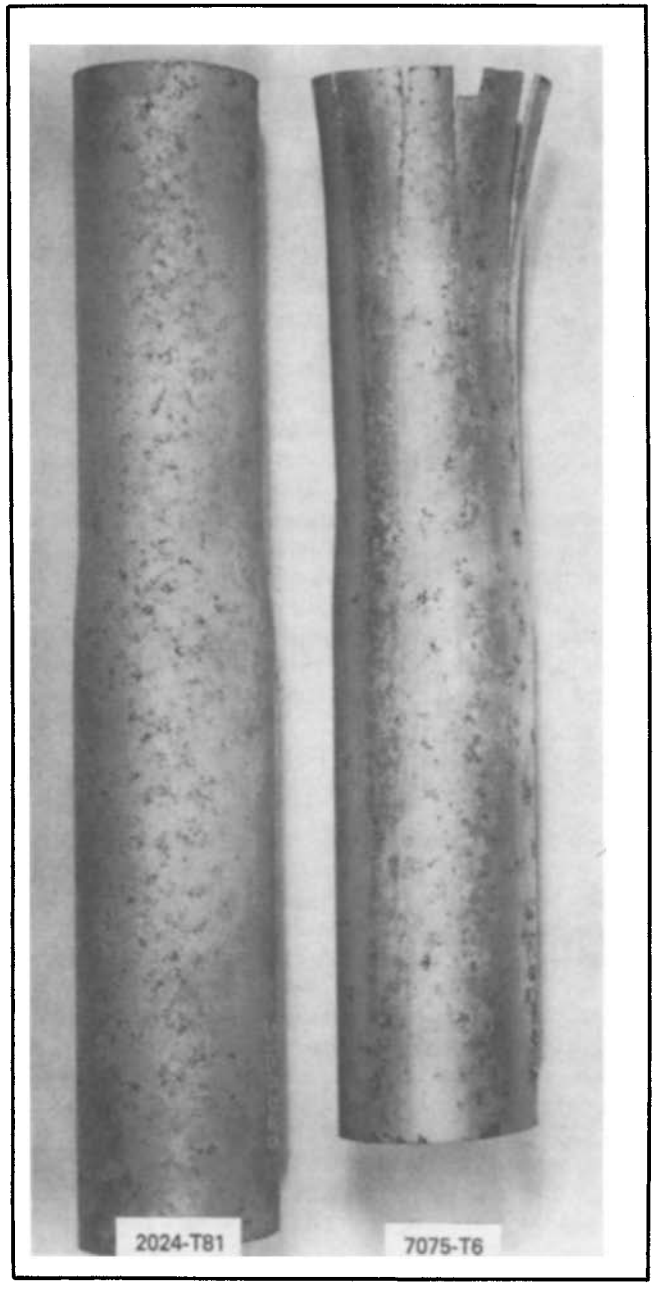

Fig. 14. Effects of cold working on the resistance of different alloys to SCC. Both drawn tubes were cold swaged and exposed for 3 months to intermittent 3.5% NaCl spray at ambient temperature. Stress-corrosion cracking occurred on the 7075-T6 samples, but not on 2024-T81 samples. (Courtesy of Alcoa Laboratories and the American Society for Metals)

Fabrication Effects. Fabrication procedures that produce torn, rough edges with attached metal fragments that have a large surface area-to-volume ratio may lead to increased corrosion. Because it is difficult for a continuous protective film to form over sharp edges, localized corrosion may develop in some environments. However, a greater danger associated with fabricating procedures such as shearing, punching, and forming is the possibility of creating high residual stresses leading to accelerated corosion; particularly to SCC in high-strength alloys. These potential problems should be given careful consideration before selection of any fabricating procedure. In many cases, the potential hazard can be avoided either by modification of the fabricating procedure, or by the use of the proper alloy and temper for the application intended (Ref 152).

Corrosion of Aluminum Joints. Methods of joining that do not involve heat, such as bolts, screws, threaded connections, cold riveting, pressure bonding, and adhesive bonding do not affect corrosion resistance, although attention may have to be paid to crevice corrosion of the assembly. Misalignment of stress-corrosion susceptible alloys must be avoided to prevent the introduction of assembly stresses. Methods that involve heat welding, brazing, and soldering can affect corrosion resistance. In brazing and soldering, alloy composition of the joint is changed appreciably and reduces corrosion resistance.

Fusion Welding. A variation in microstructure across the weld exists in fusion-welded aluminum. The central melted zone has a cast structure. On each side of this, there is a heat-affected zone, the width of which depends on the thickness of the material, the speed of welding, and the heat input from the arc. Gas (argon) shielded processes (such as MIG and TIG) are preferred to eliminate oxidation during the molten stage. A filler wire may be used (as in the MIG process), or the two parts may be melted together using an inert electrode (as in the TIG process). The filler wire may be the same alloy as the parts being joined, or may be specially selected.

The variation in microstructure and of corrosion potentials across a weld are shown in Fig. 15 for alloys 5456, 2219, and 7039. These differences can lead to localized corrosion under certain circumstances and in some environments, as demonstrated by corrosion of the HAZ of an as-welded structural member of 7005 alloy (Fig. 16). In general, the welding procedure that puts the least amount of heat into the metal has the least influence on microstructure and the least chance of reducing corrosion behavior of the weld (Ref 153).

Some alloy tempers are more suitable for welding than others. Further, some filler alloys are better than others from the standpoint of weldability and resistance to localized corrosion. Tables 4(a), (b), and (c) summarize the standard filler alloys recommended for welding various combinations of parent alloys to obtain maximum properties, including corrosion resistance. Tables 4(a) and (b) should be used together, while Table 4(c) can be used independently. With certain alloys, particularly those of the heat treatable 7XXX series, thermal treatment after welding is sometimes used to obtain maximum corrosion resistance, as shown in Fig. 16 (Ref 154 and 155).

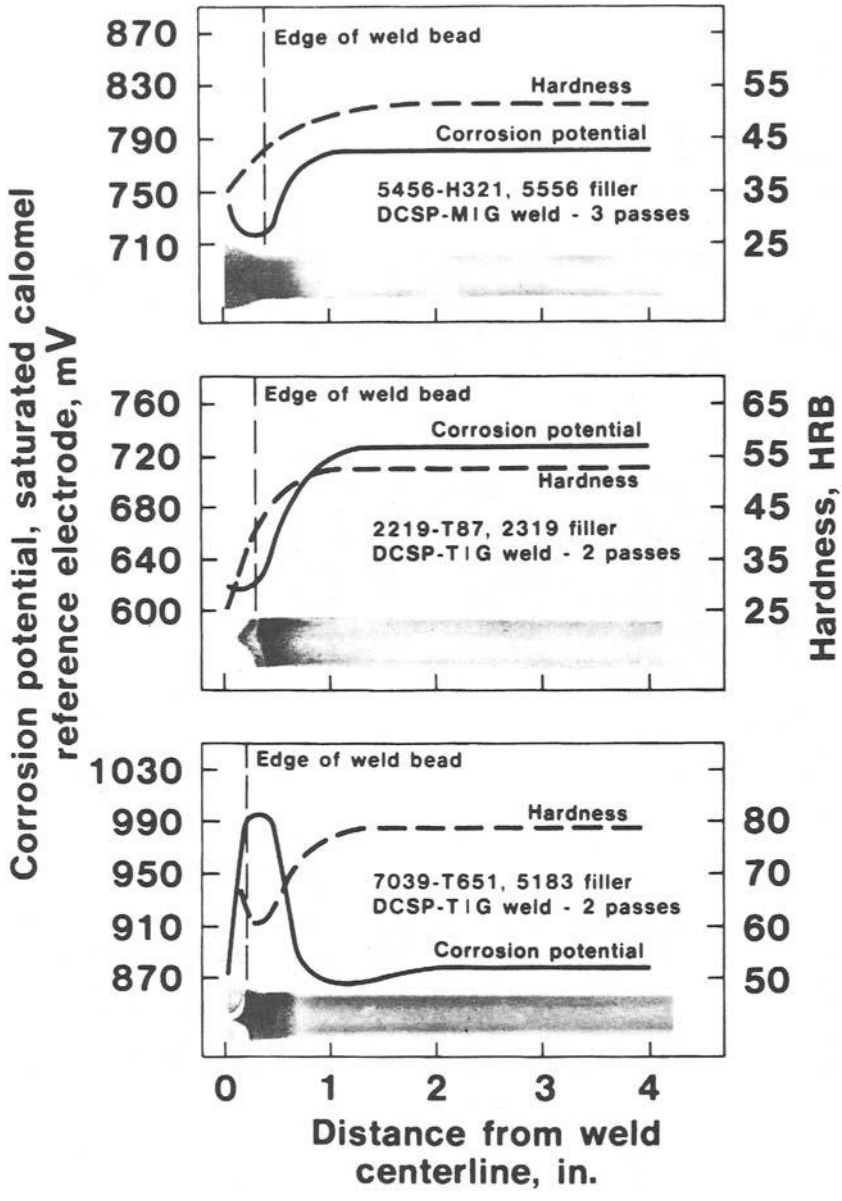

Fig. 15. Effect of the heat of welding on microstructure, hardness, and corrosion potential of welded assemblies of three alloys. The differences in corrosion potential between the HAZ and the parent alloy can lead to selective corrosion. (Courtesy of Alcoa Laboratories and the American Society for Metals)

If localized weld corrosion does occur, it may take the form of the preferential dissolution of the weld bead, or of preferential attack in the HAZ, depending on microstructure and the corrosion potentials of the constituents and matrices involved. Residual stresses are also developed

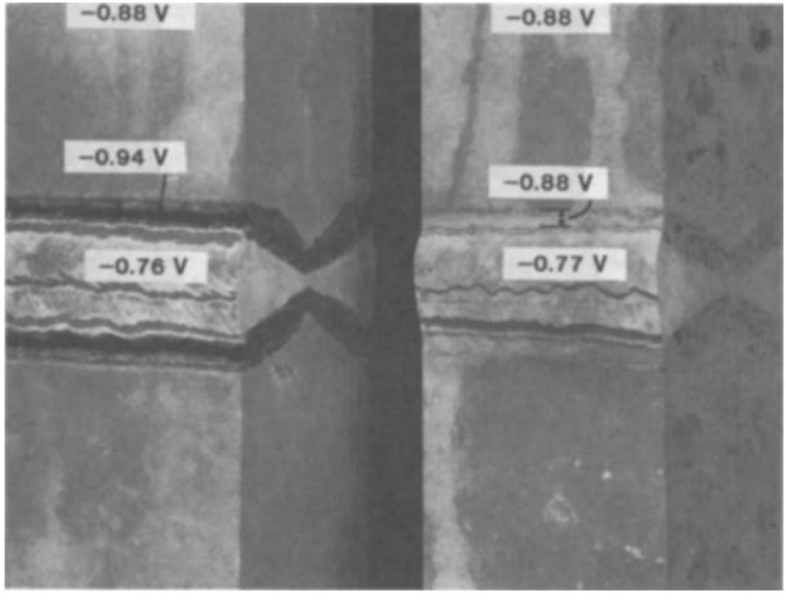

Fig. 16. Welded assemblies of 7075 alloy with 5356 filler material exposed to seawater for 1 year. (a) Exposed in the as-welded condition, shows severe localized corrosion of the HAZ. (b) Shows the beneficial effects of postweld aging. The corrosion potentials of the different areas of each are indicated where measured. They were measured in 53 g/L (6 oz/gal) NaCl plus 3 g/L (0.3 oz/gal) H_2O_2 at 25 °C (77 °F), with a 0.1N calomel reference electrode and recalculated to a saturated calomel electrode. (Courtesy of Alcoa Laboratories)

in welded structures by restraint of the metal while local regions are being heated and cooled during welding. However, SCC of aluminum alloy weldments from this cause is rare and can be avoided through design.

Resistance spot welding has been used in aircraft and other applications (Ref 154), including more recently the automotive industry (Ref 156). Generally, the resistance to corrosion of resistance spot-welded aluminum is high, but in the case of high-strength 2XXX and 7XXX alloys, selective attack of the welds may develop in corrosive service, as a result of changes in microstructure that occur during welding. Protection to alloys of this type should be provided when they are used under severe environmental conditions.

Crevice corrosion may occur in spot-welded assemblies. One approach used to solve this problem is a procedure called weld bond (Ref 157-159) that combines adhesive bonding with resistance spot welding. Usually, the pieces to be joined are first bonded by adhesives that seal the crevices, followed by resistance spot welding.

A more recent development in resistance spot welding involves joining aluminum to dissimilar metals by the use of transition joints. In this case, aluminum is first spot welded to a compatible metal that in turn is joined

Table 4a. Aluminum Filler Alloy Chart

Base alloys	Filler alloys	1060 1350 W	S	D	C	T	M	1100 W	S	D	C	T	M	2014, 2036 W	S	D	C	T	M	2219 W	S	D	C	T	M
319.0, 333.0	2319													B	A	A	A	A	A	B	A	A	A	A	A
354.0, 355.0	4043	B	A	A	A	A	A	B	A	A	A	A	A	C	C	B	C	A	A	C	C	B	C	A	A
C355.0, 380.0	4145	A	A	B	A	A	A	A	A	B	A	A	A	A	B	C	B	A	A	A	B	C	B	A	A
413.0, 443.0	4043	A	A	A	A	A	A	A	A	A	A	A	A	B	B	A	A	A	A	B	B	A	A	A	A
444.0, 356.0																									
A356.0, A357.0	4145	A	A	B	B	A		A	A	B	B	A		A	A	B	A	A		A	A	B	B	A	A
359.0																									
	5356																								
7005, 7021,	4043	A	A	C	A	A		A	A	C	A	A		B	B	A	A	A		B	B	A	A	A	
7039, 7046,	4145													A	B	A	A			A	A	B	A	A	
7146, 710.0,	5183	B	A	B	A		A	B	A	B	A		A												
711.0	5356	B	A	A	A		A	B	A	A	A		A												
	5554																								
	5556	B	A	B	A		A	B	A	B	A		A												
	5654																								
6061	4043	A	A	C	A	A		A	A	C	A	A		B	B	A	A	A		B	B	A	A	A	
6070	4145	A	A	D	B	A		A	A	D	B	A		A	A	B	A	A		A	A	B	A	A	
	5183	B	A	B			A	B	A	B			A												
	5356	B	A	A			A	B	A	A			A												
	5554																								
	5556	B	A	B			A	B	A	B			A												
	5654																								
6005	4043	A	A	C	A	A		A	A	C	A	A		B	B	A	A	A		B	B	A	A	A	
6063	4145	A	A	D	B	A		A	A	D	B	A		A	A	B	A	A		A	A	B	A	A	
6101	5183	B	A	B			A	B	A	B			A												
6151	5356	B	A	A			A	B	A	A			A												
6201	5554																								
6351	5556	B	A	B			A	B	A	B			A												
6951	5654																								
5454	4043	A	B	C	C	A		A	B	C	C	A								A	A	A	A	A	
	5183	B	A	B	B		A	B	A	B	B		A												
	5356	B	A	A	B		A	B	A	A	B		A												
	5554	C	A	A	A	A	A	C	A	A	A	A	A												
	5556	B	A	B	B		A	B	A	B	B		A												
	5654																								
514.0	4043	A	B	C	C			A	B	C	C									A	A	A	A		
513.0	5183	p	A	B	B		A	B	A	B	B		A												
512.0	5356	B	A	A	B		A	B	A	A	B		A												
511.0	5554	C	A	A	A		A	C	A	A	A		A												
5154	5556	B	A	B	B		A	B	A	B	B		A												
5154	5654	C	A	A	A		B	C	A	A	A		B												
5086	4043	A	B	C	B			A	B	C	B									A	A	A	A		
5356	5183	A	A	B	A		A	A	A	B	A		A												
	5356	A	A	A	A		A	A	A	A	A		A												
	5554																								
	5556	A	A	B	A		A	A	A	B	A		A												
	5654																								

How to Use the Filler Alloy Chart

First select the base alloys to be joined, one from the column on the left side and the other from the row at the top. Then, from the base alloys in the left column, move to the right until the block directly under the base alloy in the top row is reached. Or, from the base alloy in the top row, move down until the block directly across from the base alloy in the left column is reached.

This intersecting block contains horizontal lines of letters (A through D) that represent the filler alloys directly across from them in the box at the ends of each row. The letters in each line give the A to D rating of the characteristics listed at the top of each column—W, S, D, C, T and M.

By choosing the different filler alloys in each block, the characteristics of the weld can be varied. Trade off one characteristic for another until the most suitable filler is found.

to the dissimilar metal. This procedure improves resistance to galvanic corrosion by minimizing dissimilar metal contact (Ref 160 and 161).

Brazing. Brazed aluminum is used extensively in heat exchanger applications. There are two general types of brazing: one uses a flux and

Table 4a. Aluminum Filler Alloy Chart (Continued)

3003, Alclad 3003						3004						Alclad 3004						5005, 5050						5052, 5652						
W	S	D	C	T	M	W	S	D	C	T	M	W	S	D	C	T	M	W	S	D	C	T	M	W	S	D	C	T	M	
																														2319
B	B	A	A	A	A	B	B	A	A	A	A	B	B	A	A	A	A	B	B	A	A	A	A	A	A	A	A	A	A	4043
A	A	B	A	A	A	A	A	B	A	A	A	A	A	B	A	A	A	A	A	B	A	A	A							4145
A	A	A	A	A	A	A	A	A	A	A	A	A	A	A	A	A	A	A	A	A	A	A	A	A	B	A	A	A	A	4043
A	A	B	B	A																										4145
																								B	A	B	B		A	5356
A	B	C	A	A		A	D	C	B	A		A	D	C	B	A		A	B	C	B	A		B	D	C	B	A		4043
																														4145
B	A	B	A		A	B	A	B	A		A	B	A	B	A		A	B	A	B	A		A	A	A	B	A		A	5183
B	A	A	A		A	B	B	A	A		A	B	B	A	A		A	B	A	A	A		A	A	B	A	A		A	5356
						C	C	A	A	A	A	C	C	A	A	A	A	C	A	A	A	A	A	B	C	A	A	A	A	5554
B	A	B	A		A	B	A	B	A		A	B	A	B	A		A	B	A	B	A		A	A	A	B	A		A	5556
						C	C	A	A		B	C	C	A	A		B	C	A	A	A		A	B	C	A	A		A	5654
A	B	C	A	A		A	D	C	A	A		A	D	C	A	A		A	B	C	A	A		A	D	C	A	A		4043
A	A	D	B	A		B	C	D	B	A		B	C	D	B	A		A	B	D	B	A								4145
B	A	B			A	B	A	B			A	B	A	B			A	B	A	B			A	B	A	B	C		B	5183
B	A	A			A	B	B	A			A	B	B	A			A	B	A	A			A	B	B	A	C		A	5356
																								C	C	A	B	A	B	5554
B	A	B			A	B	A	B			A	B	A	B			A	B	A	B			A	B	A	B	C		B	5556
																								C	C	A	B		A	5654
A	B	C	A	A		A	D	C	A	A		A	D	C	A	A		A	B	C	A	A		A	D	C	A	A		4043
A	A	D	B	A		B	C	D	B	A		B	C	D	B	A		A	B	D	B	A								4145
B	A	B			A	B	A	B			A	B	A	B			A	B	A	B			A	B	A	B	C		B	5183
B	A	A			A	B	B	A			A	B	B	A			A	B	A	A			A	B	B	A	C		A	5356
																								C	C	A	B	A	B	5554
B	A	B			A	B	A	B			A	B	A	B			A	B	A	B			A	B	A	B	C		B	5556
																								C	C	A	B		A	5654
A	B	C	C	A		A	D	C	C	A		A	D	C	C	A		A	B	C	C	A		A	D	C	C	A		4043
B	A	B	B		A	B	A	B	B		A	B	A	B	B		A	B	A	B	B		A	A	A	B		B		5183
B	A	A	B		A	B	B	A	B		A	B	B	A	B		A	B	A	A	B		A	A	B	A	B		A	5356
C	A	A	A	A	A	C	C	A	A	A	A	C	C	A	A	A	A	C	A	A	A	A	A	C	C	A	A	A	A	5554
B	A	B	B		A	B	A	B	B		A	B	A	B	B		A	B	A	B	B		A	A	A	B	B		A	5556
																								B	C	A	B		B	5654
A	B	C	C			A	D	C	C			A	D	C	C			A	B	C	C			A	D	C	C			4043
B	A	B	B		A	B	A	B	B		A	B	A	B	B		A	B	A	B	B		A	A	A	B	B		B	5183
B	A	A	B		A	B	B	A	B		A	B	B	A	B		A	B	A	A	B		A	A	B	A	B		A	5356
C	A	A	A		A	C	C	A	A		A	C	C	A	A		A	C	A	A	A		A	C	C	A	A		B	5554
B	A	B	B		A	B	A	B	B		A	B	A	B	B		A	B	A	B	B		A	A	A	B	B		B	5556
C	A	A	A		B	C	C	A	A		B	C	C	A	A		B	C	A	A	A		B	B	C	A	A		B	5654
A	B	C	B			A	C	C	B			A	C	C	B			A	B	C	B									4043
A	A	B	A		A	A	A	B	A		A	A	A	B	A			A	A	B	A		A	A	A	B	A		A	5183
A	A	A	A		A	A	B	A	A		A	A	B	A	A		A	A	A	A	A		A	A	B	A	A		A	5356
																								C	C	A	A		A	5554
A	A	B	A		A	A	A	B	A		A	A	A	B	A		A	A	A	B	A		A	A	A	B	A		A	5556
																								B	C	A	A		B	5654

Legend

Filler alloys are rated on the following characteristics:

Symbol

- W Ease of welding (relative freedom from cracking)
- S Strength of welded joint (as-welded condition). (Rating applies particularly to fillet welds. All rods and electrodes rated develop presently specified minimum strengths for butt welds)
- D Ductility (Rating is based upon free bend elongation of the weld)
- C Corrosion resistance in continuous or alternate immersion in fresh or salt water
- T Recommended for service at sustained temperatures above 66 °C (150 °F)
- M Color match after anodizing

- A, B, C and D are relative ratings in decreasing order of merit. The ratings have relative meaning only within a given block
- Combinations having no rating are not usually recommended
- Ratings do not cover these alloys when heat-treated after welding

(Tables 4a, b, and c are courtesy of Alcoa Laboratories)

Table 4b. Aluminum Filler Alloy Chart

Base alloys	Filler alloys	5083, 5456					5086, 5356					514.0, A514.0, B514.0, F514.0, 5154, 5254					5454				
		W	S	D	C	T M	W	S	D	C	T M	W	S	D	C	T M	W	S	D	C	T M
319.0, 333.0, 354.0, 355.0 C355.0, 380.0	2319																				
	4043	A	A	A	A	A	A	A	A	A	A	A	A	A	A	A	A	A	A	A	A
	4145																				
413.0, 443.0 444.0, 356.0 A356.0, A357.0 359.0	4043	A	B	B	A	A	A	B	B	A	A	A	B	B	A	A	A	B	B	A	A
	4145																				
	5356	A	A	A	A	A	A	A	A	A	A	A	A	A	B	A	A	A	A	B	A
7005, 7021, 7039, 7046, 7146, 710.0, 711.0	4043																				
	4145																				
	5183	A	A	B	A	A	A	A	B	A	A	A	A	B	A	A	A	A	B	A	A
	5356	A	B	A	A	A	A	B	A	A	A	A	B	A	A	A	A	B	A	A	A
	5554											B	C	A	A	A	B	C	A	A	A
	5556	A	A	B	A	A	A	A	B	A	A	A	A	B	A	A	A	A	B	A	A
	5654											B	C	A	A	A	B	C	A	A	A
6061 6070	4043	A	D	C	A		A	D	C	A		A	D	C	A		A	D	C	B	A
	4145																				
	5183	A	A	B	A	A	A	A	B	A	A	B	A	B	C	B	B	A	B	C	A
	5356	A	B	A	A	A	A	B	A	A	A	B	B	A	C	A	B	B	A	C	A
	5554	B	C	A	A	A	B	C	A	A	A	C	C	A	B	B	C	C	A	A	A
	5556	A	A	B	A	A	A	A	B	A	A	B	A	B	C	B	B	A	B	C	A
	5654	B	C	A	A	B	B	C	A	A	B	C	C	A	B	A	C	C	A	B	B
6005 6063	4043	A	B	C	A		A	B	C	A		A	B	C	A		A	B	C	B	A
	4145																				
6101 6151 6201 6351 6951	5183	A	A	B	A	A	A	A	B	A	A	B	A	B	C	A	B	A	B	C	A
	5356	A	A	A	A	A	A	A	A	A	A	B	A	A	C	A	B	A	A	C	A
	5554	B	A	A	A	A	B	A	A	A	A	C	A	A	B	A	C	A	A	A	A
	5556	A	A	B	A	A	A	A	B	A	A	B	A	B	C	A	B	A	B	C	A
	5654	B	A	A	A	B	B	A	A	A	B	C	A	A	B	B	C	A	A	B	B
5454	4043																				
	5183	A	A	B	B	A	A	A	B	B	A	A	A	B	B	A	A	A	B	B	A
	5356	A	B	A	B	A	A	B	A	B	A	A	B	A	B	A	A	B	A	B	A
	5554	B	C	A	A	A	B	C	A	A	A	B	C	A	A	A	B	C	A	A	A
	5556	A	A	B	B	A	A	A	B	B	A	A	A	B	B	A	A	A	B	B	A
	5654											B	C	A	A	B	B	C	A	B	B
514.0 513.0 512.0 511.0 5154 5154	4043																4043				
	5183	A	A	B	A	A	A	A	B	A	A	A	A	B	B	B	5183				
	5356	A	B	A	A	A	A	B	A	A	A	A	B	A	B	A	5356				
	5554	B	C	A	A	A	B	C	A	A	A	B	C	A	A	B	5554				
	5556	A	A	B	A	A	A	A	B	A	A	A	A	B	B	B	5556				
	5654	B	C	A	A	B	B	C	A	A	B	B	C	A	A	A	5654				
5086 5356	4043													4043							
	5183	A	A	B	A	A	A	A	B	A	A			5183							
	5356	A	B	A	A	A	A	B	A	A	A			5356							
	5554													5554							
	5556	A	A	B	A	A	A	A	B	A	A			5556							
	5654													5654							

the other is fluxless (Ref 162 and 163). Many fluxes are corrosive, and must be completely removed after joining, or severe corrosion may occur in service (Ref 164). Cleaning procedures for this have been established (Ref 165 and 166). In recent years, relatively noncorrosive fluxes have been developed that minimize the necessity of their removal (Ref 167 and 168).

Assemblies joined by vacuum brazing generally have improved corrosion resistance over those brazed with flux, because the possibility of incomplete flux removal is eliminated (Ref 169). Assemblies brazed in this manner have recently been introduced to the automotive industry.

Table 4b. Aluminum Filler Alloy Chart (Continued)

6005, 6063, 6101, 6151, 6201, 6351, 6951						6061, 6070						7075, 7021, 7039, 7046, 7146, 710.0, 711.0						413.0, 443.0, 444.0, 356.0, A356.0, A357.0, 359.0						319.0, 333.0, 354.0, 355.0, C355.0, 380.0						
W	S	D	C	T	M	W	S	D	C	T	M	W	S	D	C	T	M	W	S	D	C	T	M	W	S	D	C	T	M	
																								B	A	A	A	A	A	2319
B	B	A	A	A	A	B	B	A	A	A	A	B	B	A	A	A	A	B	B	A	A	A	A							4043
A	A	B	A	A	A	A	A	B	A	A	A	A	A	B	A	A	A	A	A	B	A	A	A	A	B	B	B	A	A	4145
A	B	A	A	A	A	A	B	A	A	A	A	A	B	B	A	A	A	A	B	A	A	A	A			4043				
A	A	B	B	A		A	A	B	B	A		A	A	B	B	A		A	A	B	B	A				4145				
												A	A	A	A		B									5356				
A	D	C	B	A		A	D	C	B	A		B	D	C	B	A				4043										
																				4145										
A	A	B	A		A	A	A	B	A		A	A	A	B	A		A			5183										
A	B	A	A		A	A	B	A	A		A	A	B	A	A	A	A			5356										
B	C	A	A	A	A	B	C	A	A	A	A	B	C	A	A		A			5554										
A	A	B	A		A	A	A	B	A		A	A	A	B	A		A			5556										
B	C	A	A		A	B	C	A	A		A	B	C	A	A		A			5654										
A	C	B	A	A		A	C	B	A	A				4043																
														4145																
B	A	A	C		A	B	A	A	C		B			5183																
B	A	A	C		A	B	B	A	C		A			5356																
C	B	A	B	B	A	C	B	A	B	B	B			5554																
B	A	A	C		A	B	A	A	C		B			5556																
C	B	A	B		B	C	B	A	B		B			5654																
A	C	B	A	A				4043																						
								4145																						
B	A	A	C		A			5183																						
B	A	A	C		A			5156																						
C	B	A	B	B	A			5554																						
B	A	A	C		A			5556																						
C	B	A	B		B			5654																						

Soldering. Aluminum has been soldered for many years with relative ease. Surface preparation, fluxes, and design of the joint are important (Ref 157-161). Three types of solders are used with aluminum: (1) low-temperature lead-tin types, (2) intermediate temperature zinc-cadmium or zinc-tin types, and (3) high-temperature zinc or zinc-aluminum types (Ref 170 and 171). Characteristics of several solders for aluminum are shown in Table 5. The corrosion resistance of soldered aluminum joints varies with the type of solder used. The low-temperature lead-tin solders exhibit the lowest corrosion resistance. The high-temperature zinc solders have the highest resistance (Ref 172 and 173). The corrosion performance of the various types of soldered joints is related to the corrosion potentials existing at the solder-aluminum interface, as shown in Fig. 17 (Ref 170). Removal of fluxes from joints after soldering is essential to maximize corrosion performance. This is particularly true when fluxes containing chlorides and fluorides are used (Ref 174). More recently, noncorrosive fluxes have been developed. The removal of these fluxes by cleaning is less essential. In addition, soldering by ultrasonic methods, in which no flux is involved, has gained acceptance (Ref 175). Absence of flux eliminates the need for cleaning and greatly improves corrosion resistance.

Protection must be considered for best performance of soldered aluminum joints. Joints using the low- and medium-temperature solders must be protected (usually by painting) in all but the very mildest environ-

Table 4c. Aluminum Filler Alloy Chart

Base alloys	Filler alloys	1060, 1350					1100					2014, 2036					2219				
		W	S	D	C	T	M	W	S	D	C	T	M	W	S	D	C	T	M	W	S	D	C	T	M
5083	4083	A	B	C	B			A	B	C	B									A	A	A	A		
5456	5183	A	A	B	A		A	A	A	B	A		A												
	5356	A	A	A	A		A	A	A	A	A		A												
	5554																								
	5556	A	A	B	A		A	A	A	B	A		A												
	5654																								
5052	4083	A	B	C	A	A		A	B	C	A	A		A	A	A	A	A		A	A	A	A	A	
5652	5183	B	A	B			A	B	A	B			A												
	5356	B	A	A			A	B	A	A			A												
	5554																								
	5556	B	A	B			A	B	A	B			A												
	5654																								
5005	1100	C	B	A	A	A	A	C	B	A	A	A	A												
5050	4043	A	A	C	A	A		A	A	C	A	A		B	B	A	A	A		B	B	A	A	A	
	4145	B	A	D	B	A		B	A	D	B	A		A	A	B	A	A		A	A	B	A	A	
	5183	C	A	B			B	C	A	B			B												
	5356	C	A	B			B	C	A	B			B												
	5556	C	A	B			B	C	A	B			B												
Alclad 3004	1100	D	B	A	A	A	A	D	B	A	A	A	A												
	4043	A	A	C	A	A		A	A	C	A	A		B	B	A	A	A		B	B	A	A	A	
	4145	B	A	D	B	A		B	A	D	B	A		A	A	D	A	A		A	A	B	A	A	
	5183	C	A	B	C		B	C	A	B	C		B												
	5356	C	A	B	C		B	C	A	B	C		B												
	5554																								
	5556	C	A	B	C		B	C	A	B	C		B												
3004	1100	D	B	A	A	A	A	D	B	A	A	A	A												
	4043	A	A	C	A	A		A	A	C	A	A		B	B	A	A	A		B	B	A	A	A	
	4145	B	A	D	B	A		B	A	D	B	A		A	A	B	A	A		A	A	B	A	A	
	5183	C	A	B			B	C	A	B			B												
	5356	C	A	B			B	C	A	B			B												
	5554																								
	5556	C	A	B			B	C	A	B			B												
3003	1100	B	B	A	A	A	A	B	B	A	A	A	A												
Alclad 3003	4043	A	A	B	A	A		A	A	B	A	A		B	A	A	A	A		B	A	A	A	A	
	4145	A	A	C	B	A		A	A	C	B	A		A	A	B	A	A		A	A	B	A	A	
2219	2319													B	A	A	A	A	A	A	A	A	A	A	A
	4043	B	A	A	A	A		B	A	A	A	A		B	C	B	C	A		B	C	B	C	A	
	4145	A	A	B	A	A		A	A	B	A	A		A	B	C	B	A		A	B	C	B	A	
2014	2319													C	A	A	A	A	A			2319			
2036	4043	B	A	A	A	A		B	A	A	A	A		B	C	B	C	A				4043			
	4145	A	A	B	A	A		A	A	B	A	A		A	B	C	B	A				4145			
1100	1100	B	B	A	A	A	A	B	B	A	A	A	A			1100									
	4043	A	A	B	A	A		A	A	B	A	A				4043									
	5356															5356									
1060	1100	B	B	A	A	A	B			1100															
1350	1060	C	C	A	A	A	A			1060															
	4043	A	A	B	A	A				4043															

ments. High-temperature soldered joints usually require protection only in more severe environments.

Riveting. Historically, riveting has been a common method of joining aluminum to aluminum and to other materials (Ref 176-178). Generally, with proper selection of alloy and temper, high corrosion resistance can be anticipated with aluminum-to-aluminum joints, although higher strength aluminum-copper-magnesium and aluminum-zinc-magnesium-copper alloys should be given protection in such assemblies (Ref 179). In highly conductive environments such as seawater, careful selection of the rivet material is required. If aluminum rivets cannot be used in these environ-

Table 4c. Aluminum Filler Alloy Chart (Continued)

3003, Alclad 3003	3004	Alclad 3004	5005, 5050	5052, 5652	5083, 5456	
W S D C T M	W S D C T M	W S D C T M	W S D C T M	W S D C T M	W S D C T M	
A B C B	A C C B	A C C B	A B C B			4043
A A B A A	A A B A A	A A B A A	A A B A A	A A B A A	A A B A A	5183
A A A A A	A B A A A	A B A A A	A A A A A	A B A A A	A A A A	5356
				C C A A A		5554
A A B A A	A A B A A	A A B A A	A A B A A	A A B A A	A A B A A	5556
				B C A A B		5654
A B C A A A	A B C A A A	A C C A A A	A B C A A A	A D C B A	4043	
B A B A	B A B A	B A B A	B A B A	A A B C B	5183	
B A A A	B A A A	B B A A	B A A A	A B A C A	5356	
				C C A A A B	5554	
B A B A	B A B A	B A B A	B A B A	A A B C B	5556	
				B C A B A	5654	
C C A A A A			B A A A A	1100		
A B C A A	A B C A A	A B C A A	A B D A A	4043		
B B D B A				4145		
C A B C B	B A B A	B A B B A	B A C B	5183		
C A B C B	B A A A	B A A B A	B A B B	5356		
C A B C B	B A B A	B A B B A	B A C B	5556		
C C A A A A			1100			
A B C A A	A D D A A	A D D A A	4043			
B B D B A			4145			
C A B C A	B A C C A	B A C C A	5183			
C A B C A	B B B C A	B B B C A	5356			
	C C A B A A	C C A B A A	5554			
C A B C A	B A C C A	B A C C A	5556			
C C A A A A		1100				
A B C A A	A B D A A	4043				
B B D B A		4145				
C B C A	B A C C A	5183				
C A B C A	B B B C A	5356				
	C C A B A A	5554				
C B C A	B A C C A	5556				
B B A A A A	1100					
A A B A A	4043					
A A C B A	4145					
2319						
4043						
4145						

ments, consideration should be given to the use of protected metal rivets, such as galvanized steel or aluminized steel. Protected metal rivets are also preferred for riveting aluminum to dissimilar metals. In any case, the base metal in the rivet should be cathodic to aluminum. In addition, protective measures should be applied to avoid galvanic corrosion. Riveted joints of aluminum alloys may be subject to crevice-type corrosion. Depending upon the environment, protective measures should be considered. Adhesive bonding before riveting has been used to overcome this type of corrosion.

Adhesive Bonding. Adhesive bond joining of aluminum has been expanding steadily in recent years. It has been used extensively for the fabrication of laminates in building product applications (Ref 180) and for many aircraft, aerospace, and boat applications (Ref 181). More recently, adhesive-bonded aluminum has been considered for some automotive applications (Ref 182 and 183). The corrosion performance of adhesive-bonded aluminum is governed by the alloy, design of the joint, surface preparation, and choice of adhesive (Ref 184 and 185). Generally, the

Table 5. Characteristics of Several Solders for Aluminum

Type	Composition	Melting range °C	Melting range °F	Wetting of aluminum	Fluxes	Corrosion rating
Low temperature	91% Sn-9% Zn	205	400	Fair	Organic and salt	Fair
Low temperature	50% Sn-50% Pb	180–220	360–425	Poor	Organic and salt	Poor
Low temperature	34% Sn-63% Pb-3% Zn	170–255	340–490	Poor	Organic and salt	Poor
Intermediate temperature	70% Sn-30% Zn	200–310	390–590	Good	Salt	Fair
Intermediate temperature	40% Cd-60% Zn	265–335	510–635	Excellent	Salt	Good
Intermediate temperature	30% Sn-70% Zn	200–380	390–710	Excellent	Salt	Good
Intermediate temperature	10% Cd-90% Zn	265–400	510–750	Excellent	Salt	Good
High temperature	5% Al-95% Zn	380	720	Excellent	Salt	Excellent
High temperature	100% Zn	420	790	Good	Salt	Excellent

Courtesy of Alcoa Laboratories.

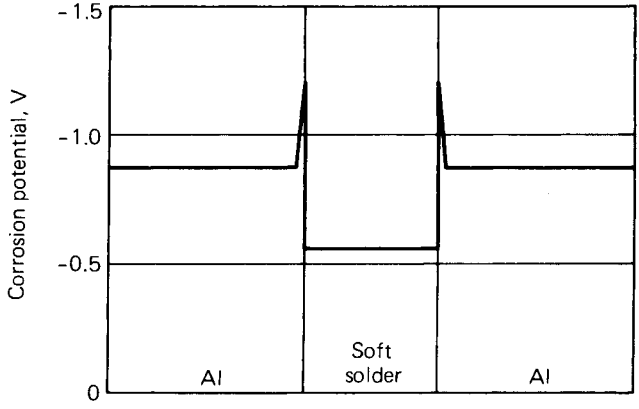

Fig. 17. Potential values across an aluminum-aluminum soft soldered joint. (Courtesy of Alcoa Laboratories)

performance of such assemblies is good, although the application of stress can have deleterious effects (Ref 186 and 187). One major advantage is that the use of an adhesive eliminates corrosion-susceptible crevices. The overall performance of these joints can be improved by the use of organic coatings and sealants.

Most adhesives are compatible with aluminum. However, there are exceptions, including the alkaline water-based latex adhesives, acetic anhydride adhesives, and adhesives that have been made electrically conductive by the addition of copper, silver, or carbon. Such adhesives should be used only with caution and with the recognition that corrosion problems could develop.

ENVIRONMENTAL FACTORS

Effect of Water. Except in cases of high-temperature oxidation, gas-metal reactions, fretting, and certain hot, anhydrous organic chemicals such as phenol and methanol, aluminum does not corrode unless water is present on the surface. The water may appear in the form of isolated droplets, as a thin film of moisture condensed on an aluminum surface that is below the dew point, or as an aqueous solution. Water in contact with air contains dissolved oxygen, which must be present for corrosion of aluminum to occur. De-aeration usually stops the corrosion reaction. The protective surface film on aluminum thickens on exposure to water. This reaction is more rapid in the absence of oxygen.

Purity of the water is another critical factor. Aluminum is highly resistant to high-purity water (distilled or demineralized) at ambient temperatures (Ref 188-190). A slight reaction occurs initially, but ceases within a few days, as the result of the development of a protective oxide film. After this conditioning period, the effect of the water on aluminum becomes negligible (Ref 189 and 191). This is demonstrated by the curves on aluminum pickup in deionized water shown in Fig. 18.

At elevated temperatures, high-purity water can have an adverse effect on many aluminum alloys. At 200 °C (390 °F), high-purity aluminum sheet disintegrates within a few days with the formation of aluminum

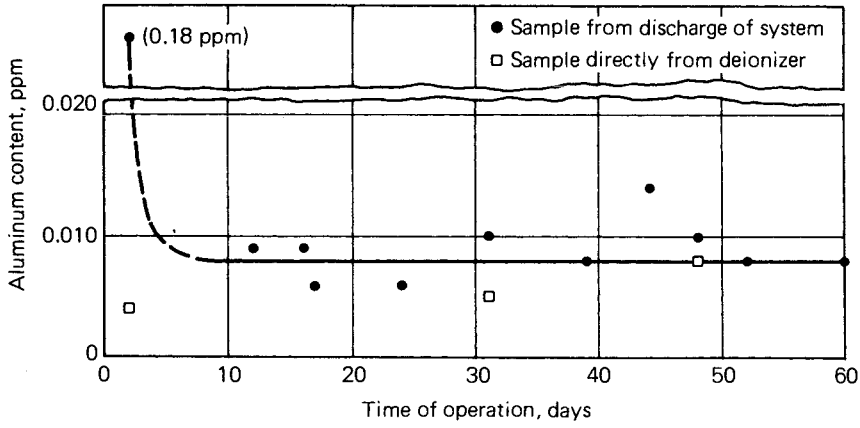

Fig. 18. Aluminum pickup in deionized water. Note steep decline after first week. (Courtesy of Alcoa Laboratories)

oxide powder. Contrary to what occurs at lower temperatures, alloying elements such as nickel and iron that usually decrease corrosion resistance result in improved corrosion resistance of alloys exposed to high-purity water at elevated temperatures. Aluminum-nickel-iron alloys have good resistance to corrosion by high-purity water at temperatures as high as 315 °C (600 °F) (Ref 192 and 193).

Aluminum resists steam condensate (Ref 194 and 195). Steam condensate is relatively pure water that is usually saturated with oxygen and carbon dioxide, making it corrosive to steel. The corrosion resistance of aluminum alloys is not decreased significantly by these dissolved gases, or by the additives used to provide the required compatibility with steel.

In some organic compounds such as phenol and methanol, the presence of a small amount of water (≈0.1%) prevents severe corrosion that might otherwise occur at elevated temperature. The corrosion behavior of aluminum in natural surface waters is covered in a previous section on fresh water pitting. Behavior in seawater is also discussed in an earlier section of this chapter.

Effect of pH. As a general rule, the protective oxide film is stable in aqueous solutions in the pH range of 4.0 to 9.0. Usually, the oxide film is readily soluble in strong acids and alkalis, and as a consequence these attack aluminum. However, there are certain acid and alkaline solutions in which aluminum is highly resistant to attack (Fig. 19). A few examples are glacial acetic acid, concentrated nitric acid, sodium disilicate, and concentrated ammonium hydroxide. For this reason, the corrosivity of an environment cannot be determined solely by pH, because the nature of the individual ions in the solution may be the controlling factor.

However, the Pourbaix potential-pH diagram for aluminum (Ref 196) shown in Fig. 20, which is based solely on theoretical thermodynamic considerations and does not provide information on corrosion rates, predicts oxide film stability and thus resistance to general dissolution in the pH range 4 to 9. Aluminum alloys have become a standard material of construction for storage and handling of hot, 83% ammonium nitrate.

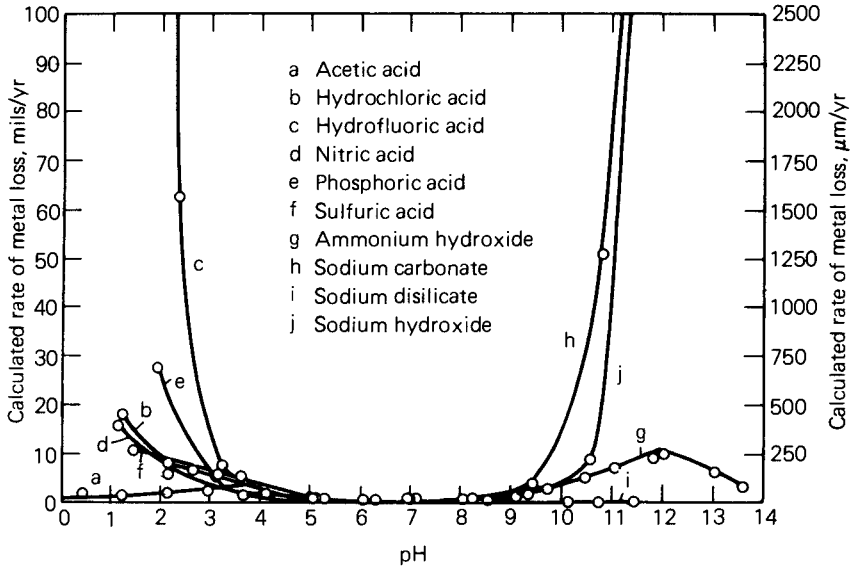

Fig. 19. Effect of pH on corrosion of 1100-H14 alloy by various chemical solutions. Observe the minimal corrosion in the pH range of 4.0 to 9.0. The low corrosion rates in acetic acid, nitric acid, and ammonium hydroxide demonstrate that the nature of the individual ions in solution is more important than the degree of acidity or alkalinity. (Courtesy of Alcoa Laboratories)

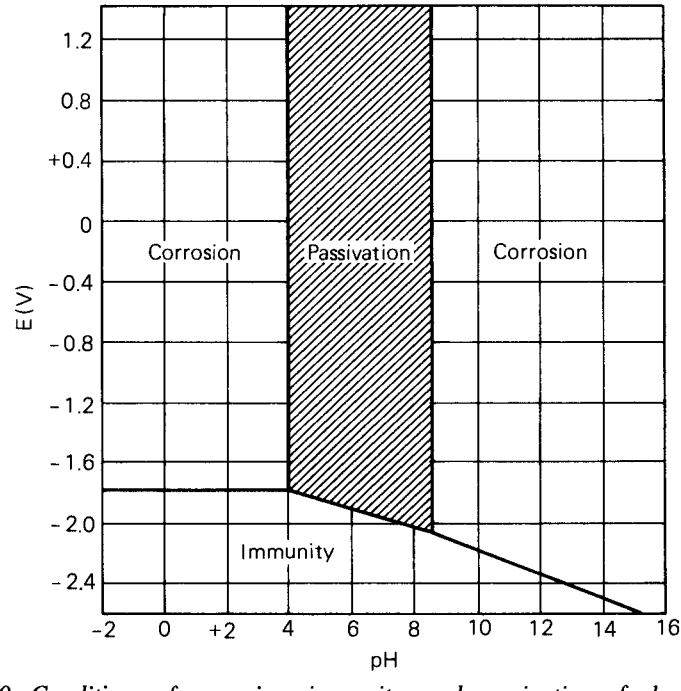

Fig. 20. Conditions of corrosion, immunity, and passivation of aluminum at 25 °C (77 °F), assuming protection by a film of Bayerite, $Al_2O_3 \cdot 3H_2O$. (Ref 196)

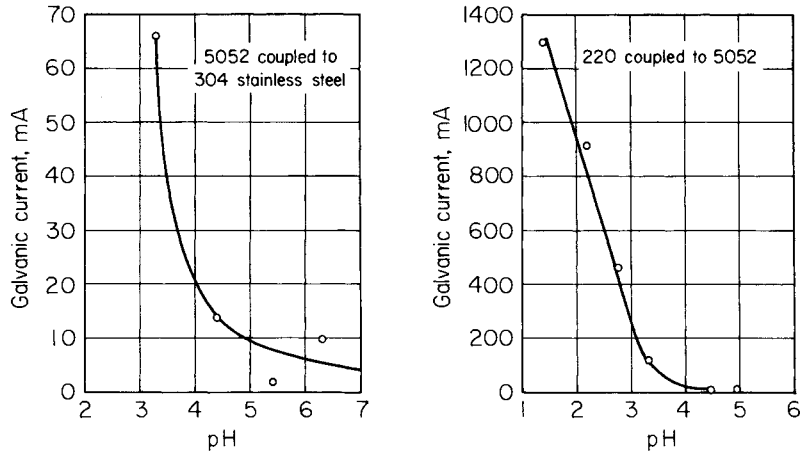

Fig. 21. Effect of pH on galvanic currents in 83% ammonium nitrate. The magnitude of the galvanic currents becomes negligible above a pH of 4.5 to 5.0. The pH values were maintained with nitric acid or ammonia, as required. 5052 coupled to 304 stainless and 220 aluminum alloy (Courtesy of Alcoa)

Under operating conditions where an excess of ammonia is present, alloys 1100, 3003, 5052, 5454, 6061, and 6063 (including welded joints) have excellent corrosion resistance.

Occasional difficulties that have arisen in ammonium nitrate service have been traceable to an acidic condition. Under hot storage conditions, excess ammonia is readily lost, lowering the pH and causing attack in the HAZ of welded 5052 alloy. The HAZ of welded 3003 alloy is not susceptible to this attack. Attack by acidic ammonium nitrate solutions is stopped by adjusting the product with ammonia to neutralize the free nitric acid.

To demonstrate the effect of pH, couples between welded 5052 and stainless steel were exposed at 88 °C (190 °F) for 83% ammonium nitrate solutions having pH values of 3 to 6. The stainless steel merely supplied a large cathodic area to the 5052. Measurements indicated the galvanic current was dependent on the pH of the solution (Fig. 21). Above a pH of 4.5, the galvanic current was insignificant. Similar measurements between couples of 5052 and other more anodic aluminum-magnesium alloys, containing higher amounts of magnesium, also indicated that the galvanic current was dependent on pH of the solution (Fig. 21). Furthermore, the addition of ammonia immediately stifled the galvanic corrosion.

Effect of Purity: Trace Elements. There are cases where aluminum has been established as suitable for use with a specific product, but the metal has corroded because of contamination of that product with trace amounts of heavy metal ions. These impurities may have virtually no effect on the product, but may cause significant pitting of aluminum alloys. An actual example was the pitting of an aluminum tank truck used to transport molasses. While molasses does not normally corrode aluminum, this particular batch had been produced in a copper kettle and

contained enough copper ions (>10 ppm) to cause deposition corrosion of the aluminum. Another similar case of pitting occurs when small amounts of copper from copper plumbing enter upstream from an aluminum system. Even smaller amounts of mercury (>0.01 ppm) entering an aluminum system, such as from a broken thermometer or mercury contact switch, can cause substantial and rapid corrosion. With respect to atmospheric corrosion, the usual good performance of aluminum alloys in saline environments can be altered by the presence of nitrogen and sulfur oxides working in combination with air-borne salt. Investigations have been made to evaluate such atmospheric effects, including their relationship to acid rain (Ref 190, 197, and 199).

Effect of Temperature. The effect of temperature on the corrosion of aluminum by high-purity water has already been mentioned. In general, an increase in temperature leads to a higher corrosion rate in many chemicals such as mineral acids, organic acids, and alkaline solutions. However, the relationship may not be simple, as shown in Fig. 22 for sulfuric acid. In other chemicals and in waters, the accelerating effect may be counteracted by the formation of a protective film. For example, in monoethanolamine (MEA), increasing the temperature reduces the rate of corrosion, as a result of surface film formation.

In the case of atmospheric exposure, elevated temperature can be beneficial by speeding up drying, reducing the length of time the surface is wet. As an example, aluminum conductors operating at temperatures slightly

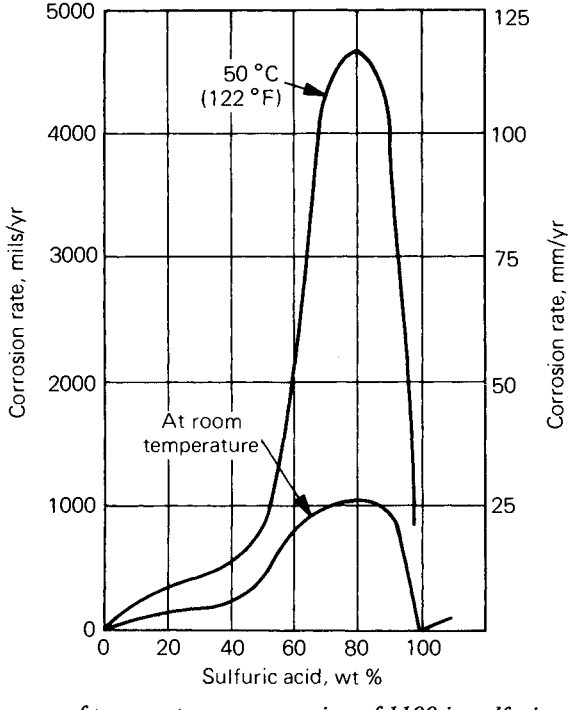

Fig. 22. Influence of temperature on corrosion of 1100 in sulfuric acid. (Courtesy of Alcoa Laboratories)

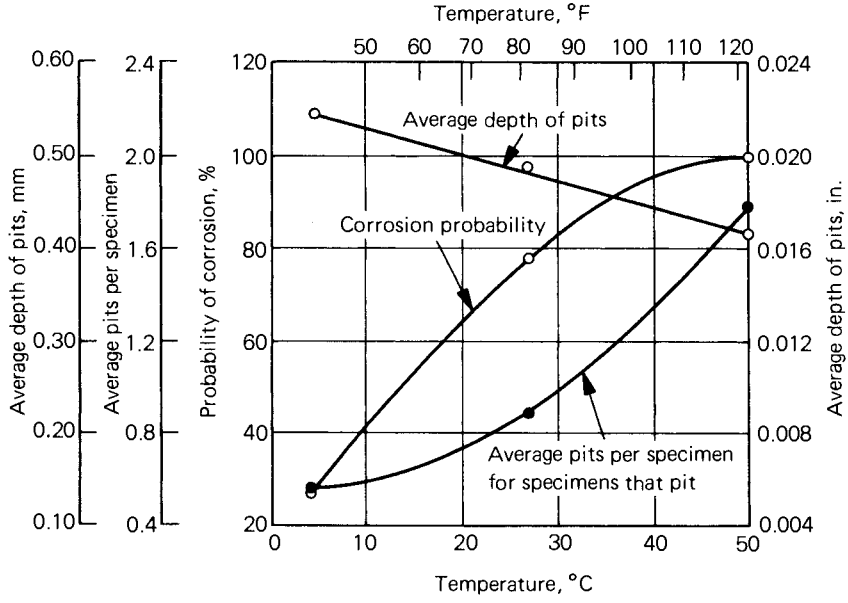

Fig. 23. Influence of temperature on pitting of aluminum.

above ambient usually suffer very little corrosion, because the elevated operating temperature keeps them dry and does not permit corrosion to occur (Ref 199).

Although very little supporting data has been published, temperature affects galvanic corrosion (Ref 200). The corrosion potential difference between 7072 and 3003 and between 7072 and 6061 alloys change with temperature, and potential reversals can occur in waters at 71 °C (160 °F) similar to the zinc-iron reversals that can occur in some waters at similar temperatures. As the temperature of a pitting-type water increases, the number of pits increases and the rate of penetration decreases (Fig. 23).

Effect of Fluid Movement. Movement of a corrosive fluid or gas (including steam) over an aluminum surface can accelerate the rate of corrosion. In some natural waters, velocities greater than 0.04 m/s (0.13 ft/s) are beneficial and may prevent pitting that might otherwise occur (Ref 201). However, at higher velocities—in the range of 5 to 6 m/s (15 to 20 ft/s)—turbulence at protrusions, such as at bends or fittings, may cause impingement or cavitation conditions that cause pitting. Corrosion caused by velocity effects is influenced by the hardness of the metal, flow rate, composition of the fluid, temperature, and pH (Ref 201 and 202). The presence of suspended solids in a moving liquid may accelerate attack by eroding away an otherwise protective film.

Effect of Surface Area-to-Metal Volume Ratio. The ratio of surface area-to-metal volume has a marked influence on the corrosion life of an aluminum product in a given environment. This is illustrated by the rate of loss of tensile strength of 1050 aluminum wires of varying diameter exposed for 5 years under shelter to an industrial-marine atmosphere in Halifax, Nova Scotia. The influence of wire diameter on corrosion life is shown in Fig. 24.

The loss of a given thickness of metal is a larger percentage of the original thickness for fine wires than for wires of larger diameter, and the reduction of breaking load for a given amount of corrosion is greater. In addition, the influence of a pit of given depth is greater, the finer the wire.

Effect of Surface Area-to-Liquid Volume Ratio. Under some conditions of exposure, the rate of corrosion of aluminum alloys varies widely, as the ratio between the metal surface area and the volume of corrodant changes (Ref 203), as illustrated graphically in Fig. 25. Under other conditions and with different solutions, the rate of corrosion is not affected significantly by changes in the area-to-volume ratio. In chemical solutions such as sulfuric acid solutions, the changes are insignificant.

An extreme case is seen in a new type of container that has been developed for inflammable and explosive fluids such as gasoline, in which the container is tightly packed with aluminum foil ribbon, about 12 m^2 (130 ft^2) surface per cubic foot of container volume. Thus, for a theoretical aluminum container cube 0.03 m^3 (1 ft^3) per side, the amount of aluminum corroded (and the amount of hydrogen produced) at a particular corrosion rate would be $^{130}/_{6}$ or 22 times as much for the foil-filled container as for the sample cube.

Effect of Pressure. Generally, pressure has not been found to significantly alter the corrosion resistance of aluminum alloys. An increase in pressure can minimize cavitation damage in special cases. The exposure of aluminum at great depths in seawater under high pressure has not shown consistent trends.

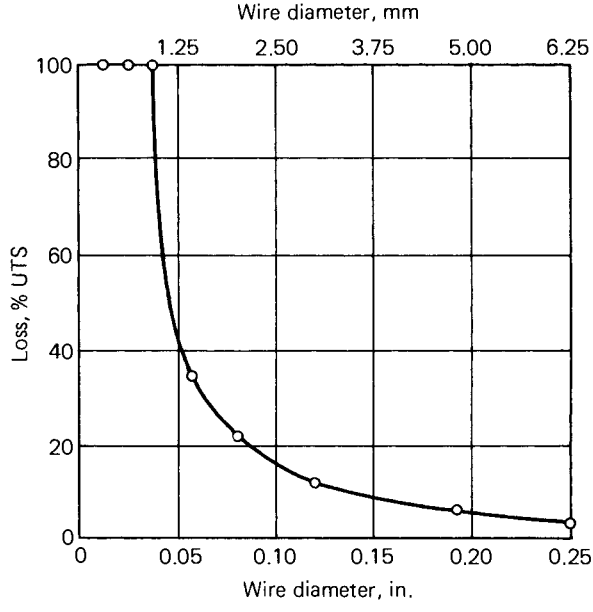

Fig. 24. Influence of diameter on corrosion life of aluminum wire under shelter in a marine-industrial atmosphere. (Courtesy of Alcan International, Kingston Laboratories)

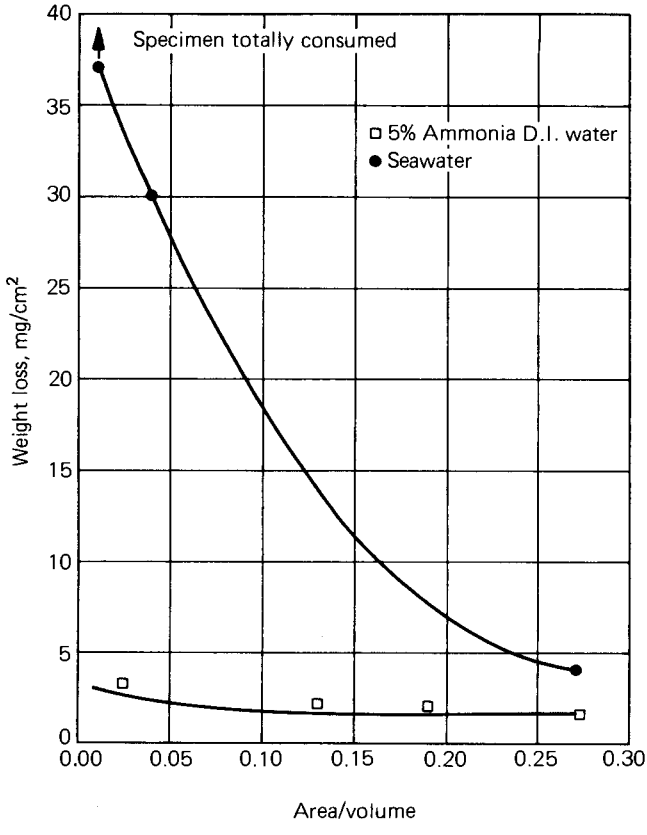

Fig. 25. Influence of surface area-to-liquid volume on rate of corrosion. (Courtesy of Alcoa Laboratories)

PREVENTIVE MEASURES

A number of corrosion preventive measures, special to a specific type of aluminum corrosion, have already been described. This section deals with the seven main methods of preventing the corrosion of aluminum equipment:

- Alloy and temper selection
- Design of equipment
- Organic coatings (and sealants)
- Inhibitors
- Cathodic protection
- Thickened surface oxide films (proprietary, conversion coatings, anodizing)
- Modification of the environment

An interesting treatise on the prevention of corrosion of metals, much of which applies to aluminum, was published by the SAE in 1964 (Ref 204).

Alloy and Temper Selection

The choice of an aluminum alloy for a given use is often based on strength, formability, ease of welding, or product availability. However, corrosion resistance must be included when making the choice.

In general, aluminum-magnesium alloys (5XXX) have the best corrosion resistance, followed by commercial-purity alloys (1XXX), aluminum-manganese alloys (3XXX), and aluminum-magnesium-silicon alloys (6XXX) in that order, with only small differences between families. These alloy families are normally used without protection, although for aesthetic reasons they are sometimes painted (house or building siding) or anodized (window frames). The aluminum-copper-magnesium alloys (2XXX) and the medium- and high-strength aluminum-zinc-magnesium-copper alloys (7XXX) are usually given a protective measure such as cladding or painting.

The importance of temper was mentioned previously in the case of exfoliation corrosion of aluminum-magnesium and aluminum-zinc-magnesium-copper alloys. The H116 temper for 5083, 5086, and 5456 gives better resistance to intergranular and exfoliation corrosion (Ref 205). In 7XXX alloys, the T-7X temper provides improved resistance to SCC, for example, the T73 and T76 tempers of 7075 alloy. These tempers are a compromise, because strength is somewhat lower than that for the T6 temper. The lower strength of these tempers in 7075 has been offset by the development of stress-corrosion resistant tempers in 7049, 7050, and 7010 alloys.

Alclad Alloys. Alclad aluminum (see Chapter 9 in this Volume) is a duplex product in which a thin surface layer of one aluminum alloy (usually 5 to 10% of the total thickness) is metallurgically bonded to the main core alloy (selected to provide the desired strength). With the exception of clad brazing alloys, the cladding layer is selected to be at least 100 mV anodic to the core, and it provides built-in cathodic protection. The surface layer is normally 1XXX (for 2XXX cores), or 7072 (for 3XXX, 5XXX, 6XXX, and 7XXX cores). The alclad aluminum alloys have maximum resistance to perforation by pitting corrosion (pits do not penetrate the core alloy) and to loss of mechanical properties on long-term exposure to corrosive atmospheres. As an example, a kitchen kettle fabricated from sheet with a 5% layer of 7072 alloy on a 3003 core alloy resisted perforation in an aggressive water for 5 to 10 times the life of an unclad 3003 alloy kettle in the same water. Another example is the alclad 3004 roofing and siding on the hangar for Howard Hughes' "Spruce Goose" in a Long Beach, CA harbor, that after 33 years had pitted only to the depth of the clad layer, 76 μm (3 mils). Further, the cladding of thin-wall (1.5 mm or 0.060 in.) irrigation pipe and culvert sheet greatly extends the time to perforation in aggressive waters.

Influence of Design

The design of equipment can have an important influence on corrosion behavior, even in environments in which aluminum is normally resistant. The three most common causes of unexpected corrosion of aluminum as

a result of poor design have been (1) improper choice of alloy or temper, such as aluminum-copper-magnesium alloys for marine service; (2) improper choice of dissimilar metals for contact with aluminum (and failure to provide the proper preventive measures when other metals must be used), which can cause galvanic corrosion; and (3) failure to use a nonhardening resilient caulking material on faying surfaces to exclude the entry of water, which can cause crevice corrosion. All three can be avoided by proper design, because the principles are well understood. Selection of the welding method and filler can influence corrosion behavior. Equipment design can affect physical variables of the environment such as temperature, fluid velocity, and impingement and cavitation and alter corrosion susceptibility.

The correction of simple design failures on large equipment can be extremely costly. For example, the rebuilding of a poorly designed aluminum-steel joint on a ship superstructure may keep the vessel out of service for an extended period. The following guidelines (Ref 206) help the designer to minimize corrosion of aluminum in service:

- Avoid contacts with dissimilar metals, but if they must be used, apply suitable protection
- Avoid crevices, but if they must be present, and if thin sections are involved, prevent ingress of moisture by application of sealants
- Join by continuous welding, rather than by skip welding or riveting
- Provide for complete draining and easy cleaning (Fig. 26 to 29)
- Avoid contact of bare aluminum surfaces with water-absorptive materials, but if they must be used together, apply suitable protection
- Avoid sharp bends in piping systems
- Avoid heat transfer hot spots
- Avoid direct impingement by fluid streams
- Avoid excessive mechanical stress concentrations
- When locating equipment, choose the least corrosive environment possible
- Eliminate sharp edges in equipment that is to be painted

Prevention of Galvanic Corrosion. The following guidelines indicate ways of minimizing galvanic corrosion of aluminum:

- The dissimilar metal should be as close as possible to aluminum in the galvanic series (Table 1)
- A fastening alloy for dissimilar metal couples should be cathodic to aluminum (for example, use steel bolts in an aluminum-steel joint, not aluminum bolts). Aluminized steel bolts (usually either hot dipped or vapor deposited) are even better
- Provide complete electrical isolation of the two metals. This can be done with nonconductive insulating gaskets, sleeves (ferrules) and washers. No external electrical path between the two metals should exist
- If paint is applied on the faying surface, it should be applied to the cathodic metal, not the aluminum. Paint applied to the aluminum may concentrate galvanic attack at pinholes because of an unfavorable cathode-anode area ratio

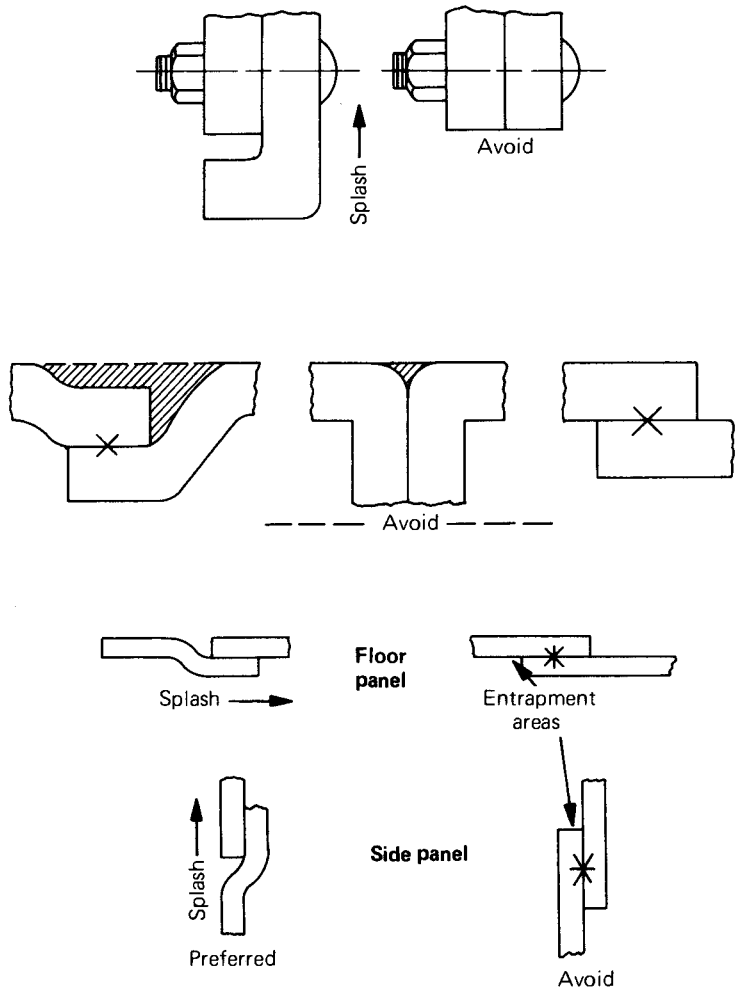

Fig. 26. Lap joint orientations to avoid entrapment areas.

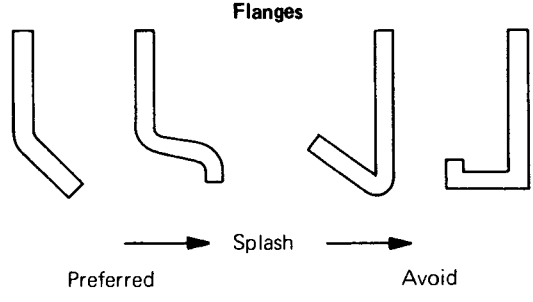

Fig. 27. Flange orientation and design to avoid entrapment of moisture and debris.

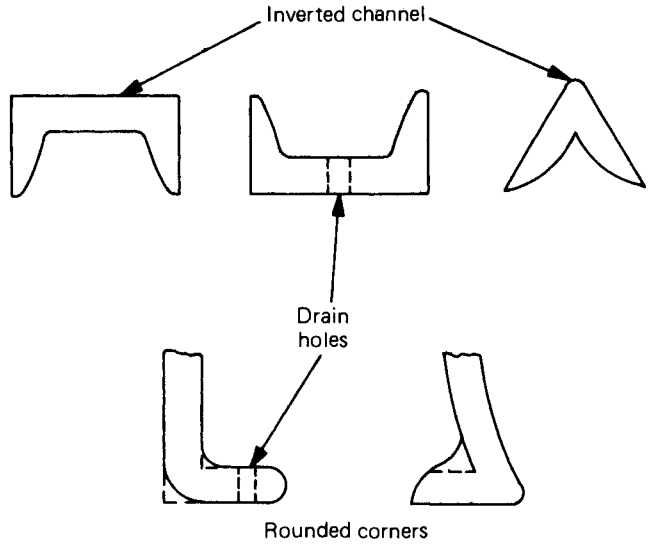

Fig. 28. Orientation and design of structural members.

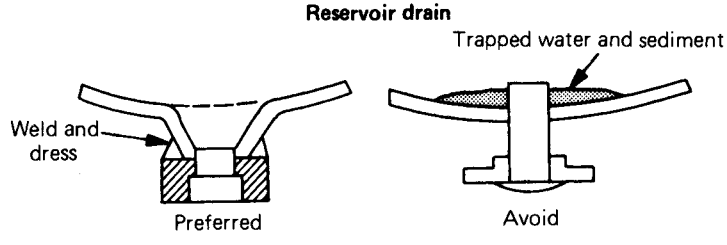

Fig. 29. Drains for liquid reservoirs should permit complete drainage.

- At aluminum pipe—other metal connections, install a thick-wall replaceable aluminum nipple section
- Also at aluminum pipe—other metal connections, avoid a threaded connection. Instead, use a flanged joint that minimizes crevices and that can be electrically insulated
- If possible, locate the dissimilar metal joint away from the corrosive environment
- In a mixed-metal, closed-loop liquid system, such as an automobile cooling system, use an inhibitor
- If there must be an external electrical connection between the dissimilar metals, separate the metals as far as possible to increase the resistance of the liquid path
- Apply cathodic protection
- Avoid unfavorable cathode-anode area ratios in a conductive environment (at least 1-to-5 in seawater)

Hardware for Aluminum. Dissimilar metal hardware such as hinges, latches, and door catches are frequently used on aluminum structures.

Aluminum hardware affixed with aluminum bolts or screws are preferred, if they are available with adequate strength. However, these items are usually available only in plated steel, plated brass, or stainless steel. In most situations, steel hardware coated with aluminum, cadmium, chromium, tin, and zinc do not cause much galvanic corrosion of aluminum until the underlying steel is exposed by deterioration of the coating, after which galvanic corrosion may be appreciable. Stainless steel hardware (AISI 300 alloys) are preferred for this reason, except on ships, where aluminized steel or painted galvanized hardware is preferred. Plated brass fasteners should be avoided.

Use of Helicoil™ Inserts for Dissimilar Metal Bolts. When a dissimilar metal bolt must be tapped into aluminum plate or castings, an 18-8 (AISI 304) stainless steel wire coil insert called a Helicoil™ (Ref 207) should be used in the drilled hole to prevent seizing of the bolts. The springs are dipped in zinc chromate primer (TT-P-1757) before insertion.

Prevention of Deposition Corrosion. The following guidelines help reduce deposition corrosion of aluminum:

- Eliminate the heavy metal parts that are providing the aggressive ion
- Paint the source metal
- Use alclad aluminum
- Use inhibitors
- Clean aluminum frequently to remove the deposited heavy metal

It may be possible to remove heavy metals from a product stream to be handled in aluminum equipment by passing it through a trap, consisting of a tank or column containing magnesium or aluminum turnings. This reportedly has been successful with seawater, but no published information has appeared.

Prevention of Crevice Corrosion. When crevice corrosion is considered possible, the crevices should be sealed with a nonhardening elastomer to prevent the entry of moisture. Some sealants become hard and crack on aging, allowing moisture entry. The elastomeric requirement is essential for joints in equipment that work in service, such as in all types of vehicles—road transport, ships, and airplanes. There are two general types of sealant: (1) one-component systems such as butyls or silicones, and (2) two-component systems such as polysulfides and epoxies. To prevent poultice corrosion, which is a special case of crevice corrosion, avoid the contact of bare aluminum surfaces with moisture-absorptive materials such as paper, cloth, wood, asbestos, and noncellular foams.

Prevention of Stress Corrosion. The SCC of high-strength aluminum alloys such as 2024, 7075, and 7079 is often caused by sustained residual or assembly tension stresses acting in the short transverse direction. The stresses developed by service loads are usually intermittent and are designed to operate in a favorable direction (longitudinal or long transverse) relative to the grain structure. The following guidelines (Ref 208-214) should be considered by the designer to minimize SCC:

- Select alloys and tempers that are resistant to SCC
- Use stress-relieved parts
- Do severe forming in the annealed condition, followed by heat treatment and aging, if required for strength

- Perform forming and straightening on freshly quenched material, W-temper, to ensure less severe effects
- Machine exterior surfaces before heat treating, because quenching causes more desirable compressive surface stresses
- Machine internal surfaces after heat treating to partially remove internal stresses
- Avoid fitup stresses by careful attention to tolerances. Poorly fitted parts and misaligned parts should not be forced into place
- Where built-in surface tensile stresses cannot be avoided, techniques such as shot peening (Ref 211) and surface rolling, or thermal stress relief from second stage aging (Ref 213), can be utilized to reduce the undesired stresses
- Postweld heat treat weldments

Location of Equipment. While aluminum equipment usually must be placed in a given location that determines the environment, there is sometimes choice in location. In these cases, the least corrosive available location should be selected.

Organic Coatings. Organic coating systems are frequently applied to aluminum for strictly decorative purposes. For example, they are applied to aluminum siding and exposed automobile body panels to obtain a desired color and to prevent natural weathering that is aesthetically unacceptable but structurally insignificant. Organic coatings may also be applied to aluminum for corrosion protection in special situations. In both cases, adequate surface preparation and careful coating selection are important to long coating life.

Most organic coatings provide corrosion protection by forming a physical barrier between the aluminum surface and the environment. Some contain inhibitors such as chromate primers. Aluminum insulation jacketing and refrigerator liners are coated on the back with a vapor barrier to prevent poultice and crevice corrosion when condensation collects between foamed insulation and the aluminum. Clear organic coatings are used where the natural aluminum surface is desired and weathering must be prevented. Temporary organic coatings are sometimes used to protect aluminum surfaces from corrosion during storage and transit. Heavy organic coatings, such as mastics and coal tars, are sometimes used to protect aluminum surfaces that are embedded in soils and concrete.

The performance of organic coating systems can be maximized by following the specific recommendations of suppliers regarding surface preparation, pretreatment, selection of compatible conversion coat, primer, and topcoat, application, and curing. If continuing maximum corrosion protection is required, the organic coating systems must be maintained periodically.

Inhibitors. The use of inhibitors to prevent the corrosion of aluminum has been reviewed by Mears and Eldredge (Ref 215), Haygood and Minford (Ref 216), Roebuck and Pritchett (Ref 217), and Roebuck and Richards (Ref 218).

Inhibitors such as chromates that reduce anodic corrosion reaction are termed anodic inhibitors, whereas those such as polyphosphates that reduce cathodic corrosion reaction are termed cathodic inhibitors. If anodic

inhibitors are used in insufficient amounts, they tend to increase pitting. Cathodic inhibitors are safer in this respect. Mixed anodic and cathodic inhibitor systems are also used.

Phosphates, silicates, nitrates, fluorides, benzoates, soluble oils, and certain other chemicals alone or in combination have been recommended for use with aluminum in some services. If copper is present in a closed system, sodium mercaptobenzothiazole may be added to prevent copper corrosion and subsequent deposition corrosion of the aluminum.

In mildly alkaline solutions (Ref 219), the corrosion of aluminum can be inhibited by additions of sodium silicate. Silicates with a high ratio of silicate to soda are widely used in alkaline cleaning solutions, soaps and dentrifrices containing amines, carbonates, and phosphates. In mixed-metal, water-handling systems, such as an automobile cooling system, inhibitor mixtures have been developed to prevent corrosion of all metals in the system, including aluminum.

Cathodic Protection. In cathodic protection, a direct electric current is caused to flow through the environment to a metal surface to prevent corrosion of that surface. The current may be supplied by a sacrificial anode such as zinc or magnesium as shown in Fig. 30, by some aluminum alloys (seawater only), or by an impressed current source such as a rectifier, using an inert anode such as graphite to feed the current into the environment. Complete protection results when the local anode current (corrosion current) is reduced to zero. The magnitude of the externally applied current sufficient to accomplish this depends upon the polarization and resistance characteristics of the system to be protected.

Cathodic protection can be used with aluminum, providing the current density on the aluminum surface does not create a highly alkaline environment, a condition of overprotection that causes cathodic corrosion. This is more likely to occur with uncontrolled impressed current systems than with sacrificial anode systems, because the polarized voltage applied to the aluminum surface can be much higher (more negative) with impressed current systems. Zinc anode systems are always safe, and magnesium anode systems are safe if properly designed. The upper safe polarization voltage is -1.20 V ($Cu/CuSO_4$).

Alclad aluminum provides built-in cathodic protection to the core alloy. National Association of Corrosion Engineers (NACE) Recommended Practice RP-01-69 provides cathodic protection criteria for buried metallic piping systems, including aluminum (Ref 220). Morgan (Ref 221) has reported that in many soils, a potential of -1.30 V can be tolerated without significant corrosion of buried aluminum. Impressed current cathodic protection systems have been used on painted aluminum boat hulls in seawater for 20 years.

Thickened Surface Oxide Films

Conversion Coatings. A number of proprietary chemical immersion treatments, such as Alodine, Bonderite, Iridite, and others are used to produce a complex surface conversion coating about 20 nm (200 Å) thick on aluminum sheet and extrusions before painting in a factory operation (5 nm or 50 Å for an untreated surface). The proprietary solutions are

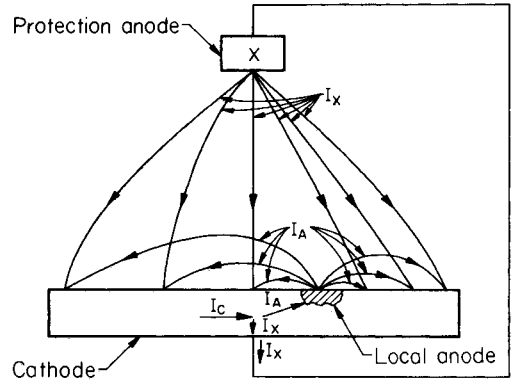

Fig. 30. Currents involved in cathodic protection with an external anode. I_x is the applied external current, I_n is the local anode current,and I_c is the total current to the anode.

acidic and contain chromates, phosphates, and other chemicals. Such films greatly improve paint adhesion.

The films, which contain chromates, have some corrosion preventive properties in their own right and are used on some aircraft and automotive components. However, they are relatively soft and can be used for corrosion prevention without overcoating only where there is no abrasion in service.

Anodic Coatings. A commercial surface treatment unique to aluminum is anodizing. The object to be treated is immersed as the anode in an acid electrolyte and a direct current is applied. Oxidation of the surface occurs to produce a greatly thickened, hard, porous film of aluminum oxide. This film is then normally immersed in boiling water to seal the porosity and render the film impermeable.

Before sealing, the film can be colored by impregnation with dyes or pigments. Special electrolytes are sometimes used to produce colored anodic films directly in the anodizing bath. The degree of protection conferred to the surface depends on the thickness of film, which may be 8 μm (0.3 mils) in the case of shiny automobile trim moldings, to 25 μm (1.0 mil) or more on the aluminum facade of a monumental building. These represent a thickening of the natural oxide film by a factor of about 1000 and 3000 times, respectively.

Architectural aluminum such as handrails, doors, windows, and facades are often anodized. The surface retains less atmospheric dirt and is much easier to clean. The anodic film has the same chemical characteristics as the natural oxide film and is corroded by strong alkalis and strong acids. In industrial atmospheres the film tends to pit, with the time to initiation depending on the film thickness. To preserve the initial appearance of anodized aluminum facades, even thick anodic films are coated with clear organic coating. The main virtues of an anodic film are its decorative appeal and the ease of cleaning. Anodizing is rarely the solution to a field corrosion problem.

During installation of anodized aluminum, components in an industrial building may be splashed by carelessly handled concrete or brick mortar.

If this occurs, the anodic film is etched in patches, and restoration of the original appearance is difficult or impossible. The best prevention is a thin film of clear organic coating that isolates the mild alkaline mortars from the anodic film. Strip-off coatings can also be used.

Prefilming in Water or Steam. The natural surface oxide film can be thickened by exposure to moving water, hot soft water, or steam. If this is done before exposure to a pitting-type environment, pitting that would otherwise occur is sometimes prevented. In one experiment, a specimen of 1200 alloy sheet that had previously been exposed for 1 year in a nonpitting fresh water (estimated film thickness of 800 nm or 800 Å) failed to pit in 16 days when immersed in a very aggressive water that produced a 965-μm (38-mil) pit on a fresh sheet specimen in the same period.

Investigation of perforations found only in certain lengths of an extensive thin-wall 1.4-mm (0.057-in.) aluminum irrigation pipe system revealed that the affected length had been produced only a month or so before the exposure, whereas the unaffected remainder of the pipe was over a year old. The difference was attributed to a thinner oxide film on the new material. Incidentally, water should be kept moving in new aluminum irrigation pipe for the first week to thicken the oxide film. The system should be drained when the water is not flowing, but prefilming helps if this is not done. Prefilming a new aluminum pot by boiling a soft water prevents the formation of a jet black surface film that occurs if a very hard water is boiled first.

Modification of the Environment. Reducing the corrosivity of an environment by slight modification is sometimes possible. For example, in a package or closed air space, maintaining the temperature above the dew point prevents corrosion that might otherwise occur, especially with rolls of aluminum sheet or foil. Adjustment of the pH of a solution to within the range 4.0 to 9.0 may render it innocuous to aluminum. If copper is present, the pH should be at least 8.0 to prevent copper dissolution and subsequent deposition on the aluminum.

The de-aeration of water greatly reduces its tendency to pit aluminum. Movement of water on an aluminum surface sometimes prevents pitting that would otherwise occur. In some chemicals such as phenol and methanol, the addition of a trace of water (0.1%) prevents vigorous corrosion that occurs in the anhydrous material at elevated temperature. In other chemicals such as liquid sulfur dioxide, traces of water promote the corrosion of aluminum.

REFERENCES

1. *Metals Handbook*, 8th ed., Vol 1, American Society for Metals, p 929
2. H.P. Godard, Ed., *The Corrosion of Light Metals*, New York: John Wiley & Sons, 1967, p 12
3. H.P. Godard, Ed., *The Corrosion of Light Metals*, New York: John Wiley & Sons, 1967, p 92
4. E.H. Dix and R.B. Mears, Symposium on *Atmospheric Exposure Tests on Nonferrous Alloys*, American Society for Testing and Materials, 1946
5. H.R. Ambler, *Journal of Applied Chemistry*, Vol 10, 1960, p 213
6. W.B. Brierly, *Journal of Environmental Sciences*, Vol 8 (No. 10), 1965, p 15

7. C.J. Walton and W. King, American Society for Testing and Materials Special Publication No. 175, 1956, p 21
8. W.H. Ailor and F.M. Reinhart, *Materials Protection*, Vol 2 (No. 6), 1963, p 30
9. W.H. Ailor, *British Corrosion Journal*, Vol 1, 1966, p 237
10. R. Harper, *Metal Industry*, 8 Dec 1961, p 454
11. W.W. Binger and C.M Marstiller, *Corrosion*, Vol 17, 1961, p 353
12. F.C. Porter and S.E. Hadden, *Journal of Applied Chemistry*, Vol 3, 1953, p 385
13. O. Sverepa, *Werkstoffe und Korrosion*, Vol 9, 1958, p 533
14. D.E. Davies, *Journal of Applied Chemistry*, Vol 9, 1959, p 651
15. L.C. Rowe and M.S. Walker, *Corrosion*, Vol 17, 1961, p 353
16. B.R. Pathak and H.P. Godard, *Nature*, Vol 218, 1968, p 893
17. P.M. Aziz, *Corrosion*, Vol 12, 1956, p 495
18. H.P. Godard, *Canadian Journal of Chemical Engineering*, Vol 38, 1960, p 167
19. D. MacIntyre, *Marine Engineering/Log*, May 1959, p 63
20. T.H. Rogers, *The Marine Corrosion Handbook*, Toronto: McGraw-Hill Ltd., 1960; *Corrosion*, Vol 15, 1959, p 403
21. C.W. Leveau, Paper presented to Southern California Section of Naval Architects and Marine Engineers, 13 Feb 1964
22. C.H. Holtyn, *et al*, *Transactions of the Society of Naval Architects and Marine Engineers*, Vol 80, 1972
23. C.H. Holtyn, *The Waterways Journal*, 27 Jan 1979
24. T.E. Wright, H.P. Godard, and I.H. Jenks, *Corrosion*, Vol 13, 1957, p 481
25. C.R. Southwell, C.W. Hummer, and A.L. Alexander, Corrosion of Metals in Tropical Environments—Part 6, Aluminum and Magnesium, U.S. Naval Research Laboratory, Report NRL 6105, 1 Dec 1964, Report AD 609, p 618
26. R.B. Mears and R.H. Brown, *Transactions of the Society of Marine Engineers*, Vol 52, 1944, p 91
27. C.J. Walton and E.T. Englehart, *Transactions of the Society of Naval Architects and Marine Engineers*, Nov 1949
28. E.T. Wanderer and D.O Sprowls, *Corrosion*, Vol 8, 1952, p 227
29. T.J. Summerson, *et al*, American Society for Testing and Materials Special Publication No. 196, 1956
30. F. Sutton, U.S. Naval Engineering Experimental Station, Annapolis, MD, R & D Report No. 910037L, PB 163, 12 June 1961, p 836
31. A. Guildhaulis, *Revue de l'Aluminium* (No. 186-188) 1952, p 85, 127 and 175; *Revue de Metallurgie*, Vol 49 (No. 11), 1952; *Revue de l'Aluminium* (No. 259 and 260); *Corrosion et Anti Corrosion*, Vol 10, 1962, p 80; and *Corrosion et Anti Corrosion*, Vol 11, 1963, p 404
32. W.H. Ailor and F.N. Reinhart, *U.S. Naval Engineering Journal*, June 1964
33. H.P. Godard and F.F. Booth, Corrosion Behavior of Aluminum Alloys in Seawater (in English), Congres International de la Corrosion Marine et des Salissures Editions du Centre de Recherches et l'Etudes Oceaniques, 1 Quai Branly, Paris 7, May 1965
34. W.H. Ailor, American Society for Testing and Materials, STP 558, 1974
35. R.S. Dalrymple, *Corrosion*, Vol 12, 1956, p 602
36. G.R. Harrison and R.N. Bassarab, Canadian Oil and Gas Industry, May 1959
37. J.F. Whiting and T.E. Wright, *Corrosion*, Vol 17 (No. 8), 1961, p 9

38. J.F. Whiting and T.E. Wright, *Materials Protection,* Vol 1 (No. 11), 1962, p 36
39. H.P. Godard, Ed., *The Corrosion of Light Metals,* New York: John Wiley & Sons, 1967, p 148
40. R.S. Dalrymple, *Oil and Gas Journal,* 11 Dec 1961, p 78
41. R.S. Dalrymple, *Materials Protection,* Vol 2 (No. 10), 1963, p 11
42. T.A. Lowe and A.H. Koepf, Highway Research Board Record
43. FHWA (US) Technical Note 5040.12, Oct 1979
44. H.P. Godard, Field and Laboratory Testing of Aluminum (in Soils), *U.S. Highway Research Record* (No. 95), 1965, p 33-39
45. J.M. Bryan, Aluminum and Aluminum Alloys in the Food Industry, U.K. Dept. of Scientific and Industrial Research, *Food Investigation Special Report* (No. 50), London: HMSO, 1948
46. *Guidelines for use of Aluminum with Food and Chemicals,* Aluminum Association, 1983
47. G.A. Nelson, Corrosion Data Survey, Shell Development Co., 1950
48. E.H. Cook, R.L. Horst, and W.W. Binger, Corrosion Studies of Aluminum in Chemical Process Specification, *Corrosion,* Vol 17, 1961, p 97
49. W.C.E. Barnes, *Aluminum—Its Applications in the Chemical and Food Industries,* London: Crosby Lockwood & Son, 1964
50. Corrosion Data Survey, NACE
51. F.L. LaQue, *Corrosion Testing,* American Society for Testing and Materials, Vol 51, 1951, p 519
52. F.A. Champion, *Corrosion Testing Procedures,* 2nd ed., London: Chapman Hall, 1965
53. W.H. Ailor, *Handbook of Corrosion Testing and Evaluation,* New York: John Wiley & Sons, 1971
54. Aluminum for More Efficient Rail Road Cars, *Aluminum Association Brochure* (No. 66), 1980, p 15
55. T.E. Wright, H.P. Godard, and I.H. Jenks, *The Engineering Journal (Montreal),* Vol 37, 1954, p 1250
56. H. Vosskuhler and E. Fischer, *Aluminium,* Vol 33, 1957, p 606
57. C.J. Walton, F.L. McGeary, and E.T. Englehart, *Corrosion,* Vol 13, 1957, p 807
58. L.H. Everett, *The Builder,* U.K., 30 March 1962
59. F.E. Jones and R.D. Tarleton, *National Building Studies Research Paper (No. 36),* U.K. Building Research Station, London: HMSO, 1963
60. R.H. Farmer and F.C. Porter, *Metallurgia,* Oct 1963, p 161
61. Wood Handbook, *Forest Products Laboratory USDA Handbook* (No. 72), 1955, p 311
62. R.H. Farmer, *Wood,* U.K., Nov 1962, p 443
63. *British Forest Product Research Bulletin,* London: HMSO, 1950, p 46
64. R.B. Mears and R.H. Brown, *Industrial and Engineering Chemistry,* Vol 33, 1941, p 1002
65. H.P. Godard and W.E. Cooke, The Analysis and Composition of Aluminum Corrosion Products, NACE Technical Committee, T-3B Report 80-5, Corrosion, Vol 16, 1960, p 181-187
66. H.P. Godard, Examining Causes of Aluminum Corrosion, *Materials Performance,* Vol 8 (No. 8), 1969, p 25-30
67. C. Edleanu and U.R. Evans, *Transactions of the Faraday Society,* Vol 47, 1951, p 1121
68. P.M. Aziz, *Corrosion,* Vol 9, 1953, p 85
69. K. Sotovdeh, *et al, Corrosion,* Vol 37, 1981, p 358

70. H.P. Godard, *The Encyclopedia of Electrochemistry*, New York: Van Nostrand Reinhold, 1964, p 925
71. Rosenfeld, *Localized Corrosion*, NACE, 1974, p 386, 389
72. H.P. Godard, Ed., *The Corrosion of Light Metals*, New York: John Wiley & Sons, 1967, p 47
73. H.P. Godard, Ed., *The Corrosion of Light Metals*, New York: John Wiley & Sons, 1967, p 46
74. American Society for Testing and Materials, Standard Definitions of Terms Relating to Corrosion and Corrosion Testing, 15 June 1979a
75. R.H. Brown, *Galvanic Corrosion*, American Society for Testing and Materials, Bulletin 126, 1944
76. W. King, G. Sowinski, and E.T. Englehart, SAE Publication (No. 750464), 1975
77. H.P. Godard, *The Engineering Journal*, Montreal, Vol 38, 1955, p 28
78. U.R. Evans and V.E. Rance, *Production Engineer*, London, Vol 27 (No. 13), 1956, p 187
79. F. Mansfeld and J.V. Kenkel, *Corrosion Science*, Vol 15, 1975, p 239
80. F. Mansfeld and J.V. Kenkel, *Corrosion Science*, Vol 15, 1975, p 183
81. F. Mansfeld and J.V. Kenkel, American Society for Testing and Materials, STP 576, 1976, p 20
82. H.P. Godard, Corrosion Behavior of Aluminum in Natural Waters, *Canadian Journal of Chemical Engineering*, 1960, p 167-176
83. W.H. Ailor, Jr., A Review of Aluminum Corrosion in Tap Waters, *Journal of Hydronautics*, Vol 3 (No. 3), 1969, p 105-115
84. W.W. Binger, R.H. Brown, and M.H. Brown, Mercury and its Compounds—A Corrosion Hazard, *Corrosion*, Vol 8, 1952, p 155-164
85. Anonymous, *Corrosion*, Vol 14 (No. 3), 1958, p 63
86. Tolstaya, *et al*, Electrocorrosion of Cables with Aluminum Casing Under the Effect of Alternating Currents, *Zashchita Metallov*, Vol 2, 1956, p 55
87. Y.N. Mikhailovski, Electrochemical Corrosion of Metals by Alternating Current, 4, Dissolution of Aluminum and Magnesium on Polarization by Alternating Current, *Zhurnal Prikladnoi Khimii*, USSR, Vol 37, 1963, p 1196-1200
88. J.F. Williams, Corrosion of Metals Under the Influence of Alternating Current, *Materials Protection*, Vol 5, 1966, p 52-53
89. W.H. French, Alternating Current Corrosion of Aluminum, *Trans IEEE*, Power Engineering Society Winter Meeting, New York, 28 Jan-2 Feb, 1973
90. M. Crook, Corrosion Killer, *Yachting*, Dec 1971, p 70
91. A.W. Peabody, Control of Pipeline Corrosion, NACE Publication, 1967
92. R.E. Brooks, A.H. Roebuck, and E. Hazan, Corrosion of Aluminum Conduit in Concrete, *Electrical Construction and Maintenance*, Feb 1965
93. R.B. Mears, R.H. Brown, and E.H. Dix, Jr., A Generalized Theory of the Stress Corrosion of Alloys, in *Symposium on Stress-Corrosion Cracking of Metals*, ASTM and AIME, 1945, p 323-344
94. D.O. Sprowls and R.H. Brown, Stress Corrosion Mechanisms for Aluminum Alloys, *Fundamental Aspects of Stress Corrosion Cracking*, NACE, 1969, p 466-506
95. M.O. Speidel, Current Understanding of Stress Corrosion Crack Growth in Aluminum Alloys, *The Theory of Stress Corrosion Cracking in Alloys*, NATO, 1971, p 289-342
96. M.O. Speidel and M.V. Hyatt, Stress-Corrosion Cracking of High-Strength Aluminum Alloys, *Advances in Corrosion Science and Technology*, Vol 2, New York: Plenum Press, 1972, p 115-335
97. H.L. Logan, *The Stress Corrosion of Metals*, New York: John Wiley & Sons, 1966

98. H.P. Godard, Ed., *The Corrosion of Light Metals*, New York: John Wiley & Sons, 1967
99. B.F. Brown, SCC Control Measures, NBS Monograph No. 156, 1977
100. R.J. Gest and A.R. Troiano, Stress Corrosion and Hydrogen Embrittlement in an Aluminum Alloy, *Corrosion*, Vol 30, 1974, p 274-279
101. J. Albrecht, Hydrogen Embrittlement in a High-Strength Aluminum Alloy, *Scripta Metallurgica*, Vol 11, 1977, p 893-897
102. G.H. Koch, Hydrogen Induced Fracture of a High Strength Aluminum Alloy, *Corrosion*, Vol 35, 1979, p 73-78
103. J.A.S. Green, H.W. Hayden, and W.G. Montague, Influence of Loading Mode on the Stress Corrosion Susceptibility of Various Alloy/Environment Systems, *Effect of Hydrogen on Behavior of Materials*, AIME, 1976, p 200-209
104. G.M. Scamans, R. Alani, and P.R. Swann, Pre-Exposure Embrittlement and Stress Corrosion Failure in Al-Zn-Mg Alloys, *Corrosion Science*, Vol 16, 1976, p 443-459
105. C.D.S. Tuck, Evidence for the Formation of Magnesium Hydride on the Grain Boundaries of Al-Mg and Al-Zn-Mg Alloys During Their Exposure to Water Vapor, Third Conference on the Effect of Hydrogen on Behavior of Materials, AIME, 1980
106. R.K. Viswanadham, T.S. Sun, and J.A.S. Green, Influence of Moisture Exposure on the Composition of Oxides on Al-Zn-Mg Alloy: An Auger Electron Spectroscopy Study, *Corrosion*, Vol 36, 1980, p 275-278
107. J.M. Chen, *et al*, *Metallurgical Transactions A*, Vol 8A, 1977, p 1935
108. R.K. Viswanadham, *et al*, *Metallurgical Transactions A*, Vol 11A, 1980, p 85
109. S. Maitra and G.C. English, Mechanism of Localized Corrosion of 7075 Alloy Plate, *Metallurgical Transactions A*, Vol 12A, 1981, p 535
110. W. Gruhl, The Stress Corrosion Behavior of High Strength Al-Zn-Mg Alloys, *Aluminium*, Vol 54, 1978, p 323-325
111. ASTM Annual Book of Standards, Part 10
112. D.O. Sprowls, *et al*, Evaluation of a Proposed Test Method of Testing for Susceptibility to Stress-Corrosion Cracking of High Strength 7XXX Series Aluminum Alloys Products, *Stress Corrosion—New Approaches*, ASTM STP 610, 1978, p 3-31
113. R.C. Dorward and K.R. Hasse, Flow Growth in High Strength Al-Zn-Mg-Cu Alloys Exposed to Stress Corrosion Environments, *Corrosion*, Vol 34, 1978, p 386-395
114. G.M. Ugiansky, *et al*, Slow Strain-Rate Stress Corrosion Testing of Aluminum Alloys, *Stress Corrosion Cracking—The Slow Strain Rate Technique*, ASTM STP 665, 1979, p 254-265
115. *Metals Handbook*, 8th ed., Vol 10, American Society for Metals, 1975, p 223
116. P.J.E. Forsyth, The Fatigue Performance of Service Aircraft and the Relevance of Laboratory Data, *Journal of the Society of Environmental Engineering*, Vol 19, 1980, p 3
117. N.L. Person, Fatigue Properties of Prior-Corroded Aluminum Sheet Alloys, *Materials Performance*, Vol 14 (No. 12), 1975, p 22
118. N.A. Miller, Some Factors Influencing the Corrosion Fatigue Behaviour of a High-Strength Aluminium Alloy, *New Zealand Journal of Science*, Vol 12, 1969, p 346
119. M. Ito and K. Takeuchi, The Effects of Atmospheric Humidity and Duration of Prior-Corrosion in Atmosphere on the Fatigue Strength of Some Aluminum Alloys, *Sumitomo Light Metals Technology Reports*, Vol 16, 1975, p 17

120. Fu-Shiong Lin, Low Cycle Corrosion Fatigue and Corrosion Fatigue Crack Propagation of High Strength 7000-Type Aluminum Alloys, Ph.D. Thesis, Georgia Institute of Technology, 1978
121. R.J. Jacko and D.J. Duquette, Hydrogen Embrittlement of a Cyclicly Deformed High Strength Aluminum Alloy, *Metallurgical Transactions A*, Vol 8A (No. 11), 1977, p 821
122. T.W. Montemarano and M.E. Wells, Improving the Fatigue Performance of Welded Aluminum Alloys, *Welding Journal*, Vol 22 (No. 6), 1980, p 21
123. N.L. Person, Effect of Shot Peening Variables on Fatigue of Aluminum Forgings, *Metal Progress*, Vol 120 (No. 2), 1981, p 33
124. H.G. Cole and R.J.M. Payne, Protection of Aluminum-Zinc-Magnesium Alloy Against Corrosion Fatigue, *Metallurgia*, Vol 66 (No. 7), 1962, p 11
125. T. Takeuchi, *Corrosion Abstracts*, Vol 13, 1957, p 13
126. W.M. Lorkovic, D. Varallayay, and R.D. Daniels, Corrosion Fatigue of Aluminum Alloys, *Materials Protection*, Vol 3 (No. 11), 1964, p 16
127. G.J. Biefer, *Corrosion Fatigue of Structural Steels in Mine Waters*, Canadian Dept. of Mines and Technical Surveys, Report No. R-167, July 1965
128. R.E. Stoltz and R.M. Pelloux, Mechanisms of Corrosion Fatigue Crack Propagation in Al-Zn-Mg Alloys, *Metallurgical Transactions A*, Vol 3 (No. 9), 1972, p 2433
129. S.E. LeBeau and D.J. Duquette, *The Effects of Corrosion and Cathodic Charging on Fatigue Crack Propagation in 7075-7851 Aluminum*, Office of Naval Research Technical Report Project No. N 00014-75-C-0466, 1978
130. M. Khobaib, E.T. Lynch, and F.W. Vahldiek, Inhibition of Corrosion Fatigue in High Strength Aluminum Alloys, *Corrosion*, Vol 37 (No. 5), 1981, p 285
131. R.J. Bucci, Selecting Aluminum Alloys to Resist Failure by Fracture Mechanisms, *Engineering Fracture Mechanics*, Vol 12 (No. 3), 1979, p 407
132. W.H. Wheeler, Mechanical Engineering Research Laboratory DSIR, East Kilbride, Glasgow, Fluids Report No. 44, 1956
133. J.M. Mousson, *Transactions of AIME*, Vol 60, 1937, p 399
134. ASTM D2809, Standard Method for Cavitation Erosion Corrosion Characteristics of Aluminum Pumps with Engine Coolants
135. R.L. Chance, Electrochemical Corrosion of an Aluminum Alloy in Cavitating Ethylene Glycol Solutions, International Symposium on State of the Art in Engine Coolant Testing, sponsored by ASTM, Atlanta, GA, April 1979
136. W.H. Anthony and J.M. Popplewell, A Study of Erosion-Corrosion in Aluminum Radiator Alloys by Jet Impingement, SAE Automotive Engineering Congress, Detroit, MI, Paper No. 72009, Jan 1972
137. C. M. Preece, A Comparison of Liquid Impact Erosion and Cavitation Erosion, *Wear*, Vol 60 (No. 2), 1980, p 269-284
138. C. M. Preece and J.H. Brumlon, Liquid Impact Erosion of Al-Mg and Al-Cu Alloys, *Wear*, Vol 60 (No. 2), 1980, p 285-304
139. G.A. Gehring, Jr., Corrosion of Aluminum Alloys in High Velocity Seawater, Fifth International Congress on Marine Corrosion and Fouling, Madrid, Spain, 1980
140. B.E. Miller and H.P. Hack, Impressed Current Cathodic Protection of Aluminum Hulled Craft, Paper No. 72-593, AIAA/SNAME/USN Advanced Vehicles Meeting, Annapolis, MD, 17-19 July 1972
141. B.E. Miller, and H.P. Hack, Impressed Cathodic Protection of Aluminum Hulled Craft, *Journal of Hydronautics*, Vol 7 (No. 3), 1973, p 108-111

142. W. Spath, Friction, Fretting and Fracture of Metals, (in German), *Metall,* Vol 7, 1953, p 34-46
143. R.B. Waterhouse, *Fretting Corrosion,* London: Pergamon Press, Biddles Wd., Surrey, U.K., 1975
144. E.H. Dix, *Corrosion of Light Metals,* American Society for Metals, 1946, p 131-176
145. P.M. Aziz and H.P. Godard, *Industrial and Engineering Chemistry,* Vol 44, 1952, p 1791
146. D.O. Sprowls and R.H. Brown, Stress Corrosion Mechanisms for Aluminum Alloys, International Conference on Fundamental Aspects of Stress-Corrosion Cracking, NACE, Houston, 1969
147. D.O. Sprowls and R.H. Brown, *Resistance of Wrought High Strength Aluminum Alloys to Stress Corrosion,* Alcoa Research Laboratories Technical Paper No. 17, 1962, p 29
148. B.W. Lifka and D.O. Sprowls, Significance of Intergranular Corrosion in High Strength Aluminum Alloy Products, Localized Corrosion—Cause of Metal Failure, ASTM STP 516, 1972, p 120-144
149. D.O. Sprowls, High Strength Aluminum Alloys with Improved Resistance to Corrosion and Stress Corrosion Alloys, Tri-Service Conference on Corrosion, 1976
150. E.H. Dix, W.A. Anderson, and M.B. Shumaker, Influence of Service Temperature on the Resistance of Wrought Aluminum-Magnesium Alloys to Corrosion, *Corrosion,* Vol 15, 1959, p 55-62
151. E.H. Dix, W.A. Anderson, and M.B. Shumaker, Development of Wrought Aluminum-Magnesium Alloys, Alcoa Research Laboratories Technical Paper No. 14, 1958
152. E.H. Spuhler and C.L. Burton, Avoiding Stress-Corrosion Cracking in High Strength Aluminum Alloy Structures, Alcoa Green Letter, April 1970
153. *Welding Aluminum,* American Welding Society—The Aluminum Association, 1972
154. J.G. Young, BWRA Experience in the Welding of Aluminum-Zinc-Magnesium Alloys, *Welding Research Supplement,* Oct 1968
155. Alcoa Aluminum Alloy 7005, Alcoa Green Letter, Sept 1974
156. Tentative Guide to Automotive Resistance Spot Welding of Aluminum, The Aluminum Association, Washington, DC, T10, Oct 1973
157. Weldbonding—An Alternate Joining Method for Aluminum Auto Body Alloys, The Aluminum Association, Washington, DC, T17, 1978
158. T.L. Wilkinson and W.H. Ailor, Joining and Testing Bimetallic Automotive Panels, SAE Technical Paper, Series No. 780254, Society of Automotive Engineers, Warrendale, PA, 1978
159. J.J. Bethke and S.J. Ketcham, Polysulfide Sealants for Corrosion Protection of Spot Welded Aluminum Joints, *Adhesives Age,* Nov 1979, p 17
160. R. Baboian and G.S. Hayes, Joining Dissimilar Metals with Transition Materials, *Automotive Engineering,* Vol 84, Dec 1976
161. Transition Spacers Developed for Dissimilar Metal Joints to Minimize Corrosion and Simplify Joining, *Welding Journal,* Vol 56, Sept 1977
162. *Metals Handbook,* 8th ed., Vol 6, American Society for Metals, 1971
163. *Aluminum Brazing Handbook,* The Aluminum Association, Washington, DC, 1979
164. W. King and W.C. Weltman, Performance of Aluminum Automotive Radiators, SAE Technical Paper Series No. 790400, Society of Automotive Engineers, Warrendale, PA, 1979
165. W.E. Cooke, T.E. Wright, and J.A. Hirschfield, Furnace Brazing of Aluminum with a Non-Corrosive Flux, SAE Technical Paper Series, No. 780300,

Society of Automotive Engineers, Warrendale, PA, 1978
166. P.B. Dickerson, Working with Aluminum? Here's What You Can Do with Dip Brazing, *Metal Progress,* Vol 87 (No. 80), May 1965
167. Non-Corrosive Flux for Brazing—Anti Corrosion Methods and Materials, London, May 1978
168. Non-Corroding Flux Averts Aluminum Brazing Problems, *Modern Metals,* Vol 34, March 1978
169. U.S. Patents 3,321,828 and 3,322,517
170. Soldering Alcoa Aluminum, Aluminum Company of America, 1972
171. J.J. Stokes, A Low Temperature Soft Solder System for Aluminum, Paper presented at American Welding Society, 55th Annual Meeting, Houston, May 1974
172. Soldering Aluminum, 2, Materials-Solders, *Welding Journal,* Vol 51 (No. 9), Sept 1972, p 643-644
173. J.F. Smith, Selecting Solders for Specific Substrates, *Materials Engineering,* Vol 80 (No. 3), Sept 1974, p 76-78
174. Soldering Aluminum, 4, Post Solder Cleaning and Finishing, *Welding Journal,* Vol 51 (No. 11), Nov 1972, p 786-787
175. Soldering Aluminum, 8, Abrasion and Ultrasonic Soldering, *Welding Journal,* Vol 52 (No. 8), Aug 1973, p 520-521
176. *Metals Handbook,* Properties and Selection of Metals, Vol 1, 8th ed., American Society for Metals, 1961
177. Fastening Aluminum, 1 and 2, *Modern Metals,* Vol 16 (No. 12), Jan 1961, Vol 17 (No. 1), Feb 1961, p 28-46
178. W.J. DeWalt and R.E. Mack, Design Considerations for Aluminum Fasteners, Society of Automotive Engineers, Technical Paper Series No. 800455, *1980 Transactions of SAE,* Sept 1981
179. R.N. Miller, Inhibitive Sealing Compounds and Coating Systems Solve Aircraft Corrosion Problems, *SAMPE Journal,* Vol 6 (No. 3), April/May 1970, p 54-58
180. J.D. Minford and E.M. Vader, Aluminum-Faced Sandwich Panels and Laminates, *Adhesives Age,* Feb 1975
181. R.J. Schliekelmann, Operational Experience with Adhesive Bonded Structures, AGARD Lecture Series 102, Bonded Joints and Preparation for Bonding, Wright-Patterson Air Force Base, Dayton, OH, Oct 1979
182. Adhesive Bonding of Aluminum Automotive Body Sheet Alloys, T-14, The Aluminum Association, 1975
183. J.D. Minford, F.R. Hoch, and E.M. Vader, SAE International Automotive Engineering Congress, Paper No. 750462, Detroit, MI, Feb 1975
184. J.D. Minford, Durability of Adhesive Bonding Aluminum Joints in Treatise of Adhesion and Adhesives, Vol III, R.L. Patrick, Ed., New York: Marcel Dekker, 1973
185. J.D. Minford, Durability or Permanence of Aluminum Adhesive Joints, Technical Report of Society of Manufacturing Engineers, ADR80-11, 1980
186. J.D. Minford, Comparison of Aluminum Adhesive Joint Durability as Influenced by Etching and Anodizing Pretreatments of Bonded Surfaces, *Journal of Applied Polymer Science,* Applied Polymer Symposium, Vol 32, 1977, p 91-103
187. J.D. Minford, Effect of Surface Preparation on Stressed Aluminum Joints in Corrosive Salt Water Exposure, *Adhesives Age,* Oct 1980
188. C.R. Schmitt, Corrosion Behavior of Aluminum in Water, *Reviews on Coatings and Corrosion,* Vol 4 (No. 1), 1979, p 95-112
189. J.E. Draley and W.E. Ruther, Aqueous Corrosion of Aluminum, Part 1—Behavior of 1100 Alloy, *Corrosion,* Vol 12 (No. 9), Sept 1956, p 441-448

190. A.A. Adams, *et al,* Synergistic Effect of Anions in the Corrosion of Aluminum Alloys, *Journal of Electrochemical Society,* Vol 119 (No. 12), Dec 1972
191. W.W. Binger and C.M. Marstiller, Aluminum Alloys for Handling High-Purity Water, *Corrosion,* Vol 13 (No. 9), Sept 1957
192. J.E. Draley and W.E. Ruther, Aqueous Corrosion of Aluminum, Part 2—Methods of Protection Above 200 °C—*Corrosion,* Vol 12 (No. 10), Oct 1956, p 480-490
193. M.H. Brown, R.H. Brown, and W.W. Binger, Alcoa Green Letter, Aluminum Alloys for Handling High Temperature Water, March 1960
194. Aluminum Alloys in Water Storage and Distribution, The Aluminum Association, Washington, DC
195. R.H. Wagner and B.M. Wyma, Aluminum Equipment for Handling High Purity Water and Steam Condensate, *Proceedings of American Power Conference,* Vol 27, 1965, p 825-834
196. M. Pourbaix, Atlas of Electrochemical Equilibria in Aqueous Solution, Oxford: Pergamon Press, 1966, p 169
197. F.H. Haynie, *et al,* Effects of Gaseous Pollutants on Materials: A Chamber Study, U.S. Dept. of Commerce, National Technical Information Service PB-251-580
198. K. Barton, *Protection Against Atmospheric Corrosion,* New York: John Wiley & Sons, 1976
199. H.P. Godard, Ed., *The Corrosion of Light Metals,* New York: John Wiley & Sons, 1967
200. D.P. Doyle and H.P. Godard, Influence of Temperature on Galvanic Corrosion, *Materials Protection,* Vol 8 (No. 8), 1969, p 40
201. E.V. Konstantinova, *et al,* Investigations of the Possibilities of Using Aluminum Alloys as Structural Materials for Distillation Equipment, *Zashchita Metallov,* Vol 12 (No. 3), May/June 1976, p 306-308
202. G.A. Gehring, Jr. and M.H. Peterson, Corrosion of 5456-H117 Aluminum in High Velocity Sea Water, Corrosion/79 Proceedings of NACE Conference, Atlanta, GA, 1979
203. R.A. Bonewitz, The Performance of Aluminum Alloys in Ammonia-Sea Water Solutions, Fifth Ocean Thermal Energy Conversion (OTEC) Conference, Miami Beach, FL, Feb 1978
204. Prevention of Corrosion of Metals, SAE HS J447a, 1964
205. C.L. Brooks, Aluminum-Magnesium Alloys 5086 and 5456-H116, *Naval Engineers Journal,* Aug 1970, p 29
206. L.D. Perrigo, Fundamentals of Corrosion Control Design, Battelle-Northwest Laboratories, BNWL-SA-5289, 5 Feb 1975
207. P.E. Wolfe and A.H. Mussnug, *Materials and Methods,* Vol 42, Oct 1955, p 11
208. D.O. Sprowls and R.H. Brown, What Every Engineer Should Know About Stress Corrosion of Aluminum, Part II, *Metal Progress,* May 1962, p 77
209. H.P. Godard, Ed., *Corrosion of Light Metals,* New York: John Wiley & Sons, Inc., 1967, p 180
210. J.D. Jackson and W.K. Boyd, Preventing Stress Corrosion Cracking of High Strength Aluminum Alloy Parts, *Materials in Design Engineering,* May 1966, p 70
211. B.W. Lifka and D.O. Sprowls, Shot Peening—A Stress Corrosion Cracking Preventive for High Strength Aluminum Alloys, National Association of Corrosion Engineers 26th Annual Conference, Paper No. 86, March 1970
212. H.L. Craig, Jr. and F.E. Loftin, Preventing Stress Corrosion Failures in Susceptible Aluminum Alloys, *Materials Protection and Performance,* Vol 10 (No. 3), 1971, p 17

213. R.S. Kaneko, RRA: Solution for Stress Corrosion Problems with T6 Temper Aluminum, *Metal Progress*, April 1980, p 41
214. B.F. Brown, Stress Corrosion Cracking Control Measures, National Bureau of Standards Monograph 156, 1977, p 23-34
215. R.B. Mears and G.G. Eldredge, *Industrial and Engineering Chemistry*, Vol 27, 1945, p 736
216. A.J. Haygood and J.D. Minford, *Corrosion*, Vol 15, 1959, p 20
217. A.H. Roebuck and T.R. Pritchett, Corrosion Inhibitors for Aluminum, *Materials Protection*, Vol 5 (No. 7), 1966, p 16
218. A.H. Roebuck and J.F. Richards, Corrosion Inhibitors for Aluminum, National Association of Corrosion Engineers, Corrosion Paper No. 134, 1975
219. H.W. McCune, Corrosion of Aluminum by Alkaline Sequestering Solutions, *Industrial and Engineering Chemistry*, Vol 50 (No. 1), 1958, p 67
220. Control of External Corrosion on Underground or Submerged Metallic Piping Systems, NACE RP-01-69, NACE, Houston, TX, 1976
221. J.H. Morgan, *Cathodic Protection*, London: Leonard Hill Books Ltd., 1959, p 28

SELECTED REFERENCES

- Alcoa Aluminum Alloy 7005, Alcoa Green Letter, Sept 1974
- Aluminum Soldering Handbook, ASH-22, Aluminum Association, Dec 1976
- R.E. Brooks, Compatibility of Aluminum with Alkaline Building Materials, *Materials Protection*, July 1962, p 44-48
- Canadian Standards Association, CSA Standard Z169-M1978, Aluminum Pipe and Pressure Piping Systems
- Canadian Standards Association, CSA Standard C22.3, No. 4-1978, Control of Electrochemical Corrosion of Underground Metallic Structures
- Canadian Standards Association, CSA Standard Z183-M1977 and Z184-M1979, Oil and Gas Pipeline Systems
- G.L. Christie, The Cathodic Protection of Aluminum—Trials with Alcan 655T Alloy, Naval Research Establishment, Dartmouth, N.S., Canada, DRB Report No. PH-85, Feb 1954
- Control of External Corrosion on Underground or Submerged Metallic Piping Systems, National Association of Corrosion Engineers, Recommended Practice RP-01-69, 1976
- Designing for Corrosion Prevention, *Automotive Engineering*, Vol 85 (No. 2), Feb 1977, p 37, 39, 41
- F.P. Ford, G.T. Burstein, and T.P. Hoar, Bare Surface Reaction Rates and Their Relation to Environment Controlled Cracking of Aluminum Alloys, *Electrochemical Society*, Vol 127, 1980, p 1325-1331
- Fu-Shiong Lin, Low Cycle Corrosion Fatigue and Corrosion Fatigue Crack Propagation of High Strength 7000-Type Aluminum Alloys, Ph.D. Thesis, Georgia Institute of Technology, 1978
- H.P. Godard, Ed., *The Corrosion of Light Metals*, New York: John Wiley & Sons, 1967, p 48
- R.J. Jacko and D.J. Duquette, Hydrogen Embrittlement of a Cyclically Deformed Aluminum Alloy, *Metallurgical Transactions A*, Vol 8A, 1977, p 1821-1827
- C. Laird and D.J. Duquette, Mechanisms of Fatigue Crack Nucleation,

Corrosion Fatigue: Chemistry, Mechanics, and Microstructure, NACE, 1972, p 88-114

- F.L. LaQue, ASTM Procedures, Vol 51, 1951, p 519
- F.L. LaQue, *Marine Corrosion, Causes and Prevention,* New York: John Wiley & Sons, 1975, p 198-200
- S.E. LeBeau and D.J. Duquette, *The Effects of Corrosion and Cathodic Charging on Fatigue Crack Propagation in 7075-T651 Aluminum,* Office of Naval Research Technical Report, Project No. N00014-75-C-0466, 1978
- R.B. Mears and H.J. Fahrney, *Transactions of AIME,* Vol 37, 1947
- R.B. Mears and R.H. Brown, *Industrial and Engineering Chemistry,* Vol 29, 1937, p 1087
- L.F. Mondolfo, Structure of the Aluminum: Magnesium: Zinc Alloys, *Metallurgical Reviews,* Vol 16, 1971, p 95-124
- R.M. Pelloux, R.E. Stoltz, and J.A. Moskovitz, Corrosion Fatigue, *Material Science Engineering,* Vol 25, 1976, p 193-200
- H.H. Uhlig, Ed., *Corrosion Handbook,* New York: John Wiley & Sons, 1948, p 416
- Schweiz Archiv fur Wissenschaft und Technik, Vol 5, 1939, p 300
- Shipbuilding and Shipping Record, Vol 105, 1965, p 214
- Soldering Aluminum, 1, Materials—Alloy Types and Fluxes, *Welding Journal,* Vol 51 (No. 8), Aug 1972, p 571-573
- Soldering Aluminum, 3, Surface Preparation, *Welding Journal,* Vol 51 (No. 10), Oct 1972, p 714-716
- Soldering Aluminum, 5, Joint Design, *Welding Journal,* Vol 51 (No. 12), Dec 1972, p 851-856
- R.E. Stoltz and R.M. Pelloux, Mechanisms of Corrosion Fatigue Crack Propagation of Al-Zn-Mg Alloys, *Metallurgical Transactions A,* Vol 3, 1972, p 2433-2441
- G.R.L. Warkings, *Light Metals,* Vol 13, 1950, p 206
- Welding Aluminum, American Welding Society, The Aluminum Association, 1972
- S.A. Westgate, Joining of Aluminum Alloy Sheet—A Literature Survey, Part I: Resistance Welding, The Welding Institute, Report No. 84, 1979
- T.E. Wright and H.P. Godard, *Corrosion,* Vol 10, 1954, p 195
- J.G. Young, BWRA Experience in the Welding of Aluminum-Zinc-Magnesium Alloys, *Welding Research Supplement,* Oct 1968

Aluminum Properties and Physical Metallurgy
John E. Hatch editor, p 320-350
DOI: 10.1361/appm1984p320

CHAPTER 8

PROPERTIES OF COMMERCIAL CASTING ALLOYS*

Aluminum alloy castings can be produced by virtually all casting processes in a range of compositions possessing a wide variety of useful engineering properties. For large production quantities, high-pressure die, permanent mold, and sand are the most important casting processes. Smaller quantities of castings are produced in plaster, investment, and composite material molds.

Unlike wrought alloys, aluminum casting alloys are not identified according to a single commercial designation system in the United States. However, the three-digit registration system of the Aluminum Association (AA) is most widely used (Ref 1). This system was adopted in 1954 and approved by the American Standards Association (now the American National Standards Institute, Inc.) as an American standard in 1957 (ANSI H-35.1). Other systems used include the proprietary nomenclatures assigned by the originators of some alloys, and the specification designations of the American Society for Testing and Materials (ASTM) (Ref 2) and the Society of Automotive Engineers (SAE) (Ref 3). Federal and military specifications for aluminum casting alloys reflect AA designations. In the Aluminum Association system, major alloying elements are indicated as follows:

Series	Alloy family
1XX	99.0% min Al
2XX	Al—Cu
3XX	Al—Si—Mg, Al—Si—Cu, Al—Si—Cu—Mg
4XX	Al—Si
5XX	Al—Mg
7XX	Al—Zn
8XX	Al—Sn

No commercial alloys are established currently in the 6XX and 9XX series. Alloys are registered by the AA, with XXX.0 representing the chemical composition limit for castings and XXX.1 and XXX.2 representing chemical composition limits for ingots. Examples can be found in Table 1.

Several AA alloy designations also include a prefix letter. Different letters used with the same alloy number distinguish alloys of a general composition that differ only in percentage of impurities or minor alloying elements, for example 356 and A356, or 380, A380, and B380 (see Table 2).

*This chapter was revised by a team comprised of J.L. Jorsted, Reynolds Metals Co.; E.L. Rooy, Aluminum Company of America; and A.B. DeRoss, Kaiser Aluminum & Chemical Corp. The original chapter was authored by W.E. Sicha, Alcoa Research Laboratories.

Table 1. Alloys Registered by the Aluminum Association

AA No.	Form	Composition, % Silicon	Iron	Copper	Manganese	Magnesium	Nickel	Zinc	Tin	Titanium	Other Each	Other Total
356.0	Sand and permanent mold	6.5–7.5	0.6	0.25	0.35	0.20–0.45	···	0.35	···	0.25	0.05	0.15
356.1	Ingot	6.5–7.5	0.50	0.25	0.35	0.25–0.45	···	0.35	···	0.25	0.05	0.15
356.2	Ingot	6.5–7.5	0.13–0.25	0.10	0.05	0.30–0.45	···	0.05	···	0.20	0.05	0.15
380.0	Die cast	7.5–9.5	2.0	3.0–4.0	0.50	0.10	0.50	3.0	0.35	···	···	0.50
380.2	Ingot	7.5–9.5	0.7–1.1	3.0–4.0	0.10	0.10	0.10	0.10	0.10	···	···	0.2

The AA chemical composition limits for aluminum alloy castings (XXX.0) are listed in Table 2. ASTM and SAE designations are also shown where applicable. Other tables in this chapter list only the AA alloy designation.

Commercial aluminum casting alloys include both heat treatable and non-heat treatable compositions (Ref 4). Castings made from non-heat treatable alloys are not appreciably affected by heat treatment and are usually marketed in the as-cast condition, identified by an F following the alloy number, or by omission of any suffix. An exception, however, is solution heat treatment (T4 temper), which specifically spheroidizes the eutectic silicon in aluminum-silicon alloys to improve ductility, such as A444-T4. Both heat treatable and non-heat treatable alloys may also be thermally stress relieved (O temper).

Alloys that respond to heat treatment provide improved combinations of mechanical properties. The nature of the treatment is identified with a suffix temper designation. The O, T4, T5, T6, and T7 tempers are normally applied to aluminum castings.

Die castings are not normally solution heat treated, because heating to the required temperature of 480 to 540 °C (900 to 1000 °F) causes blistering. However, the composition of die casting alloys such as 360, A360, 361, 364, 369, and 390 or B390 is such that they could benefit substantially from a solution heat treatment and artificial aging (T6 or T7 temper). New improvements in the die casting process have resulted in internal quality that is compatible with solution heat treatment. This has permitted the use of T6 and T7 tempers.

In addition to the effects of heat treatment on mechanical properties, heat treatments may also alter some physical properties of casting alloys. These alloys may also be affected by temper. Typical physical properties of many aluminum casting alloys are given in Table 3, including some effects of temper, where applicable.

MAJOR ALLOY SYSTEMS

In casting production, there is only one important application of commercially pure aluminum. The high electrical conductivity of aluminum is useful in collector rings and conductor bars, which are cast integrally with steel laminations to produce rotors for certain types of electric motors. Aluminum of 99.7, 99.5, and 99.0% purity provides minimum electrical conductivities of 60, 59, and 56% IACS (International Annealed Copper Standard), respectively.

Aluminum-Copper Alloys. The first aluminum casting alloy used extensively in the United States contained 8% copper and was known as 12 alloy (Ref 5). Alloys 112 and 212, containing zinc or silicon in addition

Table 2. Nominal Composition of Aluminum Alloy Castings (XXX.0)

AA No.	Former designation	Former ASTM designation	SAE designation	Products(a)
201.0	K01	SQ51A	382	S
A201.0	...	...	...	S
202.0	...	...	...	S
203.0	Hiduminium 350	...	...	S
204.0	A-U5GT	...	...	S,P
206.0	...	...	...	S,P
A206.0	...	...	...	S,P
208.0	108	CS43A	380	S,P
213.0	C113	...	...	S,P
222.0	122	CG100A	34	S,P
224.0	...	...	...	S,P
238.0	138	...	...	P
240.0	A240.0 (A140)	...	...	S
242.0	142	CN42A	39	S,P
A242.0	A142	...	...	S
243.0	ML	CS104A	...	S
249.0	X149	...	...	P
295.0	195	C4A	38	S
296.0	B295.0 (B195)	...	...	P
305.0	...	...	...	S,P
A305.0	...	...	...	S,P
308.0	A108	...	...	S,P
319.0	319, as-cast	SC64D	326	S,P
A319.0	...	...	329	S,P
B319	...	...	329	S,P
324.0	324	...	...	P
328.0	Red X-8	SC82A	327	S
332.0	F332.0 (F132)	SC103A	332	P
333.0	333	SC94A	331	P
A333.0	...	...	...	P
336.0	A332.0 (A132)	SN122A	321	P
339.0	Z332.0 (Z132)	...	334	P
343.0	X443Z	...	...	D
354.0	354	SC92A	...	P
A355.0	...	...	...	S,P
355.0	355	SC51A	322	S,P
C355.0	C355	SC51B	335	S,P
356.0	356	SG70A	323	S,P
A356.0	A356	SG70B	336	S,P
B356	...	...	...	S,P
F356.0	...	...	...	S,P
357.0	357	...	...	S,P
A357.0	A357	SG71A	...	S,P
B357.0	...	...	...	S,P
C357.0	...	...	...	S,P
358.0	B358.0 (Tens-50)	...	...	S,P
359.0	359	SG91A	...	S,P
360.0	360	SG100B	...	D
A360.0	A360	SG100A	309	D

(continued)

Table 2. (Continued)

Chemical composition(b), %						
Silicon	Iron	Copper	Magnesium	Zinc	Tin	Other
<0.10	<0.15	4.6	0.35	...	...	0.7 Ag, 0.35 Mn
<0.05	<0.10	4.5	0.25	...	...	0.7 Ag, 0.30 Mn
<0.10	<0.15	4.6	0.35	...	...	0.7 Ag, 0.4 Cr, 0.5 Mn
<0.30	<0.50	5.0	<0.10	...	...	1.5 Ni, 0.25 Mn, 0.25 Sb, 0.25 Co, 0.20 Zr, 0.20 Ti
<0.20	<0.35	4.6	0.25	...	...	...
<0.10	<0.15	4.6	0.25	...	...	0.35 Mn
<0.05	<0.10	4.6	0.25	...	...	0.35 Mn
3.0	<1.2	4.0	<0.10	<1.0	...	...
2.0	<1.2	7.0	<0.10	<2.5	...	...
<2.0	<1.5	10.0	0.25	<0.8	...	...
<0.06	<0.10	5.0	...	...	...	0.35 Mn, 0.1 V, 0.2 Zr
4.0	<1.5	10.0	0.25	<1.5	...	...
<0.50	<0.50	8.0	6.0	...	...	0.5 Mn, 0.5 Ni
<0.7	<1.0	4.0	1.5	<0.35	...	2.0 Ni
<0.6	<0.8	4.1	1.5	<0.10	...	0.2 Cr, 2.0 Ni
<0.35	<0.40	4.0	2.0	...	...	0.3 Mn, 2.1 Ni, 0.3 Cr
<0.05	<0.10	4.2	0.40	...	...	0.4 Mn, 3.0 Zn
1.1	<1.0	4.5	...	...	...	...
2.5	<1.2	4.5	...	<0.50	...	...
5.0	<0.6	1.25	...	<0.35	...	...
5.0	<0.20	1.25	...	<0.10	...	...
5.5	<1.0	4.5	<0.10	<1.0	...	...
6.0	<1.0	3.5	<0.10	<1.0	...	...
6.0	<1.2	3.5	0.3	<1.0	...	...
6.0	<1.0	3.5	<0.10	<3.0	...	...
7.5	<1.2	0.50	0.55	<1.0	...	...
8.0	<1.0	1.5	0.40	<1.5	...	0.40 Mn
9.5	<1.2	3.0	1.0	1.0	...	...
9.0	<1.0	3.5	0.3	<1.0	...	...
9.0	<1.0	3.5	0.3	<3.0	...	...
12.0	<1.2	1.0	1.0	<0.35	...	2.5 Ni
12.0	<1.2	2.25	1.0	<1.0	...	1.0 Ni
7.2	<1.2	0.7	<0.10	1.6	...	...
9.0	<0.20	1.8	0.5	...	...	...
5.0	<0.09	1.25	0.5	<0.05	...	...
5.0	<0.6	1.25	0.5	<0.35	...	...
5.0	<0.20	1.25	0.5	<0.10	...	...
7.0	<0.6	<0.25	0.35	<0.35	...	...
7.0	<0.20	<0.20	0.35	<0.10	...	...
7.0	<0.09	<0.05	0.35	<0.05	...	...
7.0	<0.20	<0.20	0.21	<0.10	...	...
7.0	<0.15	<0.05	0.55	<0.05	...	...
7.0	<0.20	<0.20	0.55	<0.10	...	0.05 Be
7.0	<0.09	<0.05	0.50	<0.05	...	...
7.0	<0.09	<0.05	0.60	<0.05	...	0.05 Be
8.1	<0.30	<0.20	0.50	<0.20	...	0.2 Be
9.0	<0.20	<0.20	0.6	...	...	...
9.5	<0.20	<0.6	0.5	...	...	...
9.5	<1.5	<0.6	0.5	...	...	...

(continued)

(a) S: sand casting; P: permanent mold casting; D: die casting. (b) Remainder: aluminum and unlisted impurities.

Table 2. Nominal Composition of Aluminum Alloy Castings (XXX.0) (Continued)

AA No.	Former designation	Former ASTM designation	SAE designation	Products(a)
361.0	...	...	...	D
363.0	363	...	...	S,P
364.0	364	...	...	D
369.0	Special K-9	...	...	D
380.0	380	SC84B	308	D
A380.0	A380	SC84A	306	D
B380.0	A380	SC84A	306	D
383.0	...	SC102A	383	D
384.0	384	SC114A	303	D
A384.0	384	...	...	D
385.0	B384.0(384)	...	...	D
390.0	390	...	...	D
A390.0	A390	...	...	S,P
B390.0	...	...	...	D
392.0	392	...	...	D
393.0	Vanasil	...	...	S,P,D
413.0	13	S12B	...	D
A413.0	A13	S12A	305	D
443.0	43	S5B	35	S,P
A443.0	43 (0.30 max Cu)	...	...	S
B443.0	43 (0.15 max Cu)	S5A	...	S,P
C443.0	A43	S5C	304	D
444.0	...	...	...	S,P
A444.0	A344	...	...	P
511.0	F514.0 (F214)	S7A	...	S
512.0	B514.0 (B214)	GS42A	...	S
513.0	A514.0 (A214)	GS242A	...	P
514.0	214	G4A	320	S
515.0	L514.0 (L214)	...	...	D
518.0	218	G8A	...	D
520.0	220	G10A	324	S
535.0	Almag 35	GM70B	...	S
A535.0	A218	...	...	S
B535.0	B218	...	...	S
705.0	603, Ternalloy 5	ZG32A	311	S,P
707.0	607, Ternalloy 7	ZG42A	312	S,P
710.0	A712.0 (A612)	ZG61B	313	S
711.0	C712.0 (C612)	ZG60A	314	P
712.0	D712.0 (D612, 40E)	ZG61A	310	S
713.0	613, Tenzaloy	ZC81A/B	315	S,P
771.0	Precedent 71A	...	...	S
772.0	B771.0 (Precedent 71B)	...	...	S
850.0	750	...	...	S,P
851.0	A850.0 (A750)	...	...	S,P
852.0	B850.0 (B750)	...	...	S,P
853.0	XC850.0 (XC750)	...	...	S,P

(continued)

Table 2. (Continued)

Chemical composition(b), %						
Silicon	Iron	Copper	Magnesium	Zinc	Tin	Other
10.0	<1.1	<0.50	0.5	...	...	0.25 Cr, 0.25 Ni
5.25	<1.1	3.0	0.30	3.8	0.25	<0.25 Pb, <0.08 Mn + Cr
8.5	<1.5	<0.20	0.30	<0.15	...	0.35 Cr, 0.03 Be
11.5	<1.3	<0.50	0.35	<1.0	...	0.35 Cr
8.5	<2.0	3.5	<0.10	<3.0	...	...
8.5	<1.3	3.5	<0.10	<3.0	...	...
8.5	<1.3	3.5	<0.10	<1.0	...	...
10.5	<1.3	2.5	<0.10	<3.0	...	...
11.3	<1.3	3.75	<0.10	<3.0	...	...
11.3	<1.3	3.75	<0.10	<1.0	...	...
12.0	<2.0	3.0	<0.30	<3.0	...	...
17.0	<1.3	4.5	0.55	<0.10	...	<0.1 Mn
17.0	<0.50	4.5	0.55	<0.10	...	<0.1 Mn
17.0	<1.3	4.5	0.55	<1.5	...	<0.5 Mn
19.0	<1.5	0.6	1.0	<0.50	...	0.4 Mn
22.0	<1.3	0.9	1.0	...	...	2.25 Ni, 0.12 V
12.0	<2.0	<1.0	<0.10	...	...	...
12.0	<1.3	<1.0	<0.10	...	...	...
5.25	<0.8	<0.6	<0.05	<0.50	...	...
5.25	<0.8	<0.30	<0.05	<0.50	...	...
5.25	<0.8	<0.15	<0.05	<0.35	...	...
5.25	<2.0	<0.6	<0.10	<0.50	...	...
7.0	<0.6	<0.25	<0.10	<0.35	...	...
7.0	<0.20	<0.10	<0.05	<0.10	...	...
0.5	<0.50	<0.15	4.0	<0.15	...	...
1.8	<0.6	<0.35	4.0	<0.35	...	...
<0.30	<0.40	<0.10	4.0	1.8	...	...
<0.35	<0.50	<0.15	4.0	<0.15	...	...
0.75	<1.3	<0.20	3.25	...	...	0.5 Mn
<0.35	<1.8	<0.25	8.0	...	...	...
<0.25	<0.30	<0.25	10.0	...	...	...
<0.15	<0.15	<0.05	6.9	...	...	0.18 Mn, 0.005 Be
<0.20	<0.20	<0.10	7.0	...	...	0.18 Mn
<0.15	<0.15	<0.10	7.0	...	...	<0.05 Mn
<0.20	<0.8	<0.20	1.6	3.0	...	0.5 Mn, 0.3 Cr
<0.20	<0.8	<0.20	2.1	4.25	...	0.5 Mn, 0.3 Cr
<0.15	<0.50	0.5	0.7	6.5	...	...
<0.30	1.0	0.5	0.35	6.5	...	...
<0.30	<0.50	<0.25	0.58	5.8	...	0.5 Cr
<0.25	<1.1	0.7	0.35	7.5	...	...
<0.15	<0.15	<0.10	0.9	7.0	...	0.13 Cr
<0.15	<0.15	<0.10	0.7	6.5	...	0.13 Cr
<0.7	<0.7	1.0	<0.10	...	6.25	1.0 Ni
2.5	<0.7	1.0	<0.10	...	6.25	0.5 Ni
<0.40	<0.7	2.0	0.75	...	6.25	1.2 Ni
6.0	<0.7	3.5	...	...	6.25	...

(a) S: sand casting; P: permanent mold casting; D: die casting. (b) Remainder: aluminum and unlisted impurities.

Table 3. Typical Properties of Aluminum Casting Alloys

These nominal properties are useful for comparing alloys, but they *should not* be used for design purposes. Properties for design *must be* obtained from appropriate material specifications, design standards, or by negotiation with the producer.

AA No.	Temper(a)	Specific gravity(b)	Density(b) kg/m³	Density(b) lb/in.³	Approximate melting range °C	Approximate melting range °F	Electrical conductivity, % IACS	Thermal conductivity, at 25 °C (77 °F), SI units	Coefficient of thermal expansion, per °C × 10⁻⁶ (per °F × 10⁻⁶) 20 to 100 °C	68 to 212 °F	20 to 300 °C	68 to 570 °F
201.0	T6 (S)	2.80	2796	0.101	570–650	1060–1200	27–32	0.29	34.7	19.3	44.5	24.7
	T7 (P)	2.80	2796	0.101	570–650	1060–1200	32–34	0.29	34.7	19.3	44.5	24.7
206.0	...	2.8	2796	0.101	570–650	1060–1200	...	0.29	...	...	...	...
A206.0	...	2.8	2796	0.101	570–650	1060–1200	...	0.29	...	...	...	...
208.0	F (S)	2.79	2796	0.101	520–630	970–1170	31	0.29	22.0	12.2	23.9	13.3
	O (S)	2.79	2796	0.101	520–630	970–1170	38	0.35	...	...	...	...
222.0	F(P)	2.95	2962	0.107	520–625	970–1160	34	0.32	22.1	12.3	23.6	13.1
	O (S)	2.95	2962	0.107	520–625	970–1160	41	0.38	...	...	...	...
	T61 (S)	2.95	2962	0.107	520–625	970–1160	33	0.31	22.1	12.3	23.6	13.1
224.0	T62 (S)	2.81	2824	0.102	550–645	1020–1190	30	0.28	...	...	...	...
238.0	F (P)	2.95	1938	0.107	510–600	950–1110	25	0.25	21.4	11.9	22.9	12.7
240.0	F (S)	2.78	2768	0.100	515–605	960–1120	23	0.23	22.1	12.3	24.3	13.5
242.0	O (S)	2.81	2823	0.102	530–635	990–1180	44	0.40	...	...	...	...
	T77 (S)	2.81	2823	0.102	525–635	980–1180	38	0.36	22.1	12.3	23.6	13.1
	T571 (P)	2.81	2823	0.102	525–635	980–1180	34	0.32	22.5	12.5	24.5	13.6
	T61 (P)	2.81	2823	0.102	525–635	980–1180	33	0.32	22.5	12.5	24.5	13.6
295.0	T4 (S)	2.81	2823	0.102	520–645	970–1190	35	0.33	22.9	12.7	24.8	13.8
	T62 (S)	2.81	2823	0.102	520–645	970–1190	35	0.34	22.9	12.7	24.8	13.8
296.0	T4 (P)	2.80	2796	0.101	520–630	970–1170	33	0.32	22.0	12.2	23.9	13.3
	T6 (P)	2.80	2796	0.101	520–630	970–1170	33	0.32	22.0	12.2	23.9	13.3
	T62 (S)	2.80	2796	0.101	520–630	970–1170	33	0.32	...	...	...	...
308.0	F (P)	2.79	2796	0.101	520–615	970–1140	37	0.34	21.4	11.9	22.9	12.7
319.0	F (S)	2.79	2796	0.101	520–605	970–1120	27	0.27	21.6	12.0	24.1	13.4
	F (P)	2.79	2796	0.101	520–605	970–1120	28	0.28	21.6	12.0	24.1	13.4
324.0	F (P)	2.67	2658	0.096	545–605	1010–1120	34	0.37	21.4	11.9	23.2	12.9
332.0	T5 (P)	2.76	2768	0.100	520–580	970–1080	26	0.25	20.7	11.5	22.3	12.4
333.0	F (P)	2.77	2768	0.100	520–585	970–1090	26	0.25	20.7	11.5	22.7	12.6
	T5 (P)	2.77	2768	0.100	520–585	970–1090	29	0.29	20.7	11.5	22.7	12.6
	T6 (P)	2.77	2768	0.100	520–585	970–1090	29	0.28	20.7	11.5	22.7	12.6
	T7 (P)	2.77	2768	0.100	520–585	970–1090	35	0.34	20.7	11.5	22.7	12.6
336.0	T551 (P)	2.72	2713	0.098	540–570	1000–1060	29	0.28	18.9	10.5	20.9	11.6
354.0	F (P)	2.71	2713	0.098	540–600	1000–1110	32	0.30	20.9	11.6	22.9	12.7
355.0	T51 (S)	2.71	2713	0.098	550–620	1020–1150	43	0.40	22.3	12.4	24.7	13.7
	T6 (S)	2.71	2713	0.098	550–620	1020–1150	36	0.34	22.3	12.4	24.7	13.7
	T61 (S)	2.71	2713	0.098	550–620	1020–1150	37	0.35	22.3	12.4	24.7	13.7
	T7 (S)	2.71	2713	0.098	550–620	1020–1150	42	0.39	22.3	12.4	24.7	13.7
	T6 (P)	2.71	2713	0.098	550–620	1020–1150	39	0.36	22.3	12.4	24.7	13.7

C355.0	T61 (S)	2.71	2713	0.098	550–620	1020–1150	39	0.35	22.3	12.4	24.7	13.7
356.0	T51 (S)	2.68	2685	0.097	560–615	1040–1140	43	0.40	21.4	11.9	23.4	13.0
	T6 (S)	2.68	2685	0.097	560–615	1040–1140	39	0.36	21.4	11.9	23.4	13.0
	T7 (S)	2.68	2685	0.097	560–615	1040–1140	40	0.37	21.4	11.9	23.4	13.0
	T6 (P)	2.68	2685	0.097	560–615	1040–1140	41	0.37	21.4	11.9	23.4	13.0
A356.0	T6 (S)	2.69	2713	0.098	560–610	1040–1130	40	0.36	21.4	11.9	23.4	13.0
357.0	T6 (S)	2.68	2713	0.098	560–615	1040–1140	39	0.36	21.4	11.9	23.4	13.0
A357.0	T6 (S)	2.69	2713	0.098	555–610	1030–1130	40	0.38	21.4	11.9	23.6	13.1
358.0	T6 (S)	2.68	2658	0.096	560–600	1040–1110	39	0.36	21.4	11.9	23.4	13.0
359.0	T6 (S)	2.67	2685	0.097	565–600	1050–1110	35	0.33	20.9	11.6	22.9	12.7
360.0	F (D)	2.68	2685	0.097	570–590	1060–1090	37	0.35	20.9	11.6	22.9	12.7
A360.0	F (D)	2.68	2685	0.097	570–590	1060–1090	37	0.35	21.1	11.7	22.9	12.7
364.0	F (D)	2.63	2630	0.095	560–600	1040–1110	30	0.29	20.9	11.6	22.9	12.7
380.0	F (D)	2.76	2740	0.099	520–590	970–1090	27	0.26	21.2	11.8	22.5	12.5
A380.0	F (D)	2.76	2740	0.099	520–590	970–1090	27	0.26	21.1	11.7	22.7	12.6
384.0	F (D)	2.70	2713	0.098	480–580	900–1080	23	0.23	20.3	11.3	22.1	12.3
390.0	F (D)	2.73	2740	0.099	510–650	950–1200	25	0.32	18.5	10.3	...	...
	T5 (D)	2.73	2740	0.099	510–650	950–1200	24	0.32	18.0	10.0	...	...
392.0	F (P)	2.64	2630	0.095	550–670	1020–1240	22	0.22	18.5	10.3	20.2	11.2
413.0	F (D)	2.66	2657	0.096	575–585	1070–1090	39	0.37	20.5	11.4	22.5	12.5
A413.0	F (D)	2.66	2657	0.096	575–585	1070–1090	39	0.37	...	...	...	...
443.0	F (S)	2.69	2685	0.097	575–630	1070–1170	37	0.35	22.1	12.3	24.1	13.4
	O (S)	2.69	2685	0.097	575–630	1070–1170	42	0.39	...	...	...	...
	F (D)	2.69	2685	0.097	575–630	1070–1170	37	0.34	...	...	...	...
A444.0	F (P)	2.68	2685	0.097	575–630	1070–1170	41	0.38	21.8	12.1	23.8	13.2
511.0	F (S)	2.66	2657	0.096	590–640	1090–1180	36	0.34	23.6	13.1	25.7	14.3
512.0	F (S)	2.65	2657	0.096	590–630	1090–1170	38	0.35	22.9	12.7	24.8	13.8
513.0	F (P)	2.68	2685	0.097	580–640	1080–1180	34	0.32	23.9	13.3	25.9	14.4
514.0	F (S)	2.65	2657	0.096	600–640	1110–1180	35	0.33	23.9	13.3	25.9	14.4
518.0	F (D)	2.53	2519	0.091	540–620	1000–1150	24	0.24	24.1	13.4	26.1	14.5
520.0	T4 (S)	2.57	2574	0.093	450–600	840–1110	21	0.21	25.2	14.0	27.0	15.0
535.0	F (S)	2.62	2519	0.091	550–630	1020–1170	23	0.24	23.6	13.1	26.5	14.7
A535.0	F (D)	2.54	2547	0.092	550–620	1020–1150	23	0.24	24.1	13.4	26.1	14.5
B535.0	F (S)	2.62	2630	0.095	550–630	1020–1170	24	0.23	24.5	13.6	26.5	14.7
705.0	F (S)	2.76	2768	0.100	600–640	1110–1180	25	0.25	23.6	13.1	25.7	14.3
707.0	F (S)	2.77	2768	0.100	585–630	1090–1170	25	0.25	23.8	13.2	25.9	14.4
710.0	F (S)	2.81	2823	0.102	600–650	1110–1200	35	0.33	24.1	13.4	26.3	14.6
711.0	F (P)	2.84	2851	0.103	600–645	1110–1190	40	0.38	23.6	13.1	25.6	14.2
712.0	F (S)	2.82	2823	0.102	600–640	1110–1180	40	0.38	23.6	13.1	25.6	14.2
713.0	F (S)	2.84	2879	0.104	595–630	1100–1170	37	0.37	23.9	13.3	25.9	14.4
850.0	T5 (S)	2.87	2851	0.103	225–650	440–1200	47	0.44	...	...	...	...
851.0	T5 (S)	2.83	2823	0.102	230–630	450–1170	43	0.40	22.7	12.6	...	...
852.0	T5 (S)	2.88	2879	0.104	210–635	410–1180	45	0.42	23.2	12.9	...	...

(a) S: sand cast; P: permanent mold; D: die cast. (b) The specific gravity and weight data in this table assume solid (void-free) metal. Because some porosity cannot be avoided in commercial castings, their specific gravity or weight is slightly less than the theoretical value.

Table 4. Typical Mechanical Properties of Aluminum Sand Casting Alloys(a)

These nominal properties are useful for comparing alloys, but they *should not* be used for design purposes. Properties for design *must be* obtained from appropriate material specifications, design standards, or by negotiation with the producer.

AA No.	Temper	Tensile strength MPa	Tensile strength ksi	Tensile yield strength(b) MPa	Tensile yield strength(b) ksi	Elongation in 50 mm (2 in.), %	Hardness(c), BHN	Compressive yield strength(b) MPa	Compressive yield strength(b) ksi	Shear strength MPa	Shear strength ksi	Endurance limit(d) MPa	Endurance limit(d) ksi	Modulus of elasticity(e) kPa × 10^6	Modulus of elasticity(e) ksi × 10^4
201.0	T43	414	60	255	37	17.0	...	...	...	...	...	...	...	...	...
	T6	448	65	379	55	8.0	130	386	56	290	42	...	...	...	...
	T7	467	68	414	60	5.5	...	...	...	...	...	97	14	...	...
A206.0	T4	354	51	250	36	7.0	...	264	38	278	40	...	...	...	...
208.0	F	145	21	97	14	2.5	55	103	15	117	17	76	11	...	...
213.0	F	165	24	103	15	1.5	70	110	16	138	20	62	9	...	...
222.0	O	186	27	138	20	1.0	80	138	20	145	21	65	9.5	...	...
	T61	283	41	276	40	<0.5	115	296	43	221	32	59	8.5	74	10.7
	T62	421	61	331	48	4.0	...	338	49	262	38	...	...	...	...
224.0	T72	380	55	276	40	10.0	123	283	41	245	35	62	9.0	72	10.5
240.0	F	235	34	200	28	1.0	90	207	30	...	...	...	...	...	...
242.0	F	214	31	217	30	0.5	...	...	...	...	...	...	...	...	...
	O	186	27	124	18	1.0	70	124	18	145	21	55	8	71	10.3
	T571	221	32	207	30	0.5	85	234	34	179	26	76	11	71	10.3
	T77	207	30	159	23	2.0	75	165	24	165	24	72	10.5	71	10.3
A242.0	T75	214	31	...	...	2.0	...	483	70	...	...	...	...	...	...
295.0	T4(f)	221	32	110	16	8.5	60	117	17	179	26	48	7	69	10.0
	T6	250	36	165	24	5.0	75	172	25	217	30	52	7.5	69	10.0
	T62	283	41	221	32	2.0	90	234	34	228	33	55	8	69	10.0
319.0	F	186	27	124	18	2.0	70	131	19	152	22	69	10	74	10.7
	T5	207	30	179	26	1.5	80	186	27	164	24	76	11	74	10.7
	T6	250	36	164	24	2.0	80	172	25	200	29	76	11	74	10.7
355.0	F	159	23	83	12	3.0	...	...	...	...	...	...	...	...	...
	T51	193	28	159	23	1.5	65	164	24	152	22	55	8	70	10.2
	T6	241	35	172	25	3.0	80	179	26	193	28	62	9	70	10.2
	T61	269	39	241	35	1.0	90	255	37	214	31	65	9.5	...	...
	T7	264	38	250	26	0.5	85	264	38	193	28	69	10	70	10.2
	T71	241	35	200	29	1.5	75	207	30	179	26	69	10	70	10.2
C355.0	T6	269	39	200	29	5.0	85	...	...	...	...	...	...	...	...
356.0	F	164	24	124	18	6.0	...	...	...	...	...	...	...	...	...
	T51	172	25	138	20	2.0	60	145	21	138	20	55	8	72	10.5

(continued)

Table 4. (Continued)

AA No.	Temper	Tensile strength MPa	Tensile strength ksi	Tensile yield strength(b) MPa	Tensile yield strength(b) ksi	Elongation in 50 mm (2 in.), %	Hardness(c), BHN	Compressive yield strength(b) MPa	Compressive yield strength(b) ksi	Shear strength MPa	Shear strength ksi	Endurance limit(d) MPa	Endurance limit(d) ksi	Modulus of elasticity(e) kPa × 10^6	Modulus of elasticity(e) ksi × 10^6
356.0	T6	228	33	164	24	3.5	70	172	25	179	26	59	8.5	72	10.5
	T7	234	34	207	30	2.0	75	214	31	164	24	62	9	72	10.5
	T71	193	28	145	21	3.5	60	152	22	138	20	59	8.5	72	10.5
A356.0	F	159	23	83	12	6.0	...	...	...	...	...	...	...	...	...
	T51	179	26	124	18	3.0	...	...	...	...	...	...	...	...	...
	T6	278	40	207	30	6.0	75	...	...	...	...	...	...	...	...
	T71	207	30	138	20	3.0	...	...	...	...	...	...	...	...	...
357.0	F	172	25	90	13	5.0	...	...	...	...	...	...	...	...	...
	T51	179	26	117	17	3.0	...	...	...	...	...	...	...	...	...
	T6	345	50	296	43	2.0	90	...	...	...	...	...	...	...	...
	T7	278	40	234	34	3.0	60	...	...	...	...	...	...	...	...
A357.0	T6	317	46	248	36	3.0	85	241	35	278	40	83	12	...	...
A390.0	F	179	26	179	26	<1.0	100	...	...	...	...	...	...	82	11.9
	T5	179	26	179	26	<1.0	100	...	...	...	...	...	...	...	...
	T6	278	40	278	40	<1.0	140	...	...	...	...	90	13	...	...
	T7	250	36	250	36	<1.0	115	...	...	...	...	...	...	...	...
443.0	F	131	19	55	8	8.0	40	62	9	97	14	55	8	71	10.3
A444.0	F	145	21	62	9	9.0	...	...	...	...	...	...	...	...	...
	T4	159	23	62	9	12.0	...	...	...	...	...	...	...	...	...
511.0	F	145	21	83	12	3.0	50	90	13	117	17	55	8	...	...
512.0	F	138	20	90	13	2.0	50	97	14	117	17	59	8.5	...	...
514.0	F	172	25	83	12	9.0	50	83	12	138	20	48	7	71	10.3
520.0	T4	331	48	179	26	16.0	75	186	27	234	34	55	8	65	9.5
A535.0	F	250	36	124	18	9.0	65	...	...	...	...	...	...	...	...
710.0	F	241	35(g)	172	25(g)	5.0(g)	75(g)	172	25	179	26	55	8	67	9.7
712.0(h)	F	241	35	172	25	5.0	75	172	25	179	26	62	9	...	...
713.0(h)	F	241	35	172	25	5.0	74	...	...	...	...	...	...	67	9.7
850.0	T5	138	20	76	11	8.0	45	76	11	97	14	...	...	71	10.3
851.0	T5	138	20	76	11	5.0	45	76	11	97	14	...	...	71	10.3
852.0	T5	186	27	152	22	2.0	65	152	22	124	18	69	10	71	10.3

(a) Tensile and hardness values determined by tests on standard 13-mm ($^1/_2$-in.) diam test specimens, without surface machining, each cast in a green sand mold. (b) Offset: 0.2%. (c) 500-kg (1102-lb) load on 10-mm (0.4-in.) ball. (d) Endurance limits based on 500 million cycles of completely reversed stresses using rotating beam-type machine and specimen. (e) Average tension and compression moduli, compression modulus is about 2% greater than tension modulus. (f) Properties of T4 approach those of T6 after standing for several weeks at room temperature. (g) Tests made approximately 30 days after casting. (h) Tests made 10 days after casting.

Table 5. Typical Mechanical Properties of Aluminum Permanent Mold Casting Alloys(a)

These nominal properties are useful for comparing alloys, but they *should not* be used for design purposes. Properties for design *must be* obtained from appropriate material specifications, design standards, or by negotiation with the producer.

AA No.	Temper	Tensile strength, MPa	Tensile strength, ksi	Tensile yield strength(b), MPa	Tensile yield strength(b), ksi	Elongation in 50 mm (2 in.), %	Hardness(c), BHN
201.0	T43	414	60	255	37	17.0	...
	T6	448	65	379	55	8.0	130
	T7	469	68	414	60	5.0	...
A206.0	T4	431	62	264	38	17.0	...
	T7	436	63	347	50	11.7	...
213.0	F	207	30	165	24	1.5	85
222.0	T52	241	35	214	31	1.0	100
	T551	255	37	241	35	<0.5	115
	T65	331	48	248	36	<0.5	140
238.0	F	207	30	165	24	1.5	100
242.0	T571	276	40	234	34	1.0	105
	T61	324	47	290	42	0.5	110
249.0	T63	476	69	414	60	6.0	...
	T7	278	62	359	52	9.0	...
296.0	T4(f)	255	37	131	19	9.0	75
	T6	276	40	179	26	5.0	90
	T7	270	39	138	20	4.5	80
308.0	F	193	28	110	16	2.0	70
319.0	F	234	34	131	19	2.5	85
	T6	276	40	186	27	3.0	95
324.0	F	207	30	110	16	4.0	70
	T5	248	36	179	26	3.0	90
	T62	310	45	269	39	3.0	105
332.0	T5	248	36	193	28	1.0	105
333.0	F	234	34	131	19	2.0	90
	T5	234	34	172	25	1.0	100
	T6	290	42	207	30	1.5	105
	T7	255	37	193	28	2.0	90
336.0	T551	248	36	193	28	0.5	105
	T65	324	47	296	43	0.5	125
356.0	F	179	26	124	18	5.0	...
	T51	186	27	138	20	2.0	...
	T6	262	38	186	27	5.0	80
	T7	221	32	165	24	6.0	70
A356.0	T61	283	41	207	30	10.0	90
357.0	F	193	28	103	15	6.0	...
	T51	200	29	145	21	4.0	...
	T6	359	52	296	43	5.0	100
A357.0	T6	359	52	290	42	5.0	100
359.0	T62	345	50	290	42	5.5	...
A390.0	F	200	29	200	29	<1.0	110
	T5	200	29	200	29	<1.0	110
	T6	310	45	310	45	<1.0	145
	T7	262	38	262	38	<1.0	120
443.0	F	159	23	62	9	10.0	45
A444.0	F	165	24	76	11	13.0	44
	T4	159	23	69	10	21.0	45
513.0	F	186	27	110	16	7.0	60
711.0	F	241	35(g)	124	18(g)	8.0(g)	70(g)
850.0	T5	159	23	76	11	12.0	45
851.0	T5	138	20	76	11	5.0	45
852.0	T5	221	32	159	23	5.0	70

(continued)

Table 5. (Continued)

AA No.	Temper	Compressive yield strength(b) MPa	Compressive yield strength(b) ksi	Shear strength MPa	Shear strength ksi	Endurance limit(d) MPa	Endurance limit(d) ksi	Modulus of elasticity(e) kPa × 10^6	Modulus of elasticity(e) psi × 10^6
201.0	T43	...	...	...	...	...	...	...	...
	T6	386	56	290	42	...	...	...	...
	T7	...	...	...	...	97	14	...	...
A206.0	T4	285	41	292	42	...	...	...	...
	T7	372	54	257	37	...	...	...	...
213.0	F	172	25	165	24	66	9.5	...	...
222.0	T52	214	31	172	25	...	...	...	...
	T551	276	40	207	30	59	8.5	74	10.7
	T65	248	36	248	26	62	9	74	10.7
238.0	F	207	30	165	24	...	...	...	...
242.0	T571	234	34	207	30	72	10.5	71	10.3
	T61	303	44	241	35	66	9.5	71	10.3
249.0	T63	...	...	...	...	...	...	...	...
	T7	414	60	276	40	55	8.0	72	10.5
296.0	T4(f)	138	20	207	30	66	9.5	70	10.1
	T6	179	26	221	32	69	10	70	10.1
	T7	138	20	207	30	63	9	70	10.1
308.0	F	117	17	152	22	90	13	...	...
319.0	F	131	19	165	24	...	...	...	...
	T6	186	27	...	...	...	...	...	...
324.0	F	...	...	...	...	...	...	...	...
	T5	...	...	...	...	...	...	...	...
	T62	...	...	...	...	...	...	...	...
332.0	T5	...	...	...	...	...	...	77	11.2
333.0	F	131	19	186	27	100	14.5	...	...
	T5	172	25	186	27	83	12	...	...
	T6	207	30	228	33	103	15	...	...
	T7	193	28	193	28	83	12	...	...
336.0	T551	193	28	193	28	93	13.5	...	...
	T65	296	43	248	36	...	...	...	...
356.0	F	...	...	...	...	...	...	...	...
	T51	...	...	...	...	...	...	...	...
	T6	186	27	207	30	90	13	72	10.5
	T7	165	24	172	25	76	11	72	10.5
A356.0	T61	221	32	193	28	90	13	72	10.5
357.0	F	...	...	...	...	...	...	...	...
	T51	...	...	...	...	...	...	...	...
	T6	303	44	241	35	90	13	...	...
A357.0	T6	296	43	241	35	103	15	...	...
359.0	T62	...	...	...	...	110	16	...	...
A390.0	F	...	...	...	...	...	...	82	11.9
	T5	...	...	...	...	...	...	...	...
	T6	414	60	...	...	117	17	...	...
	T7	359	52	...	...	100	14.5	...	...
443.0	F	62	9	110	16	55	8	71	10.3
A444.0	F	...	...	...	...	...	...	...	...
	T4	76	11	110	16	55	8	...	...
513.0	F	117	17	152	22	69	10	...	...
711.0	F	...	...	...	...	76	11	76	11.0
850.0	T5	76	11	103	15	62	9	71	10.3
851.0	T5	76	11	97	14	62	9	71	10.3
852.0	T5	159	23	148	21	76	11	71	10.3

(a) Tension and hardness values determined by tests on standard 13-mm ($^1/_2$-in.) diam test specimens, without surface machining, each cast in permanent mold. (b) Offset: 0.2%. (c) 500-kg (1102-lb) load on 10-mm (0.4-in.) ball. (d) Endurance limits based on 500 million cycles of completely reversed stresses using rotating beam-type machine and specimen. (e) Average of tension and compression moduli; compression modulus is about 2% greater than tension modulus. (f) Properties of T4 approach those of T6 after standing for several weeks at room temperature. (g) Tests made approximately 30 days after casting.

Table 6. Typical Mechanical Properties of Aluminum Die Casting Alloys(a)

These nominal properties are useful for comparing alloys, but they *should not* be used for design purposes. Properties for design *must be* obtained from appropriate material specifications, design standards, or by negotiation with the producer.

AA No.	Temper	Tensile strength MPa	Tensile strength ksi	Tensile yield strength(b) MPa	Tensile yield strength(b) ksi	Elongation in 50 mm (2 in.), %	Hardness(c), BHN
360.0	F	324	47	172	25	3.0	75
A360.0	F	317	46	165	24	5.0	75
364.0	F	296	43	159	23	7.5	...
380.0	F	331	48	165	24	3.0	80
A380.0	F	324	47	159	23	4.0	75
384.0	F	324	47	172	25	1.0	...
390.0	F	279	40.5	241	35	1.0	120
	T5	296	43	265	38.5	1.0	...
392.0	F	290	42	262	38	<0.5	...
413.0	F	296	43	145	21	2.5	80
A413.0	F	241	35	110	16	3.5	80
443.0	F	228	33	110	16	9.0	50
513.0	F	276	40	152	22	10.0	...
515.0	F	283	41	...	...	10.0	...
518.0	F	310	45	186	27	8.0	80

(continued)

to copper, subsequently replaced 12 alloy and were themselves later replaced by alloys 113 and C113 (C113 is now 213). Today, none of these five alloys is popular. Copper additions to aluminum-silicon alloys such as 319 and 333 provide moderate tensile properties, a lower specific gravity, and superior casting characteristics. Typical mechanical properties of most of the sand, permanent mold, and die casting alloys are supplied in Tables 4, 5, and 6, respectively.

A significant expansion of the use of aluminum castings occurred with the development of the heat treatable aluminum-copper alloy 295. This development afforded significantly higher mechanical properties than were available in previous alloys. Later, another variation of this 4.5% copper alloy was developed for use in permanent mold casting. Alloy 296 (formerly B195) contained 0.5% silicon, which improves resistance to hot cracking. Both 295 and 296 alloys are infrequently used today, having been replaced almost completely by alloys 355 and 356, which have similar mechanical properties, but lower specific gravities, better corrosion resistance (Ref 6), and superior casting characteristics.

The higher copper alloy 222, containing 10% copper, was developed for production of pistons for internal combustion engines. However, it has been replaced in this application by alloys 332, 336, and 339, and to a lesser extent by alloys 242 and A242. The special-purpose alloy 238 is used almost exclusively to cast soleplates for electric hand irons. This alloy has the required high hardness at elevated temperatures. Alloys 240, 242, A242, and 243 also have high strength and hardness at elevated temperatures and are used for diesel engine pistons and air-cooled cylinder heads for aircraft engines.

The more recently developed 201, A206, 224, and 249 alloys have provided tensile properties significantly higher than those of any previous

Table 6. (Continued)

AA No.	Temper	Shear strength MPa	Shear strength ksi	Endurance limit(d) MPa	Endurance limit(d) ksi	Modulus of elasticity(e) kPa × 10^4	Modulus of elasticity(e) psi × 10^4
360.0	F	207	30	131	19	71	10.3
A360.0	F	200	29	124	18	...	...
364.0	F	179	26	124	18	...	...
380.0	F	214	31	145	21	71	10.3
A380.0	F	207	30	138	20	...	...
384.0	F	207	30	145	21	71	10.3
390.0	F	...	...	138	20	82	11.9
	T5	...	...	...	...	...	...
392.0	F	234(f)	34(f)	103(f)	15(f)	...	...
413.0	F	193	28	131	19	71	10.3
A413.0	F	172	25	131	19	...	...
443.0	F	145	21	117	17	71	10.3
513.0	F	179	26	124	18	...	...
515.0	F	...	...	...	...	...	...
518.0	F	200	29	138	20	...	...

(a) Tension properties are average values determined from ASTM standard 6-mm ($^1/_4$-in.) diam test specimens cast on a cold chamber (high-pressure) die casting machine. (b) Offset: 0.2%. (c) 500-kg (1102-lb) load on 10-mm (0.4-in.) ball. (d) Endurance limits based on 500 million cycles of completely reversed stresses using rotating beam-type machine and specimen. (e) Average of tension and compression moduli; compression modulus is about 2% greater than tension modulus. (f) Estimated.

aluminum casting alloys and are being used to cast premium-quality aerospace parts. All of these aluminum-copper alloys have marginal castability relative to almost any of the alloys that contain larger quantities of silicon. They have limited fluidity and require careful gating and generous riser feeding during solidification to ensure casting soundness. In addition, pressure-tight parts of intricate design are difficult to obtain, and their resistance to hot cracking is relatively poor. They are also susceptible to stress-corrosion cracking in the fully hardened condition.

Tables 7, 8, and 9 list the mechanical properties of several casting alloys at elevated and subzero temperatures and attests to the value of copper as an alloying element to improve strength at elevated temperatures. Data in Tables 7, 8, and 9 also show that as the testing temperature for casting alloys is reduced from room temperature to −196 °C (−320 °F), the tensile and yield strengths increase, and the elongation values either remain unchanged or decrease slightly.

Aluminum-magnesium alloys include four essentially binary alloys and variations of three of these alloys. Aluminum-magnesium alloys are characterized by excellent corrosion resistance, good machinability, and attractive appearance when anodized. In comparison with aluminum-silicon alloys, all of the aluminum-magnesium alloys require more care in gating, properly located and sized risers, and greater chilling to produce sound castings. Controlled melting and pouring practices are needed to compensate for the greater oxidizing tendency of these alloys when molten.

Alloy 514 is an Al-4% Mg binary alloy, normally cast in sand. Casting characteristics of 514-type alloys are improved moderately by the addition of zinc or silicon. Alloy 513 (4% magnesium-1.8% zinc) can be per-

Table 7. Tensile Properties of Aluminum Sand Casting Alloys at Various Temperatures(a)

These nominal properties are useful for comparing alloys, but they *should not* be used for design purposes. Properties for design *must be* obtained from appropriate material specifications, design standards, or by negotiation with the producer.

AA No.	Temper	Test temperature, °C	Test temperature, °F	Tensile strength, MPa	Tensile strength, ksi	Tensile yield strength(b), MPa	Tensile yield strength(b), ksi	Elongation in 50 mm (2 in.), %
201.0	T6(c)	24	75	448	65	379	55	8.0
		150	300	379	55	359	52	6.0
		205	400	248	36	228	33	9.0
		260	500	152	22	131	19	19.0
		315	600	69	10	62	9	39.0
201.0	T7(c)	24	75	469	68	414	60	5.5
		150	300	414	60	372	54	9.0
		205	400	269	39	228	33	16.0
		260	500	110	16	90	13	25.0
		315	600	62	9	55	8	48.0
A201.0	T7	−196	−320	614	89	517	75	8.0
		−44	−112	531	77	483	70	6.0
		−8	−18	510	74	462	67	6.0
		24	75	496	72	448	65	6.0
		150	300	400	58	359	52	6.0
		205	400	165	24	124	18	25.0
		260	500	97	14	69	10	32.0
		315	600	55	8	41	6	51.0
222.0	O	24	75	186	27	138	20	1.0
		100	212	179	26	131	19	1.0
		150	300	172	25	117	17	1.0
		205	400	152	22	97	14	1.5
		260	500	117	17	76	11	3.0
		315	600	55	8	31	4.5	14.0
220.0	T551	24	75	283	41	276	40	0.5
		100	212	269	39	262	38	0.5
		150	300	248	36	241	35	1.0
		205	400	165	24	117	17	2.0
		260	500	117	17	76	11	6.0
		315	600	59	8.5	34	5	14.0
		370	700	34	5	17	2.5	30.0
224.0	T7	24	75	421	61	331	48	4.0
		150	300	338	49	255	37	5.0
		205	400	262	38	193	28	10.0
		260	500	214	31	138	20	9.0
		315	600	145	21	103	15	11.0
240.0	F(c)	−196	−320	248	36	241	35	0.5
		−44	−112	234	34	207	30	0.5
		−8	−18	234	34	200	29	1.0
		24	75	234	34	200	29	1.0
		100	212	234	34	200	29	1.0
		150	300	234	34	207	30	1.0
		205	400	228	33	172	25	1.0
		260	500	179	26	110	16	4.0
		315	600	117	17	83	12	4.0
242.0	F	24	75	214	31	207	30	<0.5
		100	212	214	31	207	30	<0.5
		150	300	207	30	186	27	0.5
		205	400	165	24	138	20	1.5
		260	500	83	12	41	6	9.0
		315	600	55	8	31	4.5	14.0
		370	700	38	5.5	21	3	36.0

(continued)

Table 7. (Continued)

AA No.	Temper	Test temperature °C	Test temperature °F	Tensile strength MPa	Tensile strength ksi	Tensile yield strength(b) MPa	Tensile yield strength(b) ksi	Elongation in 50 mm (2 in.), %
242.0	O	24	75	186	27	124	18	1.0
		150	300	159	23	103	15	1.0
		205	400	124	18	76	11	3.0
		260	500	83	12	34	5	8.0
		315	600	43	7	21	3	20.0
242.0	T571	24	75	221	32	207	30	0.5
		100	212	221	32	207	30	0.5
		150	300	207	30	193	28	0.5
		205	400	179	26	145	21	1.0
		260	500	90	13	55	8	8.0
		315	600	55	8	28	4	20.0
		370	700	34	5	21	3	40.0
242.0	T77	−196	−320	248	36	186	27	2.0
		−44	−112	214	31	172	25	1.5
		−8	−18	221	32	152	22	1.5
		24	75	207	30	159	23	2.0
		100	212	207	30	159	23	2.0
		150	300	186	27	145	21	2.0
		205	400	138	20	103	15	3.0
		260	500	90	13	55	8	6.0
		315	600	55	8	28	4	20.0
		370	700	34	5	21	3	40.0
249.0	T7	−196	−320	558	81	476	69	7.0
		−44	−112	483	70	427	62	6.0
		−8	−18	476	69	414	60	6.0
		24	75	469	68	407	59	6.0
		150	300	290	42	241	35	14.0
		205	400	186	27	159	23	20.0
295.0	T4	24	75	221	32	110	16	8.5
		100	212	207	30	103	15	5.0
		150	300	193	28	103	15	5.0
		205	400	103	15	62	9	15.0
		260	500	62	9	41	6	25.0
		315	600	28	4	21	3	75.0
		370	700	17	2.5	10	1.5	100.0
295.0	T6	24	75	248	36	165	24	5.0
		100	212	234	34	159	23	5.0
		150	300	193	28	138	20	5.0
		205	400	103	15	62	9	15.0
		260	500	62	9	41	6	25.0
		315	600	28	4	21	3	75.0
		370	700	17	2.5	10	1.5	100.0
319.0	F(c)	−196	−320	234	34	214	31	1.0
		−44	−112	207	30	179	26	1.0
		−8	−18	200	29	169	24.5	1.0
		24	75	186	27	124	18	2.0
319.0	T5(c)	−196	−320	255	37	241	35	0.5
		−44	−112	234	34	207	30	1.0
		−8	−18	224	32.5	203	29.5	1.0
		24	75	217	31.5	200	29	1.0
319.0	T7(c)	−196	−320	276	40	234	34	1.0
		−44	−112	255	37	214	31	1.0

(continued)

(a) Values are lowest properties recorded during 10,000 h at test temperatures. (b) Offset: 0.2%. (c) After 1000 h at test temperatures.

Table 7. (Continued)

AA No.	Temper	Test temperature °C	Test temperature °F	Tensile strength MPa	Tensile strength ksi	Tensile yield strength(b) MPa	Tensile yield strength(b) ksi	Elongation in 50 mm (2 in.), %
319.0	T7(c)	−8	−18	234	34	207	30	1.0
		24	75	234	34	200	29	1.0
354.0	T6	−196	−320	469	68	338	49	5.0
		−44	−112	400	58	290	42	5.0
		−8	−18	400	58	290	42	5.0
		24	75	379	55	283	41	6.0
		100	212	414	60	338	49	6.0
		150	300	290	42	241	35	6.0
		205	400	103	15	76	11	45.0
		260	500	59	8.5	41	6	65.0
355.0	T51	−196	−320	227	33	193	28	1.0
		−44	−112	200	29	176	25.5	1.5
		−8	−18	200	29	169	24.5	1.5
		24	75	193	28	159	23	1.5
		100	212	193	28	152	22	2.0
		150	300	165	24	131	19	3.0
		205	400	97	14	69	10	8.0
		260	500	66	9.5	34	5	16.0
		315	600	41	6	21	3	36.0
		370	700	24	3.5	14	2	50.0
355.0	T6	−217	−423	438	63.5	393	57	2.0
		−196	−320	407	59	321	46.5	2.0
		−44	−112	359	52	283	41	4.0
		−8	−18	...	...	...	...	...
		24	75	241	35	172	25	3.0
		100	212	241	35	172	25	2.0
		150	300	228	33	172	25	1.5
		205	400	117	17	90	13	8.0
		260	500	66	9.5	34	5	16.0
		315	600	41	6	21	3	36.0
		370	700	24	3.5	14	2	50.0
355.0	T7(c)	−196	−320	303	44	262	38	1.5
		−44	−112	279	40.5	245	35.5	2.0
		−8	−18	269	39	241	25	2.0
		24	75	262	38	249	36	0.5
355.0	T71	−196	−320	279	40.5	234	34	1.5
		−44	−112	217	31.5	207	30	1.0
		−8	−18	248	36	214	31	1.5
		24	75	241	35	200	29	1.5
		100	212	234	34	193	28	2.0
		150	300	207	30	179	26	3.0
		205	400	117	17	90	13	8.0
		260	500	66	9.5	34	5	16.0
		315	600	41	6	21	3	36.0
		370	700	24	3.5	14	2	50.0
C355.0	T6	−196	−320	386	56	255	37	7.0
		−44	−112	345	50	234	34	7.0
		−8	−18	331	48	234	34	7.0
		24	75	317	46	234	34	6.0
		100	212	317	46	276	40	7.0
		150	300	255	37	221	32	12.0
		205	400	90	13	62	9	40.0
		260	500	48	7	34	5	60.0
		315	600	31	4.5	21	3	70.0

(continued)

Table 7. (Continued)

AA No.	Temper	Test temperature °C	Test temperature °F	Tensile strength MPa	Tensile strength ksi	Tensile yield strength(b) MPa	Tensile yield strength(b) ksi	Elongation in 50 mm (2 in.), %
356.0	T5(c)	−196	−320	227	33	148	21.5	2.0
		−44	−112	193	28	141	20.5	2.5
		−8	−18	190	27.5	138	20	2.0
		24	75	172	25	138	20	2.0
356.0	T6	−196	−320	276	40	193	28	2.0
		−44	−112	241	35	172	25	2.0
		−8	−18	228	33	165	24	2.0
		24	75	228	33	165	24	3.5
		100	212	221	32	165	24	4.0
		150	300	159	23	138	20	6.0
		205	400	83	12	59	8.5	18.0
		260	500	52	7.5	34	5	35.0
		315	600	28	4	21	3	60.0
		370	700	17	2.5	14	2	80.0
356.0	T7	−196	−320	278	40	217	31.5	3.0
		−44	−112	241	35	197	28.5	3.0
		−8	−18	227	33	190	27.5	3.0
		24	75	234	34	207	30	2.0
		100	212	207	30	193	28	2.0
		150	300	159	23	138	20	6.0
		205	400	83	12	56	8.5	18.0
		260	500	52	7.5	34	5	35.0
		315	600	28	4	21	3	60.0
		370	700	17	2.5	14	2	80.0
A356.0	T6	−196	−320	372	54	248	36	10.0
		−44	−112	317	46	221	32	10.0
		−8	−18	296	43	214	31	10.0
		24	75	283	41	207	30	10.0
		100	212	262	38	228	33	12.0
		150	300	145	21	117	17	20.0
		205	400	83	12	59	8.5	40.0
		260	500	52	7.5	34	5	55.0
		315	600	28	4	21	3	70.0
A357.0	T6	−196	−320	427	62	331	48	6.0
		−44	−112	379	55	310	45	6.0
		−8	−18	372	54	303	44	6.0
		24	75	359	52	290	42	8.0
		100	212	331	48	310	45	6.0
		150	300	159	23	145	21	20.0
		205	400	69	10	52	7.5	50.0
		260	500	48	7	41	6	...
443.0	F(c)	−196	−320	179	26	69	10	8.0
		−44	−112	152	22	62	9	11.0
		−8	−18	145	21	62	9	12.0
		24	75	131	19	55	8	8.0
512.0	F(c)	−196	−320	200	29	124	18	2.5
		−44	−112	176	25.5	110	16	2.0
		−8	−18	186	27	100	14.5	3.0
		24	75	138	20	90	13	2.0
514.0	F	24	75	172	25	83	12	9.0
		100	212	165	24	83	12	9.0
		150	300	152	22	83	12	7.0
		205	400	124	18	83	12	9.0

(continued)

(a) Values are lowest properties recorded during 10,000 h at test temperatures. (b) Offset: 0.2%. (c) After 1000 h at test temperatures.

Table 7. (Continued)

AA No.	Temper	Test temperature, °C	Test temperature, °F	Tensile strength, MPa	Tensile strength, ksi	Tensile yield strength(b), MPa	Tensile yield strength(b), ksi	Elongation in 50 mm (2 in.), %
514.0.....	F	260	500	90	13	55	8	12.0
		315	600	62	9	28	4	17.0
		370	700	34	5	14	2	35.0
712.0.....	F(c)	24	75	241	35	172	25	9.0
		79	175	233	33.8	214	30.7	3.0
		120	250	203	29.5	174	25.2	2.0
		180	350	136	19.7	117	17	6.0

(a) Values are lowest properties recorded during 10,000 h at test temperatures. (b) Offset: 0.2%. (c) After 1000 h at test temperatures.

manent mold or high-pressure die cast in parts of simple design. Alloy 512 (0.4% magnesium-1.8% silicon) is usually sand cast, but can also be cast in permanent mold. Another sand casting alloy is 511 (4% magnesium-0.5% silicon). The silicon addition reduces tensile properties somewhat, but this is not of major importance because these alloys generally are used for parts in which the major requirement is corrosion resistance or decorative appearance.

Alloys 535 (7% magnesium-0.2% manganese) and B535 (7% magnesium) are normally cast in sand. Both alloys provide high tensile properties without heat treatment and are also suitable for welded assemblies. Alloys 518 (8% magnesium) and A535 (similar to 535 but less pure) are intended for high-pressure die casting; however, their oxidizing tendency and limited fluidity make them relatively difficult to cast when compared to alloys that contain silicon. Again, these alloys are used when corrosion resistance and decorative appearance are the essential requirements.

An outstanding combination of strength, ductility, and resultant high impact resistance is provided by 520-T4 (10% magnesium) alloy. This alloy is cast in sand, and good grain refinement and virtually complete removal of hydrogen and sodium are essential to attain high tensile properties. Quenching in hot oil after heat treatment, or use of an interrupted boiling water quench, is essential to provide optimum resistance to stress-corrosion cracking. After heat treatment, subsequent heating to even moderate elevated temperatures appreciably reduces both room temperature tensile properties and resistance to stress-corrosion cracking. Also, this alloy self-ages at warm ambient temperature (such as direct sunlight) and over time, it loses ductility and resultant high impact resistance.

Aluminum-Silicon Alloys (Eutectic and Hypoeutectic). Alloys with silicon as a major alloying ingredient are by far the most important commercial casting alloys, primarily because of their superior casting characteristics in comparison to other alloys. A wide range of physical and mechanical properties is afforded by these alloys. Ratings of casting alloys with respect to casting characteristics, corrosion resistance, machinability, and weldability are given in Tables 10, 11, and 12.

Binary aluminum-silicon alloys combine the advantages of high corrosion resistance, good weldability, and low specific gravity. Although castings of these alloys are somewhat more difficult to machine than the aluminum-copper or aluminum-magnesium alloys, all types of machining

Table 8. Tensile Properties of Aluminum Permanent Mold Casting Alloys at Various Temperatures(a)

These nominal properties are useful for comparing alloys, but they *should not* be used for design purposes. Properties for design *must be* obtained from appropriate material specifications, design standards, or by negotiation with the producer.

AA No.	Temper	Test temperature °C	Test temperature °F	Tensile strength MPa	Tensile strength ksi	Tensile yield strength(b) MPa	Tensile yield strength(b) ksi	Elongation in 50 mm (2 in.), %
201.0	T6(c)	24	75	448	65	379	55	8.0
		150	300	379	55	358	52	6.0
		205	400	248	36	227	33	9.0
		260	500	152	22	131	19	19.0
		315	600	69	10	62	9	39.0
201.0	T7(c)	24	75	469	68	414	60	5.0
		150	300	414	60	372	54	9.0
		205	400	267	39	227	33	16.0
		260	500	110	16	90	13	25.0
		315	600	62	9	55	8	48.0
A206.0	T7	24	75	434	63	345	50	11.7
		120	250	386	56	317	46	14.0
		180	350	331	48	303	44	17.7
222.0	T551	24	75	255	37	241	35	0.5
		100	212	234	34	227	33	0.5
		150	300	207	30	186	27	0.5
		205	400	172	25	138	20	1.0
		260	500	124	18	83	12	3.0
		315	600	59	8.5	34	5	10.0
		370	700	34	5	17	2.5	25.0
242.0	T571	24	75	276	40	234	34	1.0
		100	212	276	40	234	34	1.0
		150	300	255	37	227	33	1.0
		205	400	193	28	152	22	2.0
		260	500	90	13	55	8	15.0
		315	600	55	8	28	4	35.0
		370	700	34	5	21	3	60.0
296.0	T4	24	75	248	36	152	22	7.5
		100	212	227	33	152	22	7.5
		150	300	207	30	138	20	8.0
		205	400	103	15	62	9	12.0
		260	500	52	7.5	34	5	25.0
		315	600	28	4	17	2.5	65.0
296.0	T6	24	75	276	40	179	26	5.0
		100	212	241	35	159	23	5.0
		150	300	200	29	159	23	5.0
		205	400	117	17	76	11	15.0
		260	500	48	7	27	4	25.0
		315	600	24	3.5	17	2.5	75.0
		370	700	17	2.5	10	1.5	100.0
336.0	T551	24	75	248	36	193	28	0.5
		100	212	241	35	172	25	1.0
		150	300	214	31	152	22	1.0
		20	400	179	26	103	15	2.0
		260	500	124	18	69	10	5.0
		315	600	69	10	28	4	10.0
		370	700	34	5	21	3	45.0
332.0	T5	24	75	248	36	193	28	1.0
		100	212	227	33	186	27	1.0

(continued)

(a) Values are lowest properties recorded during 10,000 h at test temperatures. (b) Offset: 0.2%. (c) After 1000 h at test temperature.

Table 8. (Continued)

AA No.	Temper	Test temperature, °C	Test temperature, °F	Tensile strength, MPa	Tensile strength, ksi	Tensile yield strength(b), MPa	Tensile yield strength(b), ksi	Elongation in 50 mm (2 in.), %
332.0	T5	150	300	214	31	165	24	2.0
		205	400	172	25	110	16	3.0
		260	500	131	19	83	12	6.0
		315	600	83	12	55	8	15.0
		370	700	55	8	41	6	25.0
355.0	T51	−196	−320	290	42	186	27	2.0
		−44	−112	276	40	169	24.5	4.0
		−8	−18	245	35.5	155	22.5	3.0
		24	75	207	30	165	24	2.0
		100	212	193	28	165	24	3.0
		150	300	157	23	138	20	4.0
		205	400	103	15	69	10	19.0
		260	500	65	9.5	34	5	33.0
		315	600	41	6	21	3	38.0
		370	700	24	3.5	14	2	60.0
355.0	T6	−217	−423	489	71	420	61	2.0
		−196	−320	410	59.5	365	53	3.0
		−44	−112	348	50.5	314	45.5	4.0
		−8	−18	...	...	...	...	...
		24	75	290	42	186	27	4.0
		100	212	276	40	186	27	5.0
		150	300	221	32	172	25	10.0
		205	400	131	19	90	13	20.0
		260	500	65	9.5	34	5	40.0
		315	600	41	6	21	3	50.0
		370	700	24	3.5	14	2	60.0
355.0	T61	−217	−423	483	70	365	53	2.0
		−196	−320	383	55.5	338	49	3.0
		−44	−112	345	50	252	36.5	6.0
		−8	−18	...	...	...	...	...
		24	75	327	47.5	241	35	5.0
355.0	T62	−196	−320	427	62	324	47	3.0
		−44	−112	379	55	303	44	2.0
		−8	−18	372	54	296	43	3.0
		24	75	310	45	276	40	1.5
355.0	T71	−196	−320	365	53	276	40	3.5
		−44	−112	317	46	248	36	4.0
		−8	−18	310	45	245	35.5	4.5
		24	75	248	36	214	31	3.0
		100	212	227	33	200	29	4.0
		150	300	200	29	179	26	8.0
		205	400	131	19	90	13	20.0
		260	500	65	9.5	34	5	40.0
		315	600	42	6	21	3	50.0
		370	700	24	3.5	14	2	60.0
C355.0	T61	−196	−320	386	56	255	37	7.0
		−44	−112	345	50	234	34	7.0
		−8	−18	331	48	234	34	7.0
		24	75	317	46	234	34	6.0
		100	212	296	43	234	34	6.0
		150	300	262	38	234	34	10.0
		205	400	96	14	69	10	40.0
		260	500	45	6.5	38	5.5	60.0
		31	600	28	4	21	3	70.0
		37	700	24	3.5	17	2.5	90.0

(continued)

Table 8. (Continued)

AA No.	Temper	Test temperature °C	Test temperature °F	Tensile strength MPa	Tensile strength ksi	Tensile yield strength(b) MPa	Tensile yield strength(b) ksi	Elongation in 50 mm (2 in.), %
356.0.....	T6(c)	−196	−320	331	48	221	32	5.0
		−44	−112	276	40	193	28	5.0
		−8	−18	269	39	186	27	5.0
		24	75	276	40	186	27	5.0
		100	212	207	30	172	25	6.0
		150	300	145	21	117	17	10.0
		205	400	83	12	59	8.5	30.0
		260	500	52	7.5	34	5	55.0
		315	600	31	4.5	21	3	70.0
		370	700	17	2.5	14	2	80.0
356.0.....	T7	−196	−320	300	43.5	196	28.5	6.0
		−44	−112	241	35	172	25	9.0
		−8	−18	234	34	172	25	9.0
		24	75	221	32	165	24	6.0
		100	212	186	27	158	23	10.0
		150	300	145	21	117	17	20.0
		205	400	83	12	59	8.5	40.0
		260	500	48	7	34	5	55.0
		315	600	28	4	21	3	70.0
		370	700	17	2.5	14	2	80.0
A356.0....	T61	24	75	283	41	207	30	10.0
		150	300	145	21	117	17	20.0
		205	400	83	12	59	8.5	40.0
		260	500	52	7.5	34	5	55.0
		315	600	28	4	21	3	70.0
		370	700	17	2.5	14	2	80.0
		24	75	345	50	276	40	10.0
		150	300	214	31	200	29	11.0
		205	400	83	12	62	9	29.0
		260	500	42	7	41	6	...

(a) Values are lowest properties recorded during 10,000 h at test temperatures. (b) Offset: 0.2%. (c) After 1000 h at test temperature.

operations are routinely accomplished, usually using tungsten carbide tools and appropriate coolants and lubricants. Also, recently developed polycrystalline diamond tools are proving to have a very long service life when applied to alloys of the aluminum-silicon family.

Alloy 443 (5.3% silicon) may be used with all casting processes for parts in which good ductility, good corrosion resistance, and pressure tightness are more important than strength. For die casting, alloys 413 and A413 (12% silicon) also have good corrosion resistance but are superior to alloy 443 in terms of castability and pressure tightness. Alloy A444 (7% silicon-0.2% iron, maximum) also has good corrosion resistance and has especially high ductility when cast in permanent mold and heat treated to a T4 condition. This alloy is used when impact resistance is a primary consideration.

Alloys 413, 443, and 444 are the important binary aluminum-silicon alloys. Another group of aluminum-silicon alloys, however, represent the workhorse aluminum foundry alloys. In this group, silicon provides good casting characteristics and copper imparts moderately high strength and improved machinability, at the expense of somewhat reduced ductility

Table 9. Tensile Properties of Aluminum Die Casting Alloys at Various Temperatures(a)

These nominal properties are useful for comparing alloys, but they *should not* be used for design purposes. Properties for design *must be* obtained from appropriate material specifications, design standards, or by negotiation with the producer.

AA No.	Temper	Test temperature, °C	Test temperature, °F	Tensile strength, MPa	Tensile strength, ksi	Tensile yield strength(b), MPa	Tensile yield strength(b), ksi	Elongation in 50 mm (2 in.), %
360.0	F	−44	−112	334	48.5	186	27	4.0
		−8	−18	327	47.5	193	28	4.0
		24	75	324	47	172	25	3.0
		100	212	303	44	172	25	2.0
		149	300	241	35	165	24	4.0
		205	400	152	22	96	14	8.0
		260	500	83	12	52	7.5	20.0
		315	600	48	7	31	4.5	35.0
		370	700	31	4.5	21	3	40.0
A360.0	F	24	75	317	46	165	24	5.0
		100	212	296	43	165	24	3.0
		150	300	234	34	159	23	5.0
		205	400	145	21	90	13	14.0
		260	500	76	11	45	6.5	30.0
		315	600	45	6.5	28	4	45.0
		370	700	28	4	17	2.5	45.0
380.0	F(c)	−196	−320	407	59	207	30	2.5
		−44	−112	338	49	165	24	2.5
		−8	−18	338	49	165	24	3.0
		24	75	331	48	165	24	3.0
		100	212	310	45	165	24	4.0
		150	300	234	34	83	22	5.0
		205	400	165	24	110	16	8.0
		260	500	90	13	55	8	20.0
		315	600	42	7	28	4	30.0
		370	700	28	4	17	2.5	35.0
A380.0	F	24	75	324	47	159	23	4.0
		100	212	303	44	159	23	5.0
		150	300	227	33	145	21	10.0
		205	400	159	23	103	15	15.0
		260	500	83	12	48	7	30.0
		315	600	41	6	28	4	45.0
		370	700	28	4	17	2.5	45.0
384.0	F	24	75	324	47	172	25	1.0
		100	212	317	46	172	25	1.0
		150	300	262	38	165	24	2.0
		205	400	179	26	124	18	6.0
		260	500	96	14	62	9	25.0
		315	600	48	7	28	4	45.0
		370	700	31	4.5	17	2.5	45.0
413.0	F	−196	−320	372	54	179	26	4.0
		−44	−112	324	47	162	23.5	5.0
		−8	−18	321	46.5	159	23	5.5
		24	75	296	43	145	21	2.5
		100	212	255	37	138	20	5.0
		150	300	221	32	131	19	8.0
		205	400	165	24	103	15	15.0
		260	500	90	13	62	9	30.0
		315	600	14	7	31	4.5	35.0
		370	700	31	4.5	17	2.5	40.0
443.0	F	−196	−320	310	45	131	18	14.0
		−44	−112	241	35	110	16	12.0
		−8	−18	241	35	110	16	13.0

(continued)

Table 9. (Continued)

AA No.	Temper	Test temperature °C	Test temperature °F	Tensile strength MPa	Tensile strength ksi	Tensile yield strength(b) MPa	Tensile yield strength(b) ksi	Elongation in 50 mm (2 in.), %
443.0.....	F	24	75	227	33	110	16	9.0
		100	212	193	28	110	16	9.0
		150	300	152	22	103	15	10.0
		205	400	110	16	83	12	25.0
		260	500	62	9	41	6	30.0
		315	600	34	5	24	3.5	35.0
		370	700	24	3.5	17	2.5	35.0
518.0.....	F	−44	−112	352	51	145	21	14.0
		−8	−18	345	50	196	28.5	10.0
		24	75	310	45	186	27	8.0
		100	212	276	40	172	25	8.0
		150	300	221	32	145	21	25.0
		205	400	145	21	103	15	40.0
		260	500	90	13	62	9	45.0
		315	600	59	8.5	31	4.5	45.0
		370	700	34	5	17	2.5	45.0

(a) Values are lowest properties recorded during 10,000 h at test temperatures. (b) Offset: 0.2%. (c) After 1000 h at test temperatures.

and lower corrosion resistance. Alloy 319 (6% silicon-3.5% copper) is a preferred general-purpose alloy for sand foundries that also may be used in permanent mold casting; 380 alloy (8.5% silicon-3.5% copper) is preferred for die casting. Alloy 333 (9.0% silicon, 3.5% copper) was developed for permanent mold casting and is recommended for general permanent mold use. Many castings of these general-purpose alloys are supplied only in the as-cast temper. Some castings are heat treated to the T5 temper to improve hardness, machinability, and growth stability. The strength of 319 and 333 alloys can also be substantially improved by the full T6 heat treatment. Actually, 380 alloy, as well as some other die casting alloys, could benefit by a full T6 or T7 heat treatment. The nature of conventional die casting is such that they tend to blister during solution heat treatment, so such tempers are not applied to the alloys. Other aluminum-silicon-copper die casting alloys include 308, 333, 383, and 384, with variations of all of these alloys containing up to 3% zinc and other impurity elements. Ratings of permanent mold and die casting alloys with regard to castability, corrosion resistance, machinability, and weldability are given in Tables 11 and 12.

Another group of aluminum-silicon alloys are those hardened by Mg_2Si (magnesium silicide). The most popular of these is 356 alloy (7% silicon-0.3% magnesium) and the higher purity A356. The entire aluminum-silicon-magnesium silicide group of alloys has excellent casting characteristics, weldability, pressure tightness, and corrosion resistance. These alloys are heat treatable to provide various combinations of tensile and physical properties that are attractive for many applications, including aircraft and automotive parts. Alloy 357 is similar to 356 but has a higher magnesium content (0.5%) and can be heat treated to a higher strength level.

Alloys A356 and A357 are higher purity versions of 356 and 357, and A357 also contains a small amount of beryllium. Both alloys are capable

Table 10. Ratings of Aluminum Sand Casting Alloys With Regard to Castability, Corrosion Resistance, Machinability, and Weldability(a)

AA No.	Resistance to hot cracking(b)	Pressure tightness	Fluidity(c)	Shrinkage tendency(d)	Resistance to corrosion(e)	Machinability(f)	Weldability(g)
201.0	4	3	3	4	4	1	2
208.0	2	2	2	2	4	3	3
213.0	3	3	2	3	4	2	2
222.0	4	4	3	4	4	1	3
240.0	4	4	3	4	4	3	4
242.0	4	3	4	4	4	2	3
A242.0	4	4	3	4	4	2	3
295.0	4	4	4	3	3	2	2
319.0	2	2	2	2	3	3	2
354.0	1	1	1	1	3	3	2
355.0	1	1	1	1	3	3	2
A356.0	1	1	1	1	2	3	2
357.0	1	1	1	1	2	3	2
359.0	1	1	1	1	2	3	1
A390.0	3	3	3	3	2	4	2
A443.0	1	1	1	1	2	4	4
444.0	1	1	1	1	2	4	1
511.0	4	5	4	5	1	1	4
512.0	3	4	4	4	1	2	4
514.0	4	5	4	5	1	1	4
520.0	2	5	4	5	1	1	5
535.0	4	5	4	5	1	1	3
A535.0	4	5	4	4	1	1	4
B535.0	4	5	4	4	1	1	4
705.0	5	4	4	4	2	1	4
707.0	5	4	4	4	2	1	4
710.0	5	3	4	4	2	1	4
711.0	5	4	5	4	3	1	3
712.0	4	4	3	3	3	1	4
713.0	4	4	3	4	2	1	3
771.0	4	4	3	3	2	1	...
772.0	4	4	3	3	2	1	...
850.0	4	4	4	4	3	1	4
851.0	4	4	4	4	3	1	4
852.0	4	4	4	4	3	1	4

(a) For ratings of characteristics, 1 is the best and 5 is the poorest of the alloys listed. Individual alloys may have different ratings for other casting processes. (b) Ability of alloy to withstand stresses from contraction while cooling through hot-short or brittle temperature range. (c) Ability of molten alloy to flow readily in mold and fill thin sections. (d) Decrease in volume accompanying freezing of alloy and measure of amount of compensating feed metal required in form of risers. (e) Based on resistance of alloy in standard salt spray test. (f) Composite rating, based on ease of cutting, chip characteristics, quality of finish, and tool life. In the case of heat treatable alloys, rating is based on T6 temper. Other tempers, particularly the annealed temper, may have lower ratings. (g) Based on ability of material to be fusion welded with filler rod of same alloy.

of much higher ductility than their lower purity counterparts. Alloys A356 and A357 are among the premium-quality sand and permanent mold casting alloys specified for military and aircraft applications.

Other alloys of the aluminum-silicon-magnesium silicide group are 359 (9% silicon-0.6% magnesium), and the die casting alloys 360 (10.5% silicon-0.5% magnesium), A360 (lower iron than 360), and 364 (8.5% silicon-0.3% magnesium-0.4% chromium-0.03% beryllium) that provide a combination of high strength and ductility with good casting charac-

Table 11. Ratings of Aluminum Permanent Mold Casting Alloys With Regard to Castability, Corrosion Resistance, Machinability, and Weldability(a)

AA No.	Resistance to hot cracking(b)	Pressure tightness	Fluidity(c)	Shrinkage tendency(d)	Resistance to corrosion(e)	Machinability(f)	Weldability(g)
201.0	4	3	3	4	4	1	2
213.0	3	3	2	3	4	2	2
222.0	4	4	3	4	4	1	3
238.0	2	3	2	2	4	2	3
240.0	4	4	3	4	4	3	4
296.0	4	3	4	3	4	3	4
308.0	2	2	2	2	4	3	3
319.0	2	2	2	2	3	3	2
332.0	1	2	1	2	3	4	2
333.0	1	1	2	2	3	3	3
336.0	1	2	2	3	3	4	2
354.0	1	1	1	1	3	3	2
355.0	1	1	1	2	3	3	2
C355.0	1	1	1	2	3	3	2
356.0	1	1	1	1	2	3	2
A356.0	1	1	1	1	2	3	2
357.0	1	1	1	1	2	3	2
A357.0	1	1	1	1	2	3	2
359.0	1	1	1	1	2	3	1
A390.0	2	2	2	3	2	4	2
443.0	1	1	2	1	2	5	1
A444.0	1	1	1	1	2	3	1
512.0	3	4	4	4	1	2	4
513.0	4	5	4	4	1	1	5
711.0	5	4	5	4	3	1	3
771.0	4	4	3	3	2	1	...
772.0	4	4	3	3	2	1	...
850.0	4	4	4	4	3	1	4
851.0	4	4	4	4	3	1	4
852.0	4	4	4	4	3	1	4

(a) For ratings of characteristics, 1 is the best and 5 is the poorest of the alloys listed. Individual alloys may have different ratings for other casting processes. (b) Ability of alloy to withstand stresses from contraction while cooling through hot-short or brittle temperature range. (c) Ability of molten alloy to flow readily in mold and fill thin sections. (d) Decrease in volume accompanying freezing of alloy and measure of amount of compensating feed metal required in form of risers. (e) Based on resistance of alloy in standard salt spray test. (f) Composite rating, based on ease of cutting, chip characteristics, quality of finish, and tool life. In the case of heat treatable alloys, rating is based on T6 temper. Other tempers, particularly the annealed temper, may have lower ratings. (g) Based on ability of material to be fusion welded with filler rod of same alloy.

teristics. Corrosion resistance of all of these alloys is superior to the general-purpose 319 and 380 alloys previously mentioned.

Another group of alloys in the aluminum-silicon system are those that contain both magnesium and copper. The combination of magnesium and copper affords greater response to heat treatment than either element alone; however, the higher strength achieved is accomplished with some sacrifice in ductility and corrosion resistance. Representative sand and permanent mold alloys of this group are 355 (5% silicon-1.3% copper-0.5% magnesium) and a higher tensile property version of the same alloy, C355 (another premium-quality casting alloy). Products such as tank engine cooling fans and high-speed rotating parts and impellers are made of C355

Table 12. Ratings of Aluminum Die Casting Alloys With Regard to Castability, Corrosion Resistance, and Machinability(a)

AA No.	Resistance to hot cracking(b)	Pressure tightness	Fluidity(c)	Resistance to corrosion(d)	Machinability(e)	Weldability(f)
360.0	1	1	2	2	3	4
A360.0	1	1	2	2	3	4
364.0	2	2	1	3	4	3
380.0	2	1	2	5	3	4
A380.0	2	2	2	4	3	4
384.0	2	2	1	3	3	4
390.0	2	2	2	2	4	2
413.0	1	2	1	2	4	4
C443.0	2	3	3	2	5	4
515.0	4	5	5	1	2	4
518.0	5	5	5	1	1	4

(a) For ratings, 1 is the best and 5 is the poorest of the alloys listed. Individual alloys may have different ratings for other casting processes. (b) Ability of alloy to withstand stresses from contraction while cooling through hot-short or brittle temperature range. (c) Ability of liquid alloy to flow readily in mold and fill thin sections. (d) Based on resistance of alloy in standard salt spray test. (e) Composite rating based on ease of cutting, chip characteristics, quality of finish, and tool life. (f) Based on ability of material to be fusion welded with filler rod of same alloy.

alloy. When premium-strength casting principles are used, even higher tensile properties can be obtained with heat treated 354 alloy (9% silicon-1.8% copper-0.5% magnesium).

Pistons for automotive internal combustion engines are permanent mold cast of 332 alloy (9.5% silicon-3% copper-1% magnesium). Diesel engines and higher output engines often require the higher silicon 336 alloy that also contains nickel (12% silicon-2.5% nickel-1% copper-1% magnesium). This alloy has improved elevated-temperature properties, a lower expansion coefficient, and it provides improved wear resistance. It is common practice to age pistons to a T5 temper or a variation of T5, such as T551, to increase hardness, improve machinability, and provide growth stability.

When sand or permanent mold casting the aluminum-silicon alloys, it is often necessary to modify the eutectic to improve strength, ductility, pressure tightness, and machinability. Modification has traditionally been accomplished by adding a small amount of sodium (0.001 to 0.003%) to the melt; however, other additives are now used and are described later in this chapter.

Hypereutectic aluminum-silicon alloys (alloys with greater than 12% silicon) have outstanding wear resistance, a lower thermal expansion coefficient, and very good casting characteristics. Such alloys have traditionally received only limited attention and use because the presence of the extremely hard primary silicon phase reduces tool life during machining. Also, the special foundry characteristics and requirements of this alloy system, needed to properly control microstructure and casting soundness, are not nearly as well understood as are the characteristics of conventional hypoeutectic alloys.

Hypereutectic aluminum-silicon alloys have been used in Europe for heavy-duty internal combustion engine pistons and similar high-temperature applications for many years. In the United States, alloys such as 393 (22% silicon-2.3% nickel-1.3% copper-1% magnesium-0.1% van-

adium) have been used in similar applications for years.

In the early 1970's, the first all-aluminum engine block without iron liners or electroplating on the cylinder bores was die cast using 390 alloy. Since that time, the engines for five premium automobiles in Europe have been designed and manufactured using 390 alloy and the same bare-bore technology. The outstanding wear characteristics and strength of 390 alloy (17% silicon-4.5% copper-0.5% magnesium) have caused a rapid growth in its use. Today, 390 alloy is used extensively in small engines (such as for chain saws), computer disc spacers, pistons for air conditioning compressors, air compressor bodies, master brake cylinders, and pumps and other components in automatic transmissions.

The hypereutectic aluminum-silicon alloys have outstanding fluidity and excellent machinability in terms of surface finish and chip characteristics. Also, the recent introduction of polycrystalline diamond cutting tools have done much to alleviate previous problems of poor tool life when these alloys are machined. To guarantee the best machinability, mechanical properties, and performance of parts cast from hypereutectic aluminum-silicon alloys, the melt must be treated to control primary silicon size. This treatment, termed refinement, is accomplished by adding a few hundredths of a percent phosphorus to the melt. Phosphorus from this addition nucleates the primary silicon particles during solidification. Properly refined primary silicon is only 8 to 10% the size of unrefined silicon. When hypereutectic aluminum-silicon alloys are conventionally high-pressure die cast, refinement is not needed; rapid solidification and turbulence result in a fine structure even when the melt is not treated with phosphorus. Removal of sodium by fluxing is essential prior to the phosphorus addition, because sodium forms sodium phosphide. In this compound, phosphorus loses its nucleating effect on the primary silicon.

Aluminum-zinc alloys also present special desirable characteristics as well as some difficulties in casting. Generally, these alloys have good machinability and high melting points (solidus temperatures), making them suitable for castings that are to be assembled by brazing. Aluminum-zinc alloys age at room temperature to moderately high strengths in a relatively short period of time. While all of these alloys can be sand cast, carefully designed gating is required to provide the directional solidification and feeding needed to produce sound castings. Permanent mold casting of these alloys is more difficult, because hot cracking is likely to be encountered in all but the simplest shapes.

The tensile properties of the aluminum-zinc-magnesium alloys in the as-cast (F temper) condition change rapidly during the first few weeks of room temperature aging, because of natural precipitation hardening. Additional hardening continues thereafter at a progressively slower rate. Heat treatments of the T6 and T7 type may be applied to alloys of this type. Aluminum-zinc alloys self-age to a reasonable strength level without a solution heat treatment, making them useful for castings with shapes that are difficult to solution heat treat and quench without cracking or distortion.

Aluminum-Tin Alloys. The tin-containing alloys were developed for bearings and bushings with high load-carrying capacity and fatigue strength. Corrosion resistance by internal combustion engine lubricating oils is an important consideration in such applications. Aluminum-tin alloys provide superior corrosion characteristics in comparison to most other metals

for bearing composition. All four alloys of this family can be cast in both sand and permanent mold. However, careful control of gating and other casting practices are necessary to produce sound castings and to overcome a marked susceptibility to hot cracking.

Castings of the 850-type normally are heat treated to the T5 temper to increase compressive strength. Some T5 castings are then cold worked, reducing the axial dimensions 4% (T101 temper), providing a substantial increase in compressive yield strength. Alloys 850 and 851 are primarily used for connecting rods and crankcase bearings for diesel engines. Alloys 852 and 853 have higher compressive yield strengths and hardnesses and are used for truck roller bearings, large rolling mill bearings, and other bearings and bushings that are made to be heavily loaded.

MINOR ALLOYING AND IMPURITY ELEMENTS

Silicon. A low maximum silicon content is specified in some alloys of the aluminum-magnesium and aluminum-zinc-magnesium groups because silicon in these systems has a deleterious effect on tensile properties.

Iron is restricted to a maximum of 0.8 or 1% in most commercial sand and permanent mold casting alloys because higher contents impair feeding ability and mechanical properties (especially ductility). In the aluminum-magnesium alloys, iron limits in the range of 0.25 to 0.5% are imposed to permit attainment of specified tensile properties.

A maximum of 0.2% iron is stipulated for premium-strength aluminum-silicon-magnesium or aluminum-silicon-magnesium-copper alloys (see Table 2) to allow attainment of the required ductility and toughness. Iron combines with other elements in the alloys to form insoluble embrittling constituents that act as severe stress risers and, therefore, must be kept at an absolute minimum in applications requiring high ductility.

An iron content of 1% or more is considered desirable for die casting alloys to minimize die soldering. Aluminum has a natural affinity for iron and attacks and dissolves die steel, a condition commonly referred to as soldering. An iron content of approximately 1% or more minimizes the tendency of aluminum die casting alloys to solder to the steel die. The ternary aluminum-iron-silicon eutectic exists at approximately 0.8% iron. With 1% or more iron in the alloy, there is no significant driving force for the molten alloy to further dissolve steel dies.

Beryllium. Addition of a few thousandths of a percent beryllium often is used to increase the resistance of aluminum-magnesium alloy melts to oxidation. Also, adding a few hundredths of a percent beryllium to an aluminum-silicon-magnesium alloy somewhat alters the morphology of the iron phases and, therefore, improves its ductility. However, broad industry practice carefully restricts the use of beryllium for hygenic reasons. Welding restrictions may apply to some alloys containing beryllium because of tight atmospheric restrictions for beryllium fumes.

Chromium and manganese are sometimes introduced individually or together, in quantities generally of less than 1%, to improve the elevated-temperature properties of 240, 243, 328, and 392 alloys. Also, chromium and/or manganese are added to such alloys as 363, 535, 705, and 707 to alter the morphology of the aluminum-iron-silicon constituent, thereby improving mechanical properties, especially ductility, at room temperature.

Nickel. Introduction of up to 2.5% nickel increases the ability of an

alloy to resist the effects of exposure to elevated temperatures. The 1% nickel in 339 alloy, and the 2.0%+ nickel in 336, 242, A242, and 243 alloys, are examples where nickel imparts high tensile properties at elevated exposure temperatures.

Titanium, Boron, and Zirconium. Small additions of titanium are made to most sand and permanent mold casting alloys to refine the primary aluminum grain structure. Boron, in amounts of a few thousandths of a percent, is frequently added together with titanium to improve the degree of grain refinement and to increase retention of refinement during repeated remelting. Zirconium is also a grain refiner, but larger quantities are needed to achieve the same effect as titanium or titanium-boron.

Sodium, Calcium, Strontium, and Antimony. Each of these elements is employed to alter the form of the aluminum-silicon eutectic in alloys containing from 5 to 11% silicon. In the absence of modification, the eutectic is characterized by rather coarse needles or plates. As with any microstructure of this type, mechanical properties in general, and ductility as measured by percent of elongation in particular, are not as high as with a small rounded constituent.

By means of modification, the aluminum-silicon constituent can be changed from needles and plates to a fine spherical shape with improvements in casting characteristics and mechanical properties. This is normally accomplished by adding either sodium, strontium, or other modifiers to the alloy.

Sodium generally is added as the elemental metal. The most convenient method is the addition of prepackaged metallic sodium in aluminum cans. From 0.001 to 0.003% sodium is sufficient to achieve modification, depending on silicon content and whether the casting is sand or permanent mold. It usually is necessary, even under the most careful conditions of addition, to add several times the amount of sodium desired.

In adding strontium, either aluminum-strontium or aluminum-silicon-strontium master alloys are used. Strontium additions generally range from 0.01 to 0.03%.

There is a difference in behavior between sodium and strontium after addition. Both elements are lost continuously during holding of the melt, although sodium is lost more rapidly. Loss of modification occurs directly with the loss of sodium. For strontium, the degree of modification increases with holding time for several hours, after which acceptable levels of modification are retained until strontium is reduced to very low levels. Care should be taken not to add excess sodium or strontium, because overmodification may occur. This condition is not normal and generally requires additions greatly in excess of those recommended before occurrence. The concurrent use of sodium and strontium for immediate and retained modification is permissible and in some cases desirable.

Antimony changes the microstructure of aluminum-silicon to a lamellar eutectic with the advantages of conventional modification. The use of antimony has not been widely accepted as a result of hygiene and toxicological concerns; however, the effect of antimony on metallurgical structures is essentially permanent in comparison with the transient effects of either sodium or strontium.

Calcium and a number of less important chemical elements are recognized as modifiers of aluminum-silicon structures; however, modifi-

cation is neither as effective nor as reliable as in the use of the more widely accepted elements described above.

Bismuth, Lead, and Tin. Elements such as bismuth or lead form small insoluble globules in a casting microstructure and act as chip breakers that reduce the lengths of chips during machining. If present in sufficient quantities (generally 0.5% each), lead and bismuth have been shown to permit increased machining speeds and reduce the need for cutting fluids. Tin similarly is credited with improving machinability of aluminum casting alloys, but its major purpose is to improve bearing properties as previously described for the 8XX alloys.

Phosphorus. The advantage of adding 0.01 to 0.03% phosphorus in refining primary silicon particles was described relative to the hypereutectic aluminum-silicon alloys, which contain more than 12% silicon. Phosphorus combines with aluminum in a melt to form insoluble aluminum-phosphide particles that, because of their close crystallographic similarity to silicon, act as suitable nuclei for the primary silicon phase. Both aluminum-phosphide and silicon have a diamond cubic crystal habit and a similar lattice constant (silicon, 0.543 nm or 5.43 Å; aluminum-phosphorus, 0.545 nm or 5.45 Å). Phosphorus and sodium tend to interact when both are present in a melt. One sometimes renders the other ineffective. For hypereutectic alloys, sodium should be at low levels to obtain refinement of the silicon phase by phosphorus. Similarly for hypoeutectic alloys, phosphorus must be at a low level to obtain sodium modification.

ALLOY DEVELOPMENT

Several hundred aluminum casting alloys have been developed in the past half century. Many of them are now obsolete after various degrees of commercial utilization. Also, many other specific alloys that are not discussed in this chapter are used in limited quantities or are supplied to meet the specification of individual companies. To all of these can be added yet an additional number of alloys that are currently in the developmental or experimental stage.

The need will always exist for alloys having properties or characteristics required only in very special applications. The number of alloys in commercial use, however, should periodically be reduced through the concerted efforts of casting producers and casting purchasers and the suppliers of foundry ingot, affording economic advantages to all concerned.

REFERENCES

1. Registration Record of Aluminum Association Alloy Designation and Chemical Composition Limits for Aluminum Alloys in the Form of Castings and Ingot, The Aluminum Association, Washington, DC, Aug 1982
2. 1982 Annual Book of ASTM Standards, Part 7, (B275), American Society for Testing and Materials, Philadelphia, 1982
3. SAE Handbook 1980, Section 11.08, Society of Automotive Engineers, Warrendale, PA, 1980
4. W.E. Sicha, Aluminum Base Casting Alloys, in *Cast Metals Handbook,* American Foundrymen's Society, 1957, p 254-259
5. R.S. Archer, Commercial Alloys of Aluminum, in *The Aluminum Industry,* Vol 22, New York: McGraw-Hill Book Co., 1930, p 192-231
6. E.H. Dix, Jr., Corrosion of Light Metals, in *Corrosion of Metals,* American Society for Metals, 1946, p 131-177
7. J.W. Meier, Research on Premium-Quality Castings in Light Alloys, *Transactions,* American Foundrymen's Society, Vol 73, 1965, p 525-540

Aluminum Properties and Physical Metallurgy
John E. Hatch editor, p 351-378
DOI: 10.1361/appm1984p351

CHAPTER 9

PROPERTIES OF COMMERCIAL WROUGHT ALLOYS*

The designation "wrought" indicates that certain aluminum alloys are available primarily in the form of worked products, such as sheet, foil, plate, extrusions, tube, forgings, rod, bar, and wire. Working operations and thermal treatments transform the cast ingot structure into a wrought structure that may range from fully recrystallized to fibrous, as may be characteristic for the alloy and product. Structure influences strength, corrosion resistance, and various other properties.

In this chapter, wrought alloys are first considered according to method of obtaining mechanical properties (heat treated or non-heat treated), and then by end use or application. There is some degree of cross-referencing; the reader, for example, of the section on alclad products may wish to refer back to the appropriate alloy section to read more about the core or cladding alloy.

ALLOY AND TEMPER DESIGNATIONS

Under the guidance of the Aluminum Association (AA), the major aluminum producers in the United States have agreed on a four-digit numerical system for designating wrought aluminum and aluminum alloys. The first of the four digits in the designation indicates the alloy group as follows:

Designation	Major alloying element
1XXX	None(a)
2XXX	Cu
3XXX	Mn
4XXX	Si
5XXX	Mg
6XXX	Mg and Si
7XXX	Zn
8XXX	Other than above
9XXX	Unused

(a) 99.00% aluminum, minimum.

In the 1XXX group, the last two digits designate the minimum percent aluminum in excess of 99.00. In the 2XXX through 8XXX alloy groups,

*This chapter was revised by a team comprised of N.W. Nielson, B.N. Peak, and J.D. Yerger, Jr., Aloca; J. Faunce, Martin Marietta Laboratories; F.W. Gayle and D.S. Thompson, Reynolds Metals Co.; D.B. Kulp, Anaconda Aluminum Co.; D.M. Moore, Alcan International Ltd; W.A. Wong, Kaiser Aluminum & Chemical Corp. The original chapter was authored by J.A. Nock, Jr., Aloca Research Laboratories.

the last two digits have no special significance, except to identify different aluminum alloys in the group. The second digit in the designation indicates alloy modifications. For a more complete description of the alloy and temper system, see ANSI specification H35.1 (Ref 1).

National variations have composition limits that are similar but not identical to those registered by another country. They are identified by a letter following the numerical designation. Alloys with a composition that is still considered experimental have the letter X preceding their designation.

The various wrought alloys can be most readily described by adopting two basic classes: non-heat treatable and heat treatable alloys. Non-heat treatable alloys include all the various grades of pure aluminum and all other alloys in which strength is developed largely by solid solution hardening and by strain hardening from the annealed temper. The variety of properties found in non-heat treatable alloys results from elements that are present as major impurities for some alloys. For other alloys, the elements are additions. Such elements include chromium, iron, magnesium, manganese, silicon, and zinc. In addition, minor amounts of other elements such as copper may be added. The non-heat treatable alloys are in the 1XXX, 3XXX, 4XXX, and 5XXX series, although a few such alloys occur in the 7XXX and 8XXX series.

Heat treatable alloys contain one or more of the elements copper, magnesium, silicon, and zinc that are soluble in aluminum in considerable amounts at elevated temperatures, but to a much smaller degree at room temperature. This characteristic renders these alloys susceptible to heat treatment, as described in Chapter 5 in this Volume. Manganese, chromium, or zirconium may be added to retard or prevent recrystallization. The heat treatable alloys generally are found in the 2XXX, 6XXX, and 7XXX series, although a few such alloys occur in the 4XXX and 5XXX series.

Wrought alloy products are offered for sale in a variety of conditions, or tempers, that determine strength and other characteristics. Under the guidance of the AA, a temper system has been developed that generally identifies the type and sequence of mechanical and thermal operations used to produce the temper. Each temper for any given alloy-product-size combination has specific mechanical property limits, and some have other designated characteristics or properties as well. A more detailed description of the temper designation system can be found in Chapters 4 and 5 in this Volume and in ANSI specification H35.1.

Table 1 lists AA alloy designations and nominal compositions for many standard non-heat treatable aluminum alloys. Table 2 lists standard heat treatable alloys with nominal compositions. A complete and frequently updated list of alloy compositions can be obtained from the AA (Ref 2 and 3). Both heat treatable and non-heat treatable alloys are available in a wide variety of products, as illustrated below:

- *Sheet*: 1060, 1350, 1145, 1100, 2014, 2219, 2024, 2036, 3102, 3003, 3004, 3005, 3104, 3105, 4343, 5005, 5042, 5050, 5052, 5252, 5154, 5454, 5056, 5456, 5457, 5657, 5082, 5182, 5083, 5086, 6009, 6010, 6951, 6061, 7005, 7016, 7021, 7029, 7050, 7072, 7075, 7475, 7178, 8001, 8280, 8081

Table 1. Composition of Some Commercial Non-Heat Treatable Wrought Aluminum and Aluminum Alloys

Alloy	Alloying elements, wt% (nominal value)						Aluminum, minimum %
	Silicon	Copper	Manganese	Magnesium	Chromium	Other	
1199	...	...	...	...	...	...	99.99
1180	...	...	...	...	...	...	99.80
1060	...	...	...	...	...	...	99.60
1350	...	...	...	...	...	...	99.50
1145	...	...	...	...	...	...	99.45
1235	...	...	...	...	...	...	99.35
1100	...	0.12	...	...	...	...	99.00
3102	...	...	0.22	...	...	...	rem
3003	...	0.12	1.2	...	...	...	rem
3004	...	...	1.2	1.0	...	...	rem
3104	...	0.15	1.1	1.0	...	...	rem
3005	...	...	1.2	0.40	...	...	rem
3105	...	...	0.6	0.50	...	...	rem
4043	5.2	...	...	...	...	...	rem
4343	7.5	...	...	...	...	...	rem
4643	4.1	...	...	0.20	...	...	rem
4045	10.0	...	...	...	...	...	rem
4145	10.0	4.0	...	...	...	...	rem
4047	12.0	...	...	...	...	...	rem
5005	...	...	...	0.8	...	...	rem
5042	...	...	0.35	3.5	...	...	rem
5050	...	...	...	1.4	...	...	rem
5052	...	...	...	2.5	0.25	...	rem
5252	...	...	...	2.5	...	...	rem
5154	...	...	...	3.5	0.25	...	rem
5454	...	...	0.8	2.7	0.12	...	rem
5654	...	...	...	3.5	0.25	0.10 Ti	rem
5056	...	...	0.12	5.0	0.12	...	rem
5456	...	...	0.8	5.1	0.12	...	rem
5457	...	...	0.30	1.0	...	...	rem
5657	...	...	...	0.8	...	...	rem
5082	...	...	...	4.5	...	...	rem
5182	...	...	0.35	4.5	...	...	rem
5083	...	...	0.7	4.4	0.15	...	rem
5086	...	...	0.45	4.0	0.15	...	rem
7072	...	...	...	...	...	1.0 Zn	rem
8001	...	...	...	...	...	0.6 Fe, 1.1 Ni	rem
8280	1.5	1.0	...	...	...	0.45 Ni, 6.2 Sn	rem
8081	...	1.0	...	...	...	20 Sn	rem

- *Plate*: 1060, 1350, 1100, 2014, 2219, 2024, 2124, 3003, 3004, 3005, 5005, 5050, 5052, 5252, 5154, 5454, 5456, 5457, 5083, 5086, 6951, 6061, 7021, 7050, 7075, 7475, 7178, 8001, 8280
- *Foil*: 1199, 1180, 1145, 1235, 1100, 2024, 3003, 5005, 5050, 5052, 5056, 7072
- *Drawn tubing*: 1060, 1350, 1100, 2011, 2014, 2219, 2024, 3102, 3003, 3004, 5050, 5052, 5154, 5454, 5083, 5086, 6101, 6951, 6053, 6061, 6262, 6063, 7005, 7075, 7178, 8001
- *Extruded tube and pipe*: 1060, 1350, 1100, 2011, 2014, 2219, 2024, 3003, 5154, 5454, 5083, 5086, 6101, 6053, 6061, 6262, 6063, 6066, 6070, 7075, 7178, 8001

Table 2. Composition of Some Commercial Heat Treatable Wrought Aluminum Alloys

Alloy	Alloying elements, wt% (nominal value)							Aluminum
	Silicon	Copper	Manganese	Magnesium	Chromium	Zinc	Other	
2011	...	5.5	...	...	...	...	0.40 Bi, 0.40 Pb	rem
2014	0.8	4.4	0.8	0.5	...	...	...	rem
2017	0.5	4.0	0.7	0.6	...	...	...	rem
2117	...	2.6	...	0.35	...	...	...	rem
2218	...	4.0	...	1.5	...	...	2.0 Ni	rem
2618	0.18	2.3	...	1.6	...	...	1.1 Fe, 1.0 Ni, 0.07 Ti	rem
2219, 2419	...	6.3	0.30	...	...	...	0.10 V, 0.18 Zr, 0.06 Ti	rem
2024, 2124, 2224	...	4.4	0.6	1.5	...	...	...	rem
2025	0.8	4.4	0.8	...	...	...	...	rem
2036	...	2.6	0.25	0.45	...	...	...	rem
4032	12.2	0.9	...	1.0	...	...	0.9 Ni	rem
6101	0.50	...	...	0.6	...	...	...	rem
6201	0.7	...	...	0.8	...	...	...	rem
6009	0.8	0.37	0.50	0.6	...	...	...	rem
6010	1.0	0.37	0.50	0.8	...	...	...	rem
6151	0.9	...	...	0.6	0.25	...	...	rem
6351	1.0	...	0.6	0.6	...	...	...	rem
6951	0.35	0.28	...	0.6	...	...	...	rem
6053	0.7	...	...	1.2	0.25	...	...	rem
6061	0.6	...	0.28	1.0	0.20	...	...	rem
6262	0.6	0.28	...	1.0	0.09	...	0.6 Bi, 0.6 Pb	rem
6063	0.4	...	...	0.7	...	...	...	rem
6066	1.3	1.0	0.8	1.1	...	...	...	rem
6070	1.3	0.28	0.7	0.8	...	...	...	rem
7001	...	2.1	...	3.0	0.26	7.4	...	rem
7005	...	...	0.45	1.4	0.13	4.5	0.14 Zr, 0.03 Ti	rem
7016	...	0.8	...	1.1	...	4.5	...	rem
7021	...	...	...	1.5	...	5.5	0.13 Zr	rem
7029	...	0.7	...	1.6	...	4.7	...	rem
7049	...	1.6	...	2.4	0.16	7.7	...	rem
7050	...	2.3	...	2.2	...	6.2	0.12 Zr	rem
7150	...	2.2	...	2.4	...	6.4	0.12 Zr	rem
7075, 7175	...	1.6	...	2.5	0.23	5.6	...	rem
7475	...	1.6	...	2.2	0.22	5.7	...	rem
7076	...	0.6	0.50	1.6	...	7.5	...	rem
7178	...	2.0	...	2.7	0.23	6.8	...	rem

- *Extruded shapes*: 1060, 1350, 1100, 2011, 2014, 2219, 2024, 2224, 3003, 5154, 5454, 5456, 5083, 5086, 6006, 6101, 6105, 6351, 6053, 6061, 6262, 6063, 6463, 6066, 6070, 7001, 7005, 7029, 7050, 7150, 7075, 7178, 8001
- *Rolled shapes*: 2014, 5456, 6101, 6061
- *Bar*: 1199, 1060, 1350, 1100, 2011, 2014, 2017, 2024, 3003, 5052, 5154, 6101, 6951, 6061, 6262, 6066, 7001, 7075
- *Wire*: 1199, 1060, 1350, 1100, 2011, 2014, 2017, 2117, 2219, 2024, 3003, 4043, 4343, 4643, 4145, 5005, 5052, 5154, 5654, 5056, 6201, 6151, 6951, 6053, 6061, 6262, 7075, 7178
- *Rod*: 1199, 1350, 1100, 2011, 2014, 2017, 2117, 2219, 2024, 3003, 4043, 5005, 5052, 5154, 5056, 6101, 6201, 6951, 6053, 6061, 6262, 6066, 7001, 7075, 7178, 8001

- *Rivets*: 1100, 2011, 2017, 2117, 2219, 2024, 3003, 5052, 5056, 6151, 6053, 6061, 7050, 7075, 7178, 8001
- *Forgings*: 1100, 2011, 2014, 2017, 2218, 2618, 2219, 2024, 2124, 2025, 3003, 4032, 5052, 5456, 5083, 5086, 6101, 6151, 6053, 6061, 6066, 7049, 7050, 7075, 7175, 7076, 7178
- *Impacts*: 1199, 1100, 2014, 2618, 2024, 3003, 3004, 6151, 6053, 6061, 6063, 6463, 7075, 7178, 8001

NON-HEAT TREATABLE ALLOYS

Super-Purity and Pure Aluminum. The first wrought aluminum alloy produced was undoubtedly a grade of pure aluminum. It is reasonable to assume that the composition was similar to present-day commercially pure aluminum, designated 1100 alloy. Wrought products of this alloy have been available in the United States since 1888.

The various grades of pure metal were used directly as wrought products for specific applications in the early development of the industry. A high grade of pure aluminum that became available early in this century, called EC alloy, was used for electrical conductors. The pure aluminum wrought material used today for electrical conductors is of 1350 alloy, which has a minimum aluminum content of 99.50%. In addition to the purity level, small amounts of boron generally are added to offset the effects of vanadium and titanium and thereby obtain the required conductivity. Alloys containing up to 0.5% iron as a principal alloying element also are used for applications requiring high electrical conductivity. The aluminum used for household and much commercial foil varies in purity from 98.6 to 99.9% aluminum. Several high-purity grades are listed in Tables 1 and 3.

The tensile properties of the various grades of pure aluminum do not cover a very extensive range in strength when compared to the alloys discussed subsequently in this chapter. The tensile strength of annealed 99.99% aluminum, as shown in Table 3, is about 45 MPa (6.5 ksi), with a yield strength about 10 MPa (1.4 ksi), and elongation about 50%. Wrought

Table 3. Typical Mechanical Properties of Unalloyed Aluminum

Alloy	Temper	Tensile strength MPa	Tensile strength ksi	Tensile yield strength(a) MPa	Tensile yield strength(a) ksi	Elongation in 50 mm (2 in.),%	Hardness(b), BHN	Shear strength MPa	Shear strength ksi	Fatigue limit(c) MPa	Fatigue limit(c) ksi
1199	O	45	6.5	10	1.4	50	...	...	...	...	...
	H18	115	16.7	110	16.0	5	...	...	...	...	...
1180	O	60	8.7	20	2.9	45	...	...	...	...	...
	H18	125	18.1	115	16.7	5	...	...	...	...	...
1060	O	70	10.2	30	4.4	43	19	50	7.2	20	2.9
	H14	100	14.5	90	13.0	12	26	60	8.7	35	5.1
	H18	130	18.8	125	18.1	6	35	75	10.9	45	6.5
1350	O	85	12.3	30	4.4	23(d)	...	55	8.0	...	...
	H14	110	16.0	95	13.8	...	...	70	10.2	...	...
	H19	185	26.8	165	23.9	2.5(d)	...	105	15.2	...	...
1145	O	75	10.9	35	5.1	40	...	55	8.0	...	...
	H18	145	21.0	115	16.7	5	...	85	12.3	...	...

(a) Yield strength, 0.2% offset. (b) 500-kg (1102-lb) load, 10-mm (0.4-in.) ball, 30 s. (c) Based on 500 million cycles using an R.R. Moore-type rotating-beam machine. (d) Elongation in 250 mm (10 in.).

products of 99.99% aluminum in the O temper are so soft that strain hardening can be induced even during careful milling of test coupons. This strain hardening is reflected in a sharp increase of yield strength from the typical 10 MPa (1.4 ksi) level. Super-purity aluminum does not remain in the severely strain-hardened condition but partially recrystallizes at ambient temperatures.

The various grades of pure aluminum used commercially have distinctly higher strength, and stable properties are developed in the various strain-hardened tempers. The maximum strength levels occur in 1100 alloy wrought products. Properties of only a few grades of pure aluminum are given in Table 3, because only minor variations in strength occur among the various compositions with approximately the same aluminum content. In many instances, no change in strength is found, but the control of composition is related to other characteristics, such as electrical conductivity or corrosion resistance, required for a specific application. Wrought products of commercially pure aluminum are used in virtually all fields, with major consumption in the packaging, chemical, electrical, and architectural fields. An important application of pure aluminum is as cladding, to improve corrosion resistance of heat treatable alloys, or to improve finishing characteristics of non-heat treatable alloys.

Aluminum-Magnesium Alloys. The 5XXX series alloys containing up to 6% nominal magnesium form a useful series of solid solution alloys (Ref 4). Strengths in the annealed temper range from about 110 MPa (16.0 ksi) tensile strength and 40 MPa (5.8 ksi) yield strength for the Al-1% Mg alloy, to 310 MPa (45.0 ksi) tensile strength and 160 MPa (23.2 ksi) yield strength for the Al-6% Mg alloy. Elongation over this range of magnesium exceeds 25%.

General-purpose and structural alloys containing from about 1% to slightly over 5% magnesium are in widespread commercial use. Alloys containing up to about 3% magnesium are structurally stable at room and elevated temperatures, even in the hard rolled tempers, but some structural instability occurs with higher magnesium contents in severely strain-hardened tempers.

In the 1920's, limited amounts of Al-4% Mg sheet were made. No large-scale production of aluminum-magnesium alloy wrought products occurred until the 1930's, when alloys 5052 and 5154 were introduced, followed by 5056. The number of aluminum-magnesium alloys has increased rapidly since that period, as indicated by the compositions listed in Table 1. Actually, there are only a few general-purpose commercial binary aluminum-magnesium alloys, such as 5005 and 5050. Alloys 5052, 5154, and 5056 are examples of alloys with small additions of dispersion-hardening elements. To improve strength or other characteristics, the majority of the aluminum-magnesium alloys contain additions of chromium, manganese, and titanium, singly or in combination, in total amounts from about 0.25 to 1%.

The commercial aluminum-magnesium alloy with the greatest strength is 5456, closely followed by 5083, and at a lower strength level, by 5086. Other alloys of lesser strength are 5454, 5082, and 5182. The lowest strength levels occur with the binary alloys, such as 5005 and 5050, as shown in Table 4.

Wrought products of aluminum-magnesium alloys are always available in the O temper and in one or more of the basic H1, H2, or H3 tempers. The H3 temper is in general use for strain-hardened tempers of these alloys, because the H1 temper is not stable at ambient temperatures. The H3 temper, therefore, is used to produce stable properties with higher elongation levels and improved forming characteristics. In a limited number of alloys, the H2 temper is used for good corrosion resistance and for improved forming characteristics, combined with strengths higher than those available in the O temper.

The aluminum-magnesium alloys combine a wide range of strength, good forming and welding characteristics, and high resistance to general corrosion. An outstanding property is the good welding response of the higher strength alloys when commercial shielded arc processes are used. Weld strengths equal the annealed strengths of the various alloys, and the welds exhibit good ductility. Alloys with magnesium contents lower than about 3.5% are somewhat less easily welded than those with higher magnesium contents. Alloys for welding electrodes include 5356, 5554, and 5556. In general, the electrode filler alloys are similar to the base alloy being welded, but they contain an addition of titanium to refine the grain structure of the weld.

Although these alloys are classified as non-heat treatable, the amount of magnesium soluble at the annealing temperature for alloys such as 5083, 5086, 5056, and 5456 is higher than that retained in solid solution at room temperature. This instability attains a critical state in the presence of severe strain hardening, followed by long storage at room temperature or exposure to elevated temperatures, as precipitation occurs along grain boundaries or along slip planes. Precipitation promotes intergranular attack and stress-corrosion cracking in corrosive media. This situation resulted in the development of the H116 temper to eliminate or minimize instability and to use the higher strength and other qualities of these alloys (Chapter 7 in this Volume).

The many desirable characteristics of the aluminum-magnesium alloys prompt usage in numerous areas where strengths higher than those of pure aluminum are required. The higher strengths and good welding qualities make them valuable in the transportation and structural fields, in the process industries, and in military uses requiring good ballistic or cryogenic properties.

Decorative alloys with a wide range of strengths and bright surface finish capabilities are also characteristic of the aluminum-magnesium alloy system. This combination of properties contributes significantly to the extensive use of these alloys. Important examples are the use of low-iron base alloys and appropriate treatments to develop bright, durable products for automotive trim, architectural components, and other decorative applications. The alloys used in this general field include the 5X57 alloys and the general-purpose alloys 5005 and 5050. Impurity limitations in many of the 5X57 alloys are a contributing factor in developing bright, uniform finishes. The best finishes are achieved when impurities are at the lowest level, such as in alloys 5252 and 5657.

Aluminum-Manganese and Aluminum-Manganese-Magnesium Alloys. The first and only aluminum-manganese alloy of commercial sig-

Table 4. Typical Mechanical Properties of Some Non-Heat Treatable Aluminum Alloys

Alloy	Temper	Tensile ultimate strength MPa	Tensile ultimate strength ksi	Tensile yield strength(a) MPa	Tensile yield strength(a) ksi	Elongation in 50 mm (2 in.), %	Hardness(b), BHN	Shear strength MPa	Shear strength ksi	Fatigue limit(c) MPa	Fatigue limit(c) ksi
1100	O	90	13.0	35	5.1	35	23	60	8.7	35	5.1
	H14	125	18.1	115	16.7	9	32	75	10.9	50	7.2
	H18	165	23.9	150	21.8	5	44	90	13.0	60	8.7
3003	O	110	16.0	40	5.8	30	28	75	10.9	50	7.2
	H14	150	21.8	145	21.0	8	40	95	13.8	60	8.7
	H18	200	29.0	185	26.8	4	55	110	16.0	70	10.2
Alclad 3003	O	110	16.0	40	5.8	30	...	75	10.9	...	...
	H14	150	21.8	145	21.0	8	...	95	13.8	...	...
	H18	200	29.0	185	26.8	4	...	110	16.0	...	...
3004	O	180	26.1	70	10.2	20	45	110	16.0	95	13.8
	H34	240	34.8	200	29.0	9	63	125	18.1	105	15.2
	H38	285	41.3	250	36.3	5	77	145	21.0	110	16.0
	H19	295	42.8	285	41.3	2	...	...	...	...	...
Alclad 3004	O	180	26.1	70	10.2	20	...	110	16.0	...	...
	H34	240	34.8	200	29.0	9	...	125	18.1	...	...
	H38	285	41.3	250	36.3	5	...	145	21.0	...	...
	H19	295	42.8	285	41.3	2	...	...	...	...	...
3104	H19	290	42.1	260	37.7	4	...	...	...	...	...
3005	O	130	18.9	55	8.0	25	...	...	...	...	...
	H14	180	26.1	165	23.9	7	...	...	...	...	...
	H18	240	34.8	225	32.6	4	...	...	...	...	...
3105	O	115	16.7	55	8.0	24	...	85	12.3	...	...
	H25	180	26.1	160	23.2	8	...	105	15.2	...	...
	H18	215	31.2	195	28.3	3	...	115	16.7	...	...
5005	O	125	18.1	40	5.8	25	28	75	10.9	...	...
	H34	160	23.2	140	20.3	8	41	95	13.8	...	...
	H38	200	29.0	185	26.8	5	55	110	16.0	...	...
5042	H19	360	52.2	345	50.0	4.5	...	...	...	...	...
5050	O	145	21.0	55	8.0	24	36	105	15.2	85	12.3
	H34	190	27.6	165	23.9	8	53	125	18.1	90	13.0
	H38	220	31.9	200	29.0	6	63	140	20.3	95	13.8
5052	O	195	28.3	90	13.0	25	47	125	18.1	110	16.0
	H34	260	37.7	215	31.2	10	68	145	21.0	125	18.1
	H38	290	42.1	255	37.0	7	77	165	23.9	140	20.3
5252	O	180	26.1	85	12.3	23	46	115	16.7	...	...
	H25	235	34.1	170	24.7	11	68	145	21.0	...	...
	H28	285	41.3	240	34.8	5	75	160	23.2	...	...

(continued)

Table 4. (Continued)

Alloy	Temper	Tensile ultimate strength MPa	Tensile ultimate strength ksi	Tensile yield strength(a) MPa	Tensile yield strength(a) ksi	Elongation in 50 mm (2 in.), %	Hardness(b), BHN	Shear strength MPa	Shear strength ksi	Fatigue limit(c) MPa	Fatigue limit(c) ksi
5154	O	240	34.8	115	16.7	27	58	150	21.8	115	16.7
	H34	290	42.1	230	33.4	13	73	165	23.9	130	18.8
	H38	330	47.9	270	39.2	10	80	195	28.3	145	21.0
	H112	240	34.8	115	16.7	25	63			115	16.7
5454	O	250	36.3	115	16.7	22	62	160	23.2	...	...
	H34	305	44.2	240	34.8	10	81	180	26.1	...	...
	H111	260	37.7	180	26.1	14	70	160	23.2	...	...
	H112	250	36.3	125	18.1	18	62	160	23.2	...	...
5056	O	290	42.1	150	21.8	35	65	180	26.1	140	20.3
	H18	435	63.1	405	58.8	10	105	235	34.1	150	21.8
	H38	415	60.2	345	50.0	15	100	220	31.9	150	21.8
5456	O	310	45.0	160	23.2	24	...	...	...	...	...
	H112	310	45.0	165	23.9	22	...	...	...	...	...
	H116	350	50.8	255	37.0	16	90	205	29.7	...	...
5457	O	130	18.9	50	7.2	22	32	85	12.3	...	...
	H25	180	26.1	160	23.2	12	48	110	16.0	...	...
	H28	205	29.7	185	26.8	6	55	125	18.1	...	...
5657	O	110	16.0	40	5.8	25	28	75	10.9	...	...
	H25	160	23.2	140	20.3	12	40	95	13.8	...	...
	H28	195	28,3	165	23.9	7	50	105	15.2	...	...
5082	H19	395	57.3	370	53.7	4	...	...	...	...	...
5182	O	275	39.9	130	18.8	21	...	...	...	...	...
	H19	420	60.9	395	57.3	4	...	...	...	...	...
5083	O	290	42.1	145	21.0	22	...	170	24.7	...	...
	H116	315	45.7	230	33.4	16	...	...	...	160	23.2
5086	O	260	37.7	115	16.7	22	...	160	23.2	...	...
	H34	325	47.1	255	37.0	10	...	185	26.8	...	...
	H112	270	39.2	130	18.9	14	...	...	...	...	...
	H116	290	42.1	205	29.7	12	...	...	...	...	...
7072	O	70	10.2	...	...	15	...	...	...	...	...
	H113	75	10.9	...	...	15	...	...	...	...	...
8001	O	110	16.0	40	5.8	30	...	...	...	...	...
	H18	200	29.0	185	26.8	4	...	...	...	...	...
8280	O	115	16.7	50	7.2	28	...	...	...	...	...
	H18	220	31.9	205	29.7	4	...	...	...	...	...

(a) Yield strength, 0.2% offset. (b) 500-kg (1102-lb) load, 10-mm (0.4-in.) ball, 30 s. (c) Based on 500 million cycles using an R.R. Moore-type rotating-beam machine.

nificance is 3003, while 3004 is the oldest commercial aluminum-manganese-magnesium alloy in use. Alloy 3003 (Ref 5) is one of the oldest wrought alloys, having been introduced in 1906; alloy 3004 made its appearance in 1929. The strength of 3003 is measurably higher than that of 1100 alloy, and 3004 is considerably stronger than 3003. Alloy 3003 is an example of a dispersion-hardened alloy, whereas 3004 combines the dispersion hardening of manganese with the solid solution hardening of magnesium. Typical properties are shown in Table 4 and nominal compositions in Table 1. Alloy 3003 is supplied in the H1 temper, and 3004 is supplied in the stabilized H3 temper for stability and improved forming qualities. Alloy 3004 is subject to age softening in the H1 temper, but 3003 remains unchanged. Alloy 3004 is remarkable for a consistently fine grain size and general freedom from critical grain growth. These two alloys have extremely good corrosion resistance combined with moderate strength and are used in many of the applications previously mentioned for pure aluminum and aluminum-magnesium alloys. The drawn and ironed beverage can accounts for the greatest use of 3004.

Several lower strength alloys added to the aluminum-manganese-magnesium group combine in part the characteristics of the older alloys. Thus, 3005 was introduced in 1953 and 3105 in 1960. These alloys offer desirable combinations of strength, formability, and corrosion resistance for application in building and specialty products.

Miscellaneous Alloys. In the non-heat treatable class, miscellaneous alloys span a rather broad range of composition and applications. One is 8001, an aluminum-nickel-iron alloy used in atomic energy applications; resistance to corrosive attack in water at high temperature and pressure is the desired characteristic. Its mechanical properties resemble those of 3003.

Some aluminum-iron-manganese and aluminum-iron-manganese-zinc alloys are produced as thin sheet and foil for applications such as fin stock. These alloys generally exhibit ultrafine grain size. The aluminum-tin-nickel-copper alloy 8280 is used for bearings. The anti-friction qualities of this alloy are imparted by the tin; the other additions contribute to its strength, which is slightly higher than that of 3003. Another bearing alloy, 8081, was introduced in 1965. This alloy, of Al-20% Sn-1% Cu, has bearing characteristics superior to other alloys for automotive use. The nominal compositions of these alloys are shown in Table 1 and strengths in Table 4.

A number of aluminum-silicon alloys have been used for welding electrodes for many years. The oldest and most widely used is 4043, which contains 5% silicon. Other 4XXX series alloys such as 4343, containing 7.5% silicon, and 4045, containing 10.5% silicon, are used as the brazing alloy component of brazing sheet. Brazing products are discussed in greater detail later in this chapter.

Several alloys of the 7XXX series are non-heat treatable. The most widely known is 7072, an Al-1% Zn alloy used as the anodic coating on the alclad version of alloys such as 2219, 3003, 3004, 6061, 7075, and 7178. Further discussion of alclad products appears later in this chapter in the section on wrought products. Alloy 7072 is also used as a fin stock when anodic protection of the heat exchanger tubes is required.

HEAT TREATABLE ALLOYS

Discovery of the original heat treatable alloy, an aluminum-copper magnesium-manganese composition, was reported in the literature in 1911 (Ref 6). Since that time, the 2XXX series has developed along the following lines.

Aluminum-Copper Wrought Alloys. The first aluminum-copper wrought alloy developed in North America was 2025, Al-4.5% Cu (Ref 7). This alloy contains deliberate additions of silicon and manganese, but they do not contribute as precipitation hardeners. Alloy 2025 is still used extensively for forged airplane propellers.

Alloy 2219, Al-6.3% Cu, introduced in 1954 (Ref 8), provides all the properties of 2025, combined with a much wider and higher range of strength, as well as good weldability, superior resistance to stress corrosion, and higher elevated-temperature properties. Although it was introduced originally for its outstanding elevated-temperature characteristics, its excellent weldability and weld strength prompted other applications, involving the use of both plate and forgings. Nominal compositions are given in Table 2, typical properties are given in Table 5, and elevated-temperature mechanical properties are given in Tables 6, 7, and 8.

With 2219, strain hardening of the solution heat treated products accelerates the response to artificial aging and produces higher tensile strengths. This type of work-artificial aging response is used for certain aluminum-copper-magnesium alloys (Ref 9), but had not been used commercially for aluminum-copper alloys before the development of 2219. This aging response of the alloy is exploited, so that artificially aged products produced by the recommended procedures have excellent resistance to stress corrosion under high tensile stresses in the critical short transverse direction. The development of 2219 is an excellent example of a persistent pattern: characteristics not critically required for its initial application (forged engine parts) were used in subsequent applications. Later uses were structural applications, involving forgings, plate, sheet, extrusion, and even rivets. Alloy 2219 is welded with filler alloy 2319.

Good cutting and chip characteristics are necessities for high-speed production of screw-machine parts. The aluminum-copper alloy 2011 contains additions of lead and bismuth to achieve good cutting characteristics and fine, easily broken chips, thereby meeting the requirements of a free-machining alloy. It was introduced in 1934 and is presently the basic aluminum screw-machine alloy and the reference standard for machinability of aluminum alloys. In applications involving corrosive atmospheres, 2011-T8 stock should be used to obtain a higher resistance to intergranular and stress corrosion than provided by the T3 temper. Nominal compositions and typical properties of alloy 2011 are shown in Tables 2 and 5.

Aluminum-Copper-Magnesium Alloys. The first alloy of this type, introduced about 70 years ago by Wilm (Ref 6), is now designated 2017. It is an alloy of Al-4% Cu-0.6% Mg that is now in rather limited use, chiefly for rivets. After the heat treatment of aluminum alloys was established as another means of increasing strength, research efforts extended the principles to other alloy systems. Few heat treatable alloys available in the 1920's to 1930's remain in use today, but the results of

Table 5. Typical Mechanical Properties of Some Heat Treatable Aluminum Alloys

Alloy	Temper	Tensile ultimate strength, MPa	Tensile ultimate strength, ksi	Tensile yield strength(a), MPa	Tensile yield strength(a), ksi	Elongation in 50 mm (2 in.), %	Hardness(b), BHN	Shear strength, MPa	Shear strength, ksi	Fatigue limit(c), MPa	Fatigue limit(c), ksi
2011	T3	380	55.1	295	42.8	15	95	220	31.9	125	18.1
	T8	405	58.8	310	45.0	12	100	240	34.8	125	18.1
2014	O	185	26.8	95	13.8	18	45	125	18.1	90	13.1
	T4, T451	425	62.4	290	42.1	20	105	260	37.7	140	20.3
	T6, T651	485	70.1	415	60.2	13	135	290	42.1	125	18.1
Alclad 2014	O	170	24.7	70	10.2	21	...	125	18.1	...	...
	T3	435	63.1	275	39.9	20	...	255	37.0	...	...
	T4, T451	420	60.9	255	37.0	22	...	255	37.0	...	...
	T6, T651	470	68.2	415	60.2	10	...	285	41.3	...	...
2017	O	180	26.1	70	10.2	22	45	125	18.1	90	13.1
	T4, T451	425	62.4	275	39.9	22	105	260	37.7	125	18.1
2117	T4	300	43.5	165	23.9	27	70	195	28.2	95	13.8
2218	T72	330	47.9	255	37.0	11	95	205	29.7	...	...
2618	T61	435	63.1	370	53.7	10	...	...	...	130	18.8
2219	O	170	24.7	70	10.2	18	...	...	...	...	...
	T42	360	52.2	185	26.8	20	...	...	...	...	...
	T31, T351	360	52.2	250	36.3	17	100	230	33.4	...	...
	T37	395	57.3	315	45.7	11	117	255	37.0	...	...
	T62	415	60.2	290	42.1	10	115	255	37.0	105	15.2
	T81, T851	455	66.0	350	50.8	10	130	285	41.3	105	15.2
	T87	475	68.9	395	57.3	10	130	280	40.6	105	15.2
2024	O	185	26.8	75	10.9	20	47	125	18.1	90	13.1
	T3	485	70.1	345	50.0	18	120	280	40.6	140	20.3
	T361	495	71.8	395	57.3	13	130	290	42.1	125	18.1
	T4, T351	470	68.2	325	47.1	20	120	285	41.3	140	20.3
	T81,T851	485	70.1	450	65.3	6	128	295	42.8	125	18.1
	T861	515	74.7	490	71.1	6	135	310	45.0	125	18.1
Alclad 2024	O	180	26.1	76	11.0	20	...	125	18.1	...	...
	T3	450	65.8	310	45.0	18	...	275	39.9	...	...
	T361	460	66.7	365	52.9	11	...	285	41.3	...	...
	T4, T351	440	63.8	290	42.1	19	...	275	39.9	...	...
	T8, T851	450	65.3	415	60.2	6	...	275	39.9	...	...
	T861	485	70.0	455	66.0	6	...	290	42.1	...	...
2124	T351	470	68.2	325	47.1	20	120	285	41.3	140	20.3
2025	T6	400	58.0	255	37.0	19	110	240	34.8	125	18.1

(continued)

Table 5. (Continued)

Alloy	Temper	Tensile ultimate strength MPa	Tensile ultimate strength ksi	Tensile yield strength(a) MPa	Tensile yield strength(a) ksi	Elongation in 50 mm (2 in.), %	Hardness(b), BHN	Shear strength MPa	Shear strength ksi	Fatigue limit(c) MPa	Fatigue limit(c) ksi
2036	T4	340	49.3	195	28.3	24	...	...	...	...	...
4032	T6	380	55.1	315	45.7	9	120	260	37.7	110	16.0
6101	T6	220	31.9	195	28.3	15	71	140	20.3	...	...
6201	T81	330	47.9			6(d)				105	15.2
6009	T4	230	33.4	125	18.1	25	62	150	21.8	...	...
6010	T4	290	42.1	170	24.7	24	78	195	28.3	...	...
6151	T6	330	47.9	295	42.8	17	100	220	31.9	85	12.3
6351	T6,T651	340	49.3	295	42.8	13	95	200	29.0	90	13.1
6951	O	110	16.0	40	5.8	30	28	75	10.9	...	...
	T6	270	39.2	230	33.4	13	82	180	26.1	...	...
6053	O	110	16.0	55	8.0	35	26	75	10.9	55	8.0
	T6	255	37.0	220	31.9	13	80	160	23.2	90	13.1
6063	O	90	13.1	50	7.3	...	25	70	10.2	55	8.0
	T1	150	21.8	90	13.1	20	42	95	13.8	70	10.2
	T4	170	24.7	90	13.1	22	...	110	16.0	...	...
	T5	185	26.8	145	21.0	12	60	115	16.7	70	10.2
	T6	240	34.8	215	31.2	12	73	150	21.8	70	10.2
	T83	255	37.0	240	34.8	9	82	150	21.8	...	...
	T831	205	29.7	185	26.8	10	70	125	18.1	...	...
	T832	290	42.1	270	39.2	12	95	185	26.8	...	...
6463	O	90	13.1	50	7.3		25	70	10.2	55	8.0
	T1	150	21.8	90	13.1	20	42	95	13.8	70	10.2
	T5	185	26.8	145	21.0	12	60	115	16.7	70	10.2
	T6	240	34.8	215	31.2	12	74	150	21.8	70	10.2
6061	O	125	18.1	55	8.0	25	30	80	11.6	60	8.7
	T4,T451	240	34.8	145	21.0	22	65	165	23.9	90	13.1
	T6, T651	310	45.0	275	39.9	12	95	205	29.7	95	13.8
	T91	405	58.8	395	57.3	12	...	230	33.4	95	13.8
	T913	460	66.7	455	66.0	10	...	240	34.8	...	...
Alclad 6061	O	115	16.7	50	7.2	25	...	75	10.9	...	...
	T4, T451	230	33.4	130	18.8	22	...	150	21.8	...	...
	T6,T651	290	42.1	255	37.0	12	...	185	26.8	...	...
6262	T9	400	58.0	380	55.1	10	120	240	34.8	90	13.1

(continued)

(a) Yield strength, 0.2% offset. (b) 500-kg (1102-lb) load, 10-mm (0.4-in.) ball. (c) Based on 500 million cycles using an R.R. Moore-type rotating-beam machine. (d) Elongation, % in 250 mm (10 in.).

Table 5. Typical Mechanical Properties of Some Heat Treatable Aluminum Alloys (Continued)

Alloy	Temper	Tensile ultimate strength MPa	Tensile ultimate strength ksi	Tensile yield strength(a) MPa	Tensile yield strength(a) ksi	Elongation in 50 mm (2 in.), %	Hardness(b), BHN	Shear strength MPa	Shear strength ksi	Fatigue limit(c) MPa	Fatigue limit(c) ksi
6066	O	150	21.8	85	12.3	18	43	95	13.8	...	...
	T4, T451	360	52.2	205	29.7	18	90	200	29.0	...	...
	T6, T651	395	57.3	360	52.5	12	120	235	34.1	110	16.0
6070	O	145	21.0	70	10.2	20	35	95	13.8	60	8.7
	T6	380	55.1	350	50.8	10	120	235	34.1	95	13.8
7001	O	255	37.0	150	21.8	14	60	...	...	...	...
	T6, T651	675	97.9	625	90.7	9	160	...	...	150	21.8
	T75	580	84.1	495	71.8	12	...	...	...	...	...
7005	O	195	28.3	80	11.6	20	...	...	...	...	...
	W	345	50.0	205	29.7	20	...	...	...	...	...
	T6	350	50.8	290	42.1	13		215	31.2	150	21.8
7016	T5	360	52.2	315	45.7	15	96	...	...	...	...
7021	T62	420	60.9	380	55.1	13	...	...	...	138	20.0
7029	T5	430	62.4	380	55.1	15	...	...	...	...	...
7049	T73	540	78.3	475	68.9	10	146	...	...	...	...
7050	T74, T7452	510	74.0	450	65.3	13	142	...	...	...	...
7075	O	230	33.4	105	15.2	17	60	150	21.8	115	16.7
7075	T6, T651	570	82.7	505	73.3	11	150	330	47.9	160	23.2
	T73, T735X	505	73.3	435	63.1	13	...			150	21.8
Alclad 7075	O	220	31.9	95	13.8	17	...	150	21.8	...	...
	T6, T651	525	76.2	460	66.7	11	...	315	45.7	...	...
7175	T736, T74SX	550	79.8	485	70.4	12	145	...	...	...	...
	T7351	505	73.3	435	63.1	13	...	...	...	...	...
7475	T7351	505	73.3	435	63.1	14	...	...	...	...	...
7076	T61	510	74.0	470	68.2	14	150	...	...	...	...
7178	O	230	33.4	105	15.2	15	60	150	21.8	...	...
	T6, T651	605	87.8	540	78.3	10	160	360	52.2	150	21.8
	T76, T7651	570	82.7	505	73.2	9	...	...	...	...	...
Alclad 7178	O	220	31.9	95	13.8	16	...	150	21.8	...	...
	T6, T651	560	81.2	490	71.1	10	...	340	49.3	...	...

(a) Yield strength, 0.2% offset. (b) 500-kg (1102-lb) load, 10-mm (0.4-in.) ball. (c) Based on 500 million cycles using an R.R. Moore-type rotating-beam machine. (d) Elongation, % in 250 mm (10 in.).

developments during this period are reflected in 2014 and 2024. These are now the most widely used of the aluminum-copper-magnesium class. Also of note are the 2X18 series of high-temperature alloys, and 2117, a low-copper modification of 2017, also used for rivets.

The development of 2014 alloy used the characteristics of silicon to make an aluminum-copper-magnesium alloy that is more responsive to artificial aging than 2017. This response to artificial aging provides a desirable high level of strengths unobtainable in naturally aged 2017 or 2014. Although 2014 was used initially as a high-strength forging alloy to replace 2025, it is now available in a range of wrought products and is widely used in structural applications. This alloy also is available as alclad sheet and plate with a coating of aluminum-magnesium-silicon alloy.

Alloy 2024 was introduced in the 1930's as a higher strength, naturally aging alloy to replace 2017 in the aircraft field. It is one of the outstanding structural alloys in the industry and is available in virtually all wrought product forms. The hardening phase in 2024 is a complex phase of aluminum, copper, and magnesium, rather than the copper-aluminum phase of 2017. Alloys 2124 and 2224 are high-purity modifications of 2024. They contain reduced iron and silicon levels to avoid a coarse insoluble phase and to increase toughness.

The response to artificial aging of several 2XXX series alloys, notably 2X24 and 2219, is accelerated by strain hardening the solution heat treated material in excess of levels normally required for flattening, straightening, and stress relieving (Ref 10). The strength of such material after artificial aging reflects the degree of strain hardening that is induced, plus the strength increase associated with artificial aging. The resistance of these alloys to stress corrosion for tempers using cold work is so markedly improved by artificial aging (Ref 11) that their use generally is limited to the T6X and T8X tempers. Alloy 2036 is a medium-strength alloy developed for automobile body applications.

Aluminum-Magnesium-Silicon Alloys. The 6XXX alloys contain additions of magnesium and silicon, which in the heat treated and aged condition precipitate Mg_2Si (Ref 12) as a hardening phase. These elements may be present in the amounts to nominally combine as Mg_2Si, or silicon in excess of that required for Mg_2Si may be used. The excess silicon provides an appreciable increase in strength over that obtained from a specific quantity of Mg_2Si, but tends to slightly lower corrosion resistance. Many alloys in this class contain either manganese or chromium for increased strength and control of grain size. Copper also is a beneficial addition for increased strength.

The pioneer of these alloys in the United States was introduced in about 1920 and used silicon in excess of the Mg_2Si ratio. A modification presently used for forgings, 6151, contains an addition of chromium to control grain size in products requiring heat treatment after forming, or working operations producing various amounts of strain hardening. A somewhat similar alloy, 6351, contains manganese rather than chromium.

The initial balanced Mg_2Si alloy, developed in the 1930's, was 6053, containing 2% Mg_2Si and 0.25% chromium. This was followed by 6061, a balanced alloy composed of 1.5% Mg_2Si, 0.25% copper, and 0.25%

Table 6. Typical Mechanical Properties of Heat Treatable Alloys at Various Temperatures

Temperature °C	Temperature °F	Time at temperature, h	2014-T6 Tensile ultimate strength MPa	2014-T6 Tensile ultimate strength ksi	2014-T6 Tensile yield strength MPa	2014-T6 Tensile yield strength ksi	Elongation in 4D, %
−260	−436	...	710	102.9	560	81.2	12
−200	−328	...	580	84.1	495	71.8	14
−80	−112	...	510	73.9	450	65.3	13
−28	−18	...	495	71.8	430	62.4	13
24	75	...	485	70.3	415	60.2	13
100	212	0.5	435	63.1	395	57.3	14
		10	435	63.1	395	57.3	14
		100	435	63.1	400	58.0	14
		1000	440	63.8	405	58.7	15
		10,000	440	63.8	400	58.0	15
150	300	0.5	380	55.1	350	50.8	15
		10	385	55.8	350	50.8	16
		100	385	55.8	350	50.8	16
		1000	350	50.8	315	45.7	17
		10,000	275	39.9	240	34.8	20
175	350	0.5	350	50.8	325	47.1	14
		10	345	50.0	315	45.7	17
		100	310	44.9	275	39.9	18
		1000	235	34.1	205	29.7	20
		10,000	170	24.7	140	20.3	28
200	390	0.5	310	44.9	285	41.3	14
		10	285	41.3	255	36.9	18
		100	205	29.7	185	26.8	22
		1000	145	21.0	125	18.1	29
		10,000	110	15.9	90	13.1	38
260	500	0.5	170	24.7	160	23.2	18
		10	110	15.9	105	15.2	27
		100	90	13.1	75	10.9	34
		1000	75	10.9	65	9.4	43
		10,000	65	9.4	50	7.3	52
315	600	0.5	75	10.9	65	9.4	28
		10	60	8.7	50	7.3	39
		100	50	7.3	40	5.8	48
		1000	50	7.3	40	5.8	55
		10,000	45	6.5	35	5.1	65
370	700	0.5	40	5.8	35	5.1	50
		10	35	5.1	30	4.4	56
		100	35	5.1	26	3.8	62
		1000	30	4.4	26	3.8	68
		10,000	30	4.4	24	3.5	72

chromium. This intermediate-strength, general-purpose structural alloy rapidly replaced the older aluminum-silicon-magnesium alloys and is among the most important alloys ever developed (Ref 13). Strengths are shown in Table 5 and nominal compositions in Table 2.

The highest strength levels in this class of alloys are developed by 6066 and 6070. These use silicon in excess of that required to convert the magnesium present to Mg_2Si, as well as additions of copper, manganese, and chromium in various combinations to increase strength. All have strength in excess of 6061 and are used for structural applications, but

Table 6. (Continued)

2618-T61					2024-T81				
Tensile ultimate strength		Tensile yield strength		Elongation in 4D, %	Tensile ultimate strength		Tensile yield strength		Elongation in 4D, %
MPa	ksi	MPa	ksi		MPa	ksi	MPa	ksi	
...	...	...	...	...	...	...	...	...	...
530	76.9	420	60.9	12	585	84.8	540	78.3	8
460	66.7	380	55.1	11	510	73.9	475	68.9	7
440	63.8	370	53.7	10	505	73.2	470	68.2	7
440	63.8	370	53.7	10	485	70.3	450	65.3	7
435	63.1	370	53.7	10	455	65.9	430	62.4	8
435	63.1	370	53.7	10	455	65.9	430	62.4	8
435	63.1	370	53.7	10	455	65.9	430	62.4	8
435	63.1	370	53.7	10	455	65.9	430	62.4	8
430	62.4	370	53.7	10	455	65.9	430	62.4	8
400	58.0	360	52.2	14	420	60.9	400	58.0	9
400	58.0	360	52.2	14	415	60.2	395	57.3	9
395	57.3	360	52.2	14	415	60.2	395	57.3	10
380	55.1	345	50.0	14	405	58.7	380	55.1	10
345	50.0	305	44.2	14	380	55.1	340	49.3	11
365	52.9	340	49.3	15	385	55.8	360	52.2	10
360	52.2	330	47.9	15	380	55.1	350	50.8	10
345	50.0	310	44.9	15	365	52.9	330	47.9	11
315	45.7	285	41.3	16	330	47.9	305	44.2	13
285	41.3	240	34.8	17	305	44.2	255	36.9	15
330	47.9	305	44.2	16	350	50.8	330	47.9	11
310	44.9	285	41.3	17	340	49.3	310	44.9	11
290	42.1	255	36.9	18	305	44.2	270	39.2	13
255	36.9	215	31.2	20	260	37.7	220	31.9	15
220	31.9	180	26.1	24	185	26.8	140	20.3	23
235	34.1	215	31.2	19	250	36.3	220	31.9	14
205	29.7	180	26.1	22	215	31.2	185	26.8	16
180	26.1	145	21.0	27	150	21.8	110	15.9	25
130	18.9	90	13.1	35	105	15.2	75	10.9	40
90	13.1	60	8.7	50	80	11.6	60	8.7	55
140	20.3	125	18.1	26	140	20.3	115	16.7	20
110	15.9	85	12.3	40	80	11.6	70	10.2	45
85	12.3	55	7.9	55	70	10.2	55	7.9	55
60	8.7	40	5.8	65	60	8.7	45	6.5	65
50	7.3	30	4.4	80	50	7.3	40	5.8	75
60	8.7	50	7.3	45	60	8.7	45	6.5	55
50	7.3	35	5.1	80	50	7.3	35	5.1	70
40	5.8	30	4.4	95	40	5.8	30	4.4	85
35	5.1	24	3.5	110	40	5.8	25	3.6	95
35	5.1	24	3.5	120	35	5.1	25	3.6	100

have reduced elongation and toughness. Compositions and properties are given in Tables 2 and 5, respectively.

Because ease of extrusion is a prime requirement for many shapes, 6063 was introduced for the applications where mechanical strength requirements were less stringent. To develop the moderate strengths required for applications in this field, this alloy can be quenched adequately from the relatively high temperatures used during extrusion as it comes from the press. Thus, the expense of a separate solution heat treating operation is eliminated. Finishing qualities of 6063 also are distinctly su-

Table 7. Typical Mechanical Properties of Heat Treatable Alloys at Various Temperatures

Temperature °C	Temperature °F	Time at temperature, h	4032-T6 Tensile ultimate strength MPa	4032-T6 Tensile ultimate strength ksi	4032-T6 Tensile yield strength MPa	4032-T6 Tensile yield strength ksi	4032-T6 Elongation in 4D, %	7075-T6 Tensile ultimate strength MPa	7075-T6 Tensile ultimate strength ksi	7075-T6 Tensile yield strength MPa	7075-T6 Tensile yield strength ksi	7075-T6 Elongation in 4D, %
−260	−436	... ...	...	...	...	...	...	800	116.0	675	97.9	8
−200	−328	... ...	455	65.9	330	47.9	11	705	102.3	635	92.1	9
−80	−112	... ...	400	58.0	315	45.7	10	620	89.9	545	79.0	11
−28	−18	... ...	385	55.8	315	45.7	9	595	86.3	515	74.7	11
24	75	... ...	380	55.1	315	45.7	9	570	82.7	505	73.2	11
100	212	.....0.5	345	50.0	305	44.2	9	515	74.7	475	68.9	15
		10	345	50.0	305	44.2	9	525	76.1	485	70.3	14
		100	345	50.0	305	44.2	9	530	76.9	490	71.1	14
		1000	350	50.8	305	44.2	9	525	76.1	485	70.3	14
		10,000	350	50.8	310	44.9	9	485	70.3	450	65.3	14
150	300	.....0.5	315	45.7	285	41.3	9	440	63.8	415	60.2	21
		10	325	47.1	290	42.1	9	440	63.8	415	60.2	19
		100	325	47.1	290	42.1	9	385	55.8	365	52.9	20
		1000	305	44.2	275	39.9	9	285	41.3	260	37.7	23
		10,000	255	36.9	230	33.4	9	215	23.9	185	26.8	30
175	350	.....0.5	295	42.8	260	37.7	9	370	53.7	345	50.0	20
		10	295	42.8	270	39.2	9	315	45.7	295	42.8	23
		100	275	39.9	250	36.3	10	240	34.8	220	31.9	26
		1000	235	34.1	185	26.8	12	165	23.9	150	21.8	35
		10,000	140	20.3	90	13.1	16	140	20.3	125	18.1	45
200	390	.....0.5	270	39.2	240	34.8	9	290	42.1	275	39.9	18
		10	250	36.3	220	31.9	10	205	29.7	195	28.3	27
		100	205	29.7	180	26.1	15	150	21.8	140	20.3	35
		1000	140	20.3	110	15.9	22	125	18.1	110	15.9	45
		10,000	90	13.1	60	8.7	30	110	15.9	90	13.1	55
230	445	.....0.5	220	31.9	200	29.0	10	...	...	...	...	...
		10	195	28.3	170	24.7	13	...	...	...	...	...
		100	140	20.3	115	16.7	21	...	...	...	...	...
		1000	90	13.1	70	10.2	35	...	...	...	...	...
		10,000	70	10.2	50	7.3	40	...	...	...	...	...
260	500	.....0.5	170	24.7	150	21.8	12	130	18.9	125	18.1	35
		10	140	20.3	125	18.1	18	95	13.8	90	13.1	45
		100	95	13.8	75	10.9	30	80	11.6	75	10.9	50
		1000	70	10.2	50	7.3	45	80	11.6	70	10.2	55
		10,000	55	7.9	40	5.8	50	75	10.9	60	8.7	65
315	600	.....0.5	90	13.1	70	10.2	26	70	10.2	55	7.9	60
		10	70	10.2	50	7.3	40	60	8.7	50	7.3	65
		100	50	7.3	35	5.1	55	60	8.7	50	7.3	70
		1000	40	5.8	26	3.8	65	55	7.9	45	6.5	70
		10,000	35	5.1	22	3.2	70	55	7.9	45	6.5	70
370	700	.....0.5	45	6.5	35	5.1	65	40	5.8	30	4.4	70
		10	35	5.1	24	3.5	80	40	5.8	30	4.4	70
		100	29	4.2	18	2.6	90	40	5.8	30	4.4	70
		1000	23	3.3	15	2.2	90	40	5.8	30	4.4	70
		10,000	23	3.3	14	2.0	90	40	5.8	30	4.4	70

perior to the older alloys. Many minor variations from the nominal 1% Mg_2Si contained in 6063 are used to achieve increased extrusion speed and better finishing characteristics. Strengths are shown in Table 5.

Table 8. Typical Mechanical Properties for 2219-T81 Alloy at Various Temperatures

Temperature °C	Temperature °F	Time at temperature, h	2219-T81 Tensile ultimate strength MPa	2219-T81 Tensile ultimate strength ksi	2219-T81 Tensile yield strength MPa	2219-T81 Tensile yield strength ksi	Elongation in 4D, %
−260	−436	...	685	99.4	470	68.2	15
−200	−328	...	560	81.2	435	63.1	13
−80	−112	...	490	71.1	375	54.4	10
−28	−18	...	475	68.9	360	52.2	10
24	75	...	455	65.9	345	50.0	10
100	212	0.5	415	60.2	325	47.1	13
		10	415	60.2	325	47.1	13
		100	415	60.2	325	47.1	13
		1000	415	60.2	325	47.1	13
		10,000	415	60.2	325	47.1	13
150	300	0.5	375	54.4	305	42.2	15
		10	375	54.4	305	42.2	15
		100	375	54.4	305	42.2	15
		1000	360	52.2	295	42.8	15
		10,000	340	49.3	275	39.9	15
200	390	0.5	295	42.8	250	36.3	16
		10	275	39.9	235	34.1	16
		100	260	37.7	220	31.9	16
		1000	250	36.3	205	29.7	16
		10,000	250	36.3	200	29.0	16
230	445	0.5	240	34.8	205	29.7	16
		10	235	34.1	195	28.3	16
		100	230	33.4	185	26.8	16
		1000	220	31.9	185	26.8	16
		10,000	220	31.9	180	26.1	16
260	500	0.5	200	29.0	170	24.7	16
		10	200	29.0	165	23.9	16
		100	200	29.0	165	23.9	16
		1000	200	29.0	165	23.9	16
		10,000	200	29.0	165	23.9	16
290	555	0.5	170	24.7	150	21.8	16
		10	165	23.9	145	21.0	16
		100	165	23.9	140	20.3	16
		1000	160	23.2	130	18.9	16
		10,000	115	16.7	75	10.9	19
315	600	0.5	140	20.3	125	18.1	18
		10	130	18.9	115	16.7	18
		100	125	18.1	105	15.2	18
		1000	95	13.8	85	12.3	23
		10,000	45	6.5	40	5.8	55

Integral-color, hard coat anodic finishes for decorative applications are provided by various alloys of the 6XXX series. Finishes from gold to black and in various shades of gray are obtained by varying composition, fabricating practice, and anodizing conditions. Improved brightness can result from lower impurity content, particularly iron.

Free-machining alloys have been developed in the heat treatable aluminum-magnesium-silicon alloy system. The good machining characteristics are attributable to the presence of lead and bismuth, which

produce the desirable fine chips for optimum screw-machine operations. Alloy 6262 is essentially 6061 with additions of 0.50% each of lead and bismuth. Properties in the T6 temper are similar to those of 6061; a desired higher level of strength is achieved by cold working the T6 temper to produce the T9 temper. Alloy 6262-T9 screw-machine rod has higher strength and machinability that is somewhat lower than that of 2011-T3. Its resistance to stress-corrosion cracking is far superior to that of 2011-T3 and considerably superior to artificially aged 2011-T6 and T8—very important for highly stressed fittings. Alloys 6009 and 6010 have recently been introduced for automotive body sheet use. Further discussion on alloys for this end use can be found later in this chapter.

Aluminum-Zinc-Magnesium and Aluminum-Zinc-Magnesium-Copper Alloy Systems. High-strength aircraft and medium-strength, general-purpose alloys have 7XXX alloy designations. The highest room temperature strengths attained in wrought aluminum alloy products are developed by aluminum-zinc-magnesium-copper alloys. These alloys were the subject of extensive investigation for many years (Ref 14). Despite attractive tensile properties and good fabricating characteristics, originally they were not commercial because of unsatisfactory resistance to stress-corrosion cracking.

Although 7076 was introduced in 1940 as a readily forgeable alloy for aircraft propellers, sheet products of this alloy system were not available until extensive research efforts led to the development of 7075, introduced in 1943 (Ref 15). Its success was associated with the beneficial effect of chromium, which imparted good resistance to stress-corrosion cracking of sheet. A higher strength modification, 7178, appeared in 1951. The highest strength aluminum alloy ever commercially available, 7001, was introduced in 1960. However, production difficulties, poor toughness, and low T73 strength have precluded its extensive use. Nominal compositions for these and other alloys are shown in Table 2, and typical properties are shown in Table 5.

More recently, 7X49 and 7X50 alloys, as well as higher purity versions of 7075, have attained commercial significance because of high strength, improved short transverse ductility, and lower quench sensitivity in heavy sections. When these aluminum-zinc-magnesium-copper alloys are overaged (artificially aged beyond peak strength) to T7X tempers, strengths are somewhat lower than T6 levels; but virtual immunity to stress corrosion cracking is achieved (Ref 16).

Alloys 7X49, 7X50, 7175, and 7475 in T6X and particularly T7X tempers, as well as 2124, 2419, and 2048 alloys in the T8X tempers, are endowed with a remarkable combination of properties. They have high strength, high resistance to stress-corrosion cracking, and when given special thermal and mechanical treatment, high resistance to unstable crack growth, a property commonly called fracture toughness (Ref 17). Special test methods for determination of plane strain (K_{IC}) or plane stress (K_C) fracture toughness are described in ASTM specifications (Ref 18).

Within the past few years, intermediate-strength and lower strength aluminum-zinc-magnesium alloys received much attention. These alloys contain reduced amounts of zinc and magnesium, with small additions of manganese, chromium, titanium, and zirconium. Copper is generally eliminated or limited to very low amounts. This control of composition

is reflected in complete solution of the soluble elements at much lower heat treating temperatures in contrast to the high-strength aircraft alloys. The optimum strength levels are achieved even after relatively slow quench rates. The low quench sensitivity favors these alloys for massive forgings and thick plate, or permits slower quenching of thinner parts, thus reducing distortion and residual stresses. Lowest quench sensitivity is obtained when only zirconium (no chromium or manganese) is added to control grain structure.

Alloy 7039 was developed for armor applications and 7005, particularly as extrusions, was developed for various ground transportation structural applications. Alloys 7016 and 7029 were introduced for bright finishing applications, particularly bumpers. They contain moderate copper levels (0.5 to 1.0%) and no recrystallization retardants. Care must be taken to avoid grain growth, and optimum processing is necessary to control stress corrosion.

Miscellaneous Alloys. The commercial heat treatable class of alloys includes a number of compositions that involve either a combination of two alloy systems, the addition of an element to develop properties for a specific use, or the addition of elements that change the aging characteristics of an alloy system. In the discussion of the 2XXX series aluminum-copper-magnesium alloys, reference was made to 2X18 alloys. Thus, 2218 is essentially an aluminum-copper-magnesium alloy containing nickel to improve performance at elevated temperatures. Alloy 2618, also for elevated-temperature applications, is an unusual combination of aluminum, copper, and magnesium with nickel and iron in balanced amounts. The properties of 2618 are not developed if the nickel and iron additions vary from the recommended range. Alloy 2218 is used for forgings, and 2618 is used for other product forms. Nominal compositions are given in Table 2, properties are given in Table 5, and elevated-temperature mechanical properties are given in Tables 6, 7, and 8. Another miscellaneous alloy, 4032, combines silicon, magnesium, copper, and nickel, providing an elevated-temperature alloy with a low coefficient of thermal expansion. For elevated-temperature mechanical properties, see Tables 6, 7, and 8.

APPLICATIONS OF WROUGHT ALLOYS

Some products, such as clad products and foil, include both heat treatable and non-heat treatable alloys. Other products, such as those used for rigid containers and those used for automotive applications, include more than one alloy series. For these reasons, such alloys are discussed in relation to their end use.

Aluminum Alloy Foil. An extremely important and widely used wrought product, aluminum alloy foil generally is produced commercially from non-heat treatable alloys. The alloys used include 1100, 1145, 1235, 3003, 5052, and 5056. The wide range of strengths provided is shown in Table 9. Note that the 125-mm (5-in.) gage length is used for elongation. Properties reflect the influence of composition, fabricating practices, and test procedures required for foil. Aluminum honeycomb core for aircraft generally is made of 3003-H19 or 5052-H19 foil, but alloy 2024 heat treated to the T81 temper is used when long service at elevated temperature is required.

Table 9. Typical Mechanical Properties of Aluminum Alloy Foil(a)

Alloy	Temper	Tensile ultimate strength MPa	Tensile ultimate strength ksi	Tensile yield strength (0.2% offset) MPa	Tensile yield strength (0.2% offset) ksi	Elongation in 125 mm (5 in.), %
Non-Heat Treatable Foil						
1145, 1235	O	75	10.9	30	4.4	2.4
	H19	165	23.9	145	21.0	2.5
1100	H19	205	29.7	165	23.9	3.0
3003	H19	250	36.3	220	31.9	3.5
5052	H19	330	47.9	325	47.1	4.0
5056	H191	450	65.3	435	63.1	3.5
Heat Treatable Foil						
2024	T81	450	65.3	415	60.2	2.0

(a) Properties of five non-heat treatable alloy foils were determined in the longitudinal direction. Properties of 2024 heat treated foil are for the long transverse direction.

Alclad Products. Aluminum products sometimes are coated on one or both surfaces with a metallurgically bonded, thin layer of pure aluminum or aluminum alloy. If the combination of core and cladding alloys is selected so that the cladding is anodic to the core, it is called alclad. The cladding of alclad products electrochemically protects the core at exposed edges and at abraded or corroded areas. When a corrosive solution is in contact with the product, current from the anodic cladding flows through the electrolyte to the cathodic core, and the cladding tends to dissolve preferentially, thus protecting the core. Sustained protection is dependent upon obtaining the optimum quantity of current (which is influenced by the potential difference between the cladding and core), the conductivity of the corroding medium, film formation, and polarization (Chapter 7 in this Volume).

The corrosion potentials of cladding and core alloys are important in selecting a coating that is sufficiently anodic to electrochemically protect the core. Copper in solid solution in aluminum is less anodic as copper content increases. Consequently, pure aluminum is anodic to aluminum-copper-magnesium alloys in the naturally aged T3X and T4X tempers by about 0.154 V and is used as the cladding for most alclad 2XXX products. Increasing zinc in solid solution increases the anodic potential of aluminum alloys while Mg_2Si and manganese have little effect. Alloy 7072, Al-1% Zn, has a more anodic potential than pure aluminum and is used as the cladding for alclad 3003, 5052, 6061, and 7075, as well as others.

The most widely used alclad products are sheet and plate, although wire, tube, and other forms are also produced. The most generally accepted method of fabricating alclad sheet and plate consists of hot rolling to pressure weld the cladding slabs to a scalped core ingot. In fabricating alclad products, the temperature and time of thermal treatments should be minimized to avoid extensive diffusion of soluble elements from the core. This is particularly important in the 2XXX alloys, as diffusion of copper in the cladding makes it less anodic. It is less important in alloys

containing zinc and magnesium, because these elements make the cladding more anodic.

The percentage of cladding thickness is determined principally by the thickness of the finished part. Because the objective is to provide an adequate absolute thickness, the percentage for thicker parts need not be as great as the percentage for thinner parts. A listing of the most widely used alclad products is given in Table 10.

Clad Products. Clad products resemble alclad products in many respects, but they are distinguished by a cladding alloy that is not intentionally anodic to the core. Clad products are designed to provide improved surface appearance or other characteristics required for special applications. Brazing products are commercial examples of clad products in which a cladding alloy having a melting point appreciably lower than the core is used for subsequent joining of several parts into an assembly. Non-heat treatable alloy 3003 or the heat treatable Al-Mg_2Si alloy 6951 are widely used as core alloys in producing brazing sheet, and the aluminum-silicon alloy 4343 is a cladding frequently used as the low-melting brazing material for flux brazing applications. Brazing sheet products for the fluxless vacuum brazing process have an aluminum-magnesium-silicon alloy, for example 4004 (or its modification 4104 that contains about 0.1% bismuth to improve brazeability) as the cladding material. The core alloy is either 6951 or a non-heat treatable alloy from the 3XXX series.

Automotive Products. The automotive industry uses wrought aluminum for trim, bumpers, body panels, and various interior parts. Alloys for trim applications are of the aluminum-magnesium type as mentioned previously in this chapter. A variety of 7XXX series alloys has been developed for bumpers; alloy 7029 and 7016 are designed for bright anodized face bars and alloys 7129, 7021, and 7146 provide characteristics desired for chrome-plated, painted, and clear-coated face bars. Alloy 7021 was also developed for bumper reinforcements. Body panels have been produced primarily from 2036 and 5182 alloys. In recent years, alloys 6009 and 6010 were developed specifically for the body panel application. Alloys used for body panels also are used for various interior parts as are general-purpose alloys such as 3004, 5052, 6061, and 6063. For additional details on this subject, see Ref 19.

Aircraft Alloys. The need for low weight in airframes has led to the development of very high-strength aluminum alloys for use as plate, sheet, and extrusions. Alloys 2024, and especially 7075, have been the work-

Table 10. Commercial Alclad Sheet and Plate

Designation	Core	Cladding	Sides clad	Cladding thickness range,%
Alclad 2014	2014	6003	Both	2.5–10
Alclad 2024	2024	1230	Both	1.5–5
Alclad 2219	2219	7072	Both	2.5–10
Alclad 3003	3003	7072	One or both	5
Alclad 3004	3004	7072	One or both	5
Alclad 6061	6061	7072	One or both	5
Alclad 7075	7075	7072	Both	1.5–4.0
Alclad 7178	7178	7072	Both	1.5–4.0

horses of the industry for many years. Higher toughness requirements have been met through high-purity modification of alloys 2124, 2224, 7175, 7475, and 7050 (Ref 20). Additionally, 2219 is used for good weldability and high-temperature strength and is designated 2419 for higher toughness. Development of aluminum-magnesium-lithium alloys offers a real potential for high-strength alloys with lower density and higher modulus.

Rigid Container Sheet. Aluminum rigid container sheet (RCS) is used mainly for container ends or container bodies. The ends for beverage cans are made of 5182 alloy and usually have tabs made from 5042 or 5082 alloy. Alloy 5182, containing 4.5% magnesium and 0.35% manganese, has very high strength and sufficient formability to permit making the integral rivet in the easy open end.

The bodies of drawn and ironed beverage cans are fabricated of 3004 or 3104 alloy, which contains 1.25% or slightly less manganese and 1% magnesium. These alloys provide the optimum strength and forming characteristics needed to manufacture the can body and to contain the beverage at the required pressure. Alloy 5352 is used primarily for ends and drawn bodies that in turn are used for packaging meats, pudding, and fruits.

Bright Finishing Alloys. A number of alloys are produced especially for surface finishing by bright anodizing. Second-phase particles in the size range comparable to the wavelengths of visible light can be used to develop varying shades and colors in anodized products. The common bright finishing alloys are 1100, 3002, 5252, 5657, 6463, 7016, and 7029. Other alloys such as 3003, while not produced specifically for bright finishing, are capable of achieving acceptable brightness. Virtually all alloys can be chemically brightened and protected by clear organic topcoats.

Special Surface Finish Products. Selection of an alloy for special surface finish generally is directed toward achieving unusual finishing characteristics. An outstanding example is aluminum-silicon alloys. Upon anodizing, colors ranging from gray to black can be developed for architectural and other applications. Gold colors are developed in the same way from aluminum-chromium alloys.

Composites of aluminum with other metals have appeared frequently as the result of efforts to combine advantages of aluminum with those of other metals. Certain combinations of aluminum with zinc, as well as with copper, are produced in limited quantities, but continued production has not been sustained. The aluminum-zinc combination is of potential value in joining operations and the aluminum-copper combination has similar value in the electrical field.

Combinations of aluminum with ferrous materials are produced in limited amounts by rolling processes, and by explosive bonding, but generally aluminum coatings on ferrous products are produced by dipping in molten aluminum. Wire coated with aluminum powder by a rolling process is sold in substantial quantities. A combination of an aluminum alloy with stainless steel has developed into a commercial product. This stainless steel-clad aluminum in sheet form is used primarily for cooking utensils, providing the desirable characteristics of both components. Plate has considerable potential in the cryogenic field for connections between aluminum and stainless steel components of tanks and other equipment.

Commercial production was not attained until 1961, when an improved product was developed. Other metals and alloys such as nickel, Monel, and titanium can be combined with aluminum by rolling processes, but commercial production and use has not been attained.

EFFECT OF DIRECTIONALITY ON PROPERTIES

The typical mechanical properties listed in the tables in this chapter reflect the influence of composition; consequently, comparisons among alloys are reasonably direct and significant in basic tempers. The effects of strain hardening and of heat treatment are evident. These typical properties are replaced by specific minimum values for procurement and design purposes. In designing aluminum parts or structures, careful consideration must be given to the alloy and product forms of the alloy required. After these are determined, the specified minimum properties should be ascertained from material specifications or from the producers. These values are governed by the section thickness or the cross-sectional area of the wrought product of the alloy selected and, of more importance, by the direction in which the test was made.

Directionality generally is not critical in sheet and thin plate products, but it assumes importance as the section thickness increases in plate, extrusions, and forgings. In the thicker products, directionality not only influences mechanical properties, but also other characteristics such as resistance to stress-corrosion cracking. The directional effects are related to the design of the section or to the direction of working (the grain or fragment flow). The directional effects are generally measured in planes or directions, as follows:

- *Longitudinal*: Parallel to major dimension or directions of working of section.
- *Long transverse*: 90° to direction of working and parallel to width of section
- *Short transverse*: 90° to direction of working and parallel to thickness or minimum dimension of section
- *Transverse*: 90° to direction of working in product having axial symmetry

Typically, tensile strengths are higher in the longitudinal direction than in the long transverse direction. For non-heat treatable alloys, properties are generally specified for the longitudinal direction. In these alloys, formability (related to strength) is often important, and the maximum strength is of interest. In the heat treatable alloys, strength is usually of greatest importance, and properties are generally specified in the long transverse direction. These guidelines are followed in the tables on mechanical properties in this chapter.

Figures 1 and 2 illustrate directional metallurgical structures and identify grain direction in flat rolled products and rolled rod of 7075-T6 alloy. As an example of the influence of directionality on mechanical properties, minimum values are cited in Table 11 for 7075-T6 hand forgings with a thickness of 50 to 80 mm (2 to 3 in.) and a maximum cross-sectional area of 165,000 mm (6496 in.).

Because the strengths in a specific product vary with the test direction, the design of a structure and the stresses involved must be related to these

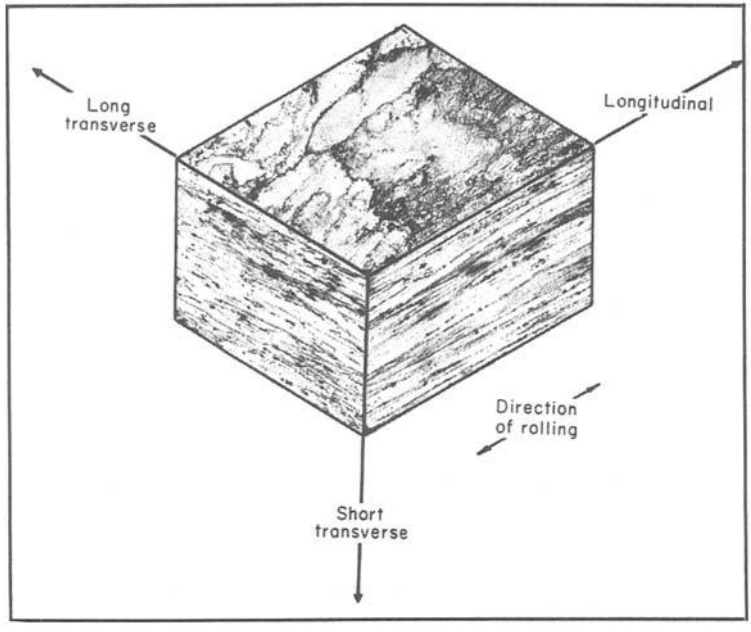

Fig. 1. Composite of micrographs of flat rolled 7075-T6 illustrating metallurgical structure directionality. (40×)

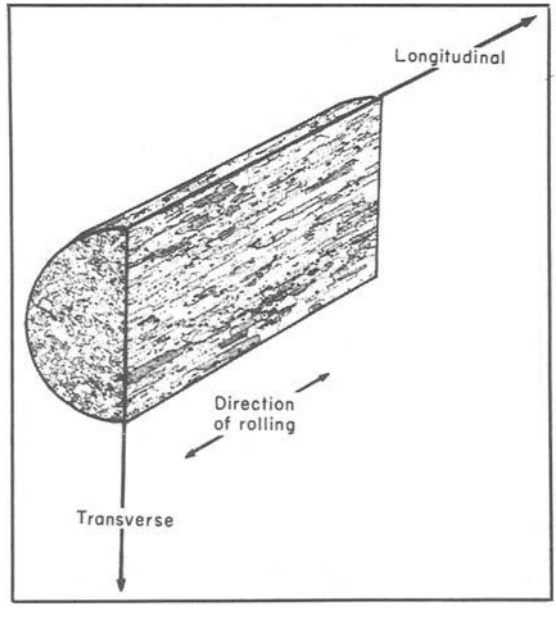

Fig. 2. Composite of micrographs of 7075-T6 rolled rod illustrating metallurgical structure directionality. (40×)

Table 11. Influence of Directionality on Mechanical Properties 7075-T6

Test direction	Tensile ultimate strength, MPa	Tensile ultimate strength, ksi	Tensile yield strength, MPa	Tensile yield strength, ksi	Elongation in 50 mm (2 in.), %
Longitudinal	505	73.2	420	60.9	9
Long transverse	490	71.1	405	58.8	4
Short transverse	475	68.9	400	58.0	3

directional effects to obtain the most efficient and reliable structure. Directional properties of one product as related to design and service may, for example, warrant the substitution of a die forging to replace a part machined from a hand forging, a thick plate, or an extrusion.

REFERENCES

1. "Aluminum Standards and Data", Aluminum Association, Washington, DC, March 1978 (Metric SI) or June 1982 (Customary)
2. "Registration Record of Aluminum Association Designations and Chemical Composition Limits for Wrought Aluminum Alloys", Aluminum Association, Washington, DC, August 1982
3. "Registration of International Alloy Designations and Chemical Composition Limits for Wrought Aluminum and Wrought Aluminum Alloys", Aluminum Association, Washington, DC, June 1980
4. E.H. Dix, Jr. and F. Keller, Equilibrium Relations to Aluminum-Magnesium Alloys of High Purity, *Transactions of AIME*, Vol 83, 1929, p 351-372
5. E.H. Dix, Jr. and W.D.Keith, Equilibrium Relations in Aluminum-Manganese Alloys of High Purity, *Proceedings of AIME*, Vol I (No. E27), 1927, p 315-335; E.H. Dix, Jr., W.L. Fink, and L.A. Willey, Equilibrium Relations in Aluminum-Manganese Alloys of High Purity, *Transactions of AIME*, Vol II (No. 104), 1933, p 335-352
6. A. Wilm, *Metallurgie*, Vol 8, 1911, p 225-227
7. E.H. Dix, Jr. and H.H. Richardson, Equilibrium Relations in Aluminum-Copper Alloys of High Purity, *Transactions of AIME*, Vol 73, 1926, p 560-580
8. J.A. Nock, Jr., M. Holt, and D.O. Sprowls, A New High-Strength Aluminum Alloy, *Metal Progress*, Vol 80 (No. 3), 1961, p 87-91
9. K.L. Meissner, The Influence of Cold Rolling on the Age Hardening of Duralumin, *Zeitschrift fuer Metallkunde*, Vol 24, 1932, p 88-89
10. P.P. Mozley, Elevated Temperature Aging of 24S Aluminum Alloy, *Journal of Aeronautical Science*, Vol 10 (No. 6), 1943, p 180-184
11. E.H. Dix, Jr., New Developments in High Strength Aluminum Alloy Products, *Transactions of ASM*, Vol. 35, 1945, p 130-155
12. E.H. Dix, Jr., F. Keller, and R.W. Graham, Equilibrium Relations in Aluminum-Magnesium-Silicide Alloy of High Purity, *Transactions of AIME*, Vol 93, 1931, p 404-420
13. J.A. Nock, Jr., Heat Treatment and Aging 61S Sheet, *Iron Age*, Vol 159, 1947, p 48-54
14. W. Sander and K.L. Meissner, Der Einfluso, der Verbindering Mg-Zn_2 und die Vergutbarkeit von Aluminum Legierungen, *Zeitschrift fuer Anorganische Chemie*, Vol 154, 1926, p 144-151
15. J.A. Nock, Jr., 75S Alcoa's New High Strength Aluminum Alloy, *Metals and Alloys*, Vol 20, 1944, p 922-925
16. M.O. Speidel, Stress Corrosion Cracking of Aluminum Alloys, *Transactions of AIME*, Vol 6A, 1975, p 631-651
17. J.T. Staley, Microstructure and Toughness of High Strength Aluminum Alloys, American Society for Testing and Materials, STP605, 1976, p 71-103
18. Specification E399-81. Test for Plane-Strain Fracture Toughness of Metallic Materials

Specification B645-78. Practice for Plane-Strain Fracture Toughness Testing of Aluminum Alloys
Specification B646-78. Practice for Fracture Toughness Testing of Aluminum Alloys
19. N.W. Smith and J.E. Grant, Reducing the Cost of Aluminum Body Panels, SAE Paper 800931, 1980
20. R.J. Bucci, Selecting Aluminum Alloys To Resist Failure By Fracture Mechanisms, *Engineering Fracture Mechanics*, Oxford: Pergamon Press Ltd., Vol 12, 1979, p 407-441

Aluminum Properties and Physical Metallurgy
John E. Hatch editor, p 379-397
DOI: 10.1361/appm1984p379

CHAPTER 10

ALUMINUM POWDER AND POWDER METALLURGY PRODUCTS*

Aluminum particulates, produced by a variety of techniques, have physical and metallurgical characteristics related to their method of manufacture and tailored to their end use. Also, aluminum particles can be consolidated into larger structural components by several powder metallurgy processes. This chapter describes aluminum particles and some applications, including two powder metallurgy technologies: pressed and sintered powder metallurgy (P/M) parts and high-strength wrought powder metallurgy products.

ALUMINUM PARTICLES

The Aluminum Association (AA) uses three broad classifications of powders that are also used in this chapter: granules, flake, and atomized. Granules are powders larger than about 74 μm (3 mils). Flake powders have one or two dimensions several hundred times larger than the third; atomized powders usually have all dimensions of the same order of magnitude. The commercially important particles and powders are listed below with brief notes concerning their method of production. A more quantitative description is given in Table 1. The name used for each category is descriptive and generic; the order is generally from large to small.

Shot is acicular or granulated particles that can vary from about 10 mm (0.4 in.) to less than 1 mm (0.04 in.). It is made by casting through screens or orifices, or by casting centrifugally. The particles are generally globular in shape, but can also be teardrop or cigar-shaped acicular. The coolant is usually air or water. Water can affect solidification rate and surface condition, causing thicker, hydrated oxide films. Shot is also produced with mechanical treatments that tend to flatten asperities and render the particles more equiaxed with mechanically worked, faceted surfaces. Composition can be in many grades or alloys.

Chopped wire is characterized by a generally cylindrical shape and is usually made from scrap wire cut to short lengths.

Machined chips, usually scrap from machining operations, are beneficated and often milled to give a desirable particulate shape and size. Composition reflects the source, which may be segregated by alloy or grade or uncontrolled; the structure is highly worked.

*This chapter was revised by a team comprised of W.S. Cebulak, Alcoa; P. Mathews, U.S. Bronze Powders, Inc.; J. Pickens, Martin Marietta, Inc.; O.R. Singleton, Reynolds Metals Co.; and W. Ullrich, Alcan Metal Powders Co. The original chapter was authored by J.P. Lyle, Alcoa Research Laboratories.

Table 1. Properties of Commercial Aluminum Particulates

Type of particulate	Shape(a)	Structure(b)	Size range(c) µm	Size range(c) mil	Mesh sizes on U.S. series	Specific surface(d), m^2/g
Air-atomized	Granular	C	1–1680	0.04–66	0–99% through 325(e)	0.1–1.0
Spherical atomized	Globular	C	1–841	0.04–33	85–100% through 325(g)	0.05–0.64
Shot	Globular	C or C-W	590–4700	23–185	0–100% through 12	0.1–0.2(h)
Acicular	Elongated	C or C-W	250–3360	10–132	Through 6 on 100	...
Granulated	Flattened globules	C	5100–17,400	201–685	Through 16 mm ($^5/_8$ in.) on 4	...
Foil granules	...	...	...	...	Through 12 on 140	0.1(j)
Flake	Flake	W	0.1–3.0 thick; 0.5–149 across	0.004–0.1 thick; 0.02–6 across	...	...
Balled foil granules	Balls	W	105–1410	4–56	...	...
Cut foil and flitter	Flat rectangles	W	115 wide, 105–1410 thick, and 150–8200 long	5 wide, 4–56 thick, and 6–323 long	...	...
Machined chips	Irregular, granular	C or W	...	...	...	0.2
Chopped wire	Cylindrical	W	25–10,000 diam	1–394 diam	...	...

(continued)

(a) Granular is approximately equidimensional nonspherical. Globular is approximately spherical. Irregular means lacking symmetry. A flake is flat or scalelike, and relatively thin. Elongated means caraway-seed shaped. (b) C: cast; C-W: cast core, wrought surface; W: wrought. (c) Individual particles. (d) Sorptometer or radiochemical. (e) Average particle diameter, Fisher Subsieve Sizer, 5 to >50 µm (0.2 to >2 mils); mass mean diameter, 7 to >90 µm (0.3 to >4 mils). (f) Also made in alloys. (g) Average particle diameter, Fisher Subsieve Sizer, 4 to 35 µm (0.2 to 1.4 mils); mass mean diameter, 8 to 48 µm (0.3 to 1.9 mils). (h) Estimated. (j) Approximate.

Table 1. (Continued)

Type of particulate	Density: Apparent g/cm³	Density: Apparent lb/in.³	Density: Tapped g/cm³	Density: Tapped lb/in.³	Oxide, %	Aluminum, %	Uses
Air-atomized	0.73–1.24	0.26–0.45	1.16–1.62	0.42–0.59	0.1–1.1	99.5+(f)	Ball-mill feed, rocket fuels, chemicals, explosives, pigments
Spherical atomized	0.54–1.41	0.2–0.51	0.89–1.70	0.32–0.6	0.1–1.7	99.5+	Rocket fuels
Shot	1.49	0.54	1.8	0.7	0.08	99.5+(f)	Chemical, metallurgical, petroleum
Acicular	1.00–1.11	0.4–0.40	1.40–1.44	0.51–0.52	0.004–0.03	99+(f)	Chemical, metallurgical
Granulated	1.3–1.5	0.5–0.5	1.5–1.7	0.5–0.6	Nil	99+	Chemical, metallurgical
Foil granules	0.54–0.68	0.2–0.25	...	...	0.1(j)	99.3+	...
Flake	...		...	...	...	...	Pigments, pyrotechnics, explosives, metallurgical
Balled foil granules	...	...	...	...	...	...	Chemical
Cut foil and flitter	0.17	0.06	0.41	0.15	Nil	99.5(f)	...
Machined chips	1.0	0.4	1.2	0.4	Nil	90–99.5+	Chemical
Chopped wire	0.5	0.2	0.6	0.2	Nil	99.5(f)	Chemical

(a) Granular is approximately equidimensional nonspherical. Globular is approximately spherical. Irregular means lacking symmetry. A flake is flat or scalelike, and relatively thin. Elongated means caraway-seed shaped. (b) C: cast; C-W: cast core, wrought surface; W: wrought. (c) Individual particles. (d) Sorptometer or radiochemical. (e) Average particle diameter, Fisher Subsieve Sizer, 5 to >50 μm (0.2 to >2 mils); mass mean diameter, 7 to >90 μm (0.3 to >4 mils). (f) Also made in alloys. (g) Average particle diameter, Fisher Subsieve Sizer, 4 to 35 μm (0.2 to 1.4 mils); mass mean diameter, 8 to 48 μm (0.3 to 1.9 mils). (h) Estimated. (j) Approximate.

Cut foil and flitter are made by chopping, cutting, or milling and are coarse in two dimensions usually above powder size. The structure is highly worked.

Balled foil granules are typically milled from either virgin or reclaimed foil sources. The product is characterized by an apparent density less than cast products of similar size. The structure is highly worked, which tends to promote chemical reactivity.

Air-atomized powders are produced directly from a melt. They are of a complex nodular shape with a cast structure. Inferred rates of solidification on the order of 10^3 to 10^6 K/s are generally encountered in atomized powder. Current commercial volume is in pure aluminum grades although all alloy types have been atomized.

Spherical atomized powders are spherical because of solidification in either inert or low oxidizing potential atmospheres. The molten metal feed can be broken up by gas aspiration, ultrasonics, or centrifugal force or gas vacuum desorption in commercial productions schemes. These products exhibit a cast structure and show inferred solidification rates on the same order as those of air-atomized powders.

Flake powders comprise an important and complex group of mechanically worked powders. Atomized powder may be a source material that is then worked to flake in a ventilated ball mill using suitable lubricants. Flake for pigment uses usually is classified as leafing or nonleafing, characterizations that are covered in Chapter 2 of this Volume. High-energy milling can be used to produce pure, prealloyed, or mechanically alloyed flake or spherical powders useful for fully dense powder metallurgy products. High oxide contents of over 2 wt% are readily obtained when the oxide is present in a finely dispersed form. Carbides may also be generated from the lubricant.

In addition to these commercially important powders, some ultrafine powders of 1 μm (0.04 mil) and less are produced by condensation or by research-type atomizers. These powders can be significant to metallurgical investigators because they are electron transparent, permitting instrumental analysis of virgin microstructures.

Safety. Before contemplating production, handling, storage, or use of aluminum in powder form, a thorough understanding and appreciation of the dangers and means for safe handling should be acquired (Ref 1–3).

APPLICATIONS OF ALUMINUM PARTICULATES AND POWDERS

The chemical activity, comparative abundance, and relatively low cost of aluminum make it useful in a variety of reactions and applications. Selection of particulate and powder surface areas for initiating and controlling reaction rates are made available through the many modes of manufacture and subsequent particle classifications. General applications in the applied fields of metallurgy, chemistry, commercial explosives, and other industries are reviewed briefly in the following sections.

Metallurgical Industries

Aluminum particulates have four broad uses in the metallurgical industry: (1) aluminothermic reactions; (2) alloying additives; (3) pressed

and sintered powder metallurgy structural parts; and (4) wrought powder metallurgy products.

Aluminothermic reactions basically are used for the reducing and heat-producing reactions obtainable from aluminum and metal oxide mixtures. Reduction reactions are quite common in the refinement and preparation of ferroalloys containing reducible oxide forms of molybdenum, columbium, tungsten, vanadium, and titanium. The distinct advantage of this class of aluminothermic reactions is that reactions are exothermic (self-sustaining), and contamination of other common furnace-type reductants such as carbon and silicon is avoided. Heat-producing (exothermic) reactions include hot topping of steels, exothermic welding, localized heating to achieve annealing, stress relieving, and powder lancing, or thermal cutting of non-oxidizing, refractory-type material such as fire brick and concrete.

Alloying Additives. Aluminum may be added to materials in a prealloyed powder form or as a compacted powder briquette of blended elemental constituents. The latter form has many advantages over cast alloy additives, such as more rapid metal solution and higher purity of individual constituents. The ratio of constituents is easily adjusted, and selection of briquette size allows for more precise alloying quantities.

The chemical industries consume thousands of tons of high-purity and custom-alloy aluminum powders every year. The complexity of processes using aluminum powder for the synthesis of organic-metallic compounds and for catalysts precludes adequate description within this text. Aluminum powders, rather than ingot forms, are preferred by the chemical industries because the high surface areas of powders and the availability of a variety of particle sizes promote rapid, controllable reaction rates. The high-purity ingot from which powders are made provides for a minimum of contaminating metallic residuals in processes during which the aluminum powder products are consumed. Significant aluminum compounds that may be manufactured using aluminum powders are aluminum alkyls, aluminum chlorophydroxide, anhydrous aluminum chloride, aluminum alkoxides, and reactions requiring nascent hydrogen. The aluminum compounds formed are used as process intermediates or final products in the manufacture of detergents, plasticizers, polymerization catalysts and antiperspirants.

Commercial Explosives and Propellants

Aluminum powder is frequently added to explosives and propellants to improve their efficiency. No gaseous products are formed in the oxidation reaction; however, the very high heat of formation of the oxide results in a considerable gain in heat of explosions, and a higher temperature is imparted to the volatile constituents. The performance effect produced by aluminum powder is used in two general categories, slurry explosives and composite propellants (Ref 4).

Slurry Explosives. Slurries consist of a saturated aqueous solution (approximately 65%) of ammonium nitrate or other nitrates. Other fuels such as fuel oil and soluble glycols are common in specific formulations, but aluminum is the most important fuel in the system. Thickeners such as

Guar gums and cross-linking agents may be included in the explosive formulation to minimize excessive flow in filling boreholes or handling rigid, packaged, tubular forms. The sensitivity (ease of ignition) of these materials may be improved further by the addition of small percentages of a fine aluminum flake or specific organic compounds.

Propellants. Aluminum powder has been and remains one of the most important fuels in solid propellants used in missiles and rockets. Propellants in which aluminum powders make up the primary fuel source are termed composites. This class of propellant essentially consists of mixtures containing an oxidizer (usually ammonium perchlorate), a binder (usually a polymer), controlling and stabilizing additives, and aluminum powders. Composites are normally cast and cured in the rocket motor chamber; however, they may be extruded into cartridge form and inserted in the motor. Burning rates and resulting thrust are controlled by propellant composition and the shape of the propellant form, combustion chamber, and nozzles. In such systems, the particle size distribution of the aluminum powder fuel is very critical because it affects the density and rheological characteristics of the propellant and overall burning rate performance.

Other industrial applications of aluminum powders take advantage of natural characteristics of the metal itself, such as attractive color, malleability, thermal conductivity, and corrosion resistance. Malleable powders converted to thin-flake form by ball-milling processes are used extensively as pigment in industrial paints, roof coatings, paper coatings, and printing inks. A high-purity, specialized form of flake pigment is used worldwide in automotive and other paint finishing applications having a rich, sparkling appearance. The plastics industries use powders in a variety of end products, including fillers in adhesives, epoxy casting compounds, cold solders, and as a thermal conductor in thermosetting type systems.

The corrosion resistance of aluminum in ambient and industrial atmospheres may be imparted to iron and steel shapes through a metallizing process. Aluminum-clad steel wire is produced by continuous cold rolling and hot rolling of a powder surface around the steel core. Other coating techniques include powder coating followed by a thermal diffusion process or thermal spraying using highly specialized applicating equipment and gases.

PRESSED AND SINTERED POWDER METALLURGY PARTS

Powder metallurgy parts, a result of consolidation of metal powders into precise shapes using pressed compaction of powder in precisely shaped metal dies, provides a means for generating low-cost parts for high-volume, small part applications. While work with aluminum powder materials for pressed and sintered applications has been under study since 1940, the work of Storchheim (Ref 5 and 6) and Dudas (Ref 7–10) resulted in a commercially viable process for compaction and sintering of aluminum powders for the production of structural components. Key elements for the P/M parts process include the following critical elements:

- Powder selection
- Compaction characteristics

- Sintering
- Secondary operations
- Heat treatment

Powder Selection. Screen analysis for base aluminum powder used in aluminum powder metallurgy premixes is shown below:

U.S. standard sieve mesh	Typical range
+50	Trace
−50 + 100	10–20
−100 + 200	20–30
−200 + 325	15–25
−325	30–40

Aluminum powder of the size and chemical analysis shown above has a desirable mixture of particle sizes, to combine characteristics of smooth, uniform flow into shape dies and good compressibility to achieve high density and good green (as-pressed) strength in pressed powder parts. An aluminum powder metallurgy blend suitable for the production of usable structural parts necessarily has other metal powders added for alloying, to promote higher strength than unalloyed aluminum could achieve. Example compositions of blends for this purpose are typified by those shown in Table 2. While mixtures of these materials alone produce an effective structural part after complete processing, ad-mixing a solid lubricant results in improved die life and reduced or eliminated galling of powder metallurgy tools. Lubricants with low moisture content and low residual ash content like those described in Table 3 have been successfully applied to powder metallurgy parts. Good die wear characteristics and minimal degradation in properties associated with the lubricant residue were achieved.

Compaction. Aluminum P/M blends are substantially more compressible than iron powder, as shown in Fig. 1. The effect of this improved compressibility results in substantially higher green densities for a given applied compaction pressure than are achieved with iron powder. The effect on part characteristics is to enhance the green strength and handling

Table 2. Nominal Composition of Several Powder Metallurgy Premixes

	Element, wt%							Lubricant, wt %	Recommended sintering temperature(b)	
Premix(a)	Copper	Silicon	Magnesium	Zinc	Chromium	Manganese	Aluminum		°C	°F
Alcoa 601AB	0.25	0.6	1.0	...	...	...	rem	1.5	620	1150
Alcoa 201AB	4.4	0.8	0.5	...	...	...	rem	1.5	590	1090
Alcan 24	4.4	0.9	0.5	...	...	0.4	rem	...	595	1100
Alcan 69	0.25	0.6	1.0	...	0.10	...	rem	...	620	1150
Alcan 76	1.6	...	2.5	5.6	0.20	...	rem	...	595	1100

(a) Manufacturer identification is not intended as an endorsement of the product. (b) Temperature of part, within ±3 °C (±5 °F).

Table 3. Lubricants Added to Aluminum Premixes for Die Wear Control

Lubricant(a)	Moisture and volatiles at 105 °C (220 °F), %	Residual ash at 800 °C (1470 °F), %	Manufacturer(a)
Acrawax C	0.08	0.00	Glyco Chemical, Inc., New York, NY
Sterotex	0.01	0.02	Capital City Products Company, Columbus, OH

(a) Manufacturer identification is not meant to endorse these specific products.

characteristics of aluminum powder green compacts and to potentially increase the size capability of parts that can be produced for a specific tonnage press.

Sintering. Aluminum powder metallurgy parts are sintered by a liquid-phase process to raise their density from the green condition and to substantially enhance bonding and raised strength of these components through uniform composition. The liquid phases are formed by heating parts to sufficiently high temperature that liquid solutions between the aluminum, copper, silicon, and magnesium are formed to promote bonding and interdiffusion of these elements. The densification and improvement in composition uniformity during sintering is illustrated by Dudas *et al* (Ref 10).

While the sintering process is primarily aimed at enhancing strength and composition uniformity, the process for aluminum is divided into several steps leading ultimately to the liquid-phase sintering operation. Green parts are charged into a sintering furnace wherein a dry, protective atmosphere can be maintained, with the atmospheric dew point maintained at −40 °C (−40 °F) or lower in the heated portions of the furnace. The initial heatup to temperatures in the range of 350 to 425 °C (660 to 800 °F) for some blends is used to volatilize the solid lubricant that is added to the powder. After lubricant volatilization, the parts are further

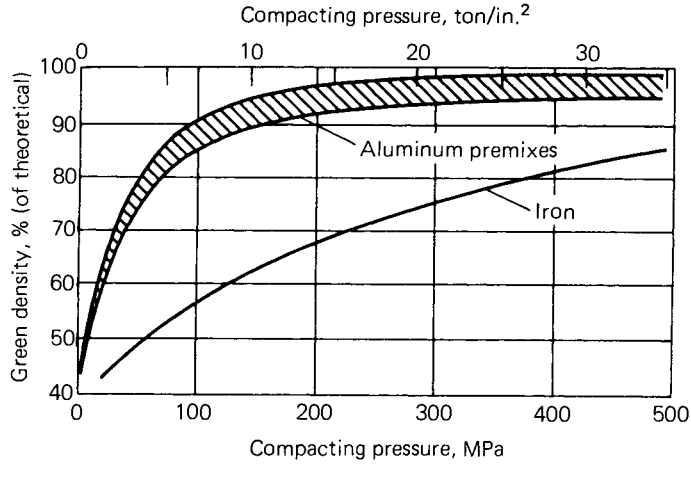

Fig. 1. Compacting pressure versus green density: compressibility comparison between typical iron powder metallurgy powders and aluminum powder metallurgy premixes.

heated to temperatures shown in Table 2 for the various P/M premix powders. Temperature uniformity is very critical in this operation because of the significant amount of liquid phase used for sintering aluminum P/M premix powders. Temperatures shown in Table 2 should be maintained within 3 °C (5 °F) for sintering. Time of sintering should be tailored to the individual part, its shape, and pressing characteristics, although sintering times ranging from 5 to 30 min are commonly used. Figure 2 illustrates the effect of sintering time on the microstructure of 201 AB sintered compacts. After sintering, the parts are cooled with atmospheric protection to a temperature in the range of 425 °C (800 °F) or less.

Secondary Operations. After parts are sintered, a number of subsequent operations can be applied to further enhance their characteristics, either in size or in performance capability. These operations can include restriking the parts to improve their dimensional characteristics or to slightly enhance densification; cold or hot forging to develop the highest possible physical and mechanical characteristics (Ref 11 and 12); and heat treatment to thermally treat certain alloys that are precipitation-strengthened to enhance mechanical properties (Ref 13).

Heat Treatment. Thermal treatments to enhance strength are a widely used secondary operation for enhancing the characteristics of aluminum P/M parts. The tempering operations commonly applied to these materials are defined by the temper designations shown below:

- T1: As-sintered
- T2: As cold formed (after sintered)
- T4: Solution heat treated plus four days minimum at room temperature
- T6: Solution heat treated plus precipitation heat treatment

These temper designations do not necessarily coincide with Aluminum Association designations. Applying these thermal treatments to various forms of P/M parts results in a variety of characteristics, depending on prior treatments. Results shown in Table 4 summarize typical mechanical property characteristics for a P/M blend alloy in a number of temper conditions. These tempering operations are metallurgically identical to similar operations used on aluminum wrought products described in Chapter 5 of this Volume.

Applications of aluminum powder metallurgy parts are extensive. They have been used to replace small aluminum castings, extrusions, and screw machine products that involve extensive machining operations. They are also being used to replace other heavier powder metallurgy materials where the lighter weight and enhanced corrosion characteristics of aluminum provide additional benefit. Figure 3 shows a number of applications where aluminum P/M parts have been applied to illustrate the range of sizes and degrees of complexity that this technology makes possible. Systems where these materials are used include business machines, automotive and truck components, power tools, hydraulic systems, military ordnance components, sewing machines, electrical systems, and appliances.

HIGH-STRENGTH WROUGHT POWDER METALLURGY PRODUCTS

Powder metallurgy provides an alternative to ingot metallurgy (I/M) for producing wrought products with superior characteristics. Powder is most often made by rapid solidification techniques such as atomization

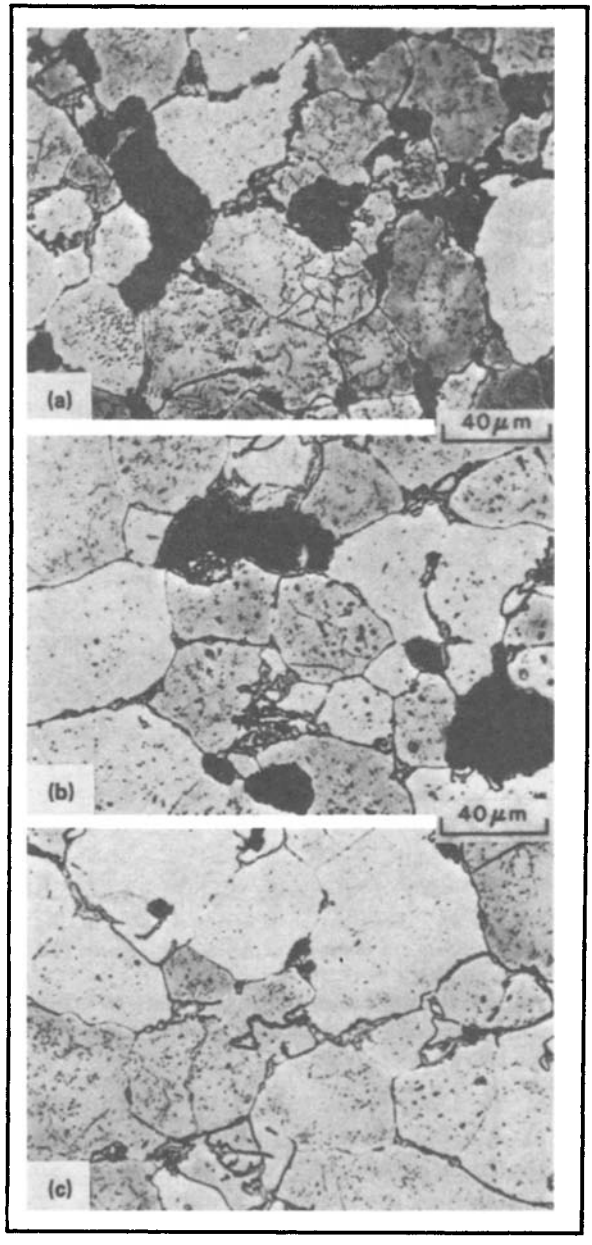

Fig. 2. Microstructures of 201AB sintered compacts, showing increased density and structure homogeneity with increased sintering time. (a) Sintered 1 min at 595 °C (1100 °F). (b) Sintered 15 min at 595 °C (1100 °F). (c) Sintered 30 min at 595 °C (1100 °F).

Table 4. Typical Product Data for Powder Metallurgy Alloys After Cold Forming and Hot Forging

601AB alloy	Tensile strength MPa	Tensile strength ksi	Yield strength MPa	Yield strength ksi	Elongation, % (in./in.)
T1(a)	145	21.0	94	13.7	6.0
Cold formed T2(b)	233	33.8	216	31.3	1.0
Cold formed T4	199	28.8	121	17.5	8.0
Cold formed T6	269	39.0	248	36.0	1.7
Hot forged T4(c)	262	38.0	138	20.0	16.0
Hot forged T6	345	50.0	317	46.0	8.0

(a) At 90% theoretical density. (b) Cold formed at 19 to 23% upset. (c) Hot forged at 50% height reduction.

(Ref 14), splat cooling (Ref 14 and 15), and molten metal spinning (Ref 16). It is then usually degassed to remove hydration water that forms upon exposure to ambient air. The powder is consolidated by any one of several techniques, including vacuum hot pressing (Ref 17), hot isostatic pressing (Ref 18), or direct powder rolling (Ref 19) or extrusion (Ref 20). The P/M technology for producing wrought products has recently been reviewed (Ref 21).

Aluminum P/M alloys are developed by rapid solidification and also mechanical attrition. The mechanical attrition techniques include sintered aluminum powder (SAP) technology (Ref 22 and 23) and mechanical alloying (Ref 24 and 25). In these techniques, powder is milled before degassing and consolidation to introduce dispersed phases and to control powder size and shape.

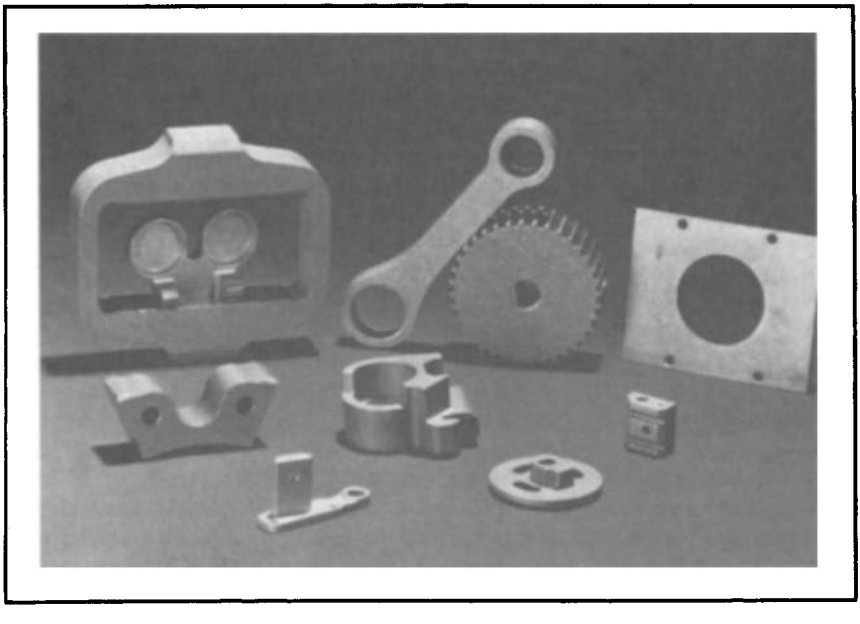

Fig. 3. Typical aluminum powder metallurgy parts.

Table 5. Nominal Composition of Aluminum Powder Metallurgy Alloys

Alloy(a)	Element, wt%								
	Zinc	Magnesium	Copper	Cobalt	Zirconium	Oxygen	Carbon	Chromium	Aluminum
7091	6.5	2.5	1.5	0.4	...	0.35	...	...	rem
7090	8.0	2.5	1.0	1.4	...	0.35	...	...	rem
MR61	8.5	2.5	1.5	0.6	0.2	<0.5	...	...	rem
IN 9051	...	4.0	...	...	...	0.6	0.75	...	rem
IN 9052	...	4.0	...	...	...	0.8	1.1	...	rem
IN 9021	...	1.5	4.0	...	...	0.8	1.1	...	rem
MR64	6.8–8.0	1.9–2.9	1.8–2.4	0.1–0.4	0.1–0.35	<0.05	<0.05	0.08–0.25	rem
1519B	6.8–8.0	1.9–2.9	1.8–2.4	...	...	<0.05	<0.05	0.1–0.5	rem

(a) 7090 and 7091 are U.S. Aluminum Association designations. MR61, MR64, and 1519B are Kaiser Aluminum Co. designations. IN 9051, IN 9052, and IN 9021 are International Nickel Co. designations.

Aluminum P/M alloy development has sought materials with improved properties in three broad areas: (1) high room temperature strength, (2) high modulus and low density, and (3) elevated-temperature strength. Powder metallurgy offers the possibility of improved properties because P/M processes: (1) refine microstructural features such as grain size and constituent particle size, (2) extend solubility limits of alloying elements, (3) permit alloying of elements that cannot be alloyed by conventional I/M, (4) enable creation of new metastable strengthening phases, and (5) allow oxide and carbide dispersion strengthening. The development efforts have been successful for several alloys, and wrought products of several aluminum P/M alloys are now available on a pilot production scale.

High-Strength Aluminum Alloys for Room Temperature Service. Aluminum alloys development using atomization has been ongoing for over 15 years, with much work concentrated on 7XXX alloys containing alloying additions that are largely insoluble in solid aluminum (Ref 26–31). This work led to the development of the recently commercialized alloys 7091* and 7090,** which are 7XXX alloys to which cobalt has been alloyed: 0.4 wt% in 7091 and 1.5 wt% in 7090.

The nominal composition of these and other aluminum P/M alloys are given in Table 5. Both 7091 and 7090 have excellent combinations of high strength and stress-corrosion cracking (SCC) resistance. Figure 4 shows the enhanced survival rate of 7090 and 7091 forgings at various strength levels in an industrial atmosphere, compared with conventional I/M alloys 7075 and 7175. The improved SCC resistance at a given strength level is attributed to the fine grain size, the presence of cobalt as a finely dispersed second phase, and the reduced segregation in 7090 and 7091—all resulting from the rapid solidification made possible by P/M.

Excellent typical strength levels have been obtained for both 7090 and 7091 in commercial-scale extrusions (Table 6) and forgings (Table 7). In addition, the toughness and strength of these alloys are superior to those of conventional I/M alloys (Fig. 5). The improved toughness and strength are possible because the rapid solidification occurring during atomization refines the size of constituent particles, which is known to affect toughness.

*Formerly called MA87 or CT91 (Aluminum Company of America designations).
**Formerly called MA67 or CT90 (Aluminum Company of America designations).

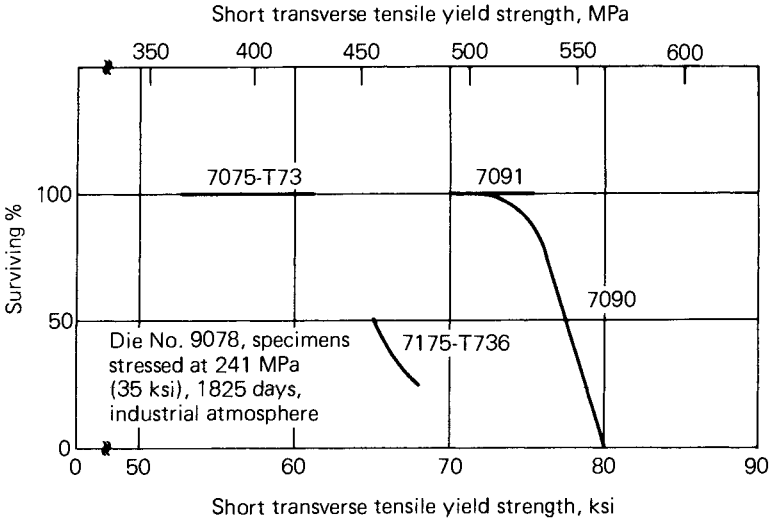

Fig. 4. Stress-corrosion cracking strength capabilities, thin, web-flange die forgings, and powder metallurgy alloys 7090 and 7091 versus ingot metallurgy alloys 7075 and 7175.

The fatigue resistance of 7090 and 7091 confers both advantages and disadvantages over I/M alloys. Results on stress versus number of cycles to failure for both notched and unnotched specimens are superior to those of P/M alloys (Ref 30). However, the fatigue crack growth rate (FCGR) at low stress-intensity levels is higher for 7090 and 7091 and for improved I/M alloys (Ref 32). This deficiency is attributed to the ultrafine grain size in these P/M alloys of 1 to 10 μm (0.04 to 0.4 mil), which is so small that the plastic zone extends over several grains (Ref 33). This means that a fatigue crack can more readily propagate from one grain to another. The FCGR can be reduced in 7090 and 7091 by grain growth (Ref 34).

MR61 is another atomized alloy similar in strength and composition to 7090 (see Table 5); however, it contains zirconium, presumably for grain refinement (Ref 35 and 36). Extrusions of MR61 were made on a pilot production scale and were used for seat tracks in Boeing 727 airliners, along with competitive P/M alloys 7090 and IN 9051. The alloy exhibits an excellent ultimate tensile strength (UTS) of 669 MPa (97 ksi) and a yield strength of 627 MPa (91 ksi) with 9.5% elongation. MR61 also has good SCC and exfoliation corrosion resistance.

Two new alloys, MR64 and 1519B, have superseded MR61. Their compositions (see Table 5) are similar, but MR64 contains cobalt and zirconium and 1519B does not. Both alloys are resistant to stress-corrosion cracking. Table 8 displays mechanical and SCC properties from forgings of these two alloys (Ref 34), and compares them with I/M 7050. These alloys are nearing the commercial stage.

Most alloy development by mechanical attrition is accomplished by mechanical alloying, a patented process that is an improved version of

Table 6. Typical Tensile Properties for Extruded Shapes of 7090 and 7091

Alloy	Orientation	Tensile strength MPa	Tensile strength ksi	Yield strength MPa	Yield strength ksi	Elongation, %—4D
7090	Longitudinal	627	91	586	85	10
	Long transverse	593	86	538	78	6
7091	Longitudinal	593	86	545	79	12
	Long transverse	552	80	510	74	8

Note: Section thickness of 6 mm (0.25 in.) to 38 mm (1.5 in.). Mechanical properties attained after solution heat treatment and aging to peak strength. 7090 was further aged for 1 to 2 h at 160 °C (325 °F). 7091 was further aged 4 h at 160 °C (325 °F).

Table 7. Typical Tensile Properties for Die Forgings of 7090 and 7091

Alloy	Orientation	Tensile strength MPa	Tensile strength ksi	Yield strength MPa	Yield strength ksi	Elongation, %—4D
7090	Longitudinal	614	89	579	84	10
	Transverse	579	84	545	79	4
7091	Longitudinal	579	84	531	77	13
	Transverse	545	79	496	72	9

Note: Section thickness of 76 mm (3.0 in.).

SAP processing (Ref 37). The high-energy milling occurring in this process enables the superimposition of many strengthening mechanisms. For example, IN 9051 is a patented (Ref 38 and 39), Al-4 wt% Mg alloy (Table 5) that is strengthened by:

- Magnesium solid solution strengthening
- Ultrafine grain size strengthening (<0.5 μm or <0.02 mil)
- Oxide dispersion strengthening
- Carbide dispersion strengthening
- Substructural strengthening

The microstructure of this alloy is quite homogeneous and precipitation strengthening is not necessary to achieve high strength levels. The alloy is non-heat treatable, and as a consequence of its refined, electrochemically passive microstructure, it has excellent general corrosion resistance and stress-corrosion resistance even when loaded close to the yield strength. IN 9052 is a similar alloy (Table 5) with higher dispersoid content that also has excellent SCC resistance.

IN 9021 is a mechanically alloyed 2XXX material that adds precipitation strengthening to the aforementioned strengthening mechanisms. Strength is increased, and corrosion and SCC resistance are still very good. The electrochemical passivity of the dispersed oxides presumably contributes to the corrosion and SCC resistance. The oxides dispersed in mechanically alloyed materials also increase elastic modulus, and the three alloys have a higher specific modulus (Young's modulus ÷ density: E/ρ) than 7075. Commercial-scale properties of forgings of three alloys are included in Table 9. Because the FCGR of IN 9021 is lower than that in 7075, the alloy has many potential applications in aircraft.

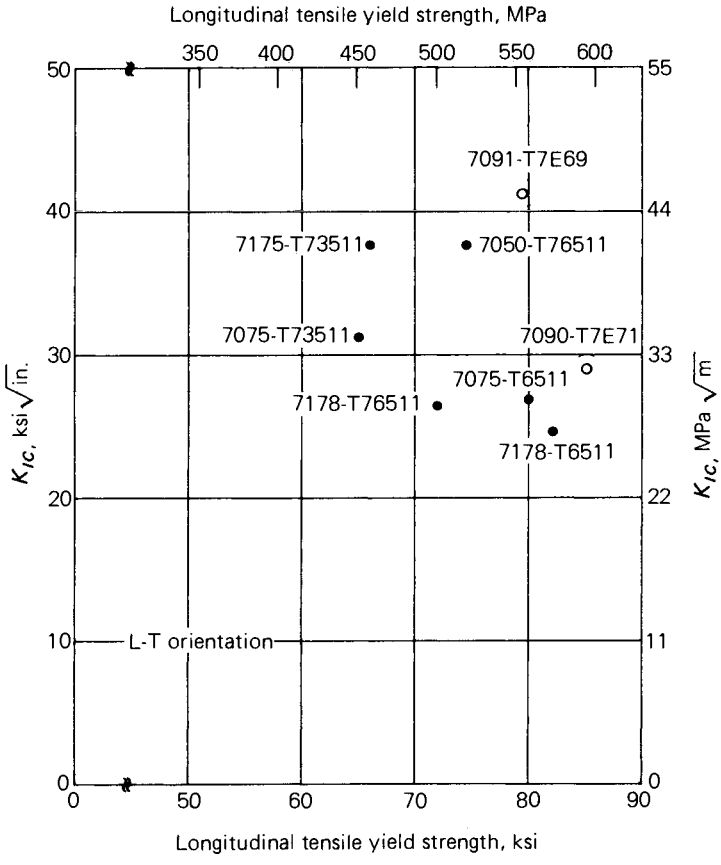

Fig. 5. Typical fracture toughness versus tensile yield strength for high-strength aluminum alloy extruded shapes 6 mm (0.25 in.) to 38 mm (1.5 in.) in thickness.

Jangg (Ref 40) and co-workers are producing SAP-type alloys with excellent room temperature strength (>700 MPa or >102 ksi) on an experimental scale. The process is called reaction milling, and the alloys produced rely primarily on carbide dispersion strengthening; the carbon is introduced as lamp black during ball milling. None of these alloys is available commercially at present.

Excellent properties have been obtained from commercial-scale extrusions and forgings of aluminum P/M alloys. However, data from plate are limited because of the technical difficulties involved in producing ingots large enough to be rolled in conventional rolling mills. Cebulak (Ref 41) has demonstrated the feasibility of manufacturing plant-scale ingots by making 1500-kg (3307-lb) ingots from an earlier version of 7091 and 7090 alloys.

High-Modulus and Low-Density Alloys. Alloying lithium to aluminum decreases density while increasing modulus, because of the formation of the δ′ phase, Al_3Li. Several aluminum and aerospace companies (Ref 42–44) are developing high E/ρ aluminum-lithium P/M alloys. At-

Table 8. Strength and SCC Data from Forgings of P/M and I/M Alloys

Alloy	Temper	Ultimate tensile strength, MPa	Ultimate tensile strength, ksi	Yield strength, MPa	Yield strength, ksi	Elongation, %	Failure, days(a)
1519B	T76	558	81	510	74	10	43
	T73	510	74	448	65	11	190
MR64	T76	600	87	552	80	6	60
	T73	558	81	496	72	9	116
I/M 7050	T73	503	73	448	65	5	23

(a) Days to failure with alternate immersion in 3.5% NaCl aqueous solution at 310 MPa (45 ksi).

tractive experimental properties have been obtained, but none of those P/M alloys is commercially available. Several aluminum companies are likely to market aluminum-lithium alloys made by I/M in the near future (Ref 34).

Dispersed intermetallics other than Al_3Li can also increase modulus. For example, an experimental, splat-cooled Al-8 wt% Fe-2 wt% Mo alloy for elevated-temperature service has a high room temperature modulus (Ref 34), because of the presence of intermetallic phases. Modulus can also be increased by dispersed oxides, as evidenced by mechanically alloyed materials. IN 9021 and IN 9052 have specific stiffness values of 5 and 8%, respectively, greater than that of I/M 7075, largely because of their dispersed oxides (Ref 34). Development of high E/ρ materials is continuing by both P/M and I/M, although no high E/ρ alloy is enjoying widespread commercial usage.

Alloys for Elevated-Temperature Service. Considerable research activity has been undertaken in the development of aluminum P/M alloys for elevated-temperature service. Air Force Wright Aeronautical Laboratories (AFWAL) has sponsored alloy development for service at 230 to 345 °C (450 to 650 °F) by atomization (Ref 45–47) and by mechanical alloying (Ref 48); NASA has sponsored development of alloys for 135 °C (275 °F) service (Ref 49), and a jet engine manufacturer has an internally funded splat-cooling program to develop aluminum alloys for use at elevated temperatures in jet engines (Ref 50 and 51). The rapid solidification approach has produced alloys with attractive elevated-temperature strength. For example, an Al-8 wt% Fe-4 wt% Ce alloy has

Table 9. Tensile Properties of Mechanically Alloyed Forgings(a)

Alloy	Orientation	Ultimate tensile strength, MPa	Ultimate tensile strength, ksi	Yield strength, MPa	Yield strength, ksi	Elongation, %
9052	Longitudinal	595	86.3	560	81.2	6
	Short transverse	568	82.4	550	79.7	2.5
9021 T4	Longitudinal	625	90.7	597	86.6	14
	Short transverse	597	86.6	585	84.8	11
I/M 7075 T7	Longitudinal	483	70	407	59	8
	Short transverse	448	65	372	54	4

(a) From Lockheed Longeron End Tie.

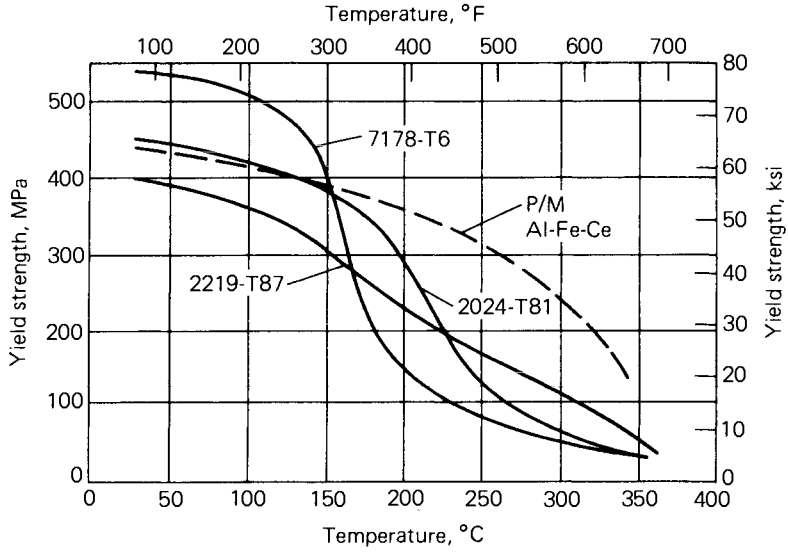

Fig. 6. Yield strength versus temperature for powder metallurgy aluminum-iron-cerium alloy, compared to various ingot metallurgy alloys after 100 h of exposure at temperatures shown.

much greater strength at elevated temperature than does I/M alloy 2219, as Fig. 6 shows (Ref 34). In addition, forgings of Al-8 wt% Fe-4 wt% Ce show only 0.05% plastic strain after 100 h at a stress of 138 MPa (20 ksi) and 230 °C (450 °F), whereas the plastic strain for I/M 2219 T851 is an order of magnitude greater. This alloy is still in the experimental stage.

An Al-8 wt% Fe-2 wt% Mo alloy under development may successfully compete with titanium alloys at 205 °C (400 °F) (Ref 34). Several experimental mechanically alloyed materials have fair strength at 425 °C (800 °F), but they are not as strong as the rapidly solidified alloys at 230 to 345 °C (450 to 650 °F) (Ref 47). Jangg (Ref 52) has had considerable success with his mechanical attrition process, reaction milling, and has obtained experimental ultimate tensile strength values around ~240 MPa (~34 ksi) at ~345 °C (~650 °F) on aluminum-carbon alloys.

Conclusion. Several new aluminum P/M alloys with very attractive properties are available on a pilot production scale in extrusions and forgings. Availability of plate of these alloys is limited because of the difficulty in making commercial-scale rolling ingots.

REFERENCES

1. Recommendations for Storage and Handling of Aluminum Pigments and Powder, Publications TR-2, the Aluminum Association, Sept 1977
2. M. Jacobson, A.R. Cooper, and T. Nagy, Explosibility of Metal Powders, V. S. Bureau of Mines, RI 6516
3. NFPA Standard 65-1180, Processing and Finishing of Aluminum, National Fire Protection Association, Inc., Boston, MA, 1980
4. R. Meyer, *Explosives*, New York: Verlag Chemie, Weinheim, 1977

5. S. Storchheim, Aluminum Powder Metallurgy Finally Made Commercially Practical, *Progress in Powder Metallurgy*, Vol 18, 1962, p 124–130
6. S. Storchheim, Porous Aluminum Bearings, *Product Engineering*, Vol 3, 1962, p 53–55
7. J.H. Dudas and W.A. Dean, The Production of Precision Aluminum P/M Parts, presented at the P/M conference and exhibit at the Park Sheraton Hotel, New York, 7 May 1969; published in the April issue of *International Journal of Powder Metallurgy*
8. J.H. Dudas and K.J. Brondyke, Aluminum P/M Parts—Their Properties and Performance, Technical Paper No. 70041, SAE, 1970
9. J.H. Dudas and D.B. Thompson, Improved Sintering Procedures for Aluminum P/M Parts, Aluminum Company of America, 1970
10. J.H. Dudas, R.H. Stevens, and B.K. Gildersleeve, Metallography and Structure Interpretation of Aluminum P/M Parts, *International Journal of Powder Metallurgy and Powder Technology*, Oct 1974
11. K.E. Buchovecky and A.L. Hurst, Fabrication and Properties of Cold-Formed Aluminum P/M Parts, prepared for MPIF International P/M Conference, Toronto, Canada, 19 July 1973
12. K.E. Buchovecky and M.R. Rearick, Aluminum P/M Forgings, *Metal Progress*, Feb 1972
13. Properties and Applications of Non-Ferrous Powder Metal Parts, *Metal Progress*, June 1981, p 65
14. N.J. Grant, in "Proceedings of the International Conference on the Rapid Solidification Process," Baton Rouge, LA: Claitor's Publishing Division, 1978, p 230
15. G. Thursfield and M.J. Stowell, *Journal of Material Science*, Vol 9, 1974, p 1644
16. C.E. Mobley, A.H. Claver, and B.A. Wilcox, *Journal of the Institute of Metals*, Vol 100, 1972, p 142
17. J.P. Lyle and W.S. Cebulak, *Metallurgical Transactions A*, Vol 6A, 1975, p 685–699
18. H. Fischmeister, *Powder Metallurgy Institute*, Vol 10, 1978, p 119
19. D.H. Ro, "Direct Rolling of Aluminum Powder Metal Strip," AFWAL Contract No. F33615-80-C-5161, interim report for period, Sept 1980–Feb 1981
20. G. Naeser, in "Modern Developments in PM," Vol 3, H.H. Hausner, Ed., 1965
21. J.R. Pickens, *Journal of Material Science*, Vol 16, 1981, p 1437–1457
22. R. Irmann, *Metallurgia*, Vol 46, 1952, p 125
23. E.A. Bloch, *Metallurgical Review*, Vol 6, 1961, p 22
24. J.S. Benjamin, *Scientific American*, Vol 234, 1976, p 40
25. J.S. Benjamin and M.J. Bomford, *Metallurgical Transactions A*, Vol 8A, 1977, p 1301
26. A.P. Haarr, U.S. Army, Frankford Arsenal Report 13-64-AP59S, Oct 1964
27. A.P. Haarr, U.S. Army, Frankford Arsenal Report 13-65-AP59S, Dec 1965
28. J.P. Lyle, W.S. Cebulak, and K.E. Buchovecky, in "Progress in PM," Vol 28, A.S. Bufferd, Ed., Metal Powder Industries Federation, New York, 1972, p 93
29. J.P. Lyle and W.S. Cebulak, *Metallurgical Engineering Quarterly*, Vol 1, 1974, p 52
30. W.S. Cebulak, E.W. Johnson, H. Markus, *International Journal of Powder Metallurgy and Powder Technology*, Vol 12, 1976, p 299
31. W.S. Cebulak and D.J. Truax, U.S. Army Contract DAAA-25-70-CO358, March 1971
32. D.R. Holloway, Master of Science Thesis, Air Force Institute of Technology, Ohio, Sept 1977
33. V. Kuo and E.A. Starke, "Effect of Processing on the Fatigue Properties of X7091," in Proceedings of Al-P/M Session of AIME Meeting," Dallas, Feb 1982
34. "Proceedings of Aerospace—Aluminum Industry Strategy Assessment Workshop," AFWAL, Dayton, OH, 30–31 July 1981

35. S.G. Roberts, Contract Report DA-04-200-507-ORD-886, US Army Department of Defense, 15 Nov 1961, p 799
36. J.W. Bohler, S.G. Roberts, and G.R. Chanani, Naval Surface Weapons Center Contract No. N60921-80-C-0238, June 1982
37. M.J. Bomford and J.S. Benjamin, US Patent 3,816,080, 11 June 1974
38. J.R. Pickens, R.D. Schelleng, S.J. Donachie, and T.J. Nichol, US Patent No. 4,292,079, 29 Sept 1981
39. J.R. Pickens, R.D. Schelleng, S.J. Donachie, and T.J. Nichol, US Patent No. 4,297,136, 27 Oct 1981
40. G. Jangg, *Metal Powder Report,* Vol 35 (No. 5), 1980, p 206–208
41. W.S. Cebulak, US Army Armament Command, Rock Island, Illinois, Contract No. DAAA25-72-C-0593 Report, April 1977
42. R.E. Lewis, Lockheed Interim Report LMSC-D674504, Palo Alto, CA, March 1979
43. R.E. Lewis, *et al.*, Lockheed Interim Report LMSC-D686125, Palo Alto, CA, Feb 1980
44. I.G. Palmer, R.E. Lewis, and D.D. Crooks, "Rapid Solidification Processing, Principles and Technologies—II," Reston, VA, 23–26 March 1980, p 342–353
45. R.R. Sawtell, W.L. Otto, and D.L. Lege, Air Force Materials Lab., USA, Contract No. F33615-77-C-5086 Report, March 1978
46. R.E. Sanders, G.J. Hildeman, and D.L. Lege, Air Force Materials Lab., USA, Contract No. F33615-77-C-5086 Report, March 1979
47. R.E. Sanders and G.J. Hildeman, Final Report on AFWAL contract No. F33615-77-C-5086, Report No. TR-81-4076, Sept 1981
48. D.L. Erich, AFML Report AFML-TR-79-4210, Contract No. F33615-76-C-5227, Jan 1980
49. G.G. Wald, NASA Contractor Report 165676, Contract No. NAS 1-14625, May 1981
50. A.R. Cox, Air Force Materials Laboratory, USA, Report FR2127, June 1979
51. A.R. Cox, Air Force Materials Laboratory, USA, Report FR11690, March 1979
52. G. Jangg and F. Kutner, *Powder Metallurgy Institute,* Vol 9, 1977, p 24